EDUARDO MANUEL HIPÓLITO PIRES MATEUS

Characterization of *Pinus* spp. needles by gas chromatography and mass spectrometry: Application to plant-insect interactions

Dissertação apresentada para obtenção do
Grau de Doutor em Ciências do Ambiente
pela Universidade Nova de Lisboa,
Faculdade de Ciências e Tecnologia

LISBOA
2008

To my grandparents Celeste, João, Isabel and Manuel

To my children Tomás and Vasco

"Everything should be made as simple as possible - but not one bit simpler"

Albert Einstein

Acknowledgements

First of all I would like to express my gratitude to my supervisor Professor Rosa Paiva for giving me the chance of working with her in the last 20 years and for all her continuous guidance, stimulus, trust and support that promoted my scientific growth and made this work possible. Very special thanks go to my co-supervisor Professor Higuinaldo Chaves das Neves, who introduced me to the chromatographic science and whose suggestions, continuous encouragement, belief in my abilities, logistic and personal support are inseparable from my work and technical growth.

I would like to express my deepest gratitude to Dr. Rui Rocha from LECO Instrumentos S.A., for all his valuable and constant support and for opening me the doors which made possible my work with GC × GC.

To Professors João Tiago Mexia (CMA/FCT/UNL) and Manuela Oliveira (DM/UE) I express my deepest gratitude for all the support in the final stage of my work, guidance and supervision with the statistical analysis of my data.

To Dr. Jitka Zrostlíková, from LECO Corporation, Prague, I would like to thank her technical assistance, support and patience during my staying at the Leco's Application Laboratory Centre, in Prague, and her advices when I was giving my first steps with ChromaTof and GC × GC analysis.

To Professor Fernando Santana and Professor Nunes dos Santos I would like to thank the valuable support at the departure of this process. To Professor Fernando Santana I am also thankful for the opportunities that he gave to me of working with him in research projects and where some of my technical skills have been developed.

I am also very thankful to Professor Maria João Cabrita, from ICAM/UE, for allowing me to use their GC/MS for the resin acids analysis, Professor Philip Marriott, from RMIT, for the GC×GC analysis of resin acids, and Professor Joaquim Vital for supplying some of the terpene standards used.

Special thanks go to Marco Gomes da Silva for his critically reading of this thesis, all the technical discussions, advices, constant support and company.

I am very grateful to Catarina José, for her work and help with the extraction, derivatization and analysis of resin acids, José Munhá for his help with the SDE work, Lena Farral for her old friendship, interesting discussions and statistical support, Ricardo Barata for the hard work with the retention indices determination, Evelyne Moura for all her help with the geographic and Apostiça data, Luz Fernandes for her technical support and constant availability to operate the GC-TOFMS, Professor Manuela Branco and Helena Santos for their support and help with the *Thaumetopoea pityocampa* tasks. I am also very grateful to Professor Zvi Mendel from the Department of Entomology/ARO, Israel for providing me the *P. halepensis* samples from Israel and Greece.

This work was possible throughout the following funding: i) the Portuguese project Project PTDC/AGR-CFL/73107/2006**,** entitled "Analysis of the ongoing evolutionary process of an insect species causing public health concern" and ii) European Project QLK5-CT-2002-00852 entitled “PROMOTH - Global change and Pine Processionary Moth: a new challenge for integrated pest management”.

A thanking thought is also due to DCEA/FCT/UNL, where I started and have always been working, which made this thesis possible.

At last but not the least, I would like to thank my Mother and Father for the love, advices, constant encouragement and strong support that they always gave me, my Father and Mother-in-law for all the precious support and encouragement, Mena for all support and help with my children, my brother João and Ana for taking care of my kids many times and my brother Miguel for his advices.

To my wife Alexandra who in the last leaps of my thesis has been my third (and sometimes fourth) arm, and during the last months have been a lonely mother, dealing with the kids and putting them to bed alone, my biggest and special gratitude for all her patience, understanding and support. For Tomás and Vasco I express my gratitude for their understanding and support, and apologies for my absence.

At the end of my acknowledgements and being aware that many people have directly or indirectly contributed to this work, I would like to apologise all those that, for some reason, I have forgotten to thank. Thank you all.

Sumário

A processionária do pinheiro *Thaumetopoea pityocampa* (Lepidoptera: Notodontidae) é considerado o desfolhador do pinhal mais importante na região mediterrânica. A sua distribuição e dinâmica populacional é influenciada pelas espécies hospedeiras, mas os mecanismos responsáveis pela sobrevivência e êxito reprodutor das populações não são ainda conhecidos. A resistência e/ou susceptibilidade das espécies hospedeiras, poderá dever-se à composição química das agulhas, ou ao "bouquet" de voláteis emitidos pelas árvores hospedeiras. Neste contexto, a caracterização da composição química das agulhas de diferentes espécies de *Pinus* constitui uma ferramenta importante para a descodificação dos processos de selecção das espécies hospedeiras e consequente, dinâmica populacional de *T. pityocampa*.

Assim, foi estudada a composição química das agulhas das espécies *Pinus pinea*, *P. pinaster*, *P. halepensis*, *P. nigra*, *P. brutia, P. patula, P. radiata, P. taeda, P. elliotti, P. kesiya, P. sylvestris* e *P. eldarica*, plantadas num arboretum na região de Abrantes. As fracções voláteis emitidas pelas agulhas foram amostradas por microextracção por fase sólida (SPME) e por destilação-extracção (SDE). Os ácidos resínicos foram extraídos por solvente e derivatizados antes de serem analisados.

As amostras foram analisadas por cromatografia gasosa unidimensional (1D-GC), cromatografia gasosa multidimensional com sistema de transferência por corte ("heart cut"; MDGC), cromatografia bidimensional abrangente (GC × GC) e espectrometria de massa com recurso a diferentes analisadores de massa. Foi também avaliado o potencial de aplicação de espectrometria de massa, utilizando ionização de campo (field ionization; 1D-GC/FI-TOFMS) como modo de ionização.

Os resultados obtidos mostraram que as capacidades analíticas da 1D-GC são parcialmente limitadas pelo poder separativo das colunas. A maior sensibilidade e a eliminação dos efeitos de distorção ("peak skewing") dos espectros de massa colectados por analisadores de massa de tempo de vôo (TOF-"time-of-flight"), em conjunto com a aplicação dos algoritmos de desconvolução espectral e de detecção de picos ("mass spectral deconvolution" e "peak find"), permitiu a detecção de componentes em quantidades vestigiais, com espectros de

massa qualitativos e a extracção qualitativa dos espectros de massa individuais de compostos que co-eluem. Estes resultados conduziram a identificações mais seguras e, consequentemente, à melhoria dos resultados obtidos por 1D-GC/MS, com recurso a analisadores de massa de quadrupolo (1D-GC/qMS).

A utilização da GC × GC resultou no aumento da eficiência de separação e da relação sinal-ruído (S/N) dos analitos, maximizando a qualidade dos espectros de massa adquiridos e melhorando a detecção e a identificação dos compostos analisados. A utilização de 1D-GC/FI-TOFMS permitiu a obtenção de informação rápida respeitante à gama de massas e à diversidade de massas moleculares existente nos extractos das diferentes agulhas de pinheiros.

A análise por componentes principais permitiu diferenciar as diferentes espécies de pinheiros, de acordo com os seus componentes voláteis e o seu perfil em ácidos resínicos. A análise por mínimos quadrados parciais (PLS) permitiu referenciar os monoterpenos *β*-pineno, terpinoleno, limoneno+*β*-felandreno, mirceno, sabineno e os enantiómeros (-)-*β*-pineno e (+)-limoneno, após cromatografia quiral, como sendo os voláteis que melhor explicam as diferenças encontradas para os níveis de ataque registados, para as diferentes espécies de pinheiros. Não foi encontrada nenhuma relação significativa entre a composição das agulhas em ácidos resínicos e a sobrevivência das larvas de *T. pityocampa.* Contudo, a detecção de diterpenos da classe dos labdanos nas agulhas forneceu pistas que poderão vir a ser exploradas em trabalhos futuros.

Este trabalho foi pioneiro na utilização de 1D-GC/TOFMS e de GC × GC/TOFMS para a análise da fracção volátil emitida por agulhas de pinheiros. A utilização de 1D-GC/TOFMS e de GC×GC/TOFMS, para a mesma amostra, permitiu detectar, respectivamente, 185 e 212 compostos voláteis, enquanto que a utilização de 1D-GC/qMS permitiu detectar 94. A análise, por GC×GC/TOFMS quiral, da composição da fracção volátil emitida pelas diferentes espécies de pinheiros permitiu a detecção de 422 compostos.

Summary

The pine processionary moth *Thaumetopoea pityocampa* (Lepidoptera: Notodontidae) is considered as the most destructive pine defoliator in the Mediterranean area. Host species appear to influence the distribution and population dynamics of the defoliator, but the mechanisms responsible for its performance are not yet understood. Tree resistance/susceptibility might be due to either the presence of some compounds present in the needles, or to specific volatile components emitted by the host trees. In this context, the characterization of the chemical composition of the needles from different pine species is an important tool to decode the process of host tree selection and performance by *T. pityocampa*.

The chemical composition of the needles of *P. pinea*, *P. pinaster*, *P. halepensis*, *P. nigra*, *P. brutia, P. patula, P. radiata, P. taeda, P. elliotti, P. kesiya, P. sylvestris* and *P. eldarica* was investigated. Headspace solid-phase microextraction and steam distillation extraction were used to collect the volatile fractions, and resin acids were solvent extracted and derivatized before analysis.

Samples were analyzed using one-dimensional gas chromatography (1D-GC), enantioselective multidimensional gas chromatography (MDGC) with heart-cutting transfer mode, comprehensive two-dimensional gas chromatography (GC × GC) and mass spectrometry (GC/MS) with different mass analyzers. The potential of mass spectrometry using field ionization as ionization mode, was also evaluated.

Results showed that the analytical capabilities of 1-D-GC are partially limited by the separation power of the columns. The high sensibility and the absence of peak skewing of the time of flight mass analyzer, with the use of automated peak finding and deconvolution algorithms, allowed for the detection of trace components with qualitative full spectra and the extraction of true mass spectra from coeluting compounds, promoting their reliable identification and thus significantly improving results obtained by 1D-GC/MS, using a quadrupole mass analyzer.

The use of GC × GC resulted in enhanced separation efficiency and increased signal to noise ratio (sensitivity) of the analytes, maximizing mass spectra quality and improving compound detection and identification.

Mass spectrometry with field ionization provided rapid information regarding the mass range, molecular weight diversity and evidence for differences due to various mass patterns in the composition of the different pine needles.

By means of principal component analysis, pine species were differentiated according to their volatile components and resin acids contents. By partial least squares regression, *β*-pinene, terpinolene, limonene+*β*-phellandrene, myrcene, sabinene and the enantiomers (-)-*β*-pinene and (+)-limonene, when quiral chromatography was performed, were identified as main volatiles explaining differences in attack level among pine species. No significant relationship was found between the needles resin acid composition and *T. pityocampa* larval performance but cues for further work emerged.

This work pioneered the use of 1D-GC/TOFMS for the analysis of pine needles volatiles, achieving the detection of 185 compounds, that is more than twice the number previously identified by standard 1D-GC/MS. The analysis by GC × GC for the same sample allowed the detection of 212 compounds. The enantio-GC × GC analysis performed for all the *Pinus* spp. under study achieved the detection of 422 diferent compounds.

Abbreviations and Symbols

1D-GC – one-dimensional gas chromatography

1D-GC/FI-TOFMS – one-dimensional gas chromatography time-of-flight mass spectrometry with field ionization

1D-GC/qMS – gas chromatography quadrupole mass spectrometry

$^{1}t_{R}$ – first dimension retention time (GC × GC)

2D – two-dimensional

$^{2}t_{R}$ – second dimension retention time (GC × GC)

3D – tri-dimensional

AL – alcohol

BGB 176 – capillary column coated with a 25% 2,3-di- methyl-6-tert-butyldimethylsilyl-*β*-cyclo-dextrin in SE-54 stationary phase (chiral)

BPX-50 – capillary column coated with a 50% phenyl polysilphenylenesiloxane stationary phase (mid polar)

CAR – carboxen

CC – carbonyl compound

CI – chemical ionization

CI-MS – chemical-ionization mass spectrometry

DB-5, ZB-5; BPX-5 or SE-52 – capillary columns with a 5 % phenyl-95% methyl-polysiloxane stationary phase (non polar)

DB-Wax – capillary column coated with a polyethylene glycol stationary phase (polar)

DiMe - capillary column coated with 0.25 μm film of 15% heptakis (2,3-di-O-methyl-6-O-*terc*-butyldimethylsilyl)-*β*-cyclodextrin in SE52

DIT – diterpene

DVB/CAR/PDMS – divinylbenzene/carboxen/poly(dimethylsiloxane)

E – ester

ECD – electro capture detector

EG – Eastern Galilee (Israel)

EI – electron ionization (formerly known as electron impact)

EI-MS – electron-ionization mass spectrometry

Equity-5 – capillary column with 5% phenyl polysilphenylenesiloxane stationary phase (non polar)

Et – ether

eV – electron volt

FD – field desorption ionization

FI – field ionization

FID – flame ionization detector

FI-TOFMS – field ionization-time-of-flight mass spectrometry

FTIR – Fourier transform infrared spectroscopy

g – gram

GC – gas chromatography

GC × GC – comprehensive two-dimensional gas chromatography

GC × GC/TOFMS – comprehensive two-dimensional gas chromatography time-of-flight mass spectrometry

GC/MS – gas chromatography mass spectrometry

H_2 – hydrogen

HC – hydrocarbon

HCA – hierarchical cluster analysis

He – Helium

HPLC – liquid chromatography/ high-performance liquid chromatography

ITD – Ion trap detector

JH – Judean Hills (Israel)

LRI – linear retention indices

$LRI_{calc.}$/ RI_{calc} – experimental linear retention indices (calculated)

$LRI_{lit.}$/ RI_{lit} – linear retention indices from reference literature or database (published)

M – monoterpene

MA – monoaromatic compound

MC – Mount Camel (Israel)

MDGC – multi-dimensional gas chromatography

min – minute

N – needles from the current year

NIST – National Institute of Standards and Technology

NPD – nitrogen phosphorous detector

ºC – degree Celsius

OM – oxygenated monoterpene

OS – oxygenated sesquiterpene

PA – poly(acrylate)

PCA – principal component analysis

PDMS – poly(dimethylsiloxane)

PDMS/CAR – poly(dimethylsiloxane)/carboxen

PDMS/DVB – poly(dimethylsiloxane)/divinylbenzene

PDMS/WAX – poly(dimethylsiloxane)/carbowax

PhE – phenyl ester

PLS – partial least squares

PTFE – polytetrafluoroethylene (Teflon)

Q2 – model predictivity (in PLS)

qMS – quadrupole Mass Spectrometry

R^2 – coefficient of determination

R2 – goodness of fit (in PLS)

R2Y – percent explained variance (in PLS)

RSD – relative standard deviation

s – second

S – sulphur compound

S/N – signal to noise ratio

SD – steam distillation

SDE – simultaneous distillation–extraction

SE – solvent extraction

SE-54 – (5%-phenyl)(1%-vinyl)-methylpolysiloxane stationary phase (non polar)

SEQ – sesquiterpene

SIM – single ion monitoring mode (in mass spectrometry)

SPME – solid phase microextraction

STO – statistical theory of overlap

TIC – reconstructed total ion current or total ion chromatogram (in mass spectrometry)

TOF – time-of-flight

V – one year old needles

vs – versus

Table of Contents

List of Figures

List of Tables

1. Introduction

1.1. General

The pine processionary moth *Thaumetopoea pityocampa* (Lepidoptera: Notodontidae) (Den. & Schifft) is considered the most destructive pine defoliator in the Mediterranean area. Severe defoliation of pine stands, caused by the caterpillars, frequently occurs resulting in economic damage and public health concern. Both indigenous and exotic *Pinus* species have been considered as host species and appear to influence the distribution and population dynamics of the defoliator, although the mechanisms responsible for its performance are not yet understood. The relative susceptibility of the host trees varies widely geographically, among different pine species and even for the same pine species. The resistance/susceptibility observed might be due to either the presence of some compounds present in the needles of the pines, or to some components of the essential oil volatiles that are emitted by the pine needles and branches, which might be responsible for the primary attraction of the females. For several phytophagous forest insects, the process of attraction and host selection has been correlated with variations in the volatile composition emitted by the trees. Chemical ecology research has mostly addressed the study of monoterpenes and sesquiterpenes, due to their importance as semiochemicals in plant–insect interactions, mainly in host selection processes. However, diterpene resin acids have also been referred as important defense compounds against insect pests and pathogens in conifers, particularly regarding insect performance after host colonization.

The characterization of the chemical composition of the needles of different pine species is an important tool to decode the process of host tree selection and performance by *T. pityocampa*. However, this task is analytically difficult, when performed by "traditional" techniques, such as one-dimensional gas chromatography, due to the high chemical complexity of the matrices, and since many structurally related compounds must be determined, demanding the development of new analytical approaches.

This work is organized in 4 chapters. It can be divided in two parts: chapters 1.1 – 1.5 - state of the art and theoretical framework, where considerations about plant-insect interactions (1.2), the genus *Pinus* (1.3), the pine processionary moth *T. pityocampa* (1.4) are approached, as well as considerations about analytical methodologies (1.5), focusing on extraction/collection methods, chromatographic methods, mass spectrometry, chromatographic and spectral resolution and two-dimensional gas chromatography. The second part of this work includes the material and methods (chapter 2), followed by the results presentation (chapter 3) and the discussion and conclusions obtained (chapter 4).

Objectives

This thesis was focused on the evaluation of new analytical approaches for the analysis of the chemical components of pine needles which can be applied to the study of plant-insect relationships, namely:

- 1D-GC/MS using a time-of-flight (1D-GC/TOFMS) mass analyzer with a high spectral acquisition rate, allowing for automated peak finding with mass spectral deconvolution;
- Comprehensive two-dimensional gas chromatography (GC × GC), using a time-of-flight (GC × GC/TOFMS) mass analyzer;
- Mass spectrometry using field ionization (FI), a soft ionization technique hyphenated with gas chromatography (GC/FI-TOFMS) and by means of direct insertion probe.

Additionally objectives were:

- To study and characterize the volatile fraction emitted by the needles of different *Pinus* species;
- To study the relationship between the volatile composition of different *Pinus* spp. located in two geographical regions, and the level of attack by *T. pityocampa*;
- To study and characterize the resin acids present in the needles of different *Pinus* species, and evaluate their relationship with the larval performance of *T. pityocampa*.

1.2. Plant-insect interactions

1.2.1. Introduction

Insect plant interactions have since long been studied (Spencer, 1988a; Khush and Panda, 1996). Insect use plants as a source of food, or shelter (Khush and Panda, 1996). A plant, upon which a phytophagous insect feeds, develops and if necessary completes its life cycle, is defined as a host plant.

Herbivorous insects can be classified according to their feeding behaviour as: **i)** monophagous if feeding on several plant species within a single genus, **ii)** oligophagous if they feed on plants of different genera but within one family or closely related families, and **iii)** polyphagous when feeding on plants from different families (Fraenkel, 1959; Bernays and Chapman, 1994a). An alternative classification divides the insects into specialists (monophagous and oligophagous) and as generalist (polyphagous) (Basset *et al*., 1996).

In order to tentatively explain the variations in host specificity among phytophagous insects, many hypotheses have been proposed based on plant-insects attributes (Bernays and Chapman, 1994b). Examples of these hypothesis, based on plant attributes, are plant defenses (Ehrlich and Raven in 1964), plant apparency (Feeny in 1976, and Rhoades and Cates also in 1976), plant abundance (Root in 1973) and plant nutritional value (Mattson and Scriber in 1987) (Bernays and Chapman, 1994b). Hypothesis based on insect traits have also been formulated and they can be exemplified by host intimacy (Mattson *et al.* in 1988), neuronal capacity of the insect (Lains and MacArthur in 1969) and the impact of generalist predators (phytophagous natural enemies) (Bernays and Graham in 1988) (Bernays and Chapman, 1994b).

The different feeding patterns are assumed to be the result of the insect specific adaptations (coevolution) to the different host plants (Spencer, 1988a; Khush and Panda, 1996). As a result of evolution, some phytophagous insects developed specialized feeding habits where

they became adapted to feed on specific plant taxa or families, while other insects feed on a large array of plants from different families (Khush and Panda, 1996). This implies that the host plant searching and selection is an active process in insects. Host plant selection is the process by which an insect detects a resource furnishing plant, amid an environment of a multitude of diversified non-host plant species (Schoonhoven, 1981; Khush and Panda, 1996). The evolution of insect plant associations has been guided to a large extent by plant chemistry, the insect's ability to identify host plants, based on their chemical composition and insect adaptation to plant chemical defenses (Schoonhoven, 1981; Renwick, 1988; Spencer, 1988; Khush and Panda, 1996).

Although visual and tactile cues are involved in the process, the host selection by an insect is mainly driven by plant chemical cues (Khush and Panda, 1996). Chemical stimuli may be perceived by olfaction (volatile compounds) and contact chemoreception (non volatile compounds) (Khush and Panda, 1996). The host plant location and selection is thus a sequential phenomenon by which an insect distinguishes between host and non-host plants, on the basis of plant chemicals that can act as attractants, arrestant and stimulants (positive response) or as repellents and deterrents (negative response) (Khush and Panda, 1996). In order to achieve that, each insect species has developed unique sensory systems to decode the important cues that will allow host recognition (Khush and Panda, 1996).

Several theories of host plant selection have been proposed (Khush and Panda, 1996):

1) *Botanical instinct theory* - In 1920, Brues hypothesized that insects are guided by specific chemical cues and that host plants were selected on the basis of specific plant odors, by larvae and adult insects, on the basis of their botanical instinct.

2) *Token (positive) stimuli theory* – Frankel, in 1959, found that host plant selection by insects was influenced not only by plant morphology and nutrients, but also by their secondary compounds. He proposed that phytophagous insects are guided to their host plants and induced to feeding by the chemical compounds in which plant differ such as glucosides, phenols, alkaloids, terpenoids and saponins. Later, in 1969, he extended the theory and included the concepts that i) insects evolved from polyphagy to monophagy to overcome adverse effects of plant chemicals, and ii) specialist insects use plant chemicals as cues to host location.

3) *Dual discrimination theory* - Kennedy and Booth proposed, in 1951, that host plant selection was based on the insect response to two types of stimuli: the flavor stimuli

and nutrient stimuli. The flavor stimuli were due to specific non nutrient chemicals of the plant, whereas the nutrient stimuli were due to nutrient constituents of the plant

4) *Nutritional imbalance theory* – Recognizes that not all plant substracts are equally nutritious. It states that the success of a phytophagous insect is stronger dependent on the proportions of plant essential nutrients than on their absolute quantities. The host selection process is not a quantitative, but a quality issue.

5) *Negative stimuli theory* – Emphasizes the role of deterrents and other negative stimuli in the food preference. Research findings supported that sensitivity to deterrents is more important in host selection than adaptation to a specific phagostimulant. This behaviour is attributed to a two-way specialization of insect chemoreceptors (receptor cells sensitive to chemicals), where it is assumed that the more they are specialized to phagostimulants, the more they are sensitive to feeding inhibitors.

6) *Chemical basis of host selection theory* - Is based on six models of host selection strategies by females for oviposition, and of the larval stages of insect groups, developed by Kogan, in 1977. He suggested that plants show different dispersion patterns and have several kinds of chemicals and, consequently, insect herbivores developed different kinds of host selection and foraging strategies. The models focused on the critical role of plant chemicals in the initiation and maintenance of oviposition and feeding. These models are supported by behavioural and electrophysiological studies, which suggested that the host selection process is diverse, at the various stage of insect life cycle, due to the interactions between plant chemicals and insect sensory systems.

Host location and selection involves several stages: searching and finding, recognition and selection and acceptance. The sequence of host plant selection mechanisms for herbivore insects can be divided in the behavioural events (Khush and Panda, 1996): **i)** dispersal, with random movements, **ii)** searching and finding with oriented movement according to visual and/or olfactory information, **iii)** plant recognition and contact-evaluation, among other mechanisms by antennation, palpation, tarsal drumming, ovipositor probing, test biting or swallowing (Khush and Panda, 1996; Karamaouna and Copland, 2000), with olfactory, mechano-sensory and gustatory information, and **iv)** host acceptance with sustained feeding, or oviposition, or host rejection with insect departure.

In the process of coevolution, with insects, plants also evolved counter-measures against insect adaptation. They developed physical barriers, such as lignified cells, trichomes or tough foliage, together with chemical defenses that use different classes of compounds such as terpenes, phenols and alkaloids, or mixtures of compound such as resins (Gardner and Agrawal, 2002; Mumm and Hilker, 2006; Chehab *et al.*, 2008). Some plants not only developed constitutively defense mechanisms, that are permanently present, such as the oleoresin in conifers, but also react to insect feeding and/or mechanical damage, in a process of induced defense, by increasing the synthesis of "toxic" compounds, releasing predator-attracting volatiles or producing proteinase inhibitors (Mumm and Hilker, 2006).

However, evolution is a dynamic process and insect herbivores also adapted to the defense mechanism of plants, upon which they became specialists, and evolved means to detoxify the defense compounds, that eventually turned feeding attractants (Harborne, 2001). Additionally, some insects such as the Lepidoptera in the larvae stage, evolved the ability to sequester and store plant defense chemicals from their host plants, and reuse them towards their own protection, avoiding predation (Harborne, 2001). An interesting example comes from the Monarch butterfly males, which convert sequestered plant pyrazine alkaloids, defence chemicals, to pheromone precursor components which became stored in the wing pencils (Harborne, 2001).

1.2.2. Plant chemicals

1.2.2.1. Primary and secondary metabolites

Plants produce a large variety of chemicals, some of which are essential to themselves, while others apparently have no direct function on plants. Plant chemicals can be divided in: **i)** primary metabolites, if they are essential for a plant and are directly involved in plant growth, development and reproduction and **ii)** secondary metabolites if no role has yet been found in plant growth, development, reproduction, or in any other "primary" functions.

Primary metabolism refers to the processes producing amino acids, carbohydrates, lipids, proteins and nucleic acids, all essential for the survival of the plant (Cseke *et al*., 2006). Primary metabolites are universal and differ very little among plant species while, secondary metabolites are not universal, but are restricted to certain plant taxa, in which they occur in a wide range of concentrations and compositions. Secondary metabolites have no apparent nutritional significance to insects, but they play an important ecological role (e.g. the selection

of host plants by phytophagous insects), and their different profiles among plants can be used to identify plant species (chemotaxonomy). More than 200 000 secondary metabolites are known (Benderoth *et al.*, 2006). A possible explanation for this vast metabolic diversity consists on a stepwise and reciprocal process of adaptation and counter-adaptation between plants and their natural enemies, driven by mutual selection (Benderoth *et al.*, 2006). In 1959, Fraenkel (1959) argued that secondary metabolites were not waste products of plant primary metabolism, which accumulated in the cells due to an inefficient excretory system, but, instead, they were "trigger" substances, which induced or avoided plant feeding by herbivore insects (Fraenkel, 1959; Harborne, 2001).

The metabolism of plant secondary metabolites is very complex and several metabolic pathways have been described such as the glycolytic pathway (conversion of glucose to pyruvate) (B13), the pentose phosphate pathway (e.g. phenols) (Magel *et al*., 2001), the acetate/mevalonate pathway (e.g. sesquiterpenes) (McGarvey and Croteau, 1995; Adam *et al*., 1998), the glyceraldehyde phosphate/pyruvate pathway (e.g. diterpenes) (Adam *et al*., 1998; Yang and Orihara, 2002), lipoxygenase pathway (e.g. green leaf volatiles) (Bate and Rothstein, 1998) and the shikimic acid pathway (e.g. tannins and methyl salicylate) (Adam *et al*., 1998; Ossipov *et al*., 2003).

According to their ecological role, if they are involved in chemical interactions between organisms, plant secondary metabolites can be classified as semiochemicals (Nordlund, 1981). Semiochemicals are divided into allelochemicals, if the interactions are interspecific, and pheromones if those are intraspecific. Allelochemicals are non-nutritional compounds produced from one species that are significant to other species. Allelochemicals are subdivided into allomones, kairomones, synomones and apneumones. Allomones are chemical compounds produced or acquired by an organism that give advantage to the emitter but not to the receiver, such as plant metabolites that act as insect repellents. Kairomones are chemicals produced or acquired by an organism that give advantage to the receiver but not to the emitter, such as plant metabolites that act as attractants or feeding stimulants for insects. Synomones are chemical compounds produced or acquired by an organism that give advantage to both sender and receiver, such as chemicals that mediate pollination. Apneumones are chemical compounds produced from a non-living source that mediate interactions between different species, such as volatiles emitted by corpses that attract necrophagic insects.

Independently of their ecological role, some chemical compounds are involved as chemical stimuli on the process of host selection by phytophagous insects. According to their effect on insect behaviour, secondary metabolites can be described as (Nordlund, 1981): arrestants, attractants, repellents, stimulants and deterrents. Arrestants are chemicals that cause an organism to aggregate in contact with it. Attractants are chemicals that promote oriented movements of insects towards its source. Repellents are chemicals that promote oriented movements of insects away from their source. Stimulants can be divided in: **i)** locomotor stimulants which are chemicals that cause organisms to disperse from an area faster than on its absence and **ii)** feeding, mating or ovipositional stimulants, which are chemicals that elicit feeding mating or oviposition in an organism. Feeding stimulant is synonymous of phagostimulant. Deterrents are chemicals that inhibit feeding, mating or oviposition when present.

1.2.2.2. Volatile compounds

Plant volatiles are usually complex mixtures, comprising several hundred compounds (Knudsen *et al*., 1993; Hick *et al*., 1999; d'Alessandro and Turlings, 2006). Most of the common plant volatiles have 5 to 20 carbon atoms and include short-chain alcohols, aldehydes, esters, ketones, aromatic phenols, lactones, phenylpropanoids, and terpenoids (Hick *et al*., 1999; Bruce *et al*., 2005; d'Alessandro and Turlings, 2006; de Bruyne and Baker, 2008).

To locate a host plant, even if it is hidden among an array of non-host plants, is fundamental for a phytophagous insect, in order to fulfill its nutritional requirements and find a suitable oviposition site (Bruce *et al*., 2005). The first chemical stimuli that insect detect in the process of host plant selection are volatiles that act as a chemical message (Visser, 1996). According to the composition of the volatile bouquet, a plant can be recognized as a host, following insect attraction or arrestment or, conversely, be recognized as a non-host, eliciting insect rejection (Bruce *et al*., 2005). Two main hypotheses have been proposed in order to understand the role of these volatile olfactory cues in host-plant location (Visser, 1996; Bruce *et al*., 2005): **i)** the species-specific odor recognition, based on the "token stimulus" theory, that suggests a plant odor recognition as a result of species specific volatile compounds and **ii)** ratio-specific odor recognition that suggests that a plant odor specificity and insect recognition is due to a specific ratio between constituent volatiles, that are common among plant species, and not due to the presence or to the absence of a particular compound.

According to Bruce *et al.* (2005), numerous electrophysiological studies, on a wide range of specialist and generalist phytophagous insects, have shown that the majority of insect peripheral receptors detect compounds that are not unique to their host plants, a result that tends to support the "ration-specific odor recognition" hypothesis. This observation means that the ratio of volatiles emitted by the plant becomes a vital component of the olfactory signal and that plant location and selection must be dependent on the recognition of its particular blend of volatiles. In consequence, Bruce and co-authors (Bruce *et al.*, 2005) proposed the theory of "coincidence detection", suggesting that an insect can identify the correct blends of host plant volatiles, even within a complex background of physiologically active non-host volatiles. An extension of this theory could be applied to plant species that change their blend of volatiles either from different parts, or over time. Those changes are often indicators of physiological changes in the host plants, reflecting differences in host suitability, or in growth stages (Hick *et al*., 1999). The insects, by identifying the associated volatile blends, are able to locate the most suitable host plants in their habitat (Bruce *et al*., 2005).

The perception of volatiles is mediated by the olfactory receptor neurons that are located in the insect antenna, which convert chemical signals into electrical signals that are directly conducted into the insect central nervous system (Visser, 1996; de Bruyne and Baker, 2008). These inputs, when originated by different compounds, are individually distinct, allowing discrimination between volatile blends (Bruce *et al*., 2005). The functional organization of co-located olfactory receptor neurons for plant volatiles, in the same olfactory sensillum on the antenna, allows a fine-scale spatio-temporal resolution of inputs to the central nervous system (Bruce *et al*., 2005). These mechanisms potentially allow an insect to differentiate odor blends, locate their source and recognize the host and non-host plants.

Although host plants are mainly selected by adult females, the larvae of some insect species are also able to detect plant volatile blends and examples of those are *Drosophila melanogaster*, *Bombyx mori* and *Spodoptera littoralis* larvae, given by Visser (1996).

Host plant volatiles can also induce pheromone production (Reddy and Guerrero, 2004) and release in some insects, such as the aggregation pheromones in bark beetles (Knudsen *et al*., 1993; Hick *et al*., 1999) and/or synergize the response to male pheromones, as shown by the boll weevil *Anthonomus grandis* (Visser, 1996; Reddy and Guerrero, 2004). An inhibitory

effect can also be induced by plant volatiles (Reddy and Guerrero, 2004). 4-allyl anisole, a common compound produced by *Pinus taeda* and other conifer species, reduces the response of *Dendroctonus frontalis* to their own pheromone (Reddy and Guerrero, 2004).

Some of the plant volatiles are not constitutively emitted by the plants but induced by insect feeding and oviposition (Baldwin *et al*., 2001; Wegener and Schulz, 2002; d'Alessandro and Turlings, 2006). Herbivore damage may induce plants to emit much larger amounts of certain volatiles (Paré and Tumlinson, 1999), change the volatile pattern (Hilker *et al.*, 2002), or even cause the *de novo* synthesis of new volatile compounds (Paré and Tumlinson, 1997). Additionally, the induced emissions are not limited to the site of damage, but can also occur systemically in other parts of the plant (Hilker *et al.*, 2002). These induced plant volatiles can play an important role in mediating interactions between plant and insect herbivores, between insect herbivores and their natural enemies and even between plants themselves (Paré and Tumlinson, 1999; Baldwin *et al*., 2001; Wegener and Schulz, 2002; Dicke *et al*., 2003). Research studies have shown that induced plant volatiles can deter oviposition by insect herbivores (Reddy and Guerrero, 2004), attract their natural enemies (parasitic and predatory insects) (Paré and Tumlinson, 1999; Hilker *et al.*, 2002), and even induce defense and volatile emission in other plants, allowing them to respond faster to future herbivore attack (Paré and Tumlinson, 1999). The chemical identity of the volatile compounds and the composition of the blends vary with the plant species and with the herbivorous insect species (Paré and Tumlinson, 1999; Kessler and Baldwin, 2001; Dicke *et al*., 2003). In spite of the differences, there is a structural similarity between the induced volatiles, which include terpenes (homo-, mono- and sesqui-), aromatic compounds and green leaf volatiles (Paré and Tumlinson, 1999; Reddy and Guerrero, 2004). This structural uniformity suggests the activation of a common set of biosynthetic pathways, common to a wide range of plants (Reddy and Guerrero, 2004). Additionally, the ability of plants to differentiate between insect damage and mechanical wounding also suggests the presence of elicitors associated with insect feeding (Reddy and Guerrero, 2004).

1.2.2.3. Terpenes

Terpenes also referred to as terpenoids or isoprenoids are the largest family of secondary metabolites (Banthorpe and Charlwood, 1994; McGarvey and Croteau, 1995). They have a high structural diversity, with more that 23000 different compounds already characterized (Sacchettini and Poulter, 1997). The terpenes are basically built from isoprene units (2-

methylbutadiene) and are classified according to their number of isoprene units (Banthorpe, 1991; Dubey *et al.*, 2003): hemiterpenes (C_5H_8, 1 isoprene unit), monoterpenes ($C_{10}H_{16}$, 2 isoprene units), sesquiterpenes ($C_{15}H_{24}$, 3 isoprene units), diterpenes ($C_{20}H_{32}$, 4 isoprene units that include resin acids and gibberelins), sesterpenoids ($C_{25}H_{40}$, 5 isoprene units), triterpenes ($C_{30}H_{48}$, 6 isoprene units that include phytosterols and saponins), tetraterpenes ($C_{40}H_{56}$, 8 isoprene units that include carotenoids) and polyterpenes (long chains of C_5, e.g. rubbers).

Terpenes are widely distributed through the whole plant kingdom (Banthorpe and Charlwood, 1994), as products of acetate-mevalonate pathway (sesquiterpenes and triterpenes) and glyceraldehyde-3-phosphate/pyruvate pathway (monoterpenes, diterpenes and tetraterpenes) (Dudareva *et al.*, 2004; Heldt and Heldt, 2005). The biosynthesis of plant terpenoids occurs in different subcellular compartments (Ayres *et al*., 1997). In general, mono- and diterpenes are preferentially formed in plastids, while sesquiterpenoids are preferentially formed in the cytosol (Ayres *et al*., 1997).

Terpenes are the largest group of specialized metabolites found in plants and play diverse physiological, metabolic and structural functions (Harborne, 2001). Some terpenes participate in primary plant processes as components of the phytol side chain of chlorophyll, phytosterols in cellular membranes, carotenoid pigments or as plant growth regulators (e.g. gibberellic acid and absicic acid) (Aharoni *et al.*, 2005; Heldt and Heldt, 2005). Plant terpenes have been extensively studied in chemical ecology and have been reported as players in almost possible plant-animal, plant-plant and plant-microorganism interactions (Harborne, 1991). As secondary metabolites terpenes either exist as constitutive compounds (e.g. oleoresin) (Phillips and Croteau, 1999), or are induced after insect damage (Arimura *et al.*, 2000; Miller *et al.*, 2005), wounding (Faldt *et al*., 2003), fungal inoculation (Chappell *et al*., 1989) or artificial induction by means of methyl jasmonate treatment (Martin *et al*., 2004).

Terpenes play an important function in plant defense as antimicrobial compounds against fungi and bacteria, allelopathic inhibitors of other plant species, repellent or antifeedant compounds to prevent herbivory, or as induced volatiles from insect wounded and damaged plants that attract phytophagous natural enemies (McGarvey and Croteau, 1995; Ayres *et al*., 1997; Harborne, 2001; Greenhagen and Chappell, 2001; Pichersky and Gershenzon, 2002; Hines, 2006; Pichersky *et al*., 2006). This function could result from the action of a specific compound, be the result of terpenoid blends that often synergize the component activities to produce the defensive effect or be directly dependent of plant terpenoid concentrations

(Harborne, 2001). Some volatile terpenes also seem to have functions in plant communication between plants (plant-plant or inter-plant) (Baldwin *et al.*, 2006). Additionally, terpenes are basic components of essential oils, and important constituents of fruit volatiles and floral scents that are involved in pollinator attraction (Harborne, 2001; Pichersky and Gershenzon, 2002).

Terpenes are the constituents of oleoresin, the constitutive defense of conifers (Phillips and Croteau, 1999). Oleoresin is a complex mixture consisting of turpentine (monoterpenes and sesquiterpenes) and rosin (diterpenes) fractions. It is composed of approximately equal molar amounts of monoterpenes and diterpenes with a smaller proportion of sesquiterpenes (Martin *et al*., 2002). Oleoresin can physically entomb attacking insects or push them out from their site of entry with its flow and seal and clean the wound from microorganisms (Keeling and Bohlmann, 2006). After the more volatile mono- and sesquiterpenoid oleoresin components have evaporated, the non-volatile diterpene resin acids harden and seal the wound, or trap the insect invaders (Phillips and Croteau, 1999; Keeling and Bohlmann, 2006).

The more volatile terpenes are the mono- and sesquiterpenes. The monoterpenes are the most simple class of terpenes and more than 1000 were already known in 1991 (Charlwood and Charlwood, 1991). Monoterpenes have been classified by Dev and co-authors (Charlwood and Charlwood, 1991) according to 38 different skeletal types. Figure 1.1 presents the structures of some monoterpenes.

Research studies on pollinator attraction, competitive phytotoxicity, defense against microbial pathogens and attraction or defense against phytophagous insects suggest an important ecological role for monoterpenes (Croteau, 1987). On their distribution through the Plant Kingdom, monoterpenoids tend to show more intraspecific variation than other classes of metabolites. This attribute makes monoterpenes useful as chemotaxonomic characters, from the genus to species level (Charlwood and Charlwood, 1991). The largest chemotaxonomic application of monoterpenes has been for the gymnosperms, such as to define species within the genus *Pinus* (Lapp and von Rudloff, 1982), and to identity hybrids in natural populations of conifers (Harborne and Turner 1984; Charlwood and Charlwood, 1991).

Sesquiterpenes are the largest class of terpenes with more than 100 known skeletal classes and thousands of compounds isolated and identified (Fraga, 1991). Figure 1.2 presents the structures of some sesquiterpenes.

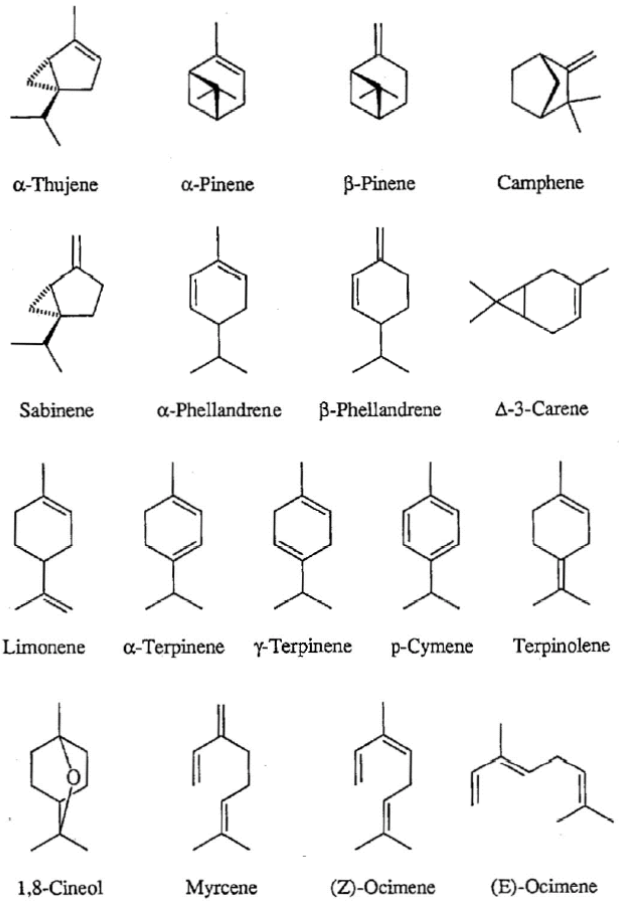

Figure 1.1 – Structures of some monoterpenes (adapted from König *et al*., 1992).

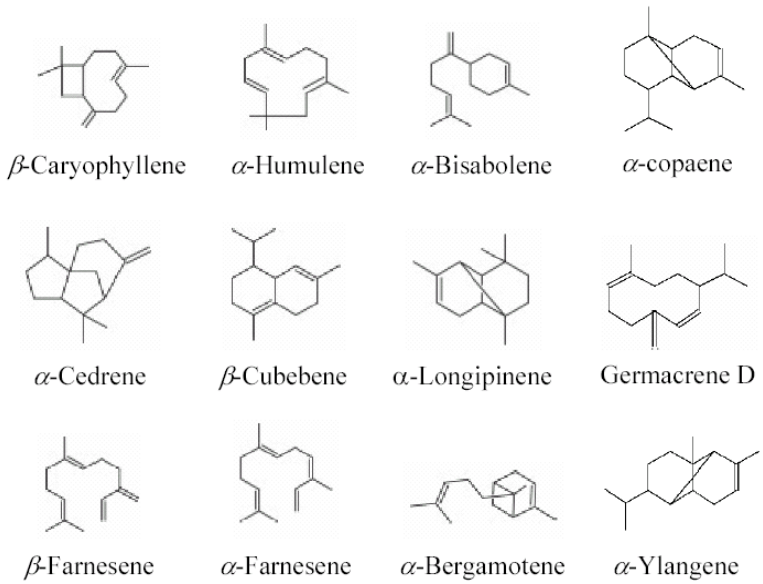

Figure 1.2 – Structures of some sesquiterpenes (adapted from Wiley library).

Diterpene resin acids are a group of C-20 bi- or tricyclic carboxylic acids of several skeletal types with diversity introduced by double-bond isomers, diastereoisomers, and additional

functionalization (Keeling and Bohlmann, 2006). Tricyclic resin acids, the most common in Pinaceae, are classified into 2 main groups, abietanes and pimaranes. Abietanes consist of abietic acid, dehydroabietic acid, neoabietic acid, levopimaric acid and palustric acid, and are classified based on their isopropyl substituent on the C-13 carbon (Carvalheiro, 1986; Carpy and Marchand-Geneste, 2003; Langenheim, 2003). Pimaranes consist of pimaric acid, isopimaric acid, and sandarocopimaric acid, and possess two substituents, vinyl and methyl on the C-13 carbon (Carpy and Marchand-Geneste, 2003). Figure 1.3 presents the structures of some diterpene resin acids.

Bicyclic diterpene acids with labdane skeletal types are also found in conifers such as agathic, isocupressic, *trans*-cummunic and pinifolic acids (Gref and Lindgren, 1984; Gardner *et al.*, 1999; Langenheim, 2003; Keeling and Bohlmann, 2006).

Considered less important in the semiochemistry of plant insect-interactions, the resin acids have been studied in less detail than the monoterpenes and sesquiterpenes (Keeling and Bohlmann, 2006). However, the resin acids are also thought to play a role in conifer defense (Keeling and Bohlmann, 2006).

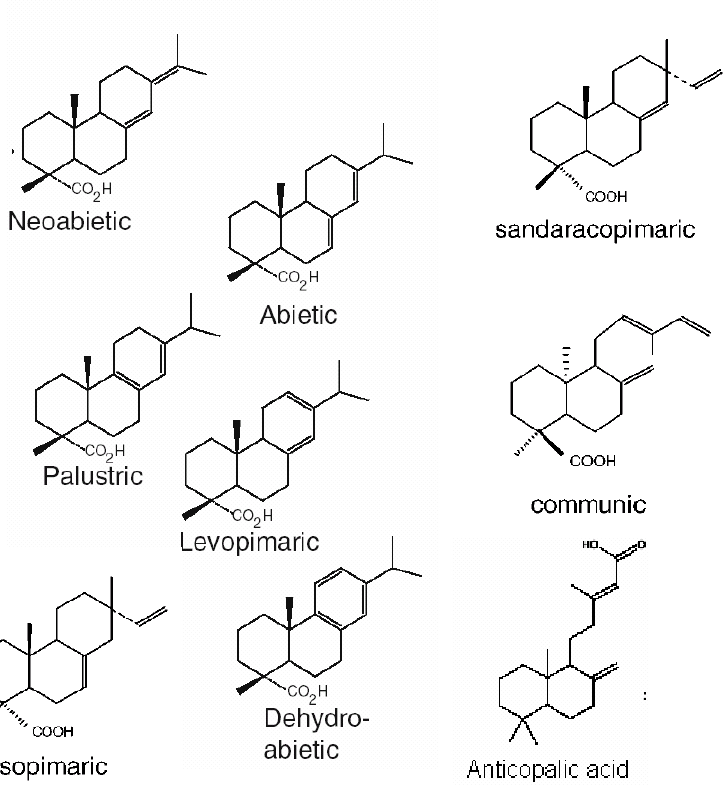

Figure 1.3 – Structures of some diterpene resin acids (adapted from Wiley library and van den Berg *et al*., 2000).

Plant emission of volatile organic compounds occurs on a global scale in a flux that is estimated to be 1150 Tg carbon (1 Tg = 10^{12}g) annually (Guenther *et al.*, 1995; Stephanou, 2007; Williams *et al.*, 2007). This biogenic emission plays an important role in atmospheric chemistry, plant physiology and plant ecology, and terpenes are responsible for 55% of the estimated emissions (Stephanou, 2007). The annual global flux is estimated to be composed by 44% of isoprene, 11% of monoterpenes and 45% of other volatile organic carbons (e.g. aldehydes, ketones, organic acids or alcohols) (Guenther *et al.*, 1995). Although sesquiterpenes emission rates have not been studied with the same detail, Tarvainen *et al.* (2005) reported that, in southern Finland, they may vary between 2 and 5% of the total monoterpenes emission rates. Both monoterpenes and isoprene react rapidly with the atmosphere primary oxidants (e.g. ozone) having life times that range from days to minutes (Lee *et al*., 2005). Sesquiterpenes are even more reactive with an atmospheric lifetime of only a few minutes, making them hardly measurable in ambient air samples (Tarvainen *et al.*, 2005). A general rule of the thumb has been that deciduous trees mainly emit isoprene, while conifers mainly emit monoterpenes (Janson *et al*., 1999). However, according to Janson *et al.* (1999), the rule fits *Pinus sylvestris* emissions, but may fail for some conifers, such as spruces. The most abundant monoterpenes emitted include α-pinene, β-pinene, myrcene, ocymene, α-terpinene, camphene, Δ-3-carene and limonene (Nunes *et al.*, 2005). Conifers monoterpenes are emitted, with diurnal and seasonal variation, continuously from storage organelles (e.g. resin ducts in leaves and axial organs) mainly as a function of leaf temperature but other factors such as light, draught, humidity and herbivore attack must also be considered (Staudt *et al*., 1997; Sabillón and Cremades; 2001; Holzke *et al*., 2006).

In the genus *Pinus*, the site of monoterpenes synthesis is the resin duct epithelium which is only active during needle elongation, in a process that is light dependent (Staudt *et al*., 1997). However, most research did not find a significant relation between light and monoterpenes emissions in conifers, as it happens with temperature (Staudt *et al*., 1997). An explanation for this absence of short term response to light may be due to the presence of large terpene reservoirs in conifer plants and thus avoiding that short-term alterations in synthesis become reflected in the emission rates (Staudt *et al*., 1997). According to Staudt *et al*. (1997), this general feature of light independence can be apparent and due to high concentration of terpenes in the needles. They suggest that together with the large terpenes pool in the resin ducts, a small light dependent poll may exist in the young needle mesophyll, linked to photosynthetic processes, that undergoes strong seasonal and diurnal alterations for some particular terpenes (Staudt *et al*., 1997).

Sesquiterpenes, in spite of being less studied than monoterpenes, have also been identified in emissions of *Pinus halepensis* (α–humulene) (Nunes *et al.*, 2005), *Pinus taeda* (β-caryophyllene, α-bergamotene, α-humulene and β-farnesene) (Helmiga *et al*., 2006) and above boreal coniferous forest (β-caryophyllene) (Hakola *et al*., 2003).

Plant emissions also contain chiral compounds, as many monoterpenes are produced in enantiomeric forms. α-pinene a common monoterpene, occurs as both (+)-α-pinene and (-)-α-pinene in *Pinus* spp. (Gomes da Silva *et al*., 2001). The importance of different enantiomers for the biological activity of a compound is well known (Pichersky and Gershenzon, 2002). Insects have olfactory receptor neurons that discriminate between enantiomers and can use them as fingerprints in host selection, or avoidance (Wise *et al*., 1998), and plants for pollinator attraction (Borg-Karlson *et al*., 1996). They can also be used as fingerprints in plant species chemotaxonomy studies (Gomes da Silva *et al.*, 2001).

Williams *et al.* (2007) reported that tropical forests and three tropical plant species, in a green house, emitted an excess of the (-) enantiomer of α-pinene in relation to the (+) enantiomer, while on Scots pine boreal forest there was a clear predominance of (+)-α-pinene and (-)-β-pinene. A similar observation was reported for the (+) enantiomer of β-pinene (Williams *et al.*, 2007). However, both enantiomers react at the same rate with atmospheric oxidants and, as a consequence, the atmospheric removal rate is the same for both of them (Stephanou, 2007). This observation supports the hypothesis that the enantiomeric difference in the air must be related to factors influencing emissions by plants, such as light and temperature (Stephanou, 2007). William *et al.* (2007) compared the concentrations of isoprene with the α-pinene enantiomers, measured in a tropical forest, and observed a correlation between (-)-α-pinene and isoprene but no correlation with (+)-α-pinene meaning that the emission of (-)-α-pinene was light dependent, like that of isoprene. On an earlier work, Tarvainen *et al.* (2005) found that with the exception of 1,8 cineol, which was both light and temperature dependent, all emission rates of the main emitted mono and sesquiterpenes were temperature dependent. However, previous studies (Faldt *et al*., 2001; Gomes da Silva *et al*., 2001) found out differences in the ratio of (+) and (-)–α-pinene in different *Pinus* species, in contrast with the spatially extensive scale homogeneity of the Williams *et al*. (2007) data. If no easy explanation can be found for the tropical forest, the data for boreal forest may simply reflect the emission patters of Scots pines. Nature uses the air as a communication medium and specific volatiles can transport chemical messages that attract insects, or act as chemical defenses (Baldwin *et al*., 2006). The predominance of a particular terpene in the forest

atmosphere may be considered as the "background noise" (Williams *et al.*, 2007) through which plant-insect interactions take place.

Research on the biosynthesis of monoterpenes and their enantiomers has shown that different enantiomers are synthesized by different enzymes (terpene cyclases), explaining its variability in different tissues and individual trees (Norin, 1996).

1.2.2.4. Green leaf volatiles

"Green leaf volatiles" (GLVs) are a blend of saturated and mono-unsaturated six-carbon aldehydes, alcohols, and their esters (Reddy and Guerrero, 2004; Matsui, 2006), produced by plants as a result of oxidative degradation of surface lipids (Reddy and Guerrero, 2004). GLVs are usually formed from linolenic and linoleic acids through the lipoxygenase pathway (Bate and Rothstein, 1998), and are commonly emitted from mechanically, or herbivore-damaged plants (d'Auria *et al.*, 2007). GLVs occur in all plants, but in different proportions among species (Hansson *et al.*, 1999). The most common GLVs found in plants and their structures are presented in Table 1.1.

Table 1.1 - Structure of main GLVs found in plants

Name	Structure
n-hexanal	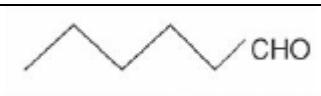
n-hexanol	
trans-2-hexenal (leaf aldehyde)	
trans-2-hexenol	
cis-3-hexenal	
cis-3-hexenol (leaf alcohol)	
trans-3 hexanal	
trans-3 hexanol	
cis-3-hexenyl acetate	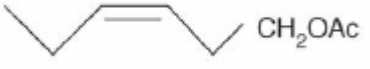

The GLVs have physiological significance. It has been suggested that they protect plants from infection, due to its antibacterial and fungicidal activities (Nakamura and Hatanaka, 2002; Matsui, 2006), and are involved in host plant location (Hansson *et al.*, 1999) and in plant induced defense, as insect deterrents, or as cues for phytophagous natural enemies (Reddy and Guerrero, 2004; Matsui, 2006). Insect detect GLVs (Hansson *et al.*, 1999), but their behavioural responses vary among species (Bruce *et al.*, 2005). Non host GLVs have been shown to inhibit the pheromone responses of several bark beetles (Reddy and Guerrero, 2004). GLVs also showed a synergistic effect, respectivelly on the aggregation and activity of the sex pheromone, for the boll weevil *Anthonomus grandis* and the diamondback moth *Plutella xylostella* (Reddy and Guerrero, 2004).

1.2.2.5. Phenolic compounds

Plant phenolic compounds are a diverse group of aromatic compounds with one, or more hydroxyl groups, that are usually formed via the shikimic acid pathway or phenylpropanoid metabolism (Ryan *et al*., 1999). Plant phenols are involved in plant defense where they act as feeding barriers (e.g. hydrolysable and condensed tannins, lignans, phenylpropanoids) (Harborne, 2001). Apparently, either classes of phenolic compounds (e.g. salicylic acid phenols), or of individual phenolic compounds (e.g. conipheryl benzoate) can act as active feeding barriers (Harborne, 2001). The effectiveness of the feeding barrier is dependent on the concentration of the phenolic compounds, on their accumulation in a particular part, or organ of the plant (Harborne, 2001), and .can be amplified by their oxidation to polymers, which reduce digestibility, palatability and nutritional value (Harborne, 2001). In conifers, together with the oleoresin terpenoids, they are the most important players in their constitutive defense mechanism (Mumm and Hilker, 2006).

Plant tannins, due to their widespread occurrence as condensed tannins (proanthocyanidins) in woody plants, and their ability to bind proteins, have been largely studied and suggested to act as powerful feeding barriers (Harborne, 2001). However, there is no consensus in the literature in what concerns herbivore-tannin interactions (Ayres *et al.*, 1997; Forkner *et al.*, 2004). Research studies divide between the hypothesis that tannins act as a defense mechanism by binding with dietary protein and digestive enzymes, thus limiting food assimilation in herbivores, or act by direct toxicity, rather than digestive inhibition, while others suggest that tannins have no detectable effect on herbivores and even can act as a feeding stimulant or nutritive substrates (Ayres *et al.*, 1997; Park *et al.*, 2004). Explanations

for this lack of uniformity, concerning tannin anti feeding activity, may be related to the tannin extensive structural diversity, tannins different oxidative activities, and on analytical difficulties to elucidate them or on physiological differences (e.g. gut chemistry) among herbivores (Ayres *et al.*, 1997; Moilanen and Salminen, 2008). However, research results can be used to describe differences in sensitivity to host plant tannins contents among phytophagous insects. According to some studies, tannins can reduce survivorship, growth and reproductive rates of phytophagous insects, but the results also suggest that only plants with high tannin concentrations (condensed and hydrolysable) are able to deter feeding (Harborne, 2001; Forkner *et al.*, 2004; Park *et al.*, 2004).

1.3. The genus *Pinus*

Since the beginning of the 20th century, a huge amount of work has been done, covering all areas of research on the genus *Pinus*, reflected by almost 22900 references on pine-related publications found in the ISI database, under the topic Pinus. This number does not take into consideration monographies, such as thesis, or technical reports (ISI Web of Knowledge, 2008).

1.3.1. Origin

Pines are coniferous trees of the genus *Pinus*, which belongs to the family *Pinaceae*, the largest family of modern conifers. Inside the *Pinaceae* they constitute the subfamily *Pinoideae* and comprise of 111 species (Price *et al*., 1998; Richardson and Rundel, 1998; Gernandt *et al*., 2005). Evidence from fossilized cones and molecular analysis suggests that the ancestors of the *Pinaceae* and *Pinus* had evolved by the Lower Cretaceous. By the Late Cretaceous, pines divided in two major subgenera: the *Strobus* (Haploxylon) and the *Pinus* (Diploxylon). The two monophyletic subgenera are distinguishable by the number of fibrovascular bundles in the needles. The Haploxylon, or soft pines, have needles with one fibrovascular bundle while the diploxylon, or hard pines, have two fibrovascular bundles in the needle (Norin, 1972; Ekundayo, 1988; Krupkin *et al.*, 1996; Millar, 1998; Willyard *et al.*, 2007).

1.3.2. Distribution

Pines have established on a wide range of habitats, from sub artic regions to the tropics. In the northern hemisphere pines often constitute the main forest components. They are the dominant trees over large parts of the boreal forest landscapes, while over large areas of southern Europe, pines can form virtually monospecific forests (Mirov and Stanley, 1959; Ekundayo, 1988; Krupkin *et al*., 1996; Richardson and Rundel, 1998; Richardson *et al*., 2007). In the Mediterranean region, pine forests comprise of 10 pine species and cover about

13 million hectares, which represents about 5% of the total regional area and about 25% of the total area forested. In the Mediterranean area, the most common species are *P. halepensis* and *P. brutia*, followed by *P. pinea*, scattered all over the region, and *P. pinaster* on the western part. *P. sylvestris* is also widespread in the region, but is more abundant in the northern regions of Europe (Barbéro *et al*., 1998; Richardson and Rundel, 1998). Since prehistoric times, the distribution of pine forests has been strongly related to land use practices, especially those affecting fire regimes and reforestation to control erosion (Barbéro *et al*., 1998; Le Maitre, 1998; Richardson *et al*., 2007).

1.3.3. Economic and ecological importance

From an economic perspective, pines are probably the most important tree genus in the world (Richardson and Rundel, 1998; Richardson *et al*., 2007), due to their value as source of timber, pulp and paper, nuts, seeds, resin, naval stores, construction materials and other products (Ekundayo, 1988; Richardson and Rundel, 1998; Richardson *et al*., 2007).

In parallel, their ecological role is highly valuable, for instance regarding the biogeochemical processes, as regulators of the hydrological cycles, fire regimes and in providing food and habitat for other animal and plant species. Pines have been intensively used in reforestation programmes, to control erosion, due to their association with acidic nutrient poor soils (Barbéro *et al*., 1998).

Nevertheless, due to pine natural expansion and commercial exploration, several species have been introduced into world regions with a wide variety of soil textures, ranging from sandy to clay-rich soils (Scholes and Nowicki, 1998), where an ecological balance with the ecosystems and /or local climatic conditions might not be achieved, originating exotic forestry enterprises, particularly in countries of the southern hemisphere (Ekundayo, 1988). Some of the introduced exotic *Pinus* species have become invasive, e.g. *P. pinaster* in South Africa, requiring extensive and costly control actions (e.g. Rouget *et al*., 2004).

1.3.4. Pines morphological characteristics

Pines have a monopodial growth and a mature large size. The largest species of pine is *P. lambertiana,* which reaches over 75 m in height and more than 5 m in diameter in Sierra Nevada, California. Pines are also among the oldest living organisms on the planet, with two

bristlecone pine trees, *Pinus longaeva* and *Pinus aristata* reaching, respectively, 5000 years and 2400 years. *P. cembra* and *P. sylvestris* are also among the longest living plants, in attaining respectively, a lifespan of 1200 and 500 years (Richardson and Rundel, 1998; Gernandt *et al.*, 2005).

Pine taxonomy can be based upon the use of several characters, such as cone and seed morphology, and foliage (Price *et al*., 1998). However, all pines share a unique morphological trait, the possession of needles as foliage. Needles are arranged in bundles, called the fascicles, or needle clusters, and can play a role as a nutrient reserve for pine growth. The number of needles per fascicle is usually constant, and is a specific characteristic of each pine species. Generally, pines species have two, three or five needles per fascicle, but other numbers are possible, such as in *P. monophylla* with one needle per fascicle, or some Mexican pines with 8 needles per fascicle. There is a wide variation in size, longevity and form of display of needles. The length of pine needles varies greatly and follows on the range of 45 cm in *P. palustris* to 2 cm in *P. banksiana* (Krupkin *et al*., 1996; Price *et al*., 1998; Richardson and Rundel, 1998; Gernandt *et al*., 2005; Lusk, 2008).

For each pine species, needle longevity is correlated with the species and with factors such as water, nutrient relations and stress of the habitat (Richardson and Rundel, 1998). Usually, tropical pines keep the needles for 2-3 years, temperate forest pines commonly retain their needles for periods of 4-6 years, and some sub-alpine pines may retain their needles for up to 30 years. Occasionally, *P. aristata* and *P. longaeva* can have physiologically active needles for periods as long as 45 years (Richardson and Rundel, 1998; Rundel and Yoder, 1998).

1.3.5. Insect pine interactions

Insect established a long evolutionary association with pines exploiting all tree parts and tissues, e.g. roots, needles and phloem, throughout their entire life cycle (de Groot and Turgeon, 1998). The insect diversity associated with pines is so large that de Groot and Turgeon (1998) estimated that in North America, native pines only, host around 1100 insect species.

Against insects, pines have evolved two types of resin-based defence mechanisms (e.g. Mumm and Hilker, 2006): **i)** the constitutive or static defence, set up by the oleoresin system,

and **ii)** the induced reaction or dynamic defence elicited by the attack, triggered in order to kill, repel or interfere with the reproduction, or development of the insect.

The resin system is located in the main stem of the tree and consists of a net of canals (resin ducts) filled with resin, a lipid-soluble mixture of volatiles and non volatile terpenoids and/or phenolic secondary compounds, that exudes when the canal rupture (de Groot and Turgeon, 1998; Björkman and Larsson, 1991; Mumm and Hilker, 2006). In pines, the resin is mainly a mixture of resin acids dissolved in mono-, sesqui- and some diterpenoids (Langenheim, 2003; Mumm and Hilker, 2006).

The physical properties of pine resins, namely total flow, rate of flow, viscosity and time to crystallization vary considerabely, are composition dependent and have been shown to contribute to the resistance of some pines to insects (Hodges *et al.*, 1979; de Groot and Turgeon, 1998). Usually resistant pines have an extremely viscous resin that crystallized slowly, and continued flowing for long periods after wounding (de Groot and Turgeon, 1998).

Dynamic defences are particularly important against organisms that invade the essential, living tissues of the tree, such as bark beetles and wood borers, which have a severe effect upon tree fitness. Success of a dynamic mechanism defence system depends on the ability of the plant to recognize the presence of an invading organism, such as the hypersensitive responses of pines to bark beetles and their symbiotic fungi where, immediately after intrusion, a necrosis is induced in the surrounding cells of the inclusion place, by the cells of phloem and xylem parenchyma. This necrosis pocket is then filled with a resin with increased concentration of terpenoids and phenolics, a mixture that is toxic to the bark beetles and inhibits the fungal growth (Gijzen *et al.*, 1993; de Groot and Turgeon, 1998; Mumm and Hilker, 2006). Resin also plays an important role in protecting the foliage (Mumm and Hilker, 2006). Resin channels are usually located near the lateral margins of the pine needles, and run parallel to the vascular bundles. Usually each needle has two resin channels, but there can be as many as 10 (Bennett, 1954; de Groot and Turgeon, 1998), and the number of channels can increase after the application of fertilizers (Otto and Geyer, 1970, referred in de Groot and Turgeon, 1998).

For insects that feed on the needles, the chemical composition of the resin may inhibit feeding, or interfere with their performance and development (McCullough and Wagner, 1993; de Groot and Turgeon, 1998).

Insects also evolved mechanisms to deal with the resin chemicals, as well as behavioural adaptations to deactivate the plant defences (de Groot and Turgeon, 1998; Mumm and Hilker, 2006). Pine sawflies are a good example of this insect strategy (de Groot and Turgeon, 1998; Björkman and Larsson, 1991; Mumm and Hilker, 2006). They may sequester resin compounds in specialized diverticular pouches in their foregut, preventing them from entering the digestive system (Eisner *et al.,* 1974; de Groot and Turgeon, 1998). They can also slit the base of the needles before oviposition, thus disrupting the resin flow in the needles canals and minimizing resin contact with its eggs. Additionally, they can use the inactivated resin compounds on their defence, as deterrent to birds, ants and spiders when regurgitated. However, sawflies ability and efficiency in using these defence strategies varies with the host species: those feeding on *P. banksiana* produce defensive secretions which have higher repellency and regurgitate greater volumes of fluid that those feeding on *P. resinosa* (Coddela and Raffa, 1995; de Groot and Turgeon, 1998). A similar effect was observed by Björkman and Larsson (1991) for the larvae of the European pine sawfly *Neodiprion sertifer,* feeding on *P. sylvestris* needles with different a resin contents. According to Björkman and Larsson (1991), larvae feeding on needles with high resin content are more effective on self defence and have higher survival rates than those feeding on low resin acid needles, when exposed to predatory ants. However, on the other hand, *N. sertifer* larvae feeding on needles with high resin content, need more time for development and has a reduced survival, when compared to larvae feeding on low resin needles (Larsson *et al*., 1986). Regarding studies on insect performance of among phenotypes and provenances of pine, Trewhella *et al*., 2000; Barre *et al*., 2002; 2003, among other authors, supply comprehensive references.

1.4. The pine processionary moth *Thaumetopoea pityocampa*

The winter pine processionary moth, *Thaumetopoea pityocampa* (Lepidoptera: Notodontidae) (Den. & Schifft) is the major pine defoliator in Portugal and in the Mediterranean area (Southern Europe, North Africa and Near East) (Avtzis, 1986; Douma-Petridou, 1990; Subchev *et al.*, 1994; Quero *et al.*, 1997; Markalas, 1998; Pérez-Contreras *et al.*, 2003; OEPP/EPPO, 2004; Petrakis *et al.*, 2005; Selfa *et al.*, 2005).

The first ecological observations on *T. pityocampa* took place in the 18th-19th centuries, being reported in the works of Ráumur and Fabre (Fabre, 1916). Since then, studies focused on biometrics, population dynamics, natural enemies and biological control (Selfa *et al.*, 2005). Presently, due to the species economic impact on pine plantations and problems caused to public health, an important part of ongoing research focus on its dispersion and distribution.

Apparently, the dependence of *T. pityocampa* on winter mild temperatures has limited its northward migration. However, recently due to global warming, the species is expanding its geographical range of distribution to northern European regions, increasing the risk of outbreaks in new areas and countries, if the host plant species distribution is favourable (Hódar *et al.*, 2003; Stastny *et al.*, 2006; Buffo *et al.*, 2007; Robinet *et al.*, 2007). Concern about the expansion, as well as the ecology and improvement of control methods of *T. pityocampa* is growing, and the period of 2001-2008 is responsible for 45.5% of all published papers on this topic, since 1954 (ISI Web of Knowledge, 2008).

1.4.1. Life cycle

1.4.1.1. Normal populations

T. pityocampa is a Lepidopteran polyphagous defoliator, with a univoltine life cycle, which develops in four life stages: egg, larvae, pupa and adult moth. The life cycle varies in relation to altitude and latitude and is dependent on weather factors, such as temperature and

insulation (Douma-Petridou, 1990; Masutti and Battisti, 1990; Schmidt, 1990; Schmidt *et al.*, 1999). In southern Portugal, according to Rodrigues (2002) the adult moths of the winter population have their emergence and flying period between July and September. Adults live for 1 - 3 days only and do not feed. Shortly after emergence, mating takes place at night, after which the females lay one egg-batch around the needles of pine host trees. The first larvae hatch is in September, after 5 - 6 weeks of embryonic development (Schmidt *et al.*, 1990) and unfolds between September and March, through five instars. Larval development can be influenced by the host plant upon which the larvae feed (Devkota and Schmidt, 1990). The larvae are very gregarious in all stages, and build silk nests attached to the branches of the host trees, where they shelter while not feeding. The instars are distinguishable by the size of the head capsule, body color and the presence of "mirrors" on the back of the larvae. During the three later instars, the larvae develop urticating hairs on the first "rings" of the abdomen (Douma-Petridou, 1990; Pérez-Contreras *et al.*, 2003) which cause serious health impacts to humans and domestic animals.

Depending on weather conditions, the last instar is generally reached between February and March, and the larvae leave the nest in procession, to pupate in the soil, where they burry themselves about 5 - 20 cm beneath the surface. A period of diapause extends until shortly before emergence, the duration of which is variable and probably influenced by climatic factors, as well as by the availability and quality of food for the larval stages (Masutti and Battisti, 1990).

1.4.1.2. Desynchronized population

In August-September of 1997 (Way *et al*., 1999; Pimentel, 2004; Santos *et al.*, 2007), a desynchronized population of *T. pityocampa* was observed and reported to the National Forestry Station (EFN) (Paiva, 1997) in Mata Nacional de Leiria (MNL), the oldest existing pinewood in Portugal, which has been continuously managed since the 14th century. The heavy defoliation observed was mostly caused by larvae of the last instar, thus indicating that larval development occurred during the summer and not during the winter, as expectable. Since 1997, the "summer" population has been continuously observed in MNL, coexisting with the "winter" population in the same pine stands and trees. A research project focused on this desynchronized population is currently under development (Project PTDC/AGR-CFL/73107/2006).

The life cycle of the winter population vs. the summer one is illustrated in Figure 1.4.

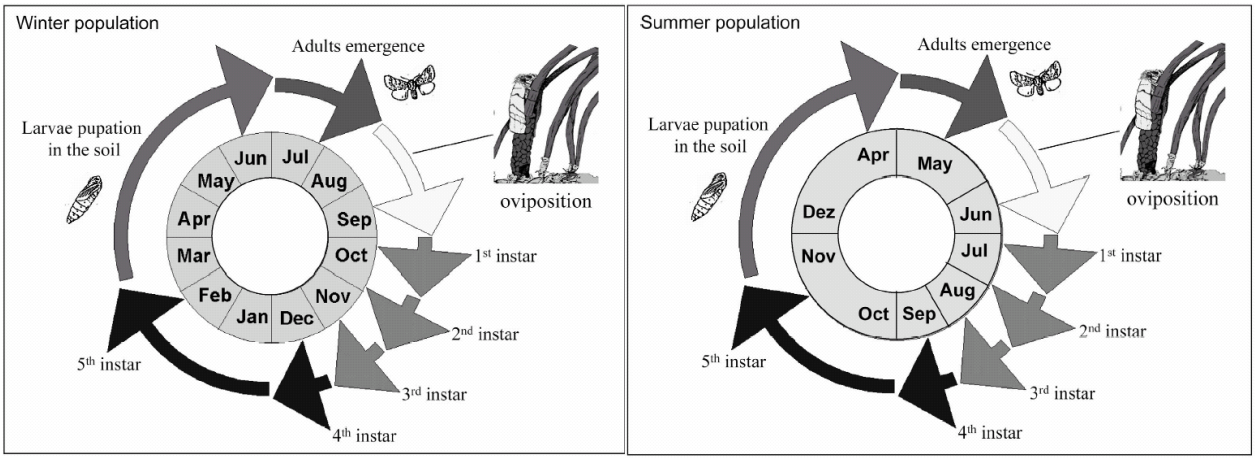

Figure 1.4 - Life cycles of the winter and summer populations of *T. pityocampa*.

Recently, Santos *et al.* (2007) studied the phenology and genetics of both populations. Results suggest that mating between the summer and winter populations does not take place, probably due to a temporal separation of the adult stage. The analysis of mitochondrial and nuclear sequences showed a short genetic divergence between both populations, suggesting that they still belong to the same species. On the other hand, preliminary results from microsatellite analysis show a significant genetic differentiation and support the hypothesis that the "summer" population will have originated by a founder effect, which resulted from the establishment of a small number of mutant individuals, followed by complete reproductive isolation due to phenological differences. They conclude that different selection pressures, and the observed genetic differentiation, may rapidly lead to a deeper divergence and to the sympatric speciation of both populations (Santos *et al*., 2007).

1.4.2. Hosts

The genus *Pinus* constitutes the main host of *T. pityocampa*, but other coniferous genera, such as *Cedrus* and *Larix* (Masutti and Battisti, 1990; Hódar *et al*., 2002a; OEPP/EPPO, 2004) are also attacked.

Among pines, both indigenous and exotic species are attacked, but both the susceptibility of the host species to the attacks, as well as the preferences of the defoliator, varies widely. In the literature, disparate accounts are abundant, among which the following can be found. The European and Mediterranean Plant Protection Organization refers the following decreasing order of host preference: *Pinus nigra* var. austriaca, *P. sylvestris*, *P. nigra* var. laricio, *P.*

pinea, *P. halepensis*, *P. pinaster*, *P. canarensis* from the genus *Pinus*, followed by *Cedrus atlantica* and *Larix deciduas* (OEPP/EPPO, 2004). Tiberi *et al.* (1999) mentioning previous works, stated that *T. pityocampa* shows a marked preference for the pines from the *Pinus nigra* group, for indigenous species in southern Europe and to *Pinus radiata* Don. Among the exotic species, Koutsaftikis (1990) ranked *Pinus* species by a different order of preference for Greece, starting with *P. halepensis*, followed by *P. pinaster*, *P. radiata*, *P. brutia*, *P. pinea*, *P. nigra* and ending with *P. canarensis*.

Apart from the host species, outbreaks of *T. pityocampa* could be influenced by forest structure and pine stand density, as well as by host factors such as tree age (Masutti and Battisti, 1990). The different level of susceptibility observed in the genus *Pinus* could result from host tree selection at the moment of oviposition, linked to the quality of the needles of the various species, or be due to a synchronism with parasitoids cycles, factors which have been reported for other insect species (Avtzis, 1986; Buxton, 1990; Devkota and Schmidt, 1990; Tiberi *et al.*, 1999; Hódar *et al*., 2002; Zhang *et al.*, 2003; Hódar *et al.*, 2004; Petrakis *et al.*, 2005; Pérez-Contreras *et al.*, 2008).

1.4.3. Damage and other negative impacts

The feeding action of *T. pityocampa* inflicts economic losses (Hódar *et al*., 2002a; OEPP/EPPO, 2004) and ecological damages to pine forests due to tree defoliation (Markalas, 1998; Shevelev *et al.*, 2001; OEPP/EPPO, 2004). Mature pine trees are rarely killed, but young trees on reforested areas may suffer injury or even death, due to severe defoliation or, indirectly, as a consequence of secondary attack by wood-boring insects (Athanassiou *et al.*, 2007). In mature trees, main losses occur in volume growth. A loss of 40 % in wood growth and of 60 % in crown growth (Branco *et al*., 2008) can be expected, because defoliation occurs in the winter, exhausting the reserves stored in the needles (Athanassiou *et al.*, 2007). The main effects of *T. pityocampa* presence in recreational (e.g. parks, golf courses) and residential areas are the damage caused to the landscape due to unaesthetic defoliation and occupational and medical risks, whose resolution or minimization require expensive actions and maintenance programmes (Moneo *et al.*, 2003; Athanassiou *et al.*, 2007; Gatto *et al*., 2008).

The most serious impact is the occupational and medical threat, due to the production and release of microscopic urticating hairs into the air (Quero *et al.*, 1997), by the last instars larvae, as well as by the remains of the larval nests (Athanassiou *et al.*, 2007).

The urticant hairs contain thaumetopoein, a protein with histamine releasing properties and are able of penetrating the epiderm and mucous membranes, due to their harpoon morphology. They seriously affect humans and other mammals, causing skin lesions, conjunctivitis and cutaneous reactions, such as dermatitis, but also allergic problems, sometimes with violent reactions, such as anaphylaxis (Lamy *et al.*, 1986; 1987; Lamy, 1990; Vega *et al.*, 1997; Moneo *et al.*, 2003; Oliveira *et al.*, 2003; Vega *et al.*, 2003; 2004).

1.4.4. Control measures

Due to the negative impacts caused, there is often a need for the application of control measures of *T. pityocampa*. The most common methods of control include the use of chemical insecticides, mechanical methods (Schmidt *et al.*, 1999) and application of *Bacillus thuringiensis* preparations (Shevelev *et al.*, 2001; Athanassiou *et al.*, 2007).

Due to growing concern about the negative environmental impacts, the use of insecticides in forest ecosystems is not a viable option. In residential and recreational areas, the application of chemicals is generally severally limited by the authorities and their use is only considered as an acceptable option when attacks originate serious problems (Athanassiou *et al.*, 2007).

Such limitations promoted research and development of "environmentaly friendly" control methods and monitoring tools, such as sex pheromones aiming at mass trapping methods for direct control (Athanassiou *et al.*, 2007) and natural biological control (Way *et al.*, 1999). Regarding the application of natural biological control the use of viruses, microorganisms, plant extracts, insect grow regulators and egg parasitoids were referred by Schmidt *et al.* (1999) and the work of Triggiani *et al.* studied the feasibility using the nematode *Steinernnema feltae* to reduce *T. pityocampa* populations (Triggiani and Tarasco, 2001; 2002). Way *et al.* (1999) and Rodrigues (2002) reported the action of the argentine ant *Linepithema humile*, as a potential control agent against *T. pityocampa*.

1.4.4.1. Biological control: natural enemies and pathogens

The natural enemies of *T. pityocampa* play an important role in the regulation of its population levels and several species have been reported as egg, larvae and pupae parasitoids and predators, in core areas. According to Mirchev *et al.* (2004), the egg parasitoids can be responsible for an egg mortality of 6 to 72%, and are thus important in reducing *T. pityocampa* populations, as well as the damage inflicted.

The most abundant egg parasitoids reported for the Iberian Peninsula are three Hymenoptera (wasps), the chalcidids *Oencyrtus pityocampae* (Mercet) and *Bariscapus servadei* (Dom.) and the trichogrammatidae *Trichogramma embryophagum* Htg (Schmidt *et al*., 1999; Arnaldo and Torres, 2006; Branco *et al*., 2008). Important parasitoids of the larvae and pupae are the tachinid flies *Phryxe caudata* Rond and *Phorocera grandis* Rond, as well as the ichneumonid wasp *Erigorgus femorator* Aubert. Additionally, the carabid beetles *Carabus graecus* Dejan and *Pristonychus* spp. have also been referred (Avci and Sarikaya, 2005). The most important predators of the eggs and larvae of *T. pityocampa* are the Tettigonidae (grasshoppers) and several birds (Buxton, 1990; Schmidt *et al.*, 1990; Tiberi, 1990; Schmidt *et al.*, 1999; Way *et al.*, 1999; Branco *et al*., 2008).

1.4.4.2. Biotechnological contol

1.4.4.2.1. The female sex pheromone

The female sex pheromone of *T. pityocampa*, *cis*-13-hexadecen-11-ynyl acetate, has been identified by Guerrero *et al.* (1981), and was the first insect pheromone reported to have an acetylenic structure. The pheromone is biosynthesized by the sexual gland of the females, from palmitic acid through sequential desaturation, acetylenation and desaturation reactions under the action of Δ-11 and Δ-13 acyl-CoA desaturases (Villorbina *et al.*, 2003; Serra *et al.*, 2007). The analysis of gland extracts showed that females produce less that 1.0 ng of pheromone, under laboratory conditions (Quero *et al.*, 1997).

In 1997, Quero *et al.* (1997) reinvestigated the active fraction of the sexual gland extract, with help of gas chromatography coupled to electroantennographic detection, in order to access the existence of possible minor active components, but without success. These results strongly suggest that *T. pityocampa* females use one single compound as sex pheromone, an uncommon situation among the Lepidoptera species (Serra *et al.*, 2007).

1.4.4.2.2. Monitoring and mass trapping

The female sex pheromone is used to bait traps of several types, apropriate for the capture of adults of *T. pityocampa* (Branco *et al.*, 2008). According to management objectives, two different strategies might be implemented: i) Monitoring: detection of the presence of adults and quantification of the population level. ii) Mass trapping: removal of large numbers of males from the population to reduce/prevent mating and thus decrease the population level of the next generation.

Barrento *et al.* (2005) using standard traps, concluded that reliable estimates can be obtained for medium and high population densities of *T. pityocampa*. Nevertheless, for low densities, results might not be accurate.

Jactel *et al.* (2006) carried out a series of field tests, in order to design a standardized and reliable pheromone trap monitoring system for *T. pityocampa*. The main variables tested were trap design, saturation and position effect, pheromone dosage and the effect of the age of the dispenser. Findings suggest that pheromone baited traps could be a suitable tool for monitoring *T. pityocampa* populations.

Information regarding the application of mass trapping applications for the control *T. pityocampa* populations is scarce. In 1994, Subchev *et al.* (1994) studied the use of the synthetic sex pheromone, and concluded that even in the presence of the pheromone isomer, the number of male captures was dependent on trap design.

Recently Athanassiou *et al.* (2007) referred the need for standardization of pheromone-baited traps, as well as of other factors, such as trap placement, pheromone source, colour of the trapping surface and trap localization, as function of the pine stand density, regarding both monitoring and mass trapping of *T. pityocampa*.

Clearly, further research is still needed, to improve the efficiency of control methods of *T. pityocampa* based on the use of the female sex pheromone.

1.4.4.3. Other methods

Until the middle of the 20th century, attemps to control the pine processionary moth relied mostly upon mechanical methods. The larval nests are detached from the trees, and burnt.

Another physical method of larval elimination consists in placing a sticky band arround the tree trunk, where the larvae get stuck when descending to pupate in the soil.

Although unpractical for application to extensive areas, mechanical methods are still recommendable for small urban parks, school yards, or isolated trees, among other cases.

1.4.5. Chemical clues in insect - host relationships

According to the authors previously referred, host selection by *T. pityocampa* females is driven by physical and chemical factors, but there is no consensus about this topic. Demolin (1969) suggested that the female moth is able of selecting the tree for oviposition, but following visual than rather chemical, or nutritional clues, while Tiberi *et al.* (1999) among other authors, suggested a negative relation between limonene and the host species selected (Demolin, 1969; Tiberi *et al.*, 1999; Hódar *et al*., 2002). Physical factors of the hosts, referred by researchers, include tree size and position in the forest, the shape of the crown and the shape and thickness of the needles. Chemical factors have been mainly studied to explain larvae development and performance, and include terpenes, phenols, tannins, and nitrogen contents of the needles.

The first study on the role of chemical clues, in the process of host selection by *T. pityocampa,* was conducted by Tiberi *et al.* (1999). Using gas chromatography (GC) hyphenated with mass spectrometry (GC-MS) and chiral GC, the qualitative and quantitative composition of the secondary metabolites produced by *P. brutia*, *P. sylvestris*, *P. Pinaster*, *P. pinea* and *P. radiata*, from two plantations in Italy, were studied, aiming at understanding the role of monoterpenes upon the behaviour of ovipositing females. Findings suggested the hypothesis that limonene, the main volatile produced by the needles of *P. pinea*, which was the less susceptible species to *T. pityocampa* attack, could be a deterrent. The enantiomers of limonene were then separately applied to the same pine plantations, and it was concluded that "limonene seems to play a decisive role" on pine host selection, acting as deterrent. The best deterrent effect was achieved by (R)-(+)-limonene, but (S)-(-)-Limonene was also effective.

Zhang *et al.* (2003) reported the first study concerning the electrophysiological responses of *T. pityocampa* to the volatile components from the "bouquet" of *P. sylvestris*. It was concluded that the main components of the volatile fraction, α-pinene, β-pinene and Δ-3-

carene, did not elicited antennal responses. However, some minor compounds, like *β*-phellandrene, myrcene, *trans*-*β*-ocimene and terpinolene, were found to be very active. Week signals were also found for limonene, *cis*-*β*-ocimene, *γ*-terpinene, as well as for some less volatile compounds, such as sesquiterpenes and oxy terpenoids. Furthermore, no antennal signal was elicited by the pure enantiomer (R)-(+)-limonene, found to be the best deterrent by Tiberi *et al*. (1999).

Stastny *et al.* (2006) studied the role of host attractiveness and suitability in the patterns of host use by *T. pityocampa*, in the Italian Alps, with *P. mugo*, *P. nigra* and *P. sylvestris*. Concerning attractiveness, results showed that on choice experiments, *P. sylvestris* was the less attractive host for oviposition and *P. nigra* was the most attractive one. *P. mugo* showed intermediate attractiveness, but closer to that of *P. nigra*. No differences were found in larval growth and mortality. However, the secondary compounds of the needles were not investigated.

Using *P. halepensis* as a model, Pérez-Contreras *et al.* (2008) analyzed the relationship between needle asymmetry and individual host vigour, and between needle asymmetry and the essential oils composition of the needles, upon host selection by *T. pityocampa*. Steam distillation and gas chromatography, hyphenated with mass spectrometry, were the techniques used for essential oil extraction and analysis. Results indicated that the relative asymmetry of the length of the needles was negatively related to limonene, and positively related to host selection, suggesting that *T. pityocampa* females selected pines with a high degree of asymmetry, due to the lower contents of defensive chemical compounds, such as limonene, a finding which is partially in accordance with the hypothesis proposed by Tiberi *et al*. (1999).

Hódar *et al*. (2002) studied the relationship between *T. pityocampa* oviposition patterns and larval performance, and the relationship between the chemical characteristics of the host plant and performance by the different larval instars. Three pine species were used, *P. pinaster*, *P. nigra salzmannii* and *P. sylvestris nevadencis*, to determine the effect of needle chemistry on larval performance, measured as food ingestion, digestibility and larval growth. The chemical parameters of the needles analyzed were total phenols content and condensed tannins, by photometric methods, and nitrogen content, using elementar analysis. No significant differences were found, among the three pine species, regarding the amount of secondary compounds present in the needles. Results suggest that nitrogen content and digestibility were the significant factors determining larval survival, on all hosts, mainly during the early stages.

More egg batches were found on *P. nigra salzmannii* and *P. sylvestris nevadensis*, than on *P. pinaster*. In the food choice experiments, larvae from second- and third instars preferred their own host species, while the fourth and fifth instar larvae preferred *P. pinaster* needles, followed by *P. nigra* and *P. sylvestris nevadencis*. However, no significant differences were found among species, either in larval growth rate, or on the needles contents of phenols and tannins.

Avtzis (1986) conducted feeding tests of *T. pityocampa* on *P. pinaster*, *P. halepensis*, *P. brutia*, *P. pinea* and *P. radiata*, concluding that the highest rate of survival was achieved on *P. radiata*, and the highest mortality on both *P. pinea* and *P. halepensis*. Additionally, the start and duration of the larval descent to pupate in the soil, was also correlated with the pine species where they fed. However, no chemical analyses were carried out.

Buxton (1990) observed that differences in the timing of pupation by *T. pityocampa* larvae, feed on two different pine species, *P. pinaster* and *P. radiata*, resulted in marked differences in their exposure to parasitism by *P. caudata*. He attributed the differences on pupation time to specific defenses against the larvae. Chemical analyses were not performed.

Devkota and Schmidt (1990) studied the influence of different host plants on the larval development of *T. pityocampa*, in Greece. Needles of *P. mugo* were used as the standard host plant, and 13 species of pines and one of larch, were tested. For each instar, significant differences in larval development and mortality were observed, in relation to the pine species upon which they fed. Mortality reached 100% on *P. parviflora* S & Z, for the first instar larvae, on *P. strobes* L. and *L. kaempferi* (Lamb.) Carr for the second instar, on *P. cembra* L. for the third instar and on *P. vallichiana* Jacks for the pupal stage. A delay in larval development on *P. strobes*, *P. parviflora*, *P. cembra*, *P. wallichiana* and *L. kaempferi* (Lamb.) was also registered. No nest building was observed on *P. parviflora*, *P. strob*es and *P. cembra*. It was hypothesised that differences in the hardness and texture of the needles, as well as of their chemical composition, could be the factors responsible for the mortality of the larvae. However, no chemical parameters were measured.

Hódar *et al*. (2004) studied larval survival in four groups of *P. sylvestris* trees, having undergone different levels of herbivory and defoliation. The parameters quantified were nitrogen, phenolics, terpenes and fibre contents of the needles. A significant relationship between the patterns of defoliation, and some of the terpenes, such as β-pinene, α-pinene,

camphene, myrcene, tryciclene and γ-cadinene, was found (Hódar *et al*., 2004). The authors suggest that larval survival was related both to the level of defoliation and to the historical profile of the trees. A positive relationship between the amounts of β-pinene and γ–cadinene in the needles of pines defoliated by *T. pityocampa* is also referred.

Petrakis *et al*. (2005) studied the feeding behaviour of the 3rd and 4th *T. pityocampa* larval stages, using feeding substrates of *P. halepensis*, impregnated with the extracts of 15 pine species, in an attempt to establish the relative contribution of the secondary metabolites. Hydro-distillation was used to obtain the essential oil fraction from the needles of each pine species, and the terpenes were analysed by gas chromatography and mass spectrometry. It was concluded that some of the terpenes contribute significantly to the separation of the profiles of different pine species, namely: caryophyllene oxide, terpinolene, myrcene, germacrene D, eudesmol, limonene, β-pinene, β-caryophyllene, α-pinene and manoyl oxide. The proposed model estimated that the chemical composition of the needle substrates had a significant role on the feeding behavioural sequence of the third and fourth larval instars, according to previously defined five feeding behavioural steps (BS), ranging from no orientation to the substrate to total consumption of the substrate. No clear antifeeding effect was found, except for β-caryophyllene, which showed to be a significant strong antifeedant of the last BS. However, as larval feeding proceeded, more terpenoids became important as feeding suppressors, such as germacrene D, which seemed to be an important, though weak, suppressor of complete feeding. For Petrakis *et al.* (2005), this observation suggests the possible absence of the type of olfactory receptor neuron that is specific for germacrene D in *T. pityocampa*, an hypothesis that does not match the findings of Zhang *et al.* (2003).

1.5. Analytical methodologies

When considering secondary compounds analysis, the first step, that is sample preparation, is probably underestimated when compared to the chromatographic separation, or to the analyte identification by mass spectrometry. In biological samples, a great chemical diversity must be expected to be present in a wide range of concentrations. The composition and quantity of the detected metabolites strongly depends on the extraction technique that is used to remove and isolate them from their matrix. The choice of a suitable extraction methodology should depend on the sample original composition and on the target compounds. However, an ideal sampling method for all kinds of compounds and matrices does not exist and no single isolation technique produces an extract that replicates the original sample (Jennings and Filsoof, 1977).

There are various techniques that can be used for the preparation of the sample analytes in biological material, such as solvent extraction by means of dipping (Hopkins *et al.,* 1997), soaking (Prudic *et al.,* 2007), sonication (Lin *et al.,* 1998), soxhlet extraction (Ekeberg *et al.,* 2006) or pressure-liquid extraction (Cho *et al.,* 2007), steam distillation and simultaneous distillation-extraction (Kim and Shin, 2005), solid phase microextraction (Santos *et al.,* 2006), dynamic headspace analysis (Mumm *et al.,* 2004), stir bar sorptive extraction (Hampel *et al.,* 2005), matrix solid-phase dispersion (Manhita *et al.,* 2006), supercritical extraction (Braga *et al.,* 2008) and microwave assisted extraction (Proestos and Komaitis, 2008).

1.5.1. Extraction / collection methods

1.5.1.1. Solvent extraction and distillation methods

Solvent extraction (SE) and steam distillation (SD) may be considered the oldest methods used to extract non volatile and volatile metabolites from their natural matrices. In 1964 simultaneous distillation-extraction (SDE) was introduced and, since then it is one of the most

cited sample preparation techniques for volatile and semi-volatile compounds (Chaintreau, 2001). All solvent and distillation methods have advantages and disadvantages. The main advantages are the possibility of obtaining relatively large amounts of material for future work and their apparent simplicity, that do not demand complex or expensive apparatus. At the end of the process, the result is generally a sample extract that, if representing the sample matrix, provides the opportunity to analyse a large number of replicates over time, at different laboratories using different techniques.

However, SE and SD methods present important disadvantages. Solvent "extracts" are usually complex mixtures of volatile and non volatile compounds, a consequence of the co-extraction of volatile compounds with heavier compounds such as cuticle lipids and chlorophyllus substances (Knudsen *et al.,* 1993). These complex sample extracts may demand one or more clean up steps, in order to isolate the active fraction, or compounds. Clean up processes are often very time consuming and prone to error. An extra source of "complexity" is due to the introduction of artifacts on the sample extracts because of solvent contamination (e.g. hydrocarbons and preservatives). Another drawback comes for volatile analysis, where the final component profiles are frequently not representative of the volatile fractions emitted by the samples. Often these complex extracts produce very complex chromatograms, which are difficult to analyse and interpret. The detection of the active compounds, that usually are present at trace levels, can be jeopardized by the peaks of interfering matrix components. This disadvantage is more evident in solvent extraction than in distillation methodologies (Figure 1.5), where the volatile compounds, emitted from the samples, do not necessarily appear in the solvent extract chromatogram, or do so at low concentrations. Additionally, less volatile compounds may deposit and accumulate in the injector liner and on the front section of the chromatographic column, producing ghost peaks, baseline drift, peak tailing, loss of chromatographic separation and analyte losses due to adsorptions (Rood, 2007).

Finally, solvent extraction usually results in extracts with a considerable volume, which must be reduced by evaporation, a process that can lead to losses of the more volatile compounds. Another issue concerns enzymatic, thermo and photochemical degradations. Enzymes released by the destruction of the sample matrix can react with the analytes and change the final composition and the profile of the samples.

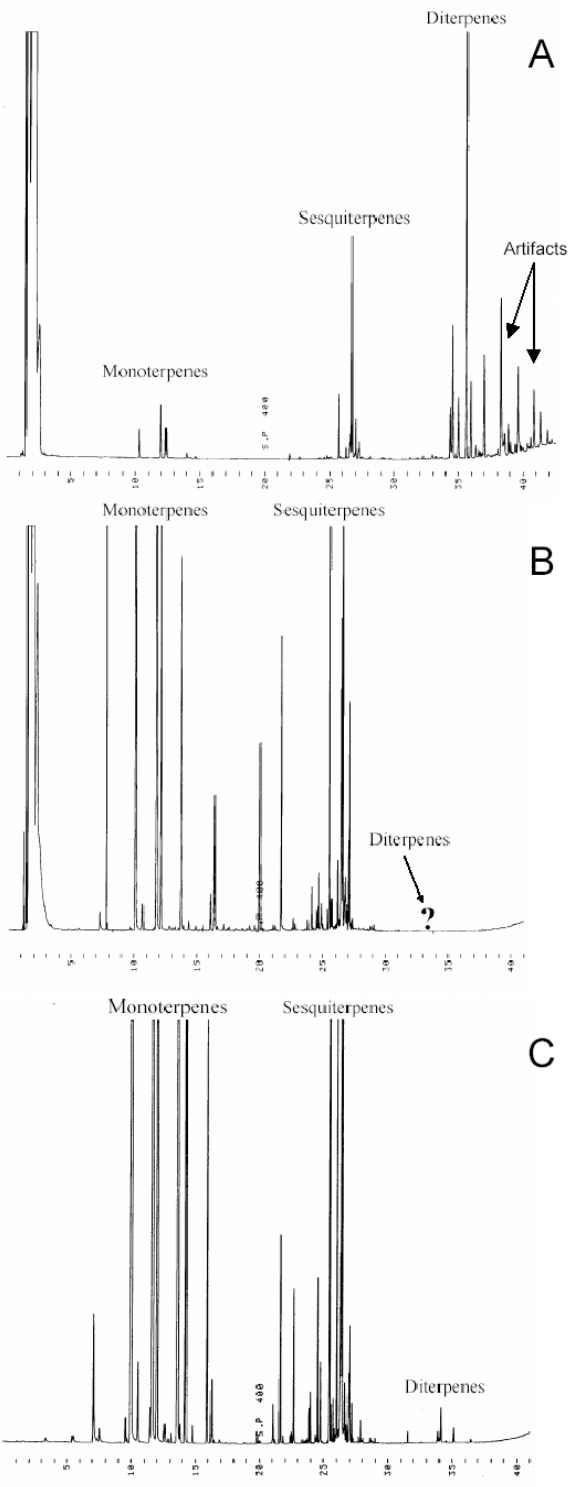

Figure 1.5 – GC-FID chromatograms of *P. pinaster* needles analysed with a DB-5 column (25 m × 0.32 i.d.; 1.0 μm): **A)** solvent extract (30 min dipped in pentane); **B)** SDE extract (2 h; pentane: diethyl ether); **C)** HS-SPME extract (100 μm PDMS fiber; 45 min).

Steam distillation, solvent extraction (soxhlet and sonication) and simultaneous distillation-solvent extraction need heat, and heat can lead to sample degradation, production of artifacts and compound rearrangements. Additionally, in distillation methods the combination of heat with the water pH can also lead to hydrolysis and rearrangement reactions of thermally labile

compounds, such as the terpene alcohol esters (Pauly *et al.*, 1973; Koedam *et al.*, 1980; Sandra and Bicchi, 1987).

SD and SDE methods can provide, for volatile analysis, a fraction free of non volatiles that can be used directly in gas chromatography. The main operational parameter to consider, when using distillation, is the length of the distillation period. The composition of the final "extract" changes unidirectionally with time (Koedam *et al.*, 1980; Sandra and Bicchi, 1987). The most volatile and water soluble compounds (e.g. oxygenated compounds) are first removed from the matrix, by hydrodiffusion, followed by the gradual removal of the low volatile and less water soluble compounds (e.g. terpenoids hydrocarbons). If SDE is used, the choice of solvent is also an important parameter. Different solvents have different affinities for the matrix components and thus they affect the final extract composition (Chaintreau, 2001).

1.5.1.2. SPME

1.5.1.2.1. Overview

The concept of solid phase microextraction (SPME) was first reported by Arthur and Pawliszyn (1990)**,** as an improvement of solid phase extraction (SPE) for aqueous samples. In that report, the main attributes of SPME, such as being a solvent-free process, reduction of extraction time, easy handling of the apparatus, simplicity, sensitivity and low operational costs, were already stated. The studies concerning process optimization and automation (Arthur *et al.,* 1992c), as well as the description of the dynamics of analyte extraction and desorption (Louch *et al.,* 1992), were published in the following years, together with applications of the technique to environmental analysis of organic pollutants in water (Arthur *et al.,* 1992a; 1992b; 1992d; Potter and Pawliszyn, 1992).

In 1993, Pawliszyn and co-workers published the theoretical fundaments for the application of SPME to headspace analysis (Arthur *et al.*, 1993; Zhang and Pawliszyn, 1993). Originally designed to be used with gas chromatography (GC) all the initial works have been carried out with volatile and semivolatile compounds. In 1995, Chen and Pawliszyn described the first interface for coupling SPME with liquid chromatography (HPLC) (Chen and Pawliszyn, 1995), opening its range of application to non-volatile and thermally unstable compounds and thus precluding the need of derivatisation steps. Since then, the technique had a fast and great expansion and has been successfully applied to several research fields, such as environmental

analysis (Ouyang and Pawliszyn, 2006), food analysis (Kataoka *et al.,* 2000), biomedical analysis (Ulrich, 2000), trace element speciation (Mester *et al.,* 2001), analysis of explosives (Gaurav *et al.,* 2007), analytical toxicology (Pragst, 2007), flavor and fragrance (Yang and Peppard, 1995; Chen *et al.,* 2006), and biological samples (Theodoridis *et al.*, 2000; Musteata and Pawliszyn, 2007). In what concerns chemical ecology, works using SPME can be found with allelochemicals (Loi and Solar, 2008) and volatile compounds emitted from plants (Yassaa and Williams, 2007), with fungal metabolites (Jelen, 2003) and with pheromones (Rochat *et al.,* 2000) and defensive compounds (Prudic *et al.,* 2007) from insects.

1.5.1.2.2. Description and use

The heart of a SPME system (Figure 1.6) consists of a 1 – 2 cm long fused silica fiber coated with an absorbent polymer material, such as poly(dimethylsiloxane), that in some cases is mixed with a solid adsorbent (e.g. a divinylbenzene polymer or porous carbon). The fiber is attached to a stainless steel plunger and assembled on a syringe-like holder. The holder, designed to be used with replaceable fiber assemblies, not only controls the exposure of the fiber during extraction and desorption (Louch *et al.,* 1992b), but also protects it during its storage and piercing of the septum on the sample vial and on the GC injector (Pawliszyn, 1997).

Two main variations of SPME can be performed: direct extraction with immersion of the fiber directly into an aqueous sample and headspace extraction (Pawliszyn, 1997). Other variants may include sample derivatisation (Pan and Pawliszyn, 1997) and sample rubbing (Monnin *et al*., 1998; Tentschert *et al*., 2002).

The SPME operating steps, sample extraction and concentration followed by the chromatographic injection, are simple and are shown in Figure 1.7. First, the SPME unit pierces the septum of the sample vial. Second the fiber is exposed to a headspace above the sample or inserted on aqueous sample and concentrates the analytes by absorption/adsorption processes. Third, after an extraction period of minutes to hours, the fiber is retracted and the SPME unit is removed from the sample vial.

For analyte desorption the SPME needle is directly inserted into the heated GC injector, the fiber exposed, the analytes thermally desorbed and injected in the GC column. For LC, an interface chamber is used (Chen and Pawliszyn, 1995) and the analytes are chemically

desorbed in an organic solvent. Finally, the SPME fiber is retracted and the unit removed from the chromatographic system. As the fiber is reusable the process could start again with the same unit.

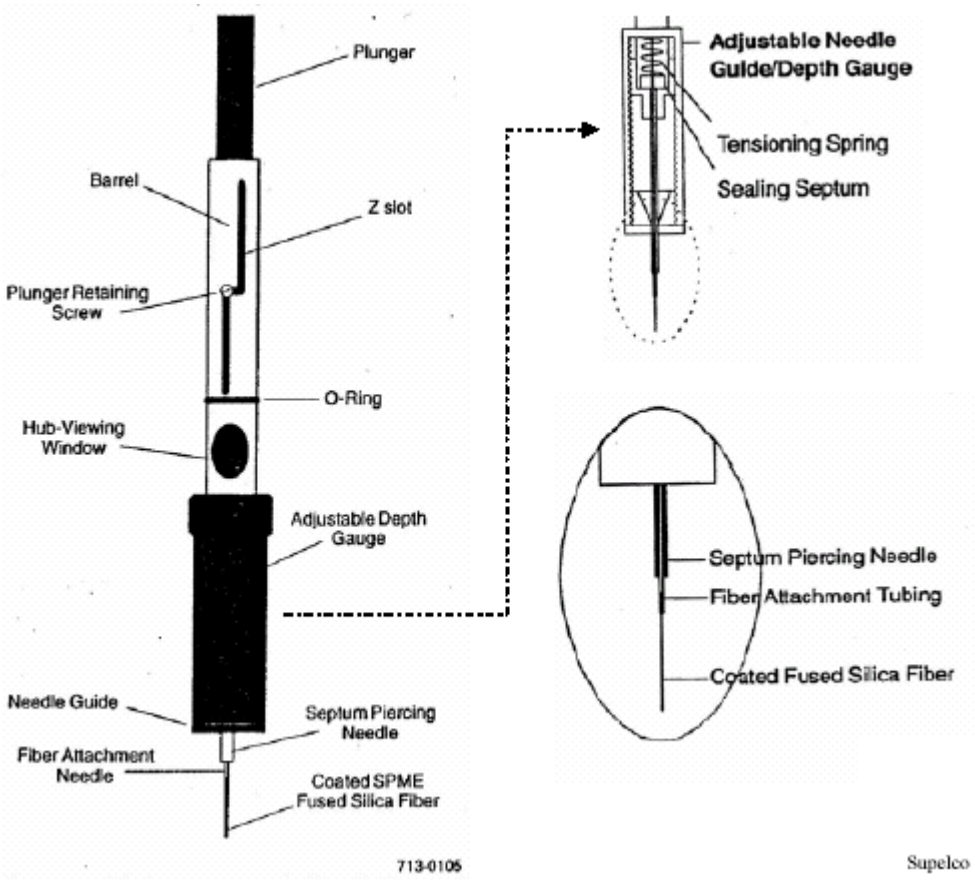

Figure 1.6 – Components of a commercial SPME manual holder and fiber assembly: general, section and detailed view (adapted from Supelco, 1995).

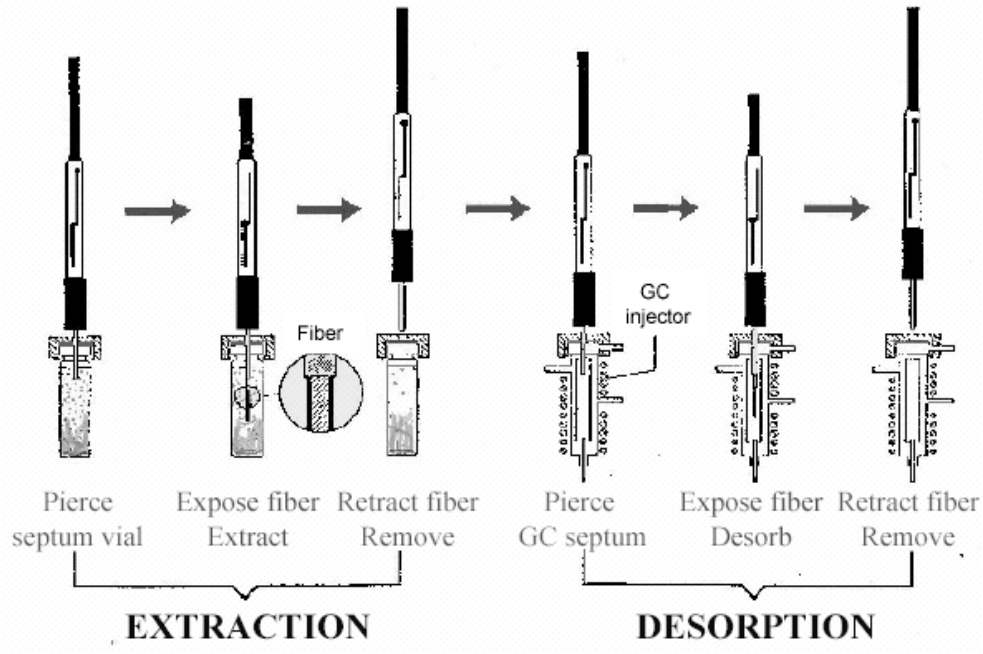

Figure 1.7 - SPME operating steps, sample extraction, and analyte desorption for chromatographic analysis.

1.5.1.2.3. Theoretical background

The theory of SPME has been extensively presented in the literature in the earlier years of the technique (Arthur *et al*., 1992c; 1992d; Louch *et al*., 1992; Zhang and Pawliszyn, 1993; Vaes *et al*., 1996). In a book published by Pawliszyn in 1997 (Pawliszyn, 1997), the compilation of the theoretical principles added to 72 pages, making up one chapter and one appendix.

Basically, the process of extraction in SPME can be divided in two stages: **i)** the kinetics of the analyte mass transfer between phases (fiber coating, headspace and sample matrix), that determines the speed of extractions and **ii)** the thermodynamic partition of the analyte between the phases (Eisert and Pawliszyn, 1997; Ulrich, 2000), that determines the amount of analyte extracted.

SPME is a multiphase equilibrium process, based on the partition of the analytes between the fiber coating and their matrices (Martos *et al.*, 1997; Saraullo *et al.*, 1997). For direct immersion the process is ruled by the equilibrium of the analyte between the aqueous phase and the fiber coating (Ulrich, 2000). For headspace extraction, the process is dependent of two equilibrium processes (Zhang and Pawliszyn, 1993): **i**) the equilibrium between the volatile analytes and their natural matrix, which is dependent of the compounds volatility and properties of the matrix, and **ii**) the equilibrium between the volatiles in the gas phase and the SPME fiber coating, which is dependent of the analytes affinity to the fiber coating. In consequence, SPME is a non exhaustive extraction method that is considered to be complete when the analyte concentration reaches the distribution equilibrium between the sample matrix and the fiber coating (Lord and Pawliszyn, 2000). At equilibrium point, theoretically, the amount of analyte extracted stays constant and is independent from further increase of the extraction time.

The amount of analyte extracted at equilibrium can be described as:

$$n = (K_{fs}\, V_f\, V_s\, C_0) / (K_{fs}\, V_f + K_{hs}\, V_h + V_s) \qquad (1.1)$$

where:

n = amount of analyte extracted by the fiber

K_{fs} = fiber coating/analyte distribution constant [K_{fs} = (Amount of analyte in the fiber)/(amount of analyte in the matrix)]

V_f = volume of the fiber coating

V_s = sample volume

C_0 = initial concentration of the analyte

V_h = volume of the headspace

K_{hs} = distribution constant of the analyte between the sample matrix and the headspace.

In other words, the amount of analyte extracted by the fiber is proportional to its initial concentration (C_0), fiber coating/analyte distribution constant, sample volume, and the volume of the fiber coating (Eisert and Pawliszyn, 1997; Lord and Pawliszyn, 2000).

However, the expression (1.1) does not give any information concerning the time needed to reach the equilibrium, which is dependent on the mass diffusion of the system.

Equation 1.2 represents the time needed to reach equilibrium:

$$T_e \approx T_{95\%} = (L_f)^2 / 2D_f \qquad (1.2)$$

where:

T_e = time needed to reach equilibrium

$T_{95\%}$ = equilibrium time achieved when 95% of the equilibrium amount of the analyte is extracted from the sample

L_f = fiber coating thickness

D_f = diffusion coefficient of the analyte in the coating layer

Due to the intrinsic experimental error associated with SPME, a change in the mass extracted can not be determined if it is smaller than the experimental error, assumed as 5%. Therefore the practical equilibrium time is assumed to be achieved when 95 % of the equilibrium amount of the analyte is extracted from the sample and $T_e \approx T_{95\%}$ (Pawliszyn, 1997).

In real samples, deviations from the theoretical model are expected, due to the nature of the matrix (gaseous or liquid) and experimental parameters, such as agitation and temperature. Consequently, not all analytes have access to the fiber coating at the same time, a phenomenon that was modulated by Pawliszyn (1997) using a hypothetical matrix boundary layer of radius δ, that depends on agitation. Thus, the time for maximal extraction, in the direct immersion mode, can be calculated from:

$$T_e \approx T_{95\%} = 3\delta K_{fs} [(L_f)^2 / D_m] \qquad (1.3)$$

where:

D_m = diffusion coefficient of the analyte in the aqueous matrix

For headspace, several variables related to the fiber coating, headspace and sample matrix have to be taken into account for the estimation of T_e (Pawliszyn, 1997; Ulrich, 2000).

A simplification of the model, assuming a very fast diffusion of the analyte on its matrix, may lead to:

$$Te \approx T_{95\%} \approx 1{,}8\ (K_{fs} / K_{hs})\ [(L_f L_{hs}) / D_{hs}] \qquad (1.4)$$

where:

K_{fs} = fiber coating/analyte distribution constant [K_{fs} = (Amount of analyte in the fiber)/(amount of analyte in the matrix)]

K_{hs} = analyte equilibrium coefficient between the gaseous phase and its matrix

L_{hs} = thickness of the headspace layer

D_{hs} = diffusion coefficient of the analyte in the headspace phase

From equations (1.2) to (1.4), it can be concluded that the time of extraction increases with fiber thickness, fiber coating/analyte distribution constants, and lower diffusion coefficients. For headspace, larger headspace volumes and low volatility of the compounds lead to higher extraction times. From the ratio (K_{fs} / K_{hs}) it can be concluded that analytes with higher K_{hs} and lower K_{fs} are more rapidly extracted (Pawliszyn, 1997).

1.5.1.2.4. Optimization

The efficiency, accuracy and precision of the SPME extraction is directly dependent on fiber attributes, such as polarity and thickness or length, and on operational parameters like extraction time, sample agitation, pH adjustment, salting out, sample or headspace volume, temperature of operation, adsorption on container walls and desorption conditions (Pawliszyn, 1997).

Extraction time can be controlled by agitation, salting out, pH control and temperature (Pawliszyn, 1997). Agitation promotes the contact and transfer of analytes from the sample matrix to the coating fiber. The form of non neutral and soluble analytes, influences the extraction efficiency, and can be controlled by changing the pH of the matrix. In general, the sample is acidified for the extraction of acidic analytes and is made alkaline for the extraction of basic analytes.

The parameter temperature is very important in headspace analysis, where it is used to increase the concentration of the analytes in the gaseous phase. The temperature affects the sensitivity and the extraction kinetics. An increase of the temperature of the system causes an increase in the extraction efficiency but, simultaneously, decreases the distribution constant. Therefore, an adequate temperature which provides satisfactory sensitivity and extraction rate should be optimized

The volume of the sample is a variable affecting the estimated distribution constants (see equation 1.1). If K_{fs} of the analytes are very high, the sensitivity will be affected by the volume ($n \approx V_s C_0$). However, the initial concentration will decrease as sample volume increases. If the sample volume is too high, the amount of analyte extracted is not dependent on V_s ($n \approx K_{fs} V_f C_0$). This makes SPME potentially usable for field sampling and analysis (Tonidandel *et al.*, 2008).

The desorption of the analytes from the fibers is dependent on the boiling point of the analytes, the thickness of the fiber, time of desorption, liner volume, depth of fiber insertion inside the hot injector zone and temperature and geometry of the injector port (Pawliszyn, 1997).

15.1.2.5. Selection of fiber coatings

There is no single fiber coating that will extract all analytes with the same efficiency (Mani, 1999). The selectivity in SPME is controlled by the chemical nature of the analytes, and is directly related to the choice and use of the most appropriated fiber coating for the target analytes. For the right selection of the fiber coating, Eisert and Pawliszyn (1997) stated that the general principle of "like dissolves like" applies, meaning that nonpolar analytes are most effectively extracted with nonpolar fiber coatings, and polar analytes with a polar coating (Supelco Inc., 1998).

The thickness of the coating plays a role in determining the equilibrium time, sample capacity and selectivity. Thicker coatings provide higher sensitivity, due to the greater mass of the analytes that can be extracted. The extraction time is smaller for thinner coatings, due to the decrease of the distribution constants, but a decrease on the amount of analyte extracted must be considered. For thickness, selectivity is accepted that volatile compounds are better

extracted with thicker coatings and thin coatings are most effective for adsorbing/desorbing semivolatile and larger analytes (Mani, 1999; Stashenko and Martínez, 2007).

However, due to diffusion kinetics, chemical interactions and concentration gradients other attributes than the polarity of the analyte, such as molecular weight, size and volatility together with the complexity of the sample matrix, should also be taken in consideration for selection of the fiber for extraction (Yang and Peppard, 1995; Shirey, 2007).

Several types of fiber coatings are available on the market, with different chemical characteristics, ranging from adsorbent to absorbent extraction mechanisms, and from polar to non polar phases, in a wide range of different thickness (7-100 μm) and operational temperatures (200-320 ºC). Commercially available fibers are summarized in Table 1.2.

Table 1.2 - Commercially available SPME fibers

Coating type	Polarity	Thickness (μm)	Operational temperature (ºC)
Polydimethylsiloxane (PDMS)	non-polar	7	220-320
		30	200-280
		100	200-280
Polyacrylate (PA)	polar	85	220-310
Carboxen/Polydimethylsiloxane (CAR/PDMS)	bi-polar	75, 85	250-310
Polydimethylsiloxane/Divinylbenzene (PDMS/DVB)	bi-polar	65	200-270
Divinylbenzene/Carboxen/Polydimethylsiloxane (DVB/CAR/PDMS)	bi-polar	50/30	230-270
Polyethylene Glycol (PEG)	polar	60	-
Carbowax/Templated Resin (CW/TPR)	polar	50	-
Carbopack-Z	polar	15	up to 340

Poly(dimethylsiloxane) (PDMS) and poly(acrylate) (PA) were the first fibers to be developed and are both pure homogeneous polymeric phases (Pawliszyn, 1997; Mani, 1999). PDMS coated fibers, that are available in tree film thickness, are usually the first choice, and the 100 μm version is the most popular phase in SPME (Pawliszyn, 1997; Mani, 1999). PDMS coating, due to its methyl groups, is nonpolar, with a high affinity for nonpolar and volatile compounds (Yang and Peppard, 1995). The PDMS is considered to be an absorptive phase

(Góreccki *et al.*, 1999), although some authors have found adsorption effects for the higher molecular weight polychlorinated biphenyls (PCBs) and polycyclic aromatic hydrocarbons (PAHs) (Yang *et al.*, 1998). It can also be applied to more-polar compounds, after optimizing extraction conditions, such as pH or salting out adjustments. The hydrophilic PA coating, due to the presence of carbonyl groups on its structure, is considered polar and shows a high affinity for polar compounds, namely phenols and alcohols (Yang and Peppard, 1995; Góreccki *et al.*, 1999) in aqueous matrices. Both PDMS and PA coatings extract the analytes mainly by absorption mechanisms (Góreccki *et al.*, 1999).

In order to improve the efficiency of SPME, for a wider range of compounds, several mixed coatings, with complementary properties to PDMS and PA, have been developed. These coatings, with bipolar properties, are mixed materials of PDMS imbedded with porous absorbent copolymers, such as divinylbenzene (PDMS/DVB) and carbowax (PDMS/WAX), and physical blends with solid adsorbents such as Carboxen (CAR), a porous activated carbon support (PDMS/CAR or DVB/CAR/PDMS) (Mani, 1999; Góreccki *et al*, 1999). In spite of their lower mechanical stability than PDMS and PA coatings, they are more selective, due to the selectivities of components, produce stronger retention of the analytes, present more extraction capacity and allow the extraction of different classes of analytes simultaneously (Mani, 1999). These attributes make mixed coatings more suited for trace level analysis (Pawliszyn, 1997). Their blending with PDMS allows for the extraction of smaller analytes and a better affinity for polar compounds than PDMS alone (Mani, 1999). Potential drawbacks are that larger molecules can be difficult to desorb or require higher desorptions temperatures, to reduce peak tailing (Mani, 1999). The primary extracting phases, of the mixed coatings, are porous solids and because of that they extract the analytes mainly by adsorption mechanisms, in opposition to the absorption mechanisms of PA and PDMS (Góreccki *et al.*, 1999).

The fundamentals of absorption for pure polymers, and adsorption mechanisms for mixed phases are different (Góreccki *et al.*, 1999). Independently of the coating, at the beginning of the SPME process, the analyte molecules become attached to its surface. However, in the absorption mechanism the analytes dissolve in the coating and migrate to its bulk during extraction. The extension of the analyte migration to the bulk of the coating is dependent of its diffusion coefficients for the coating. The diffusion coefficients are high enough, and close to those of organic solvents in PDMS and PA coatings, and allow absorption to be the primary extraction mechanism, which is a non competitive process (Góreccki *et al.*, 1999). In the

adsorption mechanisms, the analytes attach to surface of the coating. DVB and CAR have very low diffusion coefficients for organic molecules, and all molecules remain on their surfaces and adsorption become the only practical extraction mechanism for them (Góreccki *et al.*, 1999). The number of active sites at the coating surface, where adsorption can take place, is limited and due to that adsorption is a competitive process. Molecules with higher affinity for the surface sites can replace molecules with lower affinity. The consequence is that the amount of a certain analyte, extracted using porous polymers or carboxen mixed phase, is dependent on the sample matrix composition (Góreccki *et al.*, 1999). This makes quantitative analysis difficult and non reproducible, due to deviations in the linear dynamic range, except for relatively clean matrices, matrices with constant composition or with low concentrations of the target analytes. The extraction times are shorter for gaseous samples, due to the absence of diffusion to the coating bulk (Pawliszyn, 1997).

1.5.2. Chromatographic methods

Capillary gas chromatography (GC) is the most used technique for the separation and analysis of volatile and semivolatile organic compounds (Beesley *et al*., 2001), such as secondary metabolites from plant origin (Nielsen, 2007). There are a number of reasons to support this choice. First, the high complexity of the samples (Dunn and Ellis, 2005), with large amount of components, usually present in a wide range of concentrations, which need to be separated and analyzed. Second, GC has a very high resolution power that allows separation of tens of compounds in one single run and is today a simple, mature, flexible and robust method that can be used as a routine basis for qualitative and quantitative analysis (McNair and Miller, 1998; Beesley *et al*., 2001; Majors, 2003). Third, the flame ionization detector (FID), the most common detector in GC, is sensitive, has a wide linear dynamic range and is universal for organic compounds, meaning that almost all compounds in the sample are qualitative and quantitatively detected, in a wide range of concentrations, and even at relatively low concentrations (Scott, 1996; Braithwaite and Smith, 1999). Fourth, gas chromatography can be used with various detectors and hyphenated with other analytical techniques, such as mass spectrometry (GC/MS) and Fourier transform infrared spectroscopy (FTIR), and thus increase its selectivity and range of applications (Scott, 1996, Dunn and Ellis, 2005).

The essential components of a GC system are the carrier gas, the injection port to introduce the samples, an oven with controlled temperature, the analytical column, and a detector

connected to a data recorder and treatment system (e.g. computer with proper software) (McNair and Miller, 1998; Poole, 2003).

The basic principle of GC separation lies on the partition of the analytes between an inert carrier gas, the mobile phase and a solid or liquid stationary phase, which is placed inside the column (McNair and Miller, 1998; Poole, 2003).

The time elapsed between the injection and the elution (retention time) is, theoretically, an unique attribute of the analyte and can be used for its detection and potential identification and quantification. The retention time of an analyte depends on its boiling point (volatility) and the interactions between its functional groups (polarity) and those of the stationary phase (McNair and Miller, 1998).

The GC elution of the analytes present in a sample is promoted by temperature (Looser *et al*., 2005). GC runs are usually performed in the range of 40 to 325 ºC and, as the temperature rises, the analytes move in the gaseous mobile phase and through the column. However, GC runs can also be made isothermally, if the temperature is high enough to promote analytes volatility and mobility along the analytical columns (Yuwono and Indrayanto, 2004). Higher temperatures can also be used in special applications (e.g. triglycerides) and with special high-temperature columns (Wittkowski and Matissek, 1990).

There are two rules that GC analytes must fulfil. They must be volatile and be thermal stable at GC operational temperatures (Nielsen, 2007). However, non volatile compounds can be converted to volatile derivatives, allowing GC to expand its analytical capability (Dethlefs *et al*., 1996; Davis *et al*., 1968; Kleinschmidt *et al*., 1968; Dunn and Ellis, 2005; Nielsen, 2007).

The sample injection is the first stage in the chromatographic process. The sample injection technique used is an important factor and must allow reproducible and quantitative transfer of the sample to the column, minimize band broadening, analyte decomposition and adsorption on the injection port (Yuwono and Indrayanto, 2004).

The most common injection techniques in GC are split and splitless injection (Beesley *et al*., 2001; Grob, 2001; Zrostlıkova *et al*., 2001), that promote the hot vaporization of the sample. The inlet temperature is often set at 250 ºC, at which the majority of metabolites are evaporated (Beesley *et al*., 2001). At split mode, just a fraction determined by the split ratio,

of the injected sample enters the column, while the remaining is vented out. The splitless mode is performed with a split injector, and nearly all the sample vapor is transferred to the column (Grob, 2001). Split injection is the technique of choice for rather concentrated samples but is not suitable for trace analysis, when sensitivity is required (Grob, 2001). The splitless mode is used for trace level analysis, when it is necessary to transfer the maximum amount of sample to the column, in order to maximize sensitivity (Grob, 2001). However, in spite of their popularity, some potential adverse effects must be considered such as: **i)** sample backflash due to the sample vapour expansion beyond the capacity of the injector liner, **ii)** discrimination of low volatile analytes that do not vaporize in time and are vented out, and **iii)** analyte sorption and thermodegradation at the injector body (Grob, 2001; Zrostlıkova *et al*., 2001; Grob and Neukom, 2005).

Other common injection techniques are the on-column injection, used for thermo labile samples, that are directly introduced into the column at low temperatures, and temperature programmed vaporization injection (PTV), involving injection of the sample into a cold injector port, followed by rapid or programmed heating to vaporize them (Grob, 2001; Moldoveanu and David, 2002).

The analytical column is the heart of the chromatographic system and the choice of its stationary phase/polarity is the only controllable variable for selectivity in the separation process (Majors, 2003). The analytical columns generally separate the sample components based on their volatility and polarity. Chiral columns, based mainly upon modified cyclodextrins, additionally, also separate sample components according to their absolute configurations, allowing the analysis of enantiomeric compounds (Beesley and Scott, 1998; Bicchi *et al*., 1999; Looser *et al*., 2005).

The selection of a stationary phase depends on the chemical and physical properties of the analytes, but other column parameters than polarity, such as film thickness, diameter and length of the column must also be putted on equation when choosing a column. Chromatographic columns are available in a wide range of stationary phases, diameters, film thicknesses and lengths, which allow the separation of complex mixtures with compounds of different polarities and volatilities. Selecting a column stationary phase for a particular application can be done by consulting the catalogs and application notes from column vendors or by reading chromatographic guidance books (Wittkowski and Matissek, 1990; Jennings *et al*., 1997; McNair and Miller, 1998; Barry and Grob, 2007).

The nonpolar stationary phases, 100% methylsiloxane and 5% phenylmethylsiloxanes are the most popular for nonpolar compounds separation, and the polar polyethylene glycol (PEG or Wax) are preferred for more polar analytes analysis (Majors, 2003). It is accepted, as a rule of thumb, that 90% of the separation problems can be solved by using a polar and nonpolar column (Wittkowski and Matissek, 1990; Chaves das Neves and Freitas, 1996).

1.5.2.1. Detection

The vast majority of GC applications are carried out using a FID, a single channel detector, to detect the eluting analytes, on the basis of their retention times. However, the use of GC-FID data alone can not confirm the identity, or structure, of an analyte under a chromatographic peak, without complete and reproducible separation of each sample component. Retention times are a chromatographic characteristic of the analyte but they are not unique (McNair and Miller, 1998). Structural and physical-chemical similarities of several components of the samples often result in chromatographic co-elutions that are impossible to be detected by GC-FID.

The hyphenation of GC with mass spectrometry (GC/MS) introduces the identification power to the chromatographic task, and its reconstructed total ion current (TIC) results in a record output, similar to a FID chromatogram, with the advantage of the mass to charge ratio (m/z) information, in a second channel, that allows analyte structural information, which in some cases leads to tentative identification.

1.5.3. Mass spectrometry

In the GC/MS technique, the sample molecules, after eluting from the analytical columns, enter a vacuum chamber where they are ionized in the ion source. The ions thus created, ranging from molecular size to small fragment ions, are then separated according to their m/z ratio in the mass analyzer and detected. The relative abundance of each m/z is plotted as an histogram of the intensity of ions *vs*. their mass-to-charge, that is called a mass spectrum.

1.5.3.1. Electron ionization

The most widely used ionization techniques employed in GC/MS are electron ionization (EI), where analyte molecules are bombarded by high-energy electrons (-70 eV) emitted from the

electron filament. As a result, high-energy singly charged molecular ions are produced, that subsequently fragment into a series of positively charged fragment ions (Herbert and Johnstone, 2003). The efficiency of ionization and production of fragments strongly depends on the chemistry of the analyte, and the fragmentation pattern of the ions formed, at a given electron energy, are characteristic of the ionized molecules. This fragment pattern or mass spectra, obtained by electron ionization at 70 eV, is often unique for each compound, and can act like a fingerprint being used for characterization, identification and quantification of the analytes. Additionally, comparison of mass spectra with standard spectral libraries can also be used for analyte identification or confirmation.

A limitation of EI is that often the molecular ions, that give the molecular weight of the analytes, do not survive fragmentation and are not observed. One way to overcome this problem is to use a complementary technique that provides "soft" ionization of the molecules, allowing the detection of the molecular ions.

1.5.3.2. Chemical ionization

The most used “soft” ionization technique is chemical ionization (CI). In CI, the ion source is supplied by a reagent gas (e.g. methane, ammonia or isobutane) at a high pressure (0.1-100 Pa). The reagent gas molecules ionize, producing an excess of molecular ions (CH_5^+, NH_4^+, $C_4H_{11}^+$), that collide with the analyte molecules (M) which are ionized, by proton transfer. The CI ionization of the analytes occurs at much lower energy than the in EI ionization (usually less than 5 eV), resulting in $[M + H]^+$ ions with little or no fragmentation (McMaster and McMaster, 1998; Herbert and Johnstone, 2003). The mass spectra obtained by CI are much simpler than EI, but misses most of the interpretable structural information. However, the molecular ion appears as a fragment with a high intensity, being sometimes the major fragment of the spectra, and thus allowing the molecular weight determination of an analyte possible.

1.5.3.3. Field ionization/field desorption

Other “soft” ionization techniques are field ionization (FI) and field desorption (FD), that produce abundant molecular ions with minimal fragmentation (Herbert and Johnstone, 2003). These methods are based on electron tunneling from an emitter that is set at a high electrical potential (Herbert and Johnstone, 2003). Molecules can lose an electron, when placed in a

very high electric field that is created in an ion source, by applying a high voltage between a cathode and an anode, called a field emitter. The field emitter consists of a filament covered with microscopic carbon microneedles, which greatly amplify the effective field at the carbon points. The high voltage applied to that emitter promotes polarization and, finally, ionization of the molecules that come close to the tips of the microneedles, where the electric field is higher. The main difference between field ionization (FI) and field desorption ionization (FD) lies in the manner in which the sample is handled for analysis.

For FI, the sample under investigation is heated in vacuum and guided along the emitter electrode (Niessen, 2001; Herbert and Johnstone, 2003). The high local electric fields at the microneedles enable electron tunneling from the sample to the emitter and radical cations are generated with little fragmentation (Niessen, 2001), yielding mass spectra with essentially molecular ions (Hsu and Green, 2001). FI is applicable to volatile and thermally stable samples (Niessen, 2001; Dass, 2007). The samples are introduced into the ion source, using the same techniques that are common in EI-MS and CI-MS, such as by direct probe or by means of a GC effluent that passes over the emitter (Niessen, 2001; Herbert and Johnstone, 2003). The development of GC coupled with time of flight spectrometers, that allow simultaneous sampling of all masses within the spectra, provides the capability of using the FI technique for the analysis of complex mixtures (Hsu and Green, 2001).

In FD, the sample to be examined is directly placed onto the emitter, before ionization (Dass, 2007). The emitter is set to a high potential and a current is passed through the emitter, to heat up the filament. The microneedles activate the surface, which functions as the anode. The very high voltage gradients at the tips of the needles promote the electron removal from the sample analytes, being the resulting cations repelled away from the emitter. The mass spectra are acquired as the emitter current is gradually increased, and the sample is evaporated from the emitter into the gas phase. The ions generated have little excess energy so there is minimal fragmentation, and the molecular ions of the sample components are usually the only significant ions seen on the mass spectra.

1.5.3.4. Mass analysers

Mass spectrometers are usually classified by their mass analyzer, the most commonly used being the magnetic sector, quadruple filters, ion traps and time of flight instruments (TOF). In GC/MS applications the method used to obtain the spectral information on the time axis, can

be classified as scanning and array methods (Holland *et al*., 1983). The magnetic sector and quadrupole devices are scanning instruments, which produce mass spectra by sequentially measuring the intensity of individual m/z, on the range of selected masses.

The scanning mass analyzers have relatively slow acquisition rates. The maximum acquisition rate, with analytical sensitivity and resolution, for magnetic sector instruments is from 1 to 5 spectra.s^{-1} and for quadrupoles is from 5 to 10 spectra.s^{-1} (Holland and Gardner, 2002).

During the measurement of one scan, the concentration of the analyte in the ion source is not constant (Pool *et al*., 1996). Consequently, when using scanning instruments, the ion intensities across the m/z range are measured at different analyte concentrations, resulting in a spectral skewing effect where the qualitative mass spectra are different across the elution profile of the individual peaks (Figure 1.8) (Pool *et al*., 1996; Holland and Gardner, 2002; Smith, 2004). For a peak resulting from a single analyte, the average spectra over the entire peak represents the expected spectrum for that compound. However, when the chromatographic peak results from a co-elution, the ability to obtain the real spectra for each of the analytes may be compromised (Smith, 2004).

The ion trap uses a combination of scanning and array technologies, being less susceptible to the effects of peak skewing when compared with scanning instruments. The ion trap acquires the complete spectrum in sequential segments with each segment internally comprising an array, devoid of skewing (Holland and Gardner, 2002; Smith, 2004). The effective maximum spectral generation rate of the ion trap is from 10 to 15 spectra s^{-1}.

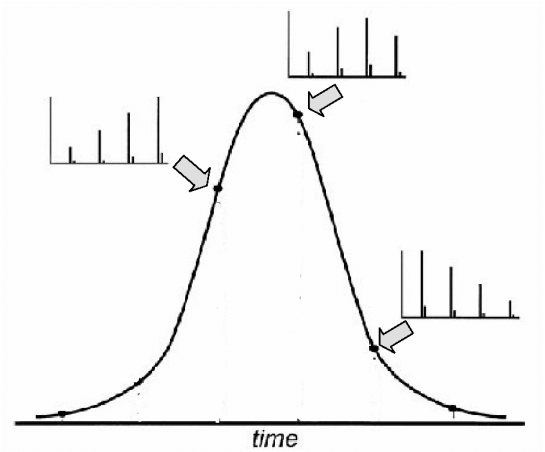

Figure 1.8 – Peak skewing due to the elution dynamics effects on mass spectra collected by scanning MS.

Array detectors, such as TOF, do not scan but rather measure all the ions across the m/z range, virtually at the same time, producing mass spectra without skewing, and allowing full range array detection (Holland and Gardner, 2002; Smith, 2004). This simultaneous acquisition, of complete spectra with a mass spectral m/z profile for the whole chromatographic peak constant, enables the application of spectral deconvolution (Smith, 2004), and potentially a more accurate use of reference libraries for identification and confirmation of analytes. Additionally, because no scanning action is involved, the time required to produce a mass spectrum in a TOF is greatly reduced. The maximum acquisition rate with adequate sensitivity for a TOF is from 50 to 200 spectra.s^{-1} (0.02 to 0.005 s.$spectra^{-1}$), but acquisition rates can be increased to 500 spectra.s^{-1}, when sensitivity is not an issue or resolution is a target (Vreuls *et al*., 1999; Holland and Gardner, 2002; LECO Corp., 2002) This fast acquisition speed makes the TOF instruments applicable as detectors, coupled to very fast or ultra fast GC separations, that produce peaks of base widths <0.3 s, allowing appropriate MS identification of complex mixtures.

1.5.4. Separation–chromatographic resolution /spectral resolution

Plant matrices originate complex samples, which are composed by volatile compounds (less than 100 m.u.), through semi-volatiles compounds (less than 300 m.u.), to more heavy compounds. These samples are essentially composed by terpenoid compounds, a group of chemical compounds with several isomeric structures, which originate mass spectra in electron ionization (E.I.) very similar or identical between some of them. These spectra are usually associated (from the chromatographic point of view) to complex peak clusters, located inside narrow ranges of retention times (Adams, 1995).

Presently GC/MS is the most frequently used hyphenate technique for the characterization and identification of volatile and semivolatile metabolites from plants. However, in spite of the continuous development of equipment, techniques and analytical methodologies, a total separation of all the sample components is still unachievable, due to the complexity of the sample and of the analysis (high number of components, structure similarities, isomers, and wide range of concentrations). High similarities are thus expectable between the retention times of several analytes, independently of the stationary phase used, that will result in co-elutions. These co-elutions are often impossible to detect and identify with some GC/MS instruments, in spite of the use of selective single ion monitoring mode (SIM), or of complex deconvolution processes. An additional problem results from the wide range of analyte

concentrations in their matrices. Consequently, the trace level analytes, that sometimes are the biological active components in the matrix under study, may never be detected, if they are co-eluting with high concentration compounds.

The development of new analytical techniques, that maximize analyte separation, has always been a target, that can be exemplified by the progression of packed column chromatography to capillary chromatography, following to multi dimensional chromatography and finally to comprehensive two-dimensional chromatography. Such advances aim at higher chromatographic capacity, in order to achieve the separation of all sample analytes (David and Sandra, 1987; Bertsch, 1999). For one dimension systems, this goal is physically and statistically limited due to the maximum number of theoretical plates of a column (Grushka, 1970; Chaves das Neves and Freitas, 1996; Bartle, 2002). Thus, the capacity of a capillary column with 50 m × 0.25 mm and d_f = 0.25 μm can be given by the following equation (Grushka, 1970):

$$n = \frac{\sqrt{N}}{4R} \cdot \ln\left(\frac{t_2}{t_1}\right) + 1 \qquad (1.5)$$

where:

n = peak capacity of a single column chromatographic system

N = number of theoretical plates of a single column

t_1 and t_2 = retention time window, t_1 and t_2 are retention times

R = resolution for the separation of two compounds with retention times t_1 and t_2.

This means that if we consider R = 1 and t_2/t_1 as 10, the considered column will be theoretically able to separate 260 analytes under ideal conditions (Grob Jr *et al.*, 1978; Grob *et al*., 1981; Bartle, 2002).

This limitation of the unidimensional chromatography (1D-GC) is even more evident when the statistical theory of overlap (STO) is applied (Davis and Giddings, 1983; Martin *et al*., 1986; Bertsch, 1999; Bartle, 2002). The capacity factor (n) from equation 1.5 represents the maximum number of analytes that the chromatographic column can theoretically separate. Statistically, this value decreases because the analytes are randomly and not discretely distributed through the chromatographic separation. Due to the potential high complexity of some of the samples, which easily reaches 100s of components that usually appear in a wide range of concentrations, the occurrence of co-elutions is inevitable.

The STO showed that in a chromatographic analysis the number of separated peaks (S) is related to the capacity factor of the column (n) and with the total number of analytes (m) in the sample (Davis and Giddings, 1983; Bertsch, 1999; Bartle, 2002) (equation 1.6).

$$S = m \exp\left(-\frac{2m}{n}\right) \tag{1.6}$$

where:

S = number of separated single peaks

n = peak capacity of a single column chromatographic system

m = number of sample components

The probability (P) of observing a peak consisting of one single component is estimated by equation 1.7:

$$P = \exp\left(-\frac{2m}{n}\right) \tag{1.7}$$

The application of equation 1.7 leads to the theoretical need of columns with capacity for 290 analytes, in order to guaranty the separation of half of the components in a 100 analytes sample (Bartle, 2002). This shows the limitation of 1D-GC, in spite of the high separation power, even under ideal separation conditions, without peak tailing or wide ranges of analyte concentration that are not considered by the STO (Bertsch, 1999).

Another issue is related to the number of possible isomeric configurations of sample components, that promote a high similarity between the mass spectra and the retention index for different analytes, which jeopardize their identifications. The existence of mass spectral similarity of terpenoid compounds, due to their structural similarity, together with retention times that do not differ significantly, or not at all on some column phases, demands the acquisition of pure mass spectra, making the identification task very difficult and sometimes even impossible.

Commercial spectral libraries are becoming increasingly more complete and specific, making GC/MS one of the most used techniques for routine identifications. However, several compounds are not yet described in library databases and, in spite of better algorithmic calculations, the databases are only reliable for target analysis, or when the compounds under study are known, characterized with a known mass spectra. Additionally, the full separation of peaks to assure clean mass spectra, in order to achieve a reliable peak analyte confirmation,

is still a necessary goal. Associating mass spectral data with compound retention indices for columns with different polarities represents an improved tool in compound identification by using GC/MS (Shibamoto, 1987; Vernin *et al*., 1987).

The time of flight MS (TOFMS), with its acquisition speed and capability of simultaneous acquisition of full spectra without spectral deformation, presently offers the possibility of using spectral resolution for the mass spectra collected, promoting effective spectral deconvolution, even in grossly co-eluting situations, which represents a true spectral resolution capability (Holland and Gardner, 2002).

The high complexity of the chromatograms points out to new ways of chromatography, such as multidimensional systems (MD-GC), where the analytes are submitted to two or more independent separation steps, in order to achieve separation. One example came from the "heart-cut" systems, using flow switching devices (Figures 1.9 and 1.10), that allowed the isolation of selected peaks, or ranges, of the chromatogram by partial transference of the selected fraction, from a pre-column to a second column of different selectivity (often chiral), where only the target analytes are submitted to chromatographic separation, avoiding the potential co-elution with the non transferred compounds (Schomburg *et al*., 1984; David and Sandra, 1987; Bertsch, 1999; Poole, 2003) (Figure 1.10).

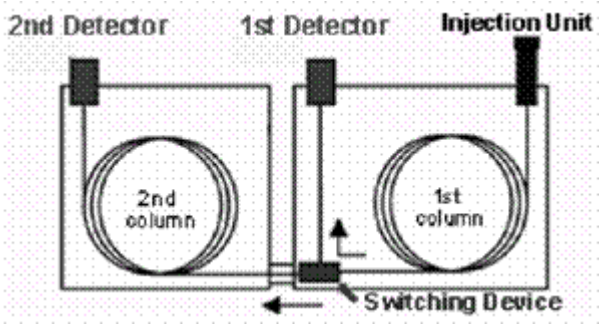

Figure 1.9 - Schematic representation of a multidimensional GC system with a heart-cut configuration, using a flow switching device.

In spite of its efficiency, the MD-GC is a time consuming technique, with long analysis times, which does not fit with the demands of routine analysis. Additionally, it is technically difficult to carry out sequential transfers in a narrow window of retentions times, since there is a likelihood of co-elutions (Poole, 2003).

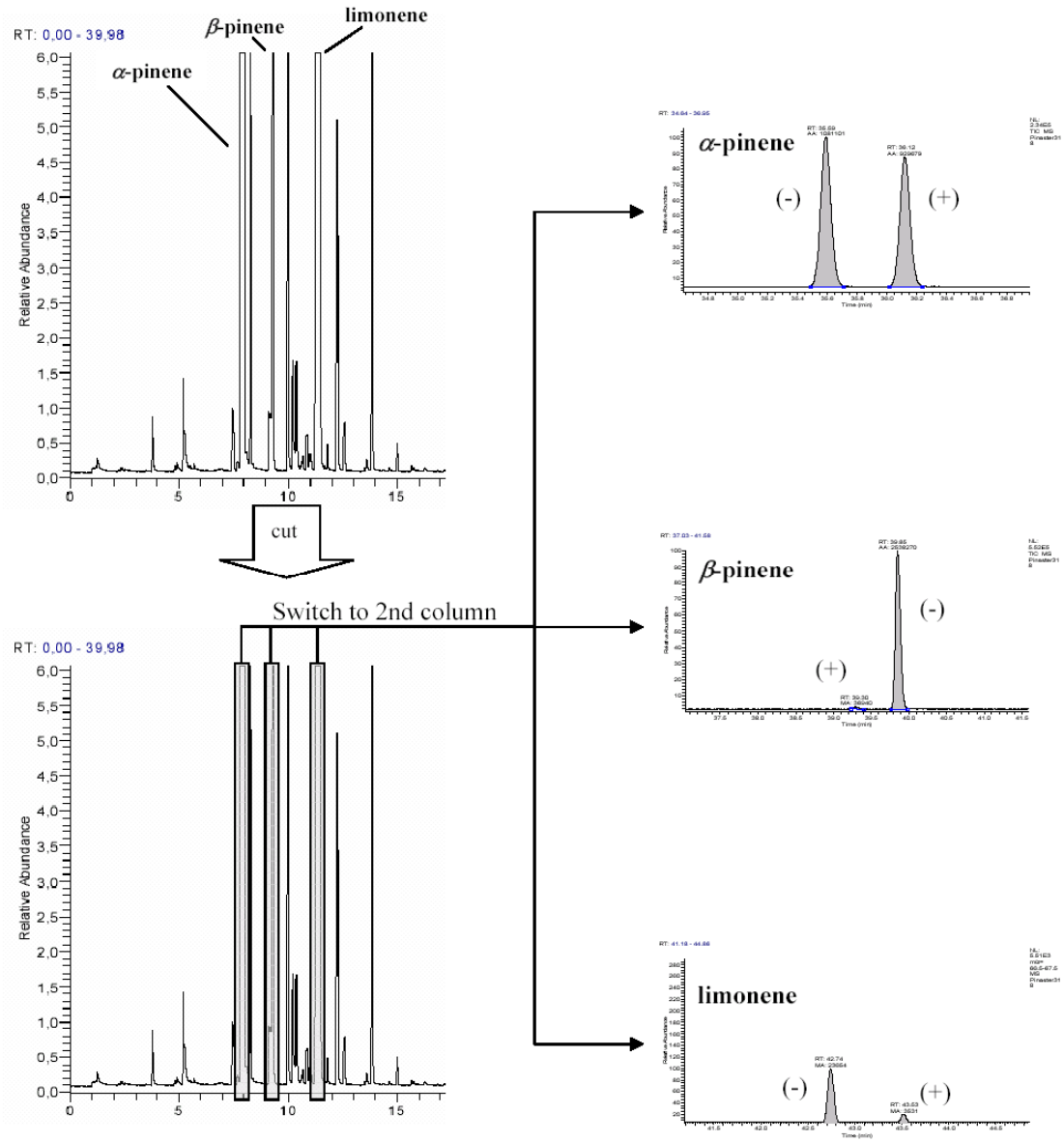

Figure 1.10 - Representation of multidimensional enantiomer-selective GC analysis of a *P. patula* sample, using a heart-cut system, where α-pinene, β-pinene and limonene, eluting on a non polar column were transferred to a chiral column for secondary analysis. The top chromatogram shows the primary separation, and the right three the resulting heart-cut chromatograms.

1.5.5. GC × GC

In 1991, comprehensive two-dimensional gas chromatography (GC × GC) was introduced by Liu and Phillips (1991). The GC × GC system consists of two columns with different selectivities, the first and second dimension columns that are serially connected through a suitable interface, which usually is a thermal modulator (Figure 1.11) (Phillips and Beens, 1999; Marriott and Shellie, 2002; Dimandja, 2003). At the GC × GC technique the entire sample separated on the first column is transferred to the second one, resulting in an enhanced chromatographic resolution into two independent dimensions, where the analytes are

separated by two independent mechanisms (orthogonal separation) (Schoenmakers *et al*., 2003).

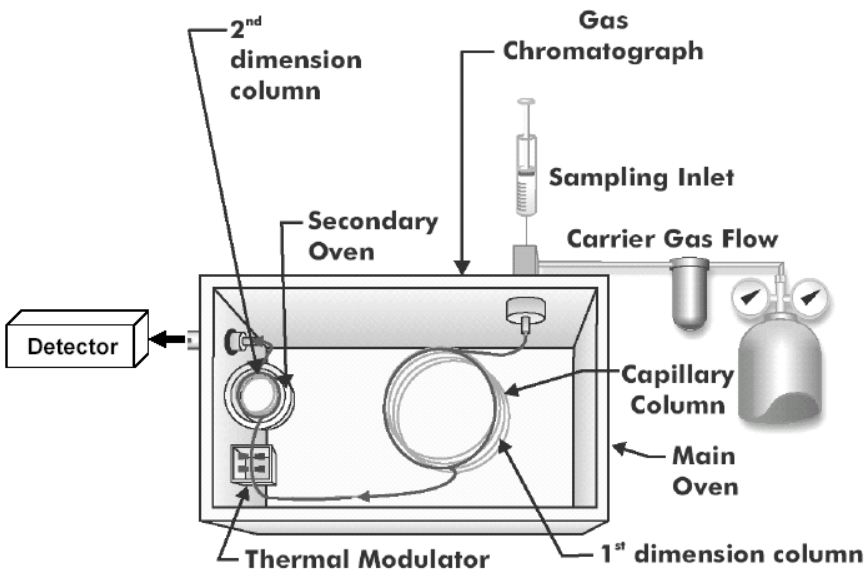

Figure 1.11 – Schematic representation of a GC × GC system (adapted from LECO Corp., 2008).

A chromatographic method is considered comprehensive if **i)** the sample transfer from the first to the second column is qualitatively and quantitatively complete; **ii)** the orthogonality principle is respected, meaning that both separation mechanisms are independent; **iii)** the separation on the first column is preserved on the second one (Bertsch, 2000; Dallüge *et al*., 2003; Schoenmakers *et al*., 2003).

Operationally, the most important component in the GC × GC system is the interface. The common interface comprises a thermal modulator, which either performs heating (to accelerate solute into a narrow band in the second column) or cooling (to retard analyte and cause on-column trapping or cryofocusing of the bands) or both, depending on the design.

The modulator cuts the effluent from the first column into small portions, which are refocused and sampled onto the second column, in the form of narrow pulses. The modulation is thus the sequential liberation of the solute from the first column onto the second column, preserving and further fractionating the separation obtained on the first column. Additionally, since the modulated zones of a peak analyte are thermally focused before the separation on the second column, in a mass conservative process, the resulting segments (peaks) of the modulation are now more intense, with higher S/N ratios, and much narrower, than in

conventional GC (Lee *et al*., 2001; Dallüge et al., 2002b), improving the detection of trace analytes and the chromatographic resolution (Figure 1.12).

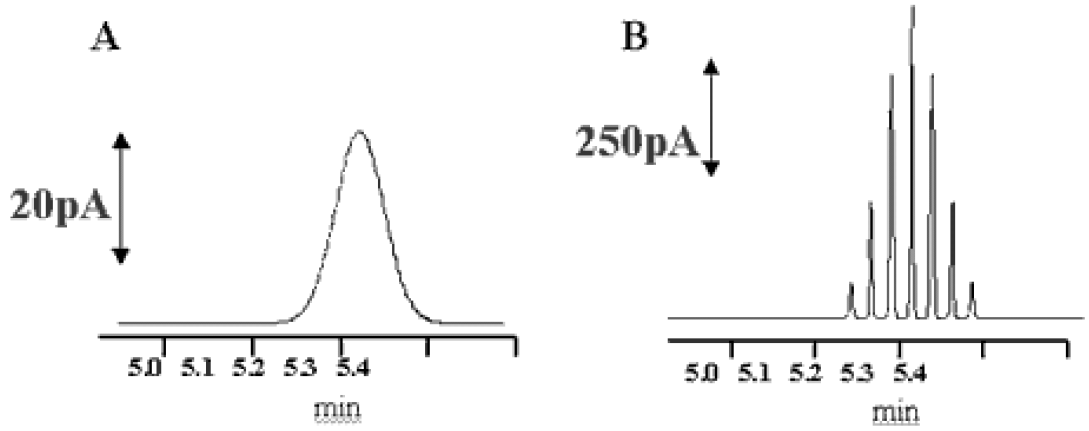

Figure 1.12 - Chromatograms of conventional 1D-GC peak (**A**), and from the same peak modulated on GC × GC (**B**), showing the peak signal increment (adapted from www.rmit.edu.au/browse; ID=ktg59442x0e6z, accessed on 04-10-08).

In theory, the total peak capacity n in GC × GC is the product of the peak capacities of the two individual columns n_1 (column 1) and n_2 (column 2), which results in separation potential $n_t = n_1 \times n_2$, that is much higher than in any other chromatographic arrangements (Figure 1.13) (Venkatramani *et al*., 1996; Bertsch, 2000).

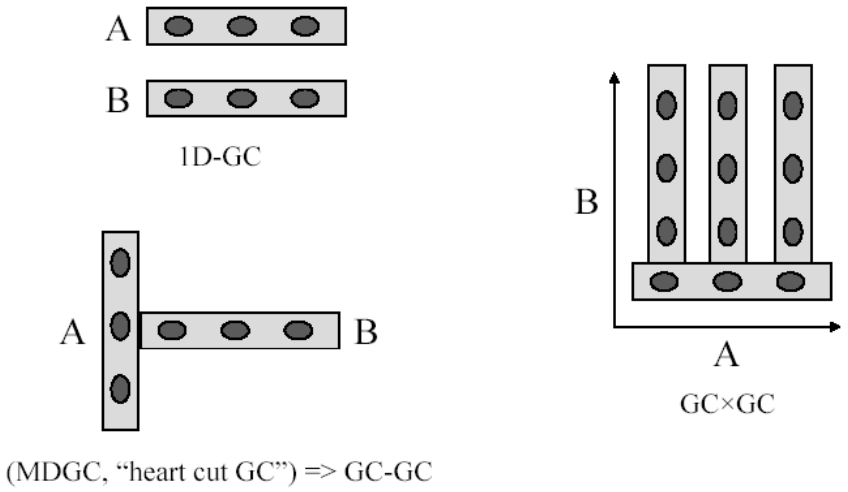

Figure 1.13 - Schematic representation of peak capacity for two individual columns A (column 1) and B (column 2) in 1D-GC and coupled for multidimensional GC using heart cut and GC × GC configurations.

In order to maximize the column peak capacities and the separation power of the GC × GC system, the separation mechanisms in both columns should be based on different and

independent physical-chemical interactions (orthogonality) (Venkatramani *et al*., 1996; Phillips and Beens, 1999; Marriott and Shellie, 2002; Dallüge *et al*., 2003; Dimandja, 2003; Schoenmakers *et al.,* 2003), meaning that stationary phases with different selectivity should be chosen for both columns. The first dimension columns have usually non-polar stationary phases and promote separation mainly due to the volatility of sample components (boiling-point separation) (Phillips and Beens, 1999; Marriott and Shellie, 2002; Dallüge *et al*., 2003). Other alternative for first dimensional columns are chiral capillary columns, coated with cyclodextrin derivatives, which additionally separate sample components according to their absolute configuration (Shellie *et al*., 2001; Shellie and Marriott, 2002). The first column is usually of standard dimensions (e.g. 30 m × 0.25 mm; d_f = 0.25 μm) and the time scale of the first dimension separation corresponds to a normal GC separation, resulting in peak widths of several seconds. The second column stationary phase is usually polar, or mid polar (Beens *et al*., 2000; de Geus *et al*., 2001; Dallüge *et al*., 2002a). Fast GC can be performed in the second dimension column, if a short narrow bore column (e.g. 1 m × 0.1 mm × 0.1 μm) is used. This configuration allows that the total time of the chromatographic run on the second column never exceeds more than a few seconds. This means that the second-column separation is performed essentially under isothermal conditions (Beens *et al*., 1998) and, therefore, analyte separation is based only on their polarity (Figure 1.14). Another consequence is that the actual total run time of both 1D-GC and GC × GC analysis, for the same sample, will be approximately the same (Marriott, and Shellie, 2002; Dallüge *et al*., 2003).

The very fast separation in the second column results in very narrow peaks with widths between 0,1 and 0,6 s (Beens *et al*., 1998; Lee *et al*., 2000; Marriott *et al*., 2000), that require high data acquisition rate detectors (50 – 100 Hz) to obtain sufficient number of data points over a chromatographic peak for its accurate description (Zrostlíková *et al*, 2003). The use of detectors, such as FID (Frysinger *et al*., 1999.), electron capture detector (ECD) (de Geus *et al*., 2000; Korytár *et al*., 2002) and nitrogen phosphorous detector (NPD) (Khummueng *et al*., 2006; Ochiai *et al*., 2007; Mateus *et al*., 2008), and mass spectrometer detectors with quadrupoles (qMS) (Song *et al*., 2004; Adahchour *et al*., 2005; Mateus *et al*., 2008) and TOF mass analysers (Dallüge *et al*., 2002c; Ma *et al.*, 2007; Mateus *et al*., 2008), on GC × GC applications, have been described in the literature. However, the fast acquisition TOF spectrometers are the detectors for this technique by excellence and have considerably enlarged the application potential of GC × GC.

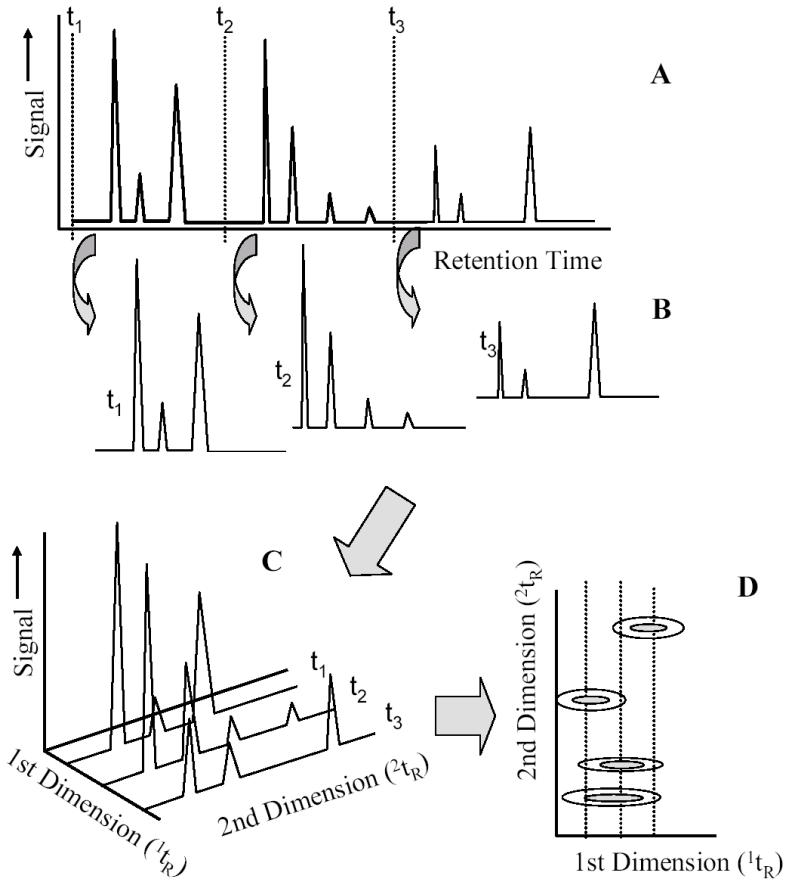

Figure 1.14 - Schematic representation of the process of a GC × GC chromatogram generation: **A)** raw linear chromatogram showing the elution profile in the first column/dimension. t_1, t_2 and t_3 point the times when re-injections on the second column occurred via the modulator; **B)** raw data are segmented into individual second-dimension chromatograms (slices); **C)** the individual second dimension chromatographic "slices" are aligned in a 3-D matrix, by the data treatment software, resulting in a second separation; **D)** the software processes the data matrix in the final GC × GC chromatogram which can be visualized as a two-dimensional contour plot.

After data acquisition, suitable software is used to generate a reconstructed two dimensional chromatogram, or a 3D plot; which is the representation of the linear modulated chromatograms projected on the second dimension for each modulation (Figure 1.14). The independent second dimension chromatograms are aligned in a bidimensional plane, the GC × GC data contour plots representing the "bird-eye view" of the chromatogram, where the X axis represents the separation on the first column, the Y axis the separation achieved on the second column and, for the 3D plots, and the Z axis the intensity of detector response (Marriott and Shellie, 2002; Dallüge *et al.*, 2003; Dimandja, 2003).

Due to the orthogonal separation occurring in both columns, the chromatograms resulting from GC × GC are ordered, producing structured chromatograms, where the analytes have their spatial location, in the contour plot, based on their structures (Phillips and Beens, 1999).

In the reconstructed 2D contour plots, characteristic patterns are obtained, in which the members of homological series with different volatilities are ordered along the first dimension axis, and the compounds are spread along the second dimension axis according to their polarity. This cluster representation of various subgroups of analytes in the GC × GC contour plots may be used as a tool for analyte class analysis and tentative identification of compounds (Frysinger and Gaines, 1999; Korytár *et al*., 2002).

2. Material and methods

2.1. Experimental plots

This study was conducted in two plots, located in two different regions of Portugal: 1) Abrantes, in central Portugal, and 2) Apostiça, on the costal area South from Lisbon (Figure 2.1). The plots are characterized on Table 2.1.

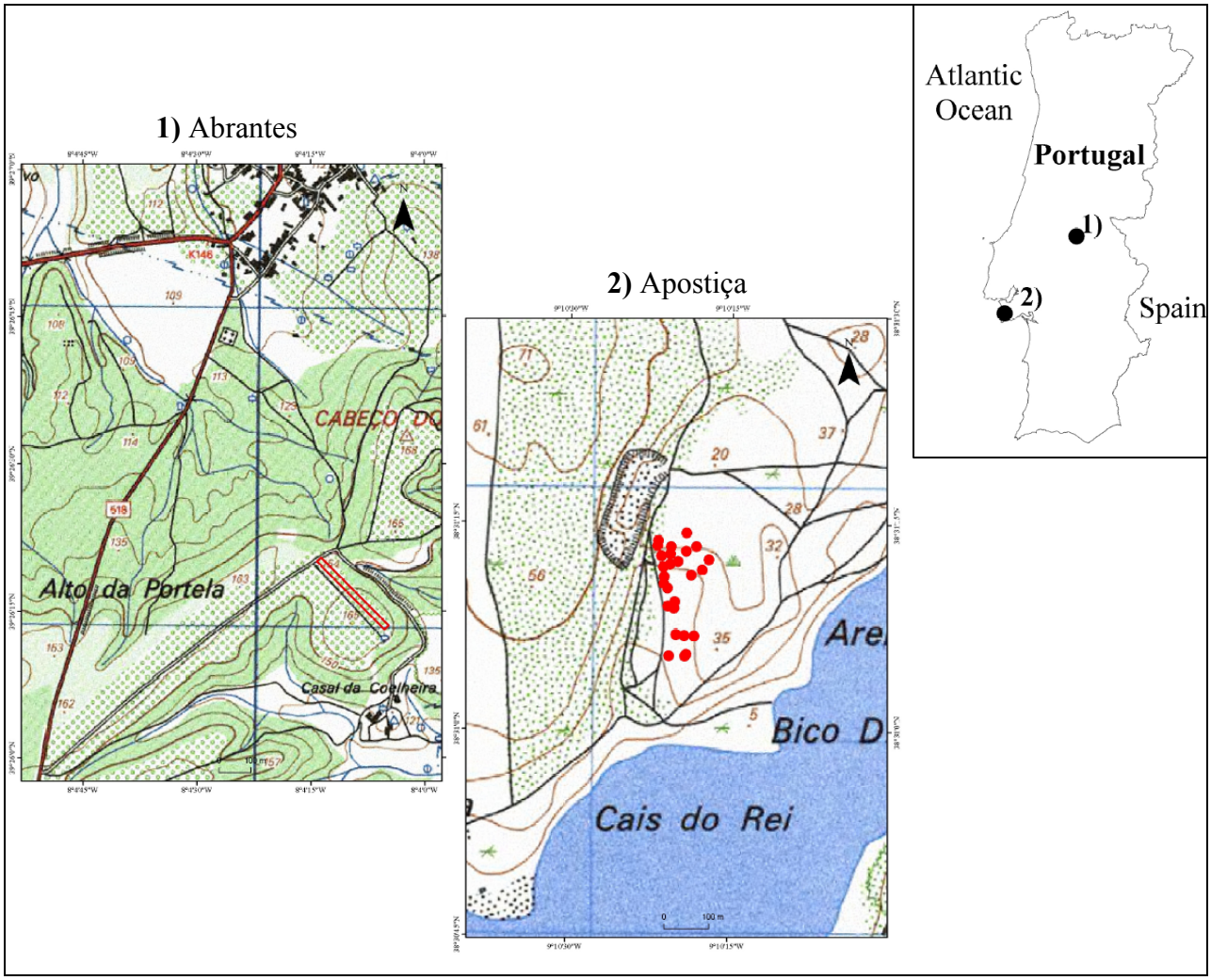

Figure 2.1 - Location of the two experimental plots.

Table 2.1 - Characterization of the experimental plots.

Parameter	Abrantes	Apostiça
Climate (data from the nearest meteorological station)	Santarém/Esc. Agrícola[a] (N 39˚15'; W 08˚42'; ca. 54 m a.s.l.)	Lisboa/Geofísico[a] (N 38˚43'; W 09˚09'; ca. 77 m a.s.l.)
Thornthwaite´s second climatic classification (for a 100 mm moisture holding capacity)	C_1 B_2' S_2 a´ Climate dry subhumid, megathermal, with a summer great water deficit and with a summer small thermal efficacy	C_2 B_2' S_2 a´ Climate rainy subhumid, megathermal, with a summer great water deficit and with a summer small thermal efficacy
Mean annual Temperature, ºC	15.9[a]	16.8[a]
Rainfall, mm	714.8[a]	750.7[a]
Parent material	Sedimentary formations: e.g. sands[b]	Sedimentary formations: e.g. sands[b]
Soil type	Orthic Podzols, associated with eutric Cambisols[c]	Eutric Regosols[c]
Pine species present	11 species, all originated from the same stand, planted in 1991	One species *P. pinaster*

References: [a]Instituto de Meteorologia (period: 1961-1990); [b]Soares da Silva, 1982; [c]Cardoso *et al*., 1973; FAO-Unesco-ISRIC, 1990.

In Abrantes, an experimental arboretum had been planted in 1991, consisting of eleven pine species, three of which endemic, *P. pinaster*, *P. pinea* and *P. halepensis*, and eight exotic: *P. brutia, P. patula, P. elliottii, P. nigra, P. radiata, P. taeda, P. kesiya* and *P. sylvestris*. The trees had been planted according to the experimental design shown in Figure 2.2. In each small plot, eight trees of the same species were planted. The same design was repeated twice (R-1 to R-3). Since all the pine species studied were originated from the same stand, planted in 1991, the influence of extrinsic factors, e.g. geographical, seasonal, and soil composition, among others, on the qualitative monoterpene composition was therefore minimized.

In Apostiça, *P. pinaster* was the only species present, representing a situation of low genetic variation. Table 2.2 shows the *Pinus* species present in each experimental plot, presenting a photograph of each one needles.

It must be referred that for resin acid analysis *Pinus spp.* samples (Table 2.2) were also sampled from other areas, although no other characteristics were studied.

The diterpene resin acid contents have been studied in two experiments.

Table 2.2 - *Pinus* species present in the experimental plots.

Pinus species		Abrantes	Apostiça	Other
P. pinaster		X	X	X
P. pinea		X		X
P. halepensis		X		X
P. brutia		X		X
P. patula		X		
P. elliottii		X		
P. nigra		X		
P. radiata		X		
P. taeda		X		
P. kesiya		X		
P. sylvestris		X		

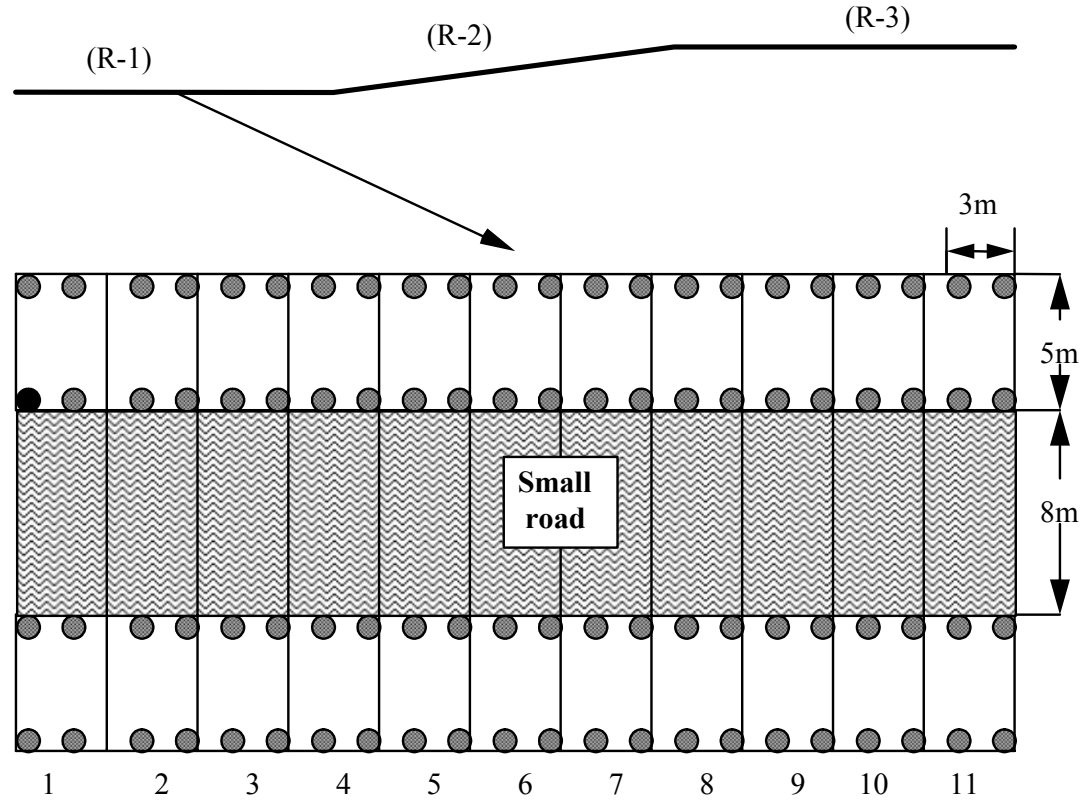

1- *Pinus pinea*	2 - *P. kesiya*	3- *P. patula*	4- *P. taeda*
5- *P. elliottii*	6- *P. sylvestris*	7- *P. radiata*	8- *P. pinaster*
9- *P. brutia*	10- *P. halepensis*	11- *P. nigra*	

Figure 2.2 – Schematic representation of Abrantes arboretum, which was used as experimental plot.

In a first experiment, the composition in diterpene resin acids of the needles of four pine species, which had been used to study the larval performance of *T. pityocampa*, was studied. *P. pinaster* and *P. pinea*, which occur naturally in the Iberian Peninsula, and two Eastern Mediterranean species, *P. halepensis* and *P. brutia.* All trees had similar vigour and age (10-15 years), except the *P. halepensis*, which was over 20 years old. All the needles were washed in a 0.53% bleach solution and with clean water afterwards, before being given to the larvae. Sub-samples of the same needles were used for chemical analysis.

In the second experiment, the composition in diterpene resin acids were studied for a set of samples comprised of *P. pinaster*, *P. pinea*, *P. brutia*, *P. kesiya*, *P. sylvestris*, *P. nigra*, *P. patula*, *P. radiata*, *P. elliottii*, *P. taeda* and 22 samples of *P. halepensis*. The *P. halepensis* needles were sampled in:

- Portugal - Trafaria and Instituto Superior de Agronomia;
- Israel - Eastern Galilee (EG), Mount Camel (MC) and Judean Hills (JH);
- Greece - unknown location.

For the *P. halepensis* originated from Israel and Greece, one year old needles (V) and current year needles (N) were sampled. The *P. pinea* needles were sampled at the Campus Caparica (UNL-FCT). The *P. pinaster* needles were sampled at Charneca da Caparica. *P. brutia* needles were sampled at Instituto Superior de Agronomia. All the others *Pinus spp.* needles were sampled at the experimental arboretum of Abrantes and kept stored at - 80 ºC in a ULT freezer, Snijders Scientific (Tilburg, Holland) until analysis

2.2. Operation mode

2.2.1. Needle sampling

After collection of the needles, the samples were stored and transported to the laboratory, under refrigeration, in hermetically sealed plastic bags. In the laboratory all samples were stored at 4 ºC until extraction. All samples were extracted within 48 h of collection.

Table 2.3 summarizes the analysis carried out for each experimental plot, followed by the description of each extraction method and of the analytical techniques used.

Table 2.3 – Analysis carried out for the pine needles from each one of the experimental plots.

Experimental plot	Target compound	Extraction method	Analytical technique	Column used
Abrantes	Volatiles	SPME SDE	GC-FID GC/MS	DB-5 DB-Wax Chiral
			GC × GC	2 column sets
Apostiça	Volatiles	SDE SPME	GC-FID (GC/MS)	DB-5 Chiral
Lisboa	Resin acids	Solvent extraction + derivatization	GC-FID FI-MS FD-MS	ZB-5 ms DB-5 ms
			GC × GC	column set

2.2.2. Standards and reagents

Monoterpene standards were purchased from Aldrich (Deisenhofen, Germany), Fluka (Neu-Ulm, Germany), Extrasynthese (Lyon, France) and Tokyo Kasei (Tokyo, Japan). All solvent used were chromatographic grade.

2.3. Extraction methods

2.3.1. Volatiles

2.3.1.1. Solid phase microextraction

Before extraction, needles from each pine species were mixed into a composite sample. Subsamples were cut, the pieces mixed, and 0.2 to 0.7 g placed inside a 7.0 mL vial (Supelco, Bellefont). The vial was closed with a hole cap sealed with a PTFE/neoprene septa. The headspace inside the vial was sampled by solid-phase microextraction (SPME) using a 100 μm polydimethylsiloxane (PDMS) coated fiber. The headspace extraction was performed at room temperature for 45 min and the trapped compounds desorbed at 250 °C in the chromatograph injection port, for 60 s. Before the analysis, the fiber was conditioned according to the manufacturer standard procedures.

2.3.1.2. Simultaneous distillation extraction (SDE)

100 g of needles from each pine species were mixed into a composite sample. Uncut needles from each pine species (10 - 20 g) were placed in a round-bottomed flask (0.5 L) with twice-distilled water (Milli-Q RG, Millipore, Molsheim, France; 350 mL). The flask was connected to a Veith and Kiwus exhaustive steam- distillation and solvent-extraction apparatus and extraction was performed for 2 h with 10 mL of pentane-ether 2:1 (v/v) (Merck, Darmstadt, Germany).

The final extract was dried with anhydrous sodium sulfate (Merck, Darmstad, Germany) and concentrated to a final volume of 1.0 mL under a gentle stream of nitrogen (Air Liquide, Lisbon, Portugal). The final extract was stored at -20 ºC until used for gas chromatographic analysis.

2.3.2. Resin acids

2.3.2.1. Extraction procedure

2.0 g of pine needles were collected from each pine species and freeze dried for 48 hours. First experiment needles were dried on a TELABE-JDF (Lisbon, Portugal) freeze drier and the second experiment needles on a freeze dryer Modulyo from Edwards (London, England). The dried needles were minced on an A-10 analytical grinding mill (IKA, Staufen, Germany) and ground to powder using a mortar and pestle.

100 mg of dried and ground needle samples were extracted twice with 10 mL of diethyl ether on an ultrasonic bath (Sonorex-KH 1024, Bandelin Electric, Germany) for 10 min. After extraction the solutions were filtered through 0.2 μm Chromafil PTFE syringe filters (Macherey – Nagel, Duren, Germany). The filtered extract was evaporated to dryness under a gentle stream of nitrogen. The final residue was redissolved to 1.0 mL with a solution of methyl *tert*-butyl ether /methanol (90:10).

2.3.2.2. Derivatization procedure

For methylation of free resin acids, diazomethane, prepared according to Vogel (1989), was used as methylation reagent.

0.5 mL of the final extract was placed inside a 1.0 mL graduated cone shaped micro reaction vessel (Supelco, Bellefonte, USA). Diazomethane was slowly added to the extract solution and the reaction proceeded at room temperature for 5 min, on a fume hood, without capping the reaction tubes. The excess diazomethane was removed by concentrating the sample to 0.2 mL under gentle stream of nitrogen, which thereafter was redissolved to 0.5 mL, using methyl *tert*-butyl ether and analysed directly by gas chromatography/mass spectrometry.

2.4. Instrumentation

2.4.1. Volatile analysis

2.4.1.1. GC - FID

The semi-quantitative analysis of the volatile compounds was performed by gas chromatography, using a HP 5890A gas chromatograph (Hewlett Packard, USA) equipped

with flame ionization detection (GC-FID). The separation was achieved on a DB-5 capillary column with 30 m × 0.32 mm I.D. and 1.0 μm thickness (J &W Scientific, Folsom, USA). The operational conditions are depicted in Table 2.4.

Table 2.4 - Operational conditions used for GC-FID.

Oven temperature program	Initial Temperature (ºC):	50
	Initial Time (min):	1.00
	Rate #1 (deg.min^{-1}):	4.0
	Final Temperature #1 (ºC):	125
	Hold Time #1 (min):	0.00
	Rate #2 (deg.min^{-1}):	6.0
	Final Temperature #2 (ºC):	250
	Hold Time #2 (min):	5.00
	Rate #3 (deg.min^{-1}):	10.0
	Final Temperature #3 (ºC):	295
	Hold Time #3 (min):	0.00
GC carrier gas	1.7 mL H_2 min^{-1} (constant pressure mode)	
Injection mode	split (1:20)	
Injection port temperature	260 ºC	
Sample volume	SPME	
Detector temperature	300 ºC	

Chromatographic data was collected using a Merck-Hitach D-2500 Chromato-integrator.

2.4.1.2. GC/MS

The analysis of pine needles volatiles was performed on three gas chromatograph/mass spectrometer systems.

The first system consisted of a Trace GC 2000 Series gas chromatograph (ThermoQuest, Rodano, Italy) coupled to a Finnigan Trace MS quadrupole mass spectrometer (ThermoQuest, Manchester, UK) Electron Impact (EI). The separation and analysis of the pine needle volatiles were performed on three different columns:

Column 1: a DB-5 (5 % phenyl-95% methyl-polysiloxane) column with 30 m × 0.32 mm i.d. and 1.00 μm film thickness (J&W Scientific, Folsom, USA).

Column 2: a DB-Wax (Polyethylene glycol – PEG) column with 60 m × 0.25 mm i.d. and 1.0 μm film thickness (J&W Scientific, Folsom, USA).

Column 3: a tailor made fused silica capillary column with 30 m × 0.25 mm I.D., coated with 0.25 μm film of 15% heptakis (2,3-di-O-methyl-6-O-terc-butyldimethylsilyl)-*β*-cyclodextrin in SE52 (DiMe). This column was used for separation of enantiomeric monoterpenes.

The operational conditions are depicted in Tables 2.5-2.7. Total ion chromatograms (TIC) were processed using the automated data processing software Xcalibur from Thermo Finnigan (ThermoFinnigan, Austin, TX, USA).

Table 2.5 - Operational conditions used for GC/MS for DB-5.

Oven temperature program	Initial Temperature (ºC):	50
	Initial Time (min):	2.00
	Rate #1 (deg.min^{-1}):	4.0
	Final Temperature #1 (ºC):	125
	Hold Time #1 (min):	0.00
	Rate #2 (deg.min^{-1}):	6.0
	Final Temperature #2 (ºC):	200
	Hold Time #2 (min):	10.00
	Rate #3 (deg.min^{-1}):	10.0
	Final Temperature #3 (ºC):	250
	Hold Time #3 (min):	1.00
GC carrier gas	1.5 mL He min^{-1} (constant flow mode)	
Injection mode	splitless (0.5 min)	
Injection port temperature	250 ºC	
Sample volume	SPME	
Ionization	Electron impact (EI+) at 70 eV	
Scan mode	Full Scan	
Scan range (amu)	40-300	
Source temperature	250 ºC	
GC interface temperature	250 ºC	

Table 2.6 - Operational conditions used for GC/MS for DB-Wax.

Oven temperature program	Initial Temperature (ºC):	50
	Initial Time (min):	2.00
	Rate #1 (deg.min^{-1}):	4.0
	Final Temperature #1 (ºC):	125
	Hold Time #1 (min):	0.00
	Rate #2 (deg.min^{-1}):	6.0
	Final Temperature #2 (ºC):	200
	Hold Time #2 (min):	10.00
	Rate #3 (deg.min^{-1}):	10.0
	Final Temperature #3 (ºC):	220
	Hold Time #3 (min):	1.00
GC carrier gas	1.5 mL He min^{-1} (constant flow mode)	
Injection mode	splitless (0.5 min)	
Injection port temperature	250 ºC	
Sample volume	SPME	
Ionization	Electron impact (EI+) at 70 eV	
Scan mode	Full Scan	
Scan range (amu)	40-300	
Source temperature	220 ºC	
GC interface temperature	250 ºC	

Table 2.7 - Operational conditions used for GC/MS for enantiomeric analysis.

Oven temperature program	Initial Temperature (ºC):	40
	Initial Time (min):	2.00
	Rate #1 (deg.min^{-1}):	15.0
	Final Temperature #1 (ºC):	70
	Hold Time #1 (min):	25.00
	Rate #2 (deg.min^{-1}):	4.0
	Final Temperature #2 (ºC):	100
	Hold Time #2 (min):	1.00
	Rate #3 (deg.min^{-1}):	10.0
	Final Temperature #1 (ºC):	200
	Hold Time #1 (min):	10.00
GC carrier gas	1.0 mL He min^{-1} (constant flow mode)	
Injection mode	splitless (1.0 min)	
Injection port temperature	250 ºC	
Sample volume	SPME	
Ionization	Electron impact (EI+) at 70 eV	
Scan mode	Full Scan	
Scan range (amu)	40-272	
Source temperature	250 ºC	
GC interface temperature	250 ºC	

The second system consists of a gas chromatograph GC System 6890N Series (Agilent Technologies, Palo Alto, CA, USA) coupled to a GCT high-resolution orthogonal time-of-flight mass spectrometer (Micromass, Manchester, UK). The separation was achieved on a ZB-5ms (5% phenyl-95% methyl-polysiloxane) column with 30 m × 0.25 mm i.d. and 0.25 μm film thickness (Phenomenex, Torrance, USA). The operational conditions are depicted in Table 2.8.

Table 2.8 - Operational conditions used for GC/TOFMS, with ZB-5ms.

Oven temperature program	Initial Temperature (ºC): 80 Initial Time (min): 0.00 Rate #1 (deg.min^{-1}): 5.0 Final Temperature #1 (ºC): 295 Hold Time #1 (min): 17.00
GC carrier gas	1.0 mL He min^{-1} (constant flow mode)
Injection mode	splitless (0.5 min)
Injection port temperature	260 ºC
Sample volume	1.0 μL
Ionization	Electron impact (EI+) at 70 eV
Scan mode	Full Scan
Scan range (amu)	40-450
Source temperature	260 ºC
GC interface temperature	290 ºC

Chloropentafluorobenzene (C_6ClF_5) was used as a reference compound and as the lock mass compound (using the 201.9609 Da ion) for mass calibration. Total ion chromatograms (TIC) were processed using the automated data processing software MassLynx from Waters-Micromass (Micromass, Manchester, UK).

The third system consisted of a gas chromatograph GC System 6890N Series (Agilent Technologies, Palo Alto, CA, USA) coupled to Pegasus III time-of-flight mass spectrometer (LECO, St. Joseph, MI, USA). The separation was achieved on two different columns:

Column 1: a DB-5ms (5% phenyl-95% methyl-polysiloxane) column with 15 m × 0.25 mm i.d. and 0.25 μm film thickness (J&W Scientific, Folsom, USA).

Column 2: an Equity-5 (5% phenyl polysilphenylenesiloxane) column with 60 m × 0.25 mm i.d. and 1.0 μm film thickness (Supelco, Bellefonte, USA).

The operational conditions are depicted in Table 2.9.

Total ion chromatograms (TIC) were processed using the automated data processing software ChromaToFTM from LECO Corp (St. Joseph, MI, USA).

Table 2.9 - Operational conditions used for Pegasus III GC/TOFMS.

Column 1 - Oven temperature program	Initial Temperature (ºC):	30
	Initial Time (min):	2.00
	Rate #1 (deg.min^{-1}):	4.0
	Final Temperature #1 (ºC):	250
	Hold Time #1 (min):	10.00
Column 2 - Oven temperature program	Initial Temperature (ºC):	40
	Initial Time (min):	1.00
	Rate #1 (deg.min^{-1}):	4.0
	Final Temperature #1 (ºC):	250
	Hold Time #1 (min):	10.00
GC carrier gas	1.0 mL He min^{-1} (constant flow mode)	
Injection mode (column 1)	split (1:50)	
Injection mode (column 2)	split (1:25)	
Injection port temperature	250 ºC	
Sample volume (column 1)	1.0 μL	
Sample volume (column 2)	SPME	
Ionization	Electron impact (EI+) at 70 eV	
Scan mode	Full Scan	
Scan range (amu)	35-350	
Source temperature	220 ºC	
Transfer line temperature	260 ºC	
Acquisition rate	7 Hz	
Detector voltage	-1750	
S/N for peak finding	5	

2.4.1.3. Enantioselective MDGC/MS

The enantioselective multidimensional gas chromatography/mass spectrometry (MDGC/MS) analysis of pine needle volatiles was performed on a Siemens SiChromat 2.8 double-oven gas chromatograph (Siemens, Karlsruhe, Germany), with independent temperature controls and equipped with a GCQ ion-trap detector (ITD) (Finnigan Mat, San Jose, USA) and a flame

ionization detector (FID). The first oven held the pre-column and the second oven held the main column.

Pre-column: a SE-52 (5 % phenyl-95% methylpolysiloxane) column with 30 m × 0.25 mm i.d. and 0.25 μm film thickness (self-prepared fused silica column).

Main column: a BGB 176 (25% 2,3-di- methyl-6-*tert*-butyldimethylsilyl-*β*-cyclo- dextrin in SE 54) column with 30 m × 0.25 mm i.d. and 0.25 μm film thickness (BGB Analytic Vertrieb, Schloßböckelheim, Germany).

The pre- and main columns were connected with a "live switching" coupling piece (live T-piece). The ITD was connected to the main column by a transfer line with an open split interface. The pre-column was connected to the flame-ionization detector. The carrier gas velocity was adjusted to give a hold up time of 60 s for methane at 100 ºC. The operational conditions are depicted in Table 2.10.

Table 2.10 - Operational conditions used for enantiomeric MDGC/MS analysis.

Pre-column: Oven temperature program	Initial Temperature (ºC):	60
	Initial Time (min):	0.00
	Rate #1 (deg.min^{-1}):	5.0
	Final Temperature #1 (ºC):	250
	Hold Time #1 (min):	0.00
Main column: Oven temperature program	Initial Temperature (ºC):	45
	Initial Time (min):	5.00
	Rate #1 (deg.min^{-1}):	5.0
	Final Temperature #1 (ºC):	220
	Hold Time #1 (min):	0.00
GC carrier gas	He (constant pressure mode) Pre-column – 2.20 bar Main column – 1.37 bar	
Injection mode	Split (1:25)	
Injection port temperature	250 ºC	
Sample volume	1.0 μL	
FID temperature	250 ºC	
ITD transfer-line temperature	250ºC	
ITD source temperature	170ºC	
Ionization	Electron impact (EI+) at 70 eV	
Scan mode	Full Scan	
Scan range (amu)	40-300	

2.4.1.4. GC × GC/TOFMS

The volatiles analysis was performed on a Pegasus 4D (LECO, St. Joseph, MI, USA) GC × GC–TOFMS system. This system comprised a HP 6890 (Agilent Technologies, USA) gas chromatograph with a dual stage jet cryogenic modulator (licensed from Zoex) and a secondary oven connected to a Pegasus III time-of-flight mass spectrometer (LECO, St. Joseph, MI, USA).

Three sets of columns have been used to perform the separations of pine volatiles.

Column set 1: The first dimension of the GC × GC column set was a DB-5ms (5% phenyl polysilphenylenesiloxane) column with 15 m × 0.25 mm i.d. and 0.25 μm film thickness (J&W Scientific, Folsom, USA), with a BPX50 (50% phenyl polysilphenylene-siloxane) column as the second dimension with 1.0 m × 0.1 mm i.d. and 0.1 μm film thickness (SGE International, Ringwood, Australia). The operational conditions are depicted in Table 2.11.

Table 2.11 - Operational conditions used for GC × GC/TOFMS, for column set 1.

Oven temperature program	Initial Temperature (ºC): 35 Initial Time (min): 2.0 Rate #1 (deg.min^{-1}): 4.0 Final Temperature #1 (ºC): 250 Hold Time #1 (min): 2.00
Secondary oven temperature program	Initial Temperature (ºC): 40 Initial Time (min): 2.0 Rate #1 (deg.min^{-1}): 4.0 Final Temperature #1 (ºC): 255 Hold Time #1 (min): 2.0
GC carrier gas	1.0 mL He min^{-1} (constant flow mode)
Injection mode	split (1:50)
Injection port temperature	300 ºC
Sample volume	1.0 μL
Ionization	Electron impact (EI+) at 70 eV
Scan mode	Full Scan
Scan range (amu)	45-600
Source temperature	220 ºC
Transfer line temperature	280 ºC
Detector voltage	-1750 V
Acquisition rate	125 Hz
Modulation period	3 s
Hot pulse	0.6 s
S/N for peak finding	10

Column set 2: The first dimension of the GC × GC column set was an Equity-5 (5% phenyl polysilphenylenesiloxane) column with 60 m × 0.25 mm i.d. and 1.0 μm film thickness (Supelco, Bellefonte, USA), with a Supelcowax-10 (Polyethylene glycol – PEG) column as the second dimension with 2.5 m × 0.1 mm i.d. and 0.1 μm film thickness (Supelco, Bellefonte, USA). The operational conditions are depicted in Table 2.12.

Table 2.12 - Operational conditions used for GC × GC/TOFMS, for column set 2.

Oven temperature program	Initial Temperature (ºC):	35
	Initial Time (min):	2.0
	Rate #1 (deg.min^{-1}):	4.0
	Final Temperature #1 (ºC):	250
	Hold Time #1 (min):	2.00
Secondary oven temperature program	Initial Temperature (ºC):	40
	Initial Time (min):	2.0
	Rate #1 (deg.min^{-1}):	4.0
	Final Temperature #1 (ºC):	255
	Hold Time #1 (min):	2.0
GC carrier gas	1.0 mL He min^{-1} (constant flow mode)	
Injection mode	split (1:50)	
Injection port temperature	300 ºC	
Sample volume	1.0 μL	
Ionization	Electron impact (EI+) at 70 eV	
Scan mode	Full Scan	
Scan range (amu)	45-600	
Source temperature	220 ºC	
Transfer line temperature	280 ºC	
Detector voltage	-1750 V	
Acquisition rate	125 Hz	
Modulation period	3 s	
Hot pulse	0.6 s	
S/N for peak finding	10	

Column set 3: This column set was used for separation of enantiomeric monoterpenes. The first dimension of the GC × GC column set was a tailor made fused silica capillary column with 30 m × 0.25 mm I.D., coated with 0.25 μm film of 15% heptakis (2,3-di-O-methyl-6-O-terc-butyldimethylsilyl)-*β*-cyclodextrin in SE52 (DiMe) with a Supelcowax-10 (Polyethylene glycol – PEG) column as the second dimension with 2.5 m × 0.1 mm

i.d. and 0.1 μm film thickness (Supelco, Bellefonte, USA). The operational conditions are depicted in Table 2.13.

Table 2.13 - Operational conditions used for GC × GC/TOFMS, for column set 3.

Oven temperature program	Initial Temperature (ºC): 40
	Initial Time (min): 1.0
	Rate #1 (deg.min^{-1}): 2.0
	Final Temperature #1 (ºC): 200
	Hold Time #1 (min): 2.00
Secondary oven temperature program	Initial Temperature (ºC): 50
	Initial Time (min): 1.0
	Rate #1 (deg.min^{-1}): 2.0
	Final Temperature #1 (ºC): 210
	Hold Time #1 (min): 2.0
GC carrier gas	1.0 mL He min^{-1} (constant flow mode)
Injection mode	split (1:4)
Injection port temperature	300 ºC
Sample volume	1.0 μL
Ionization	Electron impact (EI+) at 70 eV
Scan mode	Full Scan
Scan range (amu)	35-350
Source temperature	220 ºC
Transfer line temperature	250 ºC
Detector voltage	1700 V
Acquisition rate	100 Hz
Modulation period	5 s
Hot pulse time	1.0 s
S/N for peak finding	50

Total ion chromatograms (TIC) were processed using the automated data processing software ChromaToF^{TM} from LECO Corp (St. Joseph, MI, USA). Contour plots were used to evaluate the general quality of the separation and for manual peak identification.

2.4.1.5. GC/FI-TOFMS

The GC/FI-TOFMS experimental analyses were carried out on a Micromass GCT instrument equipped with a field ionization source. The separation of the pine needle volatiles were performed on a ZB-5ms (5% phenyl-95% methyl-polysiloxane) column, 30 m × 0.25 mm i.d.

and 0.25 μm film thickness (Phenomenex, Torrance, USA). The operational conditions used for GC/FI-TOFMS are depicted in Table 2.14.

Table 2.14 - Operational conditions used for GC/FI-TOFMS.

Oven temperature program	Initial Temperature (ºC):	40
	Initial Time (min):	2.00
	Rate #1 (deg.min^{-1}):	4.0
	Final Temperature #1 (ºC):	125
	Hold Time #1 (min):	0.00
	Rate #2 (deg/min):	5.0
	Final Temperature #2 (ºC):	250
	Hold Time #2 (min):	10.00
GC carrier gas	1.0 mL He min^{-1} (constant flow mode)	
Injection mode	split (1:5)	
Injection port temperature	250 ºC	
Sample volume	1.0 μL	
Ionization	Field Ionization (FI+)	
Scan mode	Full Scan	
Scan range (amu)	40-500	
FI emitter	10 μm tungsten with carbon microneedles	
Extraction voltage	12 kV	
Emitter current (at integration)	0.0 mA	
Flash off current	4.0 mA	
Scan duration	1.2 s	
Interscan delay	0.2 s	
Source temperature	50 ºC	
GC interface temperature	290 ºC	

During analysis, chloropentafluorobenzene (C_6ClF_5), with a monoisotopic mass of 201.9609 Da, was continuously introduced as the internal reference (lock mass compound) for accurate mass measurement. A calibration mixture containing heptacosa, pentafluorbenzene, hexafluoro-benzene, pentafluoroiodobenzene, pentafluorochlorobenzene, perfluorotrimethyl-cyclohexane, xylene, and acetone was used to calibrate, the single molecular ions generated by FI, on the mass range from 50 to 600 Da. The mixture was introduced into the ion source via a batch inlet and was pumped out after the calibration.

Total ion chromatograms (TIC) were processed using the automated data processing software MassLynx from Waters-Micromass (Micromass, Manchester, UK).

2.4.2. Resin acids analysis

2.4.2.1. GC/MS

The analysis of resin acids was performed on two gas chromatograph/mass spectrometer systems. The first system consists of a Trace GC 2000 Series gas chromatograph (ThermoQuest, Rodano, Italy), coupled to a Finnigan Trace MS quadrupole mass spectrometer (ThermoQuest, Manchester, UK) Electron Impact (EI). Separation of the resin acids methyl esters was performed on a ZB-5ms (5% phenyl-95% methyl-polysiloxane) column, 30 m × 0.25 mm i.d. and 0.25 μm film thickness (Phenomenex, Torrance, USA). The operational conditions are depicted in Table 2.15.

Table 2.15 - Operational conditions used for GC/MS, on system 1, for resin acids analysis.

Oven temperature program	Initial Temperature (ºC): 80 Initial Time (min): 0.00 Rate #1 (deg.min^{-1}): 5.0 Final Temperature #1 (ºC): 295 Hold Time #1 (min): 17.00
GC carrier gas	1.0 mL He min^{-1} (constant flow mode)
Injection mode	splitless (0.5 min)
Injection port temperature	260 ºC
Sample volume	1.0 μL
Ionization	Electron impact (EI+) at 70 eV
Scan mode	Full Scan
Scan range (amu)	40-450
Source temperature	260 ºC
GC interface temperature	290 ºC

The second system consists of a Trace GC 2000 Series gas chromatograph (ThermoQuest, Rodano, Italy) and coupled with a GCQ/Polaris ion-trap mass spectrometer (ThermoFinnigan, Austin, TX, USA) equipped with an AS3000 Liquid Autosampler (ThermoQuest, Rodano, Italy). Separation of the resin acids methyl esters weas performed on a DB-5 (5% phenyl-95% methyl-polysiloxane) column, 30 m × 0.25 mm i.d. and 0.25 μm film thickness (J&W Scientific; Folsom, USA). The operational conditions are depicted in Table 2.16.

Table 2.16 - Operational conditions used for GC/MS, on system 2, for resin acids analysis.

Oven temperature program	Initial Temperature (ºC):	80
	Initial Time (min):	0.00
	Rate #1 (deg.min^{-1}):	5.0
	Final Temperature #1 (ºC):	295
	Hold Time #1 (min):	17.00
GC carrier gas	1.0 mL He min^{-1} (constant flow mode)	
Injection mode	splitless (0.5 min)	
Injection port temperature	260 ºC	
Sample volume	1.0 μL	
Ionization	Electron impact (EI+) at 70 eV	
Scan mode	Full Scan	
Scan range (amu)	40-450	
Source Temperature	230 ºC	
GC interface temperature	290 ºC	

In both systems the data processing and instrument control was performed by Xcalibur software (ThermoFinnigan, Austin, TX, USA).

2.4.2.2. GC × GC / TOFMS

This system consists of a HP 6890 (Agilent Technologies, Burwood, Australia) gas chromatograph coupled to a Pegasus III time-of- flight mass spectrometer (LECO, St. Joseph, MI, USA).

To implement the modulation process, a longitudinally modulated cryogenic system (LMCS) from Chromatography Concepts (Doncaster, Australia) was used. The first dimension of the GC × GC column set was a BPX5 (5% phenyl polysilphenylenesiloxane) column with 30 m × 0.25 mm i.d. and 0.25 μm film thickness (df); (SGE International, Ringwood, Australia), with a BPX50 (50% phenyl polysilphenylene-siloxane) column as the second dimension with 1.0 m × 0.15 mm i.d. and 0.15 μm film thickness (SGE International, Ringwood, Australia). The transfer line column for the GC × GC/TOFMS system was a 0.50 m deactivated fused silica column with 0.1 mm i.d. (0.21 m inside the transfer line and 0.29 m inside the oven) from SGE International. The operational conditions are depicted in Table 2.17.

Table 2.17 - Operational conditions used for GC × GC/TOFMS, for resin acids analysis.

Oven temperature program	Initial Temperature (ºC):	60
	Initial Time (min):	0.20
	Rate #1 (deg.min^{-1}):	20.0
	Final Temperature #1 (ºC):	170
	Hold Time #1 (min):	5.00
	Rate #2 (deg.min^{-1}):	2.0
	Final Temperature #1 (ºC):	290
	Hold Time #1 (min):	20.00
GC carrier gas	1.0 mL He min^{-1} (constant flow mode)	
Injection mode	pulse splitless mode (50 psi for 1 min)	
Injection port temperature	300 ºC	
Sample volume	1.0 μL	
Ionization	Electron impact (EI+) at 70 eV	
Scan mode	Full Scan	
Scan range (amu)	45-600	
Source temperature	200 ºC	
Transfer line temperature	350 ºC	
Multi-channel plate voltage	1700 V	
Data storage rate	100 Hz	
Modulation period	6 s	
Cryotrap temperature	-20 ºC	
Hot pulse	1.5 s	
Cool time between stages	1.5 s	

Total ion chromatograms (TIC) were processed using the automated data processing software ChromaToFTM from LECO Corp (St. Joseph, MI, USA).

2.4.2.3. GC/FI-TOFMS

The GC/FI-TOFMS experimental analyses were carried out on a Micromass GCT instrument equipped with a field ionization source. The separation of the resin acids methyl esters was performed on a ZB-5ms (5% phenyl-95% methyl-polysiloxane) column, 30 m × 0.25 mm i.d. and 0.25 μm film thickness (Phenomenex, Torrance, USA). The operational conditions are depicted in Table 2.18.

Table 2.18 - Operational conditions used for GC/FI-TOFMS, for resin acids analysis.

Oven temperature program	Initial Temperature (ºC): 80 Initial Time (min): 0.00 Rate #1 (deg.min^{-1}): 5.0 Final Temperature #1 (ºC): 280 Hold Time #1 (min): 20.00
GC carrier gas	1.0 mL He min^{-1} (constant flow mode)
Injection mode	splitless (1.0 min)
Injection port temperature	260 ºC
Sample volume	1.0 μL
Ionization	Field Ionization (FI+)
Scan mode	Full Scan
Scan range (amu)	40-500
FI emitter	10 μm tungsten with carbon microneedles
Extraction voltage	12 kV
Emitter current (at integration)	0.0 mA
Flash off current	4.0 mA
Scan duration	1.2 s
Interscan delay	0.2 s
Source temperature	50 ºC
GC interface temperature	290 ºC

During analysis, chloropentafluorobenzene (C_6ClF_5), with a monoisotopic mass of 201.9609 Da, was continuously introduced as the internal reference (lock mass compound) for accurate mass measurement. A calibration mixture containing heptacosa, pentafluorbenzene, hexafluoro-benzene, pentafluoroiodobenzene, pentafluorochlorobenzene, perfluorotrimethyl-cyclohexane, xylene, and acetone was used to calibrate, the single molecular ions generated by FI, on the mass range from 50 to 600 Da. The mixture was introduced into the ion source via a batch inlet and was pumped out after the calibration.

Total ion chromatograms (TIC) were processed using the automated data processing software MassLynx from Waters-Micromass (Micromass, Manchester, UK).

2.4.2.4. Direct probe FI-TOFMS

The samples analyzed by FI+ were introduced into the ion source, using a quartz sample holder placed inside the direct insertion probe (solid probe). The operational conditions used are depicted in Table 2.19.

Table 2.19 - Operational conditions used for direct probe FI-TOFMS, for resin acids analysis.

Thermal gradient	Initial Temperature (ºC): 50 Pulsed temperature (ºC): 100 (manual) Final Temperature (ºC): 350
Injection mode	direct probe
Sample volume	10.0 μL
Ionization	Field Ionization (FI+)
Scan mode	Full Scan
Scan range (amu)	40-1000
FI emitter	10 μm tungsten with carbon microneedles
Extraction voltage	12 kV
Emitter current (at integration)	0.0 mA
Flash off current	8.0 mA
Scan duration	1.2 s
Interscan delay	0.2 s
Source temperature	50 ºC

During analysis, chloropentafluorobenzene (C_6ClF_5), with a monoisotopic mass of 201.9609 Da, was continuously introduced as the internal reference (lock mass compound) for accurate mass measurement. A calibration mixture containing heptacosa, pentafluorbenzene, hexafluoro-benzene, pentafluoroiodobenzene, pentafluorochlorobenzene, perfluorotrimethyl-cyclohexane, xylene, and acetone was used to calibrate, the single molecular ions generated by FI, on the mass range from 50 to 600 Da. The mixture was introduced into the ion source via a batch inlet and was pumped out after the calibration.

Mass spectra were processed using the automated data processing software MassLynx from Waters-Micromass (Micromass, Manchester, UK).

2.5. Chemical analysis

Individual compounds were detected by comparison with the retention times of pure standard solutions analysed under similar operating conditions. The compounds were identified by comparison of the mass spectra obtained, for the standards, with the correspondent spectra listed on the Wiley 7th mass spectral reference library and NIST Mass Spectral Database Version 2.0.

When no standard was available, a tentative identification of the compounds was made for all the peaks that have a spectral match quality better than 80%. The tentative identification of components was made by comparing the experimental spectra, after critical evaluation, to databases that presents the mass spectra and retention index of the most commonly occurring plant essential oils components (Adams, 1989; 2001; Joulain and Koning, 1998) and commercial mass spectral reference libraries (Wiley and NIST Mass Spectral libraries). The tentative identification assignements were, whenever applicable, supported by linear retention indices (LRI). The LRIs are calculated for each compound according to the van den Dool and Kratz equation (van den Dool and Kratz, 1963) and compared with the literature retention indices databases (Adams, 1989; 2001) or with those found reported in the literature.

Comparison of the identification and detection results, between pine species, was undertaken by "overlaying" the respective chromatograms or plots to detect/identify components that are common or that are unique to the samples. It was assumed that peaks with the same retention time or located within a small range and presenting identical mass spectrum represent the same compound.

In enantioselective MDGC analysis the order of elution and retention times of the enantiomeric compounds investigated was assigned by injection of standards and by co-injection. The retention times on the pre-column were 13.1 min for α-pinene, 15.8 min for β-pinene, and 19.4 for limonene. The operational cut-time intervals used were 12.8-13.4 min for α-pinene, 15.6-16.1 min for β-pinene, and 19.0-19.7 min for limonene.

Relative area percentage of the compounds present in the volatile fraction and analysed by GC-FID was used for data analysis.

For resin acids, a relative quantification was performed using the mass fragments m/z = 316 and m/z = 314 as selective ions and integrating the corresponding peak area.

2.6. Data treatment and statistical analysis

Statistical multivariate data analyses were performed using Statistica 6.0 software (StatSoft, Tulsa, OK, USA) and SIMCA-P version 10.0 (Umetrics, Umeå, Sweden), on the volatile profile of each *Pinus* specimen. Relative area percentage of the compounds present in the volatile fraction of pine needles was used for data analysis. Data submitted to the analysis

were arranged in a matrix, where each column corresponds to one volatile component and each row represents an individual tree, or a pine species. Prior to multivariate data analysis, the data were log transformed.

The homogeneity of data pertaining to pine species and individual trees was analyzed by hierarchical cluster analysis (HCA), using Ward's method and Euclidean distance measure. Principal component analysis (PCA) was used to evaluate similarities and differences between observations and illustrated as score plots in order to visualize the structure of the data. The relationships among the variables and how they combine to explain the observations shown in the score plot was displayed by its corresponding loading plot. The HCA and PCA analysis were performed using Statistica 6.0 software.

Multivariate data analysis using partial least squares (PLS) was performed with SIMCA-P software version 10.0, in order to examine the correlations between the volatile composition of each tree and species (X variables) to *T. pityocampa* attack (Y variable). The efficiency and reability of the PLS model was evaluated with respect to the percent explained variance (R2Y) and predictivity (Q2). The PLS model was, in addition, evaluated with respect to goodness of fit (R2).

3. Results

3.1. Volatiles

The composition of the volatile fraction emitted by the needles of eleven pine species from Abrantes arboretum (referred in Figure 2.2) was studied. The identification of the volatile components was accomplished by means of gas chromatography hyphenated with mass spectrometry (GC/MS) and by comprehensive two-dimensional gas chromatography hyphenated with mass spectrometry (GC × GC/TOFMS) (according to Table 2.3). For GC/MS two mass analyzers were used: quadrupole (GC/qMS) and time-of-flight (GC/TOFMS).

3.1.1. Identification of the components of the pine needles volatile fractions

3.1.1.1. Gas chromatography/quadrupole mass spectrometry

The relative amounts of the volatile compounds of all pine species studied were determined by GC-FID. Results show (further presented when the statistical treatment is carried out) that the composition of the volatile fraction of the needles of the 11 pine species studied was dominated by monoterpenes, that accounted for 89.2% (RSD = 6.9%), in average. The remaining 10.8% were mainly sesquiterpenes, oxygenated monoterpenes, some green leaf volatiles, phenols, alcohols, aldehydes and esters. Major monoterpenes, such as α-pinene, β-pinene, myrcene, limonene, Δ-3-carene, and β-phellandrene, and sesquiterpenes, such as *trans*-caryophyllene, germacrene D, *cis*-β-farnesene, α-copaene, β-cubebene, β-elemene, γ-muurolene, δ-amorphene and α-caryophyllene, were found in the 11 pine species (Table 3.1). The most abundant monoterpenes in the needles of all pine species were α-pinene and β-pinene, which accounted for more than half of the total volatile composition. Myrcene and limonene were the following most abundant monoterpenes. Exceptions were found for *P. pinea,* in which limonene was responsible for more than 70% of the emissions, *P patula,* in which limonene + β-phellandrene and α-pinene were the major compounds (β-pinene accounting for less than 4%), and *P. nigra*, in which myrcene was the second major constituent accounting for, in average, 18.6% of its volatile fraction.

Table 3.1 - Peak identification after HS-SPME-1D-GC-qMS analysis, with calculated and literature retention data.

					Pinus species										
PeakNo.	RT	Compound	$^{\S}RI_{calc}$	$^{\S\S}RI_{Lit}$	PE	PH	PP	PK	PPr	PPa	PN	PR	PS	PB	PT
1	8.01	cis-Hex-3-en-1-ol*	878	859	x	x	x	x	x	x	x	x	x	x	x
2	10.49	Tricyclene*	941	927	x		x	x	x	x	x		x	x	x
3	10.60	Thujene*	944	930	x	x	x	x	x	x	x	x	x	x	x
4	11.10	α-Pinene*	957	939	x	x	x	x	x	x	x	x	x	x	x
5	11.49	Camphene*	967	954	x	x	x	x	x	x	x	x	x	x	x
6	12.40	Sabinene*	990	975	x	x	x	x	x	x	x	x	x	x	x
7	12.70	β-Pinene*	998	979	x	x	x	x	x	x	x	x	x	x	x
8	13.01	Myrcene*	1006	991	x	x	x	x	x	x	x	x	x	x	x
9	13.52	3-hexenyl acetate	1018	1002	x	x	x	x	x	x	x	x	x	x	x
10	13.56	α-Phellandrene*	1019	1003	x	x	x	x	x	x	x	x	x	x	x
11	13.80	Δ-3-Carene*	1025	1011	x	x	x	x	x	x	x	x	x	x	x
12	14.03	α-Terpinene*	1031	1017	x	x	x	x	x	x	x	x	x	x	x
13	14.23	Carvomenthene	1036	1026										x	
14	14.31	*p*-Cymene*	1038	1025	x	x	x	x	x	x	x	x	x	x	x
15	14.57	Limonene*	1045	1029	x	x	x	x	x	x	x	x	x	x	x
16	14.57	β-Phellandrene*	1045	1030	x	x	x	x	x	x	x	x	x	x	x
17	14.74	*cis*-Ocimene*	1049	1037	x	x	x	x	x	x	x	x	x	x	x
18	15.16	*trans*-Ocimene*	1059	1050	x	x	x	x	x	x	x	x	x	x	x
19	15.63	γ-Terpinene*	1071	1060	x	x	x	x	x	x	x	x	x	x	x
20	16.78	Terpinolene*	1100	1089	x	x	x	x	x	x	x	x	x	x	x
21	17.11	Linalool*	1108	1097	x	x	x	x	x	x	x	x		x	x

Table 3.1 - Peak identification after HS-SPME-1D-GC-qMS analysis, with calculated and literature retention data (cont.).

					Pinus species										
PeakNo.	RT	Compound	$^{\S}RI_{calc}$	$^{\S\S}RI_{Lit}$	PE	PH	PP	PK	PPr	PPa	PN	PR	PS	PB	PT
22	17.29	Ester C10	1113	1103					x						
23	17.71	Ester C10	1123	1115					x						
24	18.23	Alloocimene	1136	1132	x	x	x	x	x		x	x	x	x	x
25	19.57	Pinocamphone isomer	1170	1163	x			x	x				x	x	x
26	19.76	Borneol isomer	1175	1169	x		x		x		x		x	x	x
27	wax 19.46	Hexyl acetate*	-	1009		x	x	x	x	x	nd	x	x	x	x
28	wax 21.88	Hexan-1-ol*	-	871	x	x		x	x	x	nd	x	x	x	x
29	wax 24.98	Acetic acid*	-	-	x	x			x	x	nd	x	x	x	x
30	20.09	Pinocamphone isomer	1185	1175			x		x			x			
31	20.15	4-Terpineol	1187	1177	x	x	x		x	x		x		x	x
32	20.69	α-Terpineol*	1201	1189	x	x			x	x	x	x		x	x
33	20.86	Myrtenol	1206	1196					x					x	
34	20.86	Methyl chavicol	1206	1196					x					x	
35	21.01	Decanal	1210	1202	x										x
36	21.96	Ester C11	1235	-					x						
37	22.05	Thymol methyl ether	1240	1235	x		x		x		x	x	x	x	x
38	22.21	Hexyl isovalerate	1245	1245				x	x						
39	22.68	Linalyl acetate	1259	1257	x		x		x	x	x			x	x
40	22.71	2-Undecanone isomer	1260	-								x	x		
41	22.79	Piperitone	1262	1253					x	x		x			
42	23.76	Bornyl acetate isomer	1290	1286/1289	x	x	x		x	x	x	x	x	x	x
43	23.82	2-Undecanone isomer	1292	1294								x	x		

Table 3.1 - Peak identification after HS-SPME-1D-GC-qMS analysis, with calculated and literature retention data (cont.).

					Pinus species										
PeakNo.	RT	Compound	$^{\S}RI_{calc}$	$^{\S\S}RI_{Lit}$	PE	PH	PP	PK	PPr	PPa	PN	PR	PS	PB	PT
44	24.00	Tridecane*	1300	1300					x	x		x			
45	24.15	Pinocarvyl acetate isomer	1302	1298/1312	x										
46	24.87	Myrtanyl acetate	1327	1327	x										x
47	25.02	n.i. (sesquieterpene)	1333	-	x		x		x			x	x		x
48	25.26	n.i. (sesquiterpene)	1341	-			x	x	x	x	x	x	x	x	x
49	25.28	δ-Elemene	1342	1338	x	x									
50	25.46	Citronellyl acetate	1348	1353		x									
51	25.50	α-Terpenyl acetate	1349	1349	x		x				x	x	x	x	x
52	25.60	α-Cubebene*	1353	1351	x	x			x			x	x	x	x
53	25.76	Neryl acetate	1359	1362	x	x	x		x	x	x			x	x
54	25.80	2-Dodecanone isomer	1360	-									x		
55	26.26	Geranyl acetate	1376	1381	x	x	x		x	x	x			x	x
56	26.37	α-Copaene*	1380	1377	x	x	x	x	x	x	x	x	x	x	x
57	26.56	2-Dodecanone isomer	1387	1391									x		
58	26.64	β-Bourbonene	1389	1388	x			x	x	x				x	
59	26.71	β-Cubebene	1392	1388	x	x	x	x	x	x	x	x	x	x	x
60	26.73	β-Elemene	1393	1391	x	x	x	x	x	x	x	x	x	x	x
61	26.84	Methyl eugenol	1396	1404					x					x	
62	27.26	Longifolene	1413	1408			x		x	x	x			x	x
63	27.29	*cis*-α-Bergamotene	1414	1413	x										
64	27.55	*trans*-Caryophyllene*	1424	1419	x	x	x	x	x	x	x	x	x	x	x

Table 3.1 - Peak identification after HS-SPME-1D-GC-qMS analysis, with calculated and literature retention data (cont.).

					Pinus species										
PeakNo.	RT	Compound	$^{\S}RI_{calc}$	$^{\S\S}RI_{Lit}$	PE	PH	PP	PK	PPr	PPa	PN	PR	PS	PB	PT
65	27.75	*cis*-β-Copaene	1432	1432	x		x	x	x	x	x		x	x	
66	27.92	*trans*-α-bergamotene	1439	1435											x
67	28.00	n.i.	1442	-								x			x
68	28.01	α-Guaiene	1442	1440						x					
69	28.05	Aromadandrene*	1444	1441					x	x			x		
70	28.12	*trans*-β-Farnesene	1447	1443	x	x	x	x	x	x	x	x	x	x	x
71	28.36	α-Caryophyllene*	1456	1455	x	x	x	x	x	x	x	x	x	x	x
72	28.55	*cis*-Muurola-4(14),5-diene	1464	1467	x		x	x	x	x	x		x	x	x
73	28.71	trans-β-farnesene	1470	1457			x	x						x	
74	28.81	γ-Muurolene	1474	1480	x	x	x	x	x	x	x	x	x	x	x
75	28.93	Phenyl ethyl 2-methyl butanoate	1479	1487		x			x		x	x		x	
76	28.99	Phenyl ethyl 3-methyl butanoate	1481	1491		x			x		x	x		x	
77	29.05	Germacrene D	1484	1485	x	x	x	x	x	x	x	x	x	x	x
78	29.13	β-Selinene	1487	1490									x		
79	29.14	*trans*-Muurola-4(14),5-diene	1487	1494					x						x
80	29.24	*epi*-Cubebol	1491	1494					x	x					
81	29.33	n.i. (coelution sesquiterpenes)	1495	-	x	x		x	x	x	x	x	x		x
82	29.41	α-Muurolene	1498	1500	x		x	x	x	x	x			x	
83	29.50	α-Amorphene	1502	1512					x		x				

Table 3.1 - Peak identification after HS-SPME-1D-GC-qMS analysis, with calculated and literature retention data (cont.).

					Pinus species										
PeakNo.	RT	Compound	$^{\S}RI_{calc}$	$^{\S\S}RI_{Lit}$	PE	PH	PP	PK	PPr	PPa	PN	PR	PS	PB	PT
84	29.68	*γ*-Cadinene	1510	1514	x		x	x	x	x	x	x	x	x	x
85	29.81	*d*-Amorphene	1515	1512	x	x	x	x	x	x	x	x	x	x	x
86	30.06	Cadina-1(2),4-diene	1526	1535									x		
87	30.13	trans-*α*-Bisabolene	1530	1530**		x			x		x			x	
88	30.19	*α*-Cadinene	1532	1539									x		
89	31.05	Germacrene D-4-ol	1570	1576	x		x		x			x	x	x	x
90	31.29	Caryophyllene oxide	1581	1583	x	x		x	x		x			x	x
91	wax 26.76	Longipinene	-	1353			x		x		nd	x		x	
92	wax 27.06	*α*-Ylangene	-	1375	x	x			x	x	nd	x		x	
93	wax 29.40	*β*-Ylangene	-	1421	x			x	x	x	nd	x		x	
94	wax 31.48	*ε*-Muurolene	-	1455**	x	x	x	x	x	x	nd	x	x	x	x

RT – compound retention time in minutes. x indicates compound found in the samples.
$^{\S}RI_{calc}$, $^{\S\S}RI_{Lit}$ - calculated and literature retention index data, respectively. The calculated retention indices were obtained based on retention times across the DB-5 column. Peaks were identified based on the comparison (similarity) of their mass spectra to chemical standards, reference mass spectral databases (Mass Spectra Library NIST version 2.0, 2005 and Wiley Registry of Mass Spectral Data 7th edition, 2000) and retention indices (Adams, 2001). nd - *P. nigra* was not analysed on the DB-Wax.

Pinus species key: PE - *P. elliottii*; PH - *P. halepensis*; PP - *P. patula*; PK - *P. kesiya*; PPr - *P. pinaster*; PPa - *P. pinea*; PN - *P. nigra*; PR - *P. radiata*; PS - *P. sylvestris*; PB - *P. brutia*; PT - *P. taeda*.The peaks identified by NIST/Wiley Libraries have a match quality spectrum of 80% or better at least in one of the species.
Wax-RT – retention time on DB-wax (compounds only detected on DB-Wax)
*Identification confirmed by chemical standard
**Data not referred in Adams (2001) and thus obtained from Joulain and Konig (1998).
The RI_{Lit} for Δ-3-Carene reports to Adams (1989).

P. sylvestris also presented α- and β-pinene as major constituents, but they were closely followed by Δ-3-carene, which in average accounted for 24.4% of total volatile content. The major sesquiterpenes found were *trans*-caryophyllene, germacrene D and α-caryophyllene. *P. halepensis* was the exception, in which germacrene D was a minor constituent that coelutes, on the DB-5 type columns, with the peaks of the two phenylethyl-methylbutanoates, and that was only detected, although in small amounts, through the analysis performed with the DB-Wax column.

Table 3.1 shows the compounds detected and identified in the *Pinus* spp. samples, using the NIST mass spectra library matching and retention index criteria. The retention times and linear retention indices (LRI) reported were obtained with the DB-5 column. The experimental linear retention indices ($LRI_{calc.}$) obtained for the *Pinus* spp. volatile compounds were plotted against the linear retention indices ($LRI_{lit.}$) reported by Adams (2001), as illustrated on Figure 3.1. The LRI_{calc} presents a linear relationship when correlated with the LRI_{ref}, described by a coefficient of determination (R^2) of 0.9996.

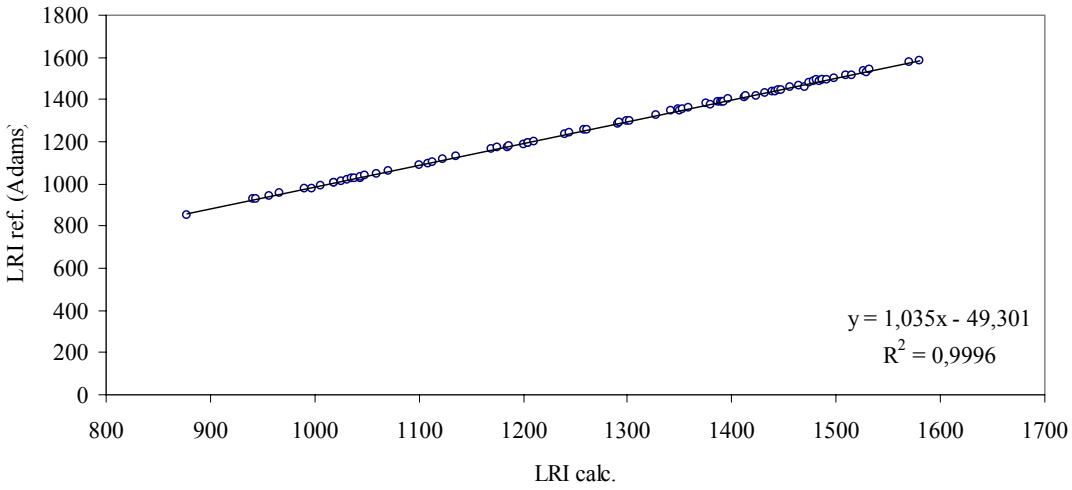

Figure 3.1 - Relation between the linear retention indices calculated for the 1D-GC/MS analysis with those reported by Adams (2001).

The separation and identification of the compounds present in the headspace of the pine needles extracted by SPME was first carried out by gas chromatography/quadrupole mass spectrometry (1D-GC/qMS), with two columns of different polarities and orthogonal separation mechanisms: **i)** a non polar DB-5ms, with 30 m length, and **ii)** a polar DB-Wax, with 60 m length (according to Table 2.3 and Tables 2.5-2.6). The two reconstructed total ion chromatograms (TIC) obtained for *P. pinaster* are presented, respectively, in Figures 3.2 and 3.3, as examples.

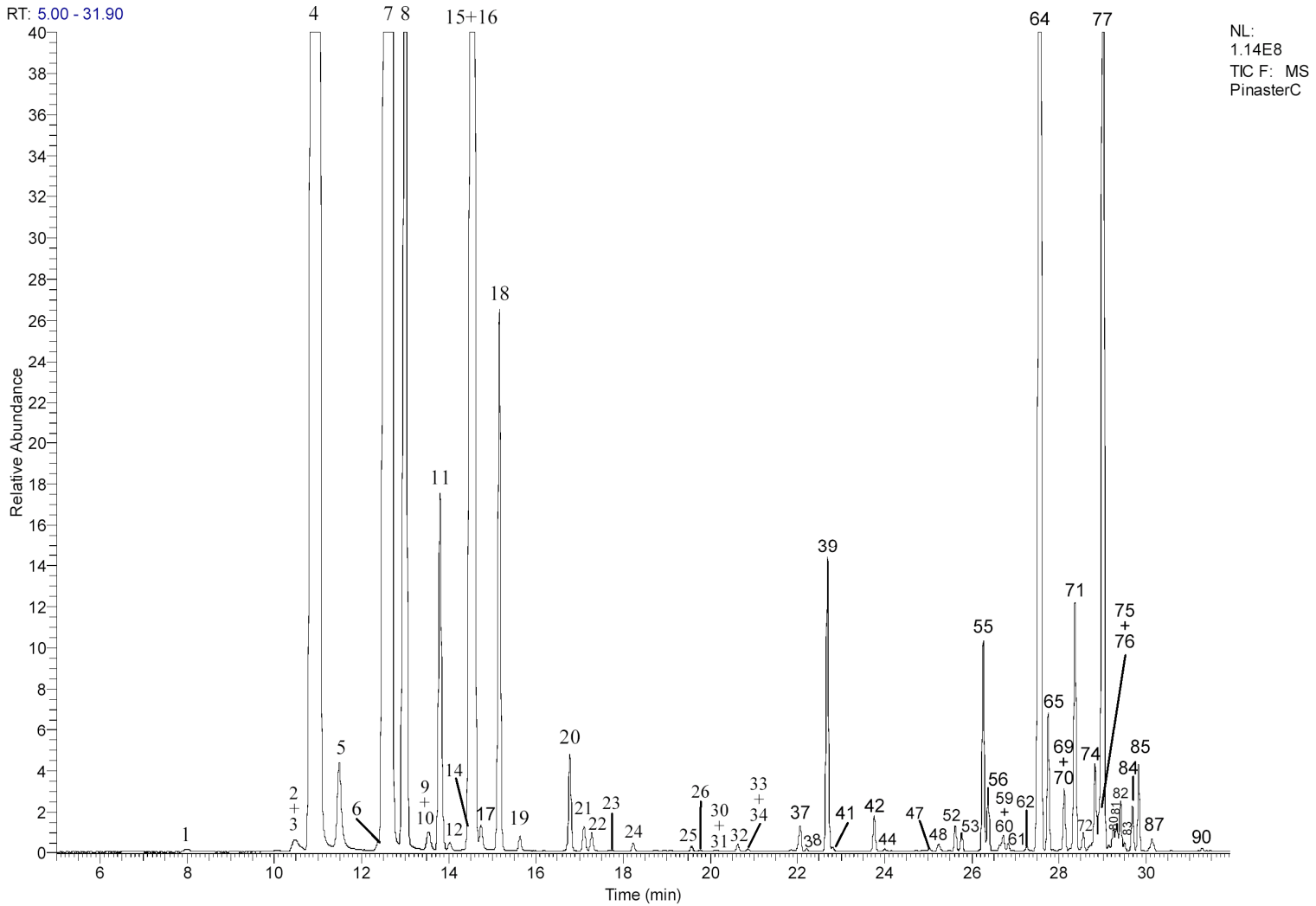

Figure 3.2 - Reconstructed total ion chromatogram from the headspace of *P. pinaster* needles analyzed on the DB-5ms column. Peaks are numbered and assigned according to Table 3.1. Operational conditions can be consulted in Chapter 2.

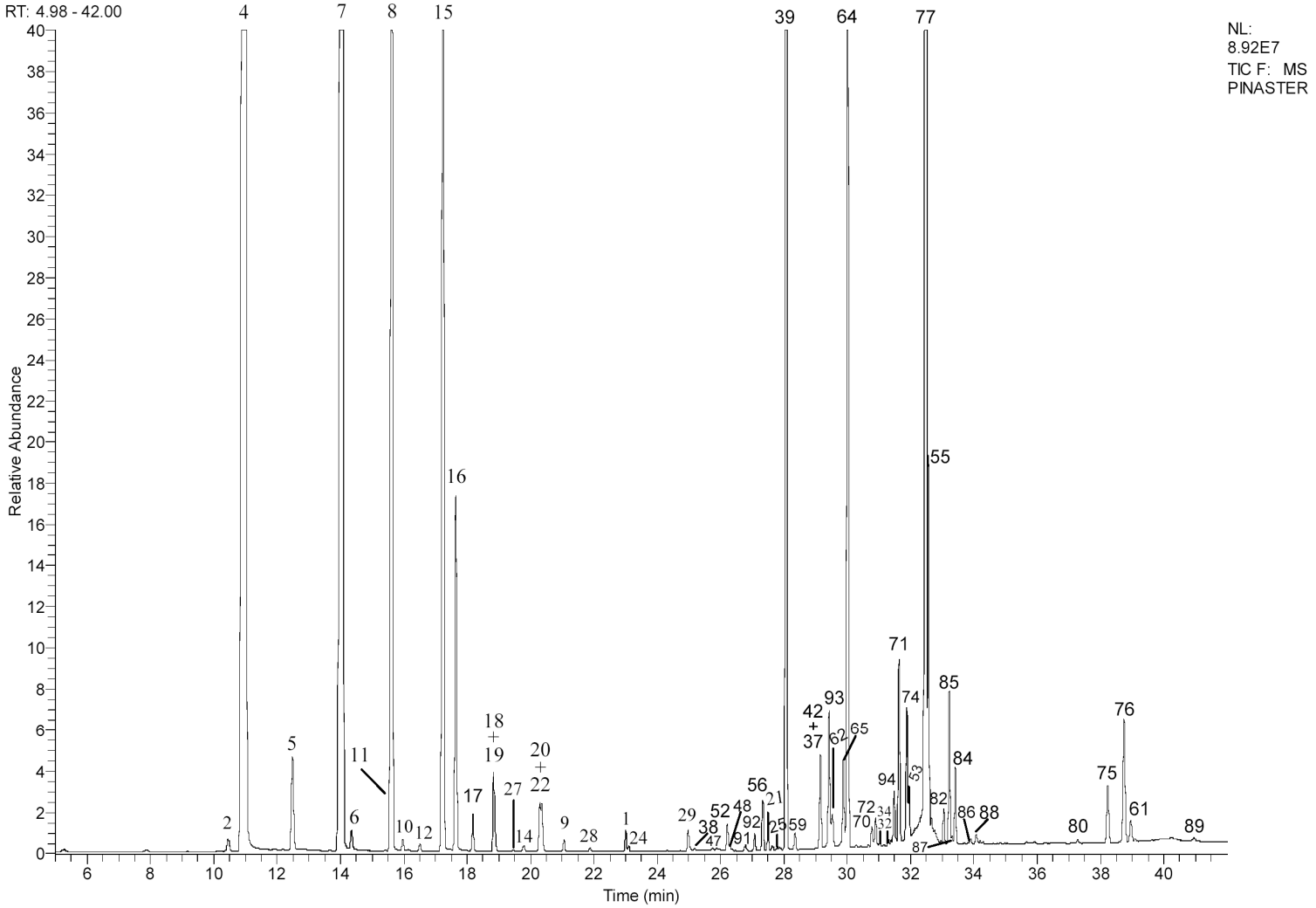

Figure 3.3 - Reconstructed total ion chromatogram from the headspace of *P. pinaster* needles analyzed on the DB-Wax column. Peaks are numbered and assigned according to Table 3.1. Operational conditions can be consulted in Chapter 2.

The numbered peaks refer to the assigned identities of detected compounds (Table 3.1). Representative TICs, obtained for the DB-5 column, for the other pine species studied, *P. pinea, P. halepensis, P. brutia, P. patula, P. elliottii, P. nigra, P. radiata*, *P. taeda, P. kesiya* and *P. sylvestris,* are presented in Appendix A.

Data analysis for the whole range of monoterpenes shows that a higher number of coelutions and partial coelutions of some compounds occurred on the DB-5 column. This observation is apparent for the final number of coelutions in both columns and results from the potential coelutions of the main components of the volatile fraction of pine needles on the 30 meters DB-5ms, which were not observed on the 60 meters DB-Wax. Examples of coeluting pairs of compounds are limonene/β-phellandrene, sabinene/β-pinene, α-phellandrene/3-hexenyl acetate ester and germacrene D/phenylethyl-3-methylbutanoate and -2-methylbutanoate. Additionally, 1,8 cineol is present at low concentrations, and also coelutes with the pair limonene/β-phellandrene. The different ratios of ion 69 from limonene and the 77 from β-phellandrene, at the beginning and at the end of peak (15 + 16), allow for the detection of both compounds. 1,8-cineol was detected by extracting the ion 154 but not identified due to the impossibility of obtaining a consistent mass spectra. The different mass spectra of the pair α-phellandrene/3-hexenyl acetate allow for the manual deconvolution of both compounds and, therefore, their identification. The pair sabinene/β-pinene is chromatographically better resolved and sabinene can be identified by mass spectra analysis at the beginning of the peak cluster. The phenylethyl-methylbutanoates that coelute with the major peak of germacrene D are detected due to their intense fragment m/z 104. They were identified after spectra subtraction at both ends on the peak obtained by extraction of the ion 104. However the ratio between these two compounds is rather variable, especially in *P. pinaster* where in some samples the amounts of phenylethyl-methylbutanoates are higher than those of germacrene D. At the DB-Wax, partial coelutions are observed between oxygenated monoterpenes and sesquiterpenes and other coelution examples can be found for the pairs terpinolene/non identified methyl ester ($C_{10}H_{20}O_2$), *trans*-ocimene/terpinolene, *cis*-hex-3-en-1-ol/alloocimene and thymol methyl ether/bornyl acetate isomer.

Peak identification was performed by standard co-injection whenever possible. When reference standards were not available, the detected peaks were tentatively identified after critical and

careful evaluation of mass spectral data, in combination with published linear retention indices and spectral information obtained from searchable and published mass spectra databases.

In spite of: **i)** the use of "reliable" available mass spectral libraries; **ii)** GC retention data bases being considered the main tool to maximize an efficient identification of the compounds; **iii)** although all the "care" put on the data evaluation, complete identification of individual components can not be guarantee and inconclusive or erroneous assignments were not uncommon.

The data reported in the published or searchable commercial databases is not free or errors, since it lacks information about its origin, which has different sources. Examples are the reported data originated from particular contributions of standards in Adams (1989; 2001) and spectra in NIST/Wiley, or from the synthesis or isolation of pure compounds which chemical structures were unambiguously established by NMR in Joulain and Koning (1998). Additionally, some of referred databases include compounds that were insufficiently characterized or incorrectly identified, and the same compounds may be reported within the same or in different libraries by different mass spectra (Figure 3.5). The operational conditions must also be critically considered, since the mass spectra reported in the libraries databases were often acquired with different conditions or with different mass analysers. An example comes from the Adams database (1989; 2001), where the author stated that as a general rule, the spectra reported in the database were chosen at the peak mid-point for small peaks and at about 0.05 min from the start of the peak for larger peaks. This situation means that, as Adams is operating with scanning mass spectrometer, the final reported spectra, for larger peaks, could present incorrections due to peak skewing. The databases themselves are "incomplete", making the identification of not previously identified compounds unreliable, with just one database or with all. Examples are the mass spectra of peaks 47 and 48 of Table 3.1, which were not found at any mass spectra library, δ-amorphene that is only reported on the 2001 Adams published database (Figure 3.6) and ε-muurolene that is only reported on Joulain and Koning database (1998). Additional difficulties for positive identification are due to mass spectral similarities, inside the terpene class, which sometimes promote incorrect library matches with an apparent match similarity higher than 80%. Examples found are such as the pair α-pinene/Δ-3carene, the terpenes α-terpinene/terpinolene/γ-terpinene and the cymene isomers. A particular example comes from the high number of isomers within the sesquiterpene

compounds, which lack of commercially available standards make their absolute identification difficult. Sesquiterpenes yield identical, or almost identical mass spectra and small variations in the mass spectra are sufficient to promote wrong identifications or identical assignments for peaks that eluting at different retention positions are reported with the same compound identity. All those compounds were only differentiable by they different retention times. These observations supported the use of chromatographic retention indices databases, such as those published by Adams, to support the identity assignments of the detected peaks. However, retention indices databases are not either error free. Published retention indices vary from source to source, and sometimes even in different editions of the same database. An example found concerns the terpene *Δ*-3-carene, which is reported with a retention index of 1031 (eluting after limonene), on the 2001 Adams database, and with a retention index of 1011 (eluting before limonene) on the 1989 Adams database. The injection of the *Δ*-3-carene standard confirmed the retention index of the 1989 Adams database, as the correct one. This observation was also additionally confirmed by the analysis of *P. sylvestris*, a *Δ*-3-carene chemotype pine species.

As previously presented, Table 3.1 shows the compounds identified, either tentatively or by means of standard injection, in the volatile fractions of the needles of the 11 different pine species. The table also shows the information regarding the average retention times for each compound, together with their linear temperature programmed retention indices (RI_{calc}), calculated according to the van den Dool and Kratz equation (van den Dool and Kratz, 1963), and their correspondent retention indices published by Adams (RI_{lit}) (2001). As already previously presented, Figure 3.1 shows the comparison between the calculated RI and the RI reported by Adams (2001) for a DB-5 type column. When identification was not possible, the compound was considered "not identified" (n.i.) and whenever possible its chemical class listed. Tentative identification was considered positive if a particular compound had a mass spectral match better than 80%, at least in one of the pine species or in one of the columns. If the spectra was absent from the searchable database, but reported on a published database, a visual comparison was made between the obtained and published spectra, together with a critical evaluation of the analyte retention indices (calculated and from the reference database). No identification was assigned for compounds whose retention index reported on the literature were not consistent with the calculated retention index.

A total of 94 compounds were detected, being 87 identified. From the identified ones, 30 were confirmed by standard injection and the remaining 57 tentatively, by means of mass spectral libraries, supported by retention index data. Seven of the compounds were only detected with the DB-Wax column. Hexyl acetate, hexan-1-ol and the acetic acid were confirmed by standard injection. The remaining 4 compounds, α- and β- ylangene, α-longipinene and ε-muurolene, were all sesquiterpenes present in minor amounts in the volatile fraction, and were tentatively identified, in a first step, by library spectra alone. The peaks α-ylangene (peak 91) and α-longipinene (peak 92) (Figure 3.4), presented at least one library match higher that 89% on the searchable Nist/Wiley/mainlib libraries.

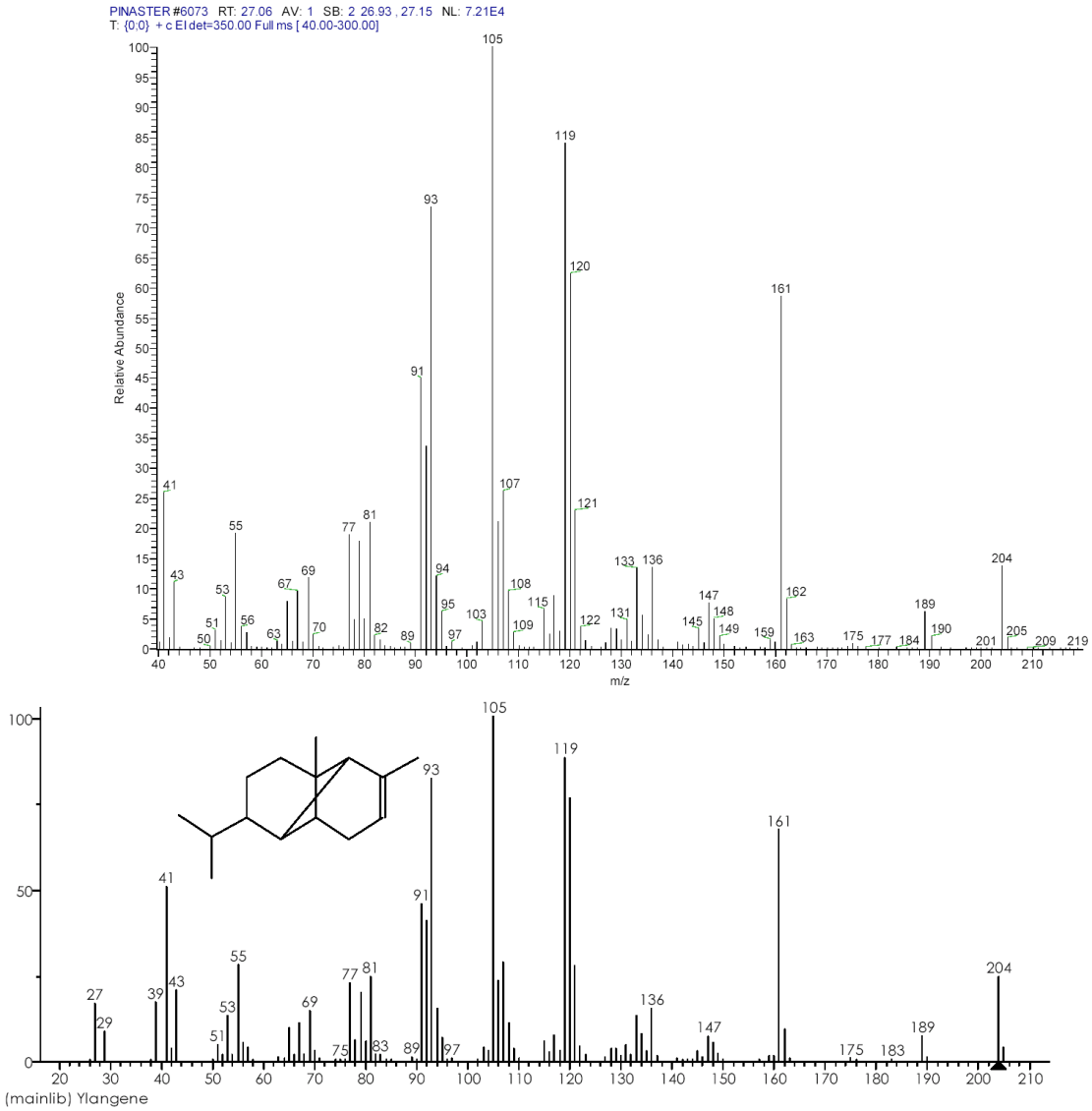

Figure 3.4 – Mass spectra of tentatively identified of α-ylangene (peak 92): (top) obtained from the *P. pinaster* sample analysed by GC-qMS; (bottom) from the NIST MS search database.

The expected retention indices, on the DB-5 column, are according to Adams, respectively 1353 and 1375. The peak of α-longipinene is always present at minor amounts and may not had been detected by the analysis performed on the DB-5 columns or may probably be coeluting with other compounds, present in larger amounts, such as neryl acetate (peak 53; RI_{lit} = 1362) and α-cubebene (peak 52; RI_{lit} = 1353) (Figure 3.2). The α-ylangene is probably coeluting, on the DB-5 column, with α-coapene (peak 56; RI_{lit} = 1377) and geranyl acetate (peak 55, RI_{lit} = 1381) (Figure 3.2). On the DB-wax column, both acetates are shifted to larger retentions times and it can be observed that α-longipinene, α-cubebene, α-ylangene and α-coapene are eluting in a close range (Figure 3.3). β-ylangene (peak 93) is an example of a compound that is reported with different spectra in different mass spectra databases (Figure 3.5).

The obtained spectrum is different from those reported by Adams and the NIST/Wiley/mainlinb databases, but almost identical to the spectra reported by Joulain and Koning (1998) database. β-ylangene has a retention index of 1421, in the Adams database, which is very close to the retention index of 1419 from *trans*-caryophyllene, the major sesquiterpene in the samples, presenting a high probability of being coeluting with it on the DB-5 column.

The ε-muurolene is only reported at the Joulain and Koning (1998) database, where it has the same retention index (1455) as α-caryophyllene, another major sesquiterpene in the 11 pine species, and both are probably coeluting on the DB-5 column. On the DB-Wax, ε-muurolene and α-caryophyllene were still observed eluting in a very close range. δ-amorphene was detected on the DB-5 column in all pine species, and was the only compound that was tentatively identified using the Adams dataset, as it was the only one reporting it. The reported retention index is 1512, and the calculated was 1515. The similarities between the obtained mass spectra with that reported by Adams, shown in Figure 3.6, together with a RI match with just 3 index units of difference, supported the tentative identification of peak 85 as δ-amorphene.

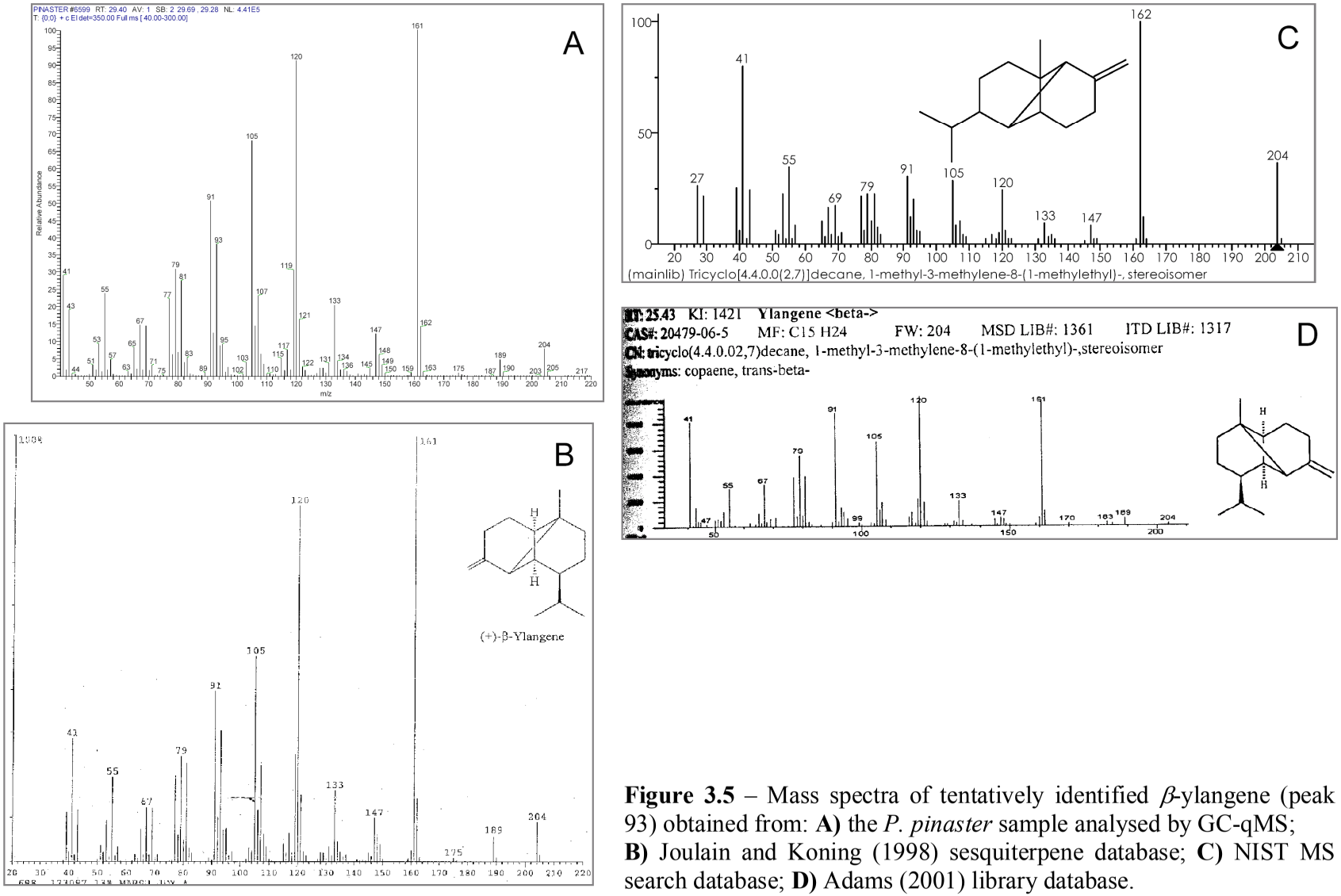

Figure 3.5 – Mass spectra of tentatively identified *β*-ylangene (peak 93) obtained from: **A)** the *P. pinaster* sample analysed by GC-qMS; **B)** Joulain and Koning (1998) sesquiterpene database; **C)** NIST MS search database; **D)** Adams (2001) library database.

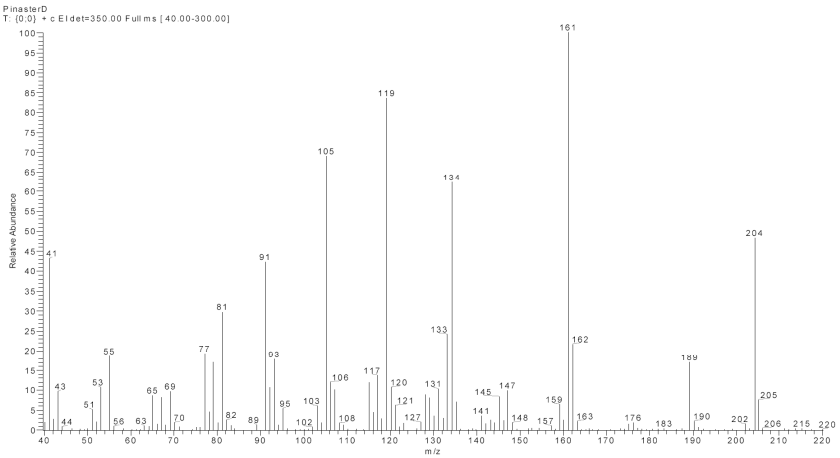

RT: 29.29 KI: 1512 **Amorphene <delta->**
CAS#: 189165-79-5 MF: C15 H24 FW: 204 MSD LIB#: 1341 ITD LIB#: 1460
CN: naphthalene,1,2,3,5,6,8a-hexahydro-4,7-dimethyl-1-(1-methylethyl)-,(1S,8aS)-
Synonyms: none

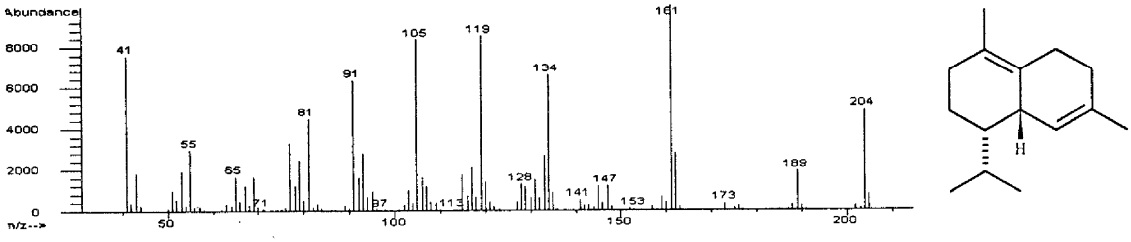

Figure 3.6 – Mass spectra of tentatively identified of δ-amorphene (peak 93): (top) obtained from the *P. pinaster* sample analysed by GC-qMS, (bottom) from the Adams library database.

3.1.1.2. Gas chromatography/time-of-flight mass spectrometry

Figures 3.7 and 3.8 present, respectively, the TIC and its expanded view obtained for a composite sample of *Pinus* spp., analysed by gas chromatography/time-of-flight mass spectrometry (1D-GC/TOFMS) (column 1; operational conditions according to the Table 2.9). In Figure 3.8, major peaks are numbered according to Table 3.1. The composite sample was made from the essential oils, obtained by SDE, of the 11 pine species under study, in order to obtain a representative sample of their composition (see section 2.3.1.2.). The sample was analyzed by the LECO Pegasus GC/TOFMS, a system with a high mass spectral acquisition rate (500 spectra.s^{-1}).

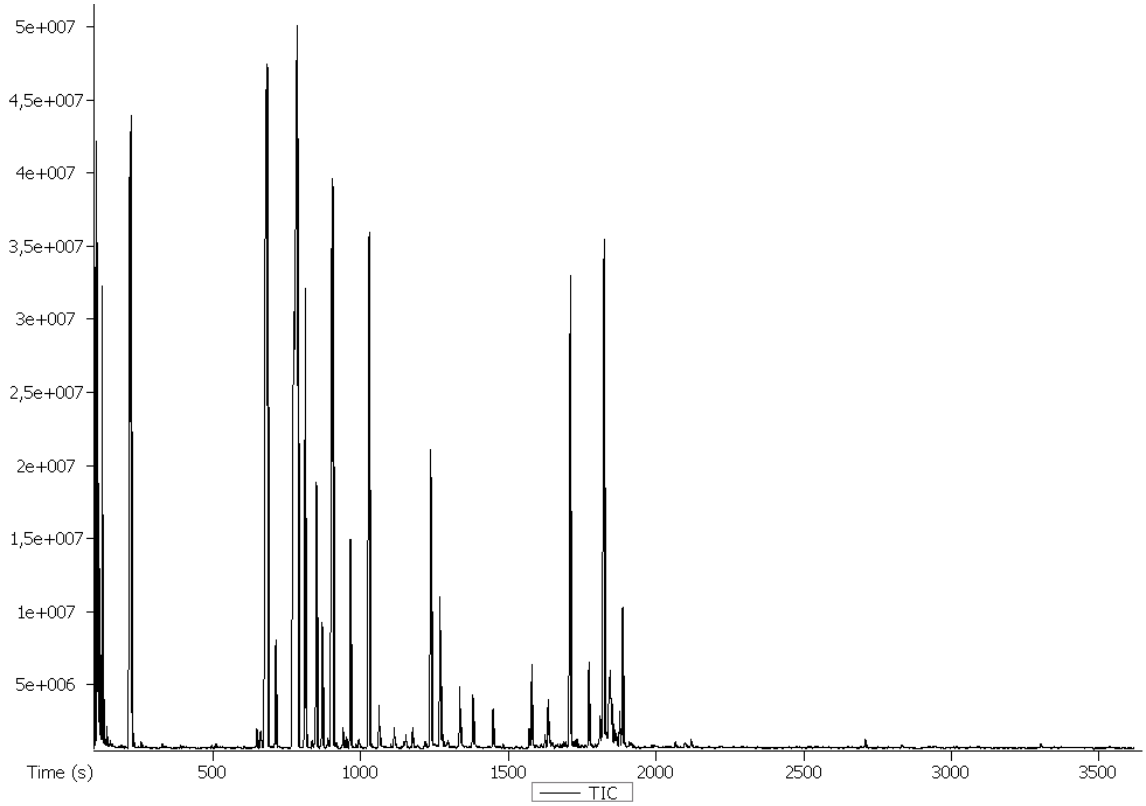

Figure 3.7 – Total ion chromatogram from a *Pinus* spp. composite sample obtained by 1D-GC/TOFMS. Operational conditions described in section 2.4.1.2.

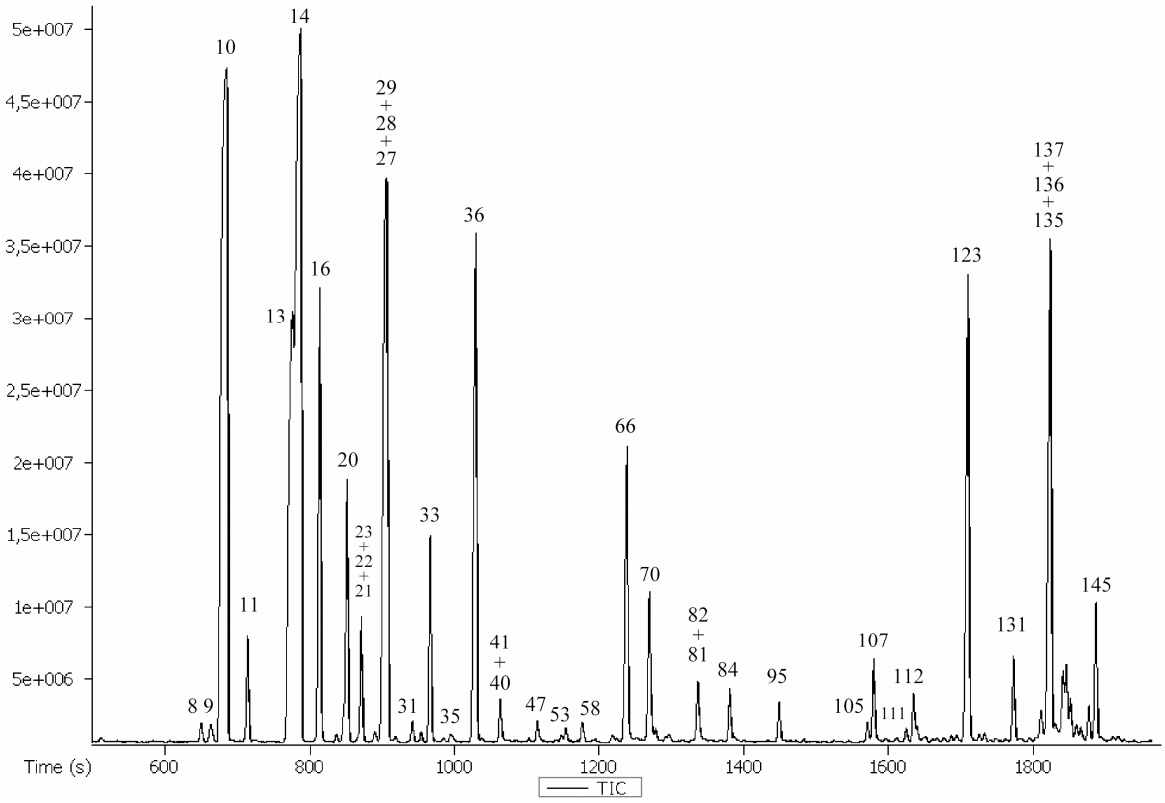

Figure 3.8 – Total ion chromatogram expanded view from a *Pinus* spp. composite sample obtained by 1D-GC/TOFMS. Compounds are numerated according to Table 3.2 (minor compounds not labeled).

The high mass spectral acquisition rate property, together with a high degree of spectral continuity across the chromatographic peaks, achieved by TOF analysers, gives an accurate representation of the ion ratios for any particular analyte through the peak, allowing for the use of automatic peak detection and deconvolution algorithms to resolve chromatographic coelutions and extract the spectrum of each analyte. This is known as spectral resolution and it was used to detect (peak find) and identify the coeluting peaks in the *Pinus* spp. composite sample.

After processing the spectral deconvolution, a number of peaks in this sample were found to be coeluting. Some coelutions are exemplified in Figures 3.9.

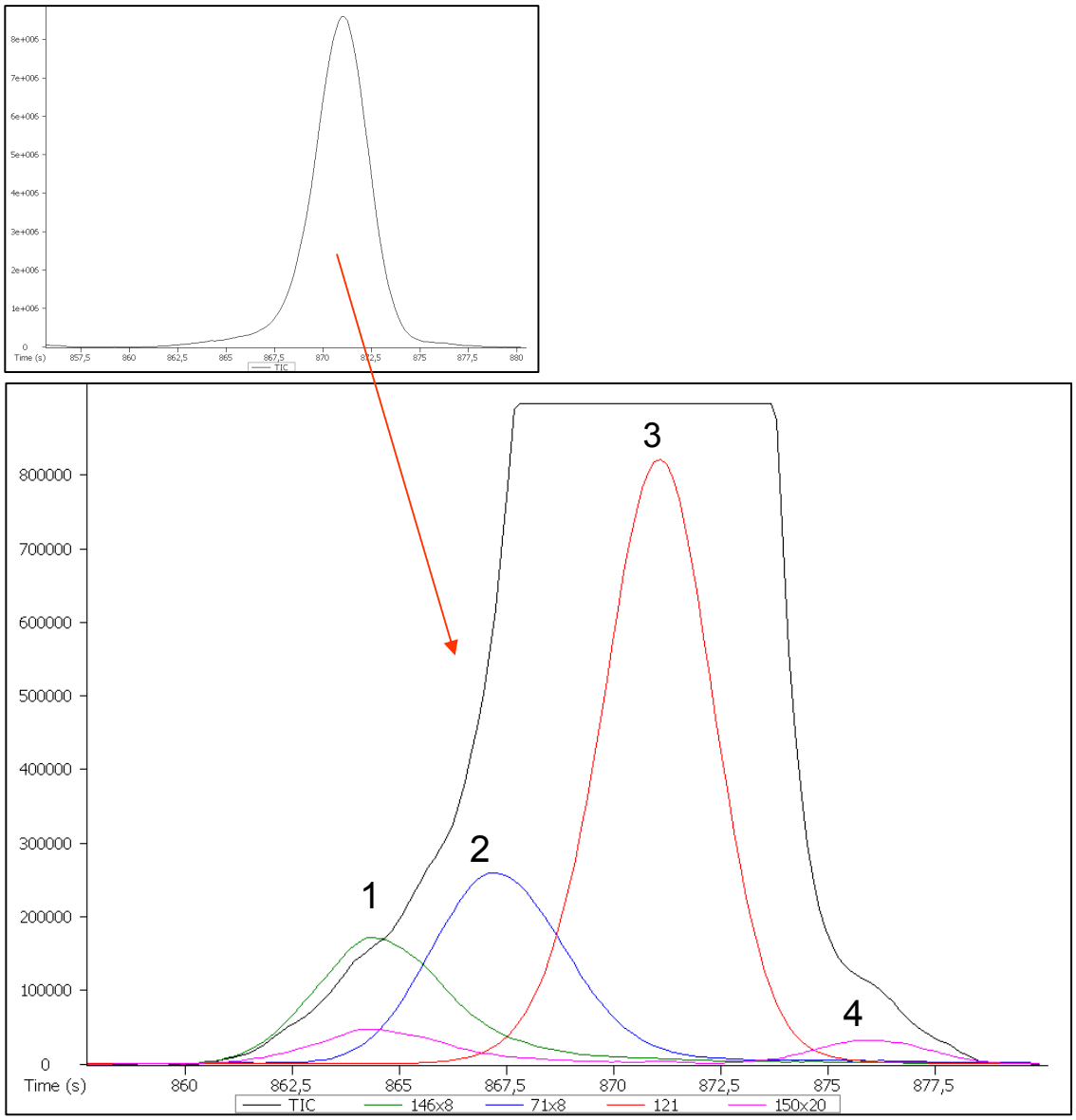

Figure 3.9 - Expanded view from an 18 second window of the *Pinus* spp. composite sample TIC, showing the deconvolution of four coeluting peaks. Peak identification is shown in Figure 3.10.

Figure 3.9 also presents an expanded view of an 18 seconds section from the chromatogram, where the TIC only shows one defined peak. In spite of the peak apparent symmetry, the use of deconvolution algorithms allowed for the detection of four peaks coeluting, and the extraction of the individual spectra for identification purposes (Figure 3.10). This shows that the TIC may be an insufficient indicator of all peaks present in the sample, showing an overall profile, because some peaks may be coeluting as single ones. By plotting their "unique" masses (m/z 146, 71, 121 and 150) together with the TIC, the presence of the coeluting peaks under the baseline of the TIC became visually evident. The intensity of m/z 146, 76 and 150 were magnified, to permit their observation on a similar scale with m/z 121 from the major peak, and the TIC baseline. The similarity of the deconvoluted spectra, after comparison with the NIST/Wiley spectral library (2000), was 765 for the dichlorobenzene isomer (peak 1), 838 for the 1.4-cineol (peak 2) and 910 for α-terpinene (peak 3). For peak 4, no valid identification was achieved with the NIST/Wiley spectral library (2000) and it was, therefore, assigned as unknown.

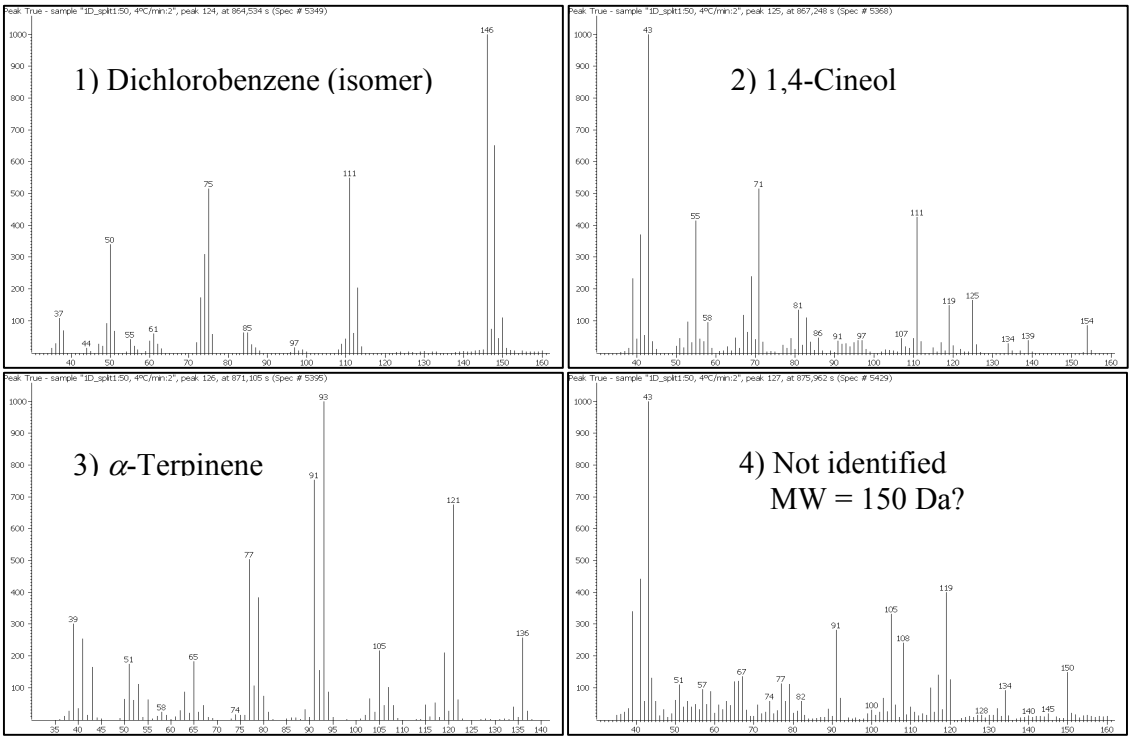

Figure 3.10 – Deconvoluted mass spectra from the peaks detected in Figure 3.9 with the assigned identification.

The use of the "peak find" and the deconvolution algorithms detected a total of 185 volatile components on the *Pinus* spp. composite sample. The results are presented in Table 3.2.

Table 3.2 - Volatile compounds tentatively identified by 1D-GC/TOFMS analysis in *Pinus* spp. composite sample.

Peak No.	RT*	Compound	Similarity	RI_{calc}§	RI_{Lit}§§
1	392	Octane	887	-	800
2	398	Hexanal	871	803	802
3	511	Hex-3-en-1-ol isomer	909	856	859
4	560	Santene	800	879	889
5	606	Nonane	(a)	900	900
6	614	Heptanal	758	904	902
7	641	Anisole	847	915	918
8	649	Tricyclene	946	920	927
9	663	α-Thujene	907	925	930
10	682	α-Pinene	926	935	939
11	714	Camphene	952	947	954
12	723	Thuja-2,4(10)-diene	755	951	960
13	773	Sabinene	888	972	975
14	787	β-Pinene	872	978	979
15	804	n.i. (ketone)	-	986	-
16	814	Myrcene	943	990	991
17	836	Hexanoic acid ethyl ester	804	1000	998
18	837	Decane	-	1000	1000
19	844	n.i.	-	1003	-
20	851	Δ-3-Carene	929	1006	1011
21	855	1,4-Dichlorobenzene	765	1008	1014
22	867	1,4-Cineol	838	1013	1015
23	871	α-Terpinene	900	1015	1017
24	876	n.i.	-	1017	-
25	885	n.i. (Menthane isomer)	-	1021	-
26	890	*p*-Cymene	939	1023	1025
27	904	Limonene	900	1030	1029
28	907	β-Phellandrene	913	1031	1030
29	909	1,8-Cineol	775	1032	1031
30	918	*cis*-Ocymene	923	1036	1037

Table 3.2 - Volatile compounds tentatively identified by 1D-GC/TOFMS analysis in *Pinus* spp. composite sample (cont.).

Peak No.	RT*	Compound	Similarity	RI_{calc}§	RI_{Lit}§§
31	942	*trans*-Ocymene	938	1046	1050
32	954	n.i.	-	1052	-
33	966	*γ*-Terpinene	914	1057	1060
34	985	n.i. (identical to peak 32)	-	1066	-
35	994	*cis*-Sabinene hydrate	747	1070	1070
36	1029	Terpinolene	933	1085	1089
37	1038	*p*-Cymenene	849	1089	1091
38	1049	n.i. (Oxygenated monoterpene)	-	1094	-
39	1059	Heptanoic acid ethyl ester	744	1098	1098
40	1063	Undecane	(a)	1100	1100
41	1063	Linalool	890	1100	1097
42	1074	Nonanal	707	1105	1101
43	1077	n.i. (C10 ester)	-	1107	-
44	1083	n.i. (Oxygenated monoterpene)	-	1109	-
45	1087	1,3,8-*p*-Menthatriene	878	1111	1110
46	1103	*endo*-Fenchol	904	1119	1117
47	1114	*cis*-*p*-Mentha-2-en-1-ol	838	1124	1122
48	1119	n.i. (Oxygenated monoterpene)	-	1126	-
49	1133	n.i.(Menthatriene isomer)	-	1133	-
50	1140	n.i. (Oxygenated monoterpene)	-	1136	-
51	1143	n.i. (Ketone)	-	1137	-
52	1148	*trans*-Pinocarveol	837	1139	1139
53	1154	*trans*-*p*-Mentha-2-en-1-ol	848	1142	1141
54	1162	n.i. (Oxygenated monoterpene)	-	1146	-
55	1166	n.i.	-	1148	-
56	1168	n.i. (Oxygenated monoterpene)	-	1149	-
57	1171	n.i.	-	1150	-
58	1177	Citronellal	941	1153	1153
59	1179	n.i. (Oxygenated monoterpene)	-	1154	-
60	1191	*trans*-Pinocamphone	821	1159	1163
61	1195	Pinocarvone	771	1161	1165

Table 3.2 - Volatile compounds tentatively identified by 1D-GC/TOFMS analysis in *Pinus* spp. composite sample (cont.).

Peak No.	RT*	Compound	Similarity	RI_{calc} §	RI_{Lit} §§
62	1215	n.i. (Ester)	-	1171	-
63	1218	Borneol	798	1172	1169
64	1219	*p*-Mentha-1,5-dien-8-ol	721	1173	1170
65	1224	*cis*-Pinocamphone	878	1175	1175
66	1238	Terpinen-4-ol	919	1181	1177
67	1249	n.i.	-	1187	-
68	1252	*p*-Cymen-8-ol	733	1188	1183
69	1259	Salicilic acid methyl ester	781	1191	1192
70	1269	α-Terpineol	927	1196	1189
71	1271	n.i. (Oxygenated monoterpene)	-	1197	-
72	1272	n.i.	-	1197	-
73	1274	n.i.	-	1198	-
74	1278	Dodecane	827	1200	1200
75	1285	n.i.	-	1203	-
76	1292	Decanal	812	1207	1202
77	1297	*trans*-Piperitol	786	1209	1208
78	1310	n.i.	-	1215	-
79	1314	n.i.	-	1218	-
80	1318	n.i.	-	1219	-
81	1337	Cittronellol	931	1228	1226
82	1338	Thymyl methyl ether	804	1229	1235
83	1368	n.i. (Oxygenated monoterpene)	-	1244	-
84	1381	Linalyl acetate	901	1250	1257
85	1384	n.i. (Oxygenated monoterpene)	-	1252	-
86	1388	Piperitone	849	1254	1253
87	1390	2-Phenylethyl acetate	777	1255	1258
88	1395	n.i.	-	1257	-
89	1401	n.i.	-	1260	-
90	1407	n.i.	-	1263	-
91	1417	n.i.	-	1268	
92	1433	1,2,4-Triethylbenzene	817	1275	-

Table 3.2 - Volatile compounds tentatively identified by 1D-GC/TOFMS analysis in *Pinus* spp. composite sample (cont.).

Peak No.	RT*	Compound	Similarity	RI_{calc}§	RI_{Lit}§§
93	1436	n.i.	-	1277	-
94	1439	n.i.	-	1279	-
95	1449	*exo*-bornyl acetate	911	1283	1286
96	1455	n.i.	-	1286	-
97	1464	n.i.(Monoterpene acetate)	-	1291	-
98	1468	n.i. (Ketone)	-	1293	-
99	1471	*trans*-pinocarvyl acetate	759	1294	1298
100	1483	Tridecane	912	1300	-
101	1525	Myrtenyl acetate	751	1322	1327
102	1529	Decanoic acid methyl ester	790	1324	1326
103	1545	n.i.(Sesquiterpene)	-	1333	-
104	1570	α-Cubebene	836	1346	1351
105	1571	Terpinyl acetate	863	1346	1349
106	1574	n.i. (Sesquiterpene)	-	1348	-
107	1580	Citronellyl acetate	920	1351	1353
108	1596	n.i. (Monoterpene Acetate)	-	1359	-
109	1607	n.i.	-	1365	-
110	1612	α-Ylangene	905	1367	1375
111	1625	α-Copaene	938	1374	1377
112	1635	Geranyl acetate	896	1380	1381
113	1640	β-Bourbonene	910	1382	1388
114	1648	β-Cubebene	783	1387	1388
115	1652	β-Elemene	887	1388	1391
116	1662	n.i. (Phenyl ester)	-	1394	-
117	1667	Decanoic acid ethyl ester	764	1396	1396
118	1674	Tetradecane	(a)	1400	1400
119	1677	n.i. (Sesquiterpene)	-	1402	-
120	1687	n.i. (Sesquiterpene)	-	1407	-
121	1694	Dodecanal	949	1411	1409
122	1698	n.i.	-	1413	-

Table 3.2 - Volatile compounds tentatively identified by 1D-GC/TOFMS analysis in *Pinus* spp. composite sample (cont.).

Peak No.	RT*	Compound	Similarity	RI_{calc} §	RI_{Lit} §§
123	1710	*trans*-Caryophyllene	945	1420	1421
124	1726	β-Copaene	834	1428	1434
125	1733	β-Bergamotene	916	1432	1435
126	1741	Aromadendrene	829	1436	1441
127	1748	Butanoic acid 2-phenylethyl ester	858	1441	1441
128	1755	n.i. (Sesquiterpene)	-	1444	-
129	1761	n.i. (Sesquiterpene)	-	1447	-
130	1764	n.i. (Sesquiterpene)	-	1449	-
131	1773	α-caryophyllene	913	1454	1455
132	1785	n.i. (Sesquiterpene)	-	1460	-
133	1795	n.i. (Sesquiterpene)	-	1466	-
134	1811	γ-Muurolene	913	1475	1480
135	1824	Germacrene D	937	1482	1485
136	1831	2-Methyl-butanoic acid 2-phenylethyl ester	807	1485	1487
137	1842	3-Methyl-butanoic acid 2-phenylethyl ester	913	1491	1491
138	1846	Bicyclogermacrene	915	1494	1500
139	1850	n.i.	-	1496	-
140	1852	α-Muurolene	932	1497	1500
141	1857	Pentadecane	(a)	1500	-
142	1859	n.i. (Sesquiterpene)	-	1501	-
143	1861	Butyl hydroxy toluene	869	1502	1516
144	1866	Germacrene A	900	1505	1509
145	1877	γ-Cadinene	917	1511	1514
146	1887	n.i. (Sesquiterpene)	-	1517	-
147	1894	n.i. (Sesquiterpene)	-	1521	-
148	1901	Dodecanoic acid methyl ester	406	1525	1526
149	1911	n.i. (Sesquiterpene)	-	1531	-
150	1918	α-Cadinene	846	1534	1539
151	1926	n.i. (Sesquiterpene)	-	1539	-
152	1948	n.i.	-	1552	-

Table 3.2 - Volatile compounds tentatively identified by 1D-GC/TOFMS analysis in *Pinus* spp. composite sample (cont.).

Peak No.	RT*	Compound	Similarity	RI_{calc} §	RI_{Lit} §§
153	1963	n.i.(Oxygenated sesquiterpene)	-	1561	-
154	1987	n.i. (Oxygenated sesquiterpene)	-	1574	-
155	1995	Caryophyllene oxide	794	1579	1583
156	2014	Salvial-4(14)-en-1-one	751	1590	1595
157	2022	Dodecanoic acid ethyl ester	-	1594	1595
158	2032	Hexadecane	(a)	1600	1600
159	2043	n.i.	-	1607	-
160	2052	n.i.	-	1612	-
161	2066	n.i.	-	1621	-
162	2073	n.i. (Oxygenated sesquiterpene)	-	1625	-
163	2097	n.i. (Oxygenated sesquiterpene)	-	1640	-
164	2098	n.i. (Phenyl ester)	-	1640	-
165	2100	n.i.	-	1642	-
166	2119	α-Cadinol	901	1653	1654
167	2133	n.i. (Oxygenated sesquiterpene)	-	1662	1667
168	2196	Heptadecane	(a)	1700	1700
169	2221	Farnesol isomer	788	1716	1718
170	2233	n.i.	-	1724	-
171	2248	n.i. (Mint sulphide)	-	1733	-
172	2300	Benzoic acid benzyl ester	833	1766	1760
173	2353	Octadecane	(a)	1800	-
174	2526	n.i. (Diterpene)	-	1912	-
175	2546	n.i.	-	1923	-
176	2576	Phthalate	-	1939	-
177	2625	n.i. (Diterpene)	-	1965	-
178	2650	n.i. (Diterpene)	-	1979	-
179	2660	n.i. (Diterpene)	-	1984	-
180	2693	n.i. (Diterpene)	-	2002	-
181	2709	n.i. (Diterpene)	-	2010	-
182	2750	n.i. (Diterpene)	-	2032	2080
183	2832	n.i. (Diterpene)	-	2076	-

Table 3.2 - Volatile compounds tentatively identified by 1D-GC/TOFMS analysis in *Pinus* spp. composite sample (cont.).

Peak No.	RT*	Compound	Similarity	RI_{calc} §	RI_{Lit} §§
184	3106	n.i. (Diterpene)	-	2192	2154
185	3302	Phthalate	-	2265	-

*RT - compounds retention times in seconds.
§RI_{calc}, §§RI_{Lit} - calculated and literature retention index data, respectively. The calculated retention indices were obtained based on retention times across the column. Peaks were identified based on the comparison (similarity) of their mass spectra to reference Mass spectral databases (Mass Spectra Library NIST version 2.0, 2005 and Wiley Registry of Mass Spectral Data 7th edition, 2000) and retention indices (Adams, 2001).
n.i. – not identified peak. (a) - Confirmed by hydrocarbon standard co-injection.

The tentative identifications (Table 3.2) were made by comparing the obtained spectra with the spectra of NIST/Wiley mass spectra database libraries, through the NIST MS Search Program, provided that the mass spectral similarity were higher than 750. The identification assignements were supported by the compound retention indices calculated using the Van den Dool and Kratz equation. When identification was not possible, the compound was counted as "not identified" (n.i.), and whenever possible its chemical class reported. All constraints related to complete compound identification were previously discussed, in section 3.1.1.1.

Figure 3.11 presents the good relationship obtained ($R^2 = 0.999$) between linear retention indices reported in literature (Adams, 2001) and the calculated ones for the compounds identified in the 1D-GC/TOFMS analysis and thus supporting the tentative identifications proposed.

From the 185 detected compounds (Table 3.2), 80 were not considered identified, mainly due to their low mass similarities with the assigned spectra from the NIST/Wiley database and deviation from the expected retention indices. The non identified compounds include 9 diterpenes, 5 oxygenated sesquiterpenes, 14 sesquiterpenes, 2 monoterpene acetates, 2 phenyl esters, 10 oxygenated monoterpenes, 2 ketones and 2 esters. A comparison between the retention time, reported in Table 3.2**,** for the non identified compounds and the TICs is shown in Figures 3.7 and 3.8, allows for their localisation mainly on the chromatogram sections where low intensity peaks are observable. As an example, 28 of the non identified compounds are located after peak 145, and 20 between peaks 66 and 105. A closer view of the chromatogram, exemplified in Figure

3.12 for peaks 78, 79 and 80, allows for the location of some of the compounds hidden in the baseline noise, being their detection only possible due to the software algorithm.

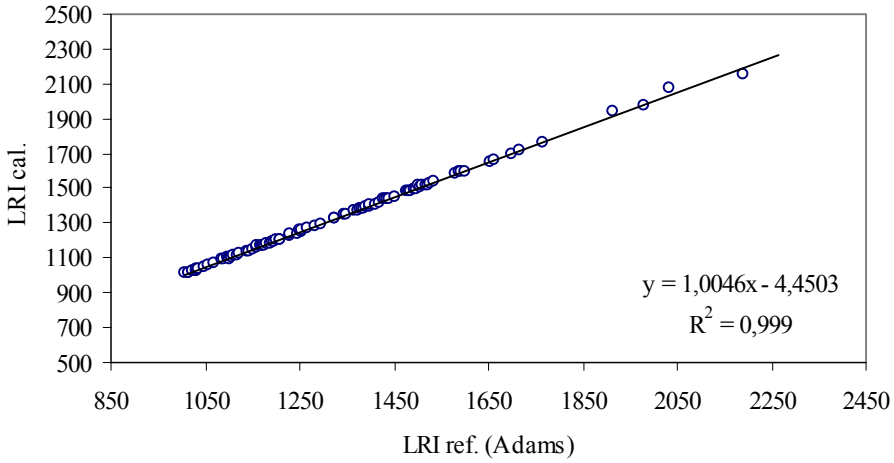

Figure 3.11 - Relationship between literature (LRI ref.) data from Adams (2001) and calculated (LRI calc.) retention index data for the compounds identified in the 1D-GC/TOFMS analysis of *Pinus* spp. composite sample.

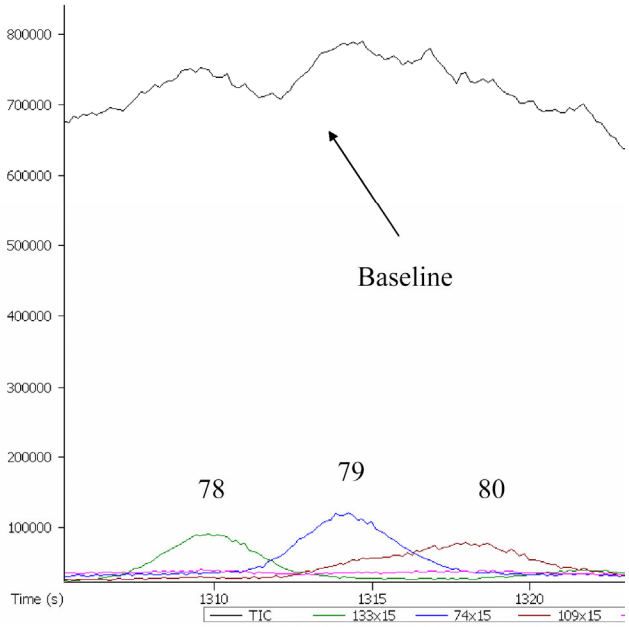

Figure 3.12 – Close view of the chromatogram baseline showing the peak extraction by the "peak find" algorithm (peak number according to Table 3.2).

This low intensity of the analytes increases the difficulty of extracting "good" mass spectra, without noise and thus explains for some of them the low similarities achieved with the NIST/Wiley spectra database. However the extracted spectra for some of the non identified compounds present characteristics diagnostic ions that allow their comparison with published mass spectra and thus manual processing aiming tentative identification supported by the experimental and published retention indices.

The manual processing allowed for the identification of 29 compounds. The results are presented in Table 3.3, and Figure 3.13 shows the relation between the experimental and the reference retention indices published by Adams.

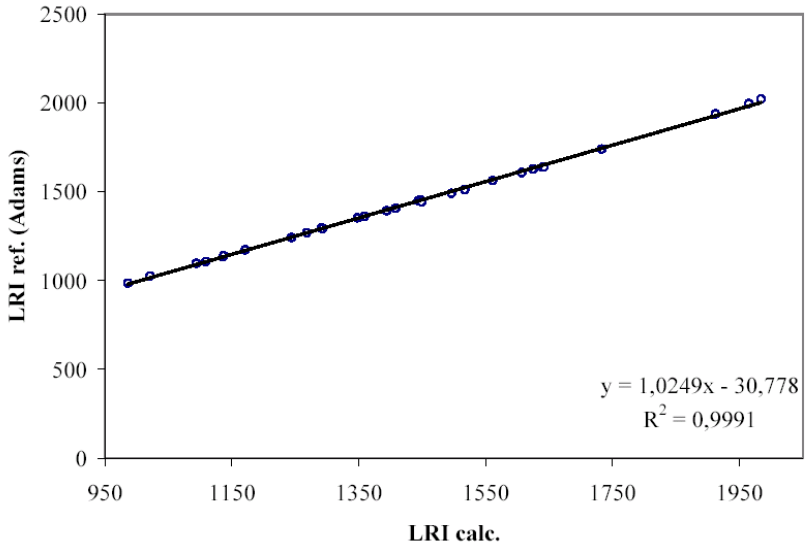

Figure 3.13 - Relationship between literature (LRI ref.) data from Adams (2001) and calculated (LRI calc.) retention index data for the compounds identified by manual processing in the 1D-GC/TOFMS analysis of *Pinus* spp. composite sample.

A set of needles from 10 pine species were analysed by 1D-GC/TOFMS, after HS-SPME, in order to study their individual composition (see section 2.3.1.1). A 60 m length column, with a 1.0 µm film thickness was used to perform the analysis (column 2; operational conditions according to the Table 2.9).

Table 3.3 – Peaks manually processed and tentatively identified by 1D-GC/TOFMS analysis in *Pinus* spp. composite sample.

Peak No.	Compound	RI_{calc}	RI_{Lit}
15	6-Methyl-hept-5-en-2-one	986	986
25	Carvomenthene	1021	1026
38	Camphen-6-one	1094	1097
44	*cis*-Rose oxide	1109	1108
50	Terpinen-1-ol	1136	1134
51	Nopinone	1137	1140
62	Benzoic acid ethyl ester	1171	1173
83	Carvone	1244	1243
91	Ethyl salicylate	1268	1270
97	3-Thujyl acetate	1291	1296
98	Undecan-2-one	1293	1294
106	α-Longipinene	1348	1353
108	Neryl acetate	1359	1362
116	Isobutanoic acid phenyl ethyl ester	1394	1394
120	β-longifolene	1408	1407
128	*cis*-Muurola-3,5-diene*	1444	1450
129	*trans*-Muurola-3,5-diene*	1447	1454
130	*trans*-β-Farnesene	1449	1443
139	Methyl isoeugenol	1496	1492
146	δ-Amorphene*	1517	1512
153	*trans*-Nerolidol	1561	1563
159	*trans*-2-Dodecen-1-ol acetate	1607	1608
162	*epi*-Cuben-1-ol	1625	1629
163	*epi*-α-Cadinol	1640	1640
164	Hexanoic acid phenyl ethyl ester	1642	1640
171	Mint sulfide	1733	1741
174	Cembrene	1912	1939
177	Manoyl oxide	1965	1998
179	Abieta-8,12-diene	1984	2023

*Compound not present in NIST/Wiley database

Table 3.4 presents the peak tentative identification achieved for the 10 *Pinus* species, after HS-SPME-1D-GC/TOFMS analysis, with calculated and literature retention data (Adams, 2001). A

total of 177 volatile compounds were detected. From these, 55 were not considered identified mainly due to their low mass similarities with the assigned spectra from the NIST/Wiley database. About 76% of the non identified compounds are located in the sesquiterpene retention time section. The identification of the sesquiterpene compounds, as previously referred in 3.111, is rather difficult due to their structural similarities and lack of available standards, which when existing are sometimes expensive. The analytical conditions provided by the 60 m column allowed for a better resolution and detection of the most volatile compounds, but also promoted the elution of the sesquiterpene compounds to higher retention times, and consequently to higher temperatures. The elution temperature of the first sesquiterpene is approximately 228 ºC (48 min), with the "column 2", in opposition to the 126 ºC and 140 ºC achieved with the used 15 m length and 30 m lenght non polar columns. The consequence was the thermal degradation of the sesquiterpenes that is observed in the chromatograms. The degradation is a dynamic process that overlaps the sesquiterpene peaks and thus produces erroneous peaks detections, by the processing algorithm, and incorrect mass spectra which lead to problems in peak identification. Another effect of the high elution temperatures can be observed, for example, for the pair myrcene/*β*-pinene, that suffers from retention cross-over, when compared with the smaller length columns. The expected elution order is *β*-pinene following myrcene, and the observed with "column 2" was myrcene following *β*-pinene. This phenomenon is mainly explained by the different temperature dependencies of the intermolecular interactions, which are responsible for the analyte retentions (Engewald, 2007a). The correlation between the column temperature (*Tc*) and the retention factor (*k*') of an analyte can be expressed as $\ln k' \propto \frac{1}{Tc}$ (Engewald, 2007a), where *k*' is the analyte retention or capacity factor, and *Tc* the absolute column temperature. The expression indicates that the analyte retention decreases logarithmically with the increase of column temperature. Structuraly, myrcene is an aliphatic hydrocarbon, and *β*-pinene is a double ring system, and thus its interaction with the phenyl modified phase of "column 2" is stronger than that of myrcene at the elution temperature of 136 ºC. The retention cross-over phenomenon has been reported in polar and non polar stationary phases by Barata (2008) and Engewald (2007a; 2007b) for compounds with different carbon skeleton, molecule geometry and functional groups. The shifts in the peak elution order on "column 2", lead to difficulties in the assignment of the relationships between the experimental and the reference retention indices such as those published by Adams (2001), which were obtained using a "standard" 30 m length column.

Table 3.4 - Peak identification after HS-SPME-1D-GC/TOFMS analysis, with calculated and literature retention data (Adams, 2001).

					Pinus species									
Peak No.	RT	Compound	RI_{calc} §	RI_{Lit} §§	PE	PH	PP	PK	PPr	PPa	PN	PR	PS	PB
1	728	Ethanol	*	427**							x			x
2	782	Acetone	*	500**			x	x	x	x	x	x	x	x
3	1036	2-Methyl-but-3-en-2-ol	*	603**								x		
4	1219	Pent-1-en-3-ol	*	680**						x	x		x	
5	1235	Pent-1-en-3-one	*	682**							x	x	x	x
6	1263	Pent-3-one	*	694**	x	x	x	x	x	x	x	x	x	x
7	1286	2-Ethyl-furan	*	707**			x	x		x	x	x	x	x
8	1436	*trans*-Pent-2-enal	*	754**									x	x
9	1466	*cis*-Pent-2-en-1-ol	*	765**						x	x	x	x	x
10	1501	Toluene	*	774**	x	x				x	x	x	x	
11	1557	*cis*-Hex-3-enal	*	800**			x	x	x	x	x	x	x	x
12	1563	Hexanal	*	802									x	x
13	1696	Hex-2-enal (isomer)	*	855							x	x	x	x
14	1705	*trans*-Hex-3-en-1-ol	*	854							x	x	x	x
15	1721	*cis*-Hex-3-en-1-ol	*	859	x	x	x	x	x	x	x	x	x	x
16	1745	Hexan-1-ol	*	871	x		x		x	x	x	x	x	x
17	1865	*cis*-2-Pentenyl acetate	*	892**	x				x	x	x	x	x	
18	1884	*trans,trans*-Hex-2,4-dienal	*	910			x	x		x	x	x	x	x
19	1889	3-Methylbut-3-enyl acetate	*	885								x		
20	1954	α-Thujene	905	930	x	x	x	x	x	x	x	x	x	x

Table 3.4 - Peak identification after HS-SPME-1D-GC/TOFMS analysis, with calculated and literature retention data (Adams, 2001) (cont.).

					Pinus species									
Peak No.	RT	Compound	RI_{calc} §	RI_{Lit} §§	PE	PH	PP	PK	PPr	PPa	PN	PR	PS	PB
21	1967	Tricyclene	913	927	x		x	x	x	x	x	x	x	x
22	1993	α-Pinene	929	939	x	x	x	x	x	x	x	x	x	x
23	2035	α-Fenchene	956	953	x		x	x	x		x		x	x
24	2044	Camphene	962	954	x	x	x	x	x	x	x	x	x	x
25	2054	2-Ethylbutenolide	968											x
26	2084	Sabinene	986	975		x		x				x	x	
27	2093	Myrcene	992	991	x	x	x	x	x	x	x	x	x	x
28	2103	3 Hexenyl acetate (isomer)	998	1002	x		x		x	x	x	x	x	
29	2106	Decane	1000	1000	x		x			x		x	x	
30	2115	3 Hexenyl acetate (isomer)	1004	1005	x	x	x	x	x	x	x	x	x	x
31	2119	β-Pinene	1005	979	x	x	x	x	x	x	x	x	x	x
32	2126	hexyl acetate	1008	1009			x	x	x	x	x	x	x	tr
33	2133	*cis*-4-hexenyl acetate	1011									x		
34	2154	n.i. (acetate)	1020									x		
35	2160	Δ-2-Carene	1022	1002									x	
36	2168	α-Phellandrene	1025	1003	x	x	x	x	x	x	x	x	x	x
37	2188	3-Carene	1034	1011***	x	x	x	x	x	x	x	x	x	x
38	2196	α-Terpinene	1037	1015	x	x	x	x	x	x	x	x	x	x
39	2203	*cis*-Ocimene	1040	1037	x	x	x	x	x	x	x	x	x	x
40	2208	1,4-Dichlorobenzene	1041	1014			x	x	x	x		x		

Table 3.4 - Peak identification after HS-SPME-1D-GC/TOFMS analysis, with calculated and literature retention data (Adams, 2001) (cont.).

					Pinus species									
Peak No.	RT	Compound	RI_{calc} §	RI_{Lit} §§	PE	PH	PP	PK	PPr	PPa	PN	PR	PS	PB
41	2214	Cymene (isomer)	1044	1025	x	x	x	x	x	x	x	x	x	x
42	2223	Sylvestrene	1048	1031									x	
43	2229	Limonene	1050	1029	x	x	x	x	x	x	x	x	x	x
44	2233	Artemisia ketone /5-Ethyl-2(*5H*)-furanone	1052	1062/984**									x	x
45	2236	*trans*-Ocimene	1053	1050		x	x		x	x	x		x	x
46	2242	*β*-Phellandrene	1055	1030	x	x	x	x	x	x	x	x	x	x
47	2249	1,8-Cineole	1058	1031	x	x		x	x	x	x	x	x	x
48	2280	Artemisia alcohol /5-Ethyl-dihydro-2(*3H*)-furanone	1071	1084/1010**									x	
49	2285	n.i.	1073										x	
50	2294	Cymene (isomer)	1077										x	
51	2295	*γ*-Terpinene	1077	1060	x	x	x	x	x	x	x	x	x	x
52	2329	n.i.	1091							x				
53	2351	Undecane	1100	1100	x		x	x	x	x	x			
54	2352	Cymenene (isomer)	1100	1085									x	
55	2362	Butanoic acid 3-methyl-pentyl ester	1105	1108 **					x					
56	2366	Linalool	1106	1097	x	x			x	x	x			x
57	2366	*Iso*-Terpinolene	1107	1088									x	
58	2374	Isopropen-1-yl-2-methylbenzene	1110								x			
59	2375	Terpinolene	1110	1089	x	x	x	x	x	x	x	x	x	x
60	2379	Perillene	1113	1101										x

Table 3.4 - Peak identification after HS-SPME-1D-GC/TOFMS analysis, with calculated and literature retention data (Adams, 2001) (cont.).

					Pinus species									
Peak No.	RT	Compound	RI_{calc} [§]	RI_{Lit} [§§]	PE	PH	PP	PK	PPr	PPa	PN	PR	PS	PB
61	2433	n.i.	1136				x							
62	2434	Alloocimene	1137	1132					x	x	x			x
63	2437	2-Phenethyl alcohol	1138	1107							x			
64	2454	2,6-Dimethyl-1,3,5,7-octatetraene (isomer)	1145						x	x	x		x	x
65	2472	*Neo*-alloocimene	1154	1144					x	x	x		x	x
66	2499	Limonene oxide (isomer)	1165	1073									x	
67	2507	*trans*-Verbenol	1169	1145									x	
68	2571	Decan-2-one	1197	1192									x	
69	2578	Pinocamphone	1200	1163	x			x	x		x		x	
70	2578	n.i.	1200										x	
71	2582	Pinocarvone	1203	1165										x
72	2582	*meta*-Cymen-8-ol	1203	1180							x		x	
73	2592	*endo*-Borneol	1207	1169	x		x	x			x		x	
74	2598	*p*-Cymen-8-ol	1210	1183			x	x					x	
75	2600	4-Terpineol	1211	1177	x	x	x	x			x	x	x	x
76	2604	Decanal	1213	1202	x									
77	2613	*p*-Methylacetophenone	1217	1183									x	
78	2615	Isopinocamphone	1218	1175								x		
79	2622	α-Terpineol	1221	1189	x	x			x	x	x	x		x
80	2631	Cryptone	1225	1186				x						

Table 3.4 - Peak identification after HS-SPME-1D-GC/TOFMS analysis, with calculated and literature retention data (Adams, 2001) (cont.).

					Pinus species									
Peak No.	RT	Compound	RI_{calc} [§]	RI_{Lit} [§§]	PE	PH	PP	PK	PPr	PPa	PN	PR	PS	PB
81	2639	Salicilic acid methyl ester	1229	1192										x
82	2646	Myrtenol	1232	1196										x
83	2656	Pentanoic acid (*Z*)-hexen-3-yl ester	1237						x			tr		
84	2657	Naphthalene	1238	1181					x	x			tr	x
85	2659	Myrtenal	1239	1196							x			x
86	2660	3-Methylbutanoic acid (*Z*)-hexen-3-yl ester	1239	1186					x					
87	2673	Isovaleric acid hexyl ester	1245						x					
88	2684	Thymol methyl ether	1250	1235			x		x		x		x	x
89	2687	Verbenone	1252	1205								x		
90	2705	Linalyl acetate	1260		x				x		x			
91	2712	Undecan-2-one (isomer)	1263										x	
92	2736	Decan-1-ol	1275	1270	x									
93	2726	n.i.	1270							x				
94	2737	Sabinene hydrate acetate (isomer)	1275	1256									x	
95	2739	2-phenylethyl acetate	1276						x		x			x
96	2743	n.i.	1278							x				
97	2763	n.i.	1287		x									
98	2761	2-Octenyl acetate	1286										x	
99	2769	n.i.	1290										x	
100	2774	Piperitone	1292	1253					x		x			

Table 3.4 - Peak identification after HS-SPME-1D-GC/TOFMS analysis, with calculated and literature retention data (Adams, 2001) (cont.).

					Pinus species									
Peak No.	RT	Compound	RI_{calc} §	RI_{Lit} §§	PE	PH	PP	PK	PPr	PPa	PN	PR	PS	PB
101	2788	Undecan-2-one	1299	1294									x	
102	2790	Tridecane	1300	1300			x							
103	2810	Acetic acid ester compound	1309								x			
104	2818	Acetic acid ester compound	1314								x			
105	2828	Acetic acid endo bornyl ester	1319	1289	x	x	x		x		x		x	x
106	2838	Acetic acid ester compound	1324	1257					x					
107	2842	Acetic acid ester compound	1326								x			
108	2849	*trans*-Pinocarvyl acetate	1330	1312							x			x
109	2869	n.i.	1340								x			
110	2882	*Iso*-ascaridole	1346	1303									x	
111	2898	Acetic acid ester compound	1354						x		x			
112	2898	n.i.	1355				x							
113	2899	n.i.	1355				x							
114	2904	Acetic acid ester compound	1358						x					
115	2910	n.i. (Sesquiterpene)	1360								x			
116	2913	Acetic acid ester compound	1362										x	
117	2917	Acetic acid ester compound	1364								x			x
118	2921	Neryl acetate	1366	1362					x		x			x
119	2928	n.i. (Sesquiterpene)	1370		x				x		x			x
120	2939	α-Terpinenyl acetate	1375	1349	x	x	x				x		x	x

Table 3.4 - Peak identification after HS-SPME-1D-GC/TOFMS analysis, with calculated and literature retention data (Adams, 2001) (cont.).

					Pinus species									
Peak No.	RT	Compound	RI_{calc} §	RI_{Lit} §§	PE	PH	PP	PK	PPr	PPa	PN	PR	PS	PB
121	2957	Geranyl acetate	1385	1381		x	x		x		x			x
122	2967	n.i. (Sesquiterpene)	1389		x	x	x	x	x		x		x	x
123	3009	α-Longipinene	1411	1353			x		x	x				
124	3018	Methyl eugenol	1417	1404	x				x		tr			
125	3019	Dodecanal	1417	1409	x									
126	3025	Butanoic acid 2-phenylethyl ester	1420	1441		x			x		x			
127	3029	n.i. (Sesquiterpene)	1422		x		x		x		x		x	x
128	3037	n.i. (Sesquiterpene)	1427		x	x	x	x	x		x		x	x
129	3038	n.i.	1428		x								x	
130	3049	n.i.	1434		x									x
131	3050	β-Elemene	1434	1391	x		x	x	x		x	x	x	x
132	3055	n.i. (Sesquiterpene)	1437		x		x		x		x		x	x
133	3065	n.i.	1443										x	
134	3066	β-Bourbonene	1443	1388	x		coelution	x	coelution		coelution		x	x
135	3078	Acetic acid non-2-enyl ester	1449										x	
136	3086	sesquiterpene	1454				x							
137	3112	β-Farnesene (isomer)	1468		x	x	x	x	x		x		x	
138	3120	α-Bergamotene (isomer)	1473		x						x			
139	3129	n.i. (Sesquiterpene)	1478		x	x	x	x	x		x	x	x	x
140	3142	*trans*-Caryophyllene	1485	1409	x	x	x	x	x	x	x	x	x	x

Table 3.4 - Peak identification after HS-SPME-1D-GC/TOFMS analysis, with calculated and literature retention data (Adams, 2001) (cont.).

					Pinus species									
Peak No.	RT	Compound	RI_{calc} [§]	RI_{Lit} [§§]	PE	PH	PP	PK	PPr	PPa	PN	PR	PS	PB
141	3149	n.i. (Sesquiterpene)	1489		x		x	x	x		x		x	x
142	3156	n.i.	1493			x	x							
143	3170	n.i. (Sesquiterpene)	1501				x		x		x		x	x
144	3178	n.i. (Sesquiterpene)	1505		x		x		x		x		x	x
145	3183	n.i.	1508				x							
146	3186	n.i. (Sesquiterpene)	1510		x				x		x		x	
147	3197	n.i.	1516								x		x	
148	3200	n.i.	1518		x						x			x
149	3203	α-Caryophyllene	1519	1455	x	x	x	x	x	x	x		x	x
150	3204	Phenylethyl ester	1520			x			x	x	x			x
151	3204	Phenylethyl ester	1520											
152	3212	n.i. (Sesquiterpene)	1525				x				x		x	x
153	3215	n.i. (Sesquiterpene)	1526		x						x		x	
154	3217	n.i. (Sesquiterpene)	1527		x	x	x	x	x		x		x	x
155	3221	n.i. (Sesquiterpene)	1530										x	
156	3224	n.i.	1532				x							
157	3225	n.i.	1532							x				
158	3229	n.i. (Sesquiterpene)	1534				x							
159	3233	n.i. (Sesquiterpene)	1536		x									
160	3234	n.i.	1537			x	x				x		x	
161	3235	n.i.	1538			x	x	x					x	

Table 3.4 - Peak identification after HS-SPME-1D-GC/TOFMS analysis, with calculated and literature retention data (Adams, 2001) (cont.).

					Pinus species									
Peak No.	RT	Compound	RI_{calc} [§]	RI_{Lit} [§§]	PE	PH	PP	PK	PPr	PPa	PN	PR	PS	PB
162	3242	n.i. (Sesquiterpene)	1542								x		x	
163	3253	n.i. (Sesquiterpene)	1548			x	x	x	x		x		x	x
164	3263	n.i. (Sesquiterpene)	1554		x		x	x			x		x	x
165	3264	n.i. (Sesquiterpene)	1555				x		x					
166	3273	n.i. (Sesquiterpene)	1559		x	x	x	x	x		x		x	
167	3280	n.i.	1564		x									x
168	3290	n.i. (Sesquiterpene)	1569		x	x	x	x	x	x	x	x	x	x
169	3298	n.i. (Sesquiterpene)	1574						x		x		x	
170	3302	*cis*-Calamenene	1576	1529			x		x	x	x		x	x
171	3307	n.i. (Sesquiterpene)	1579						x					
172	3308	*trans*-Calamenene	1580	1540					x	x	x		x	x
173	3321	n.i. (Sesquiterpene)	1587		x		x		x		x		x	x
174	3328	Cadinene isomer	1591				x	x	x		x		x	x
175	3349	*β*-Calacorene	1602	1566							x		x	
176	3358	Germacrene D-4-ol	1607	1576	x								x	
177	3436	n.i.	1648										x	

[§]RI_{calc}, [§§]RI_{Lit} - calculated and literature retention index data, respectively. The calculated retention indices were obtained based on retention times across the column. Peaks were identified based on the comparison (similarity) of their mass spectra to reference mass spectral databases (Mass Spectra Library NIST version 2.0, 2005 and Wiley Registry of Mass Spectral Data 7th edition, 2000) and retention indices (Adams, 2001). x indicates compound found in the samples.

Pinus species key: PE - *P. elliottii*; PH - *P. halepensis*; PP - *P. patula*; PK - *P. kesiya*; PPr - *P. pinaster*; PPa - *P. pinea*; PN - *P. nigra*; PR - *P. radiata*; PS - *P. sylvestris*; PB - *P. brutia*. All the peaks have a match quality spectrum better than 80%, at least in one of the species.
*Value not determined due to the absence of hydrocarbon lower than C9 (*n*-nonane); **RI_{Lit} - Data not referred in Adams (2001) and thus obtained from NIST, for equivalent columns and similar operational conditions; tr – trace amounts.

3.1.1.3. Comprehensive two-dimensional gas chromatography/time-of-flight mass spectrometry

Pinus spp. *composite sample*

The *Pinus* spp. composite sample was analyzed by comprehensive two-dimensional gas chromatography/time-of-flight mass spectrometry (GC × GC/TOFMS), and the data processed with a signal-to-noise (S/N) threshold value of 10, to maximize the detection of trace compounds. For data processing it was assumed that no spectral skew is verified during the acquisition of the mass spectra (Mateus *et al.*, 2008). Consequently, true peak finding, mass spectral deconvolution of coeluted analytes and library searching of the "true" mass spectra of individual peaks, against mass spectral database libraries, was done automatically by the ChromaTof software.

Figure 3.14 A) and B) shows the reconstructed first dimension total current chromatogram and the correspondent GC × GC contour plot chromatogram, obtained for the *Pinus* spp. composite sample. The purpose of the reconstructed 1-D chromatogram in Figure 3.14 A) is to allow for the comparison with conventional 1D-GC chromatograms, which are obtained in similar first dimension columns. In Figure 3.14 B), the X-axis represents the first dimension separation retention times, in seconds, which correspond to the reconstructed 1-D chromatogram in Figure 3.14 A). The Y-axis represents the separation retention times of the second column, in seconds, obtained for each fraction of 5 seconds of the first dimension modulation. The analyte separation on the contour plot chromatogram is a result of the orthogonal separation of the two chromatographic phases and is essentially a reflection of sample analytes on the coordinates volatility versus polarity (DB-5 versus BPX-50).

For the used column set, the least polar compounds, the linear hydrocarbons (alkanes), elute first on the second-dimension column. The other analytes elute latter, according to their polarity, and are expected to be found in the upper part of the hydrocarbons band. However, some compounds with higher polarity may have a retention time, on the second dimension, larger that the modulation period and, consequently, will elute during the second, or even third modulation period, after being introduced on the second column.

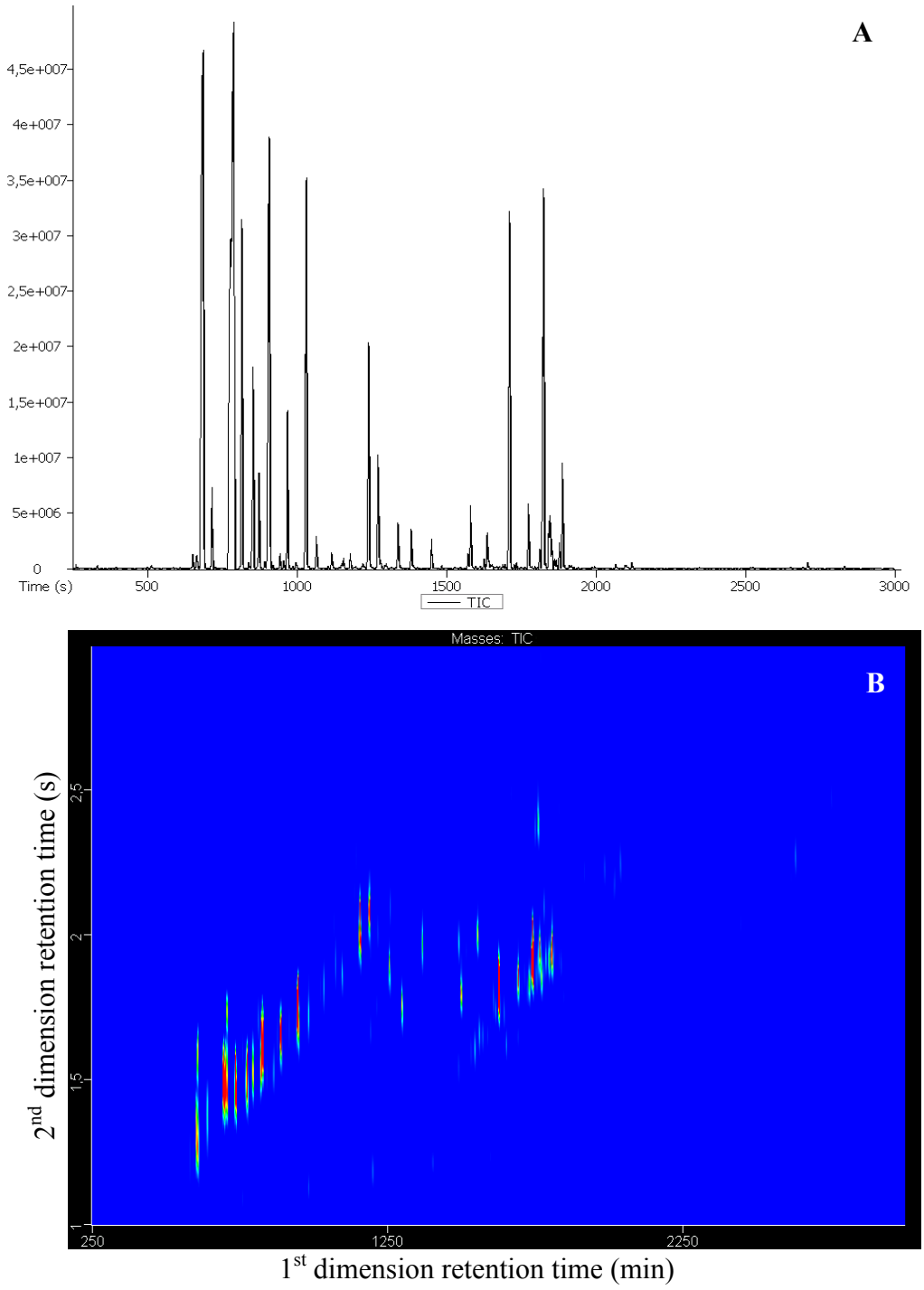

Figure 3.14 - Total current chromatograms for the *Pinus* spp. composite sample: **A)** reconstructed first dimension total current chromatogram; **B)** GC × GC contour plot chromatogram.

These compounds are usually found on GC × GC chromatograms under the alkane/ hydrocarbon band. This phenomenon is called "wrap-around" and the peaks under its effect, if overlapping other peaks, may affect the qualitative analysis of the sample. It can be avoided using longer modulation periods, but longer modulation periods lead to lower chromatographic resolution on the first column (D1).

The first results of the processed raw data resulted in the detection of over 2000 peaks. A preliminary analysis of the results showed that the majority of the peaks detected were baseline noise components, such as siloxanes/silanols from column phase bleeding, and artifact peaks from the modulation of the solvent peak tailing, together with hydrocarbons that probably come from the sample solvent. However, these interferences, due to the resolving power of the technique, were totally separated from the potential components of the essential oil, as observed in Figures 3.15 and 3.16, and thus allowing for the obtention of clear analyte spectra.

A reprocess of the sample at S/N of 50 resulted in the detection of 500 peaks. An additional processing was conducted in order to remove the siloxanes/silanols and the hydrocarbons that were still detected. The analysis of the remaining peaks led to the assignement of 200 analytes that were tentatively identified, including monoterpenes, oxygenated monoterpenes, sesquiterpenes, oxygenated sesquiterpenes, diterpenes, aldehydes, ketones and esters.

The peaks of the major monoterpenes α-pinene and β-pinene, in spite of a 1:100 split ratio, are deformed due to their overload in the chromatographic column. This can be observed on Figure 3.14 B), with both monoterpene peaks appearing with a double contour. As the two monoterpenes are well known components of all pine species, it was decided not to correct this problem, using higher split rations, in order to maximize the detectability of the minor components present in the composite sample. Nevertheless, the identification α-pinene and β-pinene was also achieved.

A preliminar analysis of the contour plot chromatogram that was performed by means of a single ion extraction in order to detect the monoterpenes (m/z 93 or m/z 136), sesquiterpenes (m/z 204) and diterpenes (m/z 272), resulted in their visualization as isolated structured clusters, according to their common mass spectral attributes, as presented in Figure 3.17.

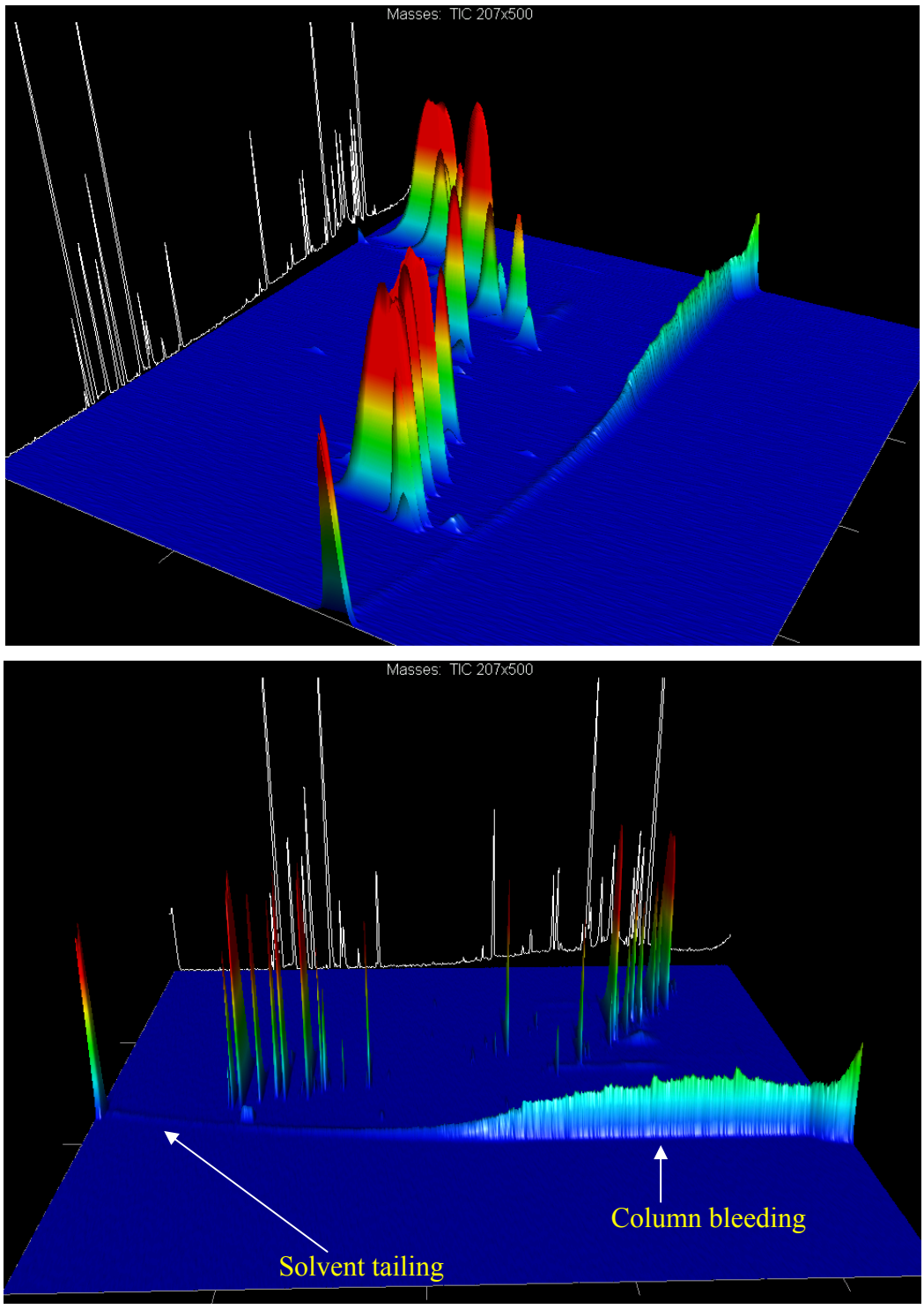

Figure 3.15 - GC × GC/TOFMS 3D surface plots obtained for the analysis of the *Pinus* spp. composite sample. The intensity of m/z 207 was magnified on the Z-axis, in order to allow the observation of the column bleeding separation from the remaining analytes.

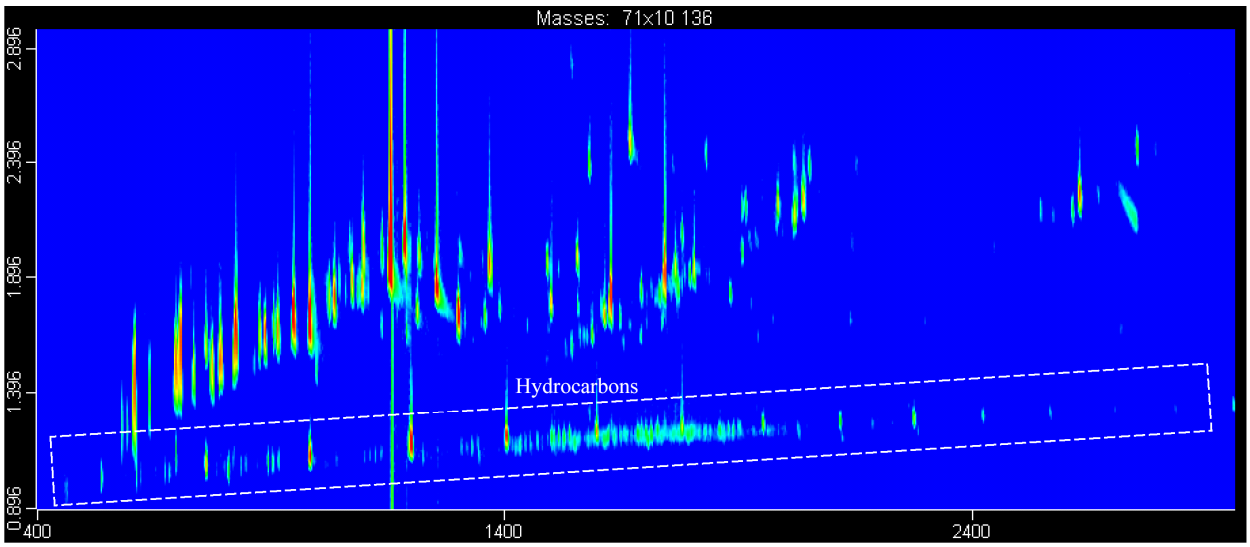

Figure 3.16 - GC × GC/TOFMS contour plot obtained for the analysis of the *Pinus* spp. composite sample showing the separation between the alkanes/hydrocarbons band (plotted by extraction of characteristic m/z 71) and the terpene compounds (plotted by extraction of m/z 136).

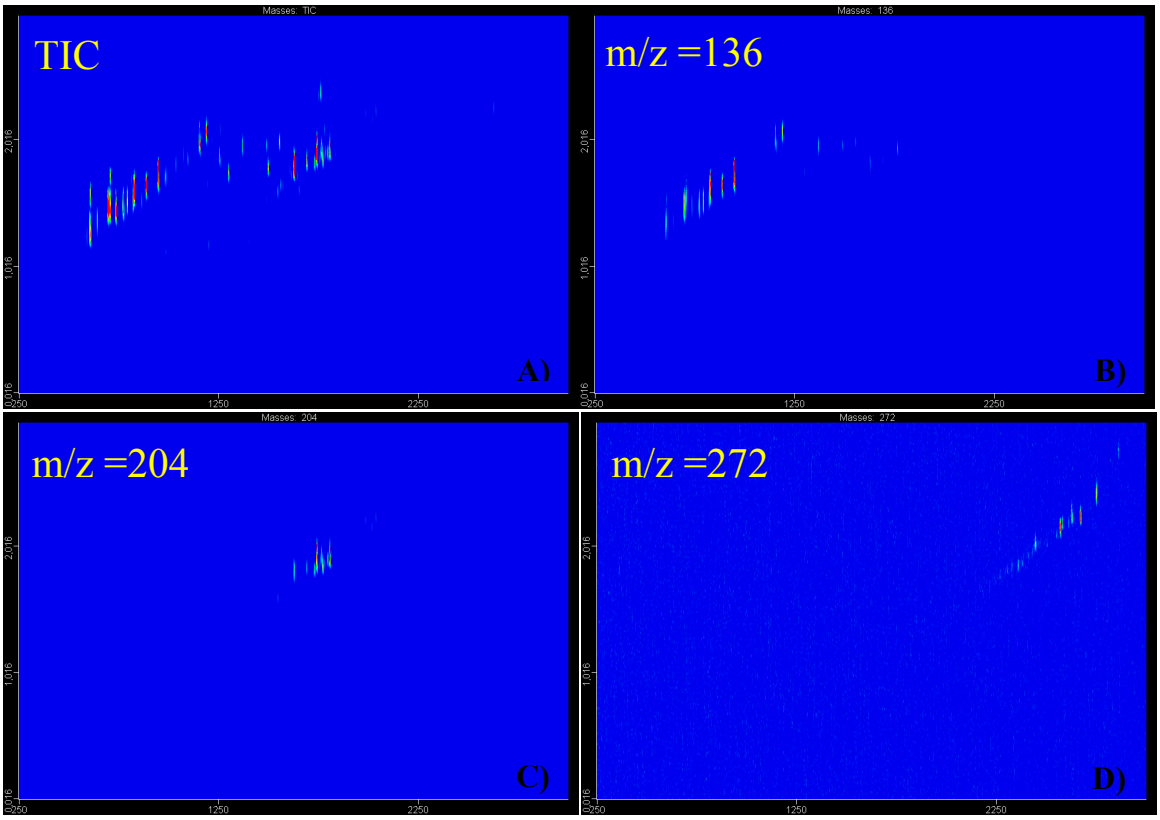

Figure 3.17 – GC × GC/TOFMS total ion chromatogram and structured ion chromatograms for terpene compounds. **A)** total ion contour plot chromatogram; **B)** monoterpenes cluster after m/z 136 extraction; **C)** sesquiterpenes cluster after m/z 204 extraction and **D)** diterpenes cluster after m/z 272 extraction.

These structured chromatograms, a result of the orthogonal separation mechanisms in GC × GC, open the possibility of spatially classifying the compounds according to their chemical classes and, therefore, to be a useful tool for analyte detection and identification purposes on the contour plot chromatograms. An example can also be visualized in Figure 3.16, with the total separation of the terpenes, based on their polarity, in the second dimension from the hydrocarbons (m/z 71).

The detailed view of the terpene bands also allows for the visualization on the second dimension (polarity) of compounds that were coeluting in the first dimension (volatility). Figure 3.18 A) presents the same 18 seconds section described before for the 1D-GC/TOFMS analysis, in which the TIC only shows one defined peak that hides a coelution of 4 compounds. On GC × GC (Figure 3.18 B), due to the different polarities of the analytes, they were separated on the second dimension with a higher chromatographic resolution than in 1D-GC.

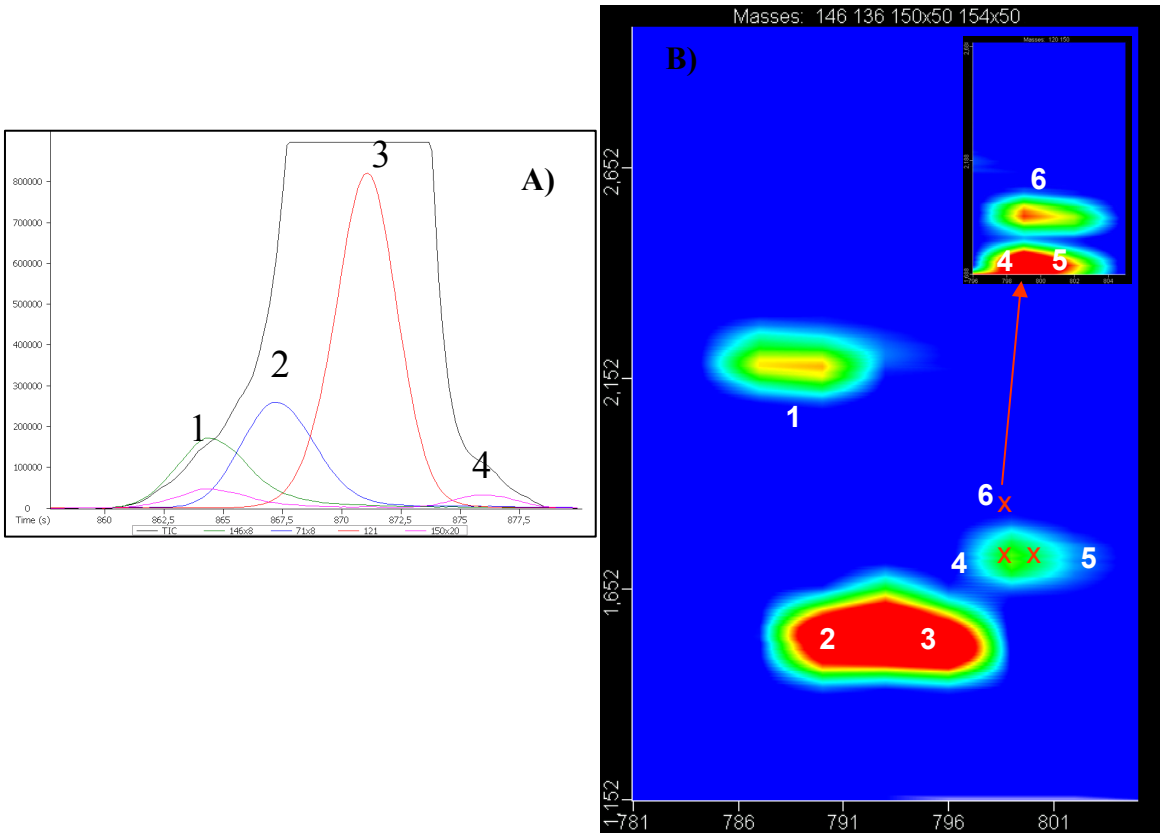

Figure 3.18 - Comparison of separation and detection of selected analytes from the *Pinus* spp. composite sample in two GC systems: **A)** 1D-GC/TOFMS system and **B)** GC × GC/TOFMS system. Marked compounds on A): 1 – dichlorobenzene isomer; 2 – 1,4-cineol; 3 – *α*-terpinene; 4 – unknown. Marked compounds on B): 1 – dichlorobenzene isomer; 2 – 1,4-cineol; 3 – *α*-terpinene; 4 – disulfite isopropyl; 5 – *o*-cimene and 6 – trimethylbenzene (pseudocumene).

Regarding peak 4, in Figure 3.18 A), it was not considered identified in the 1D-GC system, due to a low spectral match given by the library database search. In GC × GC, the peak 4 from the 1D-GC analysis, was shown to be composed of three individual compounds, peaks 4, 5 and 6, which are now separated on the second dimension. Compounds 4 and 5, on GC × GC, partially coelute on the first dimension, but are successfully deconvoluted and tentatively identified under the experimental conditions. Peak 5 is present at low concentration, but due to the improvement of its S/N ratio, a consequence of its re-focusing by the modulator, it achieved then a better separation from the system noise than on the 1D-GC, and a mass spectra record, which allowed its tentative identification. The similarities achieved by library database search were 956 for peak 1, 871 for peak 2, 895 for peak 3, 817 for peak 4, 856 for peak 6 and 430 for peak 5. A survey on the Adams data base (2001) allowed the assignment of compounds identification with their retention index (RI): 1,4-dichlorobenzene (RI = 1014), 1,4-cineol (RI = 1015), α-terpinene (RI = 1017), cymene isomer (RI = 1025) and trimethylbenzene (RI = 1026). The isopropyl disulfite was not registered at Adams database (2001). Concerning peak 5, the hypothesis of a cymene isomer presence can be assigned, based on the Adams data and the existence of cymene m/z 119 and 134 on the deconvoluted mass spectra, in spite of the low spectral similarity achieved for Wiley spectral database (2000).

Another consequence of GC × GC is the increase of the signal to noise ratio (S/N) for all the analyte peaks. The increased S/N, together with the enhaced resolving power of GC × GC, maximizes the purity of the obtained mass spectra, allowing for a more accurate identification of the sample compounds. An example is presented in Figures 3.20 and 3.21**,** for piperitone. The piperitone peak, number 3 in Figure 3.20 A), elutes on 1D-GC/TOFMS in a cluster of 4 peaks. In spite of the coelutions the extracted spectra allow for its identification, with a similarity factor of 849, as shown in Figure 3.21(left). The analysis of same section by GC × GC, as shown in Figure 3.20 B), allows for the identification of 6 compounds, in the same cluster, that are clearly separated on the second dimension. Piperitone was isolated from the other peaks, allowing the extraction of a more accurate mass spectrum, which allow for its identification, with a similarity factor of 955 (Figure 3.21; right).

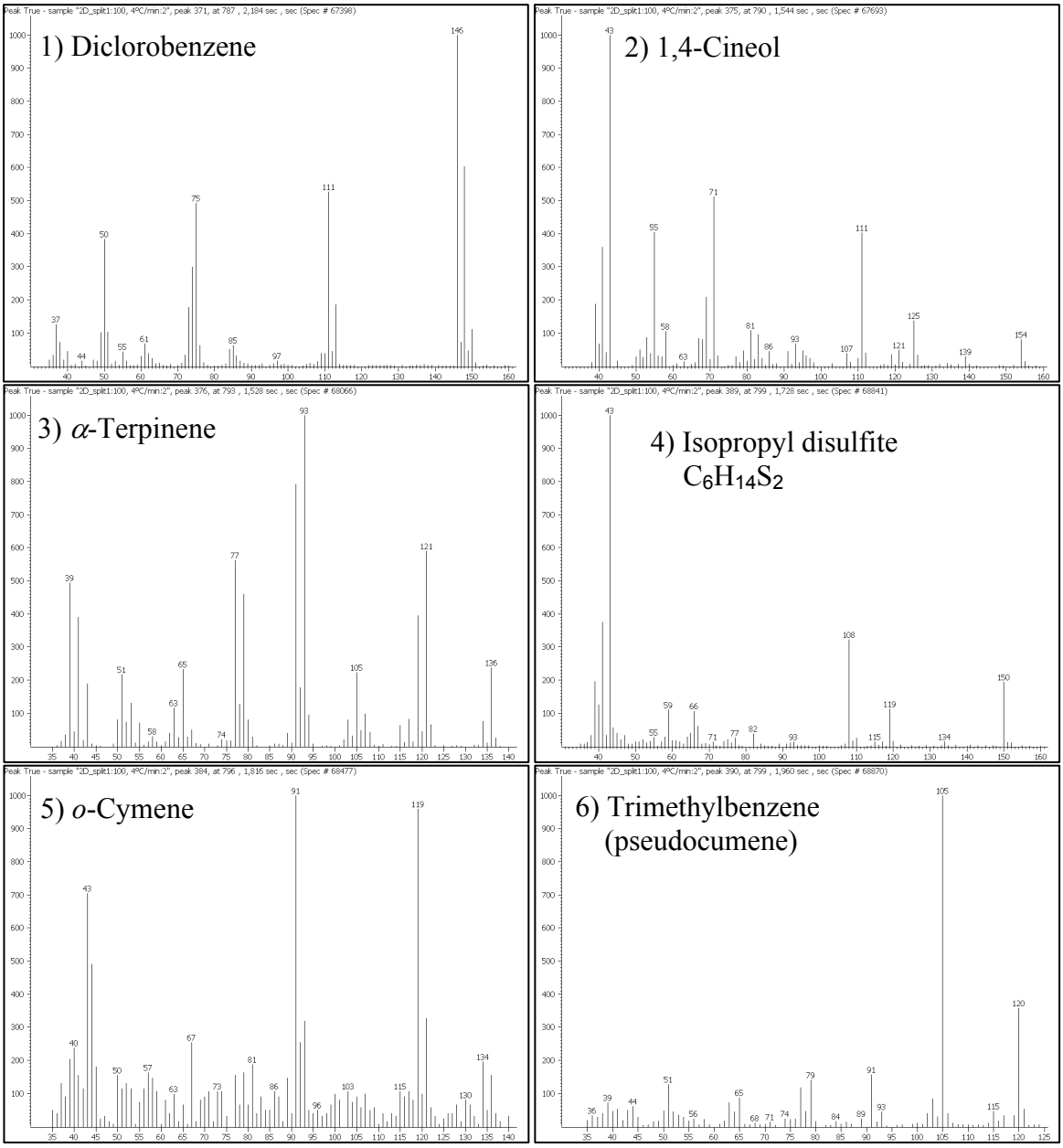

Figure 3.19 - Mass spectra of peaks 1 to 6 from Figure 3.18.

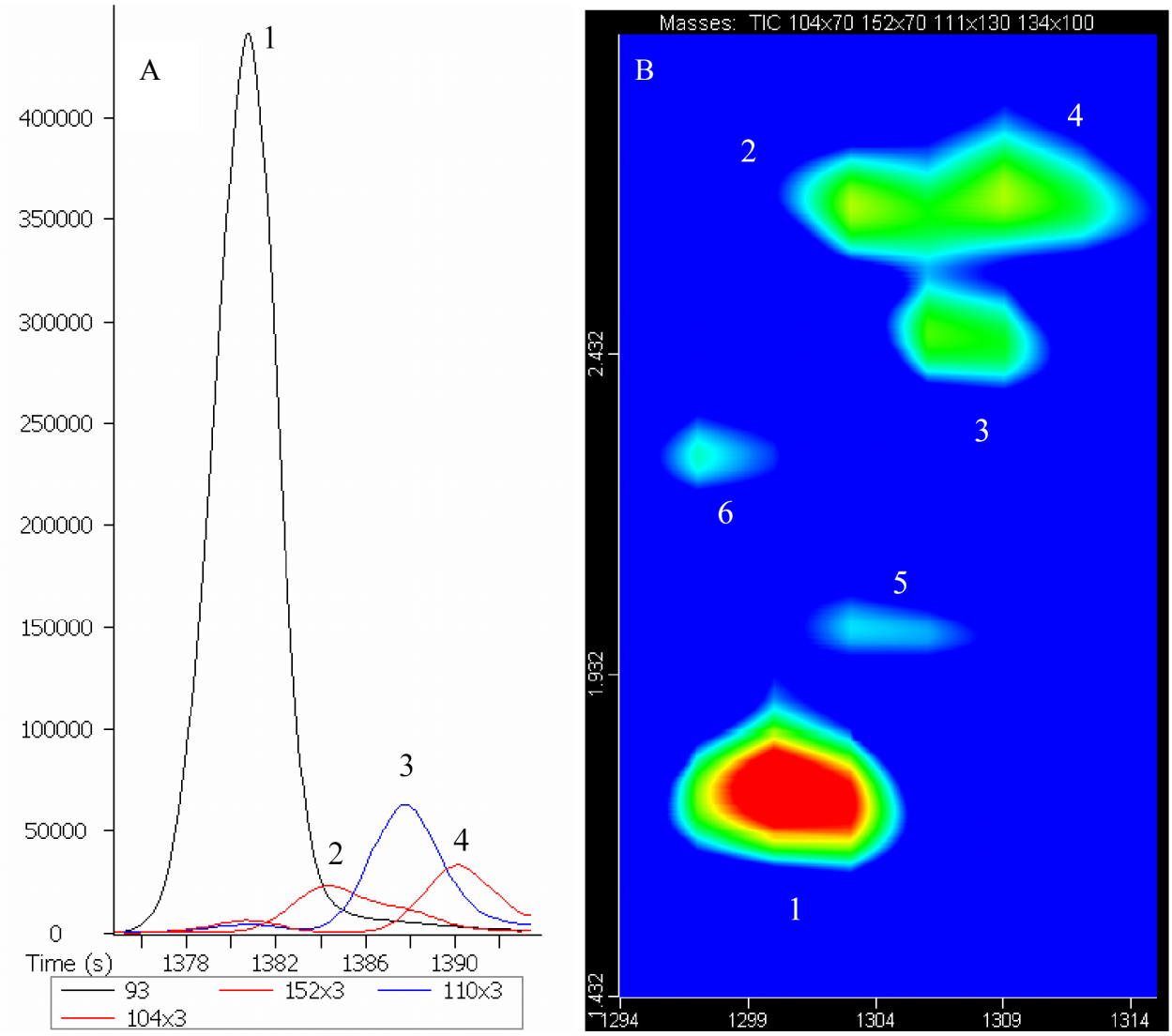

Figure 3.20 - Comparison of separation and detection of selected analytes from the *Pinus* spp. composite sample in two GC systems. **A)** 1D-GC/TOFMS system and **B)** GC × GC/TOFMS system. Peaks: 1 – linalyl acetate; 2 – 2,4-dimethoxytoluene; 3 – piperitone; 4 – 2-phenyl ethyl acetate; 5 – *trans*-geraniol; 6 – oxygenated monoterpene (S/N<50).

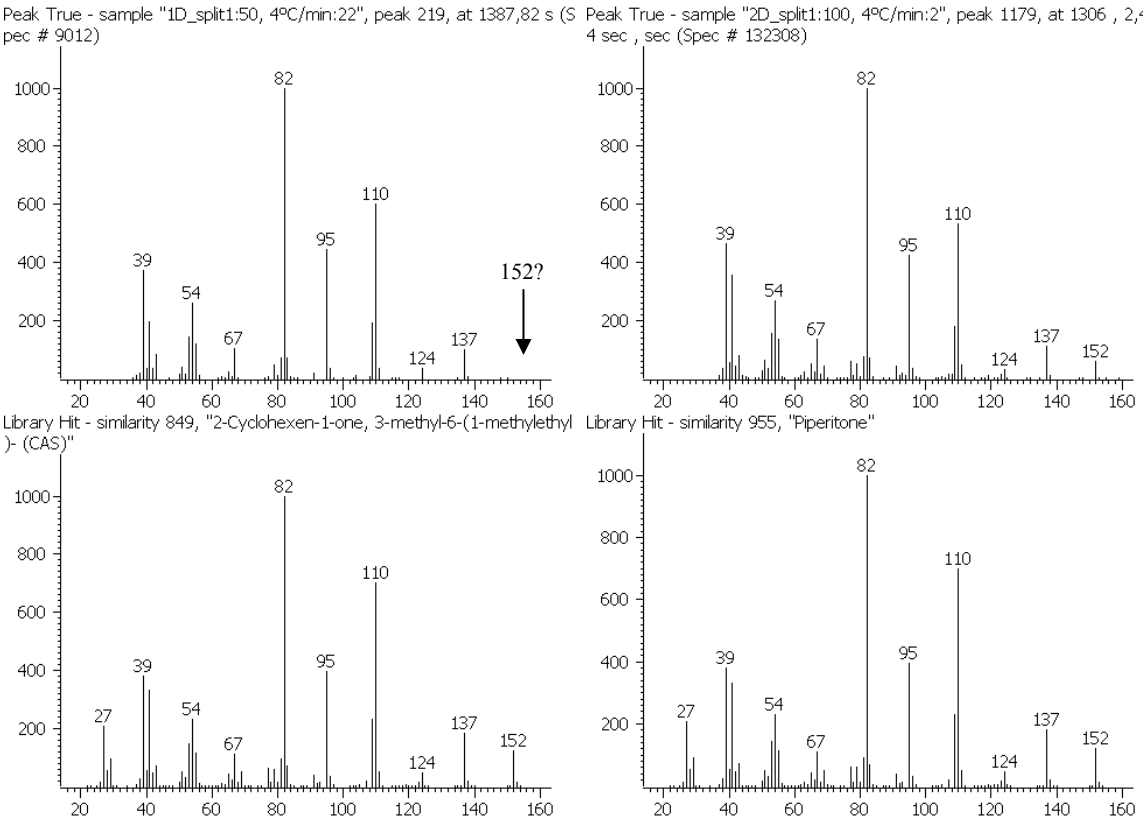

Figure 3.21 - Mass spectra of piperitone in 1D-GC/TOFMS (top left) and GC × GC/TOFMS (top right). The similarity factors obtain for piperitone, in each technique, are shown in the headers of library spectra (bottom left and right).

An unexpected achievement with the application of GC × GC concerns the degradation of sesquiterpenes, observed with the 60 m length non polar column, whose interconversion bands appear isolated from the sesquiterpene peaks on the second dimension.

An example is shown in Figure 3.22 where the slope of the degradation, observed in the linear chromatogram, form a distinct spot in the 2D plot. Figure 3.23 shows a wide view of the sesquiterpene retention time domain with 3 zones of degradation visible and the corresponding mass spectra obtained for each band that presented good similarities with the reference spectra of sesquiterpenes. These findings promote the acquisition of mass spectra free of artifact that allow for better qualitative sample chemical information.

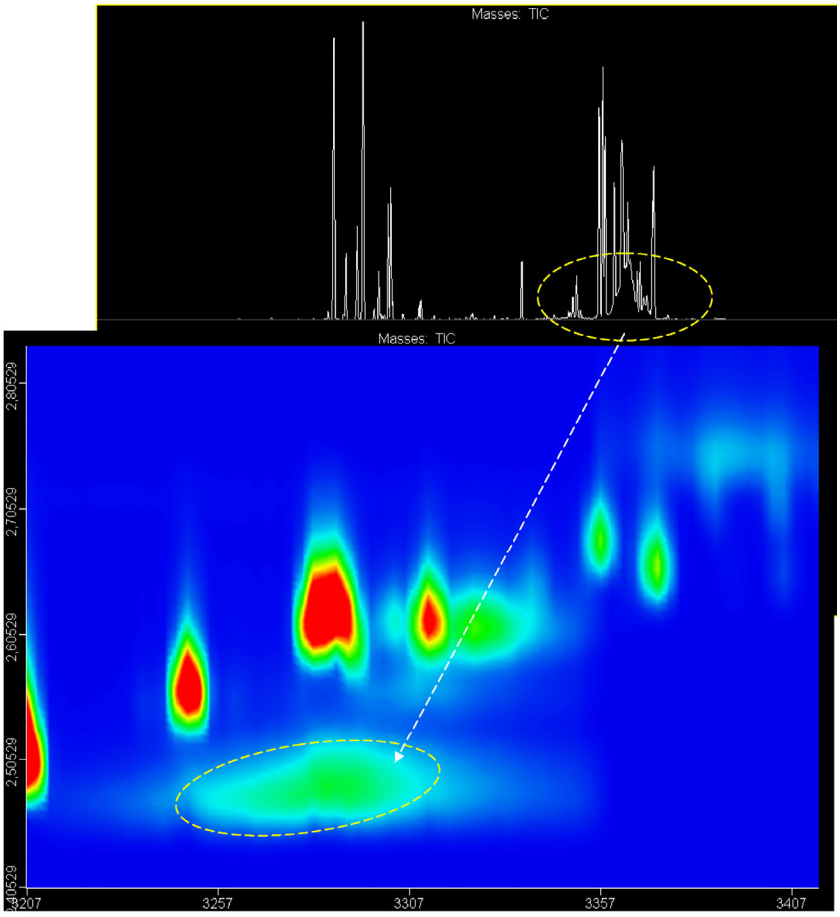

Figure 3.22 – Comparison of 1D chromatogram with the GC × GC contour plot for the degradation zone observed in the sesquiterpenes retention time domain (operational conditions according to Table 2.12).

Table 3.5 presents the volatile compounds tentatively identified by GC × GC/TOFMS analysis in *Pinus* spp. composite sample.

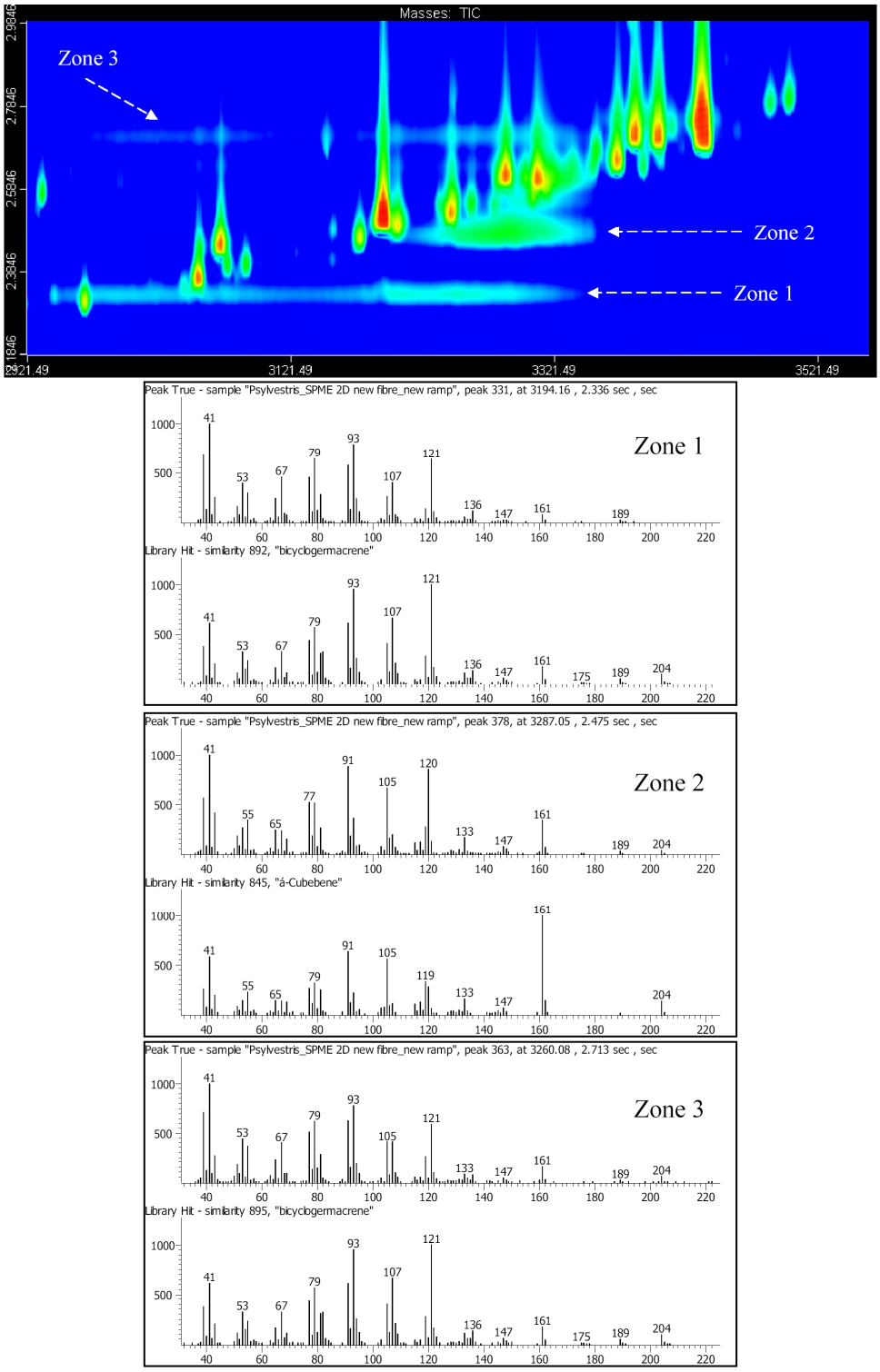

Figure 3.23 – Detail of GC × GC contour plot for the sesquiterpenes retention time domain showing 3 zones of degradation and the corresponding mass spectra obtained for each one (operational conditions according to Table 2.12).

Table 3.5 - Volatile compounds tentatively identified by GC × GC/TOFMS analyis in *Pinus* spp. composite sample.

Peak No..	$^{1}t_R$*	$^{2}t_R$**	Compound	Similarity	RI_{calc} §	RI_{Lit} §§	Compound class
1	289	1.352	Toluene	929	-	-	MA
2	340	0.928	Octane	901	800	800	HC
3	349	1.464	Hexanal	650	805	802	CC
4	436	1.384	2-Methyl-butanoic acid ethyl ester	865	848	-	E
5	454	1.592	3-Hexen-1-ol	860	858	854	AL
6	472	1.608	*p*-Xylene	807	867	-	MA
7	496	1.224	Santene	838	879	889	M
8	538	1.040	Nonane	962	900	900	HC
9	574	2.176	Anisole	644	916	918	MA
10	580	1.200	Tricyclene	943	919	927	M
11	592	1.248	α-Thujene	908	924	930	M
12	607	1.360	α-Pinene	941	931	939	M
13	640	1.384	Camphene	960	946	954	M
14	652	1.456	Verbenene	849	951	968	M
15	694	1.496	Sabinene	930	970	975	M
16	709	1.520	β-Pinene	931	977	979	M
17	730	1.904	6-Methyl-hept-5-en-2-one	854	986	986	CC
18	736	1.456	Myrcene	938	989	991	M
19	742	1.776	1,3,5-Trimethyl-benzene	900	992	996	MA
20	757	1.576	Hexanoic acid ethyl ester	945	999	998	E
21	760	1.096	Decane	930	1000	1000	HC
22	769	1.520	α-Phellandrene	899	1004	1003	M
23	775	1.800	*Z*-Hex-3-en-1-ol acetate	930	1007	1005	E
24	787	2.184	1,3-Dichloro-benzene	956	1012	1014	A
25	790	1.544	1,4-Cineole	871	1013	1015	OM
26	793	1.528	α-Terpinene	895	1015	1017	M
27	799	1.696	1-Methylethyl propyl disulfide	817	1017	-	S
28	799	1.960	1,2,4-Trimethyl-benzene	827	1017	1026	MA
29	802	1.696	***m***-Cymene	707	1019	1025	MA
30	808	1.368	Carvomenthene	601	1021	1026	OM

Table 3.5 - Volatile compounds tentatively identified by GC × GC/TOFMS analyis in *Pinus* spp. composite sample (cont.).

Peak No.	$^{1}t_R$*	$^{2}t_R$**	Compound	Similarity	RI_{calc}§	RI_{Lit}§§	Compound class
31	814	1.712	*p*-Cymene	958	1024	1025	MA
32	823	1.568	Limonene	940	1028	1029	M
33	829	1.568	*β*-Phellandrene	916	1031	1030	M
34	832	1.728	1,8-Cineole	709	1032	1031	OM
35	841	1.520	*cis*-Ocimene	951	1036	1037	M
36	865	1.544	*trans*-Ocimene	945	1047	1050	M
37	877	1.664	n.i.	798	1052	-	
38	889	1.680	*γ*-Terpinene	923	1057	1060	M
39	907	1.656	n.i.	765	1065	-	
40	916	1.664	*cis*-Sabinene hydrate	829	1069	1070	OM
41	946	1.720	Terpinolene	944	1083	1089	M
42	958	1.968	*p*-Cymenene	922	1088	1091	MA
43	985	1.128	Undecane	947	1100	1100	HC
44	985	1.720	Linalool	933	1100	1097	OM
45	994	1.720	Nonanal	931	1104	1101	CC
46	1000	1.488	3-Methyl-butanoic acid 3-methylbutyl ester	800	1107	1103	E
47	1003	1.680	*cis*-Rose oxide	785	1108	1108	OM
48	1006	1.832	1,3,8-*p*-Menthatriene	893	1110	1110	M
49	1024	1.832	*endo*-Fenchol	940	1118	1117	OM
50	1036	1.792	*cis*-*p*-Menth-2-en-1-ol	875	1124	1122	OM
51	1039	2.000	*α*-Campholenal	832	1125	1126	OM
52	1054	1.920	n.i.	870	1132	-	
53	1060	1.848	Terpinene-1-ol	899	1135	1134	OM
54	1063	2.576	Nopinone	774	1137	1140	OM
55	1069	2.064	*trans*-Pinocarveol	836	1139	1139	OM
56	1075	1.872	*cis*-*p*-Menth-2-en-1-ol	877	1142	1141	OM
57	1081	1.976	Verbenol	741	1145	1141	OM
58	1081	2.288	Camphor	861	1145	1146	OM
59	1090	2.120	n.i.	714	1149	-	
60	1093	1.848	Citronellal	905	1151	1153	OM
61	1099	2.104	n.i.	747	1154	-	

Table 3.5 - Volatile compounds tentatively identified by GC × GC/TOFMS analyis in *Pinus* spp. composite sample (cont.).

Peak No.	$^{1}t_R$*	$^{2}t_R$**	Compound	Similarity	RI_{calc}§	RI_{Lit}§§	Compound class
62	1111	2.208	*trans*-Pinocamphone	913	1159	1163	OM
63	1114	2.336	Pinocarvone	824	1161	1165	OM
64	1135	2.520	Ethyl benzoate	927	1170	1173	E
65	1138	2.056	*endo*-Borneol	916	1172	1169	OM
66	1144	2.280	*cis*-Pinocamphone (isopinocamphone)	909	1175	1175	OM
67	1156	2.024	4-Terpineol	933	1180	1177	OM
68	1159	2.888	Naphthalene	960	1182	1181	PAH
69	1168	2.568	Cryptone	848	1186	1186	OM
70	1171	2.408	*p*-Cymen-8-ol	921	1187	1183	MA
71	1180	2.632	Salicilic acid methyl ester	952	1192	1192	E
72	1186	2.080	α-Terpineol	949	1194	1189	OM
73	1186	2.472	Myrtenal	900	1194	1196	OM
74	1192	1.672	Octanoic acid ethyl ester	929	1197	1197	E
75	1192	1.936	*cis*-Piperitol	866	1197	1196	OM
76	1195	1.976	Dihydrocarveol	708	1199	1194	OM
77	1198	1.192	Dodecane	951	1200	1200	HC
78	1198	1.816	*cis*-3-Octenoic ethyl ester	743	1200	1200	E
79	1204	1.984	n.i.	829	1203	-	
80	1210	2.584	Verbenone	877	1206	1205	OM
81	1213	1.760	Decanal	941	1207	1202	CC
82	1216	2.000	*trans*-Piperitol	858	1209	1208	OM
83	1228	1.832	1,3,5-Triethyl-benzene	732	1214	-	MA
84	1234	2.208	n.i.	818	1217	-	
85	1237	2.176	*trans*-Carveol	755	1219	1217	OM
86	1246	2.280	n.i.	778	1223	-	
87	1252	1.864	α-Citronellol	954	1226	1226	OM
88	1258	2.080	Thymyl methyl ether	961	1229	1235	Et
89	1300	1.752	Linalyl acetate	906	1249	1257	E
90	1303	2.008	*trans*-Geraniol	933	1251	1253	OM
91	1303	2.672	2,4-Dimethoxytoluene	909	1251	-	MA

Table 3.5 - Volatile compounds tentatively identified by GC × GC/TOFMS analyis in *Pinus* spp. composite sample (cont.).

Peak No.	$^{1}t_R$*	$^{2}t_R$**	Compound	Similarity	RI_{calc} §	RI_{Lit} §§	Compound class
92	1306	2.464	Piperitone	955	1252	1253	OM
93	1309	2.672	2-Phenethyl acetate	892	1254	1258	PhE
94	1315	1.728	Undecan-2-one (isomer)	832	1257		CC
95	1321	2.320	2-(2-Methylpropylidene)-cyclohexanone	823	1259	-	CC
96	1327	1.904	*trans*-Decen-2-al	918	1262	1264	CC
97	1336	2.504	Salicyclic acid ethyl ester	665	1267	1270	E
98	1351	1.712	Decan-1-ol	898	1274	1270	AL
99	1354	1.992	n.i.	886	1275	-	
100	1354	2.360	n.i.	758	1275	-	
101	1369	1.976	Endobornyl acetate	953	1283	1289	E
102	1375	2.560	Anethole	866	1286	1285	MA
103	1384	1.920	n.i.	821	1290	-	
104	1390	1.760	Undecan-2-one	900	1293	1294	CC
105	1390	2.072	Acetic acid *E*-pinocarvyl ester	890	1293	1298	E
106	1405	1.216	Tridecane	954	1300	1300	HC
107	1444	2.112	Acetic acid myrtenyl ester	875	1320	1327	E
108	1447	1.928	Acetic acid dihydrocarvyl ester	891	1322	1329	E
109	1450	1.688	Decanoic acid methyl ester	940	1323	1326	E
110	1465	1.544	sesquiterpene	838	1331	-	SEQ
111	1465	1.952	4-Terpinenyl acetate	787	1331	1304	E
112	1489	1.544	α-Cubebene	902	1344	1351	SEQ
113	1492	1.968	α-Terpinyl acetate	880	1345	1349	E
114	1495	1.608	α-Longipinene	862	1347	1353	SEQ
115	1495	1.784	Citronellyl acetate	920	1347	1353	E
116	1516	1.952	Neryl acetate	911	1358	1362	E
117	1528	1.904	*trans*-dodecen-2-al	733	1364	1368	CC
118	1531	1.560	α-Ylangene	860	1366	1375	SEQ
119	1546	1.608	α-Copaene	944	1373	1377	SEQ
120	1555	1.944	Geranyl acetate	816	1378	1381	E
121	1561	1.656	β-Bourbonene	912	1381	1388	SEQ

Table 3.5 - Volatile compounds tentatively identified by GC × GC/TOFMS analyis in *Pinus* spp. composite sample (cont.).

Peak No.	$^{1}t_R$*	$^{2}t_R$**	Compound	Similarity	RI_{calc}§	RI_{Lit}§§	Compound class
122	1564	2.160	*trans*-Myrtanyl acetate	843	1383	1387	E
123	1570	1.648	sesquiterpene	866	1386	-	SEQ
124	1582	1.312	Tetradec-1-en	876	1392	1389	HC
125	1582	2.384	Butanoic acid α-phenylethyl ester	926	1392	1394	PhE
126	1588	1.648	Decanoic acid ethyl ester	919	1395	1396	E
127	1597	1.240	Tetradecane	953	1400	1400	HC
128	1597	1.696	β-Longipinene	881	1400	1401	SEQ
129	1597	2.784	Methyl eugenol	912	1400	1404	MA
130	1606	1.768	Longifolene	907	1405	1408	SEQ
131	1615	1.736	Dodecanal	953	1410	1409	CC
132	1618	1.656	*cis*-α-Bergamotene	849	1411	1413	SEQ
133	1618	2.272	2,5-Dimetoxy-*p*-cymene	800	1411	1427	MA
134	1627	1.872	*trans*-Caryophyllene	878	1416	1419	SEQ
135	1645	1.736	β-Gurjunene	914	1426	1434	SEQ
136	1651	1.768	β-Copaene	745	1430	1432	SEQ
137	1654	1.624	*cis*-α-Bergamotene	938	1431	1435	SEQ
138	1660	1.728	Aromadendrene	910	1434	1441	SEQ
139	1669	2.488	Butanoic acid α-phenylethyl ester	941	1439	1441	PhE
140	1672	1.792	sesquiterpene	891	1441	1450	SEQ
141	1681	1.808	sesquiterpene	855	1446	1454	SEQ
142	1693	1.648	*trans*-β-Farnesene	930	1452	1457	SEQ
143	1693	1.864	α-caryophyllene	944	1452	1455	SEQ
144	1705	1.824	sesquiterpene	885	1459	-	SEQ
145	1714	1.872	sesquiterpene	902	1464	-	SEQ
146	1729	1.840	9-epi-*trans*-Caryophyllene	913	1472	1466	SEQ
147	1735	1.704	Dodecan-1-ol	909	1475	1471	AL
148	1741	2.008	Germacrene D	924	1479	1485	SEQ
149	1750	2.368	Butanoic acid phenethyl-2-methyl ester	881	1484	1487	PhE
150	1753	1.872	sesquiterpene	929	1485	1490	SEQ
151	1759	2.392	3-Methyl-butanoic acid 2-phenylethyl ester	914	1489	1491	PhE

Table 3.5- Volatile compounds tentatively identified by GC × GC/TOFMS analyis in *Pinus* spp. composite sample (cont.).

Peak No.	$^{1}t_R$*	$^{2}t_R$**	Compound	Similarity	RI_{calc} §	RI_{Lit} §§	Compound class
152	1765	1.952	Bicyclogermacrene	923	1492	1500	SEQ
153	1768	2.920	*trans*-Methyl-*iso*-eugenol	900	1493	1492	MA
154	1771	1.856	α-Muurolene	924	1495	1500	SEQ
155	1780	2.096	Butylated hydroxytoluene	914	1500	1516	MA
156	1780	1.256	Pentadecane	920	1500	1500	HC
157	1786	1.712	*trans,trans*-α-Farnesene	898	1503	1506	SEQ
158	1786	1.912	β-Bisabolene	919	1503	1506	SEQ
159	1798	1.912	δ-Amorphene	892	1510	1512	SEQ
160	1804	1.968	γ-Cadinene	883	1514	1514	SEQ
161	1831	1.904	*trans*-Cadina-1(2),4-diene	897	1529	1535	SEQ
162	1837	1.904	α-Cadinene	896	1533	1539	SEQ
163	1846	1.792	sesquiterpene	888	1538	-	SEQ
164	1846	2.248	α-Calacorene	922	1538	1546	SEQ
165	1885	1.832	*trans*-Nerolidol	919	1560	1563	SEQ
166	1906	2.016	Germacrene D-4-ol	835	1572	1576	SEQ
167	1906	2.208	Spathulenol	910	1572	1578	SEQ
168	1915	2.216	Caryophyllene oxide	890	1578	1583	SEQ
169	1918	2.776	Tiglic acid phenylethyl ester	682	1579	1585	PhE
170	1924	2.072	Viridiflorol	799	1583	1593	SEQ
171	1933	2.240	Salvial-4(14)-en-1-one	835	1588	-	SEQ
172	1942	2.040	Guaiol	863	1593	1601	
173	1942	1.640	Dodecanoic acid ethyl ester	905	1593	1595	E
174	1951	2.256	Longiborneol	808	1598	1599	SEQ
175	1954	1.264	Hexadecane	942	1600	1600	HC
176	1963	2.296	Humulene epoxide II	819	1605	1608	SEQ
177	1972	2.128	1,10-di-*epi*-Cubenol	790	1611	1619	SEQ
178	1987	2.216	oxygenated sesquiterpene	831	1620	-	SEQ
179	1993	2.112	1-*epi*-Cubenol	833	1624	1629	SEQ
180	2020	2.208	τ-Muurolol	868	1640	1642	SEQ
181	2017	2.400	Hexanoic acid phenethyl ester	852	1638	1642	PhE

Table 3.5 - Volatile compounds tentatively identified by GC × GC/TOFMS analyis in *Pinus* spp. composite sample (cont.).

Peak No.	$^{1}t_R$*	$^{2}t_R$**	Compound	Similarity	RI_{calc}§	RI_{Lit}§§	Compound class
182	2038	2.288	α-Cadinol	887	1651	1654	SEQ
183	2053	2.400	7(11)-Selinen-4α-ol	836	1660	1660	SEQ
184	2119	1.272	Heptadecane	928	1700	1700	HC
185	2143	2.064	*cis*,*cis*-Farnesol isomer	918	1715	1718	SEQ
186	2152	2.392	n.i.	-	1721	-	
187	2167	2.464	Mintsulfide	652	1731	1741	S
188	2263	1.648	Tetradecanoic acid ethyl ester	500	1792	1796	E
189	2275	1.288	Octadecane	906	1800	1800	HC
190	2323	2.016	Acetic acid farnesyl ester	737	1832	1822	E
191	2425	1.304	Nonadecane	881	1900	1900	HC
192	2446	2.040	Cembrene	865	1915	1939	DIT
193	2452	2.360	Oxacycloheptadecan-2-one	800	1919	1935	CC
194	2467	2.024	n.i.	815	1930	-	
195	2497	2.872	Phthalic acid dibutyl ester	942	1951	-	E
196	2545	2.208	Manoyl oxide	805	1985	1998	DIT
197	2557	1.648	Palmitic acid ethyl ester	419	1994	1993	E
198	2566	1.320	Eicosane	585	2000	2000	HC
199	2572	2.144	n.i.	763	2005	-	
200	2581	2.200	Abieta-8,12-diene	700	2012	2023	DIT
201	2611	2.232	n.i.	812	2037	-	
202	2629	2.264	n.i.	824	2052	-	
203	2629	2.520	Abietatriene	697	2052	2057	DIT
204	2688		Heneicosane	-	2100	-	HC
205	2671	2.256	n.i.	828	2086	-	
206	2746	2.160	n.i.	791	2147	-	
207	2752	2.440	n.i.	734	2152	-	
208	2791	2.440	n.i.	698	2184	-	
209	2811		Docosane	-	2200	-	HC
210	2860	2.784	n.i.	711	2233	-	
211	2959	1.352	Tricosane	793	2300	2300	HC

Table 3.5 - Volatile compounds tentatively identified by GC × GC/TOFMS analyis in *Pinus* spp. composite sample (cont.).

Peak No.	$^{1}t_R$*	$^{2}t_R$**	Compound	Similarity	RI_{calc} §	RI_{Lit} §§	Compound class
212	3028	0.088	n.i.	745	2347	2301	

*$^{1}t_R$, **$^{2}t_R$ - retention times of the first and second dimension columns, respectively.
§RI_{calc}, §§RI_{Lit} - calculated and literature retention index data, respectively. The calculated retention indices were obtained based on retention times across the dual column set. Peaks were identified based on the comparison (similarity) of their mass spectra to reference mass spectral databases (Mass Spectra Library NIST version 2.0, 2005 and Wiley Registry of Mass Spectral Data 7th edition, 2000) and retention indices (Adams, 2001).
n.i. - non-identified peak.
MA - monoaromatic compound; HC - hydrocarbon; CC - carbonyl compound; E - ester; AL - alcohol; M - monoterpene; OM - oxygenated monoterpene; S - sulphur compound; SEQ - sesquiterpene; Et - ether; PhE - phenyl ester; DIT - diterpene

Figure 3.24 presents the good relationship obtained (R^2 = 0.99965) between linear retention indices reported by Adams (2001) and calculated retention index data for the compounds identified in the GC × GC/TOFMS analysis of *Pinus* spp. composite sample.

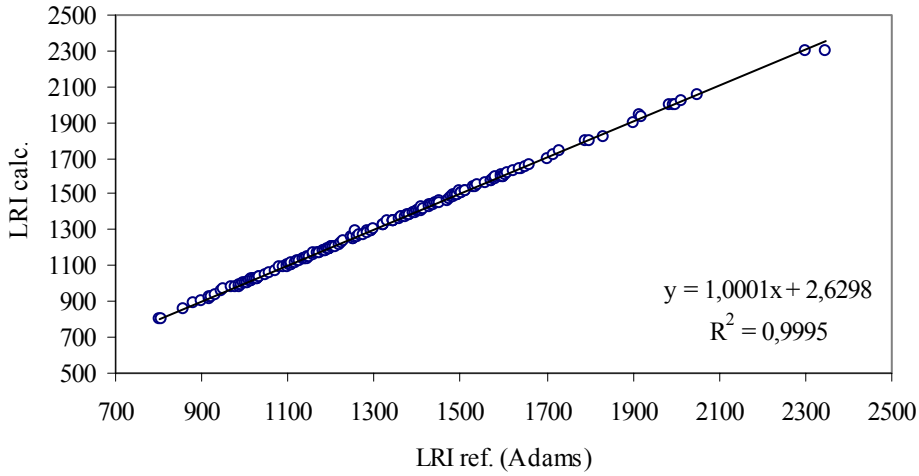

Figure 3.24 - Relationship between literature (LRI ref.) data from Adams (2001) and calculated (LRI calc.) retention index data for the identified compounds in the GC × GC/TOFMS analysis of *Pinus* spp. composite sample.

Figure 3.25 presents a color plot construted with the peaks tentatively identifieds. The plot allows for the visualization of the peaks, by chemical classes, present in the *Pinus* spp. sample and their distribution on the two dimensional chromatographic space. The column set used generated a boiling point separation in the first dimension, and a polarity separation in the

second dimension. This orthogonal separation allows for the creation of structured chromatograms, where chemical classes of compounds tend to form clusters (e.g. monoterpenes or sesquiterpenes), in specific positions of the separation plane, which can be used for component classification and identification. The results also show that the chromatographic separation observed in GC × GC was not possible to be achieved with just one dimension due to the amount of coelutions observed.

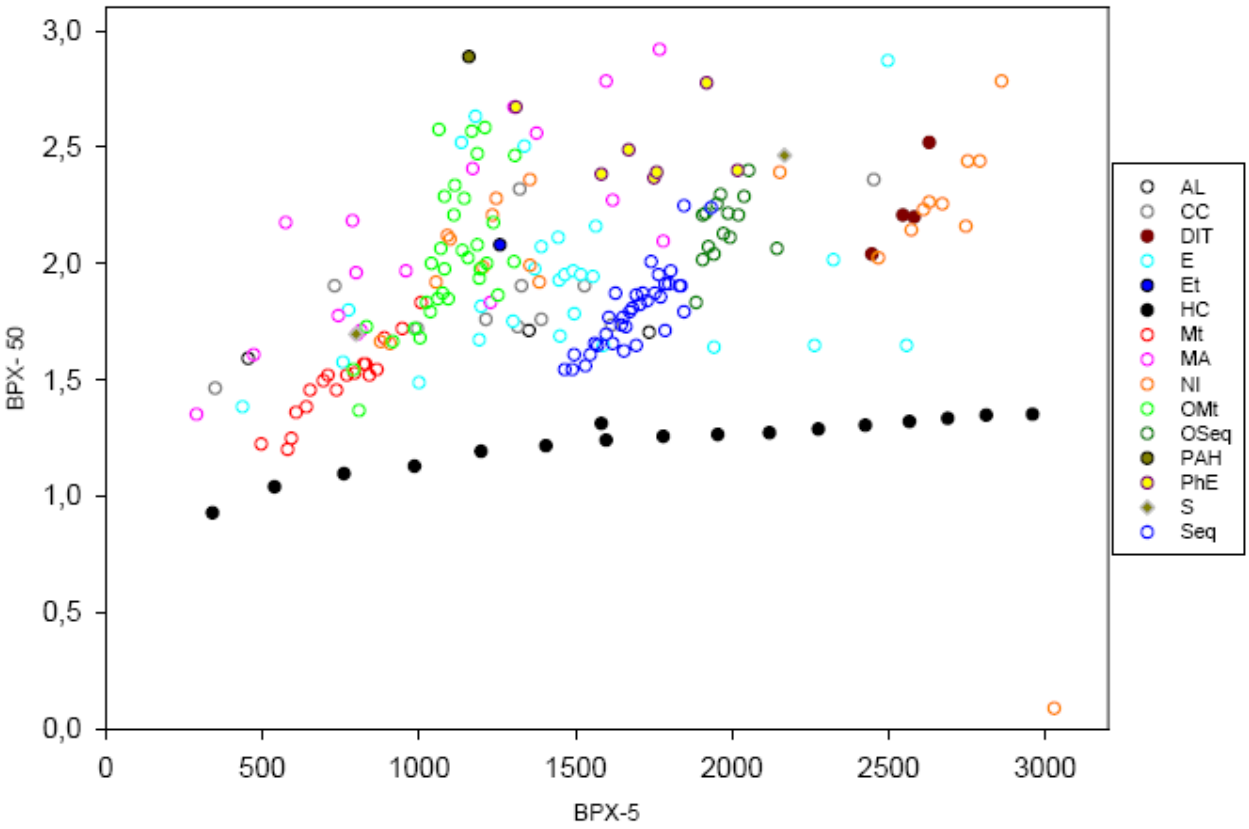

Figure 3.25 - Comprehensive two-dimensional gas chromatography/time-of-flight mass spectrometry (GC × GC/TOFMS) class separation of volatile components of *Pinus* spp. AL - alcohol; CC - carbonyl compound; DIT – diterpenes; E - ester; Et - ether; HC - hydrocarbon; Mt - monoterpene; MA - monoaromatic compound; NI – not identified; OMt - oxygenated monoterpene; OSeq – oxygenated sesquiterpenes ; PAH – polycyclic aromatic hydrocarbon; PhE - phenyl ester; S - sulphur compound; Seq – sesquiterpenes.

3.1.1.4. Enantioselective comprehensive two-dimensional gas chromatography/ time-of-flight mass spectrometry

Evaluation of the column set

The enantiomers of chiral terpenes present in the volatile blends emitted by *Pinus* spp. should analytically be considered as individual components, due to their inherent potential role in

insect-host plant relationships (Mustaparta 2002; Stranden *et al*., 2002), and in the chemical discrimination of pine species (Gomes da Silva *et al*., 2001).

The separation of enantiomeric monoterpenes by GC × GC analysis was performed with a taylor made fused silica capillary column 2,3-DiMe on the first dimension. The column was coupled to a polar column (Supelco-Wax) composing a set on columns which was never reported before in GC × GC. In order to collect information and evaluate the set performance in GC × GC, a solution with a mixture of 43 standards (Table 3.6) was analysed before the *Pinus* samples.

Table 3.6 - Chemical standards used in the evaluation of the column set used for enantioneric GC × GC/TOFMS analysis.

Peak No.	Standard	Peak No.	Standard
1	Isoamyl alcohol	23	(+)-β-Phellandrene
2	*trans*-2-Hexenal	24	γ–Terpinene
3	(-)-α-Pinene	25	Terpinolene
4	(+)-α-Pinene	26	Octan-1-ol
5	Hexan-1-ol	27	Myrtenal
6	*cis*-3-Hexen-1-ol (Leaf alcohol)	28	(-)-Verbenone
7	(-)-Camphene	29	(+)-Verbenone
8	(+)-Camphene	30	(-)-α-Terpineol
9	Myrcene	31	γ-Terpineol
10	Sabinene	32	(+)-α-Terpineol
11	(+)-β-Pinene	39	(+)-Calarene
12	*cis*-Hex-2-en-1-ol	40	*trans*-Caryophyllene
13	(-)-β-Pinene	41	α-Caryophyllene
14	α-Phellandrene	42	(+)-Aromadendrene
15	3-Carene	43	(+)-γ-Gurjunene
16	α-Terpinene	33	Citronellol
17	Hex-2-en-1-ol acetate	34	Geraniol
18	1,8-cineol (Eucalyptol)	35	(-)-α-Cubebene
19	*p*-Cymene	36	Terpinyl acetate
20	(-)-Limonene	37	(-)-α-Copaene
21	(-)-β-Phellandrene	38	(-)-α-Cedrene
22	(+)-Limonene		

Figure 3.26 shows the reconstructed first dimension TIC and the correspondent enantioselective GC × GC /TOFMS contour plot obtained for the test mixture. The first view of the elution patterns from the test mixture components, on the two dimensional plot, shows that they are separated according to their volatility and chiral discrimination on the first dimension, and according to their polarity on the second dimension. Coelutions of some compounds are still observed on the first dimension.

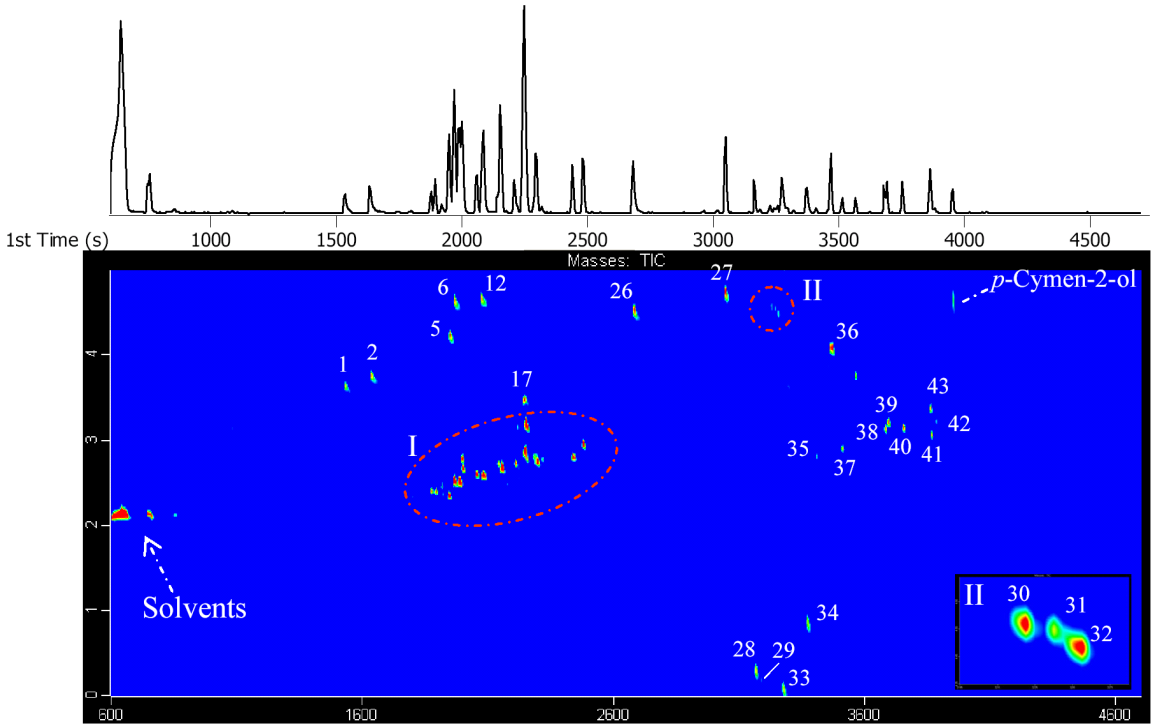

Figure 3.26 - Reconstructed first dimension TIC and the correspondent enantioselective GC×GC/TOFMS contour plot obtained for the test mixture of Table 3.6. Zone II was magnified on the left bottom corner of the contour plot.

Monoterpenes (zone I) and sesquiterpenes (peaks 35 and 37 to 43) form clusters, and the same happens for the alcohols and aldehydes (peaks 1, 2, 5, 6 and 12) on the top of second dimension. The oxygenated monoterpenes are scattered in the second dimension with the verbenone enantiomers, citronellol and geraniol eluting on the second dimension after the modulation period and thus suffering wrap around effect (Figure 3.26). On the bottom right corner of Figure 3.26, an expanded view from zone II is represented, showing the separation of α-terpineol enantiomers (peaks 30 and 31). The enantiomers of α-terpineol, with identical polarity, did not have the same second dimension retention time. The last eluted enantiomer shows a lower retention time on the second dimension. As the chromatographic analysis was performed with a temperature programmed ramp, the second enantiomer will elute at a

slightly higher elution temperature and thus its second dimension retention time will be lower than that of its pair. This observation is expected to be observed in all enantiomeric pairs and consequently it will be used as support for enantiomer pair detection.

Figure 3.27 shows an expanded view of zone I of Figure 3.26, which comprises the monoterpenes.

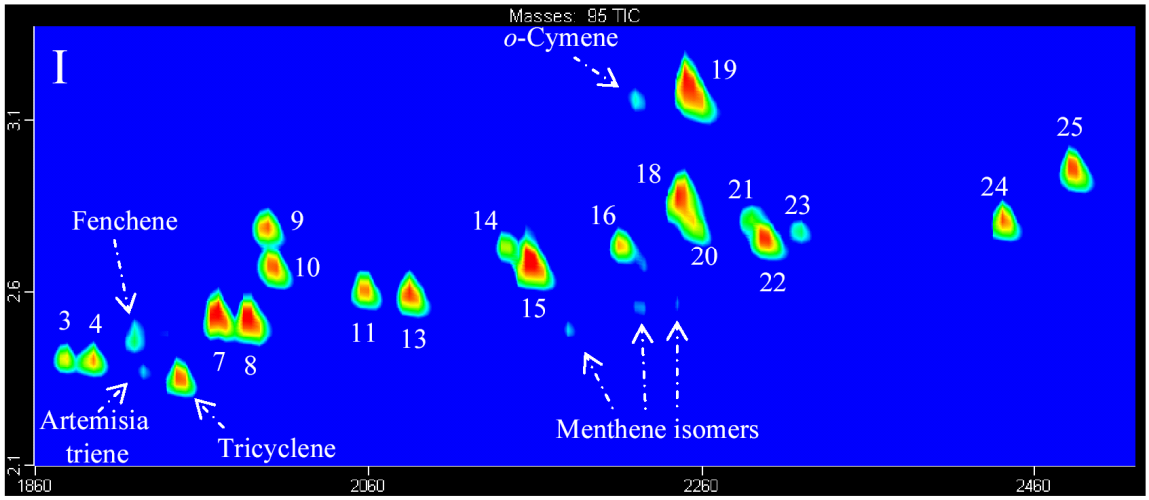

Figure 3.27 - Expanded enantioselective GC×GC/TOFMS contour plot of Zone I of Figure 3.26.

In Figure 3.27, the peak of tricyclene comes from the standard of camphene which has 10% of tricyclene. The fenchene, artemisia triene and the menthenes are impurities of the standards. The enantiomeric pairs of α-pinene, camphene, β-pinene, limonene and β-phellandrene are effectively separated on the first dimension. However, coelutions can be observed on the first dimension. One of the enantiomer of sabinene (peak 10) is coeluting with myrcene (peak 9) making not possible their evaluation in the 1D-analysis.Other coelutions or partial coelutions on the first dimension can be observed for (-)-limonene (peak 20), *p*-cymene (peak 19) and 1,8-cineol (peak 18). Those coelutions are resolved on the second dimension. Figure 3.28 shows an expansion of the plot area that comprises the limonene enantiomers. The peaks 17 to 20 and one of the menthene isomers are coeluting on the first dimension. By GC × GC these compounds are separated on the second dimension, by their polarity differences. As expected, the second enantiomer from the enantiomeric pairs of limonene (peaks 20 and 22), and β-phellandrene (peaks 21 and 23), are eluting at a lower retention time on the second dimension. Additionally, the increase of sensitivity, due to modulation, also allows for the detection of *trans*-ocimene and 1,3,4-trimethylbenzene, that is also coeluting with the peaks 17 to 20.

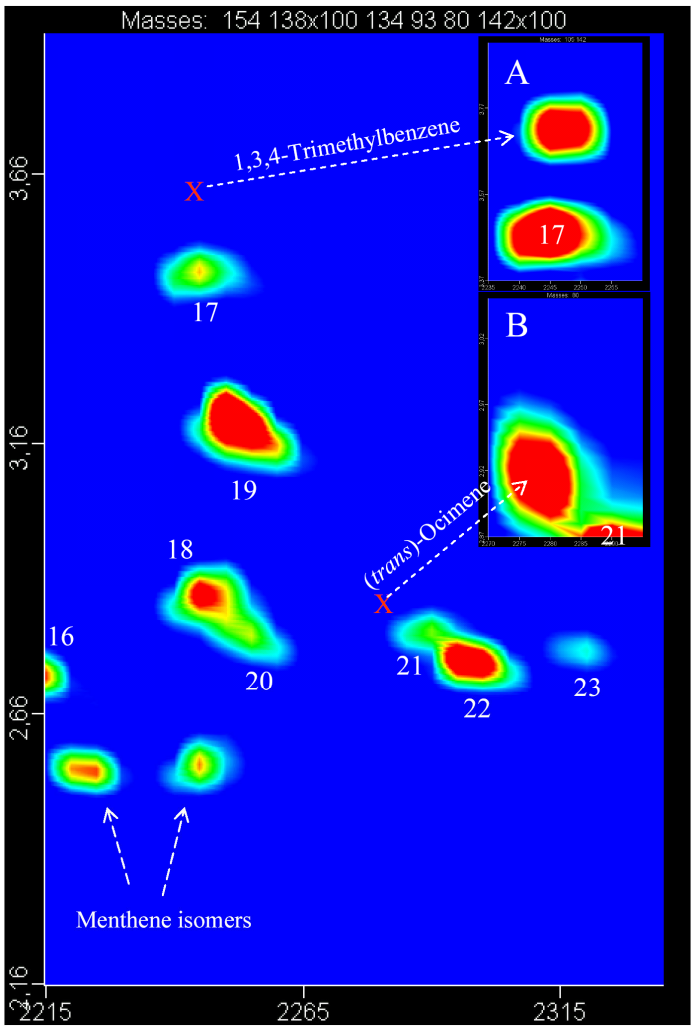

Figure 3.28 - Expanded enantioselective GC × GC/TOFMS contour plot of Figure 3.27 showing the range of the limonene enantiomers. **A)** Expanded view of the area of peak 17 and 1,2,4-trymethylbenzene; **B)** Expanded view of the area of peak 21 and *trans*-ocimene.

Figure 3.29 B) shows the 3D plot of the expanded area of Figure 3.28, where the reconstructed first dimension chromatogram only presents two peaks in opposition to the 2D and 3D plots. A section of the modulated chromatogram with the two peaks is presented on Figure 3.29 A), where different colours represent the distribution of the individual extracted ions and consequently of the coeluting compounds. Figure 3.29 C) presents the second dimension chromatogram obtained for the major modulated peak from peak 1 (^1t_R = 2250 sec.) showing its separation into five individual peaks.

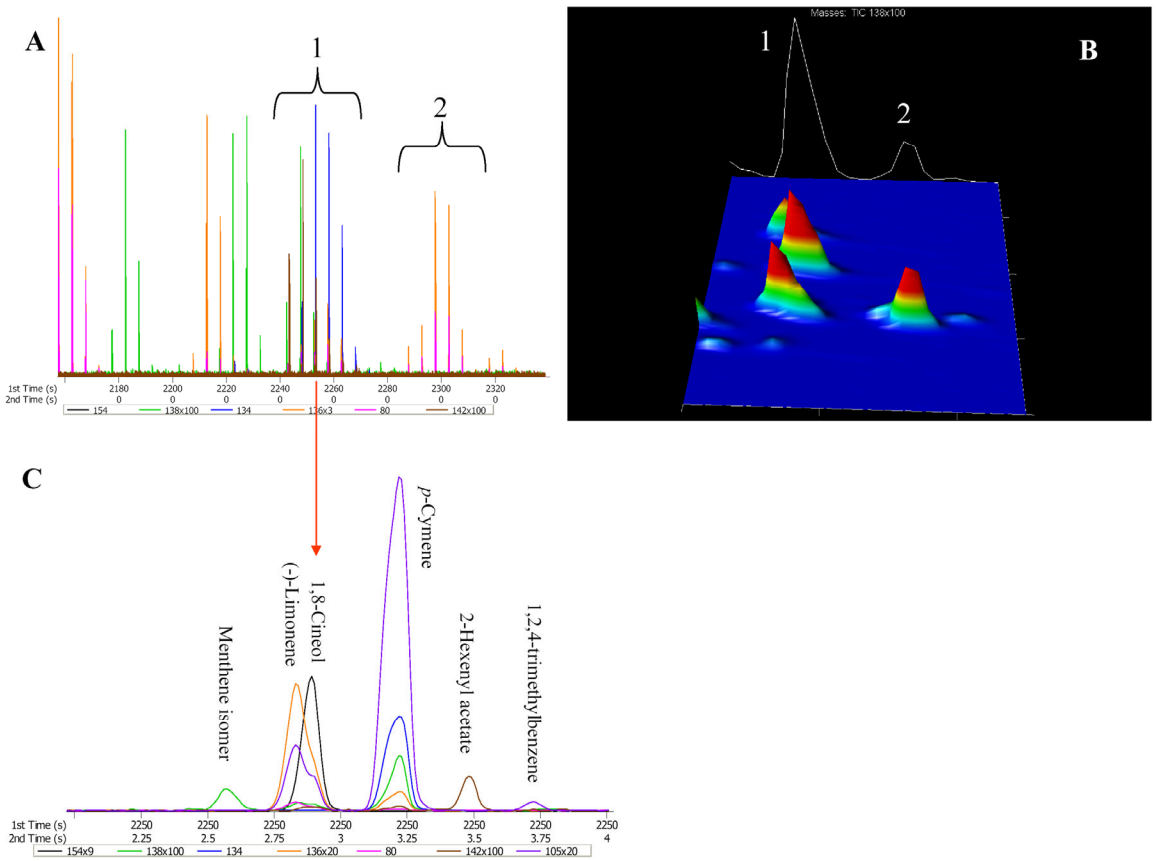

Figure 3.29 - Expanded enantioselective GC × GC/TOFMS contour plot from Figure 3.28, showing the range of the limonene enantiomers. **A)** Modulated chromatogram; **B)** 3D plot; **C)** Separation on the second dimension (^1t_R = 2250 sec.; peaks deconvoluted by ion extraction).

The results of the analysis with the 43 standards (Table 3.6) show that even samples with a small number of components can present coelutions, which may be difficult to solve using conventional one dimensional chromatography. In spite of the first enantiomeric column be the key tool for the proposed analysis, its assemblage with the polar column added more resolving power to the analysis, promoting the separation of overlapped compounds and thus making the used set suitable for the characterization of the enantiomeric volatile components of *Pinus* spp..

Characterization of the volatile fraction of Pinus spp.

A total of 10 pine species collected from Abrantes experimental plot, in the summer months, were analysed using enantioselective-GC × GC-TOF/MS.

Figures 3.30 shows, as an example, the 2D plot of an enantio-GC × GC/TOFMS analysis obtained from a *P. pinaster* sample. The signals in the contour plot are magnified in order to visualize the minor components present in the sample. Each spot on the images represents an

individual compound, for which a full mass spectrum was available. The contour plot from *P. pinaster* is rather complex due to the number of components present. However, the cluster of volatile compounds classes of can be observed, distributed through the plot producing a structured chromatogram. It is also observable the higher retention times of the oxygenated compounds on the second dimension, due to their interaction with the polar column. Oxygenated monoterpenes (alcohols and aldehydes) (OM) and linear alcohols were divided in two regions due to wrap-around effect.

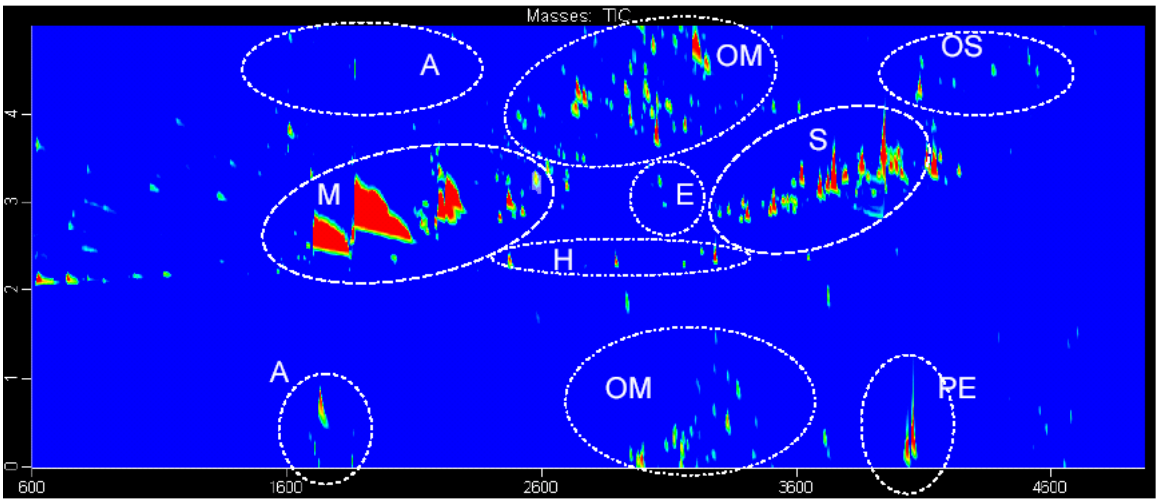

Figure 3.30 – Enantio-GC × GC/TOFMS total ion current chromatogram (TIC) data contour plot from a *P. Pinaster* sample, showing the distribution of classes of compounds in different regions of the chromatographic space: (A) Linear alcohols; (M) Monoterpenes, (OM) Oxygenated monoterpenes; (H) Hydrocarbons; (S) sesquiterpenes; (OS) Oxygenated sesquiterpenes; (PE) Phenyls esters, (E) Esters. The signal is magnified in order to allow visualization of the minor compounds.

The phenyl esters (PE), that have a high polarity, appear in a lower retention time of the second dimension, due to wrap-around effect (Figure 3.30). This effect may promote a decrease in the chromatographic resolution, since overlap of the analytes may occur. However, in this work, the observed wrap-around represents just a visual "inconvenience", since it did not affect the separation and identification of the compounds The more strongly retained components, responsible for the wrap-around, did not overlap peaks that were weakly retained in the subsequent modulation, and thus the only consequence was the maximization of the separation space with the filling of the lower region of the 2D plot.

Figure 3.31 shows an expansion of the central area of the contour plot, where the oxygenated monoterpenes are located, together with its reconstructed first dimension chromatogram, in order to illustrate the complexity of the sample under analysis, and the number of potential

coelutions that occur on the first dimension. Each spot on the 2D plot is a detected peak, and the colours represent the concentration ranking. The concentration rank is ordered from red to blue (higher concentration to lower one).

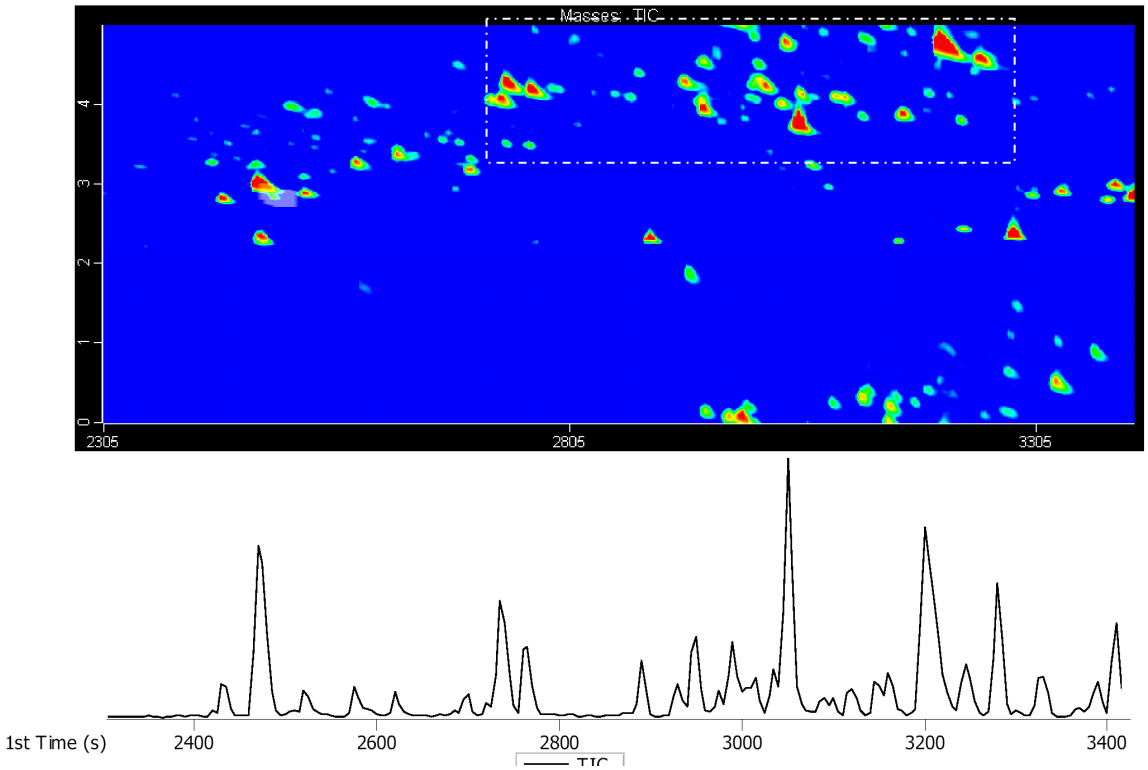

Figure 3.31 - Enantio-GC × GC/TOFMS expanded segment from Figure 3.30 and its first dimension reconstructed chromatogram, showing the section were the classes of compounds OM, E and H are distributed.

Figure 3.32 shows a 3D expanded view of the highlighted section of the contour plot shown in Figure 3.31, illustrating the good chromatographic resolution obtained, where it is possible to observe the occupation of the chromatographic space by the analytes, and thus allowing for high-quality spectral data to be produced. For sake of clarity, some peaks are presented according to Table 3.7.

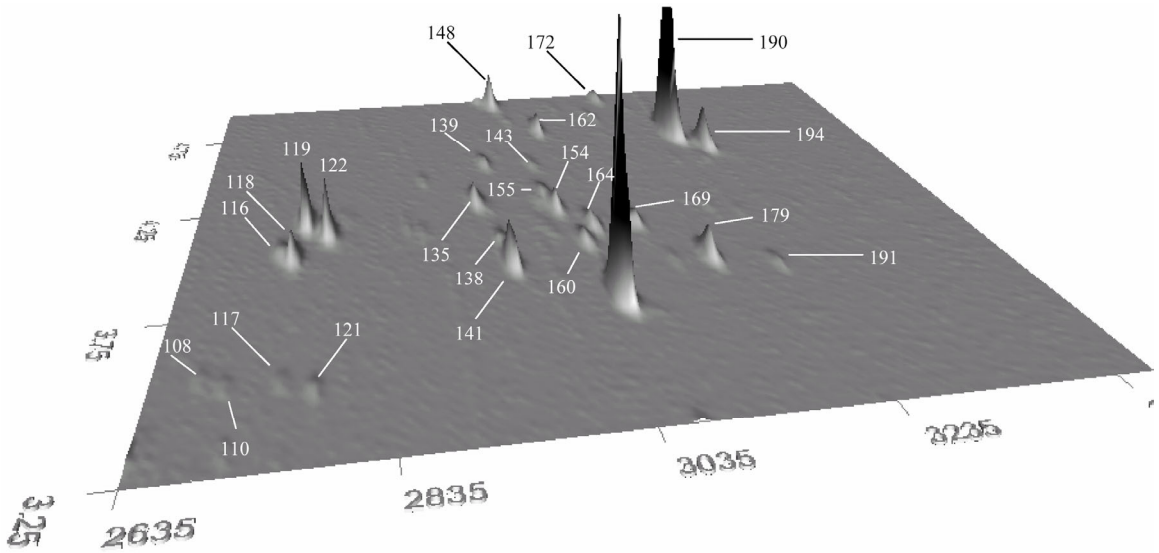

Figure 3.32 – Enantio-GC × GC/TOFMS expanded segment 3D relief plot of a *P. pinaster* sample. Compounds are numbered according to Table 3.7.

Table 3.7 presents the results obtained for all pine species, with the compound retention times in both dimensions, and retention indices calculated according to the Van den Doll and Kratz equation. As the first dimension column is a 5%-phenyl-methylpolysiloxane, similar to the DB-5 columns used by Adams and others, with a *β*-cyclodextrin phase imbibed on, the retention index from Adams and literature are also presented. These literature retention indexes were used as an indicative of the elution order of the volatile compounds present in the samples. The enantio-GC×GC analysis resulted in 422 volatile compounds detected in the 10 pine species. 54 compounds were not identified, comprising 23 sesquiterpenes, 16 oxi-terpenes, 6 diterpenes, 2 monoterpene acetates, 1 phenyl ethyl ester and 6 unknowns. With the exception of the unknowns, all the others presented library matches, that sometimes present mass spectra similarities higher than 800 (e.g. non identified sesquiterpenes) with similar compounds. Most of the 368 peak identifications reported are tentative identifications. However, all peaks indicated in more than one pine species were simultaneously found in the samples. The highest similarity value found for a compound, among the pine species, is also registered in Table3.7.

Table 3.7 - Volatiles of *Pinus* spp. detected and tentatively identified by enantiomeric GC × GC/TOFMS analysis

							Pinus species									
Peak No.	$^{1}t_R$	$^{2}t_R$	Compound	Similarity	$^{\S}RI_{calc}$	$^{\S\S}RI_{Lit}$	PE	PH	PP	PK	PPr	PPa	PR	PS	PB	PT
1	1125	2.2	Octane	940	800	800					x					
2	1505	3.31	Xylene (isomer)	965	715		x	x	x		x			x	x	x
3	1540	3.61	3-Methyl-butan-1-ol	909	707	734*					x	x				
4	1570	2.21	Nonane	949	900	900	x	x	x	x	x		x	x	x	x
5	1595	3.54	Xylene (isomer)	958	905			x		x	x	x				
6	1650	3.71	*trans*-2-Hexenal	925	917	855	x	x	x	x	x	x		x	x	
7	1660	2.38	Bornylene	902	920	896**				x				x	x	x
8	1670	4.66	*cis*-2-Penten-1-ol	876	922	774			x	x	x	x		x	x	
9	1670	4.69	3-Methyl-2-buten-1-ol	897	922	774	x		x					x		
10	1685	2.36	Santene	951	925	889	x		x		x					x
11	1685	3.29	2-Heptanone	955	925	896	x									
12	1735	2.48	α-Thujene (enantiomer)	927	936	930		x	x							
13	1750	2.47	α-Thujene (enantiomer)	932	939	930	x		x	x	x	x	x	x	x	x
14	1750	4.10	2-Ethoxyethanol acetate	976	939	907*		x		x						x
15	1760	3.21	Heptanal	935	941	902			x		x			x		
16	1810	4.79	Anisole	939	952	918	x	x	x	x	x	x		x	x	x
17	1875	2.43	α-Pinene (enantiomer)	977	966	939	x	x	x	x	x	x	x	x	x	x
18	1875	2.62	Lilac alcohol (isomer)	845	966	1209**						x				
19	1880	4.43	4-Methyl-pentanol	835	967	838				x				x	x	
20	1890	4.92	*trans*-3-Hexen-1-ol	933	970	854				x	x			x	x	x
21	1895	2.40	α-Pinene (enantiomer)	977	971	939	x	x	x	x	x	x	x	x	x	x
22	1900	2.53	α-Fenchene	951	972	953	x	x	x	x	x			x	x	x
23	1925	2.37	Tricyclene	953	977	927		x	x							
24	1925	3.31	1-Ethyl-4-methylbenzene	975	977	965*	x	x	x	x	x	x			x	x

Table 3.7 - Volatiles of *Pinus* spp. detected and tentatively identified by enantiomeric GC × GC/TOFMS analysis (cont.).

							Pinus species									
Peak No.	$^{1}t_R$	$^{2}t_R$	Compound	Similarity	$^{\S}RI_{calc}$	$^{\S\S}RI_{Lit}$	PE	PH	PP	PK	PPr	PPa	PR	PS	PB	PT
25	1935	2.50	Fenchene	936	979	953		x	x							
26	1950	2.33	Tricyclene	955	983	927	x		x	x	x	x	x	x	x	
27	1950	2.63	Lilac alcohol (isomer)	833	983	1209**						x				
28	1960	4.18	1-Hexanol	941	985	871	x	x	x		x	x		x		x
29	1970	3.77	2-Heptanol	926	987	896*	x									
30	1970	4.64	*cis*-3-Hexen-1-ol	935	987	859	x	x	x	x	x	x	x	x		x
31	1975	2.50	Camphene (enantiomer)	961	988	954	x	x	x	x	x	x	x	x	x	x
32	1980	3.46	5-Methyl-4-hepten-3-one (isomer)	893	989	1007*	x	x	x	x					x	
33	1985	2.39	*trans*-*p*-Menthane	838	990	979			x							
34	1995	2.48	Camphene (enantiomer)	958	992	954	x	x	x		x	x	x	x	x	x
35	2000	2.79	Myrcene	970	993	991	x	x	x	x	x	x	x	x	x	x
36	2005	2.65	Sabinene (isomer)	930	995	975	x	x	x		x	x		x		
37	2020	2.67	Verbenene	897	998	968	x			x	x			x		
38	2030	2.24	Decane	944	1000	1000	x	x	x	x	x	x	x	x	x	x
39	2035	2.60	Sabinene (isomer)	942	1001	975		x	x			x	x	x		
40	2035	3.69	1-Octen-3-one	875	1001	980*					x					
41	2055	2.64	(+)-β-pinene	961	1006	979	x		x	x	x		x	x	x	x
42	2060	3.56	Trimethylbenzene (isomer)	963	1007	962-1021	x	x	x	x	x	x		x	x	x
43	2065	3.06	Frontalin (enantiomer)	950	1008	949**	x					x				x
44	2085	2.58	(-)-β-Pinene	967	1012	979	x	x	x	x	x	x	x	x	x	x
45	2095	3.58	5-Methyl-4-hepten-3-one (isomer)	875	1015	1007*	x	x	x	x				x	x	x
46	2105	3.83	Sulcatone	936	1017	984*	x	x	x	x		x	x	x	x	x

Table 3.7 - Volatiles of *Pinus* spp. detected and tentatively identified by enantiomeric GC × GC/TOFMS analysis (cont).

							Pinus species									
Peak No.	$^{1}t_R$	$^{2}t_R$	Compound	Similarity	$^{\S}RI_{calc}$	$^{\S\S}RI_{Lit}$	PE	PH	PP	PK	PPr	PPa	PR	PS	PB	PT
47	2110	3.01	2-Pentylfuran	946	1018	992**	x	x	x	x		x	x	x	x	x
48	2110	3.12	*trans*-Dehydroxy linalool oxide	882	1018	993						x				
49	2120	1.88	Benzaldehyde	943	1020	960		x	x	x				x		
50	2120	3.77	2-Heptenal (isomer)	944	1020	956/961*		x	x	x		x		x		
51	2125	2.85	2,3-Dehydro-1,8-cineole (enantiomer)	845	1021	991	x	x	x	x	x	x		x	x	x
52	2135	2.89	2,6-Dimethyl-1,3,5,7-octatetraene (isomer)	927	1024			x	x	x	x			x	x	x
53	2135	3.23	Disulfide *bis*(1-methylethyl)	921	1024		x	x	x	x		x	x	x	x	x
54	2140	2.73	α-Phellandrene	959	1025	1003	x		x	x	x	x	x			x
55	2145	2.83	2,3-Dehydro-1,8-cineole (enantiomer)	781	1026	991	x			x						x
56	2155	2.76	1,4-Cineole	946	1028	1015	x	x	x	x	x	x	x	x		x
57	2160	2.64	Δ-3-Carene	950	1011	1011	x	x	x	x	x	x	x	x	x	x
58	2165	3.05	*cis*-Dehydroxylinalool oxide	913	1030	1008						x				
59	2185	3.14	Hexyl acetate	973	1035	1009			x	x	x			x	x	x
60	2200	3.29	Octanal	936	1038	999	x	x	x	x		x				x
61	2205	3.42	*cis*-3-Hexen-1-ol acetate	963	1039	1005	x	x	x	x	x	x	x	x	x	x
62	2210	2.57	1-*p*-Menthene/carvomenthene	918	1040	1026	x				x				x	
63	2210	2.73	α-Terpinene	942	1040	1017	x	x	x	x	x	x	x	x	x	x
64	2210	3.18	Cymene (isomer)	966	1040			x	x	x	x		x	x	x	
65	2235	2.85	(-)-Limonene	965	1046	1029	x	x	x	x	x	x	x	x	x	x
66	2240	3.22	Cymene (isomer)	971	1047		x	x		x	x	x		x	x	x

Table 3.7 - Volatiles of *Pinus* spp. detected and tentatively identified by enantiomeric GC × GC/TOFMS analysis (cont).

							Pinus species									
Peak No.	$^{1}t_R$	$^{2}t_R$	Compound	Similarity	$^{\S}RI_{calc}$	$^{\S\S}RI_{Lit}$	PE	PH	PP	PK	PPr	PPa	PR	PS	PB	PT
67	2240	3.50	2-Hexenyl acetate (isomer)	957	1047	1019	x	x	x	x	x		x	x	x	x
68	2240	3.75	Trimethylbenzene (isomer)	951	1047	962-1021	x			x	x	x			x	x
69	2245	2.87	1,8-Cineole	926	1048	1031	x	x						x		x
70	2250	2.85	*cis*-Ocimene	915	1049	1050		x			x				x	
71	2275	2.93	*trans*-Ocimene	953	1055	1037		x			x	x	x	x	x	
72	2285	2.83	*β*-Phellandrene (enantiomer)	949	1057	1030	x	x	x	x	x	x	x	x	x	x
73	2295	2.75	(+)-Limonene	960	1060	1029	x	x		x	x	x	x	x	x	x
74	2310	4.61	1,2-Dichlorobenzene	966	1063	1014	x	x	x	x	x	x	x	x	x	x
75	2315	2.78	*β*-Phellandrene (enantiomer)	947	1064	1030	x	x	x	x	x	x	x	x	x	
76	2320	3.44	2,2,6-Trimethylcyclohexanone	903	1065	1040*	x		x			x				
77	2335	3.25	1-Methyl-2-propylbenzene	949	1069	1074*		x		x	x	x			x	x
78	2335	3.39	Cymene (isomer)	943	1069	1025-1026	x	x		x	x	x		x		
79	2400	4.08	1-Octene-3-ol	928	1083	991				x	x	x				
80	2440	2.79	*γ*-Terpinene	960	1092	1060	x	x	x	x	x	x	x	x	x	x
81	2450	4.08	3-Methylcyclohex-3-en-1-one	837	1094	1079**		x				x		x		
82	2475	2.28	Undecane	966	1100	1100	x	x	x	x	x	x	x	x	x	x
83	2480	2.95	Terpinolene	966	1101	1089	x	x	x	x	x	x	x	x	x	x
84	2485	3.48	4-Ethyl-1,2-dimethylbenzene	960	1102	1093*	x		x	x		x		x	x	x
85	2490	2.85	2-Methylbutanoic acid isovaleryl ester	925	1104	1094*					x					
86	2490	3.80	Fenchone	929	1104	1087				x	x				x	

Table 3.7 - Volatiles of *Pinus* spp. detected and tentatively identified by enantiomeric GC × GC/TOFMS analysis (cont).

Peak No.	$^{1}t_R$	$^{2}t_R$	Compound	Similarity	$^{\S}RI_{calc}$	$^{\S\S}RI_{Lit}$	*Pinus* species									
							PE	PH	PP	PK	PPr	PPa	PR	PS	PB	PT
87	2510	3.96	Cymenene (isomer)	964	1108	1085-1091	x	x	x	x	x	x	x	x	x	x
88	2515	2.89	*Δ*-2-Carene	919	1110	1002				x				x		
89	2520	2.91	Isovaleric acid isoamyl ester	930	1111	1105*					x					
90	2525	3.66	Thuja-2,4(10)-diene	848	1112	960	x				x					
91	2530	3.90	*trans*-Linalool oxide (furanoid)	928	1113	1073	x	x	x	x	x	x		x	x	x
92	2535	3.87	2-Octenal	857	1114	1060**					x			x		
93	2550	3.43	2-Nonanone	947	1118	1090				x				x		
94	2570	4.07	2-Ethyl-hexan-1-ol	940	1123	1028*					x	x				
95	2575	3.26	Butanoic acid, 3-methyl-, 3-methyl-3-butenyl ester	881	1124	1115					x					
96	2575	3.81	*cis*-Linalool oxide (furanoid)	945	1124	1087	x	x	x	x	x	x		x	x	x
97	2580	3.10	4-*terc*-Butyltoluene	952	1125	1101*						x				
98	2580	3.25	*allo*-Ocimene (isomer)	936	1125	1132					x				x	
99	2590	4.06	Eucarvone	852	1127	1223				x	x					
100	2595	1.64	Benzeneacetaldehyde	967	1129	1042	x		x	x	x	x				x
101	2595	4.02	*cis*-Linalyl oxide (pyranoid)	928	1129	1174			x	x	x	x	x	x	x	
102	2600	3.54	Perillene	879	1130	1101		x							x	x
103	2610	3.98	*trans*-Linalyl oxide (pyranoid)	932	1132	1177		x	x	x	x	x		x		x
104	2620	3.44	2,6-Dimethyl-1,3,5,7-octatetraene (isomer)	922	1135	1134*	x	x	x	x	x			x	x	x
105	2625	3.34	Nonanal	950	1136	1101	x	x	x	x	x	x		x	x	x
106	2640	3.38	*α*-Pinene epoxide	899	1139	1095					x					

Table 3.7 - Volatiles of *Pinus* spp. detected and tentatively identified by enantiomeric GC × GC/TOFMS analysis (cont.).

							Pinus species									
Peak No.	[1]t_R	[2]t_R	Compound	Similarity	[§]RI_{calc}	[§§]RI_{Lit}	PE	PH	PP	PK	PPr	PPa	PR	PS	PB	PT
107	2650	3.77	Sabinene hydrate (isomer)	936	1142	1017-1098		x						x		
108	2670	3.56	Fenchonal (enantiomer)	844	1146					x	x					
109	2680	2.96	Butanoic acid, 3-methyl-, pentyl ester	945	1149	1108*					x					
110	2685	3.54	Fenchonal (enantiomer)	847	1150					x	x					
111	2690	3.26	*allo*-Ocimene (isomer)	913	1151	1144					x					
112	2690	4.48	1-Octanol	942	1151	1068		x	x						x	x
113	2690	4.48	Acid formic octyl ester	943	1151	1131	x				x	x		x		
114	2700	3.34	Valeric acid 3-methylbut-2-enyl ester	870	1154						x					
115	2705	3.16	6-Camphenol	847	1155	1114	x				x					x
116	2730	4.03	α-Campholenal (enantiomer)	900	1161	1126			x		x			x	x	x
117	2740	3.51	2,6-Dimethyl-1,3,5,7-octatetraene (isomer)	900	1163		x	x	x	x				x	x	x
118	2745	4.00	α-Campholenal (enantiomer)	903	1164	1126	x		x		x			x	x	x
119	2750	4.18	Linalool (enantiomer)	950	1165	1097	x	x	x	x	x	x	x		x	x
120	2765	4.95	3,7-Dimethyl-octa-1,5,7-triene-3-ol	904	1169	1101					x					
121	2770	3.48	n.i.	890	1170			x								
122	2775	4.11	Linalool (enantiomer)	952	1171	1097	x	x	x		x	x			x	x
123	2820	3.46	branched C10 ketone		1182					x				x		
124	2825	0.89	Benzoic acid ethyl ester	963	1183	1173	x									x
125	2840	4.62	Myrcenol	927	1187	1123					x				x	
126	2860	4.12	Camphor (enantiomer)	938	1192	1146					x			x		

Table 3.7 - Volatiles of *Pinus* spp. detected and tentatively identified by enantiomeric GC × GC/TOFMS analysis (cont).

Peak No.	$^{1}t_R$	$^{2}t_R$	Compound	Similarity	$^{\S}RI_{calc}$	$^{\S\S}RI_{Lit}$	*Pinus* species									
							PE	PH	PP	PK	PPr	PPa	PR	PS	PB	PT
127	2875	4.09	Camphor (enantiomer)	942	1195	1146				x	x			x		x
128	2880	4.40	*cis*-*β*-Terpineol	942	1196	1146	x	x	x		x				x	x
129	2895	2.31	Dodecane	976	1200	1200	x	x	x	x	x	x	x	x	x	x
130	2900	3.31	*trans*-2-Nonen-1-ol	855	1201	1152*										x
131	2920	430	Santolina alcohol	769	1206	1040										x
132	2935	4.66	Isophorone	867	1210	1121										x
133	2940	1.81	Naphthalene	968	1212	1181	x	x	x	x	x	x		x	x	x
134	2940	2.47	Methyl salicylate	974	1212	1192	x		x	x						x
135	2940	4.24	*α*-Fenchol	963	1212	1117	x	x	x		x			x	x	x
136	2950	3.47	2-Decanone	952	1214	1192								x		
137	2950	4.21	*β*-Fenchol	966	1214	1122				x			x	x	x	
138	2955	4.00	*E*-1-Methyl-4-(1-methylethyl)-2-cyclohexen-1-ol,	933	1215	1142*	x	x	x	x		x		x	x	x
139	2955	4.51	Nopinone	912	1215	1140	x				x				x	x
140	2960	0.11	*α*-Phellandren-8-ol (enantiomer)	910	1217	1170	x	x	x	x				x	x	
141	2960	3.88	*trans*-pinocamphone (enantiomer)	934	1217	1163	x	x		x	x	x		x	x	x
142	2965	3.80	Dill ether	895	1218	1187			x		x					
143	2965	4.06	Terpinene 1-ol	909	1218	1134		x					x	x		
144	2975	3.79	*cis*-4-Decenal	941	1221	1194	x									
145	2980	0.04	*α*-Phellandren-8-ol (enantiomer)	888	1223	1170		x						x	x	
146	2995	0.23	Methyl chavicol	963	1226	1196					x					
147	2995	3.73	*trans*-4-Decenal	903	1226	1197	x									

Table 3.7 - Volatiles of *Pinus* spp. detected and tentatively identified by enantiomeric GC × GC/TOFMS analysis (cont.).

							Pinus species									
Peak No.	$^{1}t_R$	$^{2}t_R$	Compound	Similarity	$^{\S}RI_{calc}$	$^{\S\S}RI_{Lit}$	PE	PH	PP	PK	PPr	PPa	PR	PS	PB	PT
148	3000	4.96	*trans*-Pinocarveol	916	1227	1134	x	x	x	x	x	x	x	x	x	x
149	3005	4.23	Pinocarvone (enantiomer)	832	1228	1165	x				x				x	x
150	3010	1.97	4-Methylacetophenone	959	1229	1183		x								
151	3010	4.81	Myrtenal	941	1229	1196	x			x	x			x		x
152	3015	3.20	C3-benzene	948	1231		x	x	x	x			x	x	x	x
153	3015	4.03	*cis*-pinocamphone (enantimer)	920	1231	1175				x	x		x	x	x	x
154	3015	4.21	Pinocarvone (enantiomer)	850	1231	1165	x	x	x	x	x		x	x	x	x
155	3015	4.28	Camphene hydrate	795	1231	1150	x	x	x		x			x	x	x
156	3020	4.45	*trans*-β-Terpineol	935	1232	1144	x	x	x	x	x	x			x	x
157	3025	3.87	2-Decanol	865	1233	1190*				x				x		
158	3030	3.21	*cis*-2-Methylbutanoic acid 3-hexenyl ester	890	1235						x					
159	3030	3.39	Decanal	962	1235	1202	x		x			x				x
160	3040	3.99	*cis*-pinocamphone (enantiomer)	921	1237	1175	x	x	x		x				x	x
161	3050	3.70	Linalyl acetate	953	1240	1253	x		x		x				x	x
162	3050	4.71	Myrtenal	936	1240	1196	x	x			x			x	x	x
163	3065	3.25	*cis*-3-Methylbutanoic acid 3-hexenyl ester	922	1244			x			x				x	
164	3065	4.03	Methyl thymyl ether	974	1244	1235	x		x	x	x	x	x	x	x	x
165	3080	2.98	Isovaleric acid hexyl ester	937	1247	1242*					x					
166	3085	0.26	Isopinocampheol	898	1249	1180	x				x				x	x
167	3095	4.07	4-Terpineol (enantiomer)	962	1251	1177	x	x	x	x	x	x	x	x	x	
168	3100	4.41	Cyclohexanol 4-(1-methylethyl)-	940	1253				x							x

Table 3.7 - Volatiles of *Pinus* spp. detected and tentatively identified by enantiomeric GC × GC/TOFMS analysis (cont).

Peak No.	$^{1}t_R$	$^{2}t_R$	Compound	Similarity	$^{\S}RI_{calc}$	$^{\S\S}RI_{Lit}$	*Pinus* species									
							PE	PH	PP	PK	PPr	PPa	PR	PS	PB	PT
169	3105	4.06	4-Terpineol (enantiomer)	961	1254	1177	x	x	x	x	x	x	x	x	x	
170	3120	0.43	2-Methylene-6,6-dimethyl bicyclo[3.2.0]heptan-3-ol	912	1258		x				x				x	x
171	3120	3.85	Myrtanal	898	1258	1180**	x				x				x	x
172	3120	4.70	Isoborneol	913	1258	1162	x			x	x			x	x	x
173	3125	0.29	*β*-Phellandren-8-ol (enantiomer)	916	1259	1163	x	x	x	x	x	x	x	x	x	x
174	3130	4.80	1,8-Menthadien-4-ol	869	1260	1189**	x	x	x	x	x	x		x		
175	3155	0.18	b-Phellandrene-8-ol (enantiomer)	919	1267	1163	x	x	x	x	x	x	x	x	x	x
176	3155	4.95	(+)-Borneol	939	1267	1169	x	x	x	x	x		x	x	x	x
177	3160	0.31	(-)-Verbenone	961	1268	1205	x				x					
178	3165	1.14	Nopol	955	1269	1280	x	x		x					x	x
179	3165	3.85	Bornyl acetate (isomer)	964	1269	1289	x	x	x		x	x	x	x	x	x
180	3170	4.61	(*cis*)-Piperitol	882	1271	1196	x	x	x	x	x			x	x	x
181	3185	0.00	(+)-Verbenone	967	1274	1205	x			x	x			x	x	x
182	3185	4.87	(-)-Borneol	944	1274	1169	x	x	x	x	x			x	x	x
183	3190	4.64	*d*-Terpineol	968	1276	1166				x	x			x	x	x
184	3195	0.38	Piperitone (enantiomer)	950	1277	1253		x	x	x	x	x			x	x
185	3195	0.61	Cumaldehyde	919	1277	1242	x	x			x				x	x
186	3195	4.16	*β*-Cyclocitral	895	1277	1218**	x		x			x		x	x	x
187	3210	3.43	Branched C11 ketone		1281									x		
188	3215	0.37	Piperitone (enantiomer)	808	1282	1253					x					
189	3220	3.82	Bornyl acetate (isomer)	836	1283	1289	x				x				x	x
190	3225	4.59	*α*-Terpineol (enantiomer)	968	1285	1189	x	x	x	x	x	x	x	x	x	x

Table 3.7 - Volatiles of *Pinus* spp. detected and tentatively identified by enantiomeric GC × GC/TOFMS analysis (cont.).

							Pinus species									
Peak No.	$^{1}t_R$	$^{2}t_R$	Compound	Similarity	$^{\S}RI_{calc}$	$^{\S\S}RI_{Lit}$	PE	PH	PP	PK	PPr	PPa	PR	PS	PB	PT
191	3230	4.07	*p*-Menth-1-en-9-al	891	1286	1230*	x		x		x	x		x	x	x
192	3245	4.84	Dihydrocarveol (isomer)	928	1290	1194/ 1229	x	x	x	x	x					x
193	3255	0.00	*trans*-Piperitol	892	1292	1208		x	x	x	x	x		x	x	x
194	3255	4.50	α-Terpineol (enantiomer)	960	1292	1189	x	x	x			x	x	x		
195	3260	0.81	*cis*-*p*-Mentha-1(7),8-dien-2-ol	897	1294	1231									x	
196	3265	1.46	Cymen-8-ol (isomer)	908	1295	1180		x						x	x	
197	3265	3.90	2-Octenyl acetate	848	1295									x		
198	3275	0.14	Carvone (enantiomer)	918	1297	1243					x				x	x
199	3275	0.65	Nerol (isomer)	918	1297	1230	x				x					x
200	3275	4.53	Cryptone	900	1297	1186	x		x	x	x	x		x		x
201	3280	0.07	β-Citronellol	842	1299	1226							x			
202	3280	1.09	2-Phenylethyl acetate	949	1299	1258					x				x	x
203	3285	1.46	Cymen-8-ol (isomer)	951	1300	1183	x		x	x	x	x	x	x	x	x
204	3285	2.34	Tridecane	974	1300	1300	x	x	x	x	x	x	x	x	x	x
205	3290	0.08	Carvone (enantiomer)	895	1301	1243	x		x			x				
206	3290	3.45	n.i.		1301		x									x
207	3295	4.00	2-Decenal (isomer)	923	1303	1264	x	x	x	x	x	x		x	x	x
208	3300	2.87	n.i. (sesquiterpene)		1304		x				x				x	x
209	3305	4.08	Pinocarvyl acetate isomer	914	1305	1298/ 1312	x	x			x				x	x
210	3325	1.11	*trans*-Anethole	859	1311	1253	x									
211	3325	4.11	Dihydrocarvyl acetate (isomer)	904	1311	1307	x									x
212	3330	0.99	*trans*-Carveol	948	1312	1217	x	x	x	x	x				x	x

Table 3.7 - Volatiles of *Pinus* spp. detected and tentatively identified by enantiomeric GC × GC/TOFMS analysis (cont).

Peak No.	$^{1}t_R$	$^{2}t_R$	Compound	Similarity	$^{\S}RI_{calc}$	$^{\S\S}RI_{Lit}$	*Pinus* species									
							PE	PH	PP	PK	PPr	PPa	PR	PS	PB	PT
213	3330	2.91	n.i.(sesquiterpene)		1312		x				x				x	x
214	3330	3.46	C3-Benzene (isomer)	924	1312		x	x	x	x					x	
215	3335	0.44	Myrtenol	964	1314	1196	x	x	x	x	x		x	x	x	x
216	3335	3.45	1,2-Diethyl-4,5-dimethylbenzene	928	1314			x					x	x		x
217	3335	3.51	2-Undecanone	970	1314	1294	x		x	x	x			x		x
218	3355	2.91	*d*-Elemene (enantiomer)	938	1319	1338		x				x				
219	3365	2.90	*d*-Elemene (enantiomer)	937	1322	1338		x				x				
220	3370	0.88	Nerol (isomer)	858	1323	1230	x									x
221	3370	0.88	Geraniol isomer	923	1323	1253					x				x	
222	3370	4.05	Dihydrocarvyl acetate (isomer)	945	1323	1329	x		x							x
223	3385	4.19	*cis*-Carvyl acetate	821	1327	1368					x				x	x
224	3390	2.97	α-Longipinene	932	1329	1353		x	x		x	x			x	
225	3395	4.07	n.i. (monoterpene acetate)		1330									x		
226	3410	2.81	α -Cubebene	932	1334	1351	x	x		x	x			x	x	x
227	3415	4.05	α -Ionone	817	1336	1430	x								x	x
228	3415	4.84	2,4-Decadienal (isomer)	891	1336	1293	x									
229	3420	4.55	1-Decanol	943	1337	1270	x									x
230	3430	0.16	n.i.		1340		x				x					x
231	3435	4.09	Myrtenyl acetate	931	1341	1327	x		x						x	x
232	3440	0.17	Dihydrocarveol (isomer)	917	1342					x						
233	3440	0.50	*cis*-Carveol	949	1342	1229	x	x	x	x	x				x	x
234	3470	4.09	α-Terpinenyl acetate (enantiomer)	934	1351	1349	x		x		x			x	x	x

Table 3.7 - Volatiles of *Pinus* spp. detected and tentatively identified by enantiomeric GC × GC/TOFMS analysis (cont.).

							Pinus species									
Peak No.	$^{1}t_R$	$^{2}t_R$	Compound	Similarity	$^{\S}RI_{calc}$	$^{\S\S}RI_{Lit}$	PE	PH	PP	PK	PPr	PPa	PR	PS	PB	PT
235	3480	3.63	Citronellyl acetate	940	1353	1353		x							x	
236	3495	2.88	α-Ylangene	958	1358	1375		x	x		x					
237	3495	4.42	Phellandral	938	1358	1276			x	x					x	x
238	3500	2.94	Cycloisosativene	x	1359	1371		x								
239	3505	0.02	Perilla aldehyde	901	1360	1272					x				x	
240	3505	3.66	Propionic acid isobornyl ester	895	1360	1376*								x		
241	3510	3.03	Longicyclene	899	1362	1374			x			x			x	
242	3510	4.06	Neryl acetate (isomer)	948	1362	1362	x		x		x				x	x
243	3515	2.90	α-Copaene (isomer)	961	1363	1377	x	x	x	x	x	x		x	x	x
244	3515	4.05	α-Terpinenyl acetate (enantiomer)	832	1363	1349		x							x	
245	3520	3.23	β-Elemene	926	1364	1391	x	x	x	x				x	x	x
246	3530	2.79	Isoledene	909	1367	1376	x							x		x
247	3535	0.76	*cis*-Myrtanol	942	1368	1254									x	
248	3550	3.00	β-Bourbonene	958	1373	1388	x	x	x	x	x			x	x	x
249	3565	2.93	n.i.		1377		x									
250	3565	3.01	β-Cubebene	955	1377	1388	x	x		x	x			x	x	x
251	3570	4.87	2,4-Decadienal (isomer)	931	1378	1317	x				x	x			x	x
252	3580	3.02	Sativene	926	1381	1392		x	x		x	x		x	x	
253	3585	3.22	β-Elemene	962	1382	1391	x	x	x	x	x			x	x	x
254	3585	3.55	Branched C12 ketone		1382					x				x		
255	3590	2.93	α-Copaene (isomer)	875	1384	1377	x				x	x		x	x	x
256	3605	0.46	*trans*-Myrtanol	931	1388	1261				x						

Table 3.7 - Volatiles of *Pinus* spp. detected and tentatively identified by enantiomeric GC × GC/TOFMS analysis (cont).

Peak No.	$^{1}t_R$	$^{2}t_R$	Compound	Similarity	$^{\S}RI_{calc}$	$^{\S\S}RI_{Lit}$	*Pinus* species									
							PE	PH	PP	PK	PPr	PPa	PR	PS	PB	PT
257	3605	0.68	Hydrocinnamic acid ethyl ester	948	1388	1354										x
258	3605	4.26	Myrtanyl acetate	898	1388	1387	x		x							x
259	3615	4.05	Geranyl acetate	947	1390	1381	x	x	x		x				x	
260	3615	4.05	Neryl acetate (isomer)	940	1390	1362								x		x
261	3620	3.24	Longifolene	948	1392	1408		x	x		x	x			x	
262	3620	4.45	n.i.		1392										x	
263	3625	2.90	α-Selinene	816	1393	1498		x								
264	3635	3.13	Butanoic acid octyl ester	935	1396	1372*	x									
265	3645	3.41	Undecanal	890	1399	1307										x
266	3650	2.36	Tetradecane	966	1400	1400	x	x	x	x	x	x	x	x	x	x
267	3665	3.15	α-Cedrene	861	1404	1412										x
268	3670	0.18	Valeric acid benzyl ester	874	1406						x					
269	3675	2.99	α-Bergamotene (enantiomer)	948	1407	1413/ 1435										x
270	3690	3.09	n.i. (sesquiterpene)		1411		x	x	x	x	x			x	x	x
271	3700	2.98	n.i. (sesqiterpene)		1414											x
272	3700	3.56	2-Dodecanone	947	1414	1396*								x		
273	3705	1.81	*cis*-Cinnamic acid ethyl ester	963	1416	1378	x									x
274	3705	2.96	β-Gurjunene	898	1416	1434								x		
275	3710	0.00	Benzyl isovalerate	924	1417						x					
276	3720	3.14	n.i. (sesquiterpene)		1420		x	x	x	x	x			x	x	x
277	3725	0.00	Butanoic acid 2-phenylethyl ester	919	1421	1441					x				x	x
278	3725	1.93	Methyl Eugenol	960	1421	1404	x				x				x	x

Table 3.7 - Volatiles of *Pinus* spp. detected and tentatively identified by enantiomeric GC × GC/TOFMS analysis (cont.).

							Pinus species									
Peak No.	$^{1}t_R$	$^{2}t_R$	Compound	Similarity	$^{\S}RI_{calc}$	$^{\S\S}RI_{Lit}$	PE	PH	PP	PK	PPr	PPa	PR	PS	PB	PT
279	3755	3.17	*trans*-Caryophyllene	975	1430	1419	x	x	x	x	x	x	x	x	x	x
280	3760	2.99	α-Bergamotene (enantiomer)	947	1431	1413/ 1435	x	x								x
281	3760	4.11	n.i. (monoterpene acetate)		1431				x							x
282	3765	3.56	Dodecanal	941	1433	1409		x			x					x
283	3775	3.39	α -Himachalene	926	1436	1451			x							
284	3785	3.27	n.i. (sesquiterpene)		1439			x	x		x			x		x
285	3795	3.26	n.i. (sesquiterpene)		1441		x			x	x				x	x
286	3805	3.05	α -Gurjunene	882	1444	1410		x				x		x		
287	3810	2.94	Valeric acid 2-tridecyl ester	827	1446			x								
288	3830	2.95	α -Guaiene	896	1451	1440		x				x				
289	3835	3.10	β-Farnesene (isomer)	953	1453	1443/ 1457	x	x	x	x	x	x		x	x	x
290	3840	3.53	n.i. (sesquiterpene)		1454			x	x	x						
291	3845	3.53	n.i. (sesquiterpene)		1456		x	x							x	
292	3850	3.23	n.i. (sesquiterpene)		1457		x								x	
293	3860	3.37	α-Caryophyllene	971	1460	1455	x	x	x	x	x	x	x	x	x	x
294	3865	3.07	Aromadendrene (enantiomer)	932	1461	1441	x		x	x				x		x
295	3875	3.13	β-Santalene	898	1464	1460		x								x
296	3875	4.30	Geranyl acetone	986	1464	1455	x		x	x	x	x	x		x	x
297	3880	3.30	n.i. (sesquiterpene)		1466						x					
298	3890	3.22	Aromadendrene (enantiomer)	961	1469	1441		x	x							x
299	3895	0.52	3-Methylbutanoic acid 2-phenylethyl ester	950	1470	1491					x				x	x

Table 3.7 - Volatiles of *Pinus* spp. detected and tentatively identified by enantiomeric GC × GC/TOFMS analysis (cont).

Peak No.	$^{1}t_R$	$^{2}t_R$	Compound	Similarity	$^{\S}RI_{calc}$	$^{\S\S}RI_{Lit}$	*Pinus* species									
							PE	PH	PP	PK	PPr	PPa	PR	PS	PB	PT
300	3910	3.10	n.i. (sesquiterpene)		1474						x			x		x
301	3925	3.53	branched C13 ketone	923	1479									x		
302	3940	3.43	Germacrene-D	950	1483	1485	x	x	x	x	x	x	x	x	x	x
303	3945	3.26	ε-Muurolene	954	1484	1455***			x	x	x	x		x	x	x
304	3950	3.13	n.i. (sesquiterpene)		1486			x	x	x				x		x
305	3950	3.51	n.i. (sesquiterpene)		1486			x								
306	3955	3.25	γ-Muurolene	954	1487	1480						x			x	
307	3965	3.53	Bicyclogermacrene	950	1490	1500	x		x	x	x		x	x		x
308	3975	3.39	n.i. (sesquiterpene)		1493		x	x	x							
309	3980	3.13	γ-Gurjunene	912	1494	1477		x								
310	3980	3.39	β-Himachalene	890	1494	1505		x								
311	3985	3.53	n.i. (sesquiterpene)		1496		x				x			x		
312	3995	3.34	α-Muurolene	969	1499	1500	x	x	x	x	x	x		x		x
313	4000	2.39	Pentadecane	961	1500	1500	x	x	x	x	x	x	x	x	x	x
314	4000	3.10	Allo-aromadendrene	882	1500	1460		x								
315	4005	3.50	n.i. (sesquiterpene)		1502					x	x			x		
316	4005	4.11	*trans*-2-Dodecenal	929	1502	1466	x									
317	4015	3.30	n.i. (sesquiterpene)		1505		x	x		x	x				x	
318	4020	3.54	n.i. (sesquiterpene)		1506			x	x	x					x	x
319	4025	3.30	*cis*-Cadina-1,4-diene	945	1508	1496			x					x		x
320	4030	3.24	α-Farnesene	953	1509	1506		x	x	x						x
321	4030	4.80	β-Ionone	858	1509	1489			x			x				
322	4035	3.25	n.i. (sesquiterpene)		1511		x							x		
323	4040	0.17	2,2-Dimethyl-propanoic acid 2-phenylethyl ester	938	1512			x			x				x	x

Table 3.7 - Volatiles of *Pinus* spp. detected and tentatively identified by enantiomeric GC × GC/TOFMS analysis (cont.).

							Pinus species									
Peak No.	$^{1}t_R$	$^{2}t_R$	Compound	Similarity	$^{\S}RI_{calc}$	$^{\S\S}RI_{Lit}$	PE	PH	PP	PK	PPr	PPa	PR	PS	PB	PT
324	4040	3.62	2-Tridecanone	952	1512	1496								x		x
325	4045	0.05	2-Methylbutanoic acid phenylethyl ester	891	1514		x					x				
326	4050	3.05	Anisyl acetone	940	1515	1460*				x						
327	4055	3.21	*β*-Bisabolene	914	1517	1506		x								
328	4060	0.38	3-Methyl-butanoic acid 2-phenylethyl ester	937	1518	1491		x			x				x	x
329	4060	3.19	Ledene	969	1518	1491	x		x					x		x
330	4075	2.22	*trans*-Cinnamic acid ethyl ester	958	1523	1467	x									x
331	4075	3.11	n.i. (sesqiterpene)		1523											x
332	4075	4.20	n.i. (oxi sesquiterpene)		1523		x				x					x
333	4080	2.60	*trans*-*α*-Farnesene	794	1525	1457						x				
334	4080	3.10	n.i. (sesqiterpene)		1525			x				x				
335	4090	4.24	Butylated hydroxytoluene	944	1528	1516	x	x	x	x	x	x	x	x	x	x
336	4095	4.56	n.i. (oxi sesquiterpene)		1529		x	x			x					x
337	4105	4.50	1-Dodecanol	927	1532	1409	x	x		x		x				x
338	4105	4.63	1,6-Germacradien-5-ol	839	1532		x									x
339	4110	3.48	n.i. (sesquiterpene)		1534		x				x					
340	4115	3.41	*τ*-Cadinene	965	1535	1536			x	x	x	x	x	x	x	x
341	4115	3.87	*trans*-Calamenene	935	1535	1529	x				x					x
342	4140	3.76	*cis*-Calamenene	960	1543	1540	x	x			x	x		x	x	x
343	4145	3.29	*d*-Cadinene	958	1545	1523	x	x	x	x	x	x	x	x	x	x
344	4160	4.38	*α*-Calacorene	974	1549	1546	x	x			x			x	x	x
345	4165	3.48	*α*-Cadinene	917	1551	1539			x	x	x			x	x	x

Table 3.7 - Volatiles of *Pinus* spp. detected and tentatively identified by enantiomeric GC × GC/TOFMS analysis (cont.)

Peak No.	$^{1}t_R$	$^{2}t_R$	Compound	Similarity	$^{\S}RI_{calc}$	$^{\S\S}RI_{Lit}$	*Pinus* species									
							PE	PH	PP	PK	PPr	PPa	PR	PS	PB	PT
346	4180	4.04	n.i. (oxi sesquiterpene)		1555			x								
347	4190	3.22	*trans*-α-Bisabolene	922	1558	1506	x	x		x	x				x	x
348	4195	4.38	n.i. (Oxi sesquiterpene)		1560									x		
349	4200	1.32	Cinnamic acid isopropyl ester	887	1562		x									
350	4215	1.91	4-Ethoxybenzoic acid ethyl ester	903	1566						x					
351	4215	4.36	1,5-Epoxysalvial-4(14)-ene	895	1566						x					
352	4220	4.44	Caryophyllene oxide (isomer)	820	1568	1583	x	x		x						x
353	4230	4.62	Caryophyllene oxide (isomer)	800	1571	1583	x									x
354	4240	0.40	Pentanoic acid 2-phenylethyl ester	903	1574											x
355	4240	3.33	*trans*-Cadina-1(2),4-diene	943	1574	1535	x	x	x	x	x			x	x	x
356	4255	4.46	β-Calacorene	927	1578	1566	x							x		x
357	4265	0.37	Elemol	893	1582	1550		x								
358	4265	4.73	n.i. (oxi sesquiterpene)		1582		x							x		x
359	4300	4.15	Palustrol	928	1592	1550*								x		x
360	4320	4.47	n.i. (oxi sesquiterpene)		1598		x								x	
361	4320	4.49	n.i. (oxi sesquiterpene)		1598		x		x							x
362	4320	4.58	Nerolidol (isomer)	963	1598	1563/ 1533	x		x	x						x
363	4320	4.99	Germacrene D-4-ol	905	1598	1576	x							x		x
364	4325	2.43	Hexadecane	964	1600	1600				x		x		x	x	x
365	4325	4.83	Salvial-4(14)-en-1-one	893	1600	1595									x	

Table 3.7 - Volatiles of *Pinus* spp. detected and tentatively identified by enantiomeric GC × GC/TOFMS analysis (cont.).

							Pinus species									
Peak No.	$^{1}t_R$	$^{2}t_R$	Compound	Similarity	$^{\S}RI_{calc}$	$^{\S\S}RI_{Lit}$	PE	PH	PP	PK	PPr	PPa	PR	PS	PB	PT
366	4330	3.26	Dodecanoic acid ethyl ester	903	1601	1598						x				
367	4330	4.65	n.i. (oxi sesquiterpene)		1601									x		x
368	4345	0.50	n.i. (oxi sesquiterpene)		1604		x								x	
369	4345	4.46	Caryophyllene oxide (isomer)	807	1604	1583				x		x				
370	4350	4.56	Epiglobulol	857	1605	1588**										x
371	4350	4.97	α-Guaiene	838	1605	1440	x							x		x
372	4365	4.40	n.i.		1608										x	
373	4370	4.94	Caryophyllenyl alcohol	808	1609	1572										x
374	4375	4.48	Caryophyllene oxide (isomer)	911	1610	1583	x	x	x	x	x	x		x	x	x
375	4385	1.53	n.i. (diterpene)		1612		x									
376	4395	1.49	3-Methyl-but-2-enoic acid 2-phenylethyl ester	933	1614	1487					x				x	
377	4400	0.11	Oplopenone	841	1615	1608										x
378	4420	0.38	Spathulenol (isomer)	951	1619	1578	x		x	x			x	x		x
379	4420	4.46	Caryophyllene oxide (isomer	833	1619	1583									x	x
380	4420	4.74	n.i. (oxi sesquiterpene)		1619									x		x
381	4425	4.80	n.i. (oxi sesquiterpene)		1620			x								
382	4435	4.76	Cubenol (isomer)	842	1622	1647	x							x		x
383	4440	0.01	Viridiflorol	910	1623	1593	x		x					x		x
384	4440	0.17	n.i. (oxi sesquiterpene)		1623		x									x
385	4440	0.25	2-Methyl-but-2-enoic acid 2 phenylethyl ester	899	1623	1585		x								x
386	4440	3.58	Tetradecanal	936	1623	1613					x					
387	4440	4.76	n.i. (oxi sesquiterpene)		1623			x								

Table 3.7 - Volatiles of *Pinus* spp. detected and tentatively identified by enantiomeric GC × GC/TOFMS analysis (cont.).

Peak No.	$^{1}t_R$	$^{2}t_R$	Compound	Similarity	$^{\S}RI_{calc}$	$^{\S\S}RI_{Lit}$	*Pinus* species									
							PE	PH	PP	PK	PPr	PPa	PR	PS	PB	PT
388	4460	0.22	Spathulenol (isomer)	889	1627	1578								x		x
389	4475	0.23	n.i. (oxi sesquiterpene)		1630			x								
390	4475	4.77	Guaiol (isomer)	915	1630	1601		x				x				
391	4505	4.73	n.i. (oxi sesquiterpene)		1636		x								x	
392	4510	4.63	Cubenol (isomer)	843	1637	1647	x	x	x		x			x		x
393	4545	4.50	Cubenol (isomer)	825	1644	1647	x	x	x		x			x	x	x
394	4555	0.35	γ-Eudesmol	905	1646	1632		x								
395	4555	0.66	δ-Cadinol	930	1646		x	x	x		x			x	x	x
396	4555	0.78	n.i. (diterpene)		1646					x						
397	4560	0.35	Hexanoic acid 2-phenylethyl ester	916	1647	1642	x	x							x	x
398	4580	0.88	α-Bisabolol	867	1651	1686			x							
399	4585	0.44	α-Cadinol (isomer)	924	1652	1654	x	x	x	x	x			x	x	x
400	4585	0.61	τ-Muurolol	879	1652	1647*									x	
401	4600	0.83	β-Eudesmol (enantiomer)	909	1655	1651		x								
402	4610	0.91	β-Eudesmol (enantiomer)	920	1657	1651		x								
403	4615	0.48	Guaiol (isomer)	832	1658	1601		x				x				
404	4620	1.15	Globulol	845	1659	1585								x	x	x
405	4630	2.22	Diethylphthalate	920	1661	1591						x				
406	4635	1.58	n.i. (oxi sesquiterpene)		1662		x								x	
407	4640	0.63	Isospathulenol	850	1663											x
408	4650	0.10	τ-Cadinol	918	1665	1614*	x	x	x		x			x	x	x
409	4665	1.41	2-Methylbutanoic acid 3-phenyl-2-propenyl ester (enantiomer)		1668						x					

Table 3.7 - Volatiles of *Pinus* spp. detected and tentatively identified by enantiomeric GC × GC/TOFMS analysis (cont.).

							Pinus species									
Peak No.	$^{1}t_R$	$^{2}t_R$	Compound	Similarity	$^{\S}RI_{calc}$	$^{\S\S}RI_{Lit}$	PE	PH	PP	PK	PPr	PPa	PR	PS	PB	PT
410	4680	0.55	α-Cadinol (isomer)	956	1671	1654	x	x	x		x		x	x	x	x
411	4695	0.27	Bulnesol	884	1674	1672		x								
412	4705	1.54	3-Methylbutanoic acid 3-phenyl-2-propenyl ester	913	1676						x					
413	4705	4.33	n.i. (diterpene)		1676										x	
414	4720	4.52	1-Tridecanol	937	1679	1572	x									
415	4770	0.32	n.i. (2-phenylethyl ester)		1689										x	
416	4770	4.93	Mintsulfide	838	1689	1741									x	x
417	4810	3.22	n.i. (diterpene)		1697									x		
418	4830	4.74	Muskolactone	937	1701							x				
419	4835	1.09	*cis, trans*-Farnesol	935	1702	1701	x									
420	4835	3.19	*cis*-10-Tetradecen-1-yl acetate	871	1702							x				
421	4845	1.60	n.i. (diterpene)		1705		x									
422	4960	3.17	n.i. (diterpene)		1734							x				

$^{1}t_R$, $^{2}t_R$ – compound retention time, in seconds, on the first and second dimension, respectively. x indicates compound found in the samples.
$^{\S}RI_{calc}$, $^{\S\S}RI_{Lit}$ - calculated and literature retention index data, respectively. The calculated retention indices were obtained based on retention times across the 1st dimension column. Peaks were identified based on the comparison (similarity) of their mass spectra to chemical standards, reference mass spectral databases (Mass Spectra Library NIST version 2.0, 2005 and Wiley Registry of Mass Spectral Data 7th edition, 2000) and retention indices (Adams, 2001). *RI not present in Adams and thus obtained from NIST; **RI not present in Adams and thus obtained from www.pherobase.com/database/kovats (accessed in 10 December 08); ***RI not present in Adams and thus obtained from Joulain and Koning (1998).
Pinus species key: PE - *P. elliottii*; PH - *P. halepensis*; PP - *P. patula*; PK - *P. kesiya*; PPr - *P. pinaster*; PPa - *P. pinea*; PR - *P. radiata*; PS - *P. sylvestris*; PB - *P. brutia*; PT - *P. taeda*. The peaks identified by NIST/Wiley Libraries have a match quality spectrum of 80% or better at least in one of the species.

The comparison between the calculated retention indexes with those obtained from the literature is shown in Figure 3.33. Despite the different chromatographic columns used, a coefficient of determination R^2 of 0.95 was obtained.

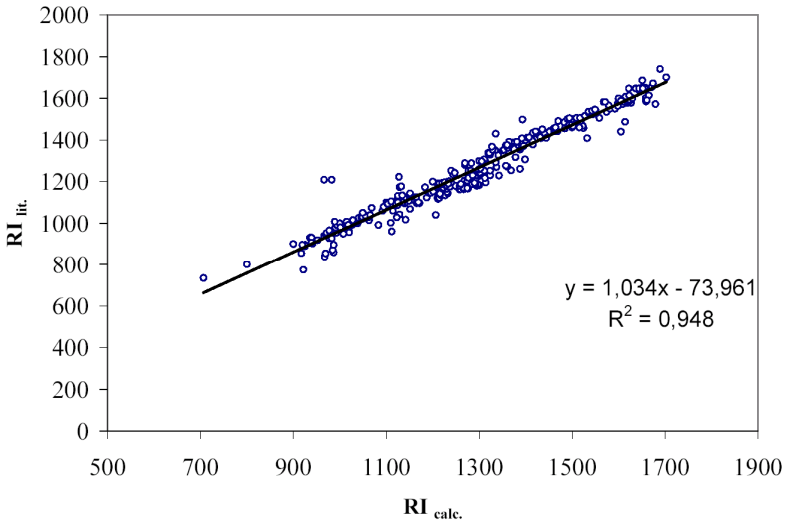

Figure 3.33 - Comparison between the retention indices from the literature and the calculated retention indices, obtained by enantioselective GC × GC/TOFMS.

3.1.1.5. Gas chromatography/field ionization - time-of-flight mass spectrometry

Pinus spp. samples were analysed by gas chromatography/time-of-flight mass spectrometry using field ionization (FI) as ion source (1D-GC/FI-TOFMS). Figure 3.34 shows the total ion chromatogram using FI obtained for the composite sample of *Pinus* spp. The X-axis is the retention time and the Y-axis is the total ion current intensity. FI is a soft ionization technique and due the low ionization voltage applied generates, for each analyte, essentially a clean mass spectrum with intense molecular ion [M^+] and minimal adducts and fragment ions. Figure 3.35 shows the mass spectra generated for α-pinene by electron ionization (EI) and by field ionization (FI). Comparing the two spectra, it can be observed that the FI spectrum is considerably simpler and easier to interpret than the spectrum generated by EI. This simplification of the mass spectrum, in spite of the loss of analytes structural information, allows for the characterization of the sample based on the distribution of the analyte molecular ions across the chromatogram.

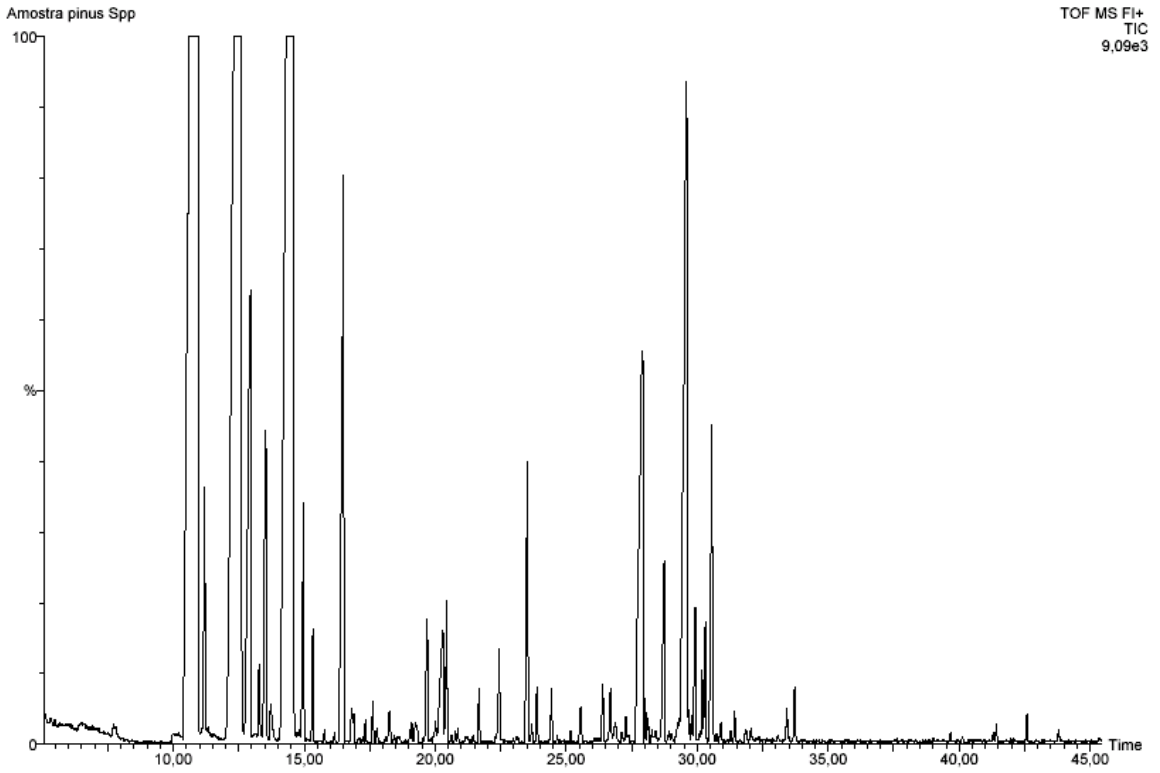

Figure 3.34 - 1D-GC/FI-TOFMS total ion chromatogram of a composite sample of *Pinus* spp.

However, since a mass spectrometer separates and detects ions of slightly different masses, it will distinguish different isotopes of a given element and therefore the fragmentation patterns of the FI spectrum will reflect the isotopic distribution of the analyte. For α-pinene, a monoterpene, with a nominal mass of 136 and chemical formula $C_{10}H_{16}$, the FI spectrum will have the isotopic fragments 136, 137 and 138 with the expected carbon isotopic abundances of 100 (^{12}C), 11.08 (^{13}C) and 0.55 (^{14}C), respectively (Figure 3.35B).

Figure 3.36 shows the average mass spectrum, from the time range between 10 and 45 minutes, for the chromatogram of Figure 3.34. The main fragments present are the m/z 136 from the monoterpenes ($C_{10}H_{16}$; M.W. 136) and m/z 204 from the sesquiterpenes ($C_{15}H_{24}$; M.W. 204). The m/z 202 comes essentially from the internal reference compound pentafluorochlorobenzene (PFCB) (C_6ClF_5; M.W. 202), which FI spectrum will have the fragments 202, 203, 204, 205 and 206 with the expected abundances of 100, 6.54, 32.14, 2.09 and 0.06, respectively. The existence of fragments with a nominal mass of 204 shared by the internal reference compound of the system and the sesquiterpenes class of compounds may be seen at first glance as a handicap of the technique due to potential nominal mass overlaps. However, the TOFMS system used provides an elevated mass resolution (7000 FWHM, at full width half maximum, according to the manufactor's specifications) and, therefore, the

differentiation of fragments 204 can be achieved, by means of their monoisotopic masses. The sesquiterpenes have a calculated monoisotopic mass of 204.188 and the PCFB fragment of 203.958 a difference of 230 mDa that requires a mass resolving power (m/Δm) of 900, for separation of the two mass spectral peaks which is achievable by the TOFMS system.

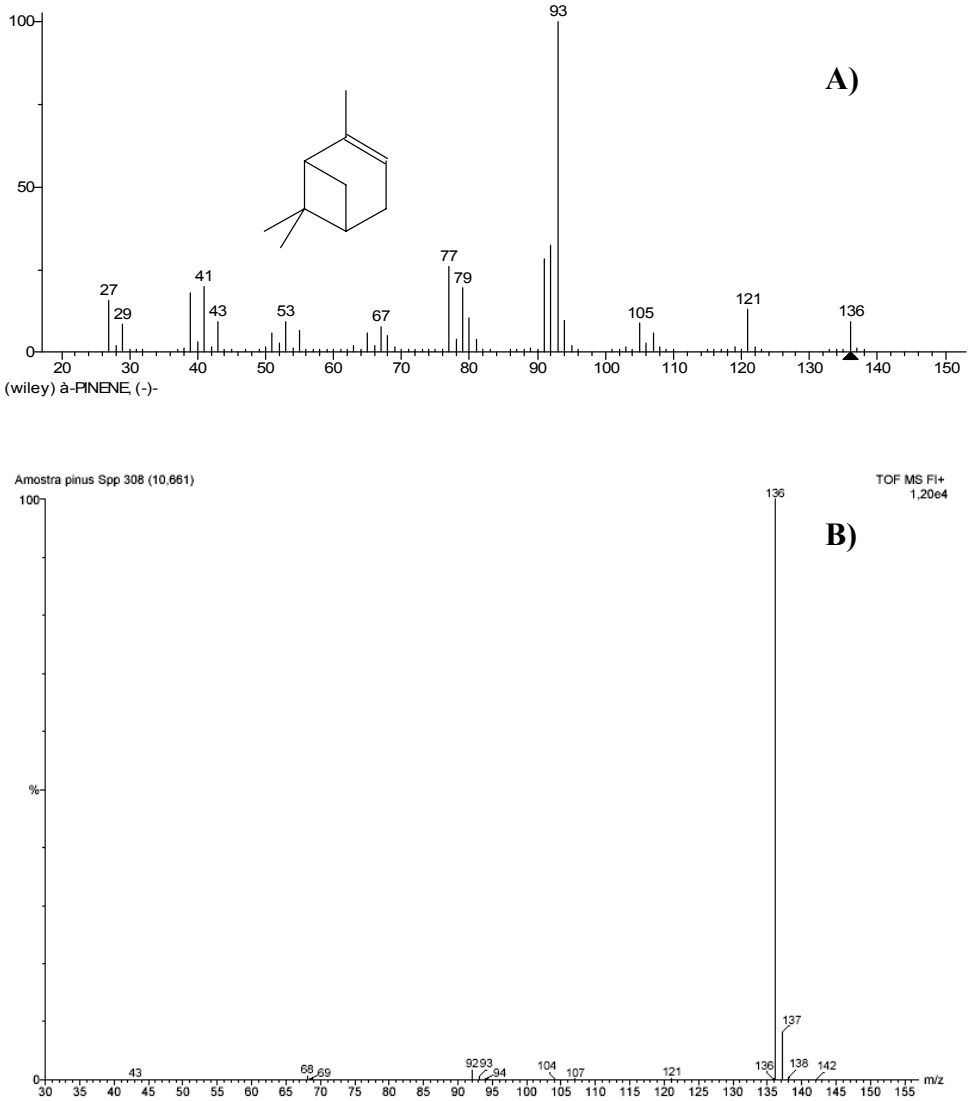

Figure 3.35 – α-pinene mass spectra generated by: **A)** by 70 eV electron ionization and **B)** field ionization.

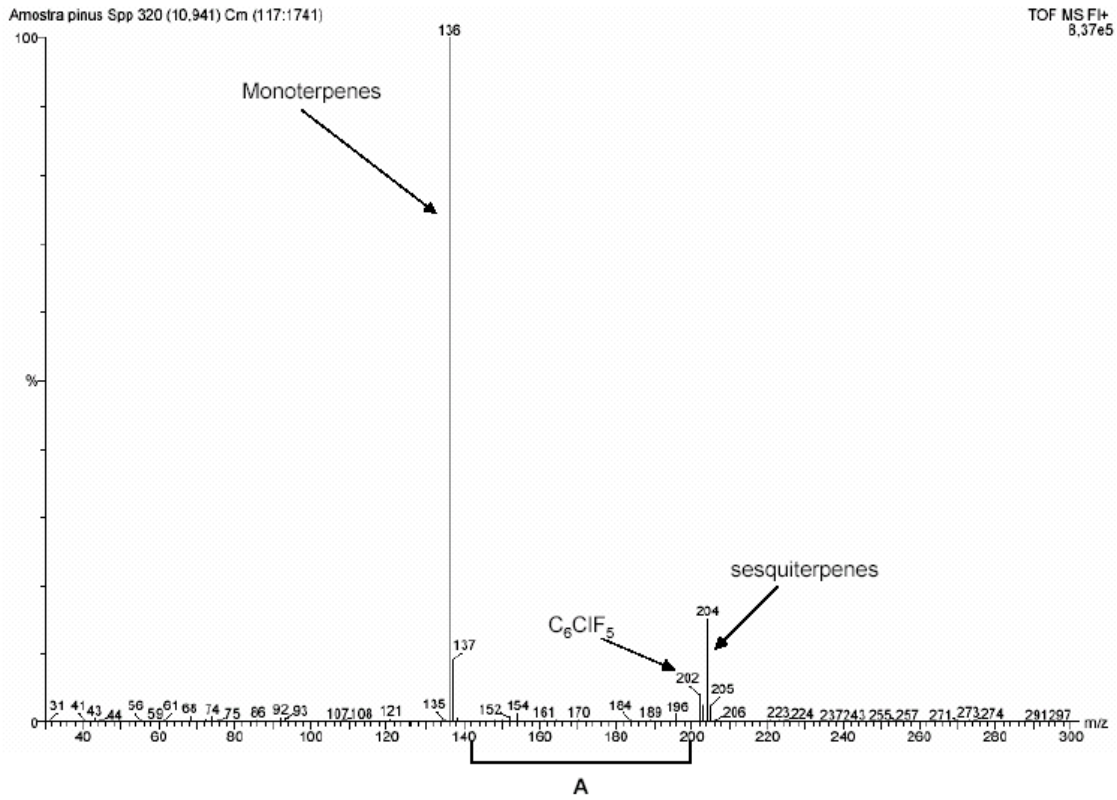

Figure 3.36 – Averaged mass spectrum from the 1D-GC/FI-TOFMS chromatogram of *Pinus* spp. composite sample (range between 10 and 45 minutes).

Figure 3.37 shows a detailed view of 200-206 mass range from a mass spectrum extracted from a sesquiterpene peak, revealing the presence of two mass peaks, 203.955 and 204.186, that have a nominal mass of 204. The sesquiterpenes and the fragment from PCFB are separated by mass spectrometry according to their monoisotopic masses.

Figure 3.38 shows an expansion of the zone A, from the averaged mass spectrum of Figure 3.36. The main fragments present are the m/z 152 and 154 from oxygenated monoterpenes, such as 1,8 cineol ($C_{10}H_{18}O$; calculated monoisotopic mass 154.136) and linalool oxide ($C_{10}H_{16}O$; calculated monoisotopic mass 152.120), and the m/z 196 of monoterpene acetates such as neryl acetate ($C_{12}H_{20}O_2$; calculated monoisotopic mass 196.146).

The m/z 161 and 189 are minor fragment ions that originate from sesquiterpene fragmentation, which appear pronounced, in the expanded range, due to the accumulated contributions of all sesquiterpene fragments. The m/z 161 and 189 are fragments that are commonly found in the EI spectrum of several sesquiterpenes. Peaks 184 and 170 are originated by dodecane ($C_{12}H_{26}$; calculated monoisotopic mass 170.202) and tridecane ($C_{13}H_{28}$; calculated monoisotopic mass 184.219).

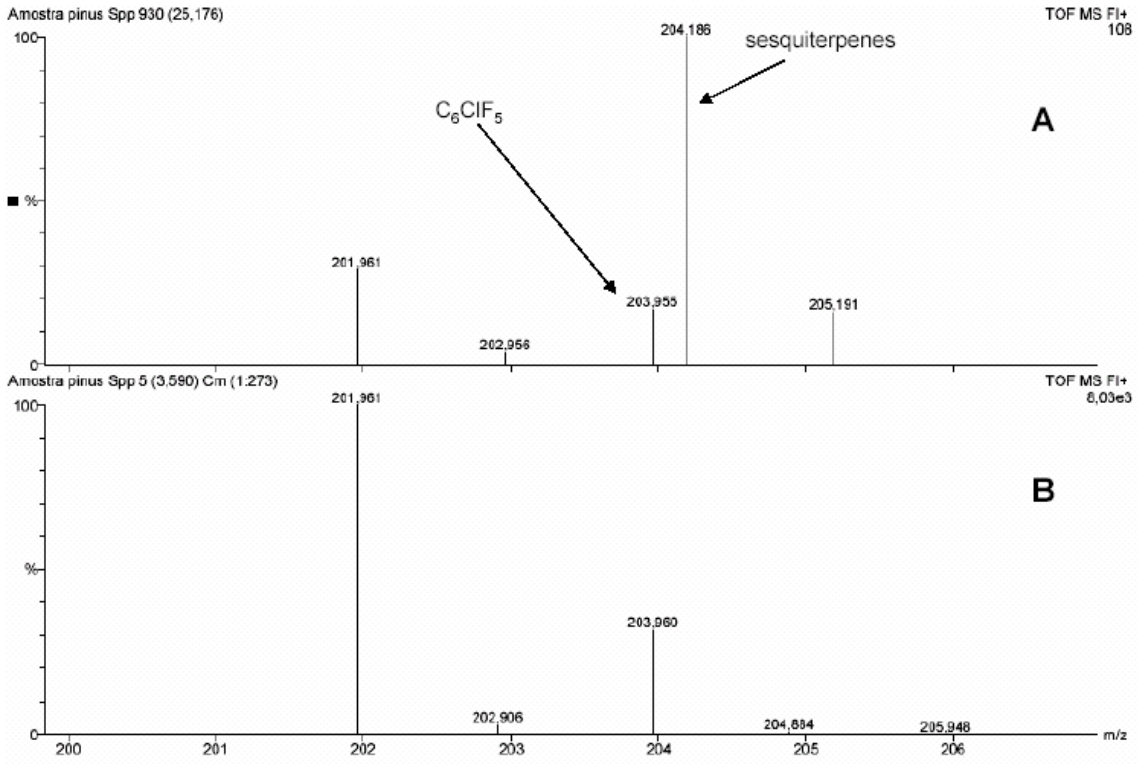

Figure 3.37 - Detailed view of 200 to 206 range of nominal masses showing exact mass present. **A**) Sesquiterpene peak; **B**) Pentafluorochlorobenzene.

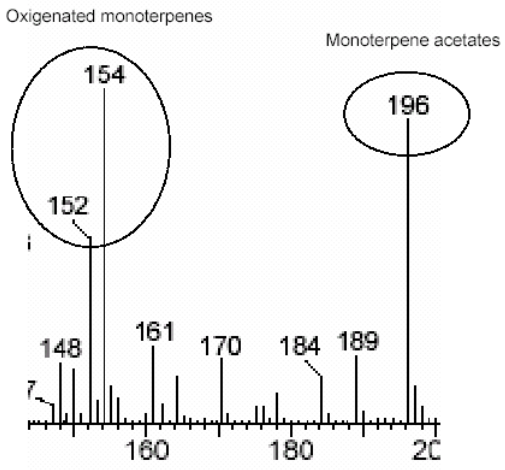

Figure 3.38 - Expansion of the averaged mass spectrum from the 1D-GC/FI-TOFMS chromatogram of *Pinus* spp. composite sample (Zone A: range between 145 and 200 amu).

Figure 3.39 shows the total ion chromatogram of *Pinus* spp. sample along with the selected ion chromatograms of masses 170 and 184. The peak label shows the exact masses of the compounds as being 170.203 and 184,212 confirming the presence of the two hydrocarbons. Alternative options for nominal mass 170 are: **i)** the compounds with the chemical formula $C_{10}H_{18}O$ (e.g. linalool oxide) that have a calculated monoisotopic mass of 170.131 and **ii)** the

compounds with the chemical formula $C_{11}H_{22}O$ (e.g. undecan-2-one) that have a calculated monoisotopic mass of 170.167. For nominal mass 184 alternatives are: **i)** the compounds with chemical formula $C_{12}H_{24}O$ (e.g. dodecan-3-one) that have a calculated monoisotopic mass of 184.183 and **ii)** compounds with chemical formula $C_{11}H_{20}O_2$ (e.g. tiglic acid hexyl ester) that have a calculated monoisotopic mass of 184.146.

Additional information that can be extracted from Figure 3.39 concerns the presence of monoterpenes (calculated monoisotopic mass 136.125), sesquiterpenes (calculated monoisotopic mass of 204.188), $C_{10}H_{18}O$ oxygenated monoterpenes (calculated monoisotopic mass 154.136) and monoterpene acetates (calculated monoisotopic mass 196.146) as major components of the sample.

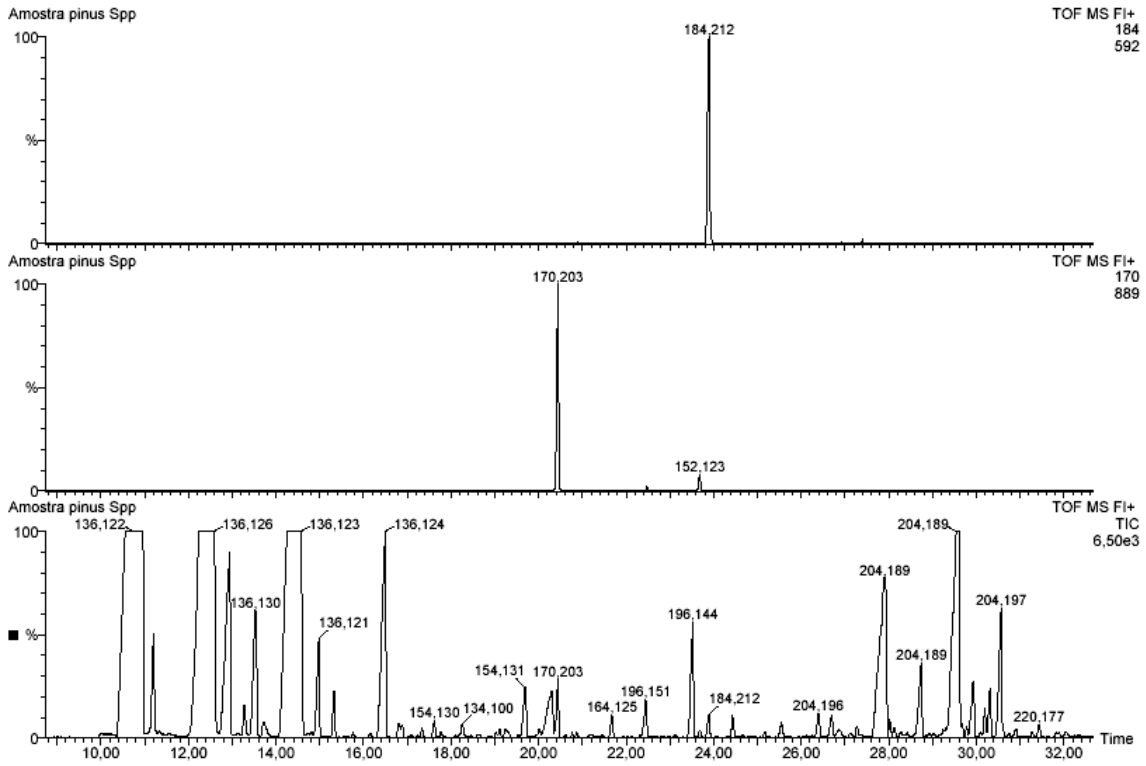

Figure 3.39 - Total ion chromatogram of *Pinus* spp. sample and selected ion chromatograms of masses 170 and 184, showing scan base peak exact masses.

In order to detect the analytes with mass 148, this ion was extracted from the TIC. The extracted ion chromatogram is shown in Figure 3.40. It can be observed that the major peak extracted is detected coeluting with the dodecane peak and other with the sesquiterpene region. Two minor peaks with base peak nominal mass of 140 are also observed following the major peak.

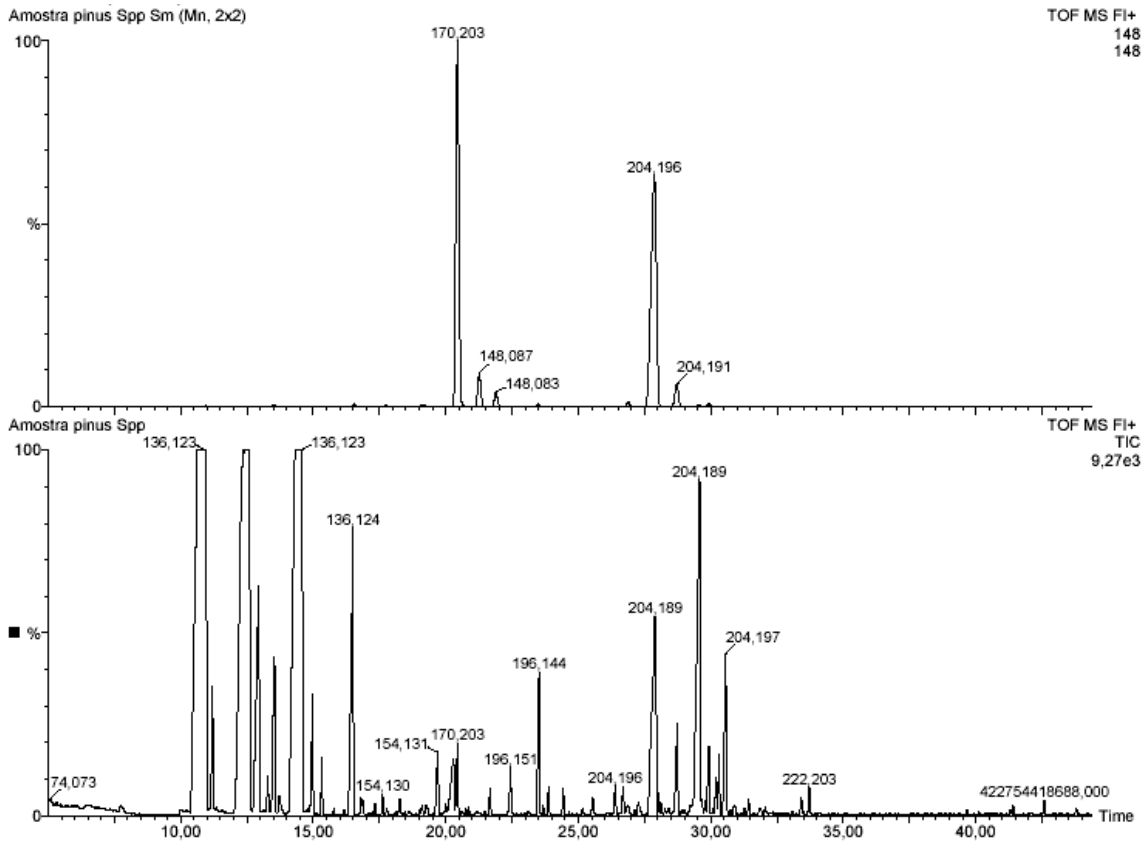

Figure 3.40 – Total ion chromatogram and extracted ion chromatogram of m/z 148 from the *Pinus* spp. composite sample.

Figure 3.41 shows the monoisotopic mass peaks from the expanded zone A of the averaged mass spectrum of Figure 3.36 compared with the averaged mass spectra of oxygenated monoterpenes and sesquiterpenes ranges. The first information given is that the odd mass fragments 189 and 161, observed on the TIC averaged spectrum, are just detected on the sesquiterpene range and the mass fragments 164 and 184 are mainly observed on the oxygenated terpene range. A closer look on the fragments with m/z 148 show that on the sesquiterpene zone their averaged monoisotopic mass is 148.114, on the dodecane zone they have an average monoisotopic mass of 148.094 and that the observed monoisotopic mass observed on the TIC is the average of 148 monoisotopic masses from both ranges. Apparently the mass fragment m/z 148.114 is a minor mass fragment that originates from sesquiterpene fragmentations, which appear pronounced, due to the accumulated contributions of all equal sesquiterpenes fragments. The m/z 148 is a fragment that is found in the EI spectrum of some sesquiterpenes such as β-caryophyllene.

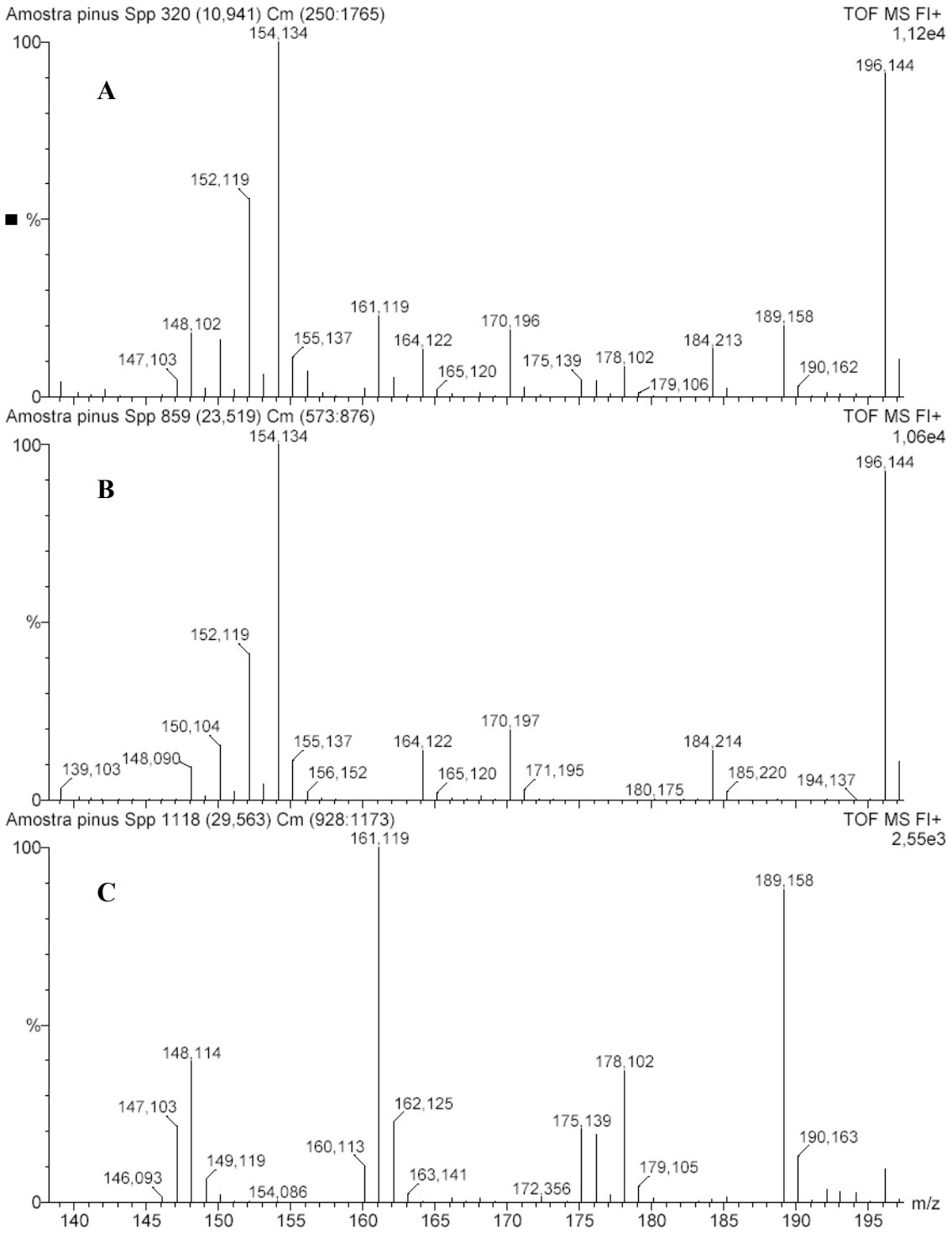

Figure 3.41 - Averaged mass spectra with the scan base monoisotopic mass peaks of: **A)** TIC expanded zone from Figure **3.36; B)** oxygenated monoterpenes range; **C)** sesquiterpene range.

Figure 3.42 shows the FI spectra of the dodecane peak. The fragments of monoisotopic masses of 170.203 from dodecane, 152.122 and 154.140 from oxygenated monoterpenes and the fragment 148 are observed. Possible hypothesis for the analyte with nominal masses are the compounds with the chemical formula $C_{10}H_{12}O$ (calculated monoisotopic mass 148.082) and silanes with chemical formula $C_5H_{16}OSi_2$ (calculated monoisotopic 148.074) and $C_6H_{16}O_2Si$ (calculated monoisotopic mass 148.092). This mean a maximum difference of 18

mDa, between the hypothesis, that requires a mass resolving power (RP) of 8000 for unequivocal separation of the mass spectral peaks which is not achievable by the TOFMS system and therefore no separation and chemical class assignment is possible by mass spectrometry.

Figure 3.43 shows the overlay chromatogram for the extracted masses 148, 152, 154 and 170, in the range of oxygenated monoterpenes, and its extended view for the dodecane peak area, in order to observe the chromatographic resolution. Assuming that each value of mass to charge is equal to the monoisotopic mass of individual analytes it can be observed, in the range of oxygenated monoterpenes, the amount of existent coelutions between the $C_{10}H_{18}O$ and $C_{10}H_{16}O$ compounds. For the dodecane peak it can be observed that the fragment 154 results from the partial coelution of the previous oxygenated monoterpene and that two potential compounds with nominal mass of 148, 152 are coeluting with dodecane. To verify this observation the same area was studied on the GC × GC data represented on Figure 3.44. Previous examination of the dodecane area on GC × GC allows for the identification of myrtenol (MW 152), piperitol (MW 154), α-terpineol (MW 154), dehydro carveol (MW 154) and the octanoic acid ethyl ester (MW 172), but no analyte with MW 148 can be found. However, the extraction of the ion 148 conducted to the detection of a compound present at low concentration on the sample (Figure 3.44 A) and B)). Consulting the Adams database (2001), a tentative identification can be proposed using the relative retention indices for the compound that has a nominal mass of 148. Dodecane has a retention index of 1200 and the closest compound, stated on the Adams database, with nominal mass 148 is methyl chavicol with a retention index of 1196. The experimental retention index for the other identified compounds in GC × GC ranged from 1194, of α-terpineol to 1200 from dodecane.

Although FI-TOFMS can not detect isomers which were not separated chromatographically, it shows great potential to separate analytes with different monoisotopic masses, even if they were not separated in the chromatographic run. Therefore this technique produces chemical information that leads to an additional characterization of complex samples, such as essential oils. On the sample analysed, it can be assumed that the analytes were submitted to two distinct separation steps. First they were separated by gas chromatography, according to their boiling point, considering that the stationary phase is an apolar column, and additionally "separated" by FI-TOFMS due to their unique monoisotopic masses. As consequence GC/FI-TOFMS may be seen as a two-dimensional analysis where the chromatographic dimension

can be represented plotted on the X–axis and the mass spectral dimension represented plotted on the Y-axis, being the signal intensity plotted on the Z–axis (Figure 3.45).

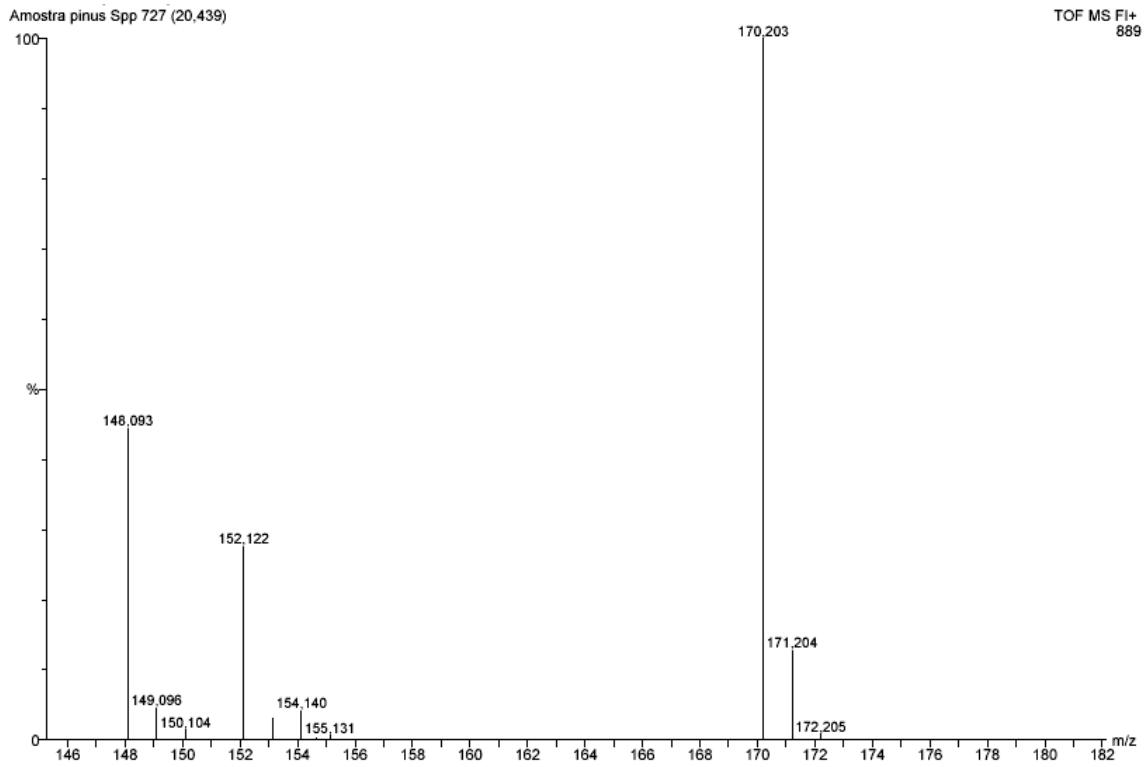

Figure 3.42 – Averaged FI mass spectrum of dodecane (MW 170) peak from *Pinus* spp. composite sample.

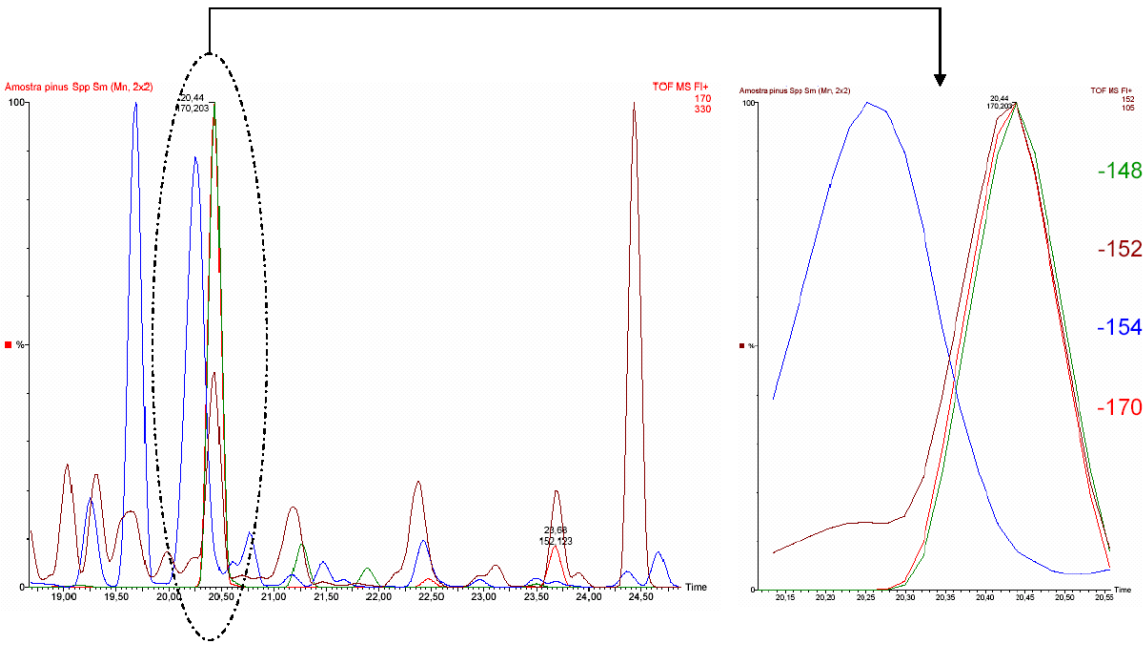

Figure 3.43 - Overlay chromatogram for the masses 148, 152, 154 and 170, in the range of oxygenated monoterpenes, and its extended view on the dodecane peak area.

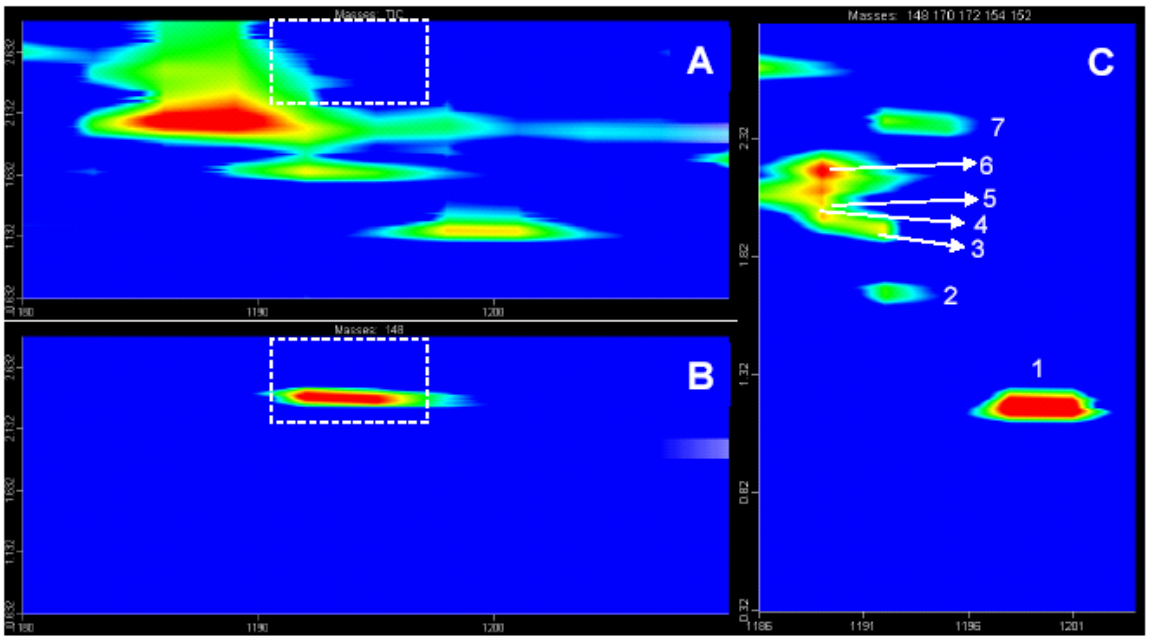

Figure 3.44 – GC × GC contour chromatograms from the dodecane area in *Pinus* spp. composite sample: **A)** Total ion chromatogram; **B)** Extracted ion chromatogram for mass 148; **C)** Extracted ion chromatogram for masses 148, 152, 154, 170 and 172. Peak identification: 1 – Dodecane; 2 – Octanoic acid ethyl ester; 3 – Dehydro carveol; 4 – Piperitol; 5 – Myrteno; 6 – α-Terpineol; 7 – compound with nominal mass 148 (Methyl chavicol).

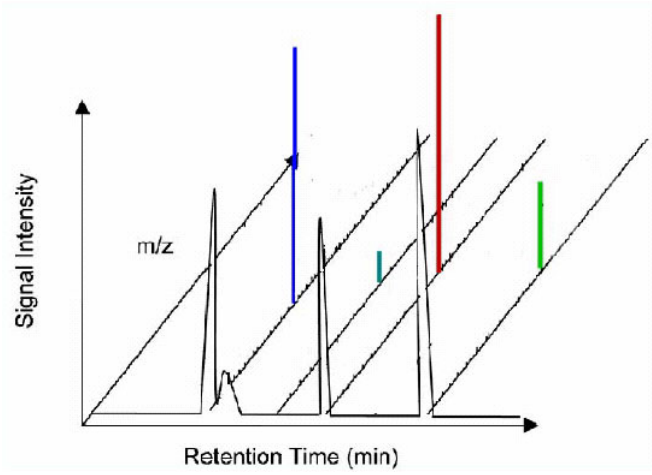

Figure 3.45 – Representation of GC/FI-TOFMS multidimensional separation.

The combination of the two methods results in a 3-D data set that provides qualitative (analyte characterization) and quantitative information (signal intensity). Additionally and according to de definition of Schoenmakers *et al.* (2003), GC/FI-TOFMS can also be seen as a comprehensive two-dimensional separation (GC×MS) because it fulfils the three requirements:

i) Every part of the sample is subjected to two different and completely independent separations (orthogonality) – analyte separation by boiling point or polarity versus analyte separation by its unique monoisotopic mass.

ii) Equal percentages (either 100%, or lower) of all sample components pass through both systems and a "faithful representation" of the chromatogram is obtained.

iii) The separation (resolution) obtained in the first dimension is essentially maintained.

In consequence, each analyte belonging to a sample analysed by GC/FI-TOFMS can be characterized by its chromatographic retention time and its unique monoisotopic mass and thus be appropriately visualized in a two-dimensional plot where the X-axis will represent the retention times and the Y-axis the monoisotopic/exact mass scale of sample analytes (Figure 3.46). The plot is constructed by extracting from the TIC, the individual monoisotopic masses of the sample analytes, based on the mass fragments found in the averaged chromatogram spectrum and recording the peaks retention time.

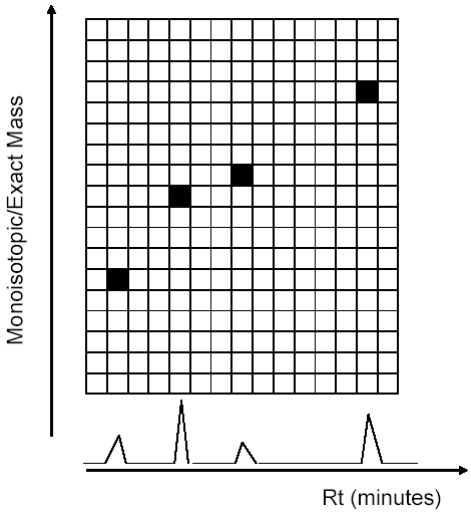

Figure 3.46 - GC/FI-TOFMS data visualization in a two-dimensional plot. The X-axis represents the retention times and the Y-axis the monoisotopic/exact mass scale of sample analytes.

Figure 3.47 shows the two-dimensional plot representation (GC × MS) of GC/FI-TOFMS data obtained for the *Pinus* spp. needle volatiles composite sample. Each detected analyte in the sample is represented by a dot in the two-dimensional plot, after plotting its nominal mass against its retention time. The stationary phase used provides separation of the sample analytes by boiling point. The first information, given by the plot visualization concerns the identification of compound classes in the sample and their chromatographic separation. The compound classes are identified in Figure 3.47, showing the presence and the chromatographic distribution of the C_6 green leaf volatiles, the monoterpenes, the oxygenated monoterpenes, the sesquiterpenes and diterpenes. Additional information concerns the

potential coelutions that can occur on the used stationary phase with the cineols and some monoterpenes and between the sesquiterpenes and oxygenated monoterpenes and sesquiterpenes. Qualitatively the combination of compound unique monoisotopic mass, which represents a unique molecular formula, with its calculated retention index is potentially a useful tool for its detection, or identification, especially if completed with data obtained with other ionization techniques (e.g. EI). The complementarity of FI in relation to EI is more evident for compounds that have a high fragmentation pattern, without visible molecular ion or with an EI spectrum that do not differentiate them from other class of compounds. An example are the monoterpene esters such as the linalyl propionate (MW 210) that produce an EI spectrum, without detectable molecular ion and almost identical to some monoterpene spectra. The analyte clustering simplifies data interpretation due to plot structure assignment and potentially allows the comparison between the composition of different samples and between the chromatographic resolutions of different stationary phases.

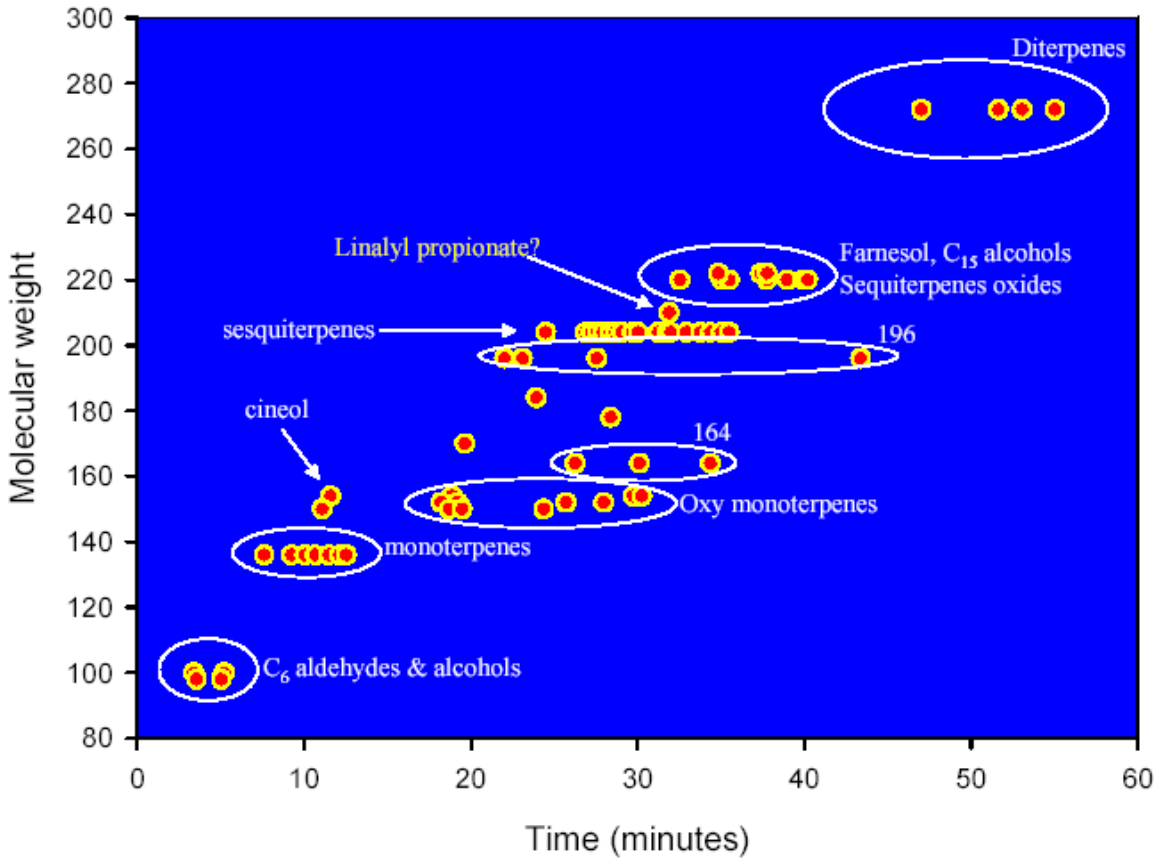

Figure 3.47 – Two-dimensional plot representation (GC × MS) of GC/FI-TOFMS data from the *Pinus* spp. needle volatiles composite sample.

3.2. Resin acids

3.2.1. Gas chromatography/mass spectrometry (1D - GC/MS)

The susceptibility to *T. pityocampa*, within the genus *Pinus*, varies both intraspecifically and interspecifically, according to the geographic location and previous defoliation history of the trees (e.g. Battisti, 1988; Devkota and Schmidt, 1990). However, contradictory results and large variations have been reported in the literature, concerning *T. pityocampa* larval survival and performance in relation to different host pine species and the physical, or chemical, characteristics of their pine needles (Avtzis, 1986; Schopf and Avtzis, 1987; Devkota and Schmidt, 1990; Hódar *et al*., 2002).

In relation to the chemical composition of the needles, their contents in silica (an hardness indicator), nitrogen, soluble carbohydrates, amino acids, terpenes and phenolic compounds have been studied and tentatively related with larval survival and performance (Schopf and Avtzis, 1987; Hódar *et al*., 2002; Hódar *et al*., 2004; Petrakis *et al*., 2005). Nevertheless, no studies concerning the contents and composition in diterpene resin acids of pine needles and *T. pityocampa* larval performance have been published.

In a first experiment, the composition in diterpene resin acids of the needles of four pine species, *P. pinaster*, *P. pinea, P. halepensis* and *P. brutia* which had been used to study the larval performance of *T. pityocampa* between the 2nd and the 5th instars, were studied by 1D-GC/MS (quadrupole) and GC × GC/TOFMS. In a second experiment, the composition of diterpene resin acids of eleven pine species were studied by means of 1D-GC/MS (ion trap). The second set of samples comprised of *P. pinaster*, *P. pinea*, *P. brutia*, *P. kesiya*, *P. sylvestris*, *P. nigra*, *P. patula*, *P. radiata*, *P. elliottii*, *P. taeda* and *P. halepensis*. For *P. halepensis* 22 samples were originating from Portugal, Israel and Greece. The reason for the inclusion of such a large and diversified number of *P. halepensis* samples, were related to previous findings (Branco *et al*., in prep.) regarding the performance of *T. pityocampa* larvae, fed on four pine species. Results showed that larvae fed on *P. halepensis* had a high mortality,

which is not in accordance with the work of Avtzis, in Greece (Avtzis, 1986), and observations in Israel, where *T. pityocampa* infestations occur in *P. halepensis* plantations and are considered a serious health problem (Solt and Mendel, 2002). The operational details and sample provenances are reported under Chapter 2, Material and methods. All resin acids were chromatographically studied in their form of methyl esters.

The 1D-GC/MS analysis of the pine needles showed that the most abundant diterpene resin acids were the tricyclic dehydroabietic and abietic acids, followed by the abietic isomers levopimaric/palustric, neoabietic and some bicyclic labdanes such as the communic acid. The labdane pinifolic acid was also found in *P. sylvestris*, where it is the major component, and at a lower level, in *P. nigra* needles. Due to the absence of available commercial standards of the diterpene resin acids, with the exception of abietic acid, their tentative identification and elution order was tentatively assessed according to literature data (Chang *et al*., 1971; Branco 1994; Li *et al*., 1996; Pfeifhofer, 2000), their molecular and characteristic mass fragments and on spectra comparison with NIST/Wiley mass spectral database. Abietic acid was identified by co-injection of its standard. All the resin acids were detected on the TIC by extraction of the molecular m/z 316 and m/z 314 which intensity is strong for the resin acids methyl esters. Dehydroabietic and neoabietic acids were confidently identified due to their predominant m/z 239 and m/z 135 mass fragments, respectively. Sandaracopimaric, pimaric and communic acids were detected by their characteristic m/z 121. Isopimaric acid was detected by its characteristic m/z 241. Levopimaric and palustric acids were not separated from each other on the DB-5 column used and were detected by the simultaneous existence of m/z 316, 43, 91, 146 and 301. A high m/z 146 is characteristic of levopimaric acid and a higher m/z ion 301 than m/z 316 is characteristic of palustric acid.

Figures 3.48 and 3.49 present, respectively, the TIC obtained for the methylated extracts of a *P. halepensis* from the second experiment and for the *P. halepensis* from the first experiment (larval performance). The numbered peaks refer to the resin acids peaks and are numbered according to the key reported in the figures.

The observation of Figure 3.48 shows that adequate resolution of the individual resin acids was not possible due to the great number of peaks present on their retention time domain. Due to the coelutions the only way to obtain information about the resin acids composition was by extraction of the molecular m/z 316 and 314. An example is presented on Figure 3.50.

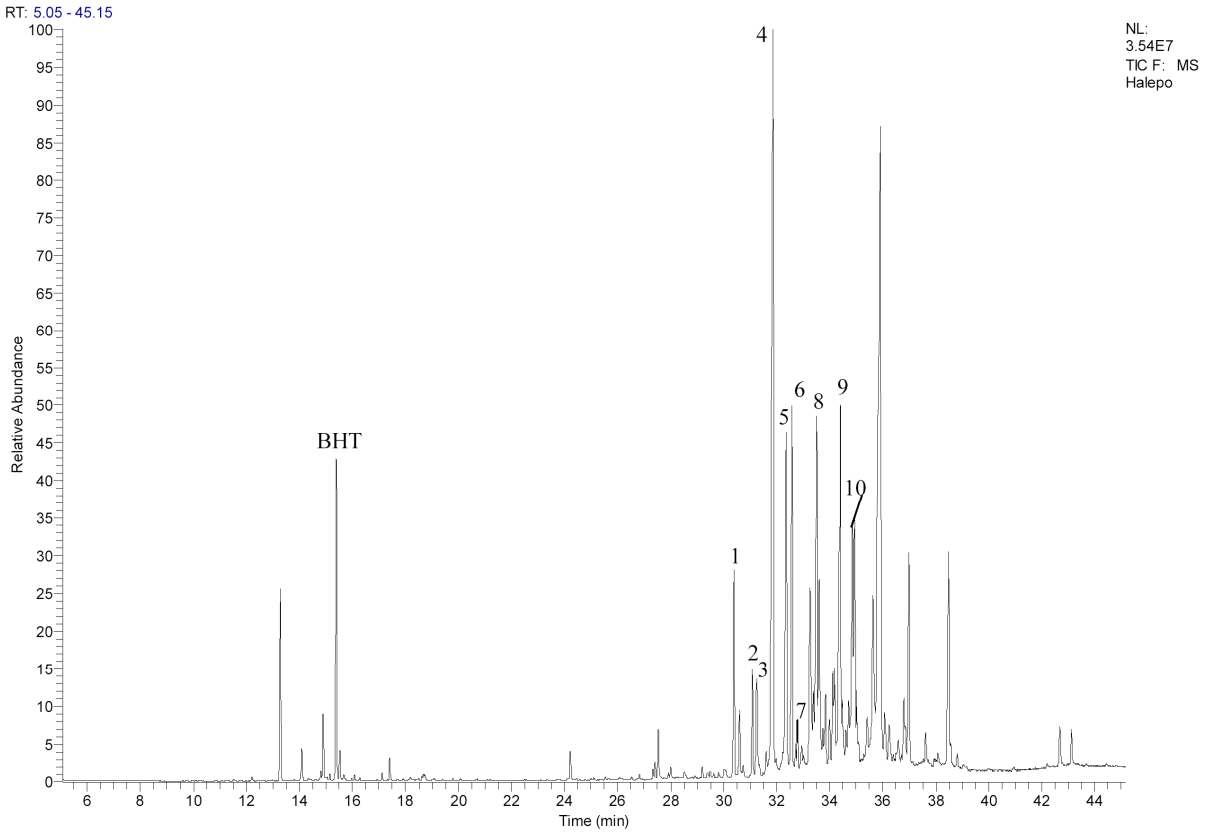

Figure 3.48 – Total reconstructed chromatogram of the non volatile fraction of *P. halepensis* from the second experiment. Key: 1 - sandaracopimaric acid; 2 - isopimaric acid; 3 - levopimaric + palustric acid; 4 - dehydroabietic acid; 5 - communic acid; 6 - abietic acid; 7 – DA2; 8 - neoabietic acid; 9 – DA3; 10 – DA4; DA - not identified diterpene acids. BHT - butylated hydroxytoluene (solvent antioxidant).

Figure 3.49 shows the TIC obtained for the *P. halepensis* needles used in the larval performance experiments. The needles extracts were characterized by the high amounts of peaks A, B and C. Peak B was tentatively identified as methyl copalate, with a similarity of 901 with the NIST/Wiley spectrum (Figure 3.51), meaning that the needles were rich in copalic acid, a labdanic diterpene acid. Peak C is non derivatized copalic acid and it results from its incomplete methylation (derivatization) on the extract. The mass spectrum of peak A presented a similarity of 836 with sclareol, a labdane diterpene, according to the NIST/Wiley database. Further sample analysis by field ionization shown that this identification was incorrect because the compound in peak A has a molecular mass of 290 while sclareol has a molecular mass of 308. Peak A has a spectrum that resembles epimanool, manool and manoyl oxide, all labdane diterpenes with molecular mass of 290. However it presents similarities lower than 800, for all of the compounds, according to the NIST/Wiley database.

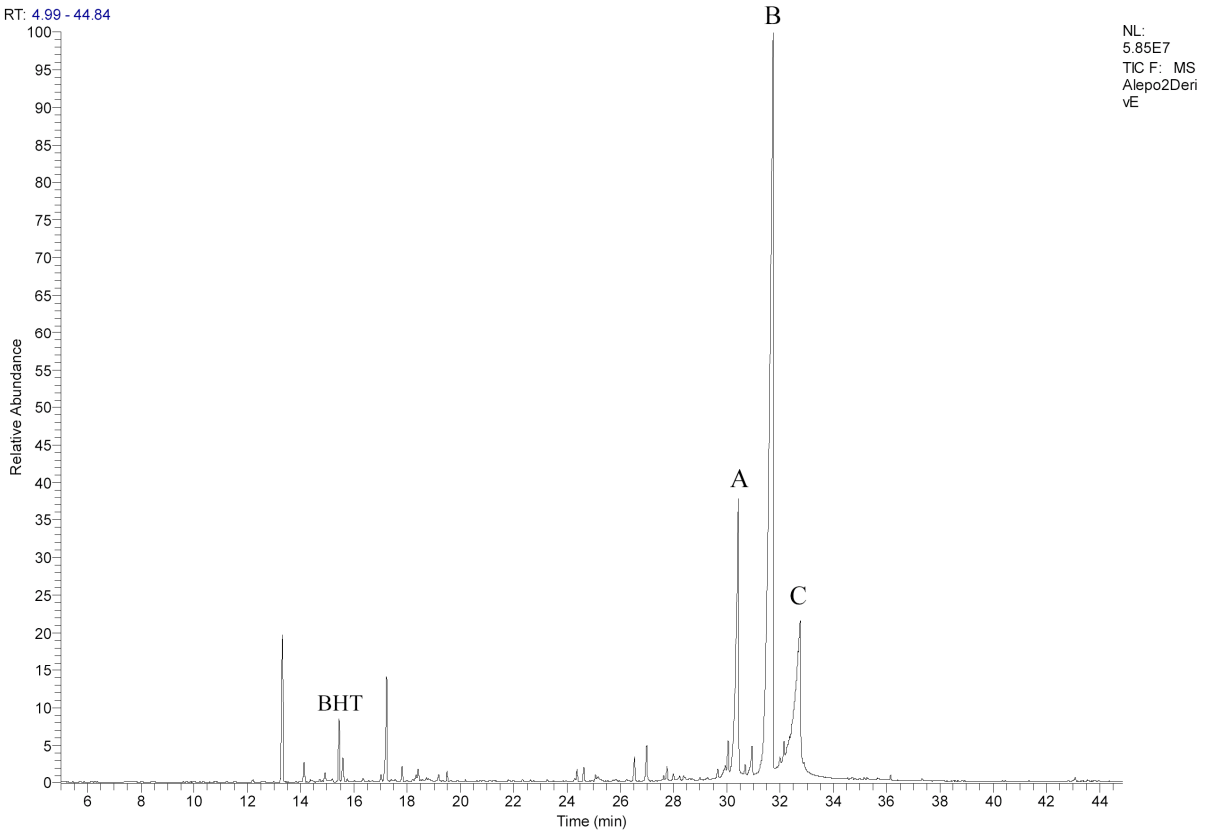

Figure 3.49 – Total reconstructed chromatogram of the non volatile fraction of *P. halepensis* used in the larval performance experience. Key: A – oxygenated labdane (MW: 290), B - Methyl copalate; C - copalic acid (not derivatized). BHT - butylated hydroxytoluene (solvent antioxidant).

The presence of peaks A, B and C (Figure 3.50) was not detected among the needles of the others *P. halepensis*, neither in all the other pine species analysed, with the exception of the *P. pinaster* needles used in the larval performance experiment. The evaluation of the amounts present in both species after integration of the peaks obtained by extraction of m/z 318 shows that the amounts of copalic acid in the *P. pinaster* needles were lower than 3.5% of those present in *P: halepensis* needles. The larval performance experiments resulted that the final larval weight and survival rate varies significantly according to the pine species were the larvae feed on. The results showed the lowest weight gain, food consumption and survival rates for the *T. pityocampa* larvae that were feeding on the *P halepensis.* The evaluation of the relationships between the amounts of copalic acid and the larvae performance resulted in a negative correlation coefficient of – 0.95 between the copalic acid and the survival rate and weight gain, although not significant (Spearman test; significant level $p<0.050$; p-value = 0.051) probably as consequence of the sample size.

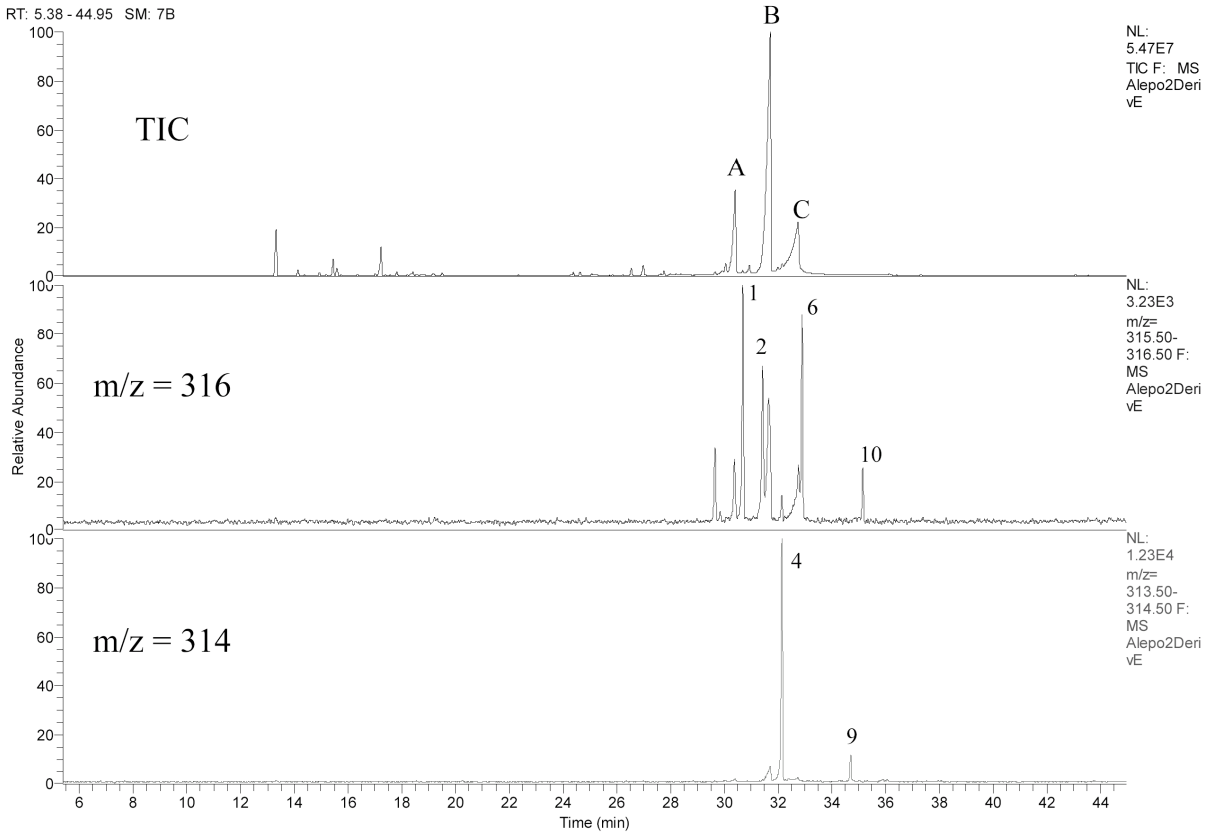

Figure 3.50 – Total reconstructed chromatogram and single ion reconstructed chromatograms for m/z 316 and 314 of the non volatile fraction of *P. halepensis* from the first experiment. Key: 1 - sandaracopimaric acid; 2 - isopimaric acid; 3 - levopimaric + palustric acid; 4 - dehydroabietic acid; 6 - abietic acid; 9 – DA3; 10 – DA4; DA - not identified diterpene acids.

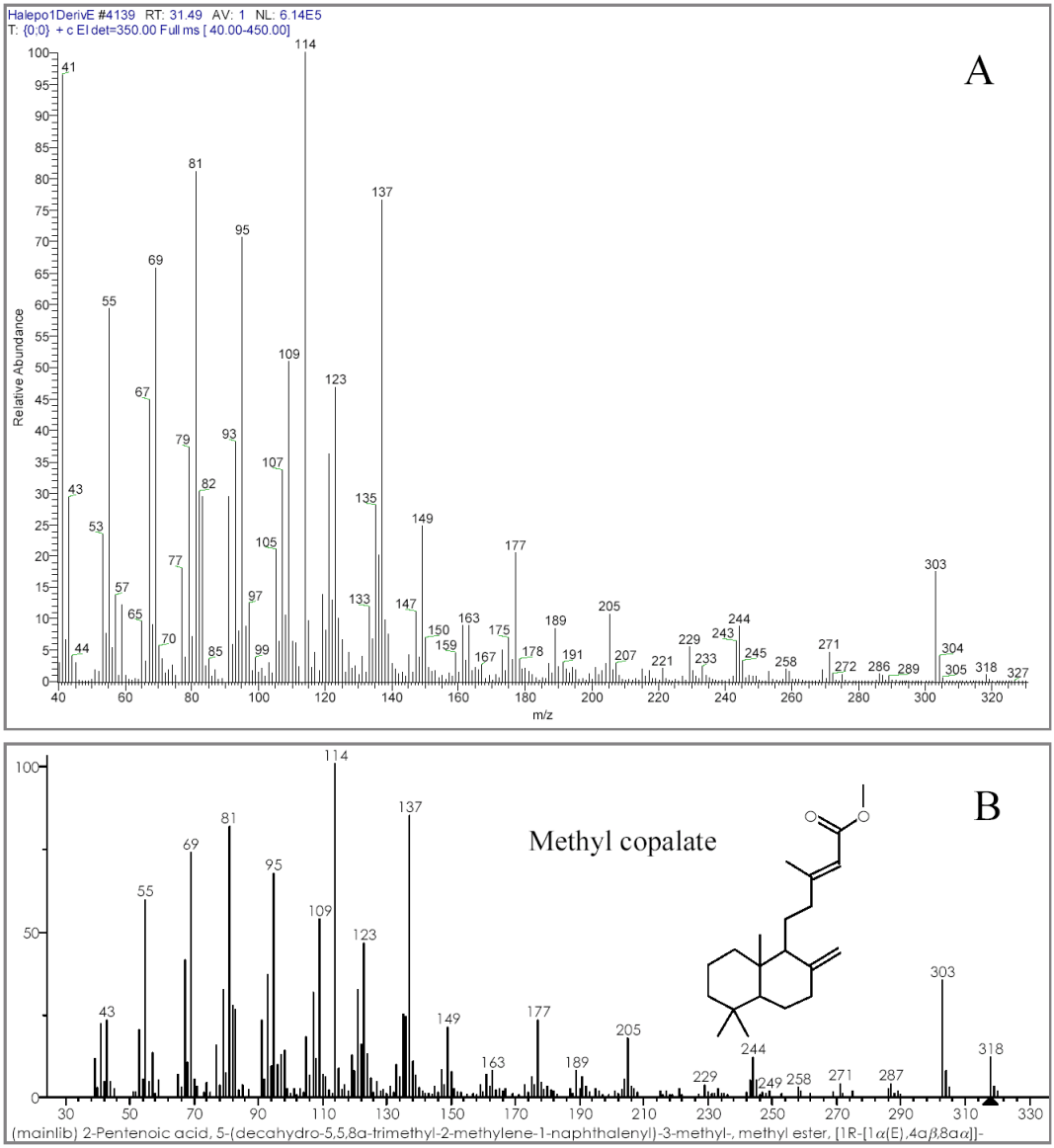

Figure 3.51 – Mass spectra of tentatively identified copalic acid (as methyl copalate) A) Mass spectra of peak B from the Figures 3.49 and 3.50; B) Mass spectra of methyl copalate from NIST/wiley database library.

3.2.2. Comprehensive two-dimensional gas chromatography/time-of-flight mass spectrometry (GC × GC/TOFMS)

The resin acids present in the pine needles extracts were analysed by GC × GC/TOFMS using a column set made that comprises a BPX-5 non-polar column (5% phenyl 95% dimethyl polysiloxane phase) on the first dimension and a BPX-50 mid polarity column (50% phenyl polysilphenylene-siloxane phase) on the second dimension.

Figure 3.52 shows a sequence of four contour plots that reflect the composition found by GC × GC in the methylated extracts from the pine needles of *P. halepensis*, *P. brutia*, *P. pinaster*

and *P. pinea* used in the larval performance bioassays. The Figure allows a simple visualization and comparison between the needles extracts from different pine species.

The compounds (black spots on the contour plot) or sectors in the plot that visually differ from sample to sample may be considered unique for each pine species at the experiment and thus can be used in a fingerprint approach evaluation. The retention time domain where the resin acids elute is highlighted on the pictures.

Among the four pine species analysed *P. halepensis* shows the highest amount of compounds and *P. pinea* and *P. brutia* the lowest amount in the resin acids retention time domain. It is also visible in the contour plot of all species that the compounds appear as isolated spots and are separated on the second dimension with some of them, located at the bottom in the middle of the plot, eluting after the modulation period and thus suffering wrap-around effect. Figure 3.53 shows an expanded view of the resin acids retention time domain. The resin acids (numbered spots) are distributed on the two dimensional plane and isolated from the other compounds that are present in the sample. The resin acids are divided in two groups according to their elution on the second dimension. Pimaric (peak 1), sandaracopimaric (peak 2) and isopimaric (peak 3) acids are grouped on the top of the second dimension axis. Dehydroabietic (peak 5) and abietic (peak 6) acids elute after the modulation period, suffering from wrap around and are located on the bottom of the second dimension axis. The peak of the pair levopimaric/palustric acids (peak 4) is split in all samples. The beginning of the peak is located on the top of the contour plot and it end is suffering wrap-around and is located at the bottom of the plot. The octadecenamides (fatty acid amides) present in *P. pinaster* and *P. halepensis* are sample contaminants. As expected by the previous visualization of Figure 3.52, *P. halepensis* present the contour plot with the highest amount of peaks with some coelutions on the first dimension visibles. The majority of the visible peaks present similar mass spectra with those of some labdane compounds such as manoyl oxide. The peaks are pointed by white arrows in the Figure 3.53. Peak 7, an intense red spot in Figure 3.53, is the methyl copalate the major compound found on the *P: halepensis* needles from the larval performance experiment. The peak is split between the top and the bottom of the plot suffering wrap around. The peak, on the first dimension, presents some tailing at its end that suffers wrap-around which due to the modulation appears sliced in the wrap-around section.

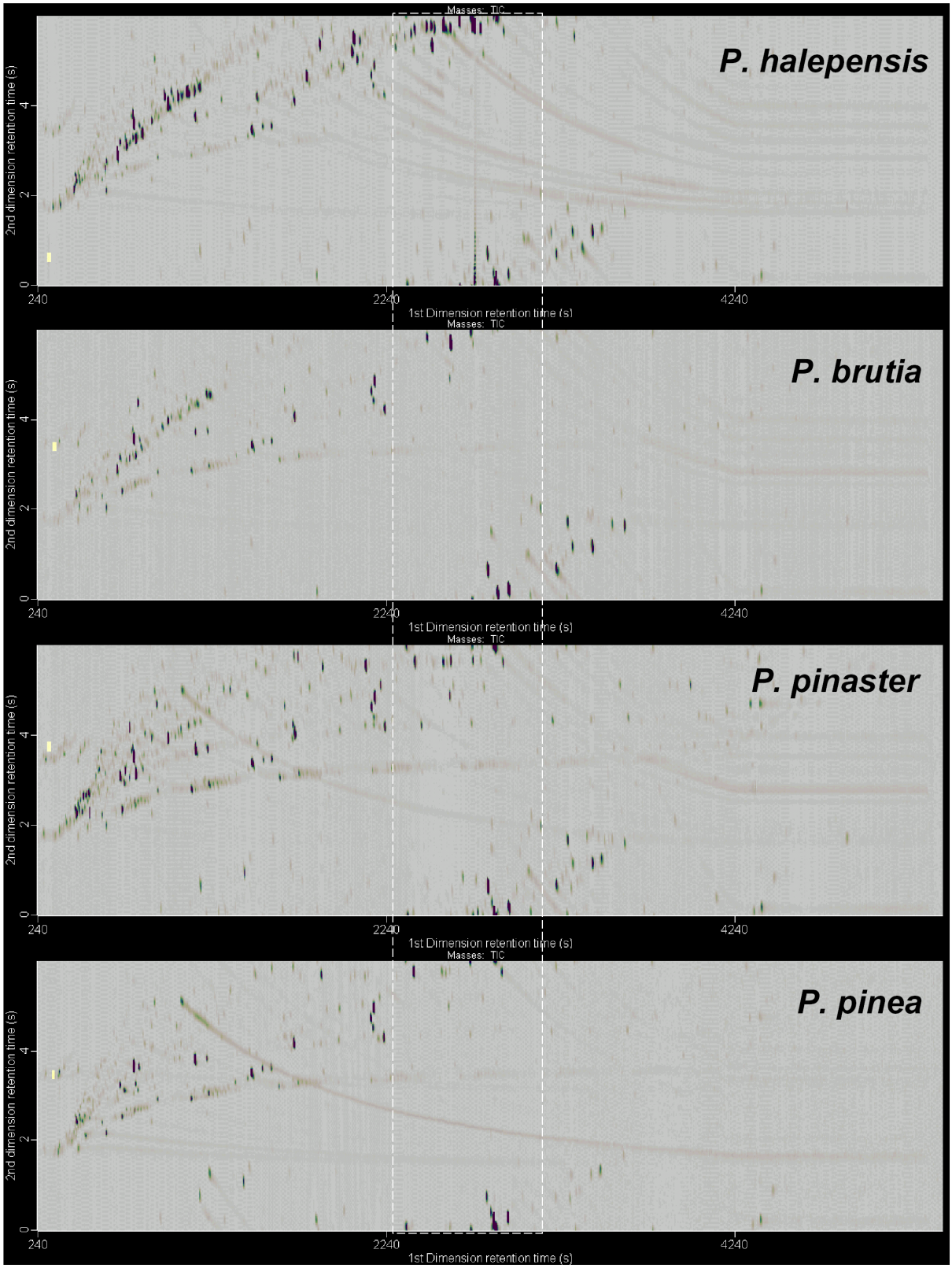

Figure 3.52 – GC × GC/TOFMS contour plots of methylated extracts from pine needles. Pine species reported in the plots. The retention time domain of resin acids is highlighted.

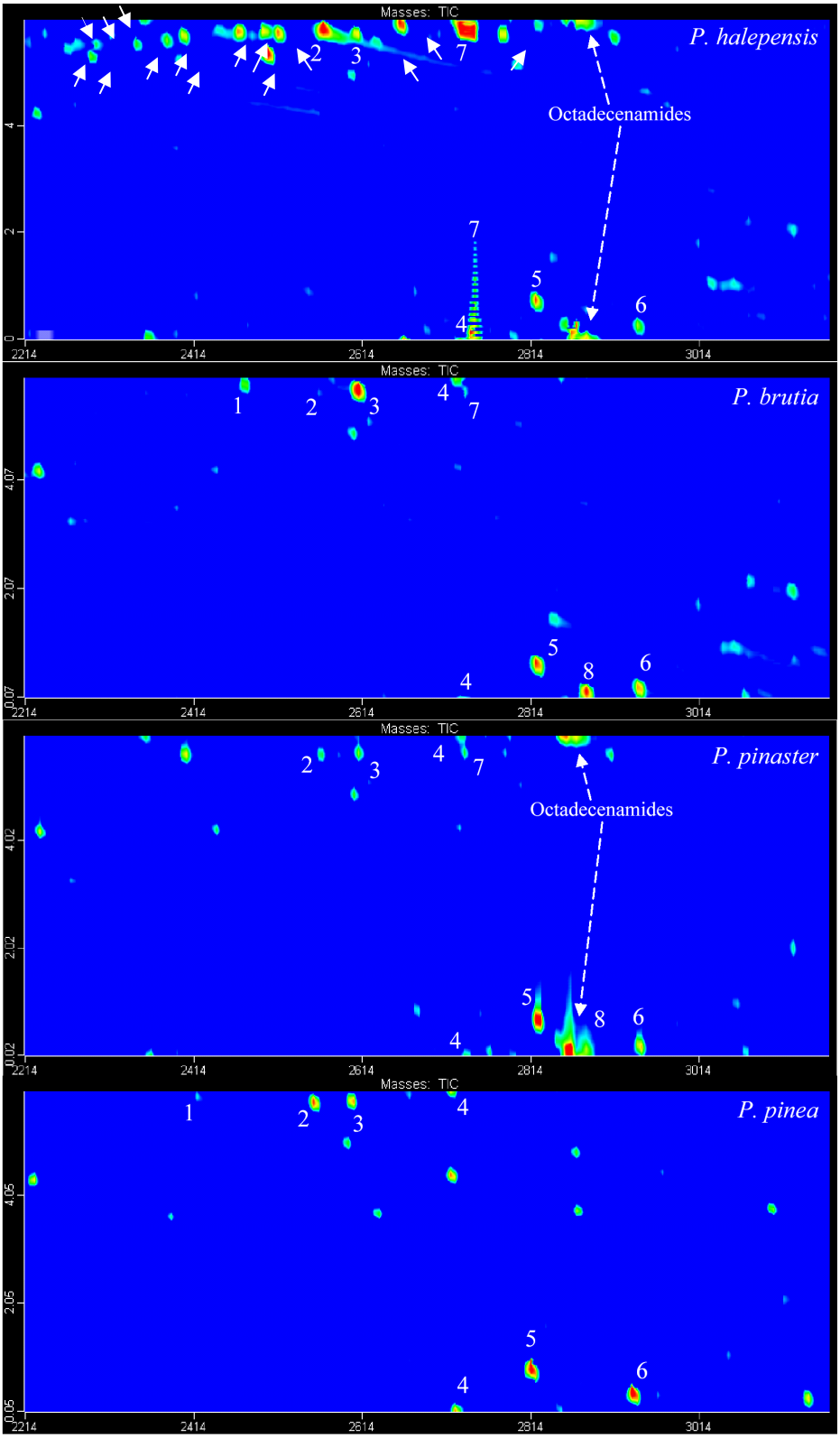

Figure 3.53 - Expanded view of the resin acids retention time domain from the GC × GC/TOFMS contour plots of Figure 3.52. Key: 1 – pimaric acid; 2 – sandaracopimaric acid; 3 – isopimaric acid, 4 – palustric/levopimaric acids; 5 – dehydroabietic acid; 6 – abietic acid; 7 – copalic acid; 8 – communic acid. White arrows – compounds with similar mass spectra.

A detailed view of the methyl copalate spot showed that is composed of two individual peaks that were not detected by 1D-GC /MS, using a non polar column, at any sample. The mass

spectral analysis, presented in Figure 3.54, showed very similar mass spectra for both compounds meaning that the two peaks are probably isomers of copalic acid. However one can observe that the NIST/Wiley library reference spectra, in spite of being catalogued as methyl copalate, present intensity shifts at m/z 114 and 137 and consequently are slightly different.

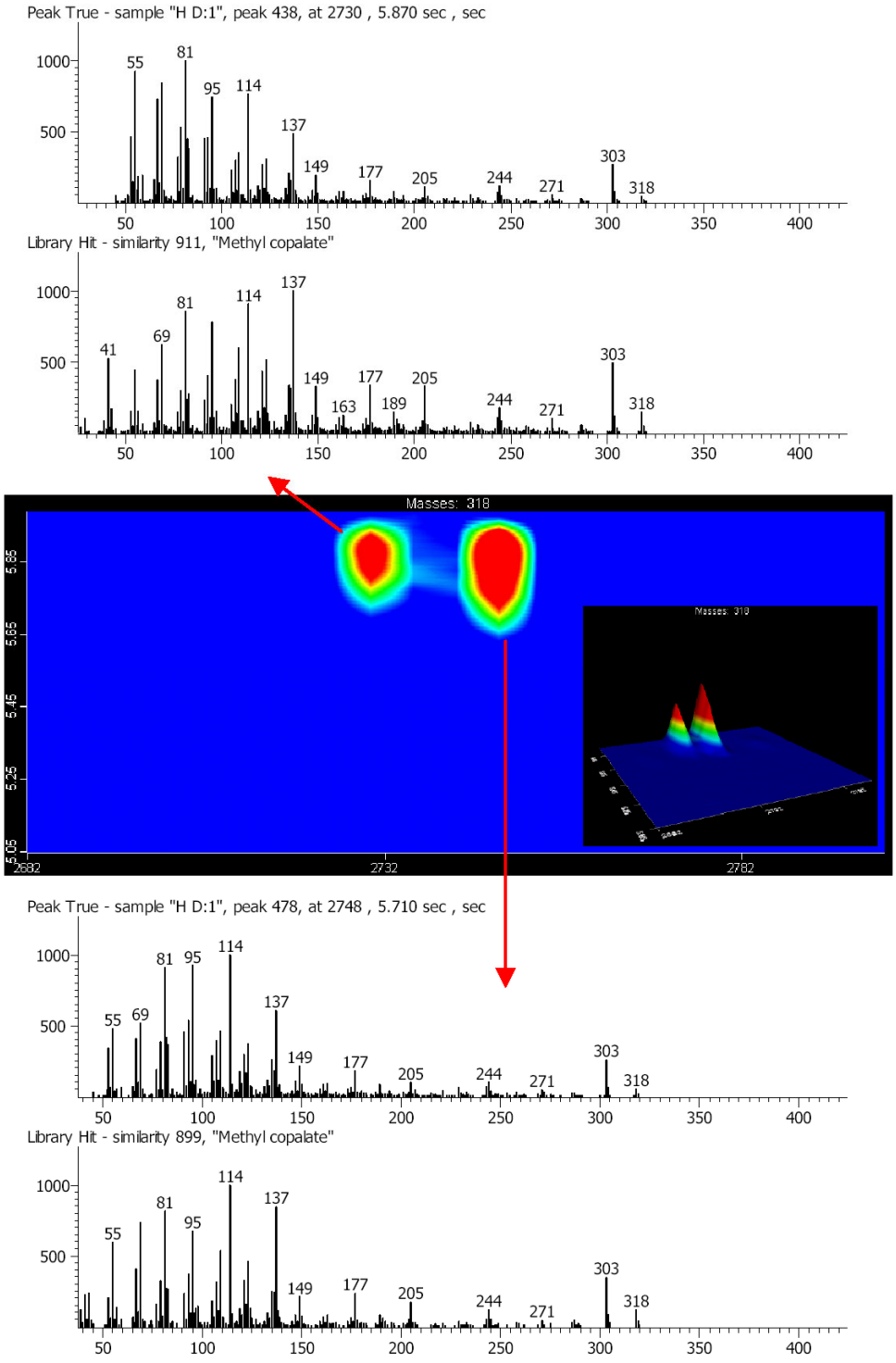

Figure 3.54 - Expanded view and 3 D relief plot of the tentatively identified copalic acid (peak 7; expressed as methyl copalate) retention time domain from the GC × GC/TOFMS contour plot of *P. halepensis* and peak mass spectra.

The NIST/Wiley database library is built on particular contributions. For methyl copalate, it reports 5 spectra, from 5 different sources. All spectra are similar although presenting some differences in the fragment intensities meaning that in spite of the good similarities achieved the methyl copalate identification cannot be assigned with total reliability.

The increased sensitivity, due to the modulation also allowed for the detection of copalic acid (expressed as methyl copalate), at trace level, on the *P. brutia* needles.

The fatty acids methyl esters are the most abundant class of compounds in the extracts, together with the sesquiterpenes and diterpenes (oxygenated and acidic) and appear on the chromatographic space separated on both dimensions, isolated from the resin acids. An example of their separation is show on Figure 3.55 for the C_{18} fatty acid methyl esters cluster. As it was not the scope of this work to proceed to the identification of the non resin acids components in the needles the fatty acids methyl esters composition were not studied.

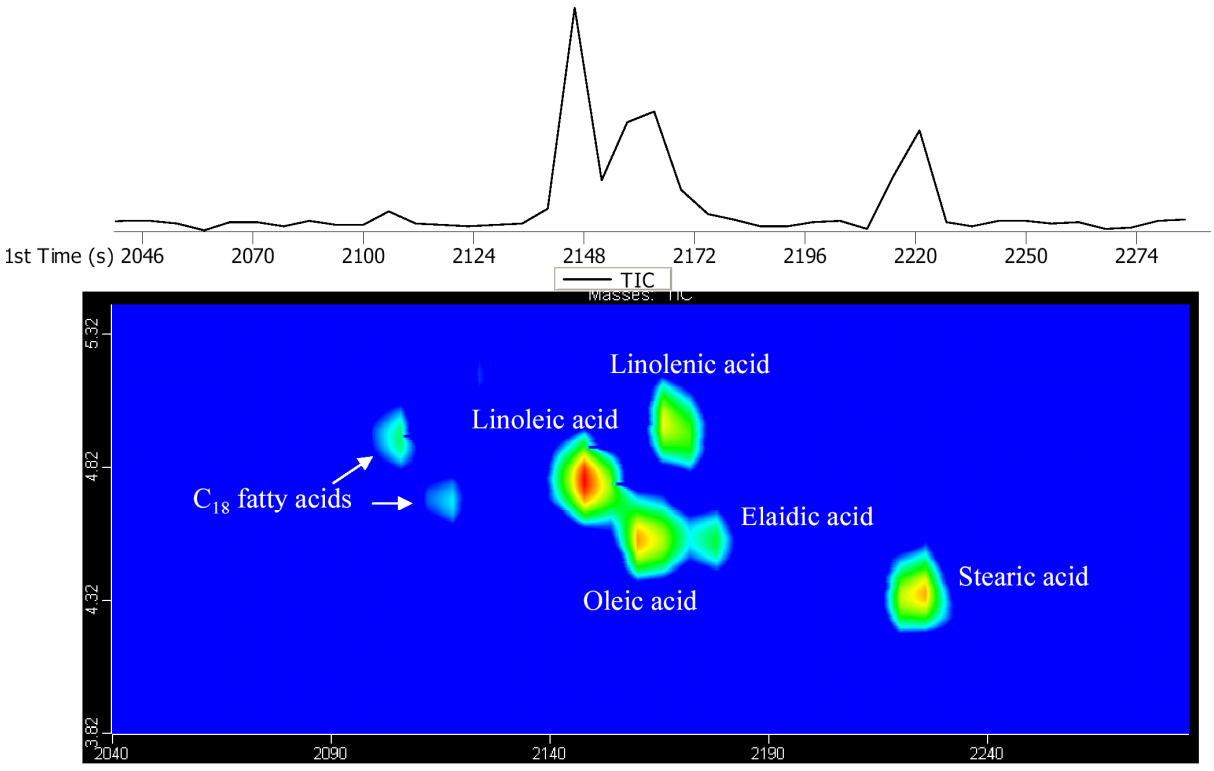

Figure 3.55 – Expansion view from the *P. pinea* GC × GC/TOFMS contour plot presenting the bidimensional separation obtained for the C_{18} fatty acid methyl esters cluster and its reconstructed first dimension TIC.

3.2.3. Gas chromatography/field ionization - time-of-flight mass spectrometry

The needles extracts from the *Pinus* spp. samples were analysed by gas chromatography/time-of-flight mass spectrometry using field ionization (FI) as ion source (1D-GC/FI-TOFMS). FI is a soft ionization technique and for each analyte a mass spectrum with an intense molecular ion [M^+], minimal adducts and fragment ions, is obtained. Figure 3.56 shows, as example, the mass spectra for methyl dehydroabietate generated by electron ionization (EI) and field ionization (FI). Therefore the obtained TIC using FI is essentially a molecular ion chromatogram and in spite of the loss of analytes structural information the technique allows a sample characterization based on the distribution of the analytes molecular ions. The concepts under the use of FI-TOFMS as an analytical tool have been described in chapter 3.1.1.5.

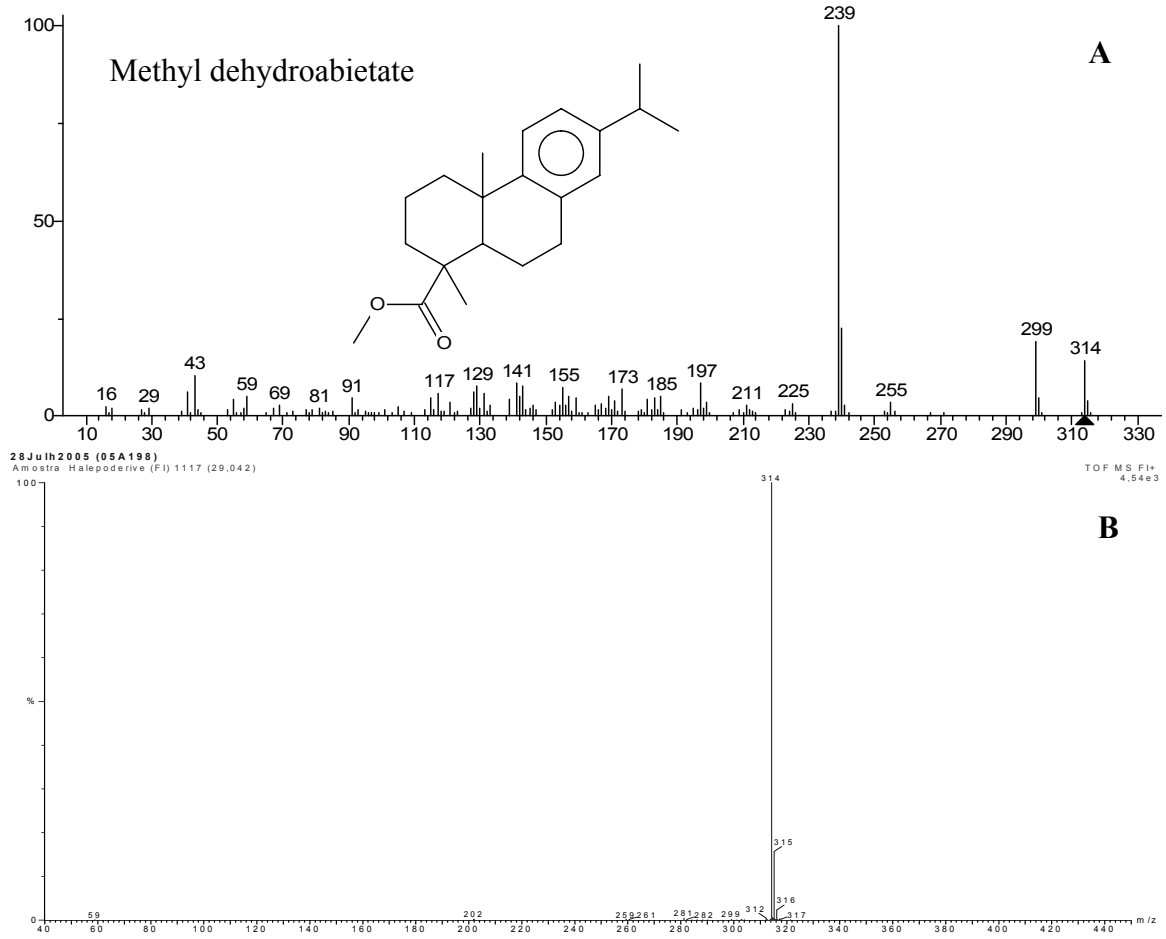

Figure 3.56 - Methyl dehydroabietate mass spectra generated by: **A)** by 70 eV electron ionization and **B)** field ionization.

Figure 3.57 presents the obtained 1D-GC/FI-TOFMS total ion chromatogram for the methylated extract of the *P. halepensis* from the first experiment (larval performance). This TIC is very similar with the TIC obtained by EI for the same sample (Figure 3.49). The peak

annotations, in Figure 3.57, report the scan base peak nominal masses. The major compounds present in the TIC have masses of 318, 304, 290 and 220. The peak with mass 318 (experimental monoisotopic mass 318.256) has been tentatively identified, using EI, as a mixture of methyl copalate acid isomers ($C_{21}H_{34}O_2$; calculated monoisotopic mass 318.256). The peak 304 (experimental monoisotopic mass 304.243) comprises the non derivatized copalic acid isomers ($C_{20}H_{32}O_2$; calculated monoisotopic mass 304.240). The peak with the mass 290 has not been identified. However its experimental monoisotopic mass of 290.265, supports the hypothesis of a compound with a chemical formula $C_{20}H_{34}O$ (calculated monoisotopic mass 290.261) such as the oxygenated diterpenes.

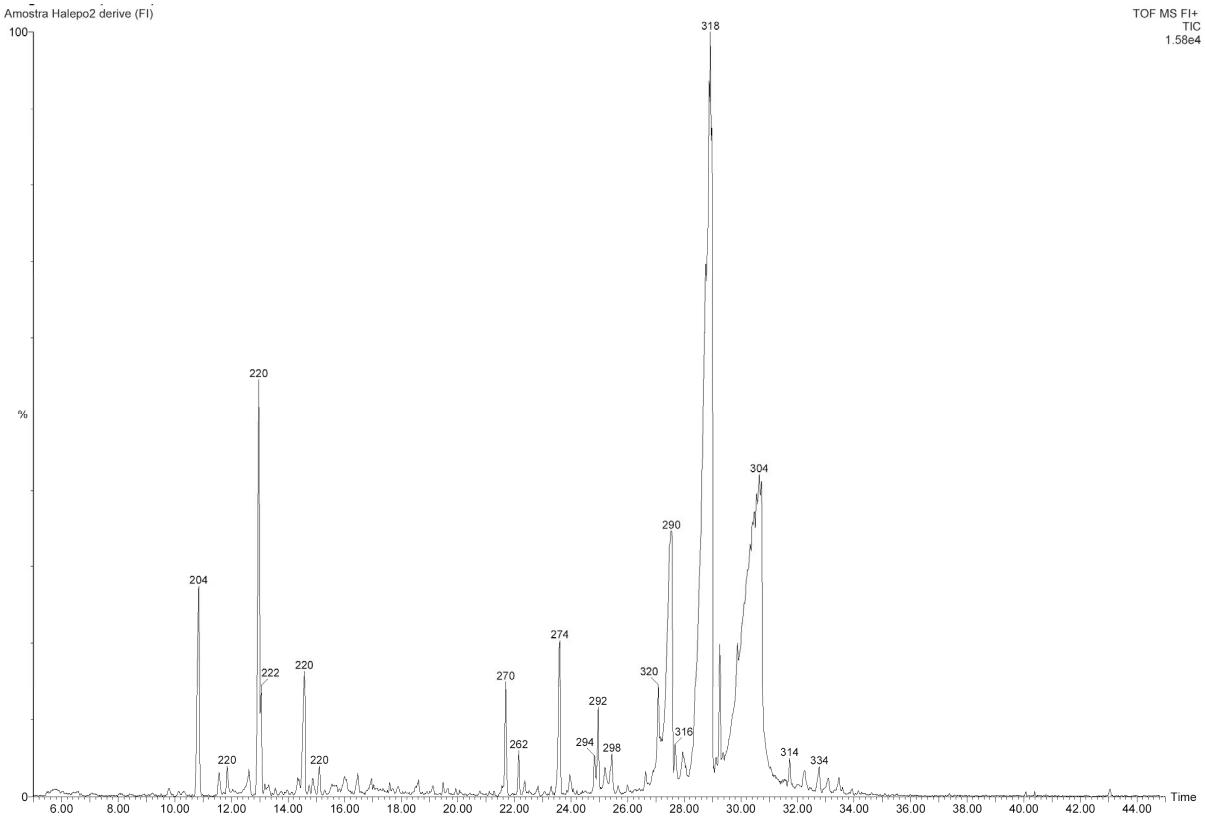

Figure 3.57 - 1D-GC/FI-TOFMS total ion chromatogram from the needles of the *P. halepensis* used in the first experience (larval performance). Peak annotations –scan base peak masses.

The mass spectrum of this peak, obtained by EI, was similar to the mass spectra of the peaks with mass 318, 320, 274 and 262. With an experimental monoisotopic mass of 320.270, the peak with mass 320 is a compound with a chemical formula $C_{21}H_{36}0_2$ (calculated monoisotopic mass 320.272) such as the diterpene acid methyl esters. The peak mass 274 has an experimental monoisotopic mass of 274.239 and differs from the peak mass 290 in 16 mass units and thus apparently the best hypothesis is to be a compound with a chemical formula $C_{20}H_{34}$, such as some diterpenes. However the calculated monoisotopic mass for

$C_{20}H_{34}$ is 274.266 which resulted in a higher difference (27 mDa) to 274.239 than the difference (9 mDa) achieved for a compound with a chemical formula $C_{19}H_{30}O$ that has a calculated monoisotopic mass of 274.230. The results suggest that the peak with nominal mass 290 has a chemical formula $C_{19}H_{30}O$. However the difference between the monoisotopic masses of both hypotheses has a maximum difference of 36 mDa that requires a mass resolving power higher than 7000 to be distinguished. This mass resolving power is not achievable by the used TOFMS system and therefore no unequivocal assignment of chemical class structure is possible by mass measurement. The peak with mass 262 has an experimental monoisotopic mass of 262.236 and the best hypothesis is to be a compound with chemical formula $C_{18}H_{30}O$ (calculated monoisotopic mass 262.230).

Concerning the other peaks, the first cluster in the TIC comprises compounds with masses 204 (sesquiterpenes), 220 and 222 (oxygenated sesquiterpenes and BHT). The first peak with mass 204 is the *trans*-caryophyllene (RI = 1419) followed by the α-caryophyllene (RI = 1455) that is located before the first peak with mass 220. The major peak with mass 220 is the BHT (RI = 1516) and the peak with mass 222 is the germacrene D-4-ol (RI = 1576). The eluting sequence was verified according to the Adams (2001) published retention indices (RI) database used before in this chapter for the volatile analysis. The second cluster comprises the peaks with masses 270, 262, 274 and a subcluster with masses 294, 292, 296 and 298. Peaks 262 and 274 have been previously discussed. The peak 270 and the peaks from the subcluster are the fatty acid methyl ester of palmitic ($C_{17}H_{24}O_2$), linoleic ($C_{19}H_{34}O_2$), linolenic ($C_{19}H_{32}O_2$), oleic ($C_{19}H_{36}O_2$) and stearic ($C_{19}H_{38}O_2$) acids. The section between ther two clusters comprises small peaks with mass such as 220 and 222 (oxygenated sesquiterpenes), 228 (tridecanoic acid methyl ester), 234 ($C_{15}H_{22}O_2$; e.g. C_7-phenylethyl esters), 234 ($C_{15}H_{24}O_2$; oxygenated sesquiterpenes such as bisabolene oxide) or 296 ($C_{21}H_{44}$ hydrocarbons). The last cluster comprises the major peaks and the diterpene acids.

Figure 3.58 shows the 1D-GC/FI-TOFMS total ion chromatogram and the reconstructed single ion chromatograms for the resin acid methyl esters masses 314 ($C_{21}H_{30}O_2$; e.g. dehydroabietic acid methyl ester), 316 ($C_{21}H_{32}O_2$; e.g. abietic acid methyl ester) and 330. For the peaks with mass 330 two hypotheses can be considered: **i)** the oxygenated diterpene acids ($C_{21}H_{30}O_3$) with a calculated monoisotopic mass of 330.220 and **ii)** the diterpene resin acids ethyl esters or methylditerpene acids methyl esters ($C_{22}H_{34}O_2$) with a calculated monoisotopic mass of 330.256. The experimental monoisotopic mass of the peaks with nominal mass 330 varies between 330.226 and 330.228 with the exception of the last one that has an

experimental monoisotopic mass of 330.257. The data suggest that the last peak with a nominal mass of 330 may be a diterpene acid ethyl ester or a methylditerpene acids methyl ester and that all the other are oxygenated diterpene acids. However with a maximum difference of 31mDa between the experimental monositopic masses the required mass resolving power needed to distinguish both masses (>7000) is not achievable by the TOFMS system and therefore no unequivocal assignment of chemical class structure is possible although their chromatographic separation.

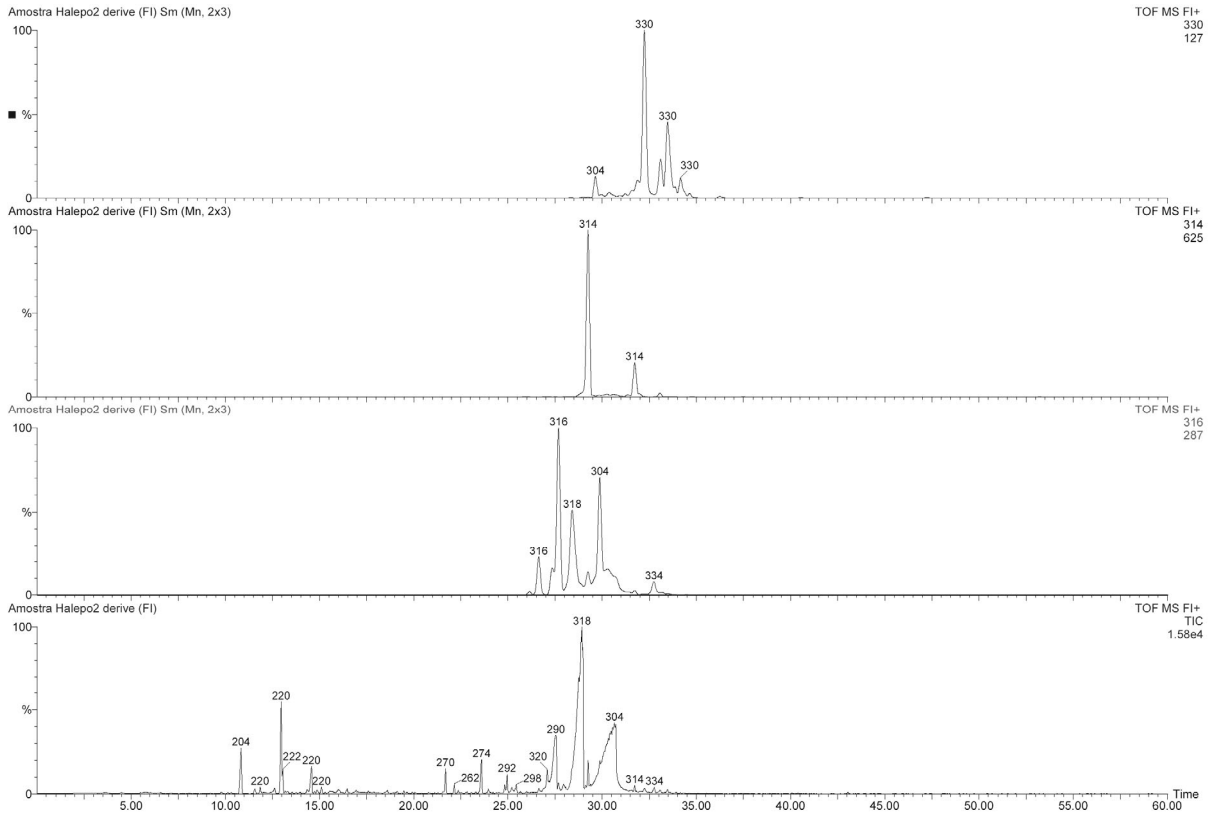

Figure 3.58 - 1D-GC/FI-TOFMS total ion chromatogram and reconstructed single ion chromatograms for the m/z 314, 316 and 330 for the sample of *P. halepensis* used in the first experiment.

Figure 3.59 shows TIC obtained by 1D-GC/FI-TOMS for the methylated extract of one of the the *P. halepensis* from the second experiment. The major compound present in the TIC have a nominal mass of 314 and has been identified has dehydroabietic acid methyl ester ($C_{21}H_{30}O_2$). The peaks with mass 318 and 304 have not been detected on the sample and thus it is confirmed that the copalic acid isomers were not present in the *P. halepensis* from the second experiment. A peak with the mass 290 has been detected at trace level on the same retention time domain but the sample analysis by EI did not confirm the presence of the compound detected in the *P. halepensis* from the first experiment.

The first cluster in the TIC, from Figure 3.59, comprises compounds with masses 204 (sesquiterpenes), 220 and 222 (oxygenated sesquiterpenes and BHT). The identity of the peaks is the same as for the *P. halepensis* from the first experiment.

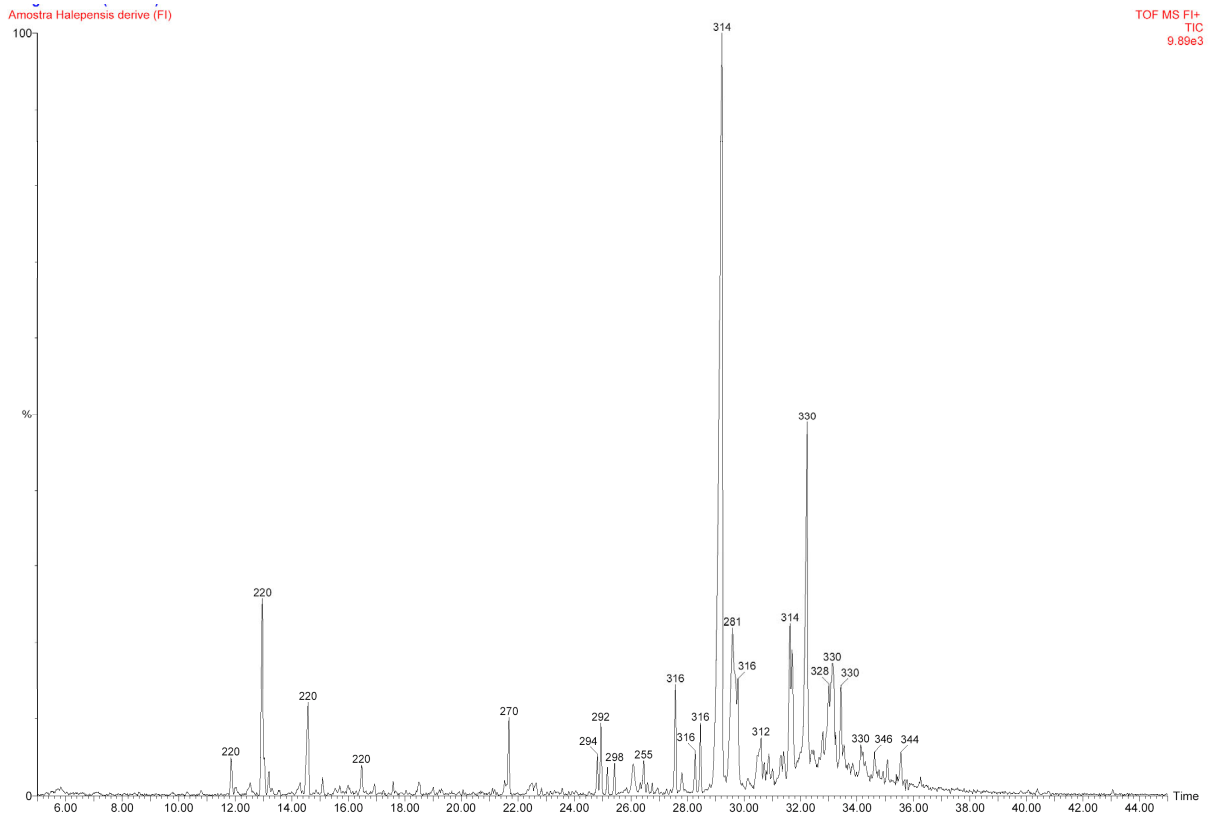

Figure 3.59 - 1D-GC/FI-TOFMS total ion chromatogram from the needles of one of the *P. halepensis* used in the second experience. Peak annotations –scan base peak masses.

The second cluster comprises the peaks with masses 270 and a subcluster with masses 294, 292, 296 and 298. The peaks 262 and 274 have not been detected on the cluster. The peak 270 and the peaks from the subcluster are the fatty acid methyl esters of palmitic, linoleic , linolenic, oleic and stearic acids previously reported for the firts *P. halepensis*. The section between ther two clusters comprises, in similar way as for the first sample, small peaks with mass such as 220 and 222 (oxygenated sesquiterpenes), 228 (tridecanoic acid methyl ester), 234 ($C_{15}H_{22}O_2$; e.g. C_7-phenylethyl esters), 234 ($C_{15}H_{24}O_2$; oxygenated sesquiterpenes such as bisabolene oxide) or 296 ($C_{21}H_{44}$ hydrocarbons). The last cluster comprises the major peaks and the diterpene acids. The peak with nominal mass is the octadecenamide, also known as oleamide and is a sample contaminant that was recently reported by McDonald *et al* (2008) to be leaking out of polypropylene plastics used in laboratory experiments.

Figure 3.60 shows the 1D-GC/FI-TOFMS total ion chromatogram and the reconstructed single ion chromatograms for the resin acid methyl esters masses 314 ($C_{21}H_{30}O_2$), 316

($C_{21}H_{32}O_2$) and 330. For the peaks with the nominal mass 330 the experimental monoisotopic mass varies the same as in the first experiment and the data suggest the last peak with a nominal mass of 330 as a diterpene acid ethyl ester or methylditerpene acids methyl ester and all the other as oxygenated diterpene acids.

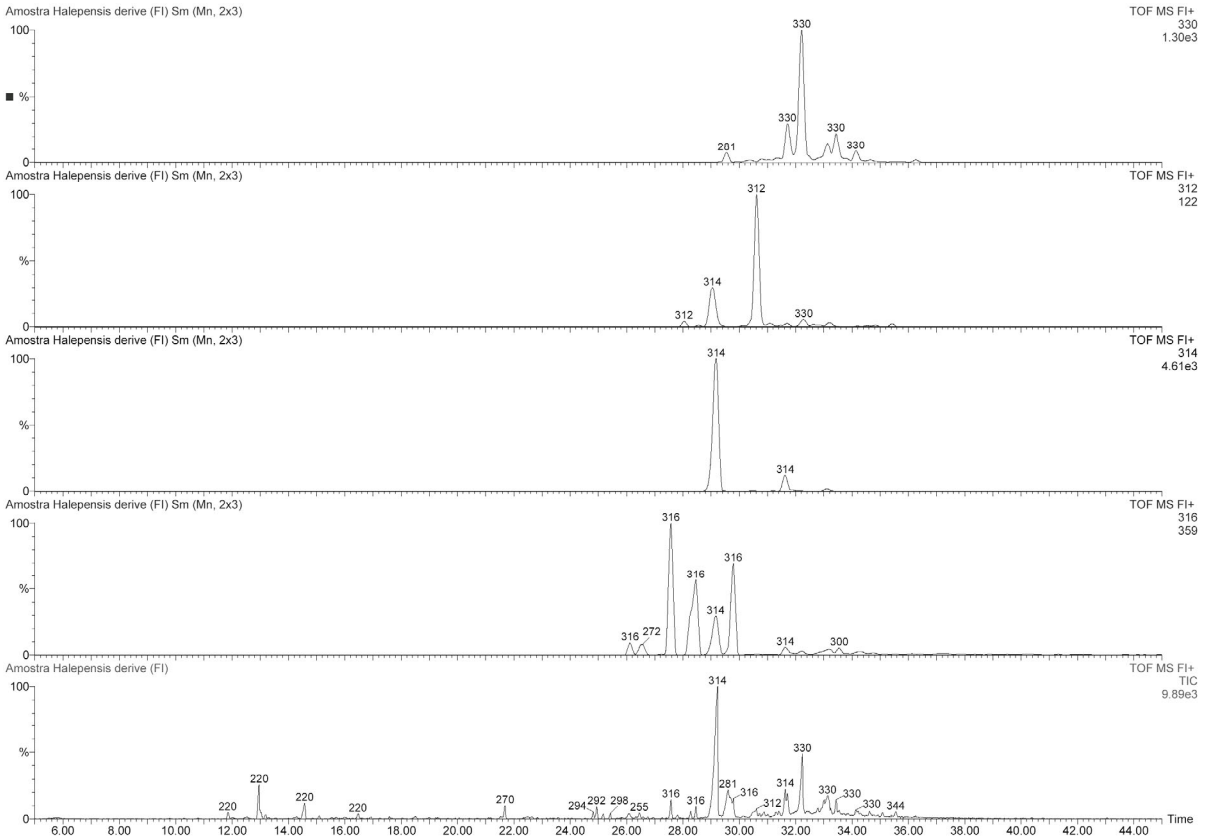

Figure 3.60 - 1D-GC/FI-TOFMS total ion chromatogram and reconstructed single ion chromatograms for the m/z 314, 316 and 330 for the sample of *P. halepensis* used in the second experiment.

3.3. Data treatment

In this section a data treatment of the *Pinus* spp. needles composition and susceptibility to *T. pityocampa* attack is carried out.

3.3.1 Abrantes experimental plot – Volatiles

Fifty four composite samples were randomly sampled from eleven pine species in an experimental plot at Abrantes, and from *P. eldarica* in a forest stand located 50 km north of Abrantes. The volatile compounds emitted by their needles were extracted by SPME and analyzed by GC-FID. The data set, with seventeen volatiles variables, was log-transformed, to allow for examination of the role of the minor volatile compounds. The volatiles separation was performed on a DB-5 column (see section 2.4.1.1), which did not separate the pair limonene and β-phellandrene. Table 3.8 shows the volatile average relative composition for each one of the pine species without log-transformation.

3.3.1 1 Hierarchical cluster analysis

A hierarchical cluster analysis (HCA), using Ward's method and Euclidean distances, was performed in order to identify similarities between the pine species sampled. The resulting HCA dendrogram, based on their volatile profiles, is shown in Figure 3.61.

Results suggest that according to their volatile chemical composition the *Pinus* species sampled can be divided in three groups, further subdivided in seven-separated clusters at a linkage distance of 6. The first group is composed by the first cluster and contains the samples of *P. halepensis*, *P. elliottii*, *P. pinaster* and *P. brutia,* that exhibit some overlap between them. The second group contain, in descending order of similarity the clusters **2)** with *P. nigra* samples and **3)** with *P. sylvestris*, *P. eldarica* samples and one overlapping *P. pinaster* sample. The third group contains in descending order of similarity the clusters **4)** with three *P. pinea* samples; **5)** with the remaining *P. pinea* samples and *P. radiata* samples but without overlapping between them; **6)** with *P. patula* samples; **7)** with *P. taeda* and *P. kesiya* samples, showing a small overlap between the last *P. taeda* and the first *P. kesiya* samples.

Table 3.8 - Volatile average relative composition for each one of the pine species present in Abrantes plot, plus *Pinus eldarica*, without log-transformation.

	Terpene volatiles																
	Th	aP	Ca	Sa	bP	My	aPh	d3C	aT	*p*-cymene	Li	cO	tO	gT	Te	Lin	Sqterp
P. halepensis	0.15	40.03	0.99	0.00	32.89	5.79	0.62	0.28	0.01	0.00	3.95	0.03	0.57	0.01	0.12	0.02	14.44
P.nigra	0.10	39.26	0.40	5.43	3.89	18.57	0.99	4.95	0.15	0.00	2.41	0.04	1.16	0.26	5.62	0.45	18.05
P.brutia	0.06	28.70	0.38	0.00	52.29	2.52	0.19	0.33	0.01	0.00	4.92	0.17	0.10	0.02	0.18	0.00	9.89
P. pinea	0.00	7.10	0.03	0.10	2.19	4.36	1.19	0.48	0.09	0.00	79.16	0.00	0.28	0.01	0.26	0.19	4.48
P. patula	0.30	24.47	1.11	0.14	3.58	3.20	1.45	0.30	0.04	0.00	42.62	0.00	0.76	0.14	1.67	0.04	20.17
P. radiata	0.00	23.91	0.31	0.02	32.34	5.21	1.43	1.18	0.03	0.00	26.96	0.31	2.42	0.53	0.34	0.58	4.43
P. eldarica	0.09	29.13	0.34	0.00	34.58	4.45	0.07	13.60	0.00	0.03	2.70	0.03	0.77	0.16	1.20	0.02	12.82
P. pinaster	0.06	35.06	0.43	0.00	42.63	7.37	0.45	0.52	0.02	0.00	3.03	0.07	0.76	0.04	0.19	0.04	9.34
P. taeda	0.39	71.27	0.95	0.00	5.14	4.39	0.24	0.35	0.02	0.01	10.37	0.05	0.04	0.15	0.24	0.05	6.34
P. elliottii	0.13	28.41	0.82	0.00	37.91	7.13	0.18	0.28	0.02	0.00	4.83	0.05	0.07	0.03	0.13	0.15	19.86
P. kesiya	0.15	76.71	1.01	0.18	1.91	2.01	0.28	0.21	0.05	0.01	11.95	0.03	0.32	0.10	0.69	0.02	4.38
P. sylvestris	0.11	33.53	1.40	0.00	26.28	3.02	0.10	24.36	0.00	0.04	2.64	0.03	0.51	0.31	2.57	0.00	5.10

Terpene volatiles key: Th – Thujene; aP – α-Pinene; Ca – Camphene; Sa – Sabinene, bP – β-Pinene; My – Myrcene; aPh – α-Phellandrene; d3C – Δ-3-Carene; aT – α-Terpinene; rC – Cymene (isomer); Li – Limonene + β-phellandrene; cO – *cis*-Ocimene; tO – *trans*-Ocimene; gT – γ-Terpinene; Te – Terpinolene; Lin – Linalool; Tsesq – total sesquiterpene.

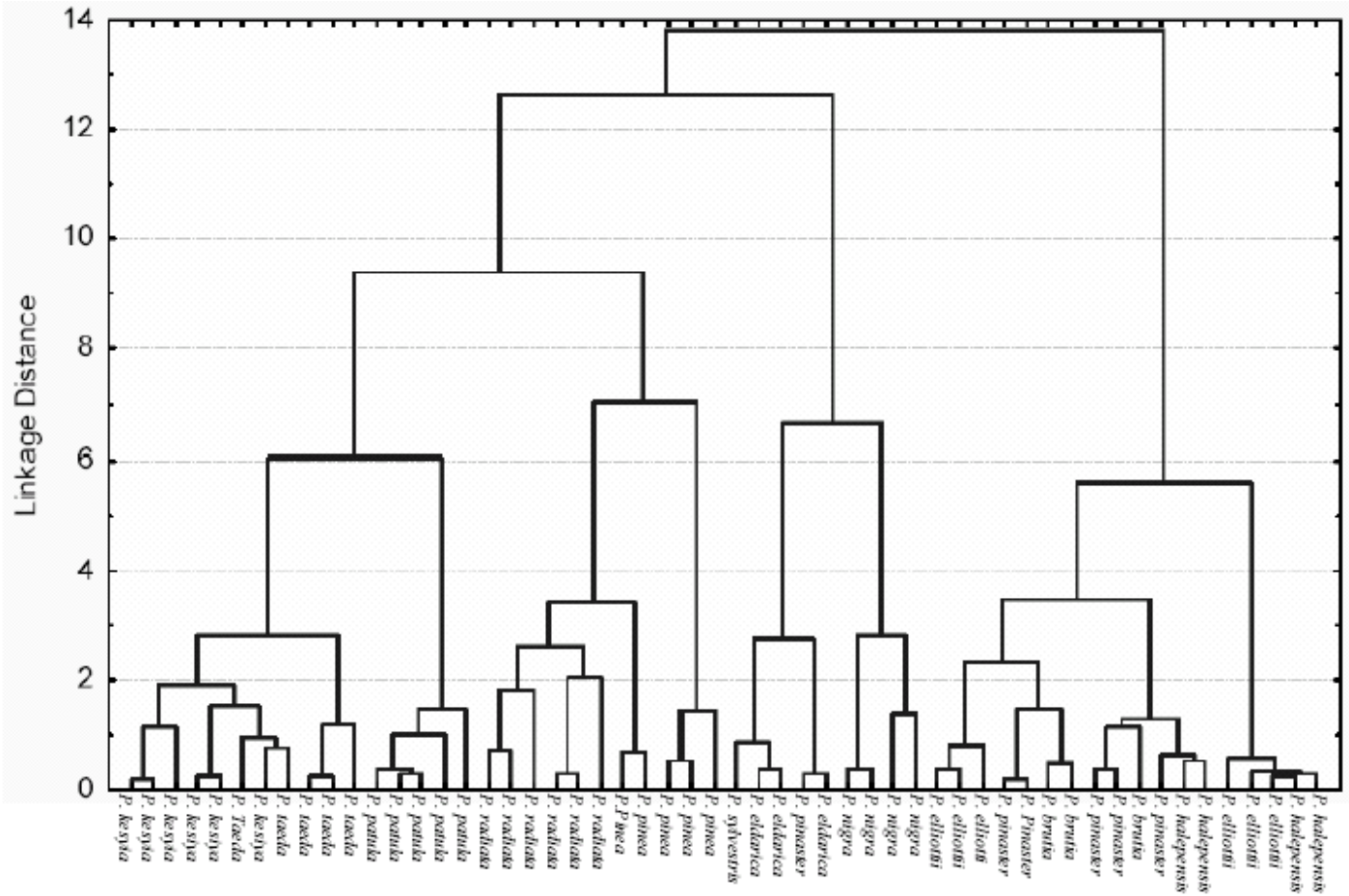

Figure 3.61 - Dendogram from the hierarchical cluster analysis for the *Pinus* species, sampled in Abrantes plot, plus *Pinus eldarica*, based on their volatile profiles.

Regarding the level of attack by *T. pityocampa*, expressed as the percentage of attacked trees, the results of the HCA classification are presented on Table 3.9.

Table 3.9 - Hierarchical cluster analysis classification for the pine species studied and percentage of attack by *T. pityocampa.*

HCA groups	Clusters	Pine species	% of attack
Group 1	1	*P. halepensis*	0*
		P. elliottii	73.90
		P. pinaster	85.00
		P. brutia	0*
Group 2	2	*P. nigra*	0*
Group 2	3	*P. eldarica*	80.00
		P. pinaster	85.00
		P. sylvestris	0*
Group 3	4	*P. pinea*	33.30
Group 3	5	*P. pinea*	33.30
		P. radiata	42.85
Group 3	6	*P. patula*	12.50
Group 3	7	*P. taeda*	57.65
		P. kesiya	14.20

*All trees belonging to pine species with 0% attack had less than 1.5 m of height

Observations of the Abrantes arboretum concluded that no trees fewer than 1.5 m in height were attacked by *T. pityocampa.* These smaller trees belonged to four species, namely *P. brutia, P. nigra*, *P. halepensis* and *P. sylvestris* and falled in the first three clusters of the dendrogram. All species, referred have been cited in literature as suffering attack by *T. pityocampa* (Hodár *et al*, 2003; Mirchev *et al*, 2004; Kanata *et al*, 2005).

The first three clusters are constituted by the pine species showing the highest levels of attack by *T. pityocampa*, in the arboretum. *P. elliottii* and *P. pinaster*, which can be mainly found in the first cluster, are the more heavily attacked pine species, with 73.4 and 85%, respectively. *P. eldarica* that was sampled outside the arboretum, with 80% attack level, followed on the third

cluster. Cluster 3 also includes one of the composite samples of *P. pinaster*. Clusters 4 and 5 include *P. pinea* and *P. radiata* samples that show an intermediate level of attack of 33.3 and 42.85%, respectively. The remaining clusters include the samples from the pine species that show the lowest attack level. *P. patula* and *P. kesiya* present an attack level of 12.5 and 14.20 % respectively, together with the samples of *P. taeda* which show an intermediate level of attack of 57.65%.

The HCA of the pine species studied, based on their volatile composition, sugests the existence of similarities among pine species according to their attack level. On the dendrogram, the attack apparently follows a trend in descending order from the first cluster to the last one. However, the information provided regarding the chemical differences between the pine species, it scarce.

3.3.1.2. Principal component analysis

In order to identify the compounds associated with the hierarchization of the samples a principal component analysis (PCA) was carried out, treating the pine species as cases and the volatile compounds as variables. The results for PCA on the log-transformed data produced are summarized on Table 3.10.

Table 3.10 - Eigenvalues and total variance from the principal component analysis using the log-transformed values for the volatile monoterpenes for the *Pinus* species from Abrantes plot.

Factor	Eigenvalue	% Total variance	Cumulative Eigenvalue	Cumulative %
1	3.38	19.86	3.38	19.86
2	3.04	17.90	6.43	37.76
3	2.13	12.52	8.55	50.28
4	2.08	12.23	10.63	62.51
5	1.49	8.77	12.12	71.28
6	1.09	6.39	13.20	77.66

The first three factors explain 50.28% of the total variance, with 19.86, 17.90, and 12.52% for components 1, 2, and 3, respectively. The log-transformed data values produced the first two-component plot shown in Figure 3.62, where only 37.76% of the variance is explained and are thus insufficient to explain the variation. To explain 80.00% of the total variance, more than six

factors were needed rendering the results difficult to analyse and, consequently, the information offered by the PCA can not be conclusive.

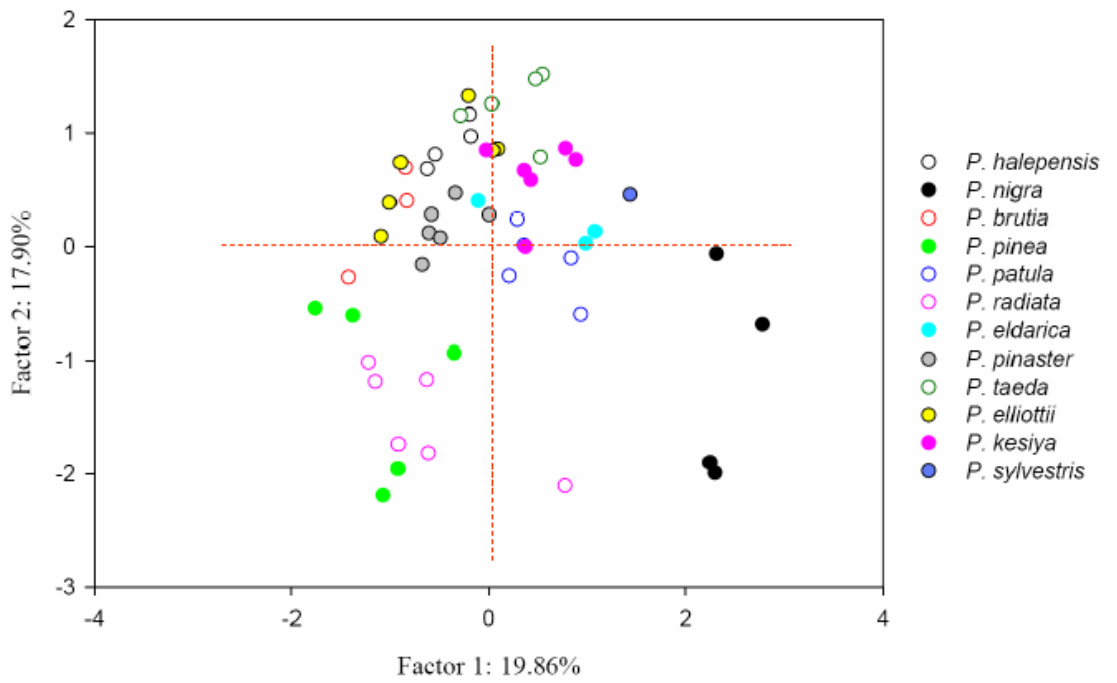

Figure 3.62 – Principal component analysis for the log-transformed volatile compounds data for the twelve pine species studied. (quadrants I to IV assigned clockwise from top left).

Nevertheless, the PCA plot shows that the fourth quadrant comprises *P. pinea* and the majority of *P. radiata* samples, which have an intermediate level of attack. The first quadrant includes *P. elliottii* and the majority of *P. pinaster* samples that registered the highest levels of attack. *P. kesyia* and *P. patula*, the pine species with the lowest attack level, are placed at close distance, on the second and third quadrants.

In spite of an apparent scattering of the score points on the plot, samples from the same pine species tend to group in the same region.

In order to identify which of the volatiles (loadings) are associated with the pine species samples (scores), the loadings projections were analyzed for the first two components. The projection of the loadings on the factor plane for the first two components is shown in Figure 3.63. The loading values for component 1 and 2 are summarized in Table 3.11.

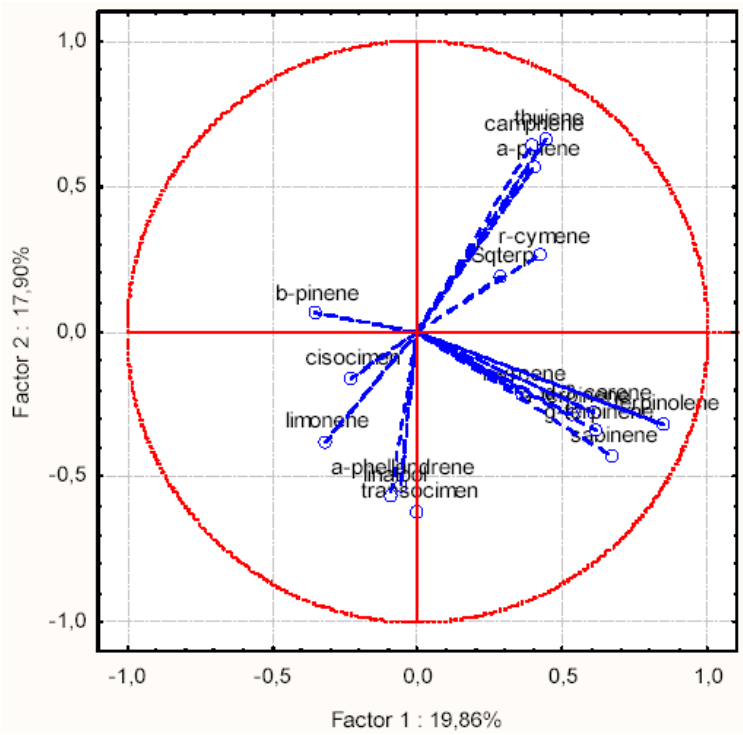

Figure 3.63 - Projection of the loadings on the factor plane for the first two components (limonene = limonene + *β*-phellandrene).

Table 3.11 - Values of the loadings from the principal component analysis using log-transformed values for the volatile compounds from the twelve pine species studied

Volatile	Factor 1	Factor 2
thujene	0.44	0.66
α-pinene	0.40	0.56
camphene	0.39	0.64
sabinene	0.67	-0.43
β-pinene	-0.36	0.07
myrcene	0.36	-0.21
α-phellandrene	-0.06	-0.53
Δ-3-carene	0.61	-0.28
α-terpinene	0.53	-0.29
ρ-cymene	0.42	0.26
Limonene + *β*-phellandrene	-0.32	-0.38
cis-ocimene	-0.23	-0.16
trans-ocimene	0.00	-0.62
γ-terpinene	0.61	-0.34
terpinolene	0.84	-0.31
linalool	-0.09	-0.57
Sqterp	0.28	0.19

The loadings data (Table 3.11 and projection plot, Figure 3.63) show that the major associations for factor 1 can be found for terpinolene, following sabinene, Δ-3-carene and γ-terpinene. Concerning factor 2, major associations can be found for thujene**,** following camphene and *trans*-ocimene.

According to the loadings data, the location of the samples on the upper left quadrant, where the pine species with the highest level of attack are grouped, is only driven by β-pinene. This observation suggests a positive association of β-pinene with the highest levels of attack.

3.3.1.3. Partial least squares regression

In order to understand the variation of the attack, expressed as percentage of trees attacked by *T. pityocampa*, on the pine species sampled (12 species; 54 observations), and study the influence of the volatile compounds, a partial least squares (PLS) regression was performed on the experimental data set. The sampled pine species are described by 17 volatile components (X variables), the predictors. The predictors are assumed to be the promoters of the effects causing the attack changes (Y variable) in the system under study. The pine species with no register of attack were omitted for the PLS analysis, considering that tree height was the main factor controlling the absence of attack. The final data set for the PLS analysis comprises eight pine species and 42 observations.

Since the variables show a range of over one order of magnitude of 10, they were logarithmically transformed in order to make their distribution more symmetrical.

The initial PLS analysis was done with all the predictor variables and the attack level expressed as percentage of attack for each pine species. The results obtained for the PLS analysis are summarized at Table 3.12.

The PLS analysis of the data extracted only one significant component according to the cross validation rule 1 (R1), that sets for PLS models a significant limit of 0.05, for models with less than 100 observations. The first component with a $Q^2 > 0.05$ is the significant component and explains 16.7% of the X variation and 82.5% of the Y variation ($R^2X = 0.167$, $R^2X = 0.825$). The same component predicts 79.0% of the Y (attack) variation ($Q^2 = 0.790$).

Table 3.12 – Summary of the partial least squares model for the data set of twelve pine species and level of attack of *T. pityocampa*.

A	R^2X	R^2X(cum)	Eigenvalue	R^2Y	R^2Y(cum)	Q^2	Q^2(cum)	Significance
1	0.167	0.167	2.84	0.825	0.825	0.790	0.790	R1
2	0.108	0.275	1.83	0.055	0.880	-0.360	0.769	NS
3	0.108	0.383	1.84	0.039	0.919	-0.110	0.746	NS
4	0.107	0.490	1.82	0.019	0.938	-0.101	0.720	NS
5	0.080	0.570	1.36	0.012	0.950	-0.151	0.692	NS
6	0.086	0.656	1.46	0.004	0.954	-0.213	0.662	N4

Number of observations: N = 42; Variables: K = 18; X(volatiles) = 17 and Y(attack) = 1

The plot of the X scores, t_1 vs. t_2 presented in Figure 3.64, shows the 42 observations grouped according to the pine species and according to the attack level that increases from left to right, on the first component. In spite of not being significant, sample dispersion on the second component can still be observed. Samples from the pines species that show a high attack level present a low dispersion on the second dimension and are closely grouped. *P. taeda*, *P. pinea* and *P. radiata*, with intermediate attack level, present a high dispersion on the second component and apparently are individually isolated from the other groups. *P. pinea* shows two groups and *P. radiata* has one isolated observation. *P. patula* and *P. kesiya* present the lowest attack ratio and are grouped on the same plot area, showing some dispersion on the second component. *P. kesiya* forms a group and is represented splited due to its proximity to the *P. patula* group and *P. pinea* subgroup. The ellipse shows the Hotellings T^2 95% confidence interval, and observations outside the confidence ellipse are considered outliers. The two *P. pinea* samples pointed as outliers are the observations with the highest percentage of limonene in the data set. Close to the ellipse edge, a third *P. pinea* sample can be observed which also contains a high percentage of limonene.

The plot of the X loadings p_1 vs. p_2 presented in Figure 3.65 shows how the variables are related and their association with the observations projected on the score plot.

The loadings plot for the PLS analysis show that the observations distribution in the first component, on scores plot, are mainly associated with β-pinene, followed by myrcene, on the attack direction and by terpinolene, limonene+β-phellandrene and sabinene in the opposite

direction (lower attack). Dispersion on the second component is mainly associated with limonene, on the negative axis and with the group of camphene, α-pinene, γ-terpinene, sqterp and thujene on the positive axis.

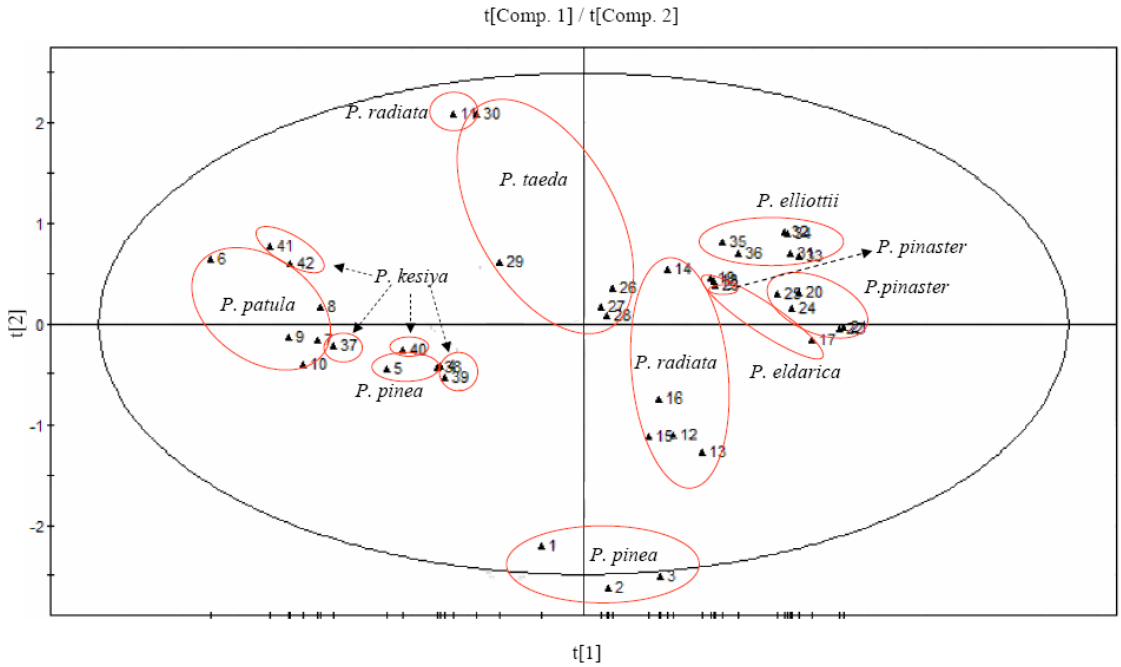

Figure 3.64 – Partial least squares scores t1 and t2 for the twelve pine species data set.

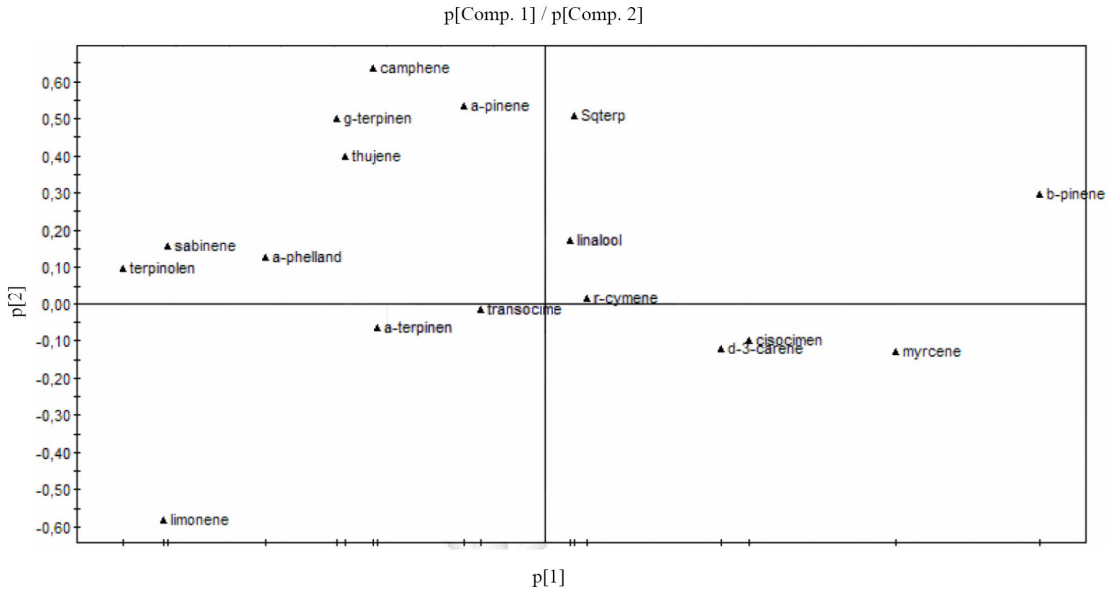

Figure 3.65 – Partial least squares loadings p1 and p2 for the twelve pine species data set (limonene = limonene + β-phellandrene).

The plot t_1 vs u_1, presented in Figure 3.66, examines the relationship between the scores of X (the observations according to the variables) and the scores of Y (the attack).

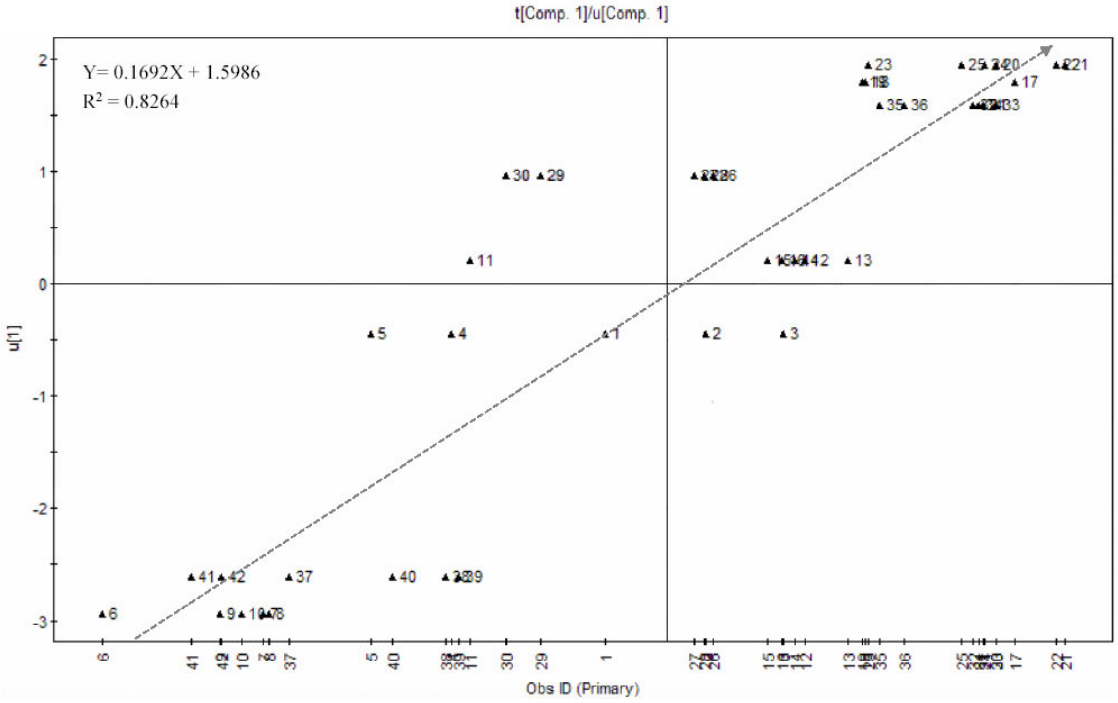

Figure 3.66 – Partial least squares scores plot t_1 vs. u_1 for the twelve pine species data set.

The scores plot t_1 vs. u_1 indicates a good relationship ($R^2 = 0.83$) between the X and Y scores but with some scattering in the data. The scattering of the data is lower for the pine species with a higher attack level, which is ≥ 74%, larger for the pine species with intermediate attack level that is between 33 and 58, and intermediate for the species less attacked. This situation, which can also be observed in the score plot, may be due to a bias in the samples that is related to the percentage of trees suffering the attack on each pine species. It can be inferred that trees from pine species with a higher level of attack, will probably be chemically more homogenous than those from species with a lower attack level.

The plot of the PLS weights w and c, presented in Figure 3.67, shows the correlation structure between the volatiles (X) and the level of ttack, and thus can be used to identify the volatile variables that exhibit a variation in parallel with the attack level.

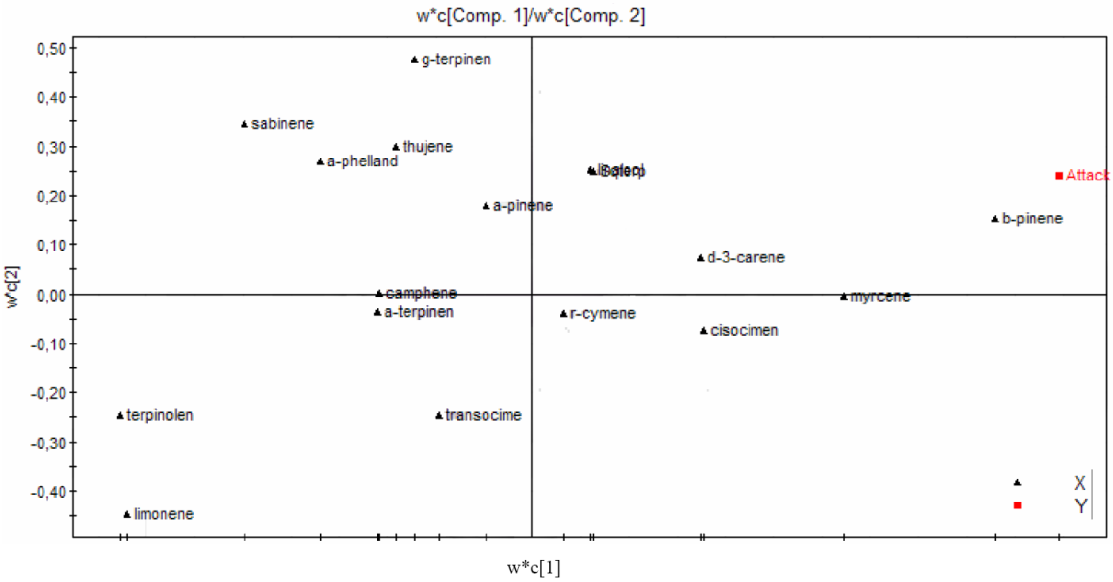

Figure 3.67 – Partial least squares weights plot w^*c_1 vs. w^*c_2 for the twelve pine species data set showing the model correlation structure (limonene = limonene + β-phellandrene).

It can be seen that the correlation between volatiles and the attack level, is related to their distance from the origin for both positive and negative sides, those further away from the origin being the ones closer correlated with the attack. The weights plot shows that the volatile with a more positive relation with the attack is β-pinene, followed by myrcene. Limonene+β-phellandrene and terpinolene are inversely related with the attack in the pine species under study.

The "variable influence on projection" (VIP) values summarize the overall contribution of each individual volatile (X variables) for the characterization of pine samples and explanation of the attack level variation (Y variable). It is assumed that VIP values higher than one, indicate the most relevant variables for explaining the model. Figure 3.68 shows the volatiles by descending VIP values. According to the plot, the most relevant variables are, by descending order, β-pinene (1.98), terpinolene (1.76), limonene+β-phellandrene (1.73), myrcene (1.33) and sabinene (1.23).

One of the goals of a PLS regression analysis is to formulate a function to model the variable Y under study. The model estimates coefficients for each volatile compound (X variable), that will be used to interpret their influence of the volatile on the attack level. Each observation will be modeled as a linear combination of all volatile compounds. Table 3.13 shows the estimated coefficients for the proposed model.

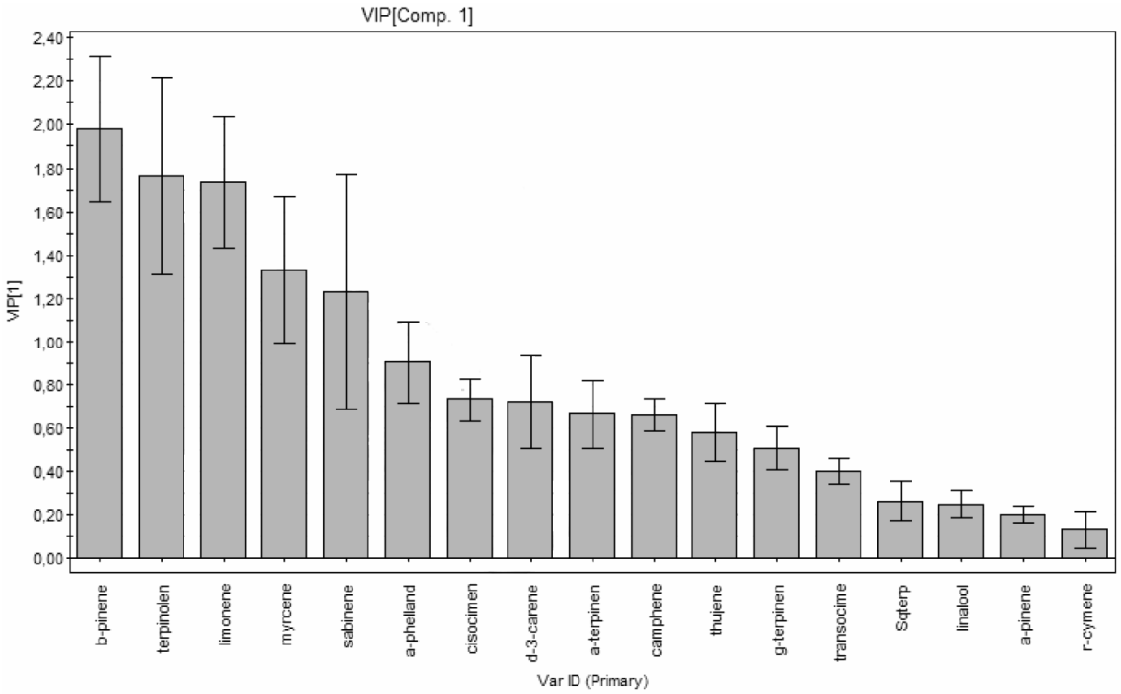

Figure 3.68 - Partial least squares variable importance, on the projection of the volatile variables for the attack level by *T. pityocampa*, in the pine species data set for the significant component. The bars indicate 95% confidence intervals based on jack-knifing (limonene = limonene + β-phellandrene).

Table 3.13 – Partial least squares regression coefficients for the combination of the volatile compounds to predict the attack. (coefficients refer to centered and scaled X, and scaled but uncentered Y) by *T. pityocampa.*

Variable	Coefficients (attack)
Thujene	-0.076
α-Pinene	-0.026
Camphene	-0.087
Sabinene	-0.162
β-Pinene	0.262
Myrcene	0.176
α-Phellandrene	-0.120
Δ–3–Carene	0.095
α-Terpinene	-0.088
ρ-Cymene	0.018
Limonene+β-phellandrene	-0.223
cis-Ocimene	0.097
trans-Ocimene	-0.053
γ-Terpinene	-0.067
Terpinolene	-0.233
Linalool	0.033
Sqterps	0.035

The agreement between the observed values and those predicted by the previous regression coefficients, estimated by the PLS model attack data, is shown in Figure 3.69

The plot of observed versus predicted attack shows a good predictive fit (R^2 = 0.8257; curve slope of 0.9964) and thus the model developed could be used to predict the attack level of the data set, using the 17 volatiles components emitted by the pine needles of the twelve species, with an estimated error for the set of 0.131. However, it must be noticed that the model shows a tendency to overestimate the attack level for *P. patula* and *P. kesiya*, the trees less attacked from all the observations.

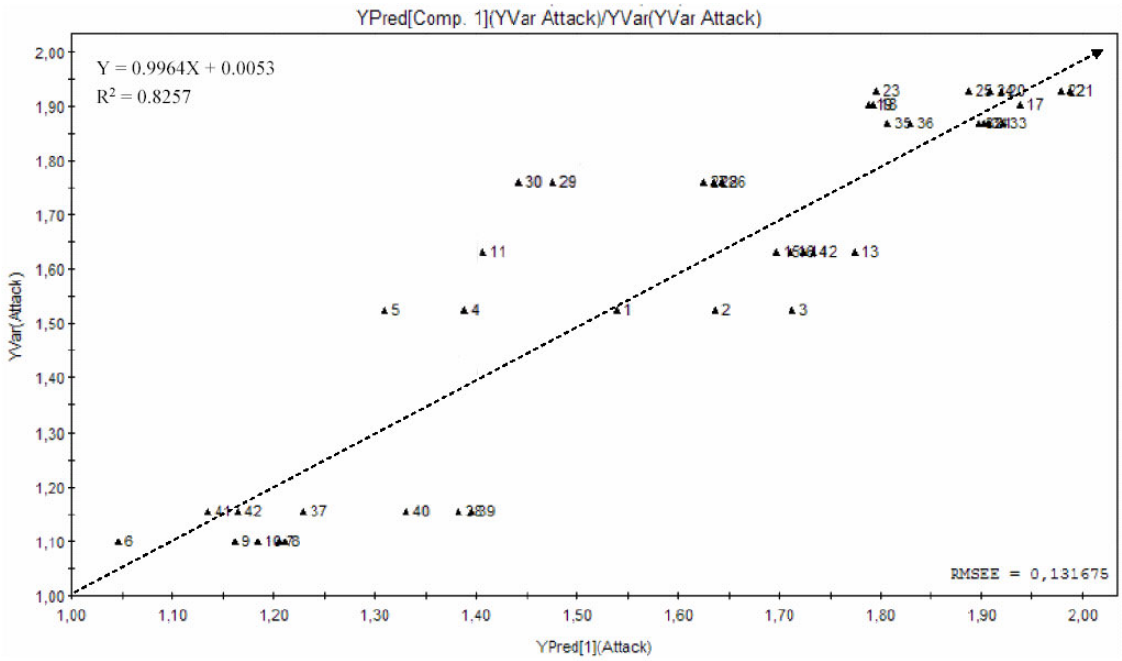

Figure 3.69 - Partial least squares predictions of the attack level by *T. pityocampa* (Y variable) plotted against the observed values.

3.3.1.4. Partial least squares regression and modeling – second analysis

The scores plot from the first PLS analysis pointed to the existence of two outliers. In order to investigate their influence in the general model for the attack, a second analysis was performed, excluding the outlier samples from the experimental data set. The new data set for the PLS analysis comprises eight pine species and 40 observations.

As the variables show a range of variation of over more than one magnitude of 10, they were logarithmically transformed in order to render their distribution more symmetrical. The results obtained for the second PLS analysis are summarized on Table 3.14.

Table 3.14 – Summary of the second partial least squares model for the data set of twelve pine species and *T. pityocampa* attack level.

A	R^2X	R^2X(cum)	Eigenvalue	R^2Y	R^2Y(cum)	Q^2	Q^2(cum)	Significance
1	0.185	0.185	3.14	0.825	0.825	0.792	0.792	R1
2	0.114	0.298	1.93	0.061	0.886	-0.354	0.771	NS
3	0.140	0.438	2.38	0.037	0.923	0.143	0.804	R1
4	0.066	0.504	1.13	0.032	0.955	0.039	0.811	NS
5	0.094	0.599	1.6	0.005	0.960	-0.197	0.792	NS
6	0.042	0.676	1.32	0.002	0.962	-0.276	0.772	N4

Number of observations: N=40; Variables: K=18; X(volatiles)= 17 and Y(attack)=1

After exclusion of the outliers, the new PLS analysis shows a slightly results improvement. Two significant components were found according to the cross validation rule 1 (R1): component 1 and component 3. The first component explains 18.5% of the X variation, 82.5% of the Y variation ($R^2X = 0.185$, $R^2Y = 0.825$) and predicts 79.2% of the Y (attack) variation ($Q^2 = 0.792$). The third component explains 14.0 % of the X variation, 3.71% of the Y variation ($R^2X = 0.14$, $R^2Y = 0.0371$) and predicts 14.3% of the Y (attack) variation ($Q^2 = 0.143$). The resulted plot of the X scores, t_1 vs. t_2 is presented in Figure 3.70.

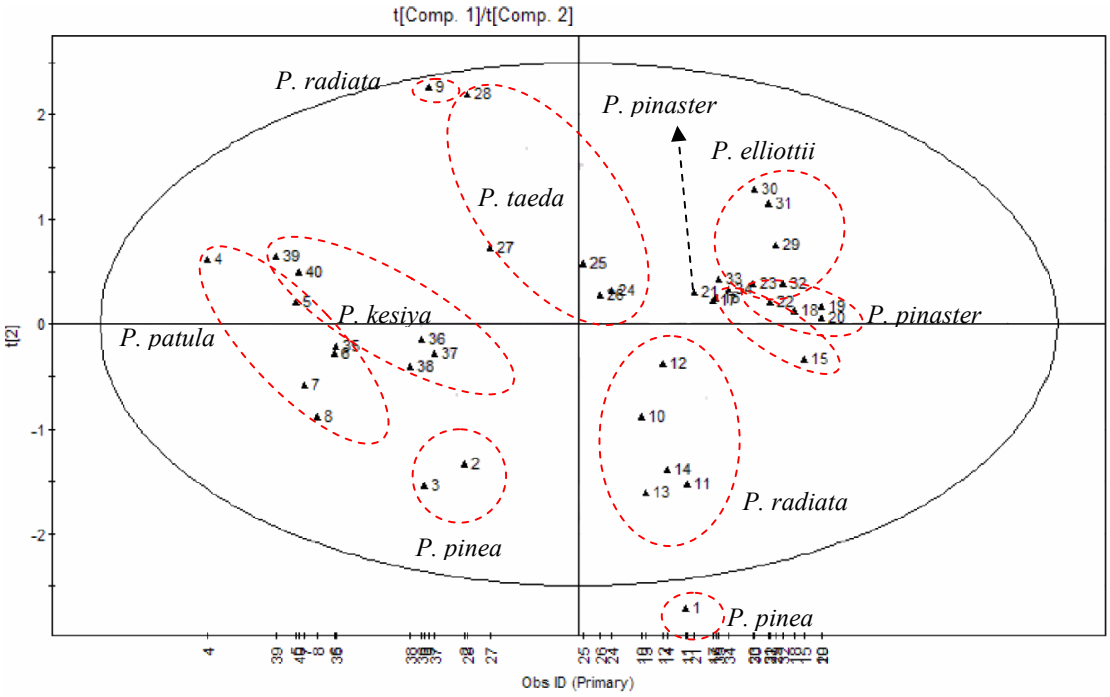

Figure 3.70 - Partial least squares scores t1 and t2 for the twelve pine species data set (second analysis).

3.3.2. Abrantes experimental plot. Chiral analysis

The enantiomeric composition of limonene, α-pinene and β-pinene, the major volatile compounds emitted by pine needles, were measured by multidimensional gas chromatography (md-GC). The samples submitted to analysis were taken from trees randomly sampled, belonging to the ten pine species, planted in the Abrantes arboretum. The data set was log-transformed, to allow for an examination of the role of the minor volatile terpenes. The attack level for each species was expressed as percentage of trees having nests from *T. pityocampa*. Table 3.15 shows the enantiomeric average regarding the relative composition of each pine species, without log-transformation.

Table 3.15 - Average enantiomeric relative composition, expressed as percentage of the total amounts, for each pine species.

	(-)-α-pinene	(+)-α-pinene	(-)-β-pinene	(+)-β-pinene	(-)-limonene	(+)-limonene
P. brutia	15.34	3.06	77.60	1.52	1.81	0.67
P. elliottii	37.09	4.03	56.02	1.29	0.95	0.62
P. halepensis	56.08	13.09	4.41	23.81	2.07	0.53
P. kesiya	4.61	90.70	0.89	0.83	2.33	0.64
P. radiata	10.16	14.40	46.08	3.98	24.54	0.84
P. pinaster	22.07	14.19	58.87	1.16	3.07	0.63
P. pinea	5.91	0.78	1.98	0.00	90.54	0.80
P. patula	66.81	8.55	0.24	0.12	22.33	1.95
P. sylvestris	18.12	64.20	15.60	0.61	0.84	0.62
P. taeda	10.94	35.46	36.17	0.84	15.97	0.61

3.3.2.1. Hierarchical cluster analysis

The data set, composed of 28 observations and six volatile compounds, was analyzed by hierarchical cluster analysis (HCA), using the Ward's method and Euclidean distances, in order to identify similarities among the samples, based on their enantiomeric volatile profiles. The resulting dendrogram from the HCA is shown in Figure 3.71.

Results show a very good separation of the samples that are grouped in the dendrogram according to the pine species they belong to. The only exception is one *P. taeda* sample, which is placed between *P. radiata* and *P. halepensis*. According to their enantiomeric composition, the 10 *Pinus* species from Abrantes arboretum are divided in three main groups: The groups subdivide, at linkage distance of 50, in nine-separated clusters that correspond to the pine species under study, with the exception of a cluster comprising both *P. pinaster* and *P. elliotti* samples. These clusters contain, by descending order of similarity: **1**) *P. brutia*, **2)** *P. elliottii* and *P. pinaster*, **3**) *P. radiata* and one tree from *P. taeda*, **4**) *P. patula*, **5**) *P. halepensis*, **6**) *P. pinea*, **7**) *P. kesiya*, **8**) *P. silvestrys* and **9**) *P. taeda* samples.

With respect to the attack level, HCA results can be visualized in Table 3.16 where each pine species is associated with its correspondent percentage of attack.

Observations of the Abrantes arboretum did not register attacks on pine species having trees with less than 1.5 m in height: *P. brutia, P. halepensis* and *P. sylvestris*. However, these species are cited in the literature as suffering attack by *T. pityocampa* (Hodár *et al*, 2003; Kanata *et al*, 2005; Mirchev *et al*, 2004). The first two clusters are constituted by pine species that are grouped in the same cluster, in the previous HCA performed for non-enatiomeric volatile compositions. *P. brutia*, in cluster one, was not attacked but *P. elliottii* and *P. pinaster*, on cluster two, have the highest level of attack by *T. pityocampa* in the arboretum. The remaining clusters include the samples from pine species that show either an intermediate or a low attack level, but without any apparent trend. In relation to the previous HCA performed for non-enantiomeric volatile composition, *P. taeda* is again on the same group as *P. kesiya.*

The information provided by the dendrogram, regarding chemical differences among pine species it scarce. However, some trends can be extrapolated from Table 3.15. The HCA of the pine species studied, based on their enantiomeric volatile composition, suggests that the aggregation on the groups/clusters is driven by (-)-β-pinene, (-)-α-pinene and (+)-α-pinene. The first group (clusters 1 to 3) comprises the pine species where (-)-β-pinene is the major enantiomeric compound, in descending order from right to left.

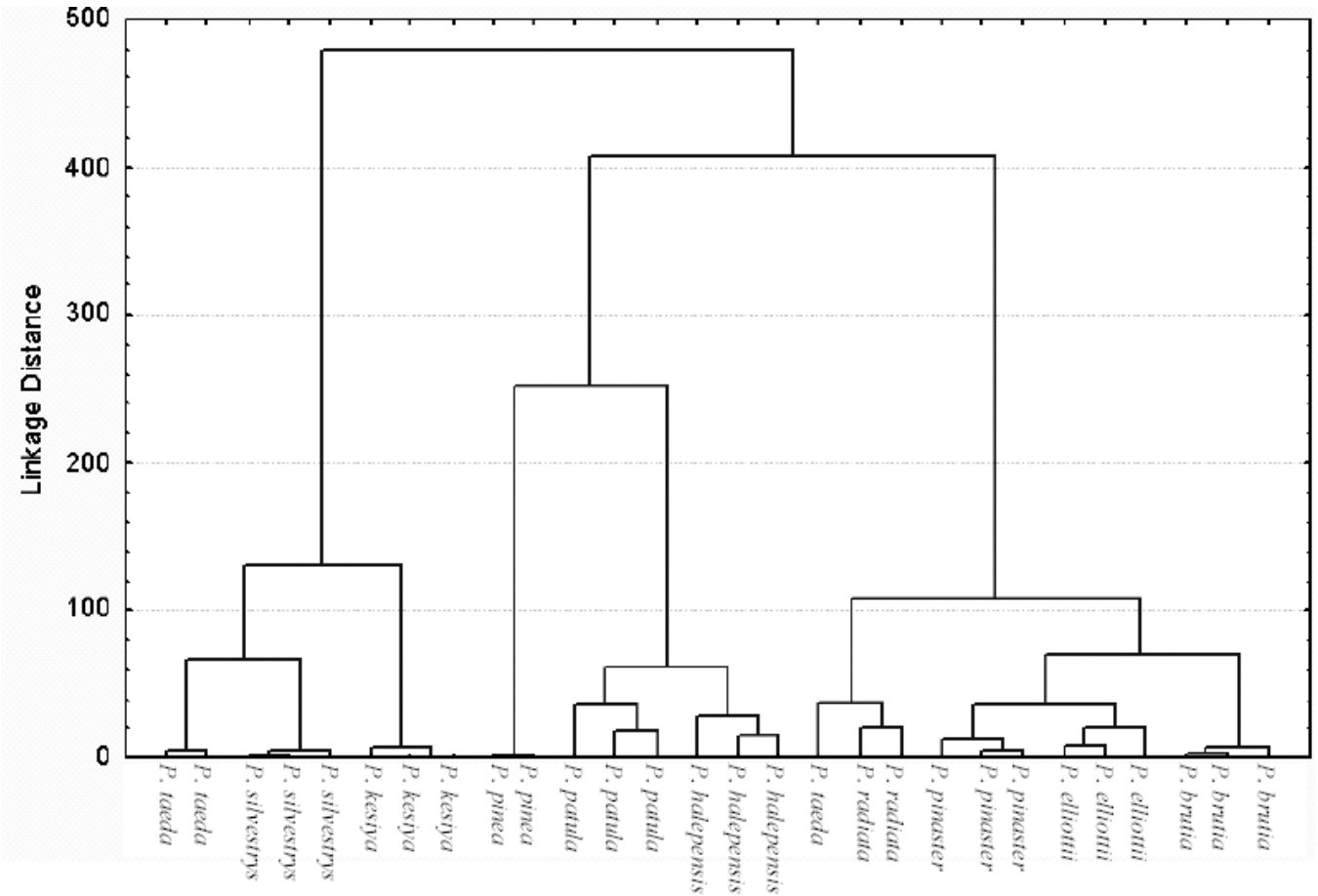

Figure 3.71 - Dendogram based on the hierarchical cluster analysis, showing the chiral profile of the ten pine species from Abrantes plot.

Table 3.16 - Hierarchical cluster analysis classification for the pine species studied, and percentage of attack by *T. pityocampa.*

HCA groups	Clusters	*Pinus* spp.	% attack
Group 1	1	*P. brutia*	0*
Group 1	2	*P. elliottii* *P. pinaster*	73.90 85.00
Group 1	3	*P. radiata* *P. taeda*	42.85 57.65
Group 2	4	*P. halepensis*	0*
Group 2	5	*P. patula*	12.50
Group 2	6	*P. pinea*	33.30
Group 3	7	*P. kesiya*	14.50
Group 3	8	*P. sylvestris*	0*
Group 3	9	*P. taeda*	57.65

*All trees belonging to pines species with 0% attack had less than 1.5 m of height
% attack $(\text{pine specie})_i = [(\text{number of trees with nests})_i/(\text{total number of trees})_i]*100$

The second group comprises in clusters 4 and 5, the pine species where (-)-α-pinene is the major enantiomeric compound. Cluster 6 comprise *P. pinea* the composition of which is strongly dominated by (-)-limonene (90.54%) followed by (-)-α-pinene (5.91%). The third group (clusters 7 to 9) comprises the pine species where (+)-α-pinene is the major enantiomeric compound. One of the samples belonging to *P. taeda* is also allocated to the first group. According to Table 3.15, *P. taeda* has very close percentages of (+)-α-pinene and (-)-β-pinene (a difference lower than 2%). Cluster 9 comprises the *P. taeda* samples where (+)-α-pinene is higher than (-)-β-pinene. On the other side, cluster 3 comprises the *P. taeda* sample where (+)-α-pinene is lower than (-)-β-pinene. This observation leads to the formulation of the hypothesis of a potential distribution of *P. taeda* samples between group one and three, and thus the aggregation of the five attacked pine species (42.85 to 85% attack level), on the first group, may be driven by their content in (-)-β-pinene.

3.3.2.2. Principal component analysis

In order to identify the compounds associated with the hierarchization of the samples, a principal component analysis (PCA) was carried out, treating the pine species as cases and the volatile

compounds as variables. The results for the PCA with the log-transformed data produced are summarized in Table 3.17.

Table 3.17 - Eigenvalues and total variance from the principal component analysis using the log-transformed values for the volatile enantiomeric data from the pine species sampled in Abrantes

PCA factor	Eigenvalue	% Total	Cumulative Eigenvalue	Cumulative %
1	2.57	42.86	2.57	42.86
2	1.29	21.43	3.86	64.29
3	1.18	19.69	5.04	83.98
4	0.44	7.40	5.48	91.39
5	0.35	5.78	5.83	97.17
6	0.17	2.83	6.00	100.00

The first three factors explain 83.98% of the total variance, with respectively 42.86, 21.43, and 19.69% for components 1, 2, and 3, and can thus be considered sufficient to explain the variation. The log-transformed data values produced the first two-component plot shown in Figure 3.72, where 64.29% of the variance is explained.

It can be further observed that *P. pinea* and *P. patula* samples, respectively on quadrant four and one, are isolated from the other samples, according to the first component. The other species, with the exception of *P. pinaster* and *P. brutia* samples that are grouped together, are separated by the second component. In comparison with the previous HCA, *P. pinea*, *P. patula* and *P. halepensis* that were grouped together on group 2, are now placed on different quadrants. Pine species from group 3 are located on quadrant 3. Pine species from group one, with the exception of *P. radiata*, are located on the second quadrant.

An interesting observation concerns the pine species and their attack level. If *P. patula* is omitted, an ascending trend according to the attack level can be observed through the second component. From bottom to top of the PCA plot, pine species can be ordered by attack level in the following sequence: *P. kesiya* (14.20%), *P. pinea* (33.30%), *P. taeda* (57.65%), *P. radiata* (42.85%), *P. pinaster* (85.00%) and *P. elliotti* (73.90%). In order to identify which enantiomers are associated with the components, the factor scores (Table 3.15) were analyzed for the first two components. The projection of the variables on the factor plane for the first two components is presented in Figure 3.73. The loading values for component 1, 2 and 3 are summarized in Table 3.18.

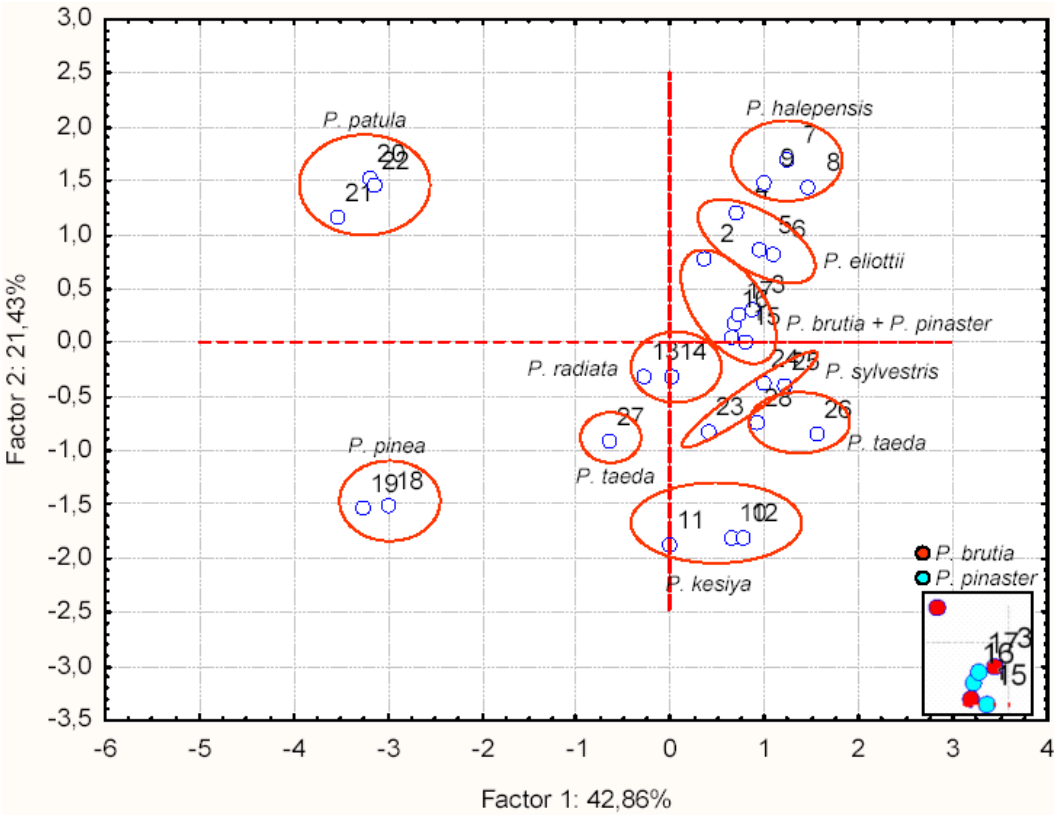

Figure 3.72 – Principal component analysis for the log-transformed volatile enantiomeric data from the pine species sampled in Abrantes.

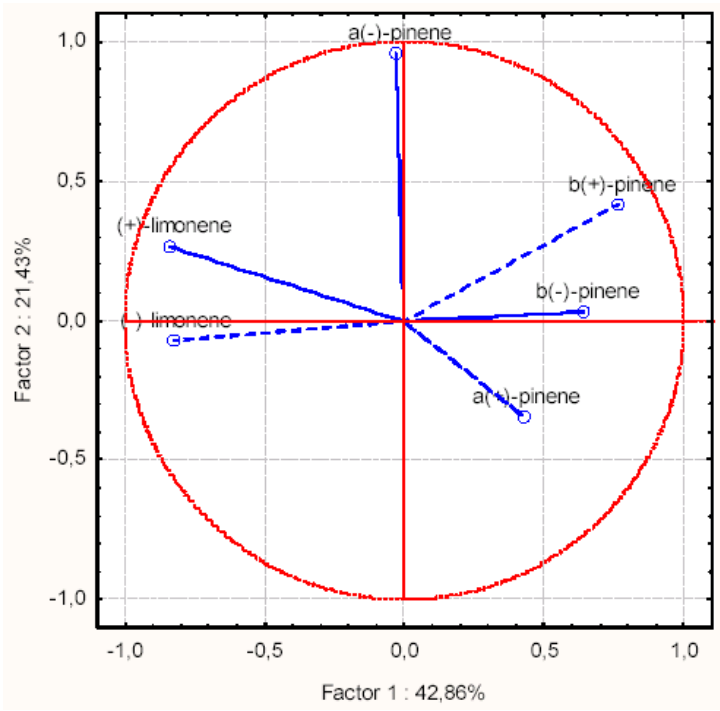

Figure 3.73 – Principal component analysis loadings for the log-transformed volatile enantiomeric data for the pine species sampled in Abrantes.

Table 3.18 - Values of loadings for the first three components from the principal component analysis using log-transformed values of the chiral monoterpenes from the *Pinus* species sampled in the Abrantes experimental plot.

Chiral terpene	Factor 1	Factor 2	Factor 3
(-)-α-pinene	-0.03	0.96	-0.15
(+)-α-pinene	0.43	-0.34	-0.77
(-)-β-pinene	0.64	0.03	0.64
(+)-β-pinene	0.77	0.41	-0.12
(-)-limonene	-0.83	-0.07	0.26
(+)-limonene	-0.84	0.26	-0.26

The loadings data (table and projection plot) show that the major associations for factor 1 can be found for both limonene and β-pinene enantiomers, in opposite influence. Concerning factor 2 the major association is found for (-)-α-pinene. The third factor is mainly associated with (+)-α-pinene and (-)-β-pinene.

According to the loadings data, the *P. patula* sample location on the first quadrant is driven by its content on (+)-limonene, which is not too high relatively to all the others enantiomers, but relatively high in relation to (-)-limonene, when compared to the other pine species. *P. pinea* is driven to quadrant four due to its high content in (-)-limonene. *P. halepensis* is driven to the second quadrant due to its major enantiomeric components (-)-α-pinene and (+)-β-pinene. Concerning the trend of the attack level, it may be observed through the second component that it is driven by (-)-α-pinene.

3.3.2.3. Partial least squares regression

In order to understand the variation of the attack, expressed as the percentage of trees attacked by *T. pityocampa* in the pine species sampled (10 species; 28 observations), and study the influence of the volatile compounds, a partial least squares (PLS) regression was performed. The pine species are described by the six enantiomers of their major volatile components (X variables). The six enantiomers are assumed to be the promoters of the effects causing the attack changes (Y variable) in the system under study. For the PLS analysis, the pine species with no register of attack were omitted, considering that tree height was the main factor controlling the absence of attack. The final data set for the PLS analysis comprises seven pine species and 19 observations.

Since the variables show a range over an order of magnitude of 10, they were logarithmically transformed in order to make their distribution more symmetrical. The results obtained for the PLS analysis are summarized on Table 3.19.

The PLS analysis of the data extracted four significant components according to the cross validation rule 1 (R1) that sets, for PLS models, a limit of significance of 0.05 for models with less than 100 observations. The four significant components of the PLS explain 90.3 % of the X variation and 97.6% of the Y variation (R^2X cum. = 0.903, R^2Y cum. = 0.976). The same components predict 92.9% of the Y (attack) variation (Q^2 = 0.922).

Table 3.19 – Summary of the partial least squares model for the data set of seven pine species and the *T. pityocampa* attack level.

A	R^2X	R^2X(cum)	Eigenvalue	R^2Y	R^2Y(cum)	Q^2	Q^2 (cum)	Significance
1	0.415	0.415	2.490	0.768	0.768	0.687	0.687	R1
2	0.275	0.689	1.650	0.157	0.926	0.613	0.879	R1
3	0.128	0.818	0.771	0.026	0.951	0.113	0.893	R1
4	0.085	0.903	0.510	0.025	0.976	0.403	0.936	R1
5	0.088	0.991	0.531	0.001	0.977	-0.187	0.929	N4
6	0.008	1	0.051	0.000	0.977	-0.124	0.922	N3

Number of observations: N=19; Variables: K=7; X (volatiles) = 6 and Y (attack) = 1

The first two components are the most significant ones, explaining 68.9% of the X variation and 92.6% of the Y variation (R^2X cum. = 0.689, R^2Y cum. = 0.926). The same components have a predictive ability of 87.9% for the Y (attack) variation (Q^2 = 0.879). In spite of this high predictive ability for the first two components, the second component only predicts 15.7% of the attack variation, contributing the first component with 76.8 % to the model predictive ability.

The plot of the X scores, t_1 *vs*. t_2, for the first two components presented in Figure 3.74, shows the seven pine species separated on both components of the plot. A trend related to the attack level is observed on the first component, increasing from left to right but not in a linear way (see Table 3.16 for the relation pine species – attack level). No observations have been found outside the Hotellings T^2 ellipse and thus no outliers are present in the data set.

The plot of the X loadings for the first two components, p_1 *vs.* p_2, presented in Figure 3.75, shows how the variables are related and their association with the observations projected on the score plot.

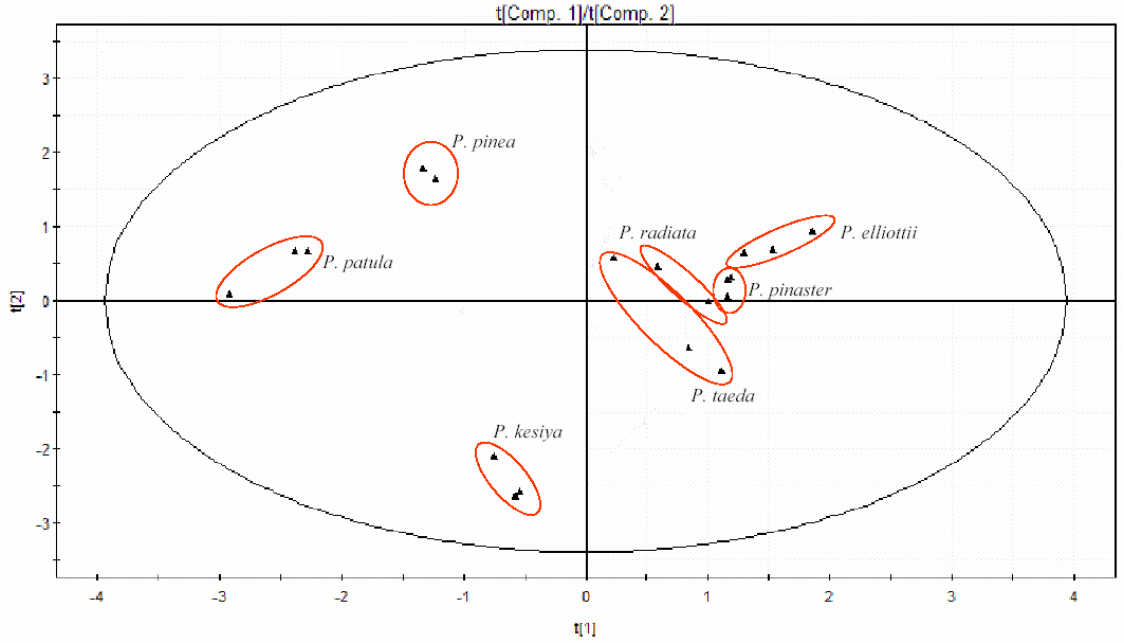

Figure 3.74 – Partial least squares scores for the first two components, t_1 *vs.* t_2, of the seven pine species enantiomeric data set.

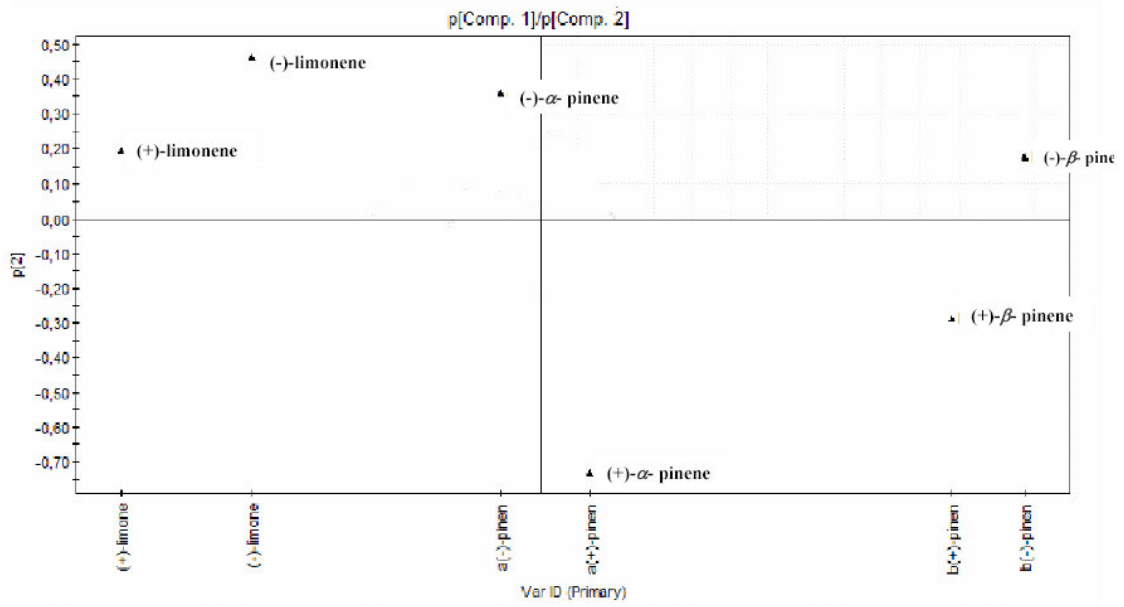

Figure 3.75 – Partial least squares loadings for the first two components, p_1 *vs.* p_2, of the seven pine species enantiomeric data set.

The loadings plot for the PLS analysis show that the observations distribution in the first component, on the scores plot, is mainly associated with the enantiomers of β-pinene and limonene. The α-pinene enantiomers are close to the origin and have almost no influence on the first component separation. The dispersion on the second component is mainly associated with the α-pinene enantiomers on both axis and with (-)-limonene on the positive axis.

The plot t_1 *vs.* u_1, presented in Figure 3.76, examines the relationship between the scores of X (the observations according to the variables) and the scores of Y (the attack).

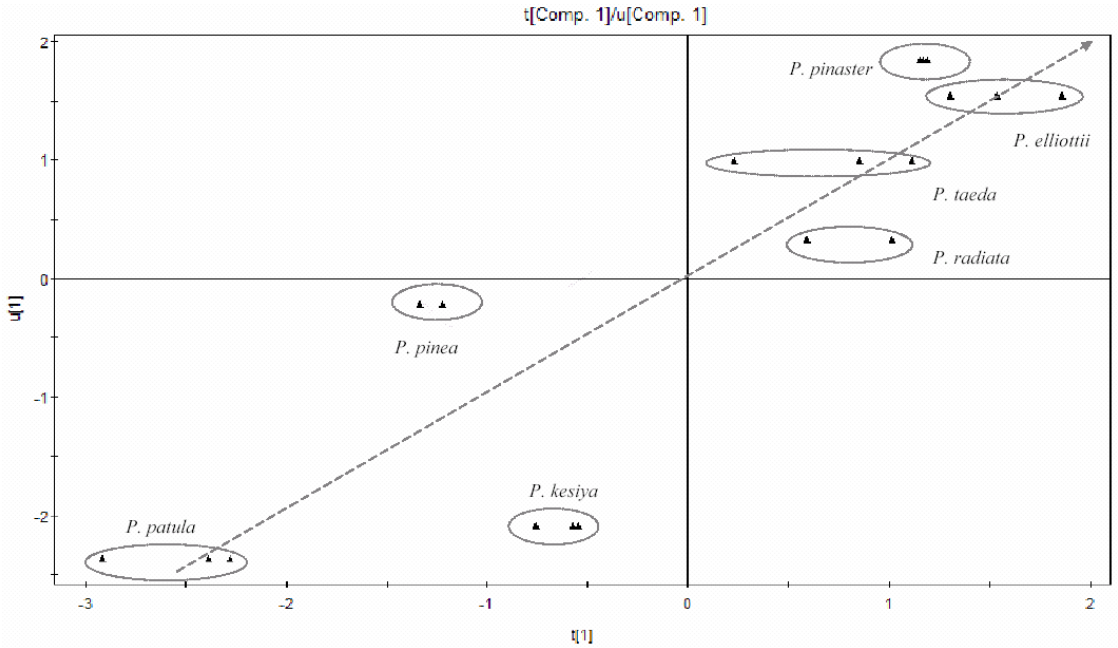

Figure 3.76 – Partial least squares scores plot t_1 *vs.* u_1 for the seven pine species data set from Abrantes.

The X-Y scores plot on the first component, t_1 *vs.* u_1, suggests a relationship between the X and Y scores but with some deviation from the *P. kesiya* and *P. pinea* samples.

The plot of the PLS weights w and c, presented in Figure 3.77, shows the correlation structure between the volatiles (X) and the attack and thus can be used to identify the variables pertaining to the volatiles which are correlated with the variation of the attack level.

The correlation of the volatiles with the attack level is related to its distance from the origin both for the positive and negative sides. The weights plot shows that the enantiomer with a more

positive relation with the attack is (-)-β-pinene followed by (+)-β-pinene. Negatively related with the attack are (+)-limonene, followed by (+)-α-pinene and (-)-limonene.

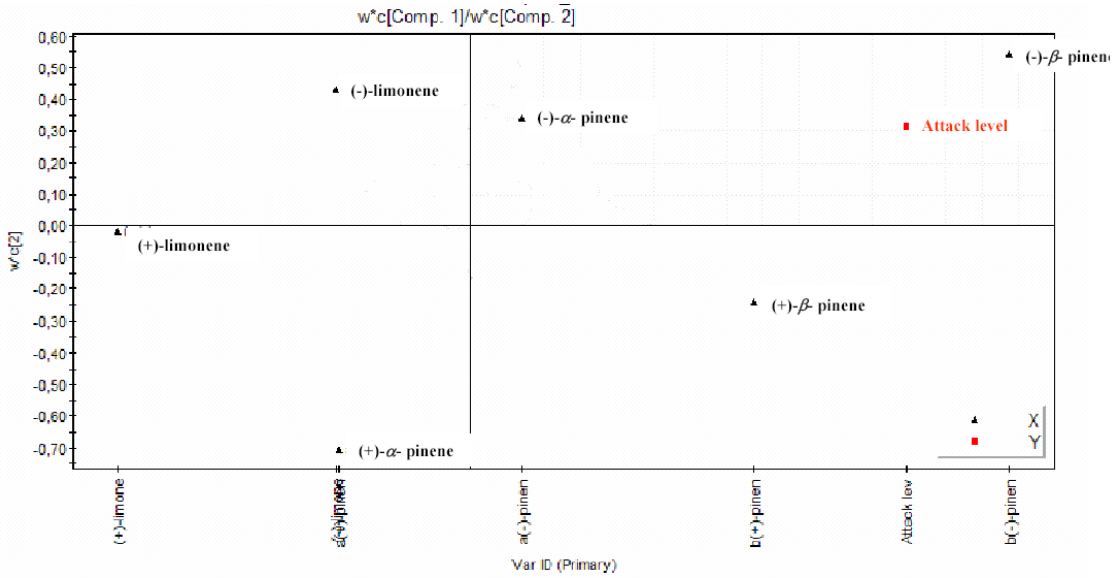

Figure 3.77 – Partial least squares weights plot w*c_1 *vs.* w*c_2 for the seven pine species data set from Abrantes, showing the model correlation structure.

The "variable influence on projection" (VIP) values summarize the overall contribution of each individual volatile (X variables) to the characterization of pine samples and explanation of the attack level variation (Y variable). It is assumed that VIP values higher than one indicate the most relevant variables for explaining the model. Figure 3.78 shows the volatiles by descending VIP values. According to the plot, the most relevant variables, by descending order, are: (-)-β-pinene (1.81), (+)-limonene (1.18) and (+)-β-pinene (0.951).

One of the goals of a PLS regression analysis is to formulate a function to model the variable Y under study. The model estimates coefficients, for each volatile compound (X variable), that will be used to interpret the influence of the volatiles upon the attack level. Each observation will be modelled as a linear combination of all volatile compounds. Table 3.20 shows the estimated coefficients for the model proposed.

The agreement between the observed values and those predicted by the previous regression coefficients, estimated by the PLS model attack data, is shown in Figure 3.79.

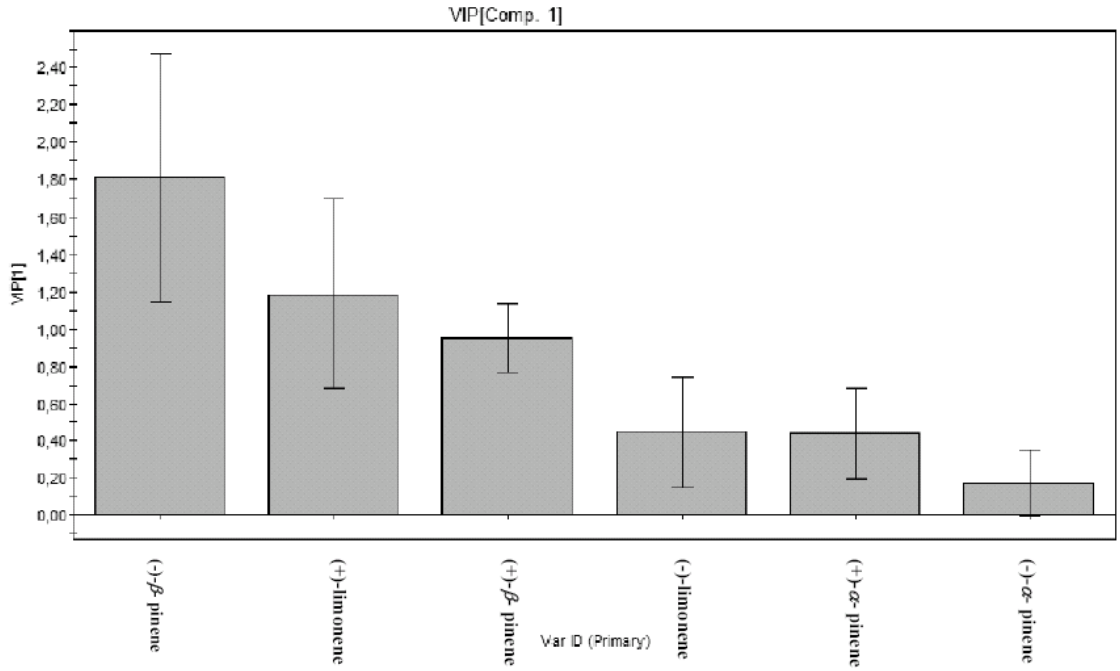

Figure 3.78 - Partial least squares variable importance on the projection of the enantiomeric volatile variables for the attack level by *T. pityocampa*, in the pine species data set for the first significant component. The bars indicate 95% confidence intervals based on jack-knifing.

Table 3.20 – Partial least squares regression coefficients for the combination of the enantiomeric volatile compounds to predict the attack (coefficients refer to centered and scaled X, and scaled but uncentered Y) level by *T. pityocampa.*

Variable	Coefficients (attack)
(-)-α-pinene	0.042
(+)-α-pinene	-0.107
(-)-β-pinene	0.440
(+)-β-pinene	0.231
(-)-limonene	-0.109
(+)-limonene	-0.288

The plot of observed *vs.* predicted attack level shows a good predictive fit (R^2 = 0.7684; curve slope of 1) and thus the model developed could be used to predict the attack level of the data set, using the enantiomeric volatiles components emitted by the pine needles of the seven species, with an estimated error for the set of 0.163. However, it must be noticed that, according to the observations, the model shows a tendency to overestimate the attack level in *P. kesiya* and to sub estimate the attack in *P. pinea*.

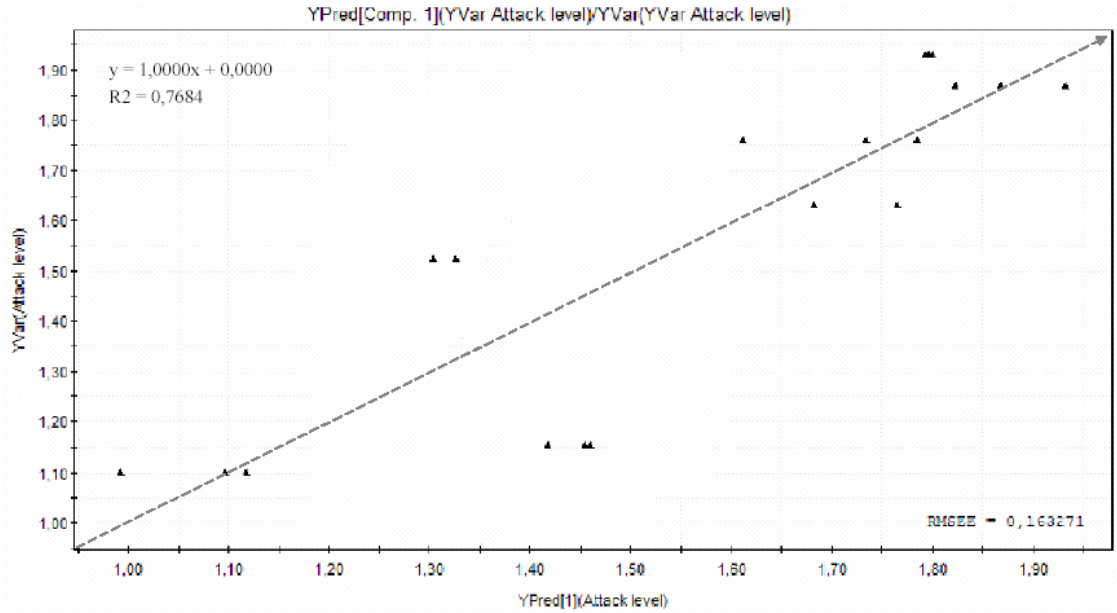

Figure 3.79 - Partial least squares predictions of the attack (Y variable) plotted against the observed values.

3.3.3 Apostiça experimental plot - Volatiles

Nineteen volatile terpenes were quantified in 21 *P. pinaster* trees, randomly sampled at Apostiça. The attack level was expressed as the number of *T. pityocampa* nests observed per tree. The nests observed were either provisional ones which are built by young larvae, or definitive ones, which are spun by larvae of the last instars. The data set obtained was log-transformed, to allow for the assessment of the role of the minor volatile terpenes. Table 3.21 shows the volatile average relative composition for each tree sampled without log-transformation. The volatiles separation was performed on a DB-5 column (see section 2.4.1.1), which did no separate the pair limonene and β-phellandrene.

3.3.3.1. Hierarchical cluster analysis

In order to identify similarities between the trees sampled a hierarchical cluster analysis (HCA), using Ward's method and Euclidean distances, was carried out. The resulting dendrogram from the HCA is shown in Figure 3.80. Results suggest that, according to their chemical composition, the *P. pinaster* trees sampled in Apostiça can be divided in two main groups, which are further subdivided into five-separated clusters, at a linkage distance of three.

Table 3.21 - Partial least squares 1 of Apostiça Data set - Mean percentages of the terpene volatiles, for each individual tree (needles composite; n = 5) of *P. pinaster*, tree characteristics and attack level by *T. pityocampa*.

							Terpene volatiles																				
Tree	Q*	A**	P§	D§§	Height	DAP	Tr	Th	aP	Ca	Sa	bP	My	3Ha	aPh	d3C	aT	Car	rC	Li	cO	tO	gT	Volat2	Te	Lin	TSes	bP/Li
1	9	0	0	0	8.85	13.7	0.06	0.07	37.59	0.15	0.14	19.30	11.70	0.04	0.05	6.95	0.04	0.10	0.04	11.23	0.02	0.04	0.09	0.02	1.23	0.05	11.27	1.72
2	9	4	2	2	8.4	18.2	0.05	0.00	35.69	0.18	0.14	35.03	5.93	0.07	0.07	0.05	0.03	0.00	0.00	8.25	0.05	2.38	0.07	0.00	0.52	0.07	11.48	4.25
3	1	3	1	2	8.00	23.60	0.07	0.00	34.72	0.55	0.22	27.63	21.65	0.52	0.33	0.37	0.06	0.00	0.00	2.30	0.10	0.86	0.00	0.00	0.76	0.23	10.72	12.01
4	9	0	0	0	8.8	12.7	0.06	0.00	35.40	0.21	0.10	32.14	14.36	0.23	0.13	0.02	0.02	0.00	0.00	2.38	0.03	0.02	0.00	0.00	0.44	0.04	13.92	13.48
59	9	5	2	3	8.75	17.9	0.06	0.00	27.31	0.16	5.91	25.89	4.26	0.05	0.04	0.05	0.03	0.00	0.00	12.46	0.05	2.25	0.00	0.00	0.24	0.02	15.53	2.08
8	1	0	0	0	3.10	4.40	0.06	0.02	36.36	0.38	0.09	39.58	5.36	0.26	0.04	0.03	0.02	0.00	0.00	8.47	0.05	0.33	0.04	0.18	0.18	0.15	8.56	4.67
91	1	6	5	1	4.60	9.00	0.05	0.04	27.81	0.19	0.09	34.62	9.03	0.11	0.06	0.05	0.04	0.00	0.00	9.49	0.04	0.94	0.05	0.00	0.32	0.08	16.99	3.65
99	9	0	0	0	7.95	12.3	0.08	0.10	24.47	0.23	0.08	31.66	14.82	0.06	0.07	0.05	0.03	0.00	0.00	6.74	0.12	2.85	0.07	0.07	0.65	0.09	18.04	4.70
17	2	11	7	4	3.80	7.00	0.07	0.06	30.21	0.27	0.07	19.16	14.58	0.09	0.05	0.03	0.03	0.00	0.00	2.76	0.09	2.06	0.05	0.00	0.20	0.03	30.25	6.95
21	9	0	0	0	8.15	12.2	0.05	0.03	23.82	0.16	0.05	23.12	9.10	0.07	0.06	0.03	0.04	0.00	0.00	9.35	0.08	3.62	0.06	0.00	1.08	0.03	29.28	2.47
22	9	14	8	6	8.95	16.1	0.05	0.02	30.10	0.25	0.07	36.43	13.74	0.08	0.07	0.04	0.04	0.00	0.00	7.44	0.03	1.84	0.05	0.00	0.68	0.03	9.17	4.89
39	9	2	1	1	6.65	14	0.05	0.08	26.85	0.21	0.11	32.37	14.94	0.04	0.05	8.81	0.06	0.00	0.00	2.61	0.04	2.62	0.14	0.03	0.73	0.02	10.28	12.41
41	9	0	0	0	3.65	5	0.22	0.46	23.63	1.21	1.01	28.19	3.06	0.28	3.41	9.45	0.01	0.08	0.01	5.19	0.17	3.62	1.05	0.36	2.06	0.09	16.90	5.43
44	9	2	1	1	8.37	19.5	0.05	0.03	24.82	0.23	0.07	35.86	6.83	0.06	0.05	0.03	0.03	0.00	0.00	5.82	0.04	2.66	0.05	0.09	0.13	0.09	23.18	6.16
45	9	0	0	0	11.75	27.8	0.07	0.04	34.95	0.17	0.09	25.26	14.06	0.07	0.05	0.04	0.03	0.00	0.00	3.11	0.07	4.19	0.05	0.70	0.48	0.05	17.11	8.12
73	9	2	1	1	9	17	0.05	0.07	32.71	0.11	0.11	19.31	14.94	0.07	0.04	8.00	0.04	0.00	0.00	1.99	0.06	3.77	0.11	0.02	0.56	0.07	18.04	9.71
88	9	3	2	1	7.35	15	0.07	0.02	34.34	0.51	0.05	28.23	9.68	0.06	0.04	0.02	0.03	0.00	0.00	13.56	0.09	1.93	0.03	0.00	0.28	0.02	11.04	2.08
107	9	5	4	1	9.5	16.2	0.05	0.04	29.18	0.21	0.10	33.54	14.12	0.06	0.06	0.03	0.05	0.00	0.00	7.39	0.06	1.84	0.10	0.00	0.40	0.07	12.76	4.54
142	9	0	0	0	10.2	13.5	0.06	0.06	33.49	0.20	0.20	25.95	15.72	0.07	4.56	5.95	0.05	0.00	0.00	2.79	0.03	2.00	0.14	0.04	1.58	0.05	8.00	9.30
157	9	4	3	1	7.65	14.8	0.06	0.02	44.24	0.25	0.09	30.54	10.05	0.05	0.05	0.03	0.04	0.00	0.00	4.04	0.03	1.95	0.06	0.00	0.26	0.18	8.03	7.55
164	9	3	3	1	6.65	10.1	0.07	0.03	37.55	0.32	0.09	28.21	10.85	0.10	0.04	0.25	0.04	0.00	0.00	2.19	0.06	0.16	0.09	0.00	1.01	0.27	18.83	12.90

*Q – quadrat; **A – Attack (total nests); §P – provisional nests; §§D – definitive nests.

Terpene volatiles key: Tr – Tricyclene; Th – Thujene; aP – α-Pinene; Ca – Camphene; Sa – Sabinene, bP – β-Pinene; My – Myrcene; 3Ha – Acetic acid hex-3-enyl ester; aPh – α-Phellandrene; d3C – Δ-3-Carene; aT – α-Terpinene; Car – Carvomenthene; rC – Cymene (isomer); Li – Limonene; cO – *cis*-Ocimene; tO – *trans*-Ocimene; gT – γ-Terpinene; Volat2 – unknown compound; Te – Terpinolene; Lin – Linalool; Tsesq – total sesquiterpene; bP/Li – ratio β-Pinene/Limonene.

Tree 59 is tree 5 from quadrat 9. Trees 91 and 99 are trees 9 from quadrats 1 and 9, respectively.

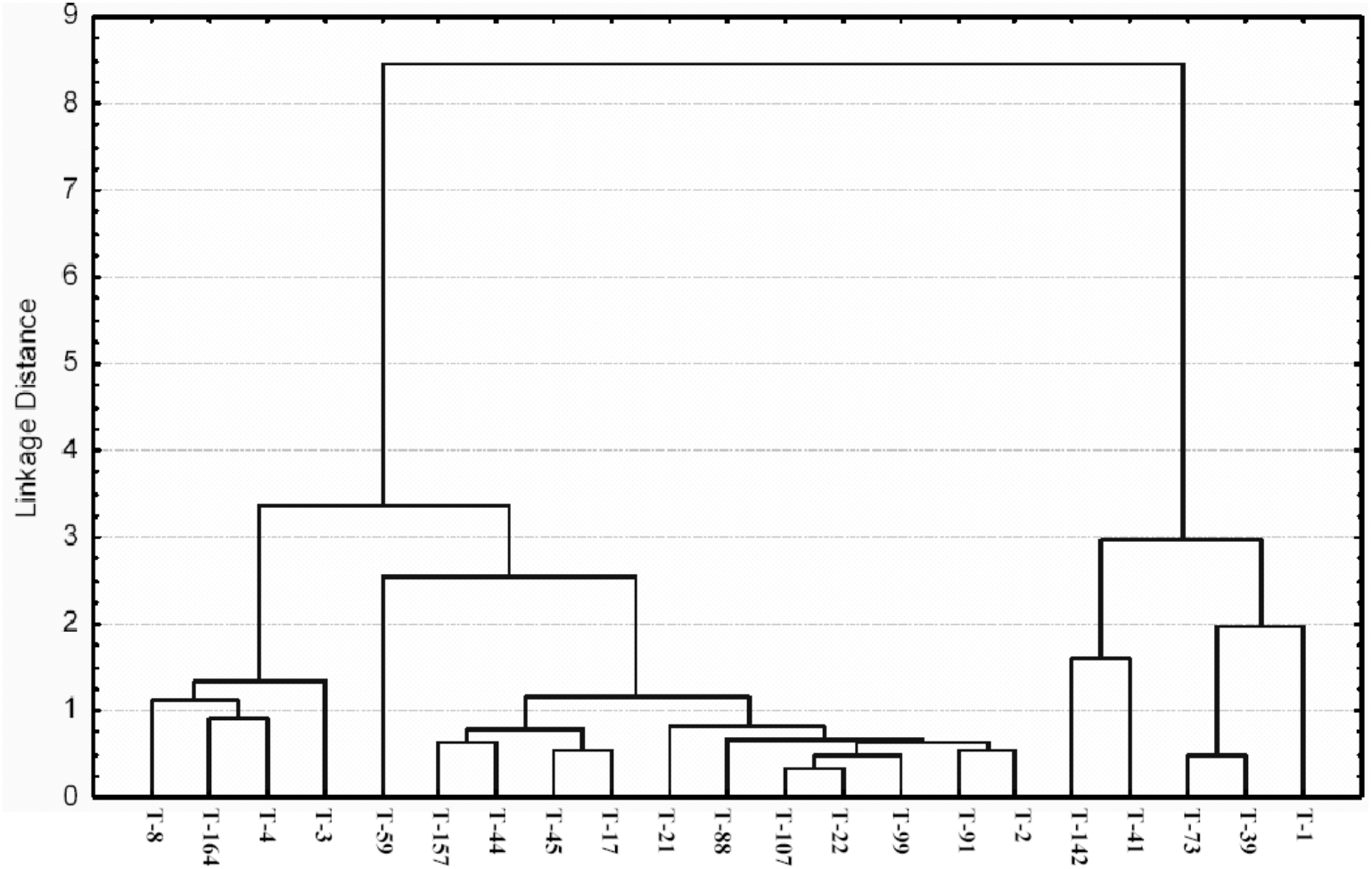

Figure 3.80 - Dendogram from the hierarchical cluster analysis for Apostiça *P. pinaster* trees based on their volatile profile.

Table 3.22 - Groups from the hierarchical cluster analysis of Apostiça trees, with correspondent number of *T. pityocampa* nests.

HCA groups	Clusters	Trees	Total tumber of nests
Group 1	1	T-1	0
		T-39	2
		T-73	2
Group 1	2	T-41	0*
		T-142	0
Group 2	3	T-2	4
		T-91	6
		T-99	0
		T-22	14
		T-107	5
		T-88	3*
		T-21	0*
		T-17	11
		T-45	0*
		T-44	2
		T-157	4
Group 2	4	T-59	5
Group 2	5	T-3	3
		T-4	0
		T-164	4
		T-8	0

* Trees foraged by the Argentinean ant *Linepithema humile.*

These clusters contain, by descending order of similarity: **1**) T-1, T-39 and T-73; **2**) T-41 and T-142; **3**) T-2, T-91, T-99, T-22, T-107, T-88, T-21, T-17, T-45, T-44 and T-157; **4**) T-59 and **5**) T-3, T-4, T-164 and T-8 trees.

It was decided to build the data set by considering the total number of provisional plus definitive nests per tree. Provisional nests indicate that egg batches were laid on the tree, although the larvae either died in the early instars, or joined other larvae from a neighbouring colony.

Table 3.22 shows the attack level by *T. pytiocampa*, expressed as the total number of nests counted on each tree. It can be seen that trees falling in cluster 1, have either zero or two nests. Similarly, cluster 5, comprises trees with zero or three-four nests. Cluster 3 contains a wide diversity of trees, supporting from zero to 14 nests, without any apparent relationship regarding the level of attack. Furthermore, three trees in this cluster, T-88, T-21 and T-45, had no nests but were not grouped together in the cluster analysis. It is however important to notice that trees T-21 and T-45 were colonized by the Argentinean ant, *Linepithema humile,* which is a highly effective predator of larvae of *T. pytiocampa* (Way *et al.*, 1999; Rodrigues, 2002), a fact that probably explains the absence of nests on these trees.

In short, the HCA of Apostiça trees, based on their volatile composition, do not suggest the existence of similarities between *P. pinaster* trees according to their attack level, and it provides scarce information regarding chemical differences among them.

3.3.3.2. Principal component analysis

In order to identify the compounds associated with the hierarchization of the trees, a principal component analysis (PCA) was carried out on a covariance matrix, treating the trees as cases and the volatile terpenes as variables. The results for the PCA on the log-transformed data produced are summarized on Table 3.23.

The first three factors explain 58.63% of the total variance, with 29.37, 15.55, and 13.71% explained respectively by components 1, 2, and 3. The log-transformed data values produced the first two-component plot shown in Figure 3.81, where only 44.91% of the variance is explained and thus is insufficient to explain the variation. To explain 80.00% of the total variance six factors were needed.

Table 3.23 - Eigenvalues and total variance from the principal component analysis using the log-transformed values for the volatile monoterpenes in the Apostiça trees.

Value number	Eigenvalue	% Total variance	Cumulative Eigenvalue	Cumulative %
1	5.58	29.37	5.58	29.37
2	2.95	15.55	8.53	44.91
3	2.61	13.71	11.14	58.63
4	2.07	10.91	13.21	69.53
5	1.47	7.72	14.68	77.25
6	1.00	5.27	15.68	82.52

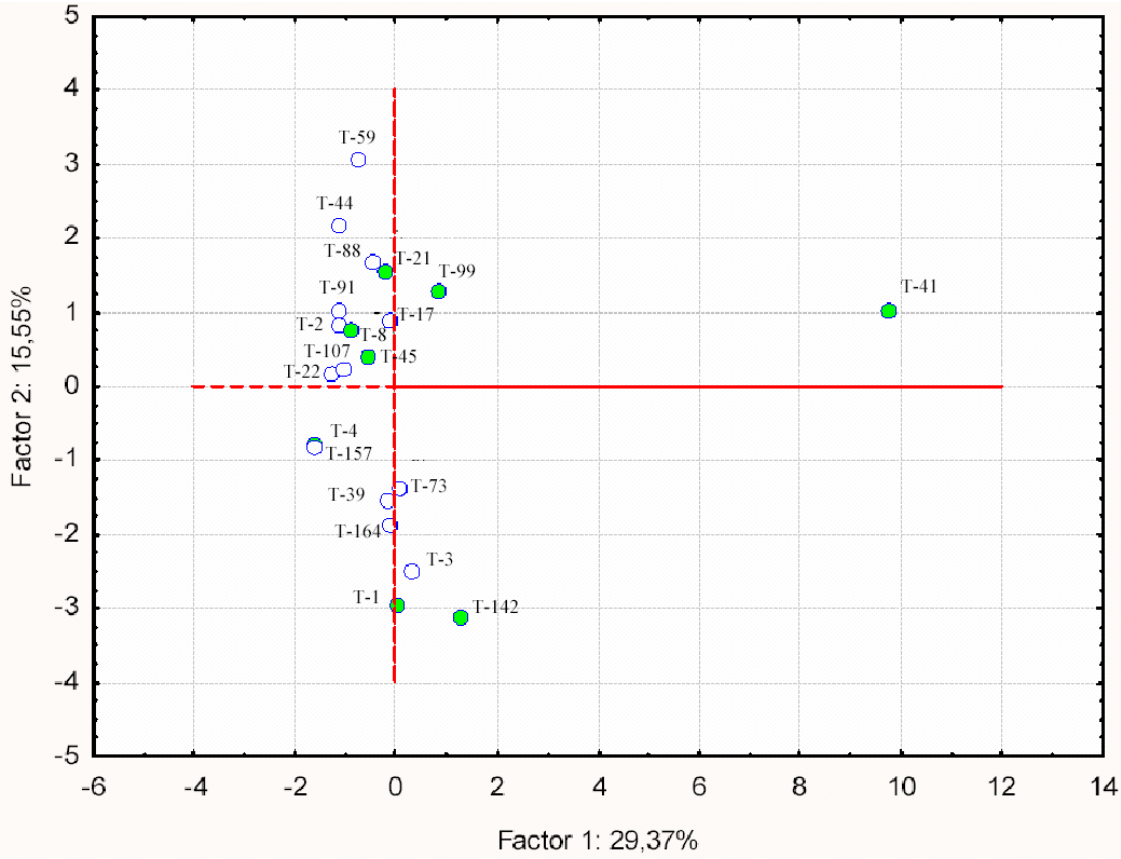

Figure 3.81 – Principal component analysis for the log-transformed volatile terpenes data from *P. pinaster* trees sampled in Apostiça (trees without nests are highlighted in green)

It can be observed in the PCA plot (Figure 3.81), that tree T-41 is totaly isolated from the other trees sampled, possibly due to its content in camphene. This isolation of tree T-41

spreads the scale of the positive side of the first component axis and thus promotes a visual illusion that the trees separation mainly occurs on the second component axis. The trees without nests, which are highlighted in green, are scattered on the plot like all the other trees and without apparent relation with the number of nests registered. The first quadrant of the plot comprises 52.4% of the trees sampled. Apparently two groups of trees can be observed in the plot. One group can be observed on the negative second component axis, and comprises all trees, with the exception of tree T-41, that was placed on the first HCA group, together with trees from the second group T-3, T-4 and T-164 (cluster five) and T-157 (cluster 3). The other group is located on the positive second component axis and comprises only samples from the second group of the HCA.

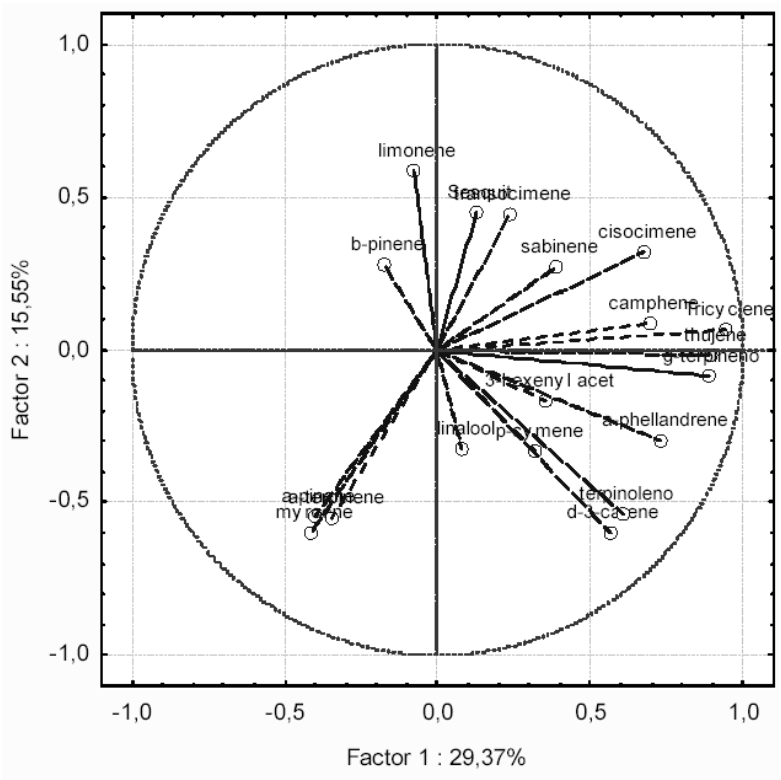

Figure 3.82 – Principal component analysis loadings for the log-transformed volatile terpenes data from *P. pinaster* trees sampled in Apostiça (limonene = limonene + β-phellandrene).

In order to identify which terpenes are associated with the components, the factor scores were analyzed for the first two components. The projection of the variables on the factor

plane for the first two components is shown in Figure 3.82. The loading values for components 1 and 2 are summarized in Table 3.24.

Table 3.24 - Values of the loadings from the principal component analysis using log-transformed values for the volatile monoterpenes of Apostiça trees

Volatile	Factor 1	Factor 2
Tricyclene	0.94	0.07
Thujene	0.90	-0.02
α-pinene	-0.40	-0.54
Camphene	0.70	0.09
Sabinene	0.39	0.27
β-pinene	-0.17	0.28
Myrcene	-0.41	-0.60
3-hexenyl acetate	0.35	-0.17
α-phellandrene	0.73	-0.29
Δ-3-carene	0.56	-0.60
α-terpinene	-0.34	-0.55
p-cymene	0.32	-0.33
Limonene+β-phellandrene	-0.08	0.59
cis-ocimene	0.67	0.32
trans-ocimene	0.23	0.44
γ-terpinene	0.89	-0.08
Terpinolene	0.61	-0.54
Linalool	0.08	-0.32
Sesquit	0.13	0.45

The loadings data show that the major associations for component 1 are found for tricyclene and thujene, two minor compounds in the volatile profile of all trees, followed by γ-terpinene. The data also show that the seven compounds with the main association with component 1 have values higher than 0.60 and are all positive. Concerning component 2, major associations are found for myrcene, Δ-3-carene and limonene+β-phellandrene, followed by α-terpinene, terpinolene and α-pinene.

According to the loadings plot, the location of 54% of the samples on the first quadrant is only driven by their contents on limonene and *β*-pinene. No association is visible from the information provided by the PCA, between the distribution of the trees in the plot, and the number of nests.

3.3.3.3. Partial least squares regression

In order to understand the variation of the attack, expressed as the number of *T. pityocampa* nests per tree on *P. pinaster* trees sampled at Apostiça (1 pine species; 21 observations), and study the influence of the enantiomeric compounds, a partial least squares (PLS) regression was carried out on the experimental data set. The trees sampled are described by 19 volatile components (X variables). These volatile components are assumed to be the promoters of the effects causing the attack changes (Y variable) in the system under study. The final data set for the PLS analysis comprises 21 observations on *P. pinaster* trees.

As the variables show a range of variation of over one magnitude of 10, they were logarithmically transformed in order to make their distribution more symmetrical. The results obtained for the PLS analysis are summarized on Table 3.25.

Table 3.25 – Summary of the partial least squares model for the data set of 21 *P. pinaster* trees and the *T. pityocampa* attack level.

A	R^2X	R^2X(cum)	Eigenvalue	R^2Y	R^2Y(cum)	Q^2	Q^2(cum)	Significance
1	0.274	0.274	5.21	0.259	0.259	-0.027	-0.027	NS
2	0.110	0.385	2.10	0.166	0.425	-0.668	-0.130	NS
3	0.091	0.475	1.72	1.04	0.529	-0.857	-0.243	NS
4	0.090	0.565	1.70	0.05	0.579	-0.806	-0.367	NS
5	0.063	0.628	1.19	0.044	0.623	-0.913	-0.503	NS
6	0.058	0.686	1.10	0.032	0.655	-0.990	-0.654	NS

Number of observations: N=19; Variables: K=7; X (volatiles) = 6 and Y (attack) = 1

The PLS analysis of the data did not extract any significant components according to the cross validation rule 1 (R1), and thus no prediction of the Y (attack) variation is achievable by the model. The first six components of the PLS only explain 68.5% of the X variation and 65.5% of the Y variation (R^2X cum. = 0.686, R^2Y cum. = 0.655), turning the results difficult to analyse and consequently the information may not be conclusive.

The first two components are the most significant components, explaining 38.2% of the X variation and 42.5% of the Y variation (R^2X cum. = 0.382, R^2Y cum. = 0.425). An exploratory analysis of the data can be visualized at the plot of the X scores, t_1 *vs.* t_2, for the first two components that are presented in Figure 3.83.

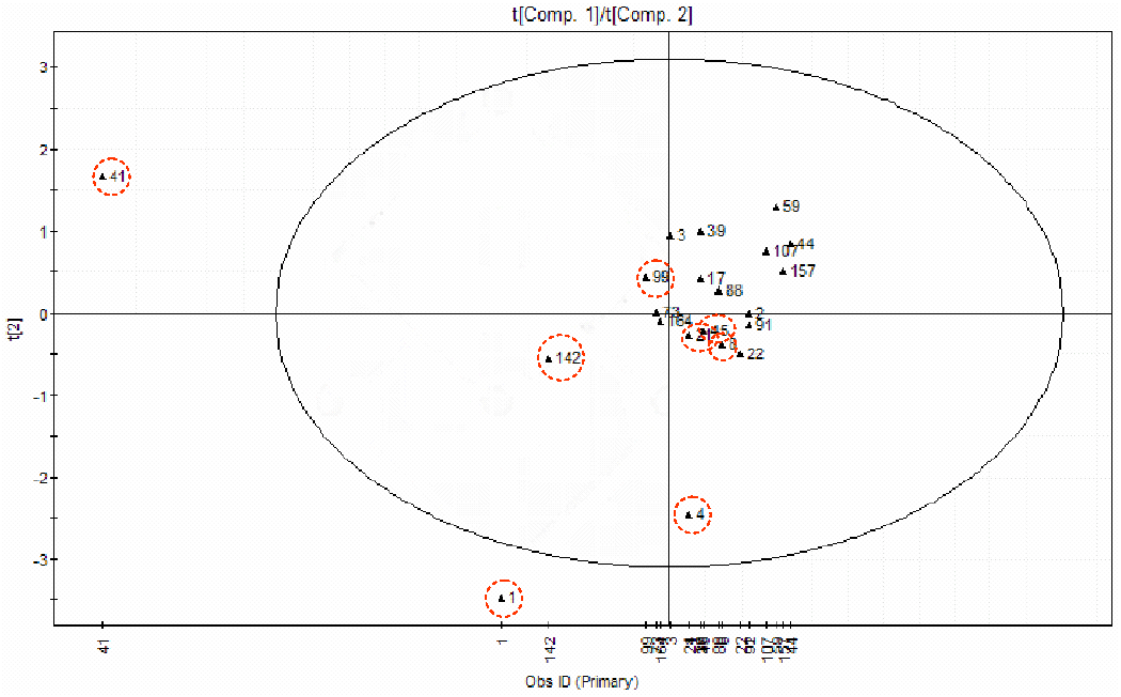

Figure 3.83 – Partial least squares scores for the first two components, t_1 *vs.* t_2, of the seven pine species enantiomeric data set. Trees with zero nests are pointed by a dotted circle.

The observation of the plot shows that the majority of the samples (70%) are located on the second and third quadrants. There are no trees with zero nests on the second quadrant. The plot of the X scores suggests a tendency of the trees without nests to be placed on the negative side of the second component axis and to be, as a group, slightly separated from

the other trees in the plot space. However, the data is not conclusive. T-22, a tree that had 14 nests, is placed very close to T-8, T-45 and T-21, trees that had no nests. T-21 and T-45 were colonized by the Argentine ant and thus the absence of nests could reflect the action of this predator. Trees T-73 (2 nests) and T-164 (3 nests) are placed very close to the origin and inside the "area" of the trees without nests. The remaining trees are separated from the previously described trees and are scattered in the plot second quadrant, but no real trend related to the number of nests is observed (see Table for relation tree – attack level). Two trees fall outside the Hotellings T^2 confidence ellipse and thus are considered, by the model, as outliers in the data set.

The plot of the X loadings for the first two components, p_1 *vs*. p_2, presented in Figure 3.84, shows how the variables are related and their association with the observations projected at the score plot.

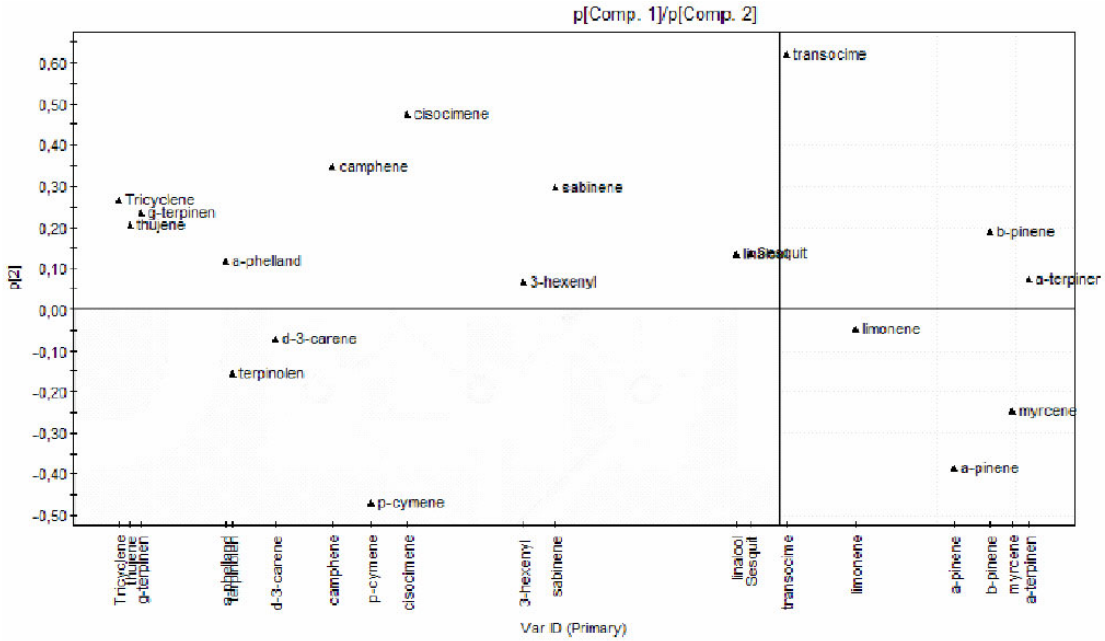

Figure 3.84 – Partial least squares loadings for the first two components, p_1 *vs*. p_2, of the *P. pinaster* trees data set.

The loadings plot for the PLS analysis show that the distribution and location of the majority of trees with nests in the second quadrant, are mainly associated with *α*-

terpinene, β-pinene and *trans*-ocimene. This observation suggests a weak association between these two volatile compounds and trees without nests.

The distribution on the third quadrant, that comprises 30% of the observed trees, is mainly driven by α-pinene and myrcene, followed by limonene+β-phellandrene. Due to the dispersion of the trees without nests across three quadrants, a clear positive association with the volatile compounds could not be established.

The plot of the PLS weights w and c, presented in Figure 3.85, shows the correlation structure between the volatiles (X) and the level of attack and thus can be used to identify the volatile variables that exhibit a variation correlated with the variation of the attack.

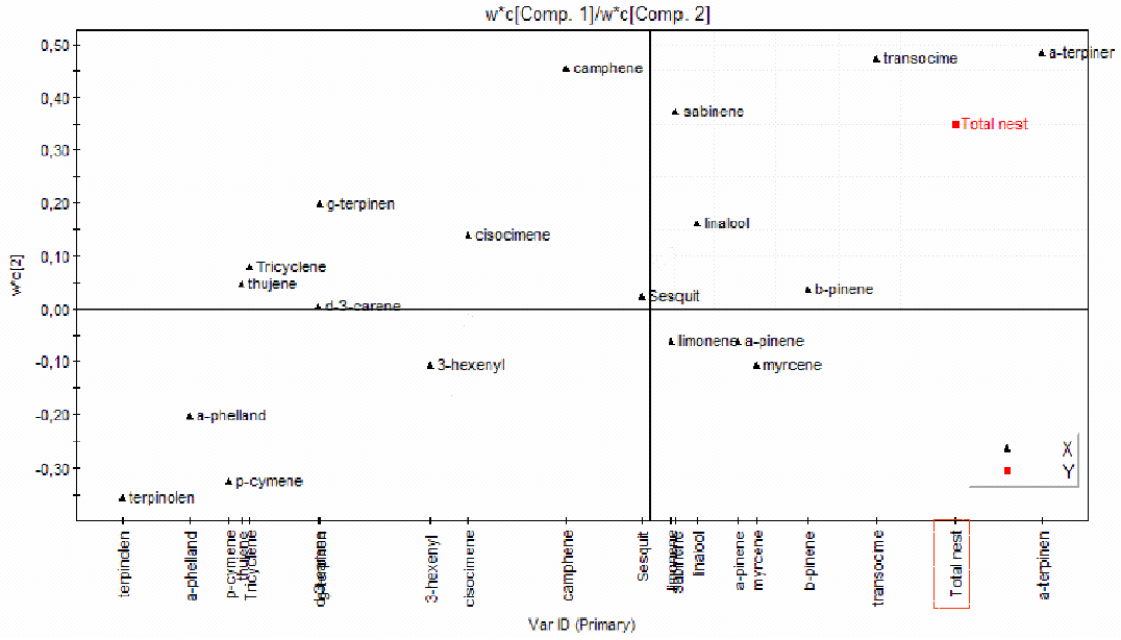

Figure 3.85 – Partial least squares weights plot w*c_1 *vs.* w*c_2 for the *P. pinaster* data set showing the model correlation structure.

The correlation between the volatile compounds analyzed and the attack level, is related to its distance from the origin, for both the positive and negative sides. The weights plot shows that the volatile compounds with more positive relation with the attack are α-

terpinene and *trans*-ocimene, followed by β-pinene. Negatively related with the attack are terpinolene, followed by α-phellandrene.

The plot t_1 *vs.* u_1, presented in Figure 3.86, examines the relationship between the scores of X (observations according to the variables) and the scores of Y (attack).

The X-Y scores plot on the first component, t_1 *vs.* u_1, did not suggest a relationship between the X and Y scores. Three groups can be observed in the plot. One group comprises the trees with no nests registered, another group the two trees with the highest amount of nests, and the last one the remaining trees. Consequently, no model can be estimated to explain the attack based on the original data set.

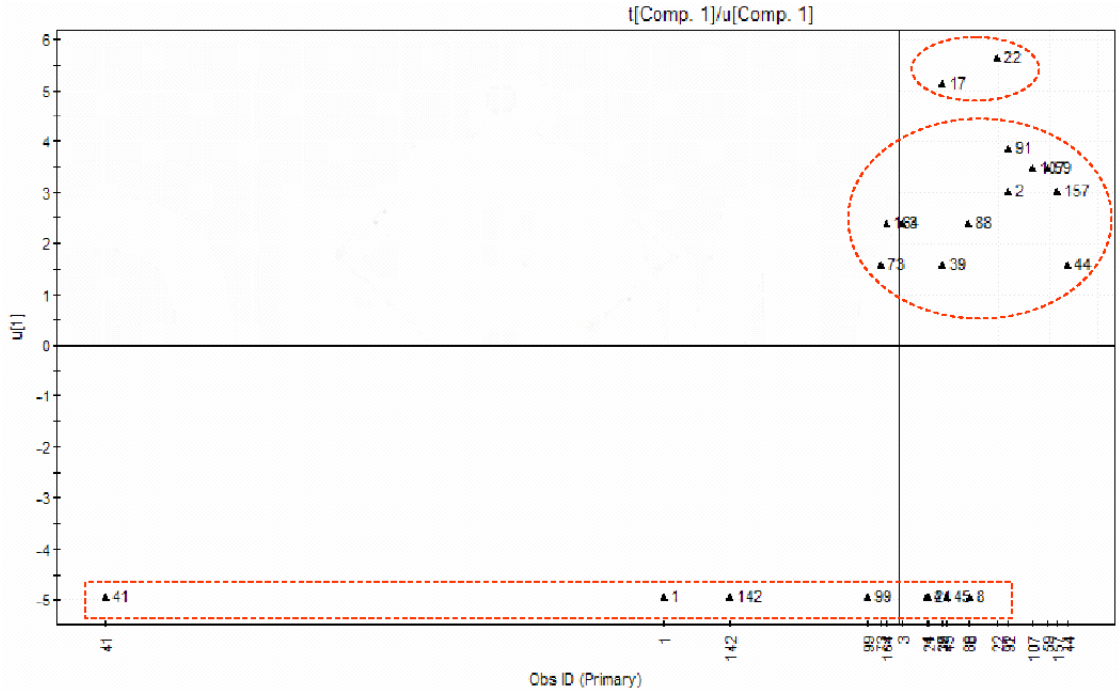

Figure 3.86 – Partial least squares scores plot t_1 *vs.* u_1 for the seven pine species data set.

3.3.4 Apostiça – Chiral

The enantiomeric composition of limonene, α-pinene and β-pinene, the main volatile compounds emitted by pine needles, were measured by multidimensional gas

chromatography (md-GC). The samples, submitted to analysis, were taken from 26 *P. pinaster* trees randomly sampled at Apostiça. The attack level was expressed as the number of observed nests from *T. pityocampa* per tree.

The data set was log-transformed, to allow for the examination of the role of the minor volatile terpenes.

Table 3.26 shows the enantiomeric average relative composition for each tree sampled, without log-transformation.

3.3.4.1. Hierarchical cluster analysis

In order to identify similarities among sampled trees a hierarchical cluster analysis (HCA), using Ward's method and Euclidean distances, was carried out. The resulting dendrogram from the HCA is shown in Figure 3.87.

The results suggest that, according to the enantiomeric composition of limonene, α-pinene and β-pinene, *P. pinaster* trees from Apostiça are divided in two main groups. The first group is subdivided in 2 separate clusters and the second group in 3 clusters. These clusters contain, in descending order of similarity: **1**) T-1, T-55, T-88 and T-21 trees, **2**) T-7, T-44, T-41, T-8, T-142, T-107, T-99, T-2 and T-91 trees, **3**) T-4, T-6, T-157, T-19, T-45, T-3, T-164, T-59, T-73 and T-17 trees, **4**) T-18 and T22 trees, and **5**) T-39 tree.

Table 3.27 shows the results regarding to the attack level, expressed as the total number of nests, where each tree code is associated with the correspondent number of total nests.

The first group is constituted by the trees with the highest percentage of (-)-limonene. It includes 72.7% of the total trees sampled without registered nests, which make up 61.5% of the trees allocated to the first group. Such results suggest the occurrence of a potential relationship between (-)-limonene and the absence of nests. However, the remaining trees show a variable level of attack, ranging from 2 to 6 nests.

Table 3.26 - Average enantiomeric relative composition (expressed as percentage) for each tree sampled in Apostiça.

Tree number	Quadrat	Total nests	(-)-α-pinene	(+)-α-pinene	(-)-β-pinene	(+)-β-pinene	(-)-limonene	(+)-limonene
1	9	0	38.04	8.78	34.03	0.93	17.52	0.70
4	9	0	32.77	13.34	51.94	1.06	0.77	0.11
6	5	0	28.17	7.84	61.69	1.19	0.56	0.55
7	5	0	36.71	12.13	45.63	1.10	3.79	0.63
8	1	0	30.81	11.56	50.91	0.98	5.16	0.58
99	9	0	35.10	7.16	51.92	0.97	4.55	0.30
21	9	0	23.30	12.86	48.99	0.86	13.68	0.31
41	9	0	33.09	8.27	51.52	0.98	5.39	0.74
45	9	0	35.58	14.29	47.94	0.97	0.51	0.71
142	9	0	31.81	13.47	47.74	1.05	5.32	0.61
55	5	0	25.77	9.65	47.07	0.90	16.04	0.58
39	9	2	0.39	12.12	84.43	1.61	1.00	0.44
44	9	2	30.52	10.08	53.55	1.06	4.16	0.63
73	9	2	33.06	18.14	46.81	0.98	0.59	0.43
3	1	3	37.21	10.85	49.87	1.01	0.47	0.59
88	9	3	28.16	9.52	42.48	1.08	18.17	0.60
164	9	3	30.57	14.81	52.50	1.07	0.51	0.54
2	9	4	27.26	7.25	56.52	1.07	7.22	0.68
19	2	4	28.78	5.53	62.84	1.25	0.89	0.71
157	9	4	42.69	8.98	46.24	1.10	0.60	0.40
59	9	5	33.83	14.07	50.04	1.14	0.44	0.48
107	9	5	24.14	13.12	55.63	1.10	5.43	0.59
91	1	6	26.24	5.16	59.89	1.18	6.82	0.71
18	2	9	28.84	13.99	55.72	0.11	0.58	0.76
17	2	11	32.94	20.65	44.55	0.71	0.70	0.45
22	9	14	27.01	14.19	57.49	0.23	0.55	0.53

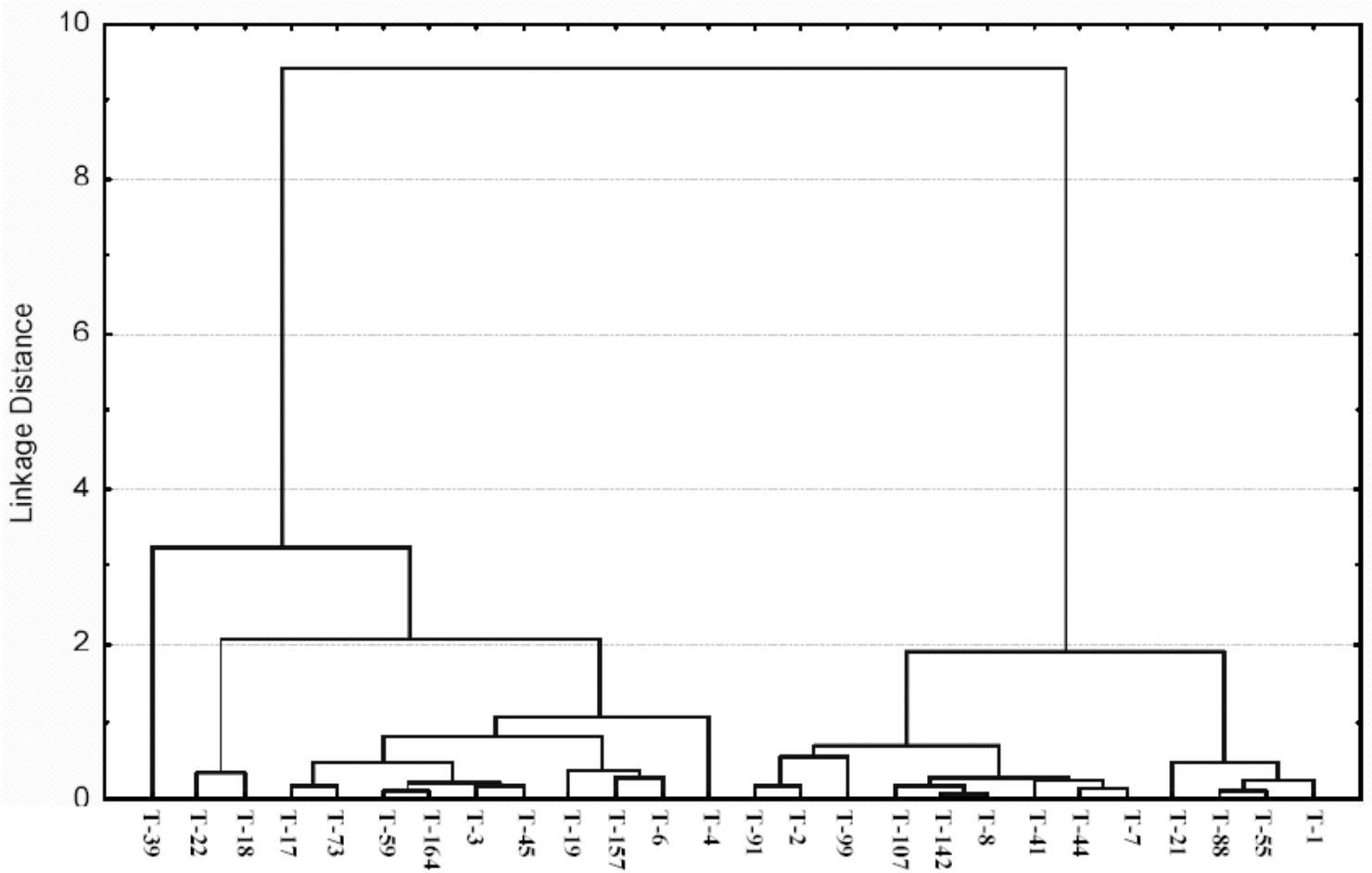

Figure 3.87 - Dendrogram from the hierarchical cluster analysis for 26 *P. pinaster* trees sampled at Apostiça, based on the enantiomeric volatile profiles of the main monoterpenes.

The second group includes the trees with the highest number of nests (T-17, T18 and T-22) that are grouped at close distance in the dendrogram. Trees T-4, T-6 and T 45 have no nests, but tree T-45 is registered as being colonized by the Argentine ant, *L. humile*. Tree T-39 which is characterized by the lowest percentage of (-)-α-pinene and the highest percentage of (-)-β-pinene found in all trees, is separated from all other clusters. The remaining trees show a highly variable level of attack, ranging from 2 to 5 nests.

Table 3.27 - Groups from the hierarchical cluster analysis of Apostiça trees, with the correspondent number of *T. pityocampa* nests.

HCA groups	Clusters	Trees	Total number of nests
Group 1	1	T-1	0
		T-55	0
		T-88*	3
		T-21*	0
Group 1	2	T-7	0
		T-44	2
		T-41*	0
		T-8	0
		T-142	0
		T-107	5
		T-99	0
		T-2	4
		T-91	6
Group 2	3	T-4	0
		T-6	0
		T-157	4
		T-19	4
		T-45*	0
		T-3	3
		T-164	3
		T-59	5
		T-73	2
		T-17	11
Group 2	4	T-18	9
		T-22	14
Group 2	5	T-39	2

*Trees colonized by the Argentine ant *Linepithema humile*.

3.3.4.2. Principal component analysis

In order to identify the compounds associated with the hierarchization of the samples, a principal component analysis (PCA) was carried out, treating *P. pinaster* trees as cases and the enantiomeric volatile compounds as variables. The results for PCA on the log-transformed data are summarized in Table 3.28.

Table 3.28 - Eigenvalues and total variance from the principal component analysis using the log-transformed values for the volatile enantiomeric data from *P. pinaster* trees sampled in Apostiça.

Value number	Eigenvalue	% Total variance	Cumulative Eigenvalue	Cumulative %
1	1.80	30.01	1.80	30.01
2	1.69	27.80	3.47	57.81
3	1.12	18.71	4.59	76.52
4	0.69	11.55	5.28	88.08
5	0.58	9.62	5.86	97.70
6	0.14	2.30	6.00	100.00

The first three factors explain 76.5% of the total variance, with 30.0, 27.8, and 18.7% explained by components 1, 2, and 3, respectively. Using the log-transformed data values, the first two-component plot were produced - Figure 3.88, where 57.8% of the variance is explained. To explain over 80.0% of the total variance, four factors were needed.

It can be observed in the PCA plot (Figure 3.88), that tree T-39 is completely isolated from the other trees sampled, which spreads the scale of the first component axis and thus promotes a visual illusion that tree separation mainly occurs on the second component axis. Trees without nests, which are placed on the first group of the HCA, are located on the first quadrant, or on its border. The trees with the highest number of nests are grouped, but divided by quadrants 3 and 4. The remaining trees are scattered on the two components, without any apparent relation with the number of nests.

In order to identify which enantiomeric terpenes are associated with the trees, separation on the factor scores plot, the loadings projections, were analyzed. The projection of the variables on the factor plane, for the first two components, is presented in Figure 3.89.

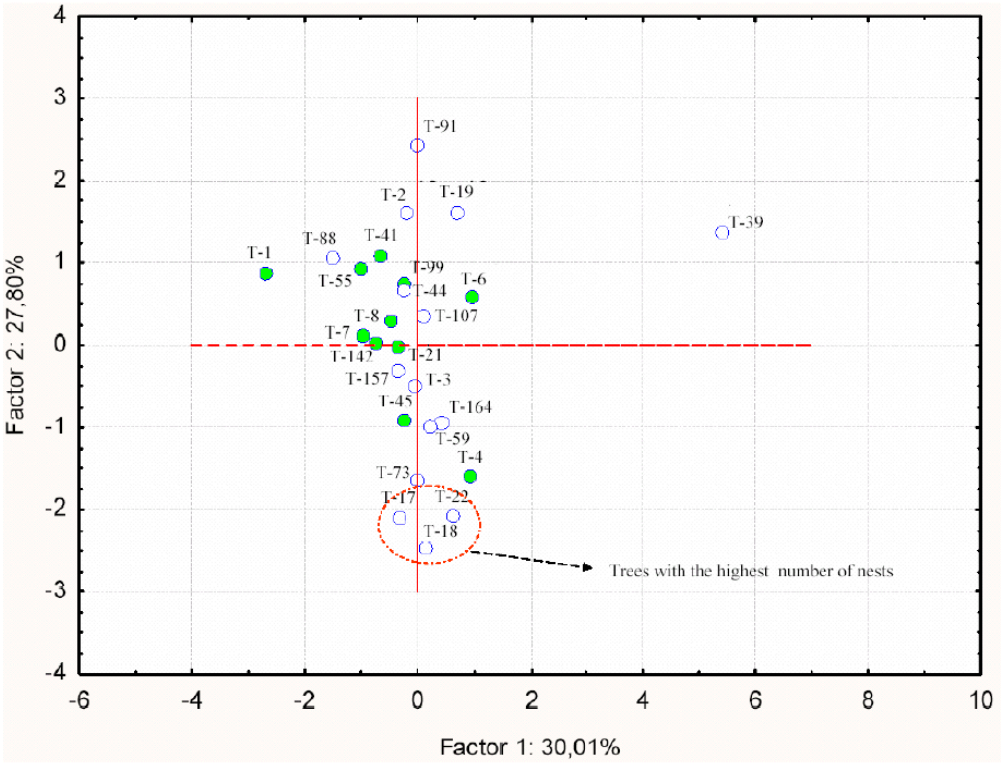

Figure 3.88 – Principal component analysis for the log-transformed volatile enantiomeric data from *P. pinaster* trees sampled in Apostiça (trees without nests are highlighted in green).

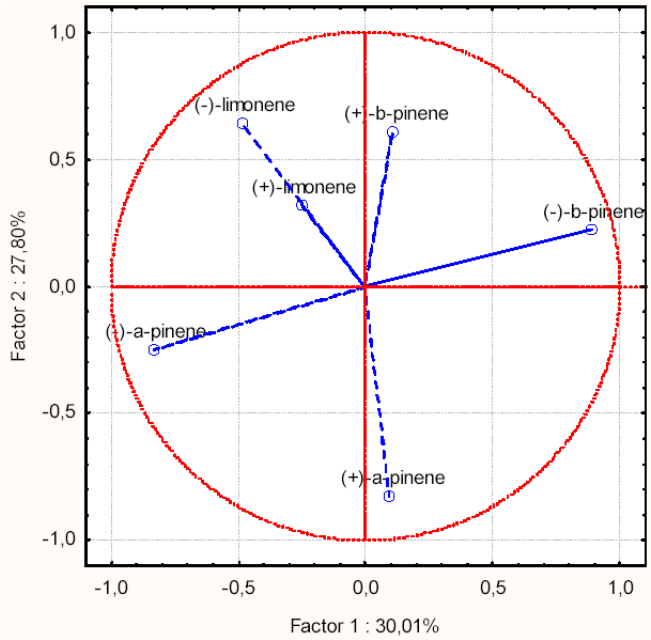

Figure 3.89 – Principal component analysis loadings for the log-transformed volatile terpenes data from *P. pinaster* trees sampled in Apostiça.

The loading values for component 1, 2 and 3 are summarized in Table 3.29.

Table 3.29 - Values of loadings from the principal component analysis using log-transformed values for the volatile monoterpenes in Apostiça trees.

Chiral terpene	Factor 1	Factor 2	Factor 3
(-)-α-pinene	-0.83	-0.25	0.00
(+)-α-pinene	0.10	-0.82	0.16
(-)-β-pinene	0.89	0.22	-0.26
(+)-β-pinene	0.11	0.60	0.62
(-)-limonene	-0.49	0.64	0.11
(+)-limonene	-0.26	0.32	-0.80

The loadings data (table and projection plot) show that the major associations for factor 1 is found for (-)-β-pinene and (-)-α-pinene enantiomers, in opposite influence. Concerning factor 2, the major association is found for (+)-α-pinene followed by (-)-limonene and (+)-β-pinene. The third factor is mainly associated with (+)-limonene followed by (+)-β-pinene.

According to the loadings data, the location of samples on the first quadrant is only driven by their contents on (-)-limonene and (+)-limonene, and thus limonene enantiomers can be associated with 72% of the trees without registered nests that are located in the quadrant. Trees with the highest number of nests, group on the negative side of the second component axis, apparently due to their content in (+)-α-pinene. The remaining trees are scattered across the four quadrants without an apparent relation with the number of nests. Tree T-39 is driven to the second quadrant due to its major enantiomeric component (-)-β-pinene and lower content in (-)-α-pinene.

3.3.4.3. Partial least squares regression

In order to understand the variation of the attack, expressed as number of *T. pityocampa* nests per tree, for the *P. pinaster* trees sampled in Apostiça (1 pine species; 26

observations), and study the influence of the enantiomeric compounds, a partial least squares (PLS) regression was performed. The trees sampled are described by the six enantiomers of their major volatile components (X variables). The six enantiomers are assumed to be the promoters of the effects causing the changes in attack level (Y variable) in the system under study.

As the variables show a range of variation over one magnitude of 10, they were logarithmically transformed in order to make their distribution more symmetrical. Results for the PLS analysis are summarized in Table 3.30.

Table 3.30 – Summary of the partial least squares model for the data set of 26 *P. pinaster* trees and *T. pityocampa* attack level.

A	R^2X	R^2X(cum)	Eigenvalue	R^2Y	R^2Y(cum)	Q^2	Q^2(cum)	Significance
1	0.25	0.250	1.5	0.281	0.281	0.0339	0.0339	NS
2	0.222	0.472	1.33	0.018	0.299	-0.236	-0.0627	NS
3	0.152	0.624	0.911	0.001	0.301	-0.195	-0.169	N4
4	0.241	0.865	1.45	0.000	0.301	-0.212	-0.286	N4
5	0.065	0.93	0.39	0.000	0.301	-0.197	-0.414	N4
6	0.07	1	0.42	0.000	0.301	-0.053	-0.49	N3

Number of observations: N=19; Variables: K=7; X (volatiles) = 6 and Y (attack) = 1

The PLS analysis of the data did not extract any significant components according to the cross validation rule 1 (R1), and thus no prediction of the Y (attack) variation is achievable by the model. However, the first four components of the PLS explain 86.5% of the X variation but only 30.1% of the Y variation (R^2X cum. = 0.865, R^2Y cum. = 0.301).

The first two components are the most significant ones, explaining 47.2% of the X variation and 29.9% of the Y variation (R^2X cum. = 0.472, R^2Y cum. = 0.299). An exploratory analysis of the data can be visualized on the X scores plot, t_1 *vs*. t_2, for the first two components that presented in Figure 3.90.

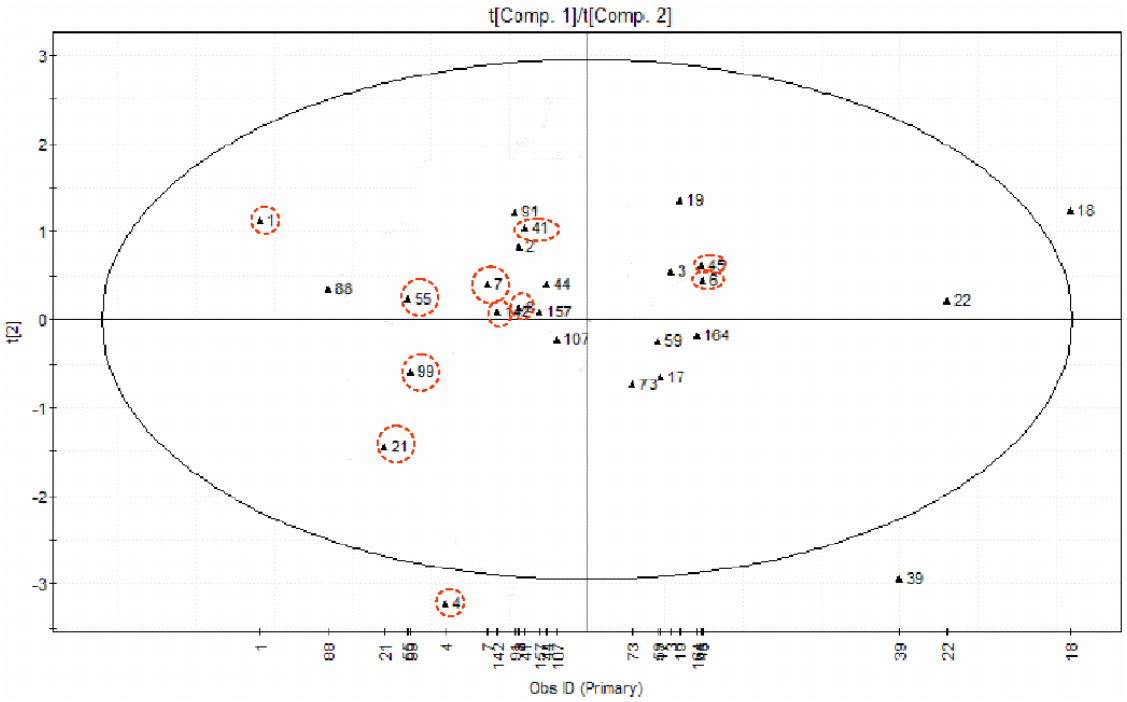

Figure 3.90 – Partial least squares scores for the first two components, t_1 *vs.* t_2, of the seven pine species enantiomeric data set. Trees with zero nests are pointed by a dotted circle.

The plot of the X scores shows that the majority of trees without nests (81%) are placed on the negative side of the first component axis. The two other trees with registered nests are grouped together on the second quadrant. One of them, tree T-45, is colonized by the Argentine ant. The remaining trees are scattered on the plot and no trend related to the attack level is observed (see Table 3.26 for relation tree – attack level). Three trees are observed outside the Hotellings T^2 confidence ellipse and are thus considered, by the model, as outliers in the data set.

The plot of the X loadings for the first two components, p_1 *vs.* p_2, presented in Figure 3.91, shows how the variables are related and their association with the observations projected on the score plot.

The loadings plot for the PLS analysis show that the distribution of the observations in the first component, on the scores plot, is mainly associated with (-)-limonene followed by (+)-*β*-pinene on the negative axis and with (-)-*β*-pinene on the positive axis. The

dispersion on the second component is mainly associated with the (+)-limonene and (+)-α-pinene enantiomers. According to the loadings plot, trees with zero nests are mainly driven on the scores plot by their content in (-)-limonene.

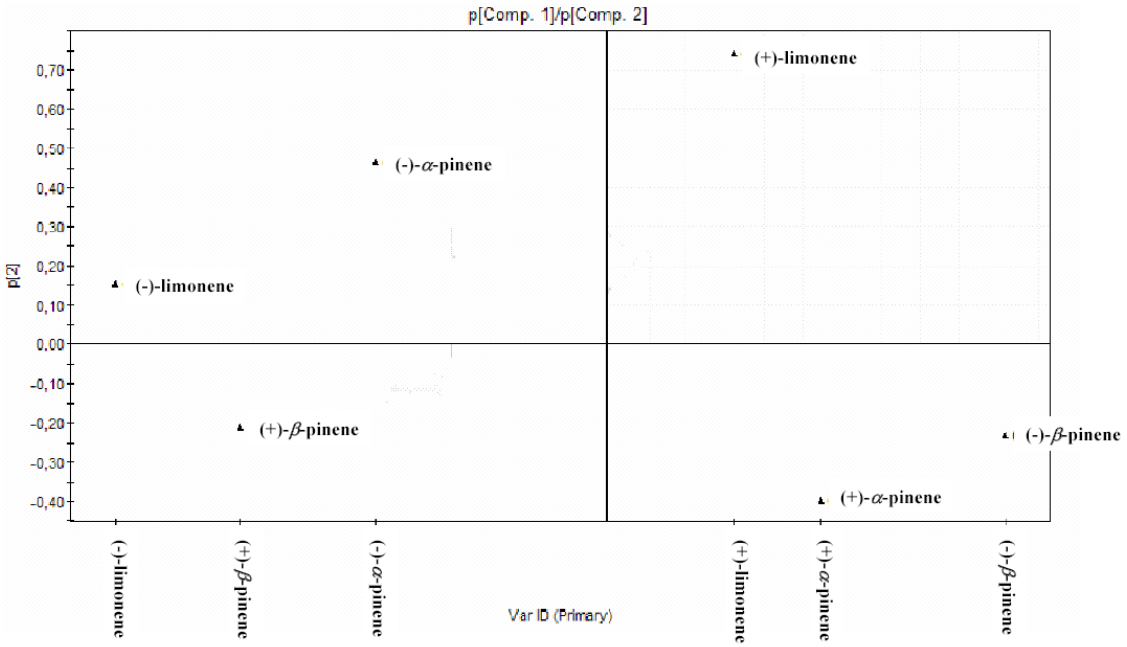

Figure 3.91 – Partial least squares loadings for the first two components, p_1 *vs*. p_2, of the seven pine species enantiomeric data set.

The plot of the PLS weights w and c, presented in Figure 3.92, shows the correlation structure between the volatiles (X) and the attack level and can thus be used to identify the volatile variables that exhibit a variation correlated with the variation of the attack level. The correlation of the enantiomeric compounds, with the attack level, is related to its distance from the origin for both the positive and negative sides. The weights plot shows that the enantiomer with a more positive relation with the attack is (-)-β-pinene followed by (+)-limonene. Negatively related with the attack are (-)-limonene followed by (+)-β-pinene. (-)-limonene shows the largest distance from the origin and, consequently, has the strongest correlation with the attack. An opposite result was here observed, in relation to the data pertaining to different pine species, where the different enantiomers from limonene and β-pinene acted synergistically in relation to the attack

level. In fact, the (-) enantiomeric forms of limonene and *β*-pinene predominate over their (+) enantiomeric forms (see Table 3.26), and both have an opposite relation with the attack level, in accordance with the previous model for different pine species.

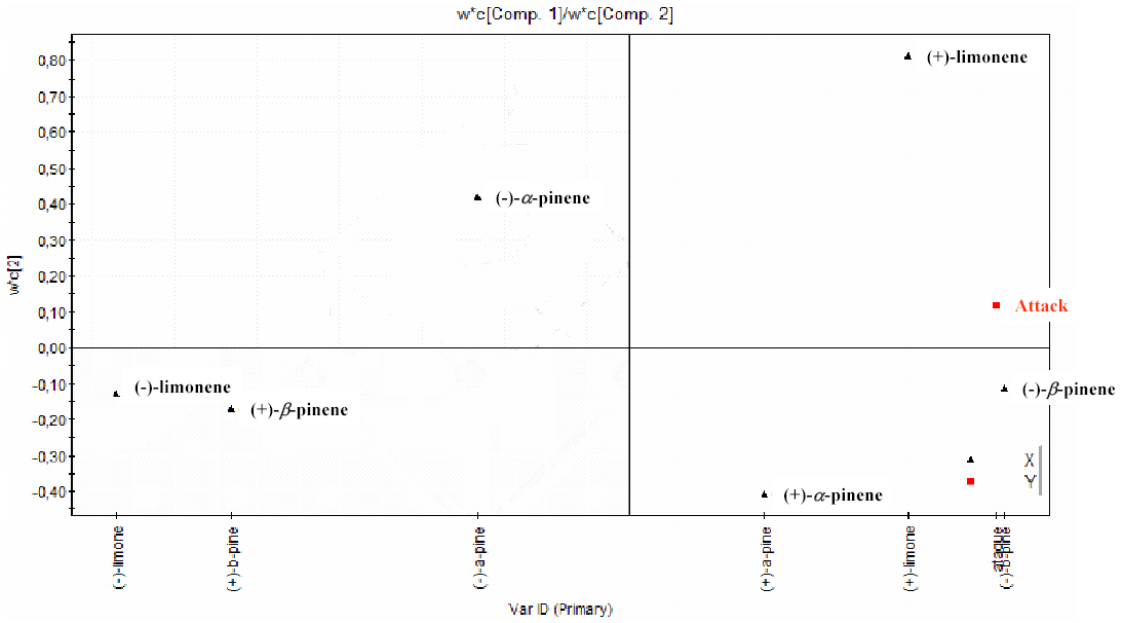

Figure 3.92 – Partial least squares weights plot w*c_1 *vs.* w*c_2 for the *P. pinaster* data set showing the model correlation structure.

The plot t_1 vs u_1, presented in Figure 3.93, examines the relationship between the scores of X (the observations according to the variables) and the scores of Y (the attack).

The X-Y scores plot on the first component, t_1 *vs.* u_1 did not suggest the presence of a relationship between the X and Y scores. Two groups can be observed in the plot: one comprising the trees with no nests, and another one with the remaining trees, so consequently a model can not be proposed to explain the attack.

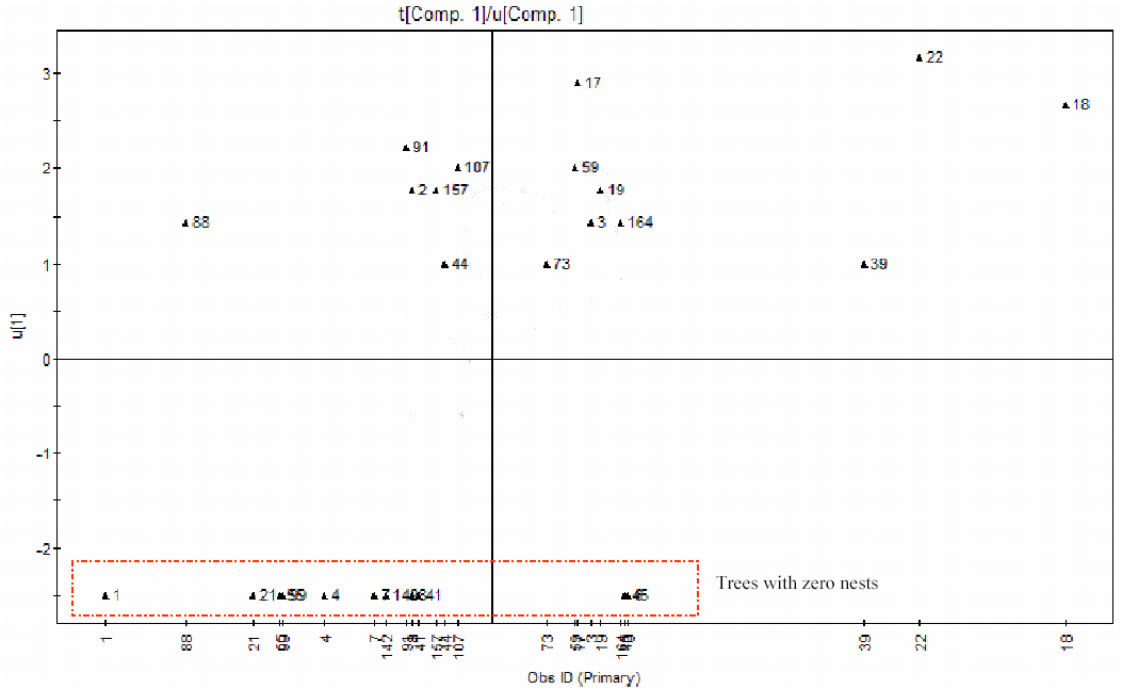

Figure 3.93 – Partial least squares scores plot t_1 *vs*. u_1 for the seven pine species data set.

3.3.5. Resin acids

The composition of the resin acids present in the studied *Pinus* spp. needles, of both data sets, were measured by 1D-GC/MS.

The needles of the first set submitted to analysis were subsamples from the needles used in an experimental assay, with second instar of *T. pityocampa* larvae fed on a host species diet of *P. pinaster*, *P. pinea*, *P. halepensis* and *P. brutia,* in order to study their effect upon larval performance (e.g. larval survival and grow rate). Nine resin acids were considered to be measured on the first set: pimaric, sandarocopimaric, isopimaric, dehydropimaric, abietic, neoabietic, levopimaric/palustic and two not identified RA-1 and RA-2.

The second set of needles analysed were taken from trees randomly sampled, belonging to 11 pine species with different provenances (see Chapter 2, Material and methods). Twelve resin acids were considered to be measured: pimaric, sandarocopimaric,

isopimaric, dehydropimaric, abietic, neoabietic, levopimaric/palustic, cummunic and four non identified DA-1, DA-2, DA-3 and DA-4. The two sample sets were analyzed with different mass analyzers (set 1 by quadrupole and set 2 by ion trap) and for this reason were notpulled for statistical analysis. Both data sets were square root-transformed before analysis.

3.3.5.1. Hierarchical cluster analysis. First set

In order to identify similarities between the *Pinus* spp. used for the *T. pityocampa* larval performance experiments, a hierarchical cluster analysis (HCA) was performed based on their resin acids profile, listed in Table 3.31. The data set, composed of 12 observations and 9 resin acid compounds, was analyzed using Ward's method and Euclidean distances. The resulting dendrogram from the HCA is shown in Figure 3.94.

Table 3.31 – Resin acids relative composition (expressed as percentage) for each sampled pine species.

	Pim	San	Iso	Dha	Abi	RA-1	RA-2	Lev/Pal	Neo
P. pinaster	2.79	11.43	3.03	14.68	62.97	3.72	1.39	0	0
P. pinaster	1.62	13.00	2.03	15.24	63.83	2.63	1.66	0	0
P. pinaster	2.52	13.59	2.28	16.96	60.83	2.61	1.21	0	0
P. pinea	2.72	0.00	4.46	15.73	77.09	0.00	0.00	0	0
P. pinea	1.68	0.72	4.33	17.77	73.26	1.12	1.12	0	0
P. pinea	1.66	0.81	2.89	11.39	79.42	2.30	1.53	0	0
P. halepensis	0.00	9.27	5.44	49.12	19.69	11.17	5.32	0	0
P. halepensis	0.00	13.99	11.62	54.66	12.15	4.86	2.72	0	0
P. halepensis	0.00	13.38	6.45	43.60	19.66	10.24	6.67	0	0
P. brutia	0.00	29.52	1.07	29.19	26.95	6.31	6.97	1.36	0.00
P. brutia	0.00	24.19	1.04	32.30	23.10	12.99	6.38	1.58	3.33
P. brutia	0.00	25.64	1.02	31.16	26.92	7.69	7.57	1.22	0.00

The results show a very good separation among samples that are grouped in the dendrogram according to the pine species they belong and thus suggesting that according to their resin acids composition, each pine species constitutes a chemotype. The dendrogram is divided in two groups that are subdivided in four separated clusters at a linkage distance of 7, which correspond to the pine species under study. The first group is composed by the clusters that contain the samples of *P. pinaster* and *P. pinea*. The second group contains, by descending order of similarity, the clusters with *P. halepensis* and *P. brutia* samples. Results suggest that *P. pinaster*, *P. pinea*, *P. brutia* and *P. halepensis* could be classified using their resin acids as chemosystematic markers.

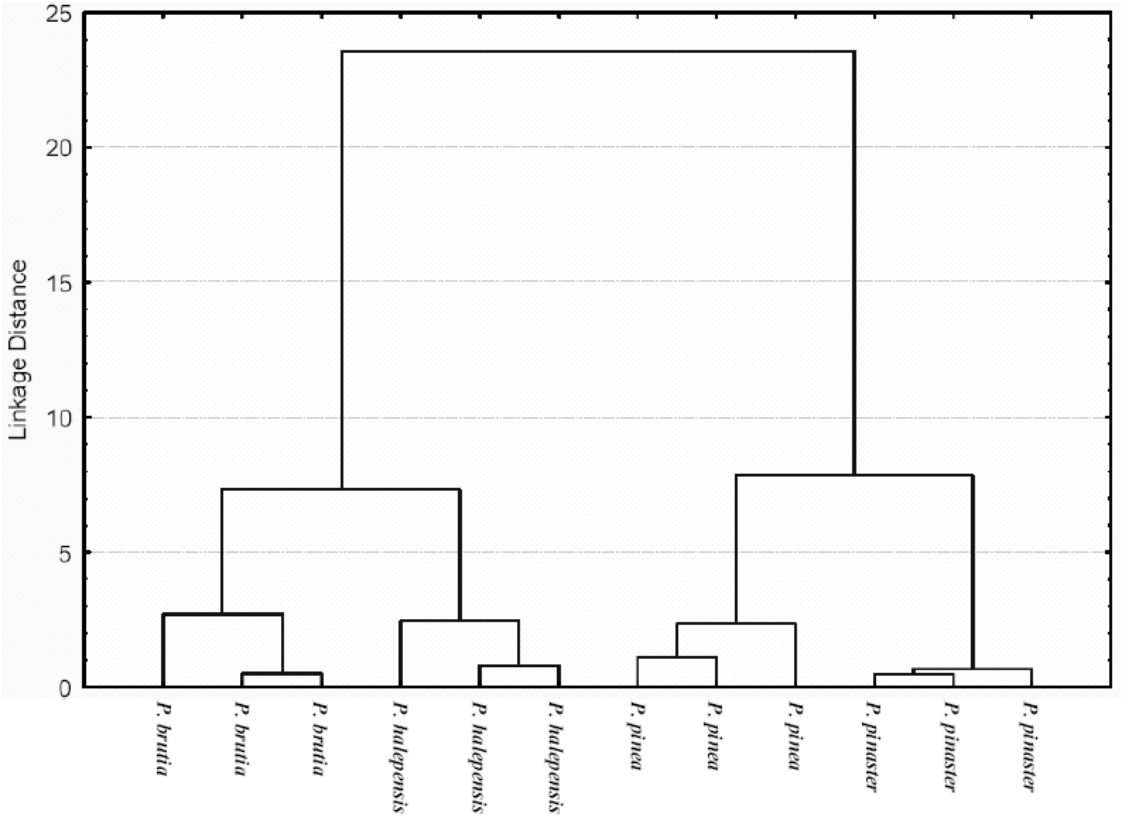

Figure 3.94 - Dendogram from the hierarchical cluster analysis for the pine species used to study the performance of *T. pityocampa* larvae, based on their resin acids profile

3.3.5.2. Principal component analysis. First set

In order to identify the compounds associated with the hierarchization of the sample, a principal component analysis (PCA) was carried out, treating the pine species as cases,

and the resin acids compounds as variables. The results for the PCA on the square root-transformed data produced are summarized on Table 3.32.

Table 3.32 - Eigenvalues and total variance from the principal component analysis using the root square-transformed values for the resin acids present in *Pinus* species used for the larval performance experiment with *T. pityocampa.*

Factor	Eigenvalue	% Total variance	Cumulative Eingenvalue	Cumulative %
1	9.45	75.76	9.45	75.76
2	2.07	16.56	11.52	92.32

The first two factors account for 92.32% of the total variance of the data set. The first two-component plot produced by square root-transformed data values is shown in Figure 3.95.

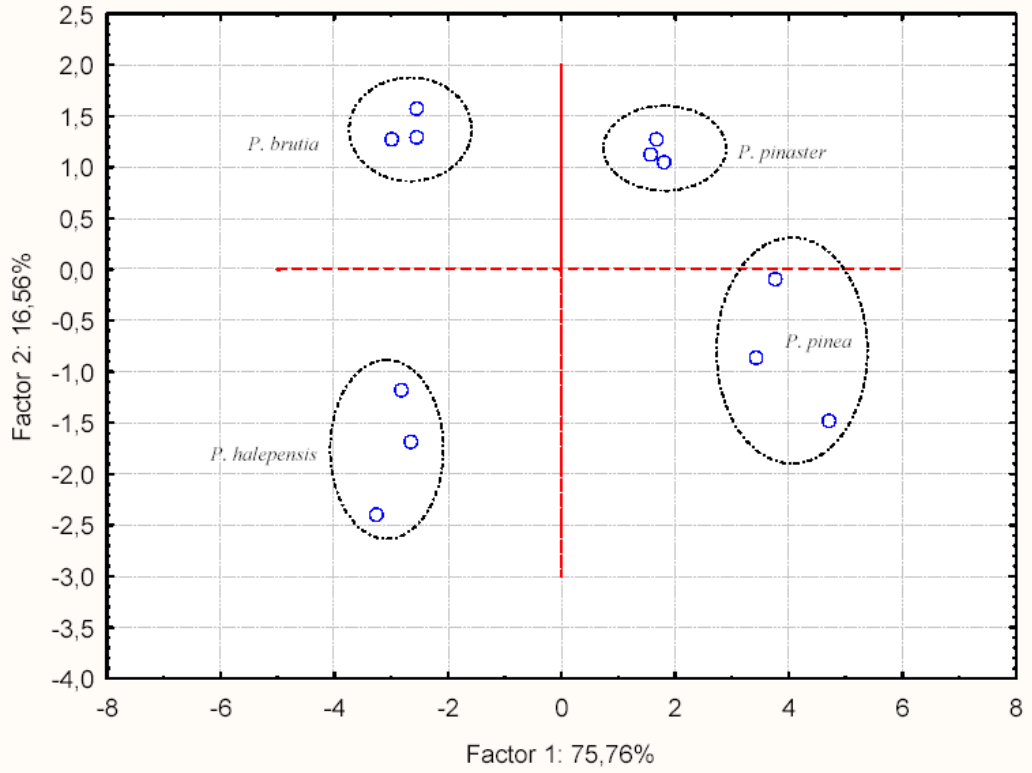

Figure 3.95 – Principal component analysis for the square root-transformed data for the resin acids present in the pine species used in the larval performance experiments with *T. pityocampa*

The PCA plot presents a clear structure, where each pine species is clearly separated from the others on both components and placed in different quadrants, according to its resin acid contents. The first axis separates *P. pinaster* and *P. pinea* from *P. brutia* and *P. halepensis,* while the second further separates *P. pinaster* from *P. pinea*, and *P. halepensis* from *P. brutia.* This observation agrees with the results of the previous HCA.

The projection of the variables on the factor plane for the first two components is presented in Figure 3.96. The loading values for the first two components are summarized in Table 3.33.

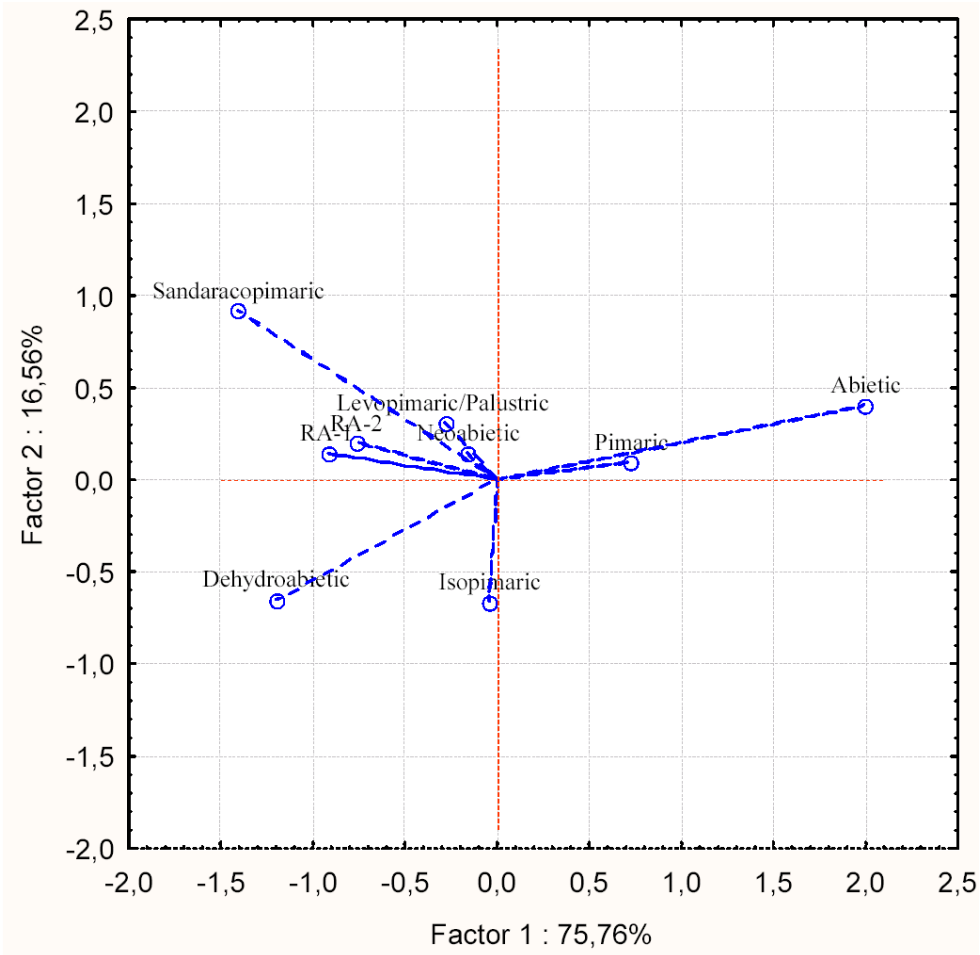

Figure 3.96 – Principal component analysis loadings for the square root-transformed data from the resin acids present in the pine species used in the larvae performance experiments with *T. pityocampa.*

Table 3.33 - Values of the loadings from the principal component analysis using square root-transformed data from the resin acids present in the pine species used in the larvae performance experiments with *T. pityocampa.*

Resin acid	Factor 1	Factor 2
Pimaric	0.73	0.10
Sandaracopimaric	-1.41	0.92
Isopimaric	-0.04	-0.66
Dehydroabietic	-1.20	-0.65
Abietic	1.99	0.41
RA-1	-0.92	0.15
RA-2	-0.76	0.20
Levopimaric	-0.28	0.31
Neoabietic	-0.16	0.15

The loadings data (Table 3.33, and projection plot, Figure 3.96) show that the major associations for factor 1 can be found for abietic and dehydroabietic acids, in opposite influence. Concerning factor 2, the major association is found for sandaracopimaric acid followed by isopimaric and dehydroabietic acids.

The loadings plot highlights that the location of *P. brutia* samples in the first quadrant is driven by their content on the sandarocopimaric acid, which together with abietic and dehydroabietic acids, are the main constituents on the needles. *P. pinaster* is driven to the second quadrant due to its high content in abietic acid. *P. pinea* is driven to the third quadrant apparently due to its content in abietic, dehydroabietic and isopimaric acids. *P. halepensis* is driven to the fourth quadrant due to its major component dehydroabietic acid.

3.3.5.3. Hierarchical cluster analysis. Second set

A hierarchical cluster analysis (HCA) was performed in order to identify similarities, among different pine species used by *T. pityocampa* as host, based on their resin acids composition. The data set, listed in Table 3.34, is composed of 41 observations and 12 resin acid compounds, and was analyzed using Ward's method and Euclidean distances. The resulting dendrogram from the HCA is shown in Figure 3.97.

Table 3.34 - Resin acids relative composition (expressed as percentage) for the pine species sampled in the second experiment.

	Resin acid											
Pinus spp.	Pim	DA1	San	Iso	Lev/Pal	Dha	Com	Abi	DA2	Neo	DA3	DA4
P. pinaster	0.66	0.00	1.85	0.16	3.52	30.02	0.97	54.43	0.00	0.15	4.29	4.62
P. pinaster	0.56	0.00	1.61	0.09	3.25	26.61	0.78	54.49	1.01	0.16	4.88	7.11
P. pinea	1.76	0.00	1.02	4.80	0.31	13.69	0.00	72.74	0.00	0.82	4.07	2.55
P. pinea	1.31	0.00	1.35	3.11	0.27	12.42	0.00	74.78	0.00	0.00	4.75	3.31
P. brutia	0.00	0.00	2.34	0.96	3.11	32.52	3.00	33.45	0.49	1.08	11.64	11.41
P. brutia	0.00	0.00	2.74	1.30	1.18	34.19	1.22	29.80	0.77	0.16	15.64	12.99
P. halepensis	0.00	0.00	2.79	0.52	12.06	17.42	1.69	13.08	1.09	34.43	11.34	5.58
P. halepensis	0.00	0.00	2.05	0.68	20.01	16.66	1.10	11.75	0.78	33.51	9.68	3.77
P. halepensis	0.00	0.00	2.64	0.72	1.36	32.05	0.30	16.58	0.69	5.71	25.69	14.25
P. halepensis	0.00	0.00	2.16	1.83	12.07	23.44	1.20	12.25	1.05	24.69	13.23	8.08
P. halepensis	0.00	0.00	5.25	0.58	2.05	32.65	1.03	21.34	1.89	10.75	15.23	9.23
P. halepensis	0.00	0.00	2.98	0.78	5.56	19.62	1.81	16.80	1.05	27.90	15.46	8.04
P. halepensis (ISA)	0.00	2.74	10.08	17.46	0.00	22.61	0.20	15.71	0.64	5.13	18.23	7.21
P. elliottii	0.00	1.32	2.25	2.08	8.01	8.68	6.45	47.56	0.00	0.61	10.88	12.16
P. elliottii	0.00	0.78	1.87	1.40	4.54	12.15	4.01	43.08	1.01	0.16	15.78	15.23
P. kesiya	0.00	3.37	2.65	2.03	0.95	36.97	0.10	17.04	0.27	0.15	16.49	19.99
P. kesiya	0.00	0.13	1.78	3.78	6.67	41.71	9.11	11.02	0.29	0.00	9.43	16.07
P. nigra	0.00	0.00	3.23	0.51	5.30	38.90	0.00	39.02	0.90	0.00	7.60	4.53
P. nigra	0.59	0.00	2.82	0.49	6.16	41.24	0.00	34.87	0.94	0.18	6.47	6.84
P. patula	0.00	0.00	5.72	2.58	3.08	52.95	0.48	29.71	0.00	0.00	3.22	2.26
P. patula	0.00	0.00	10.34	2.19	1.80	47.49	0.00	36.34	0.00	0.00	0.00	1.85
P. radiata	0.68	0.00	2.44	7.06	9.99	36.74	10.35	26.25	0.00	0.00	3.63	3.53
P. sylvestris	0.00	0.00	2.31	0.31	11.81	25.83	0.00	17.91	1.30	5.98	20.41	14.14
P. sylvestris	0.00	0.00	2.68	0.32	11.78	26.20	0.00	18.33	1.26	3.30	21.79	14.36

Table 3.34 - Resin acids relative composition (expressed as percentage) for the pine species sampled in the second experiment (cont.)

	Resin acid											
Pinus spp.	Pim	DA1	San	Iso	Lev/Pal	Dha	Com	Abi	DA2	Neo	DA3	DA4
P. taeda	0.11	0.00	3.54	0.34	2.69	23.57	6.75	32.62	1.96	0.65	12.73	15.15
P. taeda	0.10	0.00	2.55	0.22	2.24	22.83	2.96	38.94	1.79	2.05	11.88	14.53
P. halepensis (Israel/Greece)												
EG1_N	0.01	0.00	4.91	0.85	2.63	40.23	1.20	19.59	1.25	4.09	17.62	7.63
EG1_V	0.00	0.00	3.77	0.49	3.79	36.51	2.24	14.65	1.39	10.69	21.75	4.72
EG2_N	0.00	1.09	4.78	3.96	1.85	33.68	1.36	17.94	1.70	1.82	20.38	11.45
EG2_V	0.00	0.56	3.30	2.14	6.85	21.02	1.11	12.83	1.09	24.79	16.13	10.17
EG3_N	0.00	1.29	4.69	0.95	2.29	32.11	0.41	23.06	2.18	8.53	14.22	10.28
EG3_V	0.00	1.29	3.89	0.85	3.38	32.80	0.90	16.74	1.69	11.00	19.26	8.21
GreekN	0.01	0.00	4.18	1.10	1.30	33.04	0.30	22.88	0.60	1.26	22.25	13.07
JH1_N	0.77	0.00	5.99	0.61	1.79	38.33	0.83	20.62	1.38	0.87	15.06	14.51
JH1_V	0.64	0.00	4.60	0.47	2.94	28.31	0.55	16.37	1.24	17.96	15.44	12.14
MC1_N	0.02	3.77	0.06	3.37	3.89	32.12	0.80	18.83	1.35	14.08	13.53	8.21
MC1_V	0.00	3.87	0.07	2.68	3.88	35.26	1.63	19.19	1.03	9.76	14.25	8.37
MC2_N	0.00	0.23	3.98	1.17	2.41	34.25	0.47	19.23	0.82	7.53	15.45	14.45
MC2_V	0.00	0.24	3.93	0.96	4.16	35.72	1.56	17.91	0.99	8.08	17.44	9.01
MC3_N	0.00	0.05	3.19	2.45	5.19	34.28	1.31	13.48	1.17	13.51	17.68	7.68
MC3_V	0.00	0.01	2.58	0.96	11.64	31.96	2.60	9.72	0.78	18.56	15.50	5.69

All resin acids characterized as methyl esters.
Key: Pim - pimaric acid; Sam - sandaracopimaric acid; Iso - isopimaric acid; Lev/Pal - levopimaric + palustric acid; Dha - dehydroabietic acid; Com - communic acid; Abi - abietic acid; Neo - neoabietic acid; DA - not identified diterpene acids

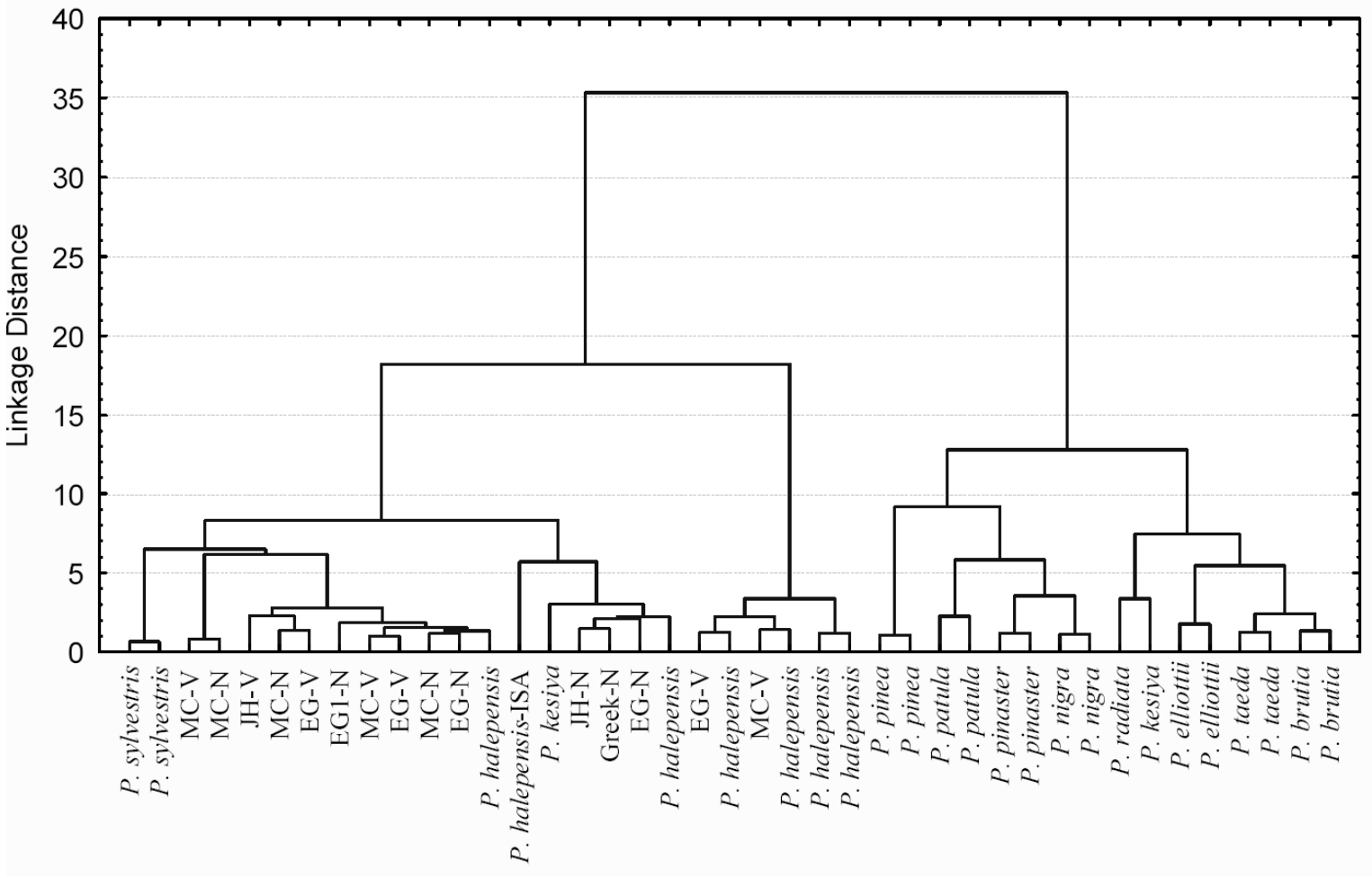

Figure 3.97 - Dendogram from the hierarchical cluster analysis for pine species based on their resin acids profiles.

Results show a good separation among samples that are grouped on the dendrogram according to the pine species they belong to. The only exception is one *P. kesiya* sample, which is placed among the *P. halepensis* samples.

Results suggest that according to their resin acids composition, the *Pinus* species samples can be divided in two main groups. One group comprises all *P. halepensis* and *P. sylvestris* samples, together with one *P. kesiya* sample, while the other includes all the other pine species under analysis. If a linkage distance of 5 is considered, the two groups may be further subdivided in 11 clusters. The first group is composed by the first 5 clusters and contains by decreasing order of similarity the samples of *P. brutia* and *P. taeda* in the first cluster, *P. elliottii* in the second, *P. nigra* and *P. pinaster,* in the third, one *P. kesiya* sample and the *P. radiata* sample in the fourth cluster and *P. pinea* and *P. patula* in the fifth cluster. All species are separated in the first group. The second group contains, by descending order of similarity 6 clusters. With the exception of the last cluster, which contains the *P. sylvestris* samples, and the seventh cluster that contains one of the *P. kesiya* samples, all other clusters are composed by the *P. halepensis* samples originated from Portugal, Israel and Greece, highlighting a similarity in resin acids composition among samples originating from different provenances. However, it is observed that the majority of *P. halepensis* samples collected in Portugal are grouped in the sixth cluster. The sole *P. halepensis* sample used in the larval performance experiments, is placed alone in cluster eight.

3.3.5.4. Principal component analysis. Second set

In order to identify the compounds associated with the hierarchization of the samples, a principal component analysis (PCA) was carried out, treating the pine species as cases and the resin acids as variables. The results for PCA on the square root-transformed data produced are summarized in Table 3.35.

The first four factors explain 82.70% of the total variance, with 47.10 and 15.62%.for components 1 and 2 respectively. The square root-transformed data values produced the first two-component plot shown in Figure 3.98, where 62.72% of the variance is explained. It can be observed that *P. halepensis* samples are separated from the other species on the first component. The exceptions are the *P. sylvestris* samples which, in accordance with the previous HCA results,

are placed inside the *P. halepensis* group. One sample of *P. kesiya* that in the HCA clustered together with *P. halepensis*, now forms a group separated from the *P. halepensis* samples. The remaining pine species show a good separation that is mainly observed on the second dimension. The exceptions are *P. taeda* and *P. brutia*, which show some overlap.

Table 3.35 - Eigenvalues and total variance from the principal component analysis using the root square-transformed values from pine species.

Factor	Eigenvalue	% Total variance	Cumulative Eingenvalue	Cumulative %
1	5.06	47.10	5.06	47.10
2	1.68	15.62	6.74	62.72
3	1.19	11.10	7.93	73.83
4	0.95	8.87	8.88	82.70

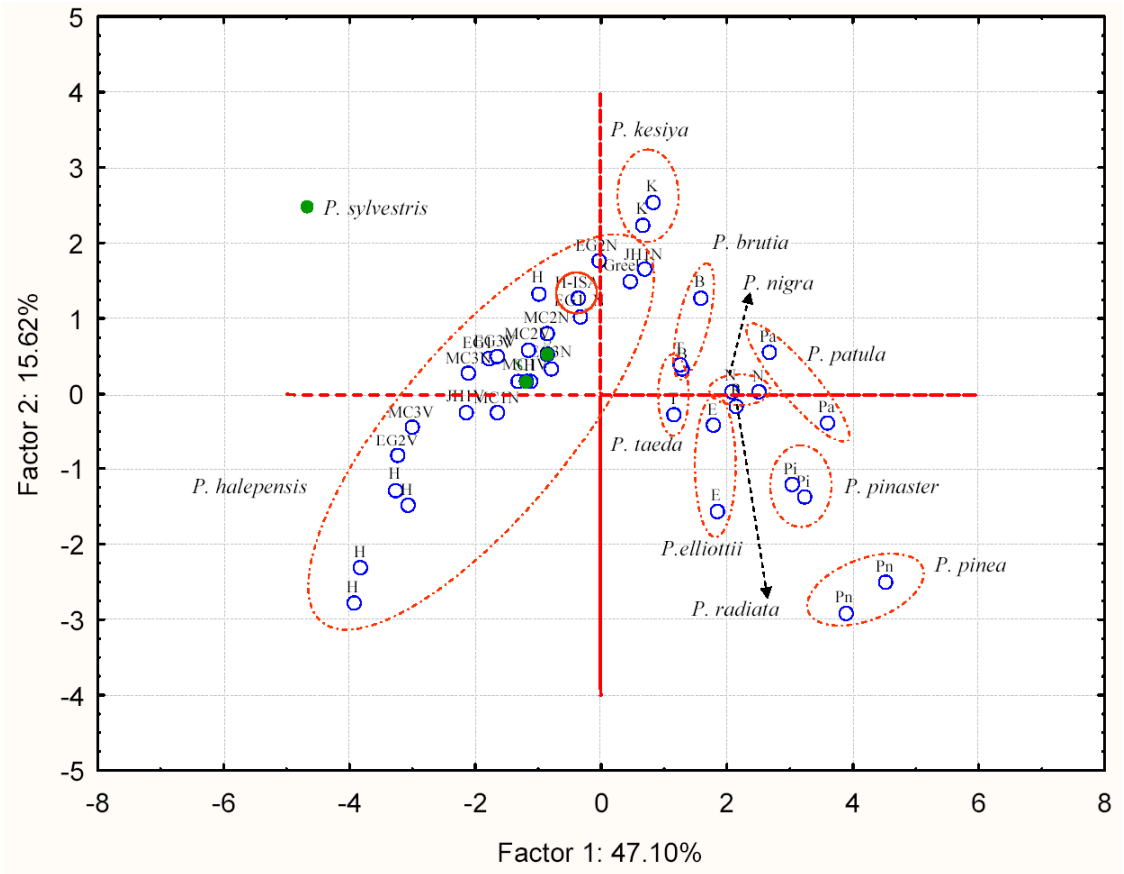

Figure 3.98 – Principal component analysis for the square root-transformed data from the resin acids present in eleven pine species. The outlines of the groups and the green dots for *P. sylvestris* samples have been added manually to aid interpretation.

In order to identify which of the resin acids are associated with the components, the factor scores (Table 3.35) were analyzed for the first two components. The projection of the variables on the factor plane for the first two components is presented in Figure 3.99. The loading values for component 1 and 2 are summarized in Table 3.36.

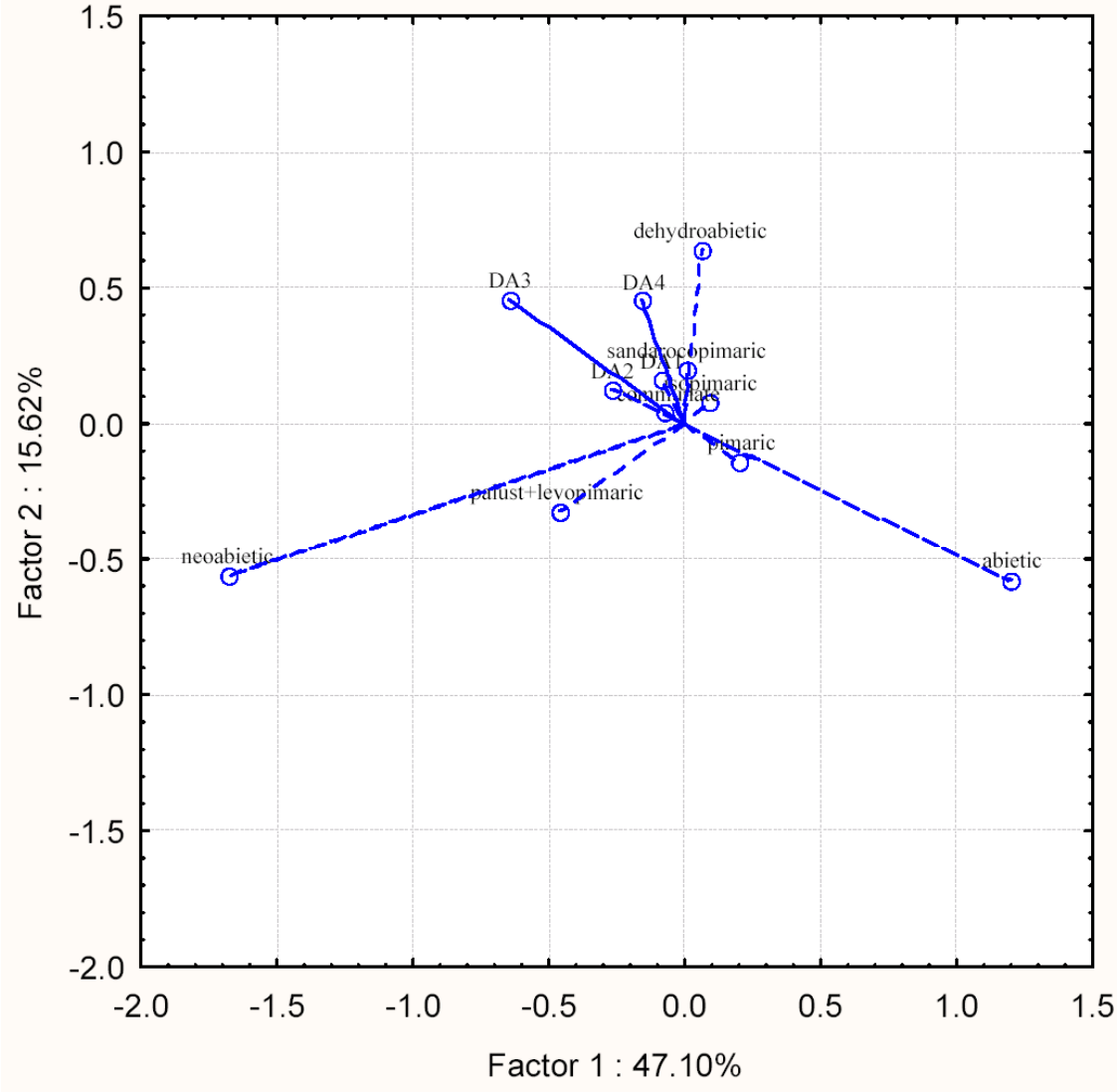

Figure 3.99 – Principal component analysis loadings for the square root-transformed data from the resin acids present in the pine species used for performance experiments with larvae of *T. pityocampa.*

The loadings data (Table 3.36 and projection plot Figure 3.99) show that the major associations for factor 1 can be found for abietic and neoabietic acids, with opposite influence. Concerning factor 2, the major association is found for dehydoabietic, abietic and neoabietic acids.

Table 3.36 - Values of the loadings from the principal component analysis using square root-transformed data from the resin acids present in the pine species used in the larvae performance experiments with larvae of *T. pityocampa.*

Resin acids	Factor 1	Factor 2
pimaric	0.09	-0.11
DA1	-0.04	0.12
sandarocopimarico	0.00	0.16
isopimaric	0.04	0.06
palust-levop	-0.21	-0.25
dehydroabietic	0.03	**0.49**
communate	-0.03	0.03
abietic	**0.53**	**-0.44**
DA2	-0.12	0.10
neoabietic	**-0.75**	**-0.43**
DA3	-0.29	0.35
DA4	-0.07	0.35

The examination of the loadings plot suggests that the predominant location of *P. halepensis* samples on the negative side of the first component (first and fourth quadrants) is driven by its content in neoabietic acid. *P. pinaster*, *P. pinea* and *P. elliottii* are driven to the third quadrant, due to their content in abietic acid. Species placed on the second quadrant are driven by their content in dehydroabietic acid.

4. Discussion and conclusions

Previously to this work, the main established technique to performe qualitative analysis of complex matrices such as essential oils or plant volatile emissions, was one-dimensional-gas chromatography hyphenated with mass spectrometry (1D-GC/MS) and, to a reduced extent, gas chromatography hyphenated with Fourier transform infrared spectroscopy (GC-FTIR). However, the analysis of the resulting matrices was dependent on the assumption that chromatographic separation was maximized and that different mass fragmentation patterns, or unique ions, were produced, in order to allow for manual deconvolution of the components and thus its individual detection and/or identification.

In this work the chemical composition of the volatile fraction of the needles of pine species were analyzed, for the first time, by means of 1D-GC/MS using a time-of-flight (1D-GC/TOFMS) mass analyzer, with a high spectral acquisition rate, that allowed for automated peak finding with mass spectral deconvolution and thus increasing analytical resolution by adding spectral resolution to the chromatographic resolution. Also for the first time, the chemical composition of the needles of pine species, both volatile (chiral and non chiral) and non volatile, were studied by comprehensive two-dimensional gas chromatography (GC × GC) hyphenated with mass spectrometry using a time-of-flight (GC × GC/TOF-MS) mass analyzer. Previously to the application of 1D-GC/TOFMS and GC × GC, the chemical composition of the needles of eleven pine species were studied and analyzed by classical 1D-GC/MS using the quadrupole and ion trap mass analyzers and by enantioselective multidimensional gas chromatography (MDGC), with heart-cutting transfer mode.

The use of the classical 1D-GC/MS allowed for the detection of 94 compounds in the pine needles volatile fraction, where 87 have been identified either tentatively or by standard injection. By means of 1D-GC/TOFMS analysis, 185 compounds were assigned to the pine needles volatile fraction, with 65% of them showing library match factors higher than 80%, and retention index agreement were tentatively identified. The highest sensibility of the TOF and the automated peak finding allowed for the detection of trace components with qualitative

full spectra, and the deconvolution algorithm the extraction of true mass spectra of compounds that coelute on the analytical column, promoting their reliable identification.

The GC × GC showed to be a powerful technique for the analysis of the chemical components of the needles of the pine species, considering both the volatile and non volatile fractions. The use of GC × GC resulted in enhanced separation efficiency and in an increased signal to noise ratio (S/N) from the analyte peaks, which maximizes the purity of the mass spectra obtained, making possible a more accurate tentative identification of the pine needles components. Due to the nature of the matrix under study, in which several constituents present similar mass spectra, and tend to coelute on the first dimension column, the increased sensitivity and improved separation power were important factors to achieve their characterization in different pine species. Additionally, the increased S/N allowed for the detection of trace components in the volatile fraction. Apparent baseline noises observed in 1D-GC resulted in clear components visualized on the 2D plot. This may be an important achievement in chemical ecology, where insect host specialization probably allows for the detection of host volatile compounds at trace level. By means of GC × GC, and just considering peaks with S/N > 50, over 200 compounds were detected with the non-chiral analysis, and more than 400 with the chiral analysis. The analysis of the mass spectra data, together with the analytes retention times and their positioning in the 2D plot, allowed for the tentative identification of more than 70% of the detected compounds. The mass spectra obtained by GC × GC showed a better quality than those obtained by 1D-GC/TOFMS, providing higher match library factors with the NIST/Wiley searchable libraries, and thus a stronger identification of the compounds present in the samples than by one-dimensional GC analysis.

All column sets used efficiently separated the analytes from each other, as well as from system artifacts and matrix constituents. This conclusion can be highlighted by the results obtained for theresin acids analysis, which usually produces complex 1D-chromatograms, where information regarding the chemical composition of the matrix is scarce. The use of GC × GC resulted in a clear separation of the resin acids under study from the other matrix components. For the volatile analysis, the worst results were achieved when using the non polar column with 60 m, due to analyte retentions cross-over and to the thermal degradation of some sesquiterpenes, which promoted the finding of some false positive peaks by the software on 1D-GC/TOFMS. However, on GC × GC using the same column in a set with a polar column, the degradation bands were separated from the analytes, reinforcing the separation power of this technique.

Volatile components identified in the needles of the pine species by all methods, include monoterpene hydrocarbons, oxygenated monoterpenes, phenyl esters, hydrocarbons, esters, alcohols, carbonyl, aromatics and sulfur compounds, and sesquiterpene hydrocarbons. Some of them, such as 1,4-cineol, mint sulphide, undecan-2-one were reported for the first time in the needles of studied pine species.

In spite of the higher mass spectral quality achieved, the mass spectra of several chromatographic peaks did not match either any of the reference spectra, or similar spectra which were not consistent with their retention index. These findings show the limitation of the spectral libraries and databases presently available, and highlight the need for the establishment of more comprehensive mass spectral libraries and databases, that may allow for complete identifications, especially in view of new technologies like GC × GC, leading to a new level of analytical information.

Although good linear relationships were found between the linear retention indices calculated and those reported by Adam (2001) or Joulain and Konig (1998) for the compounds tentatively identified, which constituted a valuable tool, it was not possible to assure the accuracy of the assignments reported, although they were confirmed by different mass spectrometric (qMS and ToF-MS) and chromatographic techniques (1D-GC and GC × GC). Nevertheless, the results obtained constitute a first contribution to the detailed knowledge of the chemical composition of the needles of the important *Pinus* species.

By means of principal component analysis (PCA) it was possible to differentiate the pine species studied by their major chiral and non chiral volatile components, as well as by their resin acids contents.

In order to study the role of the volatile compounds upon the observed variations in the intensity attack by *T. pityocampa*, a partial least squares regression (PLS) was performed for the eleven pine species present in Abrantes experimental plot, as well as for the *P. pinaster* trees sampled in Apostiça.

At intraspecific level, in Apostiça, results did not show any significant relationship between the volatile composition of the *P. pinaster* trees and the intensity of attack by *T. pityocampa*. However, at interspecific level for the Abrantes plot, the PLS extracted significant

components and estimated that the most important volatiles explaining the differences in attack among pine species, were *β*-pinene, terpinolene, limonene plus *β*-phellandrene, myrcene and sabinene. Concerning the enantiomeric composition of the monoterpenes, (-)-*β*-pinene and (+)-limonene were estimated as the most important volatiles to explain the differences in attack.

Zhang *et al.* (2003) studied the electrophysiological responses of *T. pityocampa* females to host volatiles using cut branches of *P. sylvestris* only, concluding that volatiles could be divided in three groups:

i) Antennally inactive compounds, comprising the major volatiles *α*-pinene, *β*-pinene, *Δ*-3-carene, together with (+)-limonene.
ii) Compounds which elicited strong antennal responses, comprising myrcene, trans-ocimene, *β*-phellandrene and terpinolene.
iii) Compounds which elicited weak antennal responses, comprising (-)-limonene, *cis*-ocimene, *γ*-terpinene plus other 15 volatile compounds, such as the sesquiterpenes germacrene D, *trans*-caryophyllene and *a*-caryophyllene.

Findings of Zhang *et al.* (2003) are in accordance with the present results, since for the interspecific analysis, Abrantes plot, myrcene and terpinolene were two of the most significant components estimated by the PLS, pointing to the role played by the two monoterpenes in the host selection process by the insect. On the other hand in Apostiça, where only one pine species was present, *trans*-ocimene was one of the compounds showing a stronger correlation with the intensity of attack (Figure 3.85).

Additionally, the three sesquiterpenes germacrene D, *trans*-caryophyllene and *α*-caryophyllene reported by Zhang *et al.* (2003) as weak antennal elicitors, were present in all pine species included in the present study, and might be envisaged as signalizing to T. pityocampa the location of suitable host genus.

Finally, *β*-phellandrene reported as a strong antennal elicitor, was in the present study found coeluting with limonene, and thus could not be correlated with the findings of Zhang *et al.* (2003), who did not perform an enantiomeric analysis of the headspace samples of *P. sylvestris*. From the present study it can be concluded that the amounts of *β*-phellandrene found in the needles of all Pinus species, is overwhelmingly due to one of the enantiomers,

probably (-)-*β*-phellandrene (Table 4.1). Figure 4.1 shows the relationship detected between the two enantiomers for the Pinus species studied, plus *Pseudotsuga* sp., as a representative of another conifer genus. Results strongly suggest that *β*-phellandrene might be considered as a chemomarker, for the Pinus species studied.

Table 4.1 - Relative content (%) of *β*-Phellandre enatiomeric pair for the studied pine species plus *Pseudotsuga* sp. determined by 1D enantioselective GC and GC × GC

	1D-GC/qMS*	1D-GC/qMS*	GC × GC*	GC × GC*
	(-)-*β*-Phellandrene	(+)-*β*-Phellandrene	(-)-*β*-Phellandrene	(+)-*β*-Phellandrene
P. halepensis	95.60	4.40	99.40	0.60
P. brutea	98.75	1.25	99.00	1.00
P. pinea	99.94	0.06	99.50	0.50
P. patula	99.97	0.03	100.00	0.00
P. radiata	97.61	2.39	97.70	2.30
P. pinaster	98.78	1.22	98.90	1.10
P. taeda	99.56	0.44	100.00	0.00
P. elliottii	98.9	1.10	98.80	1.20
P. kesiya	99.45	0.55	99.90	0.10
P. sylvestris	97.50	2.50	97.70	2.30
Pseudotsuga sp.	93.67	6.33	95.20	4.80

*Operational conditions according to 2.4.1.2 (Table 2.7) and 2.4.2.2. (Table 2.13).

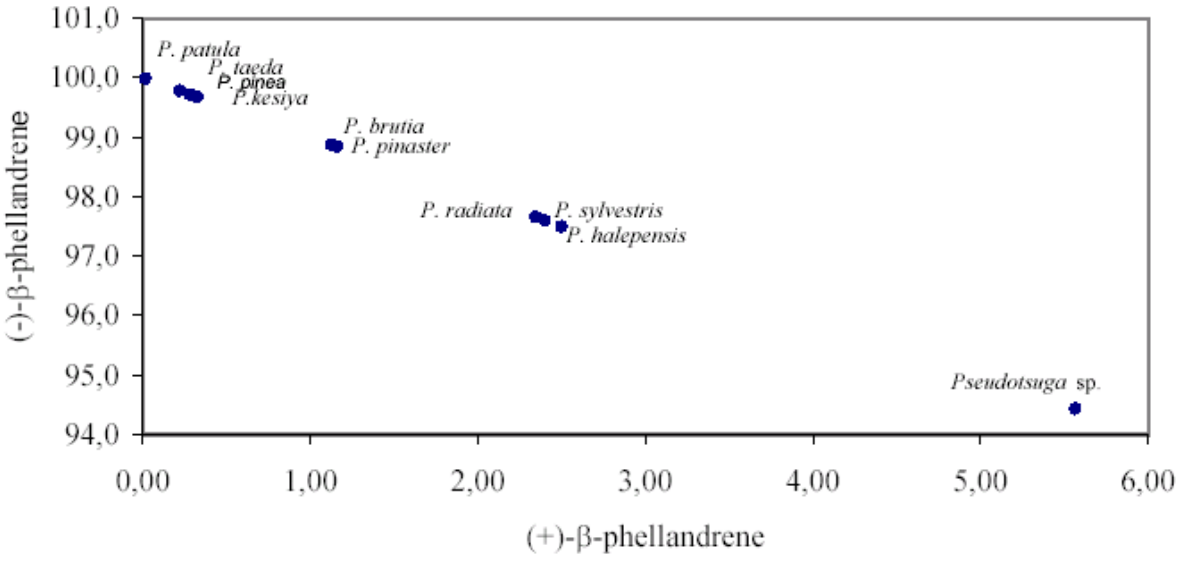

Figure 4.1 - Relationship between the *β*-phellandrene enatiomeric pair for the studied pine species plus *Pseudotsuga* sp.

Although no significant relationship was found between the resin acid composition in the needles of the pine species used in the bioassay and the larval performance of *T. pityocampa*, the presence of a diterpene labdanic acid, tentatively identified as copalic acid, was only detected in the needles of *P. halepensis* and *P. pinaster,* the species which promoted the worst larval performance. *P. halepensis*, the species leading to the lowest larval performance, presented the highest content of copalic acid.

The use of GC/TOFMS, using field ionization as a soft ionization method (GC/FI-TOFMS), permited the characterization of the needles based on the molecular weight of their components. It provided rapid information regarding the mass range, molecular weight diversity and evidence for significant differences due to different mass patterns in the composition of the needles. This information, together with the separation provided by gas chromatography, can turn the GC/FI-TOFMS in a two-dimensional technique through data analysis, providing an effective visualization of the composition of the needles of the pine species. It also provided extra information, which can be used to identify compound classes, as well as to support compound identification performed by other ionization methods and chromatographic techniques. As this information reports to exact molecular weights, it can be used to assign, or confirm, the presence of particular compounds, or compound classes, in the needles and thus providing a tool for their future characterization.

5. References

Adahchour, M.; Brandt, M.; Baier, H.-U.; Vreuls, R. J. J.; Batenburg, A. M. ; Brinkman, U. A. Th. 2005. Comprehensive two-dimensional gas chromatography coupled to a rapid-scanning quadrupole mass spectrometer: principles and applications. *Journal of Chromatography A*, **1067**(1-2): 245-254.

Adam, K.-P.; Thiel, R., Zapp, J.; Becker, H. 1998. Involvement of the mevalonic acid pathway and the glyceraldehyde-pyruvate pathway in terpenoid biosynthesis of the Liverworts *Ricciocarpos natans* and *Conocephalum conicum*. *Archives of Biochemistry and Biophysics*, **354**(1): 181-187.

Adams, R. P. 1989. *Identification of essential oils by ion trap mass spectroscopy*. Academic Press, San Diego, California, USA, 302 pp.

Adams, R. P. 1995. In: *Identification of Essential Oil Components by GC/MS*. Allured Publishing Corporation.

Adams, R. P. 2001. *Identification of essential oil components by gas chromatography/ quadrupole mass spectroscopy*. 3rd edition, Allured Publishing Corporation, Illinois, USA.

Aharoni, A.; Jongsma, M. A.; Bouwmeester, H. J. 2005. Volatile science? Metabolic engineering of terpenoids in plants. *Trends in Plant Science*, **10**(12): 594-602.

Arimura, G.; Ozawa, R.; Shimoda, T.; Nishioka, T.; Boland, W.; Takabayashi, J. 2000. Herbivory-induced volatiles elicit defence genes in lima bean leaves. *Nature*, **406**: 512-515.

Arnaldo, P. S.; Torres, L. M. 2006. Effect of different hosts on *Thaumetopoea pityocampa* populations in Northeast Portugal. *Phytoparasitica*, **34**(5):523-530.

Arthur, C. L.; Pawliszyn, J. 1990. Solid-phase microextraction with thermal desorption using fused silica optical fibers. *Analytical Chemistry*, **62**: 2145–2148.

Arthur, C. L.; Potter, D. W.; Buchholz, K. D.; Motlagh, S.; Pawliszyn, J. 1992d. Solid-phase microextraction for the direct analysis of water: theory and practice. *LC•GC*, **10**(9): 656–661.

Arthur, C. L; Chai, M.; Pawliszyn, J. 1993. Solventless injection technique for microcolumn separations. *Journal of Microcolumn Separations*, **5**: 51-56.

Arthur, C. L; Killam, L. M.; Buchholz, K. D.; Pawliszyn, J. 1992c. Automation and optimization of solid-phase microextraction. *Analytical Chemistry*, **64**: 1960–1966.

Arthur, C. L; Killam, L. M.; Motlagh, S.; Lim, M.; Potter, D. W; Pawliszyn, J. 1992a. Analysis of substituted benzene compounds in groundwater using solid-phase microextraction *Environmental Science & Technology*, **26**: 979–983.

Arthur, C. L; Pratt, K.; Motlagh, S.; Pawliszyn, J.; Belardi, R. P. 1992b. Environmental-analysis of organic-compounds in water using solid-phase microextraction and gas-chromatography ion trap mass-spectrometry. *HRC-Journal of High Resolution Chromatography*, **15**(11): 741–744.

Athanassiou, C. G.; Kavallieratos, N. G.; Gakis, S. F.; Kyrtsa, L. A.; Mazomenos, B. E.; Gravanis, F. T. 2007. Influence of trap type, trap colour, and trapping location on the capture of the pine moth, Thaumetopoea pityocampa**.** *Entomologia Experimentalis et Applicata*, **122**(2): 117-123.

Avci, M.; Sarikaya, O. 2005. Expansion, damage and natural enemies of pine processionary moth in Turkey. Proceedings of the Final Meeting of Global change and pine processionary moth: a new challenge for integrated pest management (PROMOTH QLK5-CT-2002-00852), Belgodère, Calvi, Corsica, France, 23-27 September 2005.

Avtzis, N. 1986. Development of *Thaumetopoea pityocampa* Schiff. (Lepidoptera, Thaumetopoeidae) in relation to food consumption. *Forest Ecology and Management,* **15**: 65-68.

Ayres, M. P.; Clausen, T. P.; Maclean, JR., S. F.; Redman, A. M.; Reichardt, P. B. 1997. Diversity of structure and antiherbivore activity in condensed tannins. *Ecology***, 78**(6): 1696–1712.

Baldwin, I. T.; Halitschke, R.; Kessler, A.; Schittko, U. 2001. Merging molecular and ecological approaches in plant-insect interactions. *Current Opinion in Plant Biology*, **4**(4): 351-358.

Baldwin, I. T.; Halitschke, R.; Paschold, A.; von Dahl, C. C.; Preston, C. A. 2006. Volatile signaling in plant-plant interactions: ‘‘talking trees’’ in the genomics era. *Science*, **311**: 812-815.

Banthorpe, D. V. 1991. Classification of terpenoids and general procedures for their characterisation. In: *Methods in Plant Biochemistry*, Vol. 7: Terpenoids. B. V. Charlwood, D. V. Banthorpe (Eds.), Academic Press, pp. 1-35.

Banthorpe, D. V.; Charlwood, D. V. 1994. The isoprenoids. In: *Natural Products: Their Chemistry and Biological Significance*. J. Mann, S. Davidson, J. Hobbs, D. Banthorpe, J. Harborne, Prentice Hall, pp. 185-191.

Barata, R. C. 2008. *Aplicação de índices de retenção lineares na identificação de substâncias por chromatografia gás-líquido em matrizes naturais*. M.Sc. Thesis. Faculdade de Ciências e Tecnologia, Universidade Nova de Lisboa, Lisbon, Portugal.

Barbéro, M.; Loisel, R.; Quézel, P.; Richardson, D. M.; Romane, F. 1998. Pines of the Mediterranean basin. *In: Ecology and Biogeography of P*inus. D. M. Richardson (Ed.), Cambridge University Press, Cambridge, UK, pp. 153-170.

Barre, F.; Goussard, F.; Géri, C. 2003. Variation in the suitability of *Pinus sylvestris* to feeding by two defoliators, *Diprion pini* (Hym., Diprionidae) and *Graellsia isabellae galliaegloria* (Lep., Attacidae). *Journal of Applied Entomology*, **127**(5): 249-257.

Barre, F.; Milsant, F.; Palasse, C.; Prigent, V.; Goussard, F.; Géri, C. 2002. Preference and performance of the sawfly *Diprion pini* on host and non-host plants of the genus *Pinus*. *Entomologia Experimentalis et Applicata*, **102**(3): 229-237.

Barry, E. F.; Grob, R. L. 2007. Apendix B. Column selection. *In*: *Columns for Gas Chromatography. Performance and Selection*. Wiley-Interscience, John Wiley & Sons, Inc. pp. 277-280.

Bartle, K. D. 2002. *In*: *Multidimensional Chromatography*, L. Mondello, A.C. Lewis, K.D. Bartle (Eds.), John Wiley & Sons Ltd., pp. 3-15.

Baser, K. H. C.; Demirci, F. 2007. Chemistry of essential oils. *In*: *Flavours and Fragances. Chemistry, Bioprocessing and Sustainability*. R. G. Berger (Ed.), Springer, pp. 43-86.

Basset, Y.; Samuelson, G. A.; Allison, A.; Miller, S. E. 1996. How many species of host-specific insects feed on a species of tropical tree? *Biological Journal of the Linnean Society*, **59**: 201-216.

Bate, N. J.; Rothstein, S. J. 1998. C6-volatiles derived from the lipoxygenase pathway induce a subset of defense-related genes. *The Plant Journal*, **16**(5): 561–569.

Battisti, A. 1988. Host-plant relationships and population dynamics of the pine processionary caterpillar *Thaumetopoea pityocampa* (Denis and Schiffermueller). *Journal of Applied Entomology*, **105**: 393-402.

Beens, J.; Blomberg, J.; Schoenmakers, P. J. 2000. Proper tuning of comprehensive two-dimensional gas chromatography (GC × GC) to optimize the separation of complex oil fractions. *Journal of High Resolution Chromatography*, **23**: 182-188.

Beens, J.; Boelens, H.; Tijssen, R.; Blomberg, J. 1998. Quantitative aspects of comprehensive two-dimensional gas chromatography (GC × GC). *Journal of High Resolution Chromatography*, **21**: 47-54.

Beesley, T. E.; Buglio, B.; Scott, R. P. W. 2001. *Quantitative Chromatographic Analysis*. Marcel Dekker, Inc. New York, USA.

Beesley, T. E.; Scott, R. P. W. 1998. *Chiral Chromatography*. John Wiley & Sons, New York, USA, pp. 156-164.

Benderoth, M.; Textor, S.; Windsor, A. J.; Mitchell-Olds, T.; Gershenzon, J.; Kroymann, J. 2006. Positive selection driving diversification in plant secondary metabolism. *Proceedings of the National Academy of Sciences of the United States of America*, **103**: 9118-9123.

Bennett, W. H. 1954. The effect of needle structure upon the susceptibility of hosts to the pine needle miner (*Exoteleia pinifoliella* (Chamb.)) (Lepidoptera: Gelechiidae). *The Canadian Entomologist*, **86**: 49-54.

Bernays, E. A.; Chapman, R. L., 1994a. Patterns of host-plant use. In: *Host-Plant Selection by Phytophagous Insects*, Chapman and Hall, New York, USA, pp. 4-13.

Bernays, E. A.; Chapman, R. L., 1994b. Chemicals in plants. In: *Host-Plant Selection by Phytophagous Insects*, Chapman and Hall, New York, USA, pp. 14-60.

Bertsch, W. J. 1999. Two-Dimensional gas chromatography. Concepts, instrumentation, and applications - Part 1: Fundamentals, conventional two-dimensional gas chromatography, selected applications. *Journal of High Resolution Chromatography*, **22**(12): 647-665.

Bertsch, W. J. 2000. Two-dimensional gas chromatography. Concepts, instrumentation and applications – Part 2: Comprehensive two-dimensional gas chromatography. *Journal of High Resolution Chromatography*, **23**: 167-181.

Bicchi, C.; D'Amato, A.; Rubiolo, P. J. 1999. Cyclodextrin derivatives as chiral selectors for direct gas chromatographic separation of enantiomers in the essential oil, aroma and flavour fields. *Journal of Chromatography A*, **843**: 99-121.

Björkman, C.; Larsson, S. 1991. Pine sawfly defence and variation in host plant resin acids: a trade-off with growth. *Ecological Entomology*, **16**: 283-289.

Borg-Karlson, A.-K.; Unelius, C. R.; Valterová, I.; Nilsson, L. A. 1996. Floral fragrance chemistry in the early flowering shrub *Daphne mezereum*. *Phytochemistry*, **41**(6): 1477-1483.

Braga, M. E. M.; Santos, R. M. S.; Seabra, I. J.; Facanali, R.; Marques, M. O. M.; Sousa, H. C. 2008. Fractioned SFE of antioxidants from maritime pine bark. *The Journal of Supercritical Fluids*, **47**: 37-48.

Braithwaite, A.; Smith, F. J. 1999. *Chromatographic Methods*, 5th edition. Kluwer Academic Publishers, Dordrecht.

Branco, M.; Mateus, E. P.; Barrento, M. J.; Santos, M. H.; Paiva, M. R. Effect of pine needle composition on larval performance of *Thaumetopoea pityocampa* (in prep.).

Branco, M.; Valente, C.; Paiva, M. R. 2008. *Pragas e doenças em pinhal e eucaliptal - desafios para a sua gestão integrada* [pests and diseases in pine and eucalyptus woods – challenges for their integrated management. Port., with Abstracts in Eng.]. ISApress, Lisbon. (approx.) 300 pp., in press.

Branco; M. I. P. 1994. *Isomerização de ácidos resínicos - estudo cinético*. Ph.D Thesis. Faculdade de Ciências e Tecnologia, Universidade Nova de Lisboa, Lisbon, Portugal.

Breuer, M.; Devkota, B. 1990. Control of *Thaumetopoea pityocampa* (Den. & Schiff.) by extracts of Melia azedarach L. (Meliaceae). *Journal of Applied Entomology*, **110**: 128-135.

Bruce, T. J. A.; Wadhams, L. J.; Woodcock, C. M. 2005. Insect host location: a volatile situation. *Trends in Plant Science*, **10**(6): 269-274.

Buffo, E.; Battisti, A.; Stastny, M.; Larsson, S. 2007. Temperature as a predictor of survival of the pine processionary moth in the Italian Alps. *Agricultural and Forest Entomology*, **9**: 65-72.

Buxton, R. D. 1990. The influence of host tree species on timing of pupation of *Thaumetopoea pityocampa* Schiff. (Lep., Thaumetopoeidae) and its exposure to parasitism by *Phryxe caudate* Rond. (Dipt., Laevaevoridae). *Journal of Applied Entomology*, **109**: 302-310.

Cardoso, J. C.; Bessa, M. T.; Marado, M. B. 1973. Carta de solos de Portugal (1:1000000). Estação Agronómica Nacional. *Separata da Agronomia Lusitana*, **XXXIII** (I-IV): 481-602.

Carpy, A.; Marchand-Geneste, N. 2003. Molecular characterization of retene derivatives obtained by thermal treatment of abietane skeleton diterpenoids. *Journal of Molecular Structure (Theochem)*, **635**(1-3): 45-53.

Carvalheiro, B. G. 1986: *Química dos Ácidos Resínicos*. Nº 8. Laboratório Nacional de Engenharia e Tecnologia Industrial, Lisboa, 121 pp..

Cazes, J. (Ed.). 2001. Encyclopedia of Chromatography. CRC Press, 927 pp..

Chaintreau, A. 2001. Simultaneous distillation-extraction: from birth to maturity-review. *Flavour and Fragance Journal*, **16**: 136–148.

Chang, T.-L.; Mead, T. E.; Zinke, D. F. 1971. Mass spectra of diterpene resin acid methyl esters. *Journal of the American Oil Chemists' Society*, **48**(9): 455-461.

Chappell, J.; Von Lanken, C.; Vogeli, U.; Bhatt, P. 1989. Sterol and sesquiterpenoid biosynthesis during a growth cycle of tobacco cell suspension cultures. *Plant Cell Reports*, **8**: 48-52.

Charlwood, B. V.; Charlwood, K. A. 1991. Monoterpenoids. In: *Methods in Plant Biochemistry*, Vol. 7: Terpenoids. B. V. Charlwood, D. V. Banthorpe (Eds.), Academic Press, New York, USA, pp. 43-91.

Chaves das Neves, H. J.; Freitas, A. M. C. 1996. *Introdução à Cromatografia Gás-Líquido de Alta Resolução*. Dias de Sousa, Ltd.

Chehab, E. W.; Kaspi, R.; Savchenko, T.; Rowe, H.; Negre-Zakharov, F.; Kliebenstein, D.; Dehesh, K. 2008. Distinct roles of jasmonates and aldehydes in plant-defense responses. *PLoS ONE*, **3**(4): e1904, 10 pp..

Chen, J.; Pawliszyn, J. 1995. Solid phase microextraction coupled to high-performance liquid chromatography. *Analytical Chemistry*, **67**: 2530–2533.

Chen, Y.; Begnaud, F.; Chaintreau, A.; Pawliszyn, J. 2006. Quantification of perfume compounds in shampoo using solid-phase microextraction. *Flavour and Fragance Journal*, **21**: 822–832.

Cho, S-K.; El-Aty, A. M.; Choi, J.-H.; Kim, M. R.; Shim, J. H. 2007. Optimized conditions for the extraction of secondary volatile metabolites in *Angelica* roots by accelerated solvent extraction. *Journal of Pharmaceutical and Biomedical Analysis*, **44**: 1154–1158.

Claeyssen, E.; Rivoal, J. 2007. Isozymes of plant hexokinase: Occurrence, properties and functions. *Phytochemistry*, **68**(6): 709-731.

Codella, S. G.; Raffa, K. F. 1995. Host plant influence on chemical defense in conifer sawflies (Hymenoptera: Diprionidae). *Oecologia*, **104**: 1-11.

Croteau, R. 1987. Biosynthesis and catabolism of monoterpenoids. *Chemical Reviews*, **87**(5): 929-954.

Cseke, L. J.; Kirakosyan, A.; Kaufman, P. B.; Warber, S.; Duke, J. A.; Brielmann, J. A. (Eds.) 2006. *Natural Products from Plants*. 2nd edition, CRC Press, 611 pp..

d'Auria, J. C.; Pichersky, E.; Schaub, A.; Hansel, A.; Gershenzon, J. 2007. Characterization of a BAHD acyltransferase responsible for producing the green leaf volatile (Z)-3-hexen-1-yl acetate in *Arabidopsis thaliana*. *The Plant Journal*, **49**, 194-207.

d'Alessandro, M.; Turlings, T. C. J. 2006. Advances and challenges in the identification of volatiles that mediate interactions among plants and arthropods. *Analyst*, **131**(1): 24-32.

Dallüge, J.; Beens, J.; Brinkman, U. A. Th. 2003. Comprehensive two-dimensional gas chromatography: a powerful and versatile analytical tool. *Journal of Chromatography A*, **1000**(1-2): 69-108.

Dallüge, J.; van Rijn, M.; Beens, J.; Vreuls, R. J. J.; Brinkmann, U. A.Th. 2002a. Comprehensive two-dimensional gas chromatography with time-of-flight mass spectrometric detection applied to the determination of pesticides in food extracts *Journal of Chromatography A*, **965**: 207-217.

Dallüge, J.; van Stee, L. L. P.; Xu, X.; Williams, J.; Beens, J.; Vreuls, R. J. J.; Brinkman, U. A. Th. 2002c. Unravelling the composition of very complex samples by comprehensive gas chromatography coupled to time-of-flight mass spectrometry: Cigarette smoke. *Journal of Chromatography A*, **974**(1-2): 169-184.

Dallüge, J.; Vreuls, R. J. J.; Beens, J.; Brinkmann, U. A. Th. 2002b. Optimisation and characterisation of comprehensive two-dimensional gas chromatography with time-of-flight mass spectrometric detection. *Journal of Separation Science*, **25**: 201-214.

Dass, C. 2007. Fundamentals of Contemporary Mass Spectrometry. Wiley-Intersience, John Wiley & Sons, Inc., Hoboken, New Jersey, pp. 28-30.

David, F.; Sandra, P. 1987. *In: Capillary Gas Chromatography in Essential Oil Analysis*, P. Sandra, C. Bicchi (Eds.), Huething Verlag, pp. 387.

Davis, J. M.; Giddings, J. C. 1983. Statistical theory of component overlap in multicomponent chromatograms. *Analytical Chemistry*, **55**: 418–424.

Davis, L. A.; Heinz, D. E.; Addicott, F. T. 1968. Gas-liquid chromatography of trimethylsilyl derivatives of abscisic acid and other plant hormones. *Plant Physiology*, **43**: 1389-1394.

de Bruyne, M; Baker, T. C. 2008. Odor detection in insects: volatile codes. *Journal of Chemical Ecology*, **34**(7): 882-897.

de Geus, H. J.; Aidos, I.; de Boer, J.; Luten, J. B.; Brinkman, U. A. Th. 2001. Characterisation of fatty acids in biological oil samples using comprehensive multidimensional gas chromatography. *Journal of Chromatography A*, **910**: 95-103.

de Geus, H.-J.; Schelvis, A.; de Boehr, J.; Brinkman, U. A. Th. 2000. Comprehensive two-dimensional gas chromatography with a rotating thermal desorption modulator and independently temperature programmable columns. *Journal of High Resolution Chromatography*, **23**: 189-196.

de Groot, P.*;* Turgeon, J. J. 1998. Insect-pine interactions. *In: Ecology and Biogeography of Pinus*. D. M. Richardson (ed.), Cambridge University Press, Cambridge, UK, pp. 354-406.

Dethlefs, F.; Gerhardt, K. O.; Stan. H.-J. 1996. Gas chromatograph/mass spectrometry of 13 resin acids as their PFB esters. *Journal of Mass Chromatography*, **31**: 1168-1168.

Deursen, M. D.; Beens, J.; Reijenga, J.; Lipman, P.; Cramers, C. 2000. Group type identification of oil samples using comprehensive two-domensional gas chromatography coupled to a time-of-flight mass spectrometer (GC×GC–TOF). *Journal of High Resolution Chromatography*, **23**: 507-510.

Devkota, B.; Schmidt, G. H. 1990. Larval development of *Thaumetopoea pityocampa* (Den. & Schiff.) (Lep., Thaumetopoeidae) from Greece as influenced by different host plants under laboratory conditions. *Journal of Applied Entomology*, **109**: 321-330.

Dicke, M.; de Boer, J. G.; Hofte, M.; Rocha-Granados, M. C. 2003. Mixed blends of herbivore-induced plant volatiles and foraging success of carnivorous arthropods. *Oikos*, **101**: 38-48.

Dimandja, J. M. D. 2003. A new tool for the optimized analysis of complex volatile mixtures: Comprehensive two-dimensional gas chromatography/time-of-flight mass spectrometry. *American Laboratory*, **25**(3): 42-53.

Douma-Petridou, E. 1990. European *Thaumetopoea* species (Lep., Thaumetopoeidae): Characteristics and life-cycles. Proceedings of the Thaumetopoeidae-Symposium, 5-7 July 1989, at Neustadt a. Rbge near Hannover, Germany, 12-19.

Dubey, V. S.; Bhalla, R.; Luthra, R. 2003. An overview of the non-mevalonate pathway for terpenoid biosynthesis in plants. *Journal of Biosciences*, **28**(5): 637-646.

Dudareva, N.; Pichersky, E.; Gershenzon, J. 2004. Biochemistry of plant volatiles. *Plant Physiology*, **135**: 1893-1902.

Dunn, W. B.; Ellis, D. I. 2005. Metabolomics: Current analytical platforms and methodologies. *Trends in Analytical Chemistry*, **24**(4): 285-294.

Eisert, R.; Pawliszyn, J. 1997. New trends in solid-phase microextraction. *Critical Reviews in Analytical Chemistry*, **27**(2): 103–135.

Eisner, T.; Johnessee, J. S.; Carrel, J.; Hendry, L. B.; Meinwald, J. 1994. Defensive use by an insect of a plant resin. *Science*, **184**(4140): 996 – 999.

Ekeberg, D.; Flaete, P.-O.; Eikenes, M.; Fongen, M.; Naess-Andresen, C. F. 2006. Qualitative and quantitative determination of extractives in heartwood of Scots pine (*Pinus sylvestris* L.) by gas-chromatography. *Journal of Chromatography A*, **1109**: 267–272.

Ekundayo, O. 1988. Volatile constituints of *Pinus* needle oils. *Flavour and Fragrance Journal*, **3**: 1-11.

El-Sayed, A. M. 2008. *The Pherobase: Database of Insect Pheromones and Semiochemicals*. http://www.pherobase.com/database/kovats, accessed in November 2008.

Engewald, W. 2007a. Retention cross-over phenomenon in gas chromatography—Can the mystery be revealed? Part 1. *Restek Advantage Chromatography Newsletter*, **2**: 2-3.

Engewald, W. 2007b. Retention cross-over phenomenon in gas chromatography—Can the mystery be revealed? Part 2. *Restek Advantage Chromatography Newsletter*, **3**: 2-3.

Fabre, J. H. 1916. The Life of the Caterpillar. Dodd, Mead and Company, Inc., New York, USA.

Faldt, J.; Arimura, G.; Gershenzon, J.; Takabayashi, J.; Bohlmann, J. 2003. Functional identification of *AtTPS03* as (E)-*β*-ocimene synthase: a monoterpene synthase catalyzing jasmonate- and wound-induced volatile formation in *Arabidopsis thaliana*. *Planta*, **216**: 745–751.

Faldt, J.; Sjodin, K.; Persson, M.; Valterová, I.; Borg-Karlson, A.-K. 2001. Correlations between selected monoterpene hydrocarbons in the xylem of six *Pinus* (Pinaceae) species. *Chemoecology*, **11**: 97–106.

FAO-Unesco-ISRIC 1990. *Soil map of the world*. Revised Legend. Reprinted with corrections. World Soil Resources Report no. 60. Food and Agriculture Organization of the United Nations, Rome, Italy, 119 pp..

Forkner, R. E.; Marquis, R. J.; Lill, J. T. 2004. Feeny revisited: condensed tannins as anti-herbivore defences in leaf-chewing herbivore communities of *Quercus*. *Ecological Entomology*, **29**: 174–187.

Fraenkel, G. S. 1959. The raison d'être of secondary plant substances: These odd chemicals arose as a means of protecting plants from insects and now guide insects to food. *Science*, **129**(3361): 1466-1470.

Fraga, B. M. 1991. Sesquiterpenoids. In: *Methods in Plant Biochemistry*, Vol. 7: Terpenoids. B. V. Charlwood, D. V. Banthorpe (Eds.), Academic Press, New York, USA, pp. 145-170.

Frysinger, G. S.; Gaines, R. B. 1999. Comprehensive two-dimensional gas chromatography with mass spectrometric detection (GC × GC/MS) applied to the analysis of petroleum. *Journal of High Resolution Chromatography*, **22**: 251-255.

Frysinger, G. S.; Gaines, R. B.; Ledford Jr., E. B. 1999. Quantitative determination of BTEX and total aromatic compounds by comprehensive two-dimensional gas chromatography. *Journal of High Resolution Chromatography*, **22**: 195-200.

Gardner, D. R.; Panter, K. E.; James, L. F. 1999. Pine needle abortion in cattle: Metabolism of isocupressic acid. *Journal of Agricultural and Food Chemistry*, **47**(7): 2891-2897.

Gardner, S. N.; Agrawal, A. A. 2002. Induced plant defense and the evolution of counter-defenses in herbivores. *Evolutionary Ecology Research,* **4**: 1131-1151.

Gatto, P.; Zocca, A.; Battisti, A.; Barrento, M. J.; Branco, M.; Paiva, M. R. 2008. Economic assessment of managing processionary moth in pine forests: A case-study in Portugal. *Journal of Environmental Management*, doi:10.1016/j.jenvman.2008.01.007.

Gaurav; Kaur, V.; Kumar, A.; Malik, A. K.; Rai, P. K. 2007. SPME-HPLC: a new approach for analysis of explosives. *Journal of Hazardous Materials*, **147**(3): 691–697.

Gernandt, D. S.; López, G. G.; García, S. O.; Liston, A. 2005. Phylogeny and classification of Pinus. *Taxon*, **54**(1): 29-42.

Giddings, J. C. 1987.Concepts and comparisons in multidimensional separations. *Journal of High Resolution Chromatography*, **10**: 319-323.

Gijzen, M.; Lewinsohn, E.; Savage, T. J.; Croteau, R. B. 1993. Conifer monoterpenes: Biochemistry and bark beetle chemical ecology. Chap. 2. *In: Bioactive Volatile Compounds from Plants.* Teranishi, R.; Buttery, R. G.; Sugisawa, H. (Eds.), ACS Symposium. Series 525, American Chemical Society, pp. 9-22.

Gomes da Silva, M. D. R.; Mateus, E. P.; Munhá, J.; Drazyk, A.; Farrall, M. H.; Paiva, M. R.; Chaves das Neves, H. J.; Mosandl, A. 2001. Differentiation of ten pine species from central Portugal by monoterpene enantiomer-selective composition analysis using multidimensional gas chromatography. *Chromatographia*, **53**: S412-S416.

Góreccki, T.; Yu, X.; Pawliszyn, J. 1999. Theory of analyte extraction by selected porous polymer SPME fibres. *Analyst*, **124**: 643–649.

Greenhagen, B.; Chappell, J. 2001. Molecular scaffolds for chemical wizardry: Learning nature's rules for terpene cyclases. *Proceedings of the National Academy of Sciences of the United States of America*, **98**(24): 13479–13481.

Gref, R.; Lindgren, D. 1984. The inheritance of pinifolic-acid in Scotch pine (*Pinus sylvestris* L.) needles. *Silvae genetica*, **33**(6): 235-237.

Griffiths, W. J. (Ed.) 2008. Metabolomics, Matabonomics and Metabolite Profiling. RSC Publishing, pp. 256-259.

Grob Jr., K.; Grob, G.; Grob, K. 1978. Comprehensive, standardized quality test for glass capillary columns. *Journal of Chromatography A*, **156**(1): 1-20.

Grob, K. 2001. *Split and Splitless Injection in Capillary Gas Chromatography: Concepts, Processes, Practical Guidelines, Source of Error*. Wiley VCH, 4th, completed revised edition., 480 pp..

Grob, K. 2005. Stability of the FID sensitivity during an analysis in capillary GC. *Journal of High Resolution Chromatography*, **3**(6): 286-290.

Grob, K.; Grob, G.; Grob Jr., K. 1981. Testing capillary gas chromatographic columns. *Journal of Chromatography A*, **219**(1): 13-20.

Grob, K.; Neukom, H. P. 2005. Pressure and flow changes in vaporizing GC injectors during injection and their impact on split ratio and discrimitanation of sample components. *Journal of High Resolution Chromatography*, **2**(9): 563-569.

Grob, K.; Rennhard, S. 2005. Evaluation of syringe handling techniques for injections into vaporizing GC injectors. *Journal of High Resolution Chromatography*, **3**(12): 627-633.

Grushka, E. 1970. Chromatographic peak capacity and the factors influencing it. *Analytical Chemistry*, **42**(11): 1142-1147.

Guenther, A.; Hewitt, C. N.; Erickson, D.; Fall, R.; Geron, C.; Graedel, T.; Harley, P.; Klinger, L.; Lerdau, M.; Mckay, W. A.; Pierce, T.; Scholes, B.; Steinbrecher, R.; Tallamraju, R.; Taylor, J.; Zimmerman; P. 1995. A global model of natural volatile organic compound emissions. *Journal of Geophysical Research*, **100**(D5): 8873-8892.

Guerrero, A.; Camps, F.; Coll, J.; Riba, M.; Einhorn, J.; Descoins, Ch.; Lallemand, J. Y. 1981. Identification of a potential sex pheromone of the processionary moth, *Thaumetopea pityocampa* (lepidoptera, notodontidae). *Tetrahedron Letters*, **22**(21): 2013-2016.

Hakola, H.; Tarvainen, V.; Laurila, T.; Hiltunen, V.; Hellén, H.; Keronen, P. 2003. Seasonal variation of VOC concentrations above a boreal coniferous forest. *Atmospheric Environment*, **37**: 1623–1634.

Hampel, D.; Mosandl, A.; Wust, M. 2005. Biosynthesis of mono- and sesquiterpenes in carrot roots and leaves (*Daucus carota* L.): metabolic cross talk of cytosolic mevalonate and plastidial methylerythritol phosphate pathways. *Phytochemistry*, **66**: 305–311.

Hansson, B. S.; Larsson, M. C.; Leal, W. S. 1999. Green leaf volatile-detecting olfactory receptor neurones display very high sensitivity and specificity in a scarab beetle. *Physiological Entomology*, **24**(2): 121-126.

Harborne, J. B. 1991. Recent advances in the ecological chemistry of plant terpenoids. In: *Ecological Chemistry and Biochemistry of Plant Terpenoids*, J. B. Harborne (Ed.), Oxford University Press, Oxford, UK, pp. 399-426.

Harborne, J. B. 2001. Twenty-five years of chemical ecology. *Natural Products Report*, **18**: 361-379.

Heldt, H.-W.; Heldt, F. 2005. *Plant Biochemistry*. An update and translation of the German 3rd edition, Elsevier Academic Press, London, UK.

Helmiga, D.; Ortegaa, J.; Guenther, A.; Herrick, J. D.; Geron, C. 2006. Sesquiterpene emissions from loblolly pine and their potential contribution to biogenic aerosol formation in the Southeastern US. *Atmospheric Environment*, **40**: 4150–4157.

Herbert, C. G.; Johnstone, R. A. W. 2003. *Mass Spectrometry Basics*, CRC Press, Boca Raton, Florida, USA, pp. 23-27.

Hick, A. J.; Luszniak, M. C.; Pickett, J. A. 1999. Volatile isoprenoids that control insect behaviour and development. *Natural Products Report*, **16**: 39-54.

Hilker, M.; Kobs, C.; Varama, M.; Schrank, K. 2002. Insect egg deposition induces *Pinus sylvestris* to attract egg parasitoids. *The Journal of Experimental Biology*, **205**: 455-461.

Hines, P. J. 2006. The invisible bouquet. *Science*, **311**: 803.

Hódar, J. A.; Castro, J.; Zamora, R. 2003. Pine processionary caterpillar *Thaumetopoea pityocampa* as a new threat for relict Mediterranean Scots pine forests under climate warming. *Biological Conservation*, **110**: 123–129.

Hódar, J. A.; Zamora, R.; Castro, J. 2002. Host utilisation by moth and larval survival of pine processionary caterpillar *Thaumetopoea pityocampa* in relation to food quality in three *Pinus* species. *Ecological Entomology*, **27**: 292–301.

Hódar, J. A.; Zamora, R.; Castro, J.; Baraza, E. 2004. Feast and famine: previous defoliation limiting survival of pine processionary caterpillar *Thaumetopoea pityocampa* in Scots pine *Pinus sylvestris*. *Acta Oecologica*, **26**: 203-210.

Hodges, J. D.; Elam, W.W.; Watson, W. F.; Nebeker, T. E. 1979. Oleoresin characteristics and susceptibility of four southern pines to southern pine beetle (Coleoptera: Scolytidae) attacks. *The Canadian Entomologist*, **111**: 889-896.

Holland, J. F.; Enke, C. G.; Allison, J.; Stults, J. T.; Pinkston, J. D.; Newcome, B.; Watson, J. T. 1983. Mass spectrometry on the chromatographic time scale: realistic expectations. *Analytical Chemistry*, **55**: 997A.

Holland, J. F.; Gardner, B. D. 2002. The advantages of GC-TOMS for flavor and fragrance analysis. In: *Flavor, Fragrance and Odour Analysis*, Marsili, R. (Ed.) Marcel Dekker, New York, USA, pp. 107.

Holzke, C.; Hoffmann, T.; Jaeger, L.; Koppmann, R.; Zimmer, W. 2006. Diurnal and seasonal variation of monoterpene and sesquiterpene emissions from Scots pine (*Pinus sylvestris* L.). *Atmospheric Environment*, **40**: 3174–3185.

Hopkins, R. J.; Birch, A. N. E.; Griffiths, D. W.; Baur, R.; Stadler, E.; McKinlay, R. G. 1997. Leaf surface compounds and oviposition preference of Turnip root fly *Delia floralis*: the role of glucosinolate and nonglucosinolate compounds. *Journal of Chemical Ecology*, **23**(3): 629-643.

Hsu, C. S.; Green, M. 2001. Fragment-free accurate mass measurement of complex mixture components by gas chromatography/field ionization-orthogonal acceleration time-of-flight mass spectrometry: an unprecedented capability for mixture analysis. *Rapid Communications in Mass Spectrometry*, **15**(3): 236-239.

ISI Web of Knowledge, 2008. Search on the topic "*Pinus*", "*pityocampa*", accessed in 5th August 2008.

Jactel, H.; Menassieu, P.; Vétillard, F.; Barthélémy, B.; Piou, D.; Frérot, B.; Rousselet, J.; Goussard, F.; Branco, M.; Battisti, A. 2006. Population monitoring of the pine processionary moth (Lepidoptera: Thaumetopoeidae) with pheromone-baited traps. *Forest Ecology and Management*, **235**(1-3): 96-106.

Janson, R.; De Serves, C.; Romero, R. 1999. Emission of isoprene and carbonyl compounds from a boreal forest and wetland in Sweden. *Agricultural and Forest Meteorology,* **98-99**: 671-681.

Jelen, H. H. 2003. Use of solid phase microextraction (SPME) for profiling fungal volatile metabolites. *Letters in Applied Microbiology*, **36**: 263–267.

Jennings, W. G.; Filsoof, M. 1977. Comparison of sample preparation techniques for gas-chromatographic analysis. *Journal of Agricultural Food Chemistry*, **25**(3): 440–445.

Jennings, W.; Mittlefehldt, E.; Stremple, P. 1997. *Analytical Gas Chromatography*. 2nd edition. Academic Press, New York, USA.

Joulain, D.; Konig, W. A. 1998. *The atlas of spectral data of sesquiterpene hydrocarbons*. E. B. Verlag, Hamburg, 661 pp.

Kanata, M.; Almab; M. H.; Sivrikayaa, F. 2005. Effect of defoliation by *Thaumetopoea pityocampa* (Den. & Schiff.) (Lepidoptera: Thaumetopoeidae) on annual diameter increment of *Pinus brutia* Ten. in Turkey. *Annals of Forest Science*, **62**: 91-94.

Karamaouna, F.; Copland, M. J. W. 2000. Oviposition behaviour, influence of experience on host size selection, and niche overlap of the solitary *Leptomastix epona* and the gregarious *Pseudaphycus flavidulus*, two endoparasitoids of the mealybug *Pseudococcus viburni*. *Entologia Experimentalis et Applicata*, **97**: 301-308.

Kataoka, H.; Lord, H. L.; Pawliszyn, J. 2000. Applications of solid-phase microextraction in food analysis. *Journal of Chromatography A*, **880**: 35–62.

Keeling, C. I.; Bohlmann, J. 2006. Diterpene resin acids in conifers. *Phytochemistry*, **67**: 2415–2423.

Kessler, A.; Baldwin, I. T. 2001. Defensive function of herbivore-induced plant volatile emissions in nature. *Science*, **291**: 2141-2144.

Khummueng, W.; Trenerry, C.; Rose, G.; Marriott, P. J. 2006. Application of comprehensive two-dimensional gas chromatography with nitrogen-selective detection for the analysis of fungicide residues in vegetable samples. *Journal of Chromatography A*, **1131**(1-2): 203-214.

Khush,G. S.; Panda, N. 1996. Host plant selection. In: *Host Plant Resistance to Insects*, *CAB* International, UK, pp.104-150.

Kim, Y.-S.; Shin, D.-H. 2005. Volatile components and antibacterial effects of pine needle (*Pinus densiflora* S. and Z.) extracts. *Food Microbiology*, **22**: 37–45.

Kitson, F. G.; Larsen, B. S.; McEwen, C. N. 1997. *Gas Chromatography and Mass Spectrometry. A Practical Guide*. Academic Press, San Diego, CA, USA.

Kleinschmidt, M. G.; Dobrenz, A. K.; McMahon, V. A 1968. Gas chromatography of carbohydrates in Alfalfa nectar. *Plant Physiology*, **43**: 665-667.

Knudsen, J. T.; Tollsten, L.; Bergström, G. 1993. Floral scents- a checklist of volatile compounds isolated by headspace techniques. *Phytochemistry*, **33**: 253–280.

Koedam, A.; Scheffer, J. C.; Svendsen, A. B. 1980. Monoterpe nes in the volatile leaf oil of *Abies x arnoldiana* Nitz.. *Journal of Agricultural Food Chemistry*, **28**: 862–866.

König, W. A.; Krüger, A.; Icheln, D.; Runge, T. 1992. Enantiomeric composition of the chiral constituents in essential oils. Part 1: Monoterpene hydrocarbons. *Journal of High Resolution Chromatography*, **15**(3): 184–189.

Korytár, P.; Leonards, P. E. G.; de Boer, J.; Brinkman, U. A. Th. 2002. High-resolution separation of polychlorinated biphenyls by comprehensive two-dimensional gas chromatography. *Journal of Chromatography A*, **958**: 203-218.

Koutsaftikis, A. 1990. Geographische Verbreitung europaischer *Thaumetopoea*-Arten, insbesondere in Griechenland, und ihre Wirtspflanzen. Proceedings of the Thaumetopoeidae-Symposium, 5-7 July 1989, at Neustadt a. Rbge near Hannover, Germany, 8-11.

Krupkin, A. B.; Liston, A.; Strauss, S. H. 1996. Phylogenetic analysis of the hard pines (Pinus subgenus Pinus, Pinaceae) from chloroplast DNA restriction site analysis. *American Journal of Botany*, **83**(4): 489-498.

Lagalante, A. F.; Montgomery, M. E. 2003. Analysis of terpenoids from Hemlock (*Tsuga*) Species by solid-phase microextraction/gas-chromatography/ion-trap mass-spectrometry. *Journal of Agricultural and Food Chemistry*, **51**: 2115–2120.

Lamy, M. 1990. Contact dermatitis (erucism) produced by processionary caterpillars (Genus *Thaumetopoea*). *Journal of Applied Entomology*, **110**: 425-437.

Lamy, M.; Novak, F. 1987. The oak processionary caterpillar (*Thaumetopoea processionea* L.) an urticating caterpillar related to the pine processionary caterpillar (*Thaumetopoea pityocampa* Schiff.) (Lepidoptera, Thaumetopoeidae). *Experientia*, **43**: 456-458.

Lamy, M.; Pastureaud, M.-H.; Novak, F.; Ducombs, G.; Vincedeau, P.; Maleville, J.; Texier, L. 1986. Thaumetopoein: An urticating protein from the hairs and integument of the pine processionary caterpillar (*Thaumetopoea pityocampa* schiff., Lepidoptera, Thaumetopoeidae). *Toxicon*, **24**(4): 347-356.

Langenheim, J. H. 2003. *Plant Resins: Chemistry, Evolution, Ecology and Ethnobotany*. Timber Press, Portland, Cambridge, USA, pp. 23-50.

Larsson, S.; Björkman, C.; Gref, R. 1986. Responses of *Neodiprion sertifer* (Hym., Diprionidae) larvae to variation in needle resin acid concentration in Scots pine. *Oecologia*, **70**: 77-84.

Le Maitre, D. C. 1998. Pines in cultivation: a global view. *In: Ecology and Biogeography of P*inus. D. M. Richardson (ed.), Cambridge University Press, Cambridge, UK, pp. 407-449.

LECO Corp., 2008. LECO Corporation brochure "Pegasus 4D GC × GC TOFMS"; form nº 209-183.

LECO Corp., 2002. Pegasus GC-TOFMS (Form No 203-990-000), Leco Corp, St. Joseph, MI, USA, pp. 1-8.

Lee, A. L.; Bartle, K. L.; Lewis, A. C. 2001. A model of peak amplitude enhancement in ortoghonal twodimensional gas chromatography. *Analytical Chemistry*, **73**:1330-1335.

Lee, A. L.; Lewis, A. C.; Bartle, K. D.; McQuaid, J. B.; Marriott, P. J. 2000. A comparison of modulating interface technologies in comprehensive two-dimensional gas chromatography (GC × GC). *Journal of Microcolumn Separation*, **12**: 187-193.

Lee, A.; Schade, G. W.; Holzinger, R.; Goldstein, A. H. 2005. A comparison of new measurements of total monoterpene flux with improved measurements of speciated monoterpene flux. *Atmospheric Chemistry and Physics*, **5**: 505–513.

Li, K.; Chen, T.; Bicho, P.; Breui, C.; Saddler, J. N. 1996. Factors affecting gas chromatographic analysis of resin acids present in pulp mill effluents. *Toxicological and Environmental Chemistry*, **57**:1-16.

Lin, S.; Binder, B. F.; Hart, E. R. 1998. Isolation, identification, and quantification of potential defense compounds in the Viceroy butterfly and its larval host-plant, *Carolina willow*. *Journal of Chemical Ecology*, **24**(11): 1791–1802.

Liu, Z.; Phillips, J. B. 1991. Comprehensive two-dimensional gas chromatography using an on-column thermal modulator interface. *Journal of Chromatographic Science*, **29**: 227-231.

Loi, R. X.; Solar, M. C. 2008. Solid-phase microextraction method for in vivo measurement of allelochemical uptake. *Journal of Chemical Ecology*, **34**: 70–75.

Looser, R.; Krotzky, A. J.; Trethewey, R. N. 2005. Metabolite profiling with GC-MS and LC-MS. A key tool for contemporary biology. In: *Metabolome Analyses: Strategies for Systems Biology*. Vaidyanathan, P. S.; Harrigan, G. G.; Goodacre, R. (Eds.), Springer, New York, USA, pp. 103-106.

Lord, H.; Pawliszyn, J. 2000. Evolution of solid-phase microextraction technology. *Journal of Chromatography A*, **885**: 153-193.

Louch, D.; Motlagh, S.; Pawliszyn, J. 1992. Dynamics of organic compound extraction from water using liquid-coated fused silica fibers. *Analytical Chemistry*, **64**: 1187–1199.

Lusk, C. 2008. Constraints on the evolution and geographical range of *Pinus*. *New Phytologist*, **178**(1): 1-3.

Ma, C.; Wang, H.; Lu, X.; Li, H.; Liu, B.; Xu, G. 2007. Analysis of Artemisia annua L. volatile oil by comprehensive two-dimensional gas chromatography time-of-flight mass spectrometry. *Journal of Chromatography A*, **1150**(1-2): 50-53.

Magel, E. A.; Hillinger, C.; Wagner, T.; Höll, W. 2001. Oxidative pentose phosphate pathway and pyridine nucleotides in relation to heartwood formation in *Robinia pseudoacacia* L. *Phytochemistry*, **57**(7): 1061-1068.

Majors, R. E. 2003. Response to the 2003 gas chromatography. User study - trends in column use and techniques. *LC•GC North America*, **21**(10): 960.

Makkar, H. P. S.; Siddhuraju, P.; Becker, K. 2007. *Plant Secondary Metabolites*, Methods in Molecular Biology 393, Humana Press Inc., New Jersey, USA.

Manhita, A. C.; Teixeira, D. M.; Costa, C. T. 2006. Applications of sample disruption methods in the extraction of anthocyanins from solid or semi-solid vegetable samples. *Journal of Chromatography A*, **1129**: 14–20.

Mani, V. 1999. Properties of commercial SPME coatings. Chapter 5. In: *Applications of Solid Phase Microextraction*, Pawliszyn, J. (Ed.). RSC Chromatography Monographs, The Royal Society of Chemistry: Cambridge, UK, pp. 57-72.

Markalas, S. 1989. Influence of soil moisture on the mortality, fecundity and diapause of the pine processionary moth (*Thaumetopoea pityocampa* Schiff.). *Journal of Applied Entomology*, **107**: 211-215.

Markalas, S. 1998. Biomass production of *Pinus pinaster* after defoliation by the pine processionary moth (*Thaumetopoea pityocampa* Schiff.). Proceedings: *Population Dynamics, Impacts, and Integrated Management of Forest Defoliating Insects*. M. L. McManus and A. M. Liebhold (Eds.), USDA Forest Service General Technical Report NE-247, pp. 292-302.

Marriott, P. J.; Kinghorn, R. M.; Ong, R.; Morrison, P. 2000. Comparison of thermal sweeper and cryogenic modulator technology for comprehensive gas chromatography *Journal of High Resolution Chromatography*, **23**: 253-258.

Marriott, P.; Shellie, R. 2002. Principles and applications of comprehensive two-dimensional gas chromatography. *Trends in Analytical Chemistry*, **21**(9-10): 573-583.

Marsili, R. 2002. *Flavor, Fragance and Odor Analysis*. Marcel Dekker, Inc. New York, USA.

Martin, D. M.; Faldt, J.; Bohlmann, J. 2004. Functional characterization of nine norway spruce *TPS* genes and evolution of gymnosperm terpene synthases of the *TPS-d* subfamily. *Plant Physiology*, **135**: 1908–1927.

Martin, D.; Tholl, D.; Gershenzon, J.; Bohlmann, J. 2002. Methyl jasmonate induces traumatic resin ducts, terpenoid resin biosynthesis, and terpenoid accumulation in developing xylem of Norway Spruce stems. *Plant Physiology*, **129**: 1003–1018.

Martin, M.; Herman, D. P.; Guiochon, G. 1986. Probability distributions of the number of chromatographically resolved peaks and resolvable components in mixtures. *Analytical Chemistry*, **58**: 2200–2207.

Martos, P A.; Saraullo, A; Pawliszyn, J. 1997. Estimation of air/coating distribution coefficients for solid-phase microextraction using retention from linear temperature-programmed capillary gas chromatography. Application to the sampling and analysis of total petroleum hydrocarbons in air. *Analytical Chemistry*, **69**: 402–408.

Masutti, L.; Battisti, A. 1990. *Thaumetopoea pityocampa* (Den. & Schiff.) in Italy: bionomics and perspectives. *Journal of Applied Entomology*, **110**: 229-234.

Mateus, E. P.; Gomes da Silva, M. D. R.; Ribeiro, A. B.; Marriott, P. J. 2008. Qualitative mass spectrometric analysis of the volatile fraction of creosote-treated railway wood sleepers by using comprehensive two-dimensional gas chromatography. *Journal of Chromatography A*, **1178**(1-2): 215-222.

Matsui, K. 2006. Green leaf volatiles: hydroperoxide lyase pathway of oxylipin metabolism. *Plant Biology*, **9**: 274–280.

McCullough, D. G.; Wagner**,** M. R. 1993. Defusing host defenses: Ovipositional adaptations of pine sawflies to plant resins. *In*: *Sawfly Life History Adaptations of Woody Plants*. M. Wagner and D. F. Raffa (eds.), Academic Press, New York, USA, pp. 157-172.

McDonald, G. R.; Hudson, A. L.; Dunn, S. M. J.; You, H.; Baker, G. B.; Whittal, R. M.; Martin, J. W.; Jha, A.; Edmondson, D. E.; Holt, A. 2008. Bioactive contaminants leach from disposable laboratory plasticware. *Science*, **322**(5903): 917.

McGarvey, D. J.; Croteau, R., 1995. Terpenoid metabolism. *Plant Cell*, **7**(7): 1015–1026.

McMaster, M.; McMaster, C. 1998. GC/MS: A Practical User's Guide, Wiley-VCH.

McNair, H. M.; Miller, J. M. 1998. Basic Gas Chromatography. John Wiley & Sons. Inc. New York, USA.

Mester, Z.; Sturgeon, R.; Pawliszyn, J. 2001. Solid-phase microextraction as a tool for trace element speciation. *Spectrochemica Acta part B*, **56**: 233–260.

Millar, C. I. 1998. Early evolution of pines. *In: Ecology and Biogeography of P*inus. D. M. Richardson (ed.), Cambridge University Press, Cambridge, UK, pp. 69–94.

Millar, J. G.; Haynes, K, F. (Eds.) 1998. Methods in Chemical Ecology. Kluwer Academic Publishers, Boston, USA.

Miller, B.; Madilao, L. L.; Ralph, S.; Bohlmann, J. 2005. Insect-induced conifer defense. white pine weevil and methyl jasmonate induce traumatic resinosis, de novo formed volatile emissions, and accumulation of terpenoid synthase and putative octadecanoid pathway transcripts in Sitka spruce. *Plant Physiology*, **137**: 369–382.

Mirchev, P.; Schmidt, G. H.; Tsankov, G.; Avci, M. 2004. Egg parasitoids of *Thaumetopoea pityocampa* (Den. & Schiff.) (Lep., Thaumetopoeidae) and their impact in SW Turkey. *Journal of Applied Entomology*, **128**(8): 533-542.

Mirov, N. T.; Stanley, R. G. 1959. The pine tree. *Annual Review of Plant Physiology***, 10**: 233–238.

Moilanen, J.; Salminen, J.-P. 2008. Ecologically neglected tannins and their biologically relevant activity: chemical structures of plant ellagitannins reveal their in vitro oxidative activity at high pH. *Chemoecology*, **18**: 73–83.

Moldoveanu, S. C.; David, V. 2002. Sample preparation in chromatography. *Journal of Chromatography Library*, **65**: 165-211.

Moneo, I.; Vega, J. M.; Caballero, M. L.; Vega, J.; Alday, E. 2003. Isolation and characterization of Tha p 1, a major allergen from the pine processionary moth *Thaumetopoea pityocampa*. *Allergy,* **58**: 34-37.

Monnin, T.; Malosse, C.; Peeters, C. 1998. Solid-phase microextraction and cuticular hydrocarbon differences related to reproductive activity in Queenless ant *Dinoponera quadriceps*. *Journal of Chemical Ecology*, **24**(3): 473–490.

Mumm, R.; Hilker, M. 2006. Direct and indirect chemical defence of pine against folivorous insects. *Trends in Plant Science*, **11**(7): 351-358.

Mumm, R.; Tiemann, T.; Schulz, S.; Hilker, M. 2004. Analysis of volatiles from black pine (*Pinus nigra*): significance of wounding and egg deposition by herbivorous sawfly. *Phytochemistry*, **65**: 3221–3230.

Mustaparta, H. 2002. Encoding of plant odour information in insects: peripheral and central mechanisms. *Entomologia Experimentalis et Applicata*, **104**: 1–13.

Musteata, F. M.; Pawliszyn, J. 2007. *In vivo* sampling with solid-phase microextraction. *Journal of Biochemical and Biophysical Methods*, **70**: 181–193.

Nakamura, S.; Hatanaka, A. 2002. Green-leaf-derived C6-aroma compounds with potent antibacterial action that act on both gram-negative and gram-positive bacteria. *Journal of Agricultural and Food Chemistry*, **50**: 7639-7644.

Nielsen, N. 2007. *Metabolomics: a Powerful Tool in Systems Biology*. Springer-Verlag, Berlin and Heidelberg GmbH & Co., Germany, pp. 10-14.

Niessen, W. M. A. 2001. *Current Practice of Gas Chromatography-Mass Spectrometry*. Marcel Dekker, Inc., New York, USA, pp.13.

NIST, 2005. NIST Standard Reference Database Number 69, June 2005 Release, http://webbook.nist.gov/chemistry, accessed in April 2007.

Nordlund, D. A. 1981. Semiochemicals: a review of the terminology. In: *Semiochemicals. Their Role in Pest Control*. D. A. Nordlund, R. L. Jones, W. J. Lewis. John Wiley and Sons, New York, USA, pp. 13-28.

Norin, T. 1972. Some aspects of the chemistry of the Order Pinales. *Phytochemistry***, 11**: 1231-1242.

Norin, T. 1996. Chiral chemodiversity and its role for biological activity. Some observations from studies on insect/insect and insect/plant relationships. *Pure and Applied Chemistry*, **68**(11): 2043-2049.

Nunes, F. M. N.; Veloso, M. C. C.; Pereira, P. A. 2005. Gas-phase ozonolysis of the monoterpenoids (S)-(+)-carvone, (R)-(-)-carvone, (-)-carveol, geraniol and citral. *Atmospheric Environment*, **39**: 7715–7730.

Ochiai, N.; Ieda, T.; Sasamoto, K.; Fushimi, A.; Hasegawa, S.; Tanabe, K.; Kobayashi, S. 2007. Comprehensive two-dimensional gas chromatography coupled to high-resolution time-of-flight mass spectrometry and simultaneous nitrogen phosphorous and mass spectrometric detection for characterization of nanoparticles in roadside atmosphere. *Journal of Chromatography A*, **1150**(1-2): 13-20.

OEPP/EPPO, 2004. Diagnostic protocols for regulated pests *Thaumetopoea pityocampa*. Specific scope. European and Mediterranean Plant Protection Organization PM 7/37(1). *Bulletin OEPP/EPPO,* **34**: 295 –297.

Oliveira, P.; Arnaldo, P. S.; Araújo, M.; Ginja, M.; Sousa, A. P.; Almeida, O.; Colaço, A. 2003. Cinco casos clínicos de intoxicação por contacto com a larva *Thaumetopoea pityocampa* em cães. *Revista Portuguesa de Ciências Veterinárias*, **98**(547): 151- 156.

Ossipov, V.; Bonner, C.; Ossipova, S.; Jensen, R. 2000. Broad-specificity quinate (shikimate) dehydrogenasefrom *Pinus taeda* needles. *Plant Physiology and Biochemistry*, **38**(12): 923-928.

Ossipov, V.; Salminena, J.-P.; Ossipova, S.; Haukioja, E.; Pihlaja, K. 2003. Gallic acid and hydrolysable tannins are formed in birch leaves from an intermediate compound of the shikimate pathway. *Biochemical Systematics and Ecology***, 31**(1): 3-16.

Otto, D.; Geyer*,* W. 1970*.* Zur Bedeutung des Kiefern- nadelharzes und des Kiefernnadeloles fur die Entwicklung nadelfressender insekten. *Arch Forstwes***, 19**: 151-167 [original not seen].

Ouyang, G.; Pawliszyn, J. 2006. SPME in environmental analysis. *Analytical and Bioanalytical Chemistry*, **386**: 1059–1073.

Paiva, M. R. 1997. Personal communication.

Pan, L.; Pawliszyn, J. 1997. Derivatization/solid-phase microextraction: new approach to polar analytes. *Analytical Chemistry*, **69**: 196–205.

Paré, P. W.; Tumlinson, J. H. 1999. Plant volatiles as a defense against insect herbivores *Plant Physiology*, **121**(2): 325-332.

Paré; P. W.; Tumlinson, J. H. 1997. De novo biosynthesis of volatiles induced by insect herbivory in cotton plants. *Plant Physiologist*, **114**: 1161-1167.

Park, C. G.; Lee, K. C.; Lee, D. W.; Choo, H. Y.; Albert, P. J. 2004. Effects of purified persimmon tannin and tannic acid on survival and reproduction of bean bug, Riptortus clavatus. *Journal of Chemical Ecology*, **30**(11): 2269-2283.

Pauly, G.; Gleizes, M.; Dagan, B., M. 1973. Identification des constituents de l´essence des aiguilles de *Pinus pinaster*. *Phytochemistry*, **12**(6): 1395–1398.

Pawliszyn, J. 1997. *Solid Phase Microextraction: Theory and Practice*. Wiley-VCH, Inc., New York, USA, 242 pp..

Pérez-Contreras, T.; Soler, J. J.; Soler, M. 2003. Why do pine processionary caterpillars *Thaumetopoea pityocampa* (Lepidoptera, Thaumetopoeidae) live in large groups? An experimental study. *Annales Zoologici Fennici,* **40**: 1-11.

Pérez-Contreras, T.; Soler, J. J.; Soler, M. 2008. Needle asymmetry, pine vigour and pine selection by the processionary moth *Thaumetopoea*. *Acta Oecologica,* **33**: 213-221.

Petrakis, P. V.; Roussis, V.; Papadimitriou, D.; Vagias, C.; Tsitsimpikou, C. 2005. The effect of terpenoid extracts from 15 pine species on the feeding behavioural sequence of the late instars of the pine processionary caterpillar *Thaumetopoea pityocampa*. *Behavioural Processes*, **69**: 303–322.

Pfeifhofer, H. W. 2000. Composition of the essential oil of *Pinus canariensis* Sweet ex Sprengel. *Flavour and Fragrance Journal*, **15**(4): 266-270.

Phillips, J. B.; Beens, J. 1999. Comprehensive two-dimensional gas chromatography: a hyphenated method with strong coupling between the two dimensions. *Journal of Chromatography A*, **856**: 331-347.

Phillips, M. A.; Croteau, R. B. 1999. Resin-based defenses in conifers. *Trends in Plant Science*, **4**(5): 184-190.

Pichersky, E.; Gershenzon, J. 2002. The formation and function of plant volatiles: perfumes forpollinator attraction and defense. *Current Opinion in Plant Biology*, **5**: 237-243.

Pichersky, E.; Noel, J. P.; Dudareva, N. 2006. Biosynthesis of plant volatiles: nature's diversity and ingenuity. *Science*, **311**: 808-811.

Pimentel, C. S. M. G. 2004. *Pine processionary moth (Thaumetopoea pityocampa) and great tit (Parus major) in Portugal: population dynamics and interactions*. Ph.D Thesis. Faculdade de Ciências e Tecnologia, Universidade Nova de Lisboa, Lisbon, Portugal, 171 pp..

Pimentel, C.; Calvão, T.; Santos, M.; Ferreira, C.; Neves, M.; Nilsson, J.-A. 2006. Establishment and expansion of a *Thaumetopoea pityocampa* (Den. & Schiff.) (Lep. Notodontidae) population with a shifted life cycle in a production pine forest, Central-Coastal Portugal. *Forest Ecology and Management*, **233**(1): 108-115.

Pool, W. G.; de Leeuw, J. W.; van de Graaf, B. 1996. A rapid routine to correct for skewing in gas chromatography/mass spectrometry. *Journal of Mass Spectrometry*, **31**: 213-215.

Poole, C. F. 2003. *The Essence of Chromatography*. Elsevier, Boston, USA.

Potter, D. W; Pawliszyn, J. 1992. Detection of substituted benzenes in water at the PG/ML level using solid-phase microextraction and gas-chromatography ion trap mass-spectrometry. *Journal of Chromatography*, **625**(2): 247–255.

Pragst, F. 2007. Application of solid-phase microextraction in analytical toxicology. *Analytical and Bioanalytical Chemistry*, **388**: 1393–1414.

Price, R. A.; Liston, A.; Strauss, S. H. 1998. Phylogeny and systematics of *Pinus*. *In: Ecology and Biogeography of P*inus. D. M. Richardson (ed.), Cambridge University Press, Cambridge, UK, pp. 49-68.

Proestos, C.; Komaitis, M. 2008. Applications of microwave-assisted extraction to the fast extraction of plant phenolic compounds. *LWT Food Science and Technology*, **41**: 652–659.

Prudic, K. L.; Khera, S.; Sólyom, A.; Timmermann, B. N. 2007. Isolation, identification, and quantification of potential defense compounds in the Viceroy butterfly and its larval host-plant, Carolina Willow. *Journal of Chemical Ecology*, **33**: 1149–1159.

Quero, C.; Malo, E. A.; Fabriàs, G.; Camps, F.; Lucas, P.; Renou, M.; Guerrero, A. 1997. Reinvestigation of female sex pheromone of processionary moth (*Thaumetopoea pityocampa*): no evidence for minor components. *Journal of Chemical Ecology*, **23**(3): 713-726.

Reddy, G. V. P.; Guerrero, A. 2004. Interactions of insects pheromones and plant semiochemicals. *Trends in Plant Science*, **9**: 253-261.

Renwick, J. A. A. 1988. Comparative mechanismis of host selection by insects attacking pine trees and crucifers. In: *Chemical Mediation of Coevolut*ion, Kevin C. Spencer (Ed.), Academic Press, San Diego, Ca, USA, pp. 303-316.

Richardson, D. M.; Rundel, P. W. 1998. Ecology and biogeography of Pinus: an introduction. *In: Ecology and Biogeography of P*inus. D. M. Richardson (ed.), Cambridge University Press, Cambridge, UK, pp. 3–48.

Richardson, D. M.; Rundel, P. W.; Jackson, S. T.; Teskey, R. O.; Aronson, J.; Bytnerowicz, A.; Wingfield, M. J.; Proches, S. 2007. Human impacts in pine forests: Past, present, and future. *Annual Review of Ecology Evolution and Systematics*, **38**: 275-297.

Robinet, C.; Baier, P.; Pennerstorfer, J.; Schopf, A.; Roques, A. 2007. Modelling the effects of climate change on the potential feeding activity of *Thaumetopoea pityocampa* (Den. & Schiff.) (Lep., Notodontidae) in France. *Global Ecology and Biogeography*, **16**: 460-471.

Rochat, D.; Ramirez-Lucas, P.; Malosse, C.; Aldana, R. Kakul, T.; Morin, J.-P. 2000. Role of solid-phase microextraction in the identification of highly volatile pheromones of two Rhinoceros beetles *Scapanes australis* and *Strategus aloeus* (Coleoptera, Scarabaeidae, Dynastinae). *Journal of Chromatography A*, **885**: 433–444.

Rodrigues, E. B. P. M. 2002. *Interacções produtividade/fitófagos para o ecossistema pinhal.* Ph.D Thesis. Faculdade de Ciências e Tecnologia, Universidade Nova de Lisboa, Lisbon, Portugal, 217 pp..

Rood, D. 2007. *The Troubleshooting and Maintenance Guide for Gas-chromatographers*. 4th revised and updated edition, WILEY-VCH Verlag GmbH & Co. KGaA, Weinheim, Germany.

Rouget, M.; Richardson, D. M.; Milton, S. J.; Polakow, D. 2004. Predicting invasive dynamics of four alien *Pinus* species in a highly fragmented semi-arid shrubland in South Africa. *Plant Ecology*, **152**: 79-92.

Rundel, P. W.*;* Yoder, B. J. 1998. Ecophysiology of *Pinus*. *In: Ecology and Biogeography of P*inus. D. M. Richardson (ed.), Cambridge University Press, Cambridge, UK, pp. 296-340.

Ryan, D.; Robards, K.; Prenzler, P.; Antolovich, M. 1999. Applications of mass spectrometry to plant phenols. *Trends in Analytical Chemistry*, **18**(5): 362-372.

Sabillón, D.; Cremades; L. V. 2001. Diurnal and seasonal variation of monoterpene emission rates for two typical Mediterranean species (*Pinus pinea* and *Quercus ilex*) from field measurements-relationship with temperature and PAR. *Atmospheric Environment*, **35**: 4419–4431.

Sacchettini, J. C.; Poulter, C. D. 1997. Creating isoprenoid diversity. *Science*, **277**(5333), 1788-1789.

Salas, J. J.; García-González, D. L.; Aparicio, R. 2006. Volatile compound biosynthesis by green leaves from an *Arabidopsis thaliana* hydroperoxide lyase knockout mutant. *Journal of Agricultural and Food Chemistry*, **54**: 8199-8205.

Sandra, P.; Bicchi, C. (Eds.) 1987. *The Capillary Gas Chromatography in Essential Oil Analysis*. Dr. Alfred Huethig Verlag, Heidelberg, Germany.

Santos, A. M.; Vasconcelos, T.; Mateus, E. P.; Farrall, M. H.; Gomes da Silva, M. D. R.; Paiva, M. R.; Branco, M. 2006. Characterization of the volatile fraction emitted by phloems of four pinus species by solid-phase microextraction and gas-chromatography-mass-spectrometry. *Journal of Chromatography A*, **1105**: 191–198.

Santos, H.; Rousselet, J.; Magnoux, E.; Paiva, M-R.; Branco, M.; Kerdelhué, C. 2007. Genetic isolation through time: allochronic differentiation of a phenologically atypical population of the pine processionary moth. *Proceedings of the Royal Society B*, **274**: 935-941.

Saraullo, A.; Martos, P A.; Pawliszyn, J. 1997. Water analysis by solid phase microextraction based on physical chemical properties of the coating. *Analytical Chemistry*, **69**: 1992–1998.

Schmidt, G. H. 1990. Life cycles of *Thaumetopoea* species distribution in different regions of Europe, north Africa and near east. Proceedings of the Thaumetopoeidae-Symposium, 5-7 July 1989, at Neustadt a. Rbge near Hannover, pp. 20-34.

Schmidt, G. H.; Breuer, M.; Devkota, B.; Bellin, S. 1990. Life cycle and natural enemies of *Thaumetopoea pityocampa* (Den. & Schifft.). Proceedings of the Thaumetopoeidae-Symposium, 5-7 July 1989, at Neustadt a. Rbge near Hannover, 36-40.

Schmidt, G. H.; Tanzen, E.; Bellin, S. 1999. Structure of egg-batches of *Thaumetopoea pityocampa* (Den. and Schiff.) (Lep., Thaumetopoeidae), egg parasitoids and rate of egg parasitism on the Iberian Peninsula. *Journal of Applied Entomology*, **123**: 449-458.

Schoenmakers, P.; Marriott, P.; Beens, J. 2003. Nomenclature and conventions in comprehensive multidimensional chromatography. *LC•GC Europe*, **16**: 335-339.

Scholes, M. C.*;* Nowicki, T. E. 1998. Effects of pines on soil properties and processes. *In: Ecology and Biogeography of P*inus. D. M. Richardson (Ed.), Cambridge University Press, Cambridge, UK, pp. 341-353.

Schomburg, G.; Husmann, H.; Hübinger, E.; König, W. 1984. Multidimensional capillary gas chromatography-enantiomeric separations of selected cuts using a chiral second column. *Journal of High Resolution Chromatography*, **7**: 404– 410.

Schoonhoven, L. M. 1981. Chemical mediators between plants and phytophagous insects. In: *Semiochemicals. Their Role in Pest Control*. D. A. Nordlund, R. L. Jones, W. J. Lewis. John Wiley and Sons, New York, USA, pp. 31-50.

Schopf, R.; Avtzis, N. 1987. Die bedeutung von Nadelinhalsstoffen für die disposition von fünf kiefernarten gegenüber *Thaumetopoea pityocampa* (Schiff.). *Journal of Applied Entomology*, **103**: 340-350.

Scott, R. P. W. 1996. *Chromatographic Detectors. Design, Function, and Operation*. Marcel Dekker, Inc. New York, USA.

Scott, R. P. W. 2002. Split /splitless injector. *In*: *Encyclopedia of Chromatography.* Cazes, J. (Ed.), Marcel Dekker, New York, USA.

Selfa, J.; López-Sebastián, E.; Guara, M.; Pujade-Villar, J.; Dilata, J. 2005. Some aspects of the life cycle of the moth species *Thaumetopoea pityocampa* at four Mediterranean forests (Lepidoptera: Notodontidae). *Entomologia Generalis*, **28**(2): 121-138.

Serra, M.; Piña, B.; Abad, J. L.; Camps, F.; Fabriàs, G. 2007. A multifunctional desaturase involved in the biosynthesis of the processionary moth sex pheromone. *PNAS*, **104**(42): 16444-16449.

Shellie, R.; Marriott, P. 2002. Comprehensive two-dimensional gas chromatography with fast enantioseparation. *Analytical Chemistry*, **74**: 5426 5430.

Shellie, R.; Marriott, P.; Cornwell, C. 2001. Application of comprehensive twodimensional gas chromatography (GC × GC) to the enantioselective analysis of essential oils. *Journal of Separation Science*, **24**: 823-830.

Shellie, R.; Mondello, L.; Marriot, P.; Dugo, G. 2002. Characterisation of lavender essential oils by using gas chromatography-mass spectrometry with correlation of linear retention indices and comparison with comprehensive two-dimensional gas chromatography. *Journal of Chromatography A*, **970**: 225-234.

Shevelev, A. B.; Battisti, A.; Volynskaya, A. M.; Novikova, S. I.; Kostina, L. I.; Zalunin, I. A. 2001. Susceptibility of the pine processionary caterpillar *Thaumetopoea pityocampa* (Lepidoptera: Thaumetopoeidae) toward δ-endotoxins of *Bacillus thuringiensis* under laboratory conditions. *Annals of Applied Biology*, **138**: 255-261.

Shibamoto, T. 1987. *In: Capillary Gas Chromatography in Essential Oil Analysis*. P. Sandra, P.; Bicchi, C. (Eds.), Huethig Verlag, Heidelberg, Germany, pp. 259.

Shirey, R. 2007. Selecting the appropriate SPME fiber coating. Effect of analyte molecular weight and polarity. *The Reporter,* **28**: 13-15.

Smith, R. M. 2004. *Understanding Mass Spectra: A Basic Approach*. 2nd edition, Wiley-Interscience, John Wiley & Sons, Inc., USA.

Soares da Silva, A. M. 1982. Carta Litológica (1:1000000). Comissão Nacional do Ambiente, Lisboa, Portugal.

Solt, I.; Mendel, Z. 2002. The pine processionary caterpillar, *Thaumetopoea pityocampa*. *Harefuah*, **141**(9): 810-814.

Song, S. M.; Marriott, P.; Wynne, P. 2004. Comprehensive two-dimensional gas chromatography-quadrupole mass spectrometric analysis of drugs. *Journal of Chromatography A*, **1058**(1-2): 223-232.

Spencer, K. C. 1988a. Introduction: chemistry and coevolution. *In*: *Chemical Mediation of Coevolut*ion, Kevin C. Spencer (Ed.), Academic Press, San Diego; CA, USA, pp. 1-11.

Spencer, K. C. 1988b. The chemistry of coevolution. In: *Chemical Mediation of Coevolut*ion, Kevin C. Spencer (Ed.), Academic Press, San Diego; CA, USA, pp. 581-587.

Stashenko, E. E.; Martínez, J. R. 2007. Sampling volatile compounds from natural products with headspace/solid-phase micro-extraction. *Journal of Biochemical and Biophysical Methods*, **70**(2): 235-242.

Stastny, M.; Battisti, A.; Petrucco-Toffolo, E.; Schlyter, F.; Larsson, S. 2006. Host-plant use in the range expansion of the pine processionary moth, *Thaumetopoea pityocampa***.** *Ecological Entomology*, **31**: 481-490.

Staudt, M.; Bertin, N.; Hansen, U.; Seufert, G.; Ciccioli, P.; Foster, P.; Frenzel, B.; Fugit, J.-L. 1997. Seasonal and diurnal patterns of monoterpene emissions from *Pinus pinea* (L.) under field conditions. *Atmospheric Environment*, **31**: 145-156.

Stephanou, E. G. 2007. A forest air of chirality. *Nature,* **446**: 991.

Stranden, M.; Borg-Karlson, A.-K.; Mustaparta, H. 2002. Receptor neuron discrimination of the germacrene D enantiomers in the moth *Helicoverpa armigera*. *Chemical Senses*, **27**: 143-152.

Subchev, M. A.; Moskova, R.; Tzankov, G. 1994. Attraction of *Thaumetopoea pityocampa* Denis & Schiff. by synthetic sex pheromone in the field. *Pheromones*, **4**(1-2): 3–10.

Supelco Inc., 1998. Solid phase microextraction: theory and optimization of conditions (Bulletin 923), Supelco, Bellefonte, PA, USA, pp. 1-8.

Supelco Inc., 1995. Supelco T713019A data sheet, Supelco, Bellefonte, PA, USA, pp. 1-2.

Tarvainen, V.; Hakola, H.; Hellén, H.; Back, J.; Hari, P.; Kulmala, M. 2005. Temperature and light dependence of the VOC emissions of Scots pine. *Atmospheric Chemistry and Physics*, **5**: 989–998.

Tentschert, J.; Bestmann, H. J.; Heinze, J. 2002. Cuticular compounds of workers and queens in two *Leptothorax* ant species -a comparison of results obtained by solvent extraction, solid sampling, and SPME. *Chemoecology*, **12**: 15–21.

Theis, N.; Manuel Lerdau, M. 2003. The evolution of function in plant secondary metabolites. *International Journal of Plant Sciences*, **164**: S93–S102.

Theodoridis, G.; Koster, E. H. M.; de Jong, G. J. 2000. Solid-phase microextraction for the analysis of biomedical samples. *Journal of Chromatography B*, **745**: 49–82.

Tholl, D.; Boland, W.; Hensel, A.; Loreto, F.; Rose, U. S. R.; Schnitzler, J. P. 2006. Practical approaches to plant volatile analysis. *The Plant Journal*, **45**: 540-560.

Tiberi, R. 1990. Egg parasitoids of the pine processionary caterpillar, *Thaumetopoea pityocampa* (Den. & Schiff.) (Lep., Thaumetopoeidae) in Italy: distribution and activity in different areas. *Journal of Applied Entomology*, **110**: 14-18.

Tiberi, R.; Niccoli, A.; Curini, M.; Epifano, F.; Marcotullio, M. C.; Rosati, O. 1999. The role of the monoterpene composition in *Pinus* spp. needles, in host selection by the pine processionary caterpillar, *Thaumetopoea pityocampa*. *Phytoparasitica*, **27**(4): 263-272.

Tittiger, C. 2003. Molecular biology of bark beetle pheromone production and endocrine regulation. In: *Insect Pheromone Biochemistry and Molecular Biology. Biosynthesis and detection of pheromones and plant volatiles*, G. J. Blomquist, R. G. Vogt (Eds.), Elsevier Academic Press, London, UK, pp. 201-230.

Tonidandel, L.; Sartori, E.; Traldi, P. 2008. Assessing the benefits of a "hike in the mountains" using SPME. *Reporter*, **31**: 8–10.

Trewhella, K. E.; Leather, S. R.; Day, K. R. 2000. Variation in the suitability of *Pinus contorta* (lodgepole pine) to feeding by three pine defoliators, *Panolis flammea*, *Neodiprion sertifer* and *Zeiraphera diniana*. *Journal of Applied Entomology,* **124**: 11-17.

Triggiani, O.; Tarasco, E. 2001. Priliminary attempts to control overwintering populations of *Thaumetopoea pityocampa* (Den. et Schifft.) (Lepidoptera: Thaumetopoeidae) with *Steinernema feltiae* (Filipjev, 1934) (Nematoda: Steinernematidae)*. *Entomologica,* **35**: 7-15.

Triggiani, O.; Tarasco, E. 2002. Efficacy and persistence of entomopathogenic nematodes in controlling larval populations of *Thaumetopoea pityocampa* (Lepidoptera: Thaumetopoeidae). *Biocontrol Science and Technology,* **12**: 747-752.

Ulrich, S. 2000. Solid-phase microextraction in biomedical analysis. *Journal of Chromatography A*, **902**: 167–194.

Vaes, W. H. J.; Hamwijk, C.; Ramos, E. U.; Verhaar, H. J. M.; Hermens, J. L. M. 1996. Partitioning of organic chemicals to polyacrylate-coated solid phase microextraction fibers: kinetic behaviour and quantitative structure-property relationships. *Analytical Chemistry*, **68**: 4458–4462.

van den Berg, K. J.; Boon, J. J.; Pastorovay, I.; Spetter, L. F. M. 2000. Mass spectrometric methodology for the analysis of highly oxidized diterpenoid acids in old master paintings. *Journal of Mass Spectrometry*, **35**: 512–533.

van den Dool, H.; Kratz, P. D. J. 1963. A generalization of retention index system including linear temperature programmed gas-liquid partition chromatography. *Journal of Chromatography*, **11**: 463–471.

Vega, J. M.; Moneo, I.; Armentia, A.; Lopez-Rico, R.; Curiel, G.; Bartolomé, B.; Fernández, A. 1997. Anaphylaxis to the pine caterpillar. *Allergy*, **52**: 1244-1245.

Vega, J. M.; Vega, J.; Veja, M. L.; Moneo, I.; Armentia, A.; Sánchez, B. 2003. Skin reactions to pine processionary caterpillar. *Allergy,* **58**: 87-88.

Vega, J.; Vega, J. M.; Moneo, I.; Armentia, A.; Caballero, M. L.; Miranda, A. 2004. Occupational immunologic contact urticaria from pine processionary caterpillar (*Thaumetopoea pityocampa)*: experience in 30 cases. *Contact Dermatitis*, **50**: 60–64.

Venkatramani, C. J.; Xu, J.; Phillips, J. B. 1996. Separation orthogonality in temperature-programmed comprehensive two-dimensional gas chromatography. *Analytical Chemistry*, **68**: 1486-1492.

Vernin, G.; Petitjean, M.; Metzger, J.; Fraisse, D.; Suon, K. N.; Scharff, C. 1987. *In*: *Capillary Gas Chromatography in Essential Oil Analysis*. P. Sandra, P.; Bicchi, C. (Eds.), Huethig Verlag, Heidelberg, Germany, 1987, pp. 287.

Villorbina, G.; Rodríguez, S.; Camps, F.; Fabriàs, G. 2003. Comparative sex pherome biosynthesis in *Thaumetopoea pityocampa* and *T. processionea*: a rationale for the phenotypic variation in the sex pherome within the Genus *Thaumetopoea*. *Insect Biochemistry and Molecular Biology*, **33**: 155–161.

Visser, J. H. 1996. Host odor perception in phytophagous insects. *Annual Review of Entomology*, **31**: 121-144.

Vogel, A. I. 1989. *In*: *Vogel's textbook of practical organic chemistry*, Longman Scientific and Technical, London, pp. 430.

Vreuls, R. J.; Dallüge, J.; Brinkman, U. A. Th. 1999. Gas chromatography-time-of-flight mass spectrometry for sensitive determination of organic mictrocontaminants. *Journal of Microcolumn Separation*, 11: 663-675.

Wagner, M. R; Clancy, K. M.; Tinus, R. W. 1990. Seasonal patterns in the allelochemicals of *Pseudotsuga. menziesii*, *Picea engelmanii* and *Abies concolor*. *Biochemical Systematics and Ecology*, **18**(4): 215-220.

Way, M. J.; Paiva, M. R.; Cammell, M. E. 1999. Natural biological control of the pine processionary moth *Thaumetopoea pityocampa* (Den. & Schiff.) by the Argentine ant *Linepithema humile* (Mayr) in Portugal. *Agricultural and Forest Entomology*, **1**: 27–31.

Wegener, R.; Schulz, S. 2002. Identification and synthesis of homoterpenoids emitted from elm leaves after elicitation by beetle eggs. *Tetrahedron*, **58**(2): 315-319.

Wiley Registry of Mass Spectral Data 7th Edition, 2000.

Williams, J.; Yassaa, N.; Bartenbach, S.; Lelieveld, J. 2007. Mirror image hydrocarbons from Tropical and Boreal forests. *Atmospheric Chemistry and Physics*, **7**: 973–980.

Willyard, A.; Syring, J.; Gernandt, D. S.; Liston, A.; Cronn, R. 2007. Fossil calibration of molecular divergence infers a moderate mutation rate and recent radiations for *Pinus*. *Molecular Biology and Evolution*, **24**(1): 90-101.

Wise, A.; Borg-Karlson, A.-K.; Persson, M.; Norin, T.; Mustaparta, H. 1998. Enantiomeric composition of monoterpene hydrocarbons in some conifers and receptor neuron discrimination of a-pinene and limonene enantiomers in the pine weevil, *Hylobius abietis*. *Journal of Chemical Ecology*, **24**(2): 273-287.

Wittkowski, R.; Matissek, R. (Eds). 1990. *Capillary Gas Chromatography in Food Control Research*. Technomic Publishing Co, Inc, Lancaster, U.K.

Yang, J.-W.; Orihara, Y. 2002. Biosynthesis of abietane diterpenoids in cultured cells of *Torreya nucifera* var. *radicans*: biosynthetic inequality of the FPP part and the terminal IPP. *Tetrahedron*, **58**(7): 1265-1270.

Yang, X.; Peppard, T. 1995. Solid-phase microextraction flavor compounds – a comparison of two fiber coatings and a discussion of the rules of thumb for adsorption. *LC•GC*, **13**(11): 882–886.

Yang, Y.; Hawthorne, S. B.; Miller, D. J.; Liu, Y.; Lee, M. L. 1998. Adsorption versus absorption of polychlorinated biphenyls onto solid-phase microextraction coatings. *Analytical Chemistry*, **70**: 1866–1869.

Yassaa, N.; Williams, J. 2007. Enantiomeric monoterpene emissions from natural and damaged Scots pine in a boreal coniferous forest measured using solid-phase microextraction and gas-chromatography/mass-spectrometry. *Journal of Chromatography A*, **1141**: 138–144.

Yuwono, M.; Indrayanto, G. 2004. Gas Chromatography system instrumentation. In: *Encyclopedia of Chromatography*. Cazes, J. (Ed.). Marcel Dekker.

Zhang, Q.-H.; Schlyter, F.; Battisti, A.; Birgersson, G.; Anderson, P. 2003. Electrophysiological responses of *Thaumetopoea pityocampa* females to host volatiles: implications for host selection of active and inactive terpenes. *Journal of Pest Science*, **76**: 103–107.

Zhang, Z.; Pawliszyn, J. 1993. Headspace solid-phase microextraction. *Analytical Chemistry*, **65**: 1843–1852.

Zrostlíková, J.; Hajslová, J.; Cajka, T. 2003. Evaluation of two-dimensional gas chromatography–time-of-flight mass spectrometry for the determination of multiple pesticide residues in fruit. *Journal of Chromatography A*, **1019**(1-2): 173-186.

Zrostlíková, J.; Hajslová, J.; Godula, M.; Mastovska, K. 2001. Performance of programmed temperature vaporizer, pulsed splitless and on-column injection techniques in analysis of pesticide residues in plant matrices. *Journal of Chromatography A*, **937**: 73–86.

Appendices

Appendix A – Representative TICs for the studied *Pinus* spp.

Appendix B – Chemical standards used for analyte identification.

Appendix C – *T. pityocampa* final weight, biomass consumption, faeces produced, food assimilated and survival, observed in the experiment of larvae performance (Branco *et al.*, in prep.).

Appendix A

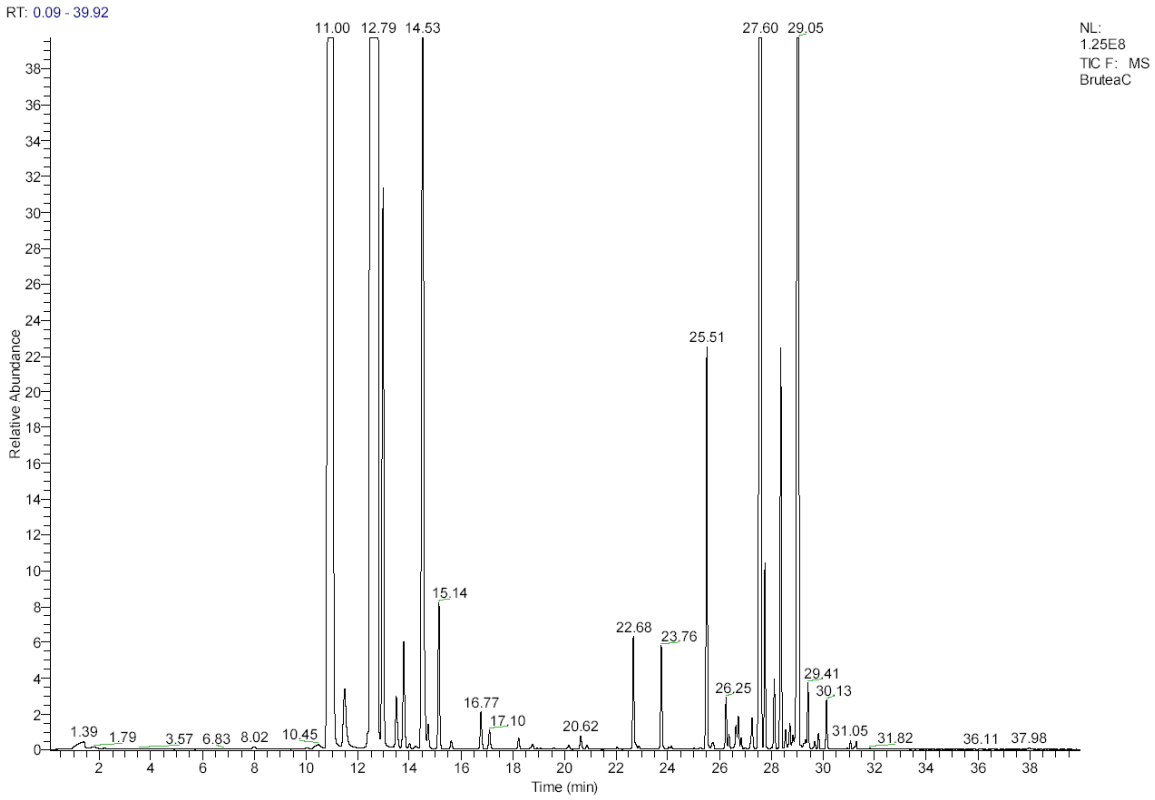

Figure A.1 - Reconstructed total ion chromatogram from the headspace of *P. brutia* needles analyzed on the DB-5ms column.

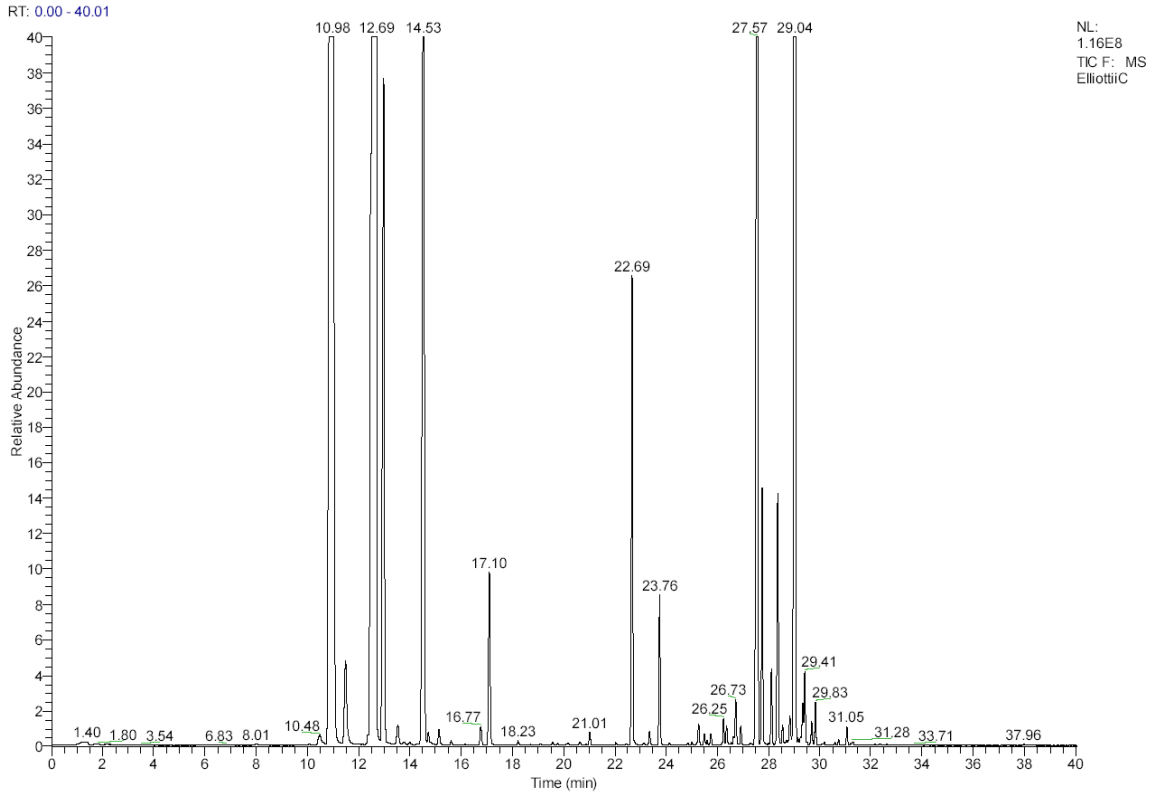

Figure A.2 - Reconstructed total ion chromatogram from the headspace of *P. elliottii* needles analyzed on the DB-5ms column.

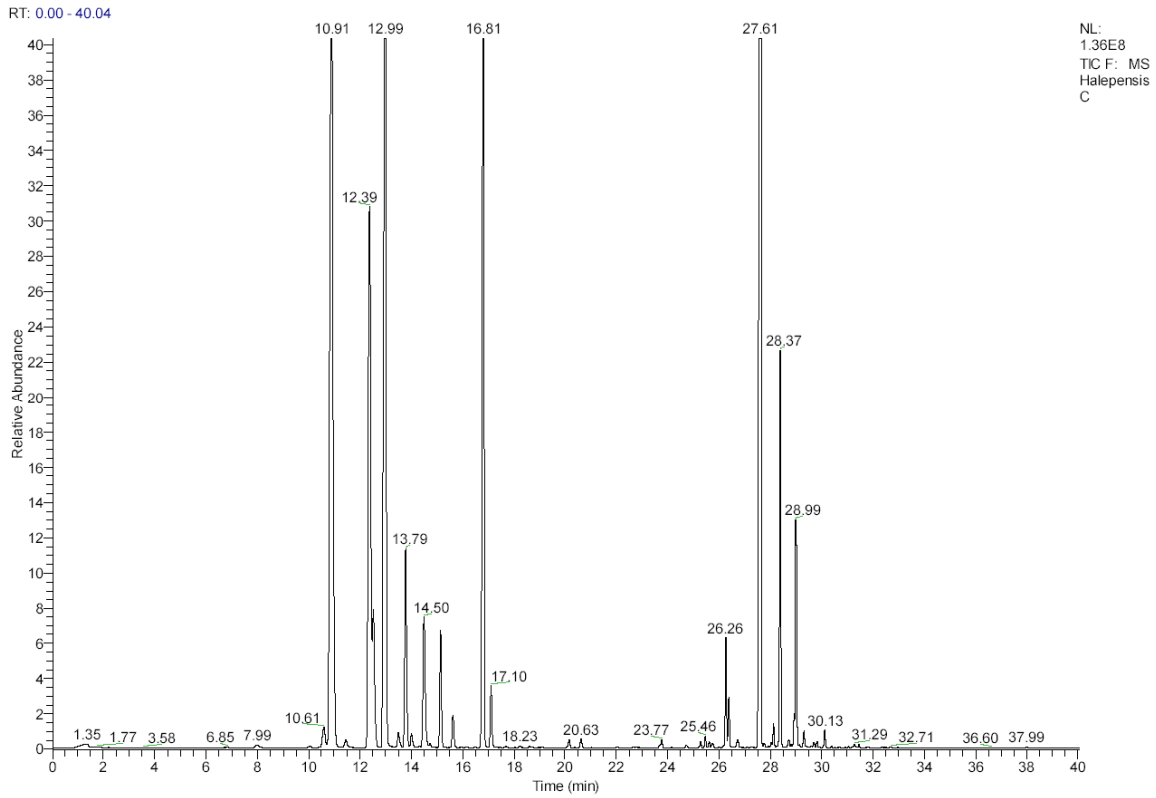

Figure A.3 - Reconstructed total ion chromatogram from the headspace of *P. halepensis* needles analyzed on the DB-5ms column.

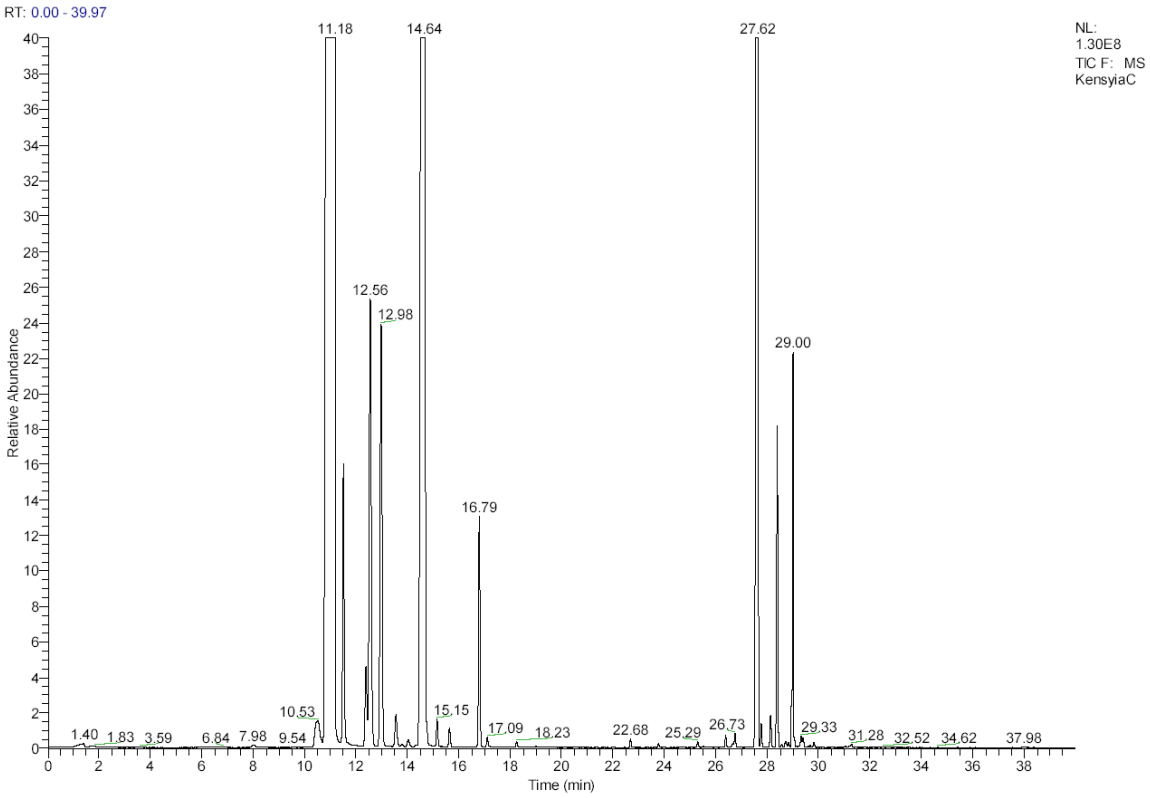

Figure A.4 - Reconstructed total ion chromatogram from the headspace of *P. kesiya* needles analyzed on the DB-5ms column.

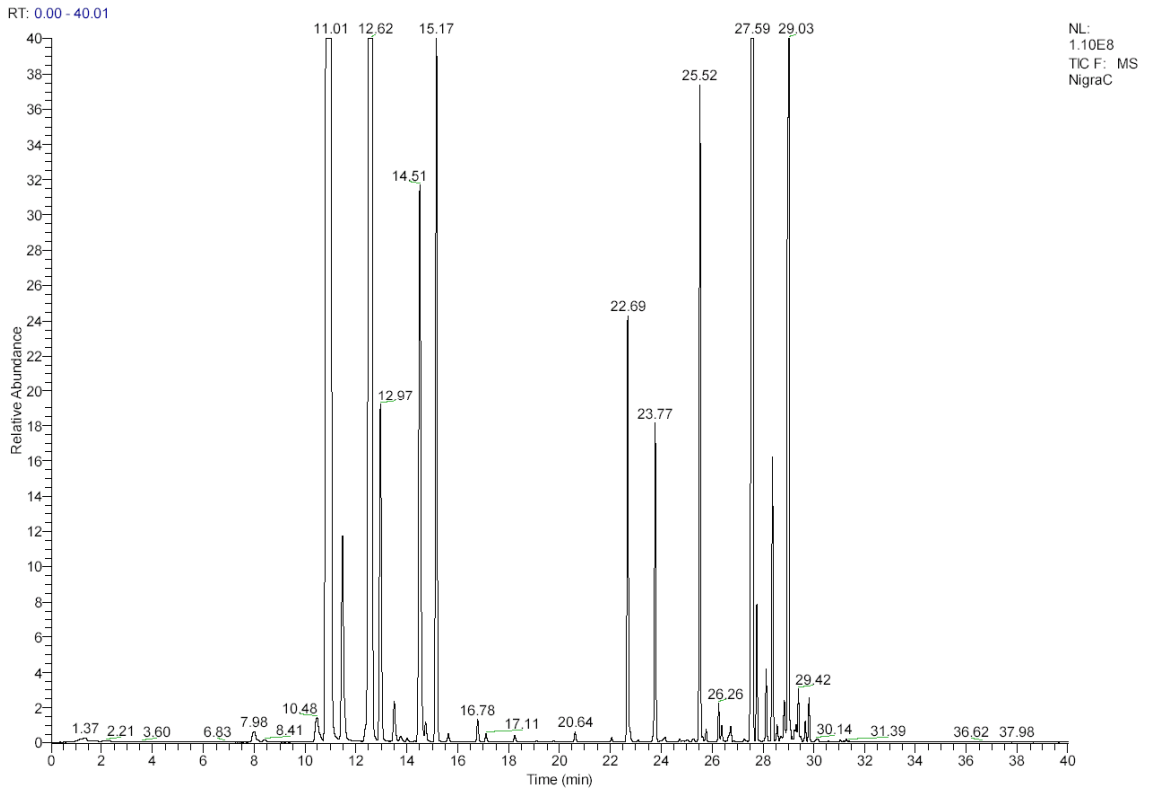

Figure A.5 - Reconstructed total ion chromatogram from the headspace of *P. nigra* needles analyzed on the DB-5ms column.

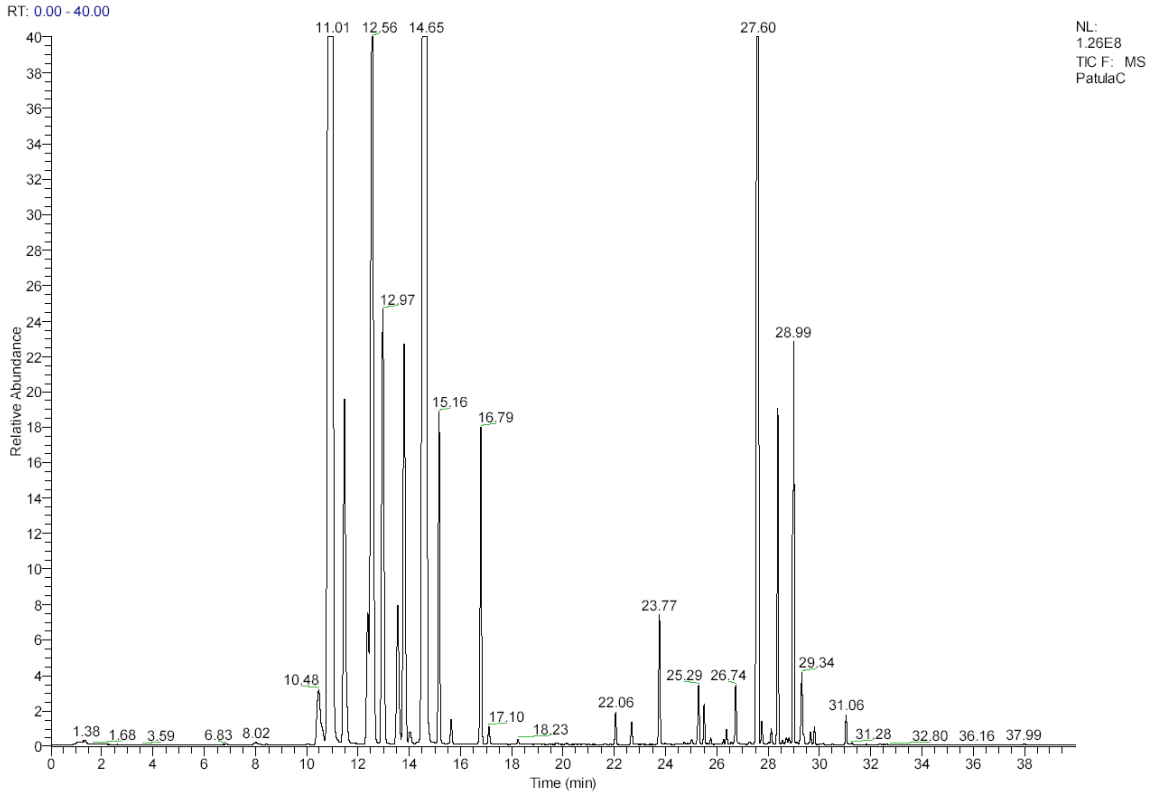

Figure A.6 - Reconstructed total ion chromatogram from the headspace of *P. patula* needles analyzed on the DB-5ms column.

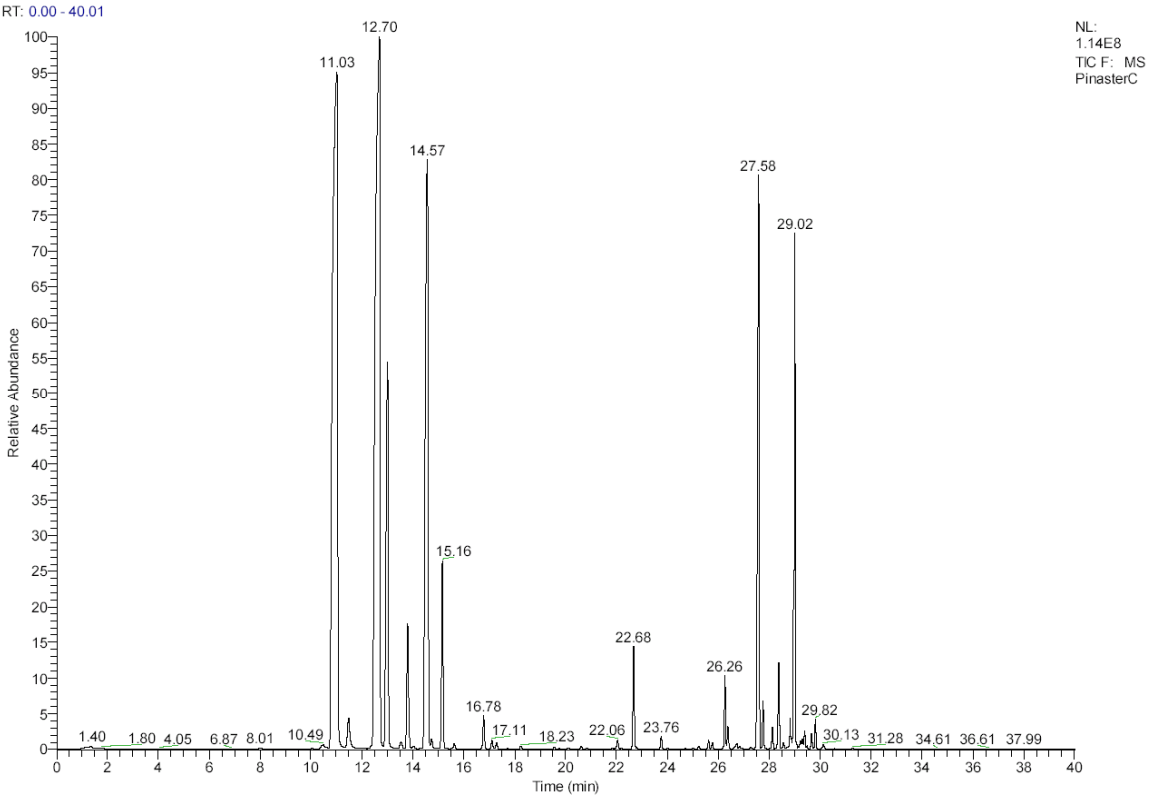

Figure A.7 - Reconstructed total ion chromatogram from the headspace of *P. pinaster* needles analyzed on the DB-5ms column.

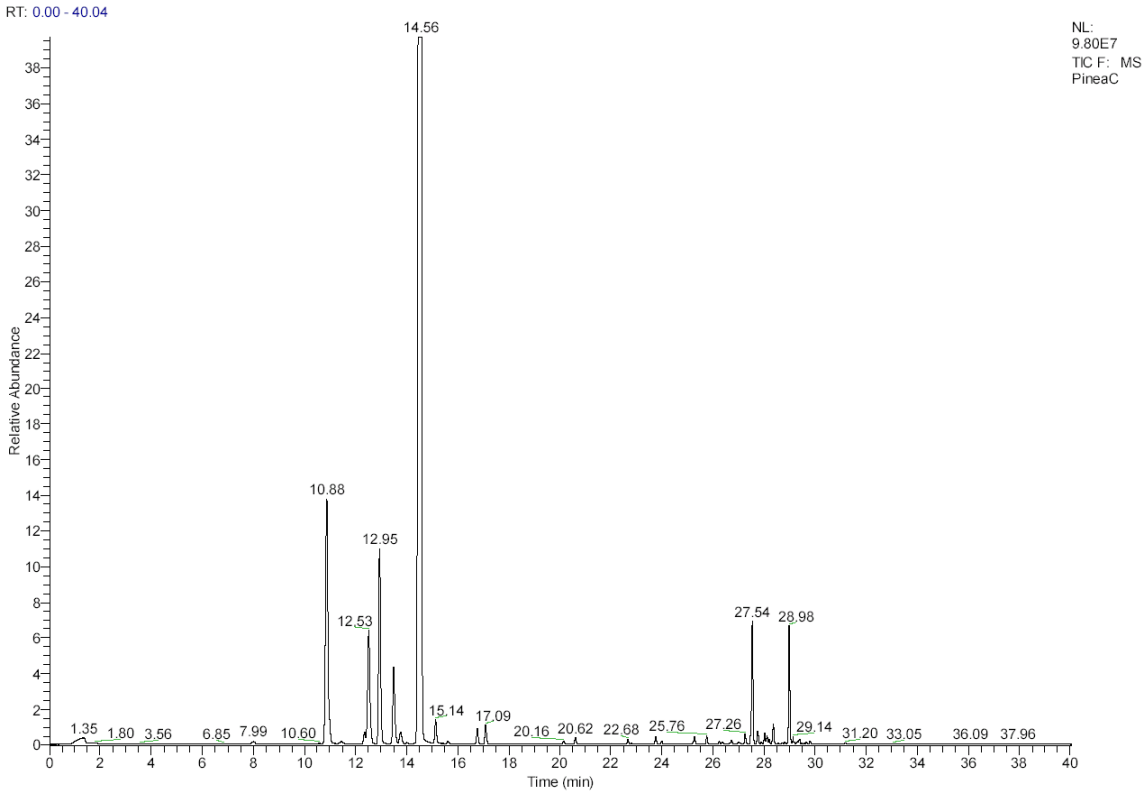

Figure A.8 - Reconstructed total ion chromatogram from the headspace of *P. pinea* needles analyzed on the DB-5ms column.

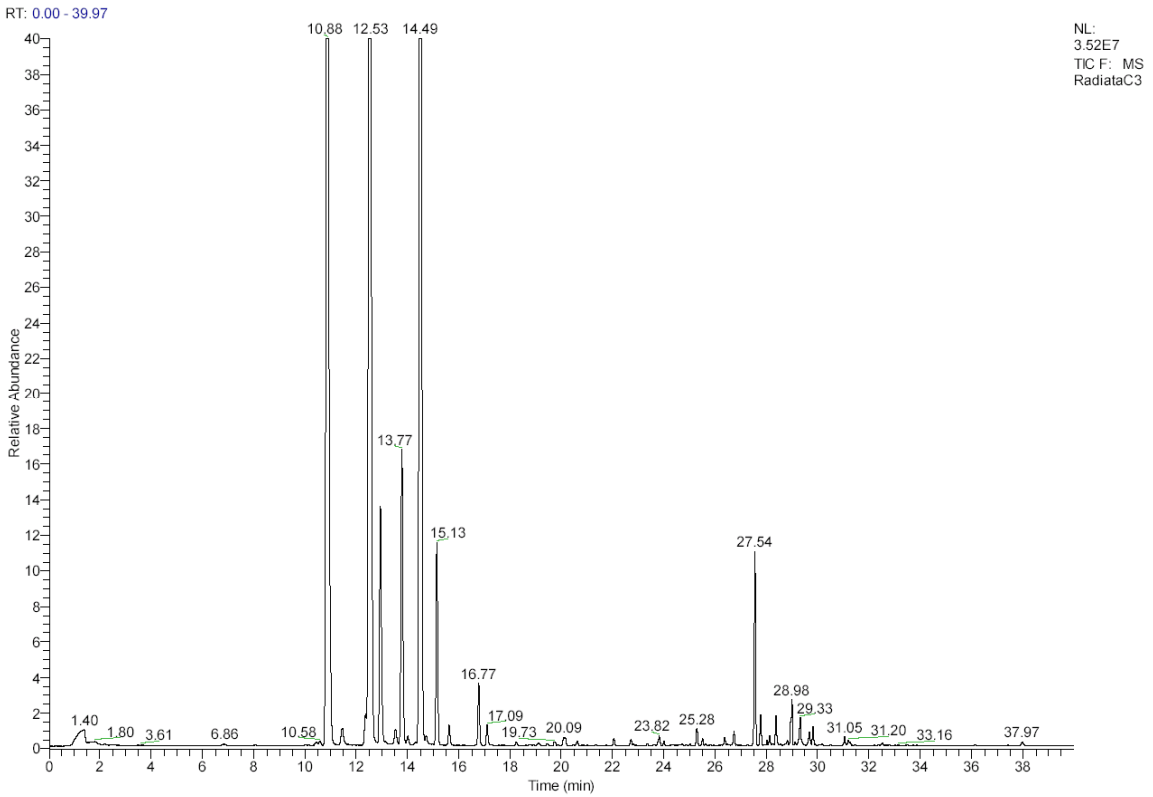

Figure A.9 - Reconstructed total ion chromatogram from the headspace of *P. radiata* needles analyzed on the DB-5ms column.

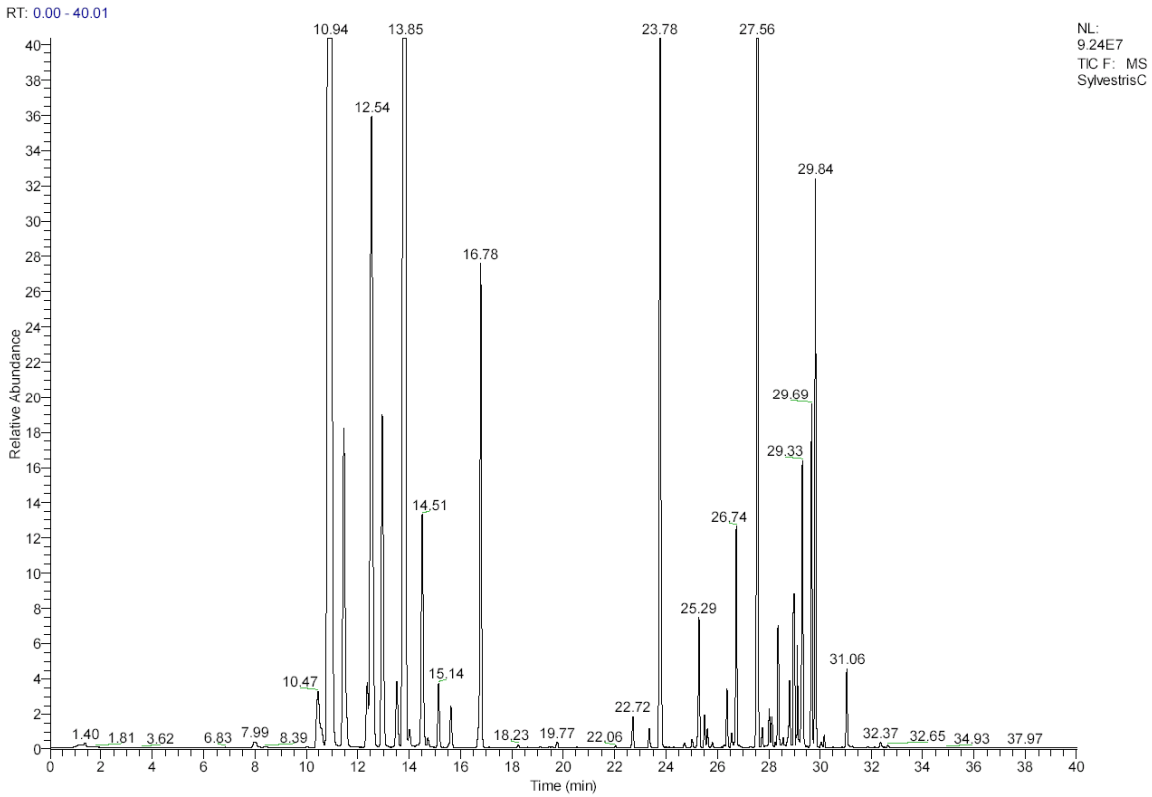

Figure A.10 - Reconstructed total ion chromatogram from the headspace of *P. sylvestris* needles analyzed on the DB-5ms column.

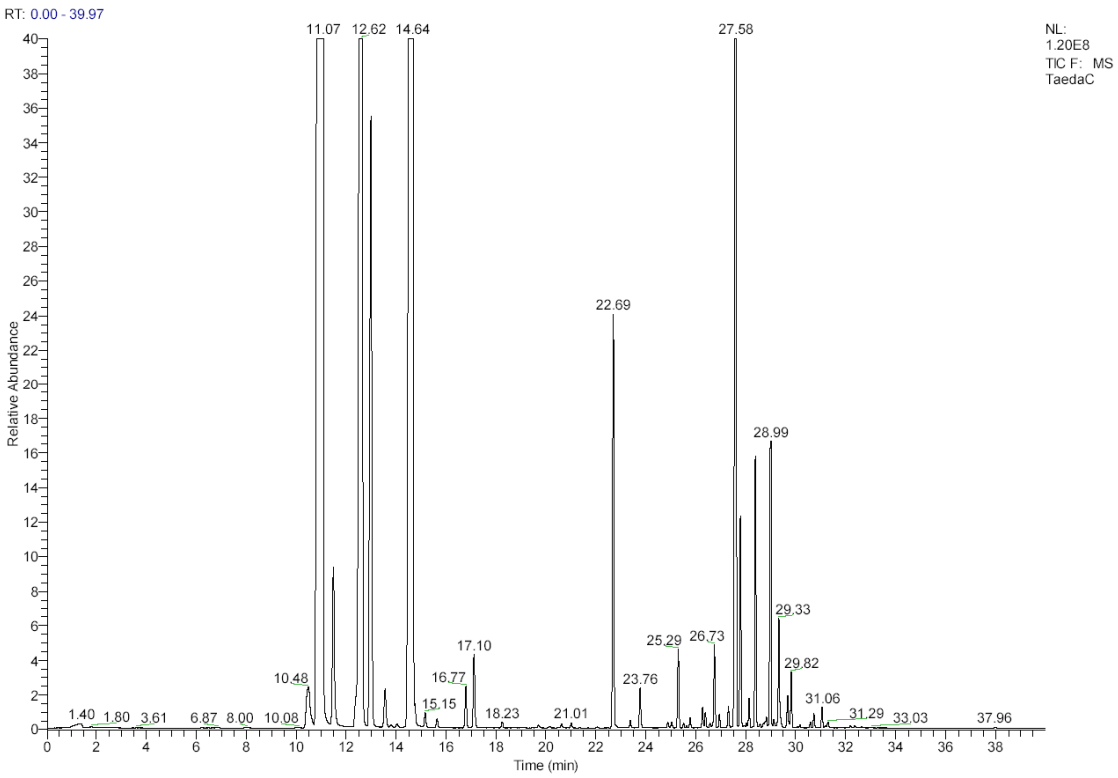

Figure A.11 - Reconstructed total ion chromatogram from the headspace of *P. taeda* needles analyzed on the DB-5ms column.

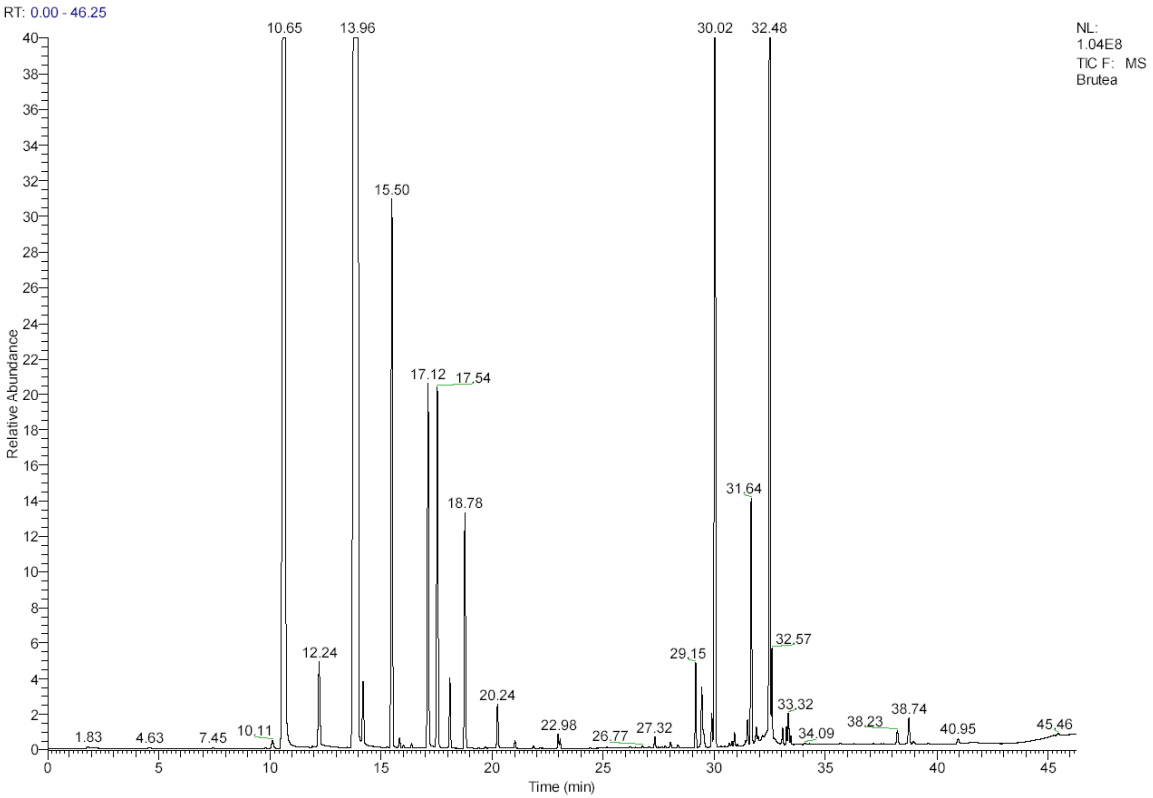

Figure A.12 - Reconstructed total ion chromatogram from the headspace of *P. brutia* needles analyzed on the DB-Wax column.

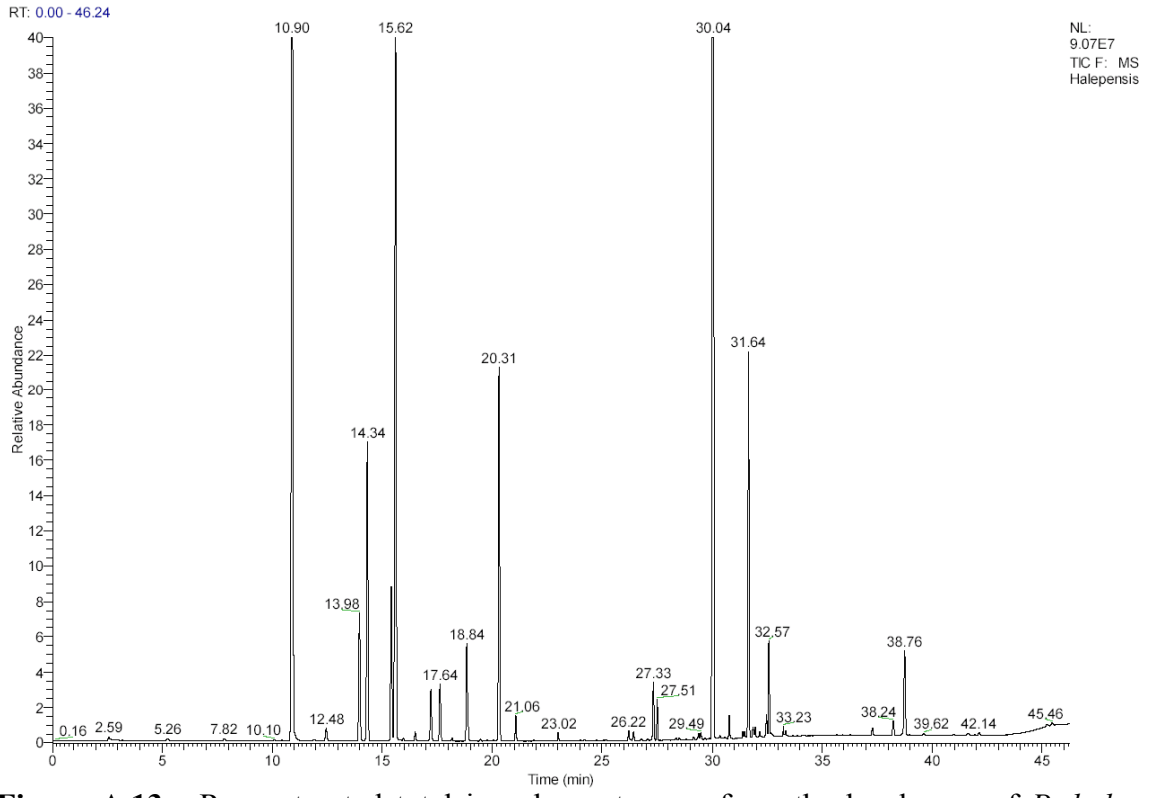

Figure A.13 - Reconstructed total ion chromatogram from the headspace of *P. halepensis* needles analyzed on the DB-Wax column.

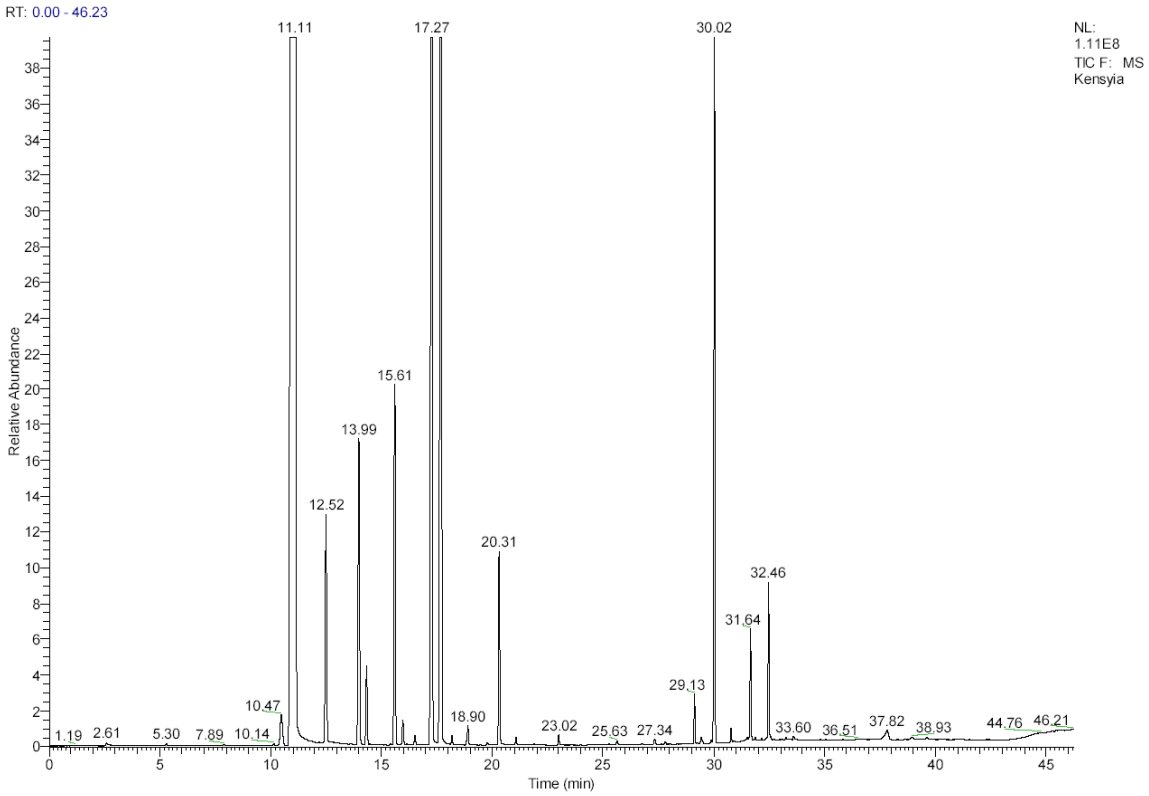

Figure A.14 - Reconstructed total ion chromatogram from the headspace of *P. kesiya* needles analyzed on the DB-Wax column.

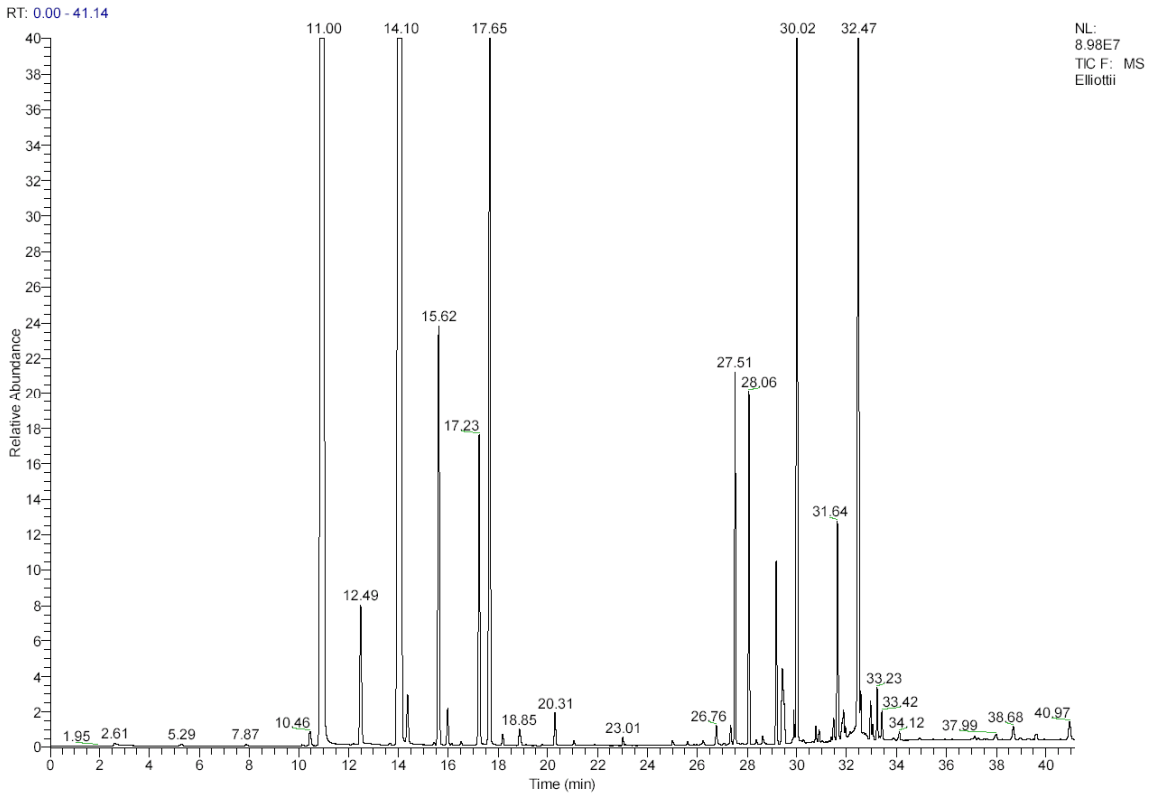

Figure A.15 - Reconstructed total ion chromatogram from the headspace of *P. kesiya* needles analyzed on the DB-Wax column.

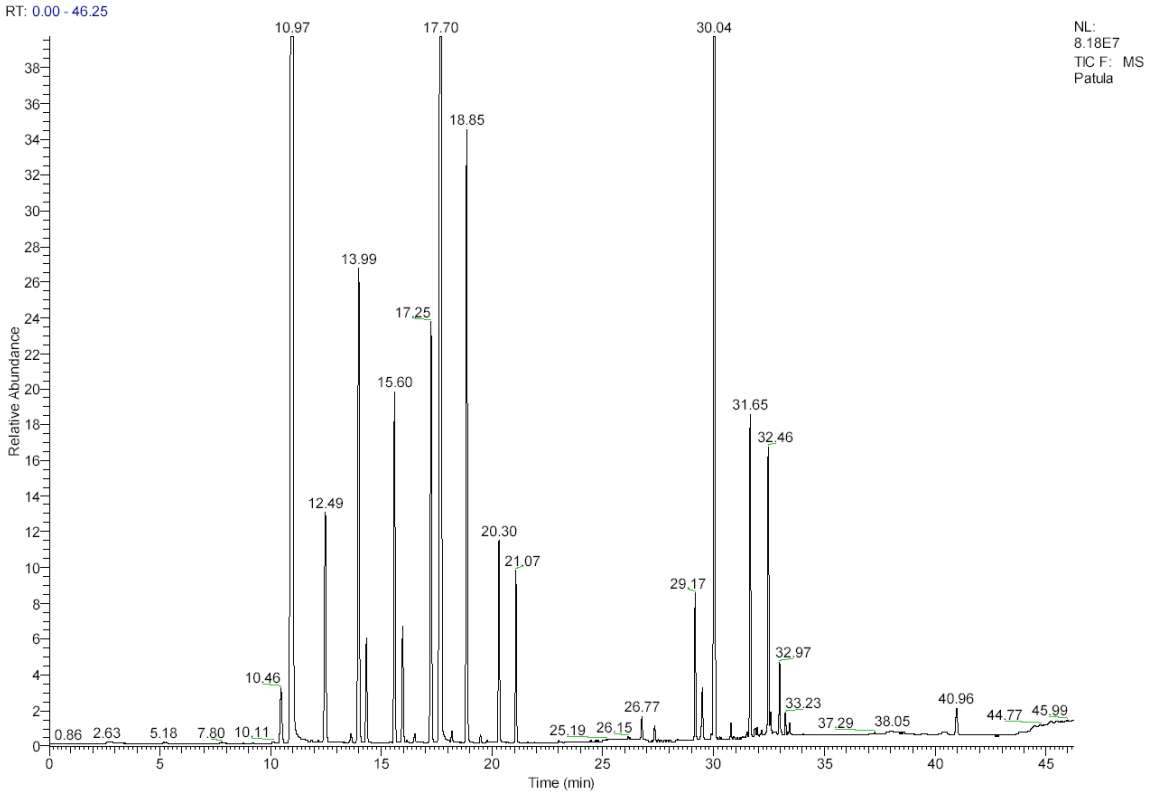

Figure A.16 - Reconstructed total ion chromatogram from the headspace of *P. elliotti* needles analyzed on the DB-Wax column.

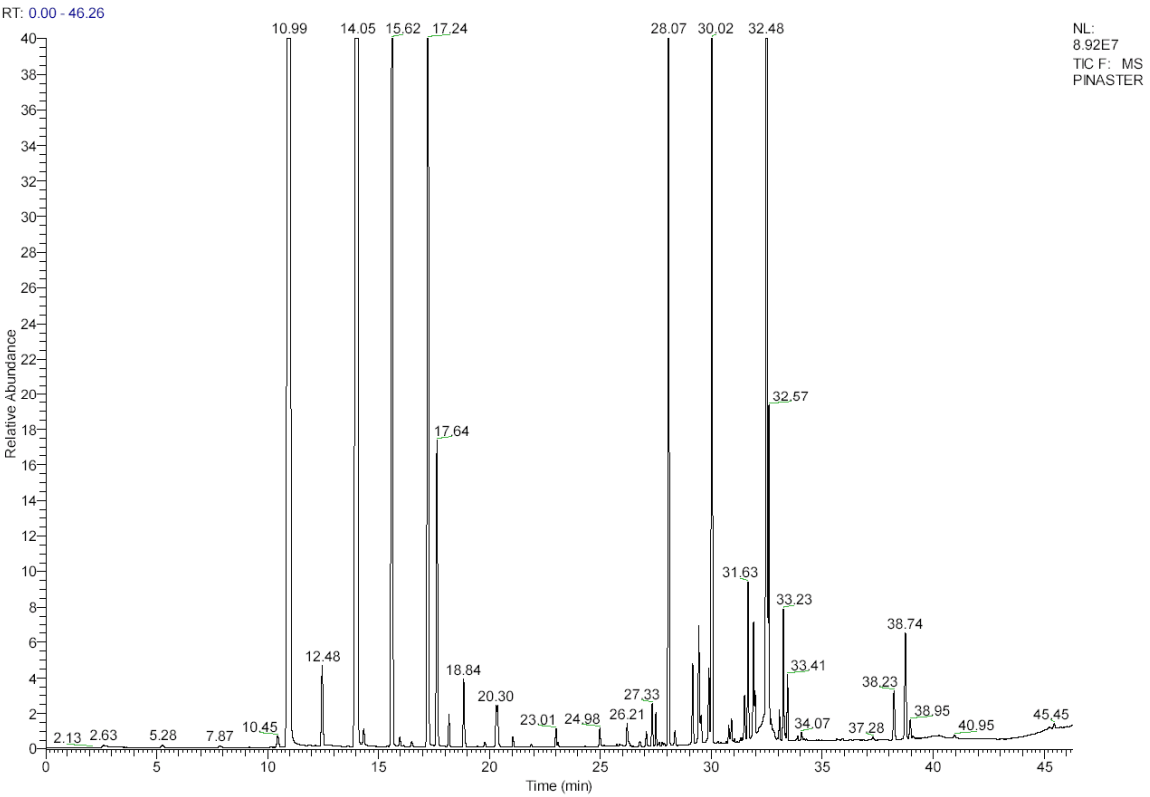

Figure A.17 - Reconstructed total ion chromatogram from the headspace of *P. pinaster* needles analyzed on the DB-Wax column.

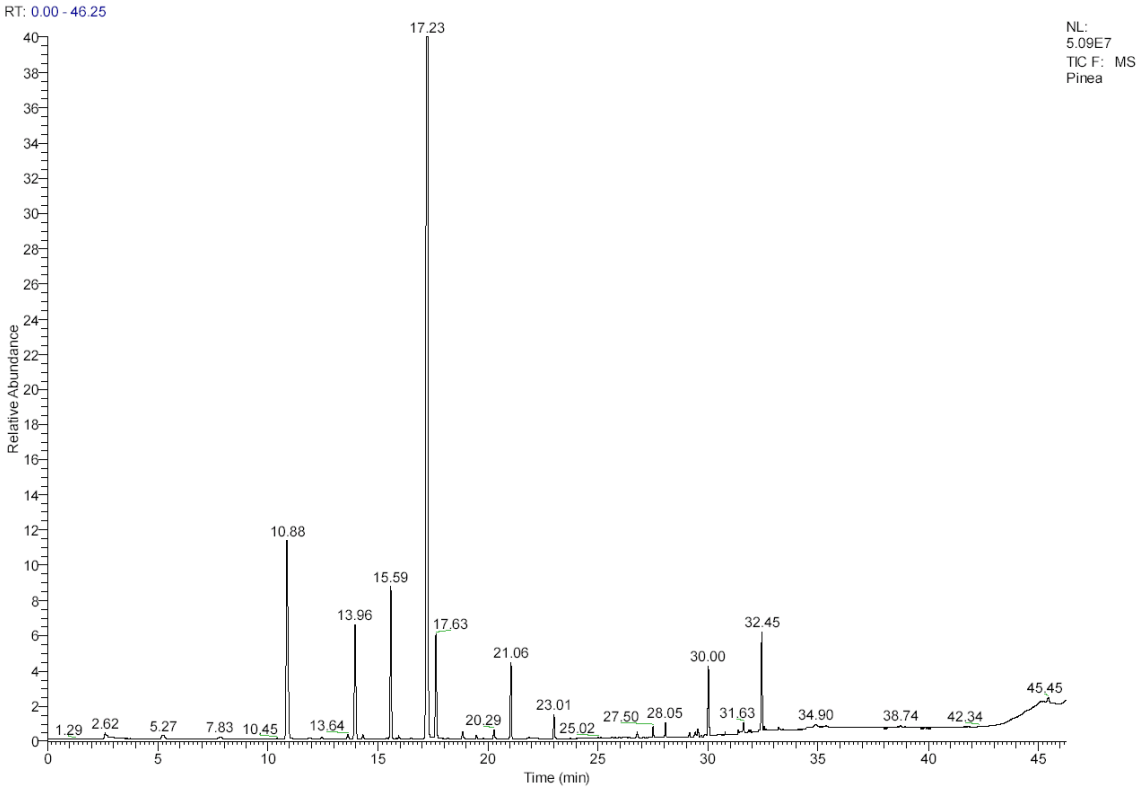

Figure A.18 - Reconstructed total ion chromatogram from the headspace of *P. pinea* needles analyzed on the DB-Wax column.

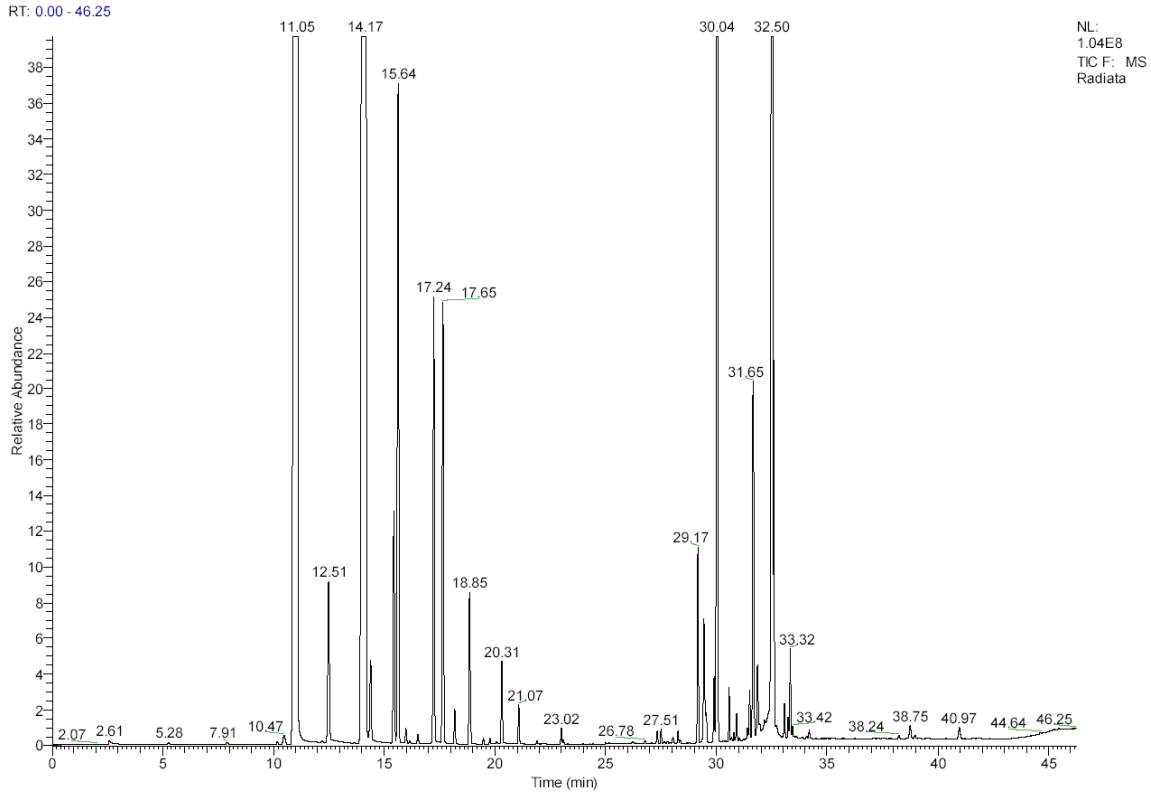

Figure A.19 - Reconstructed total ion chromatogram from the headspace of *P. radiata* needles analyzed on the DB-Wax column.

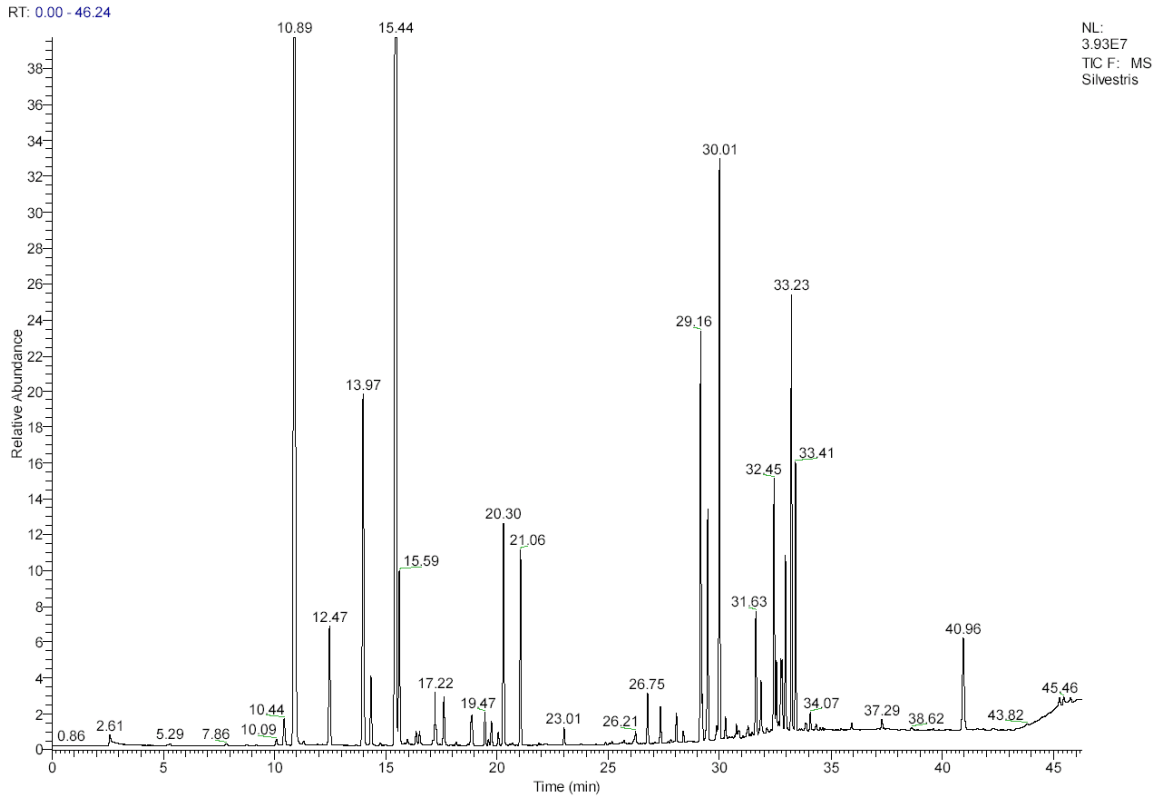

Figure A.20 - Reconstructed total ion chromatogram from the headspace of *P. sylvestris* needles analyzed on the DB-Wax column.

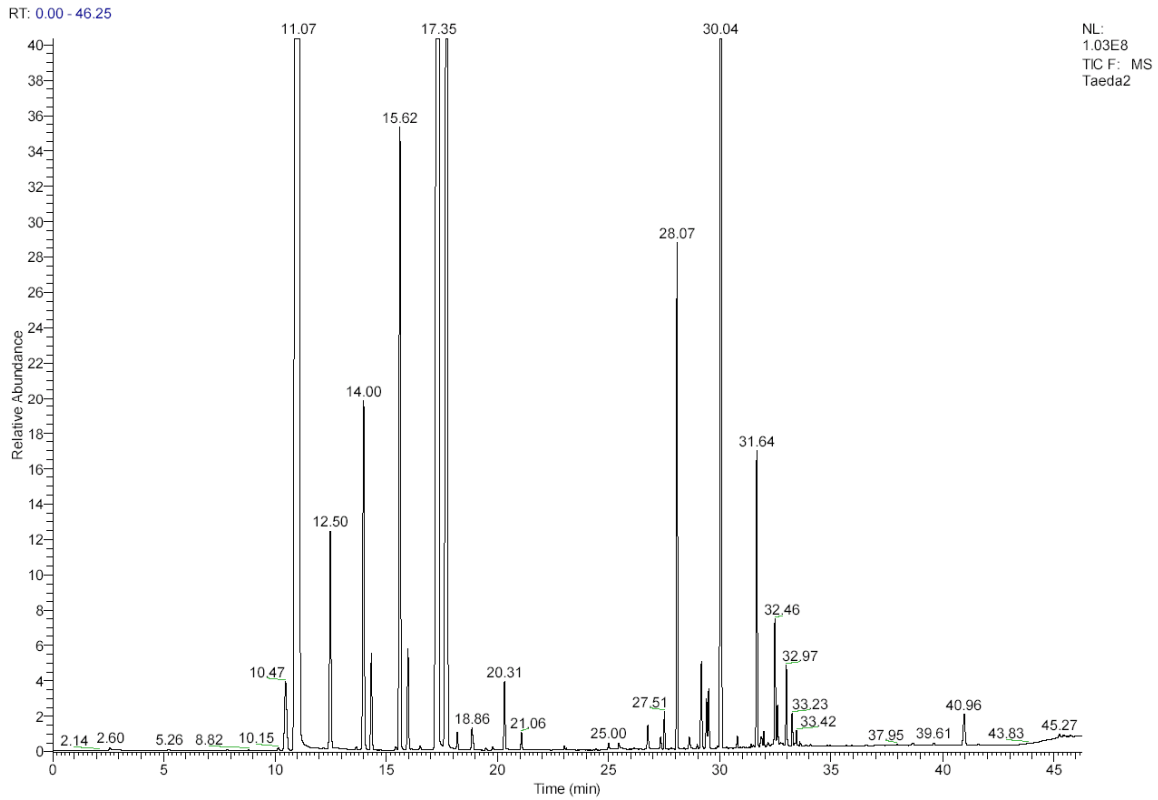

Figure A.21 - Reconstructed total ion chromatogram from the headspace of *P. taeda* needles analyzed on the DB-Wax column.

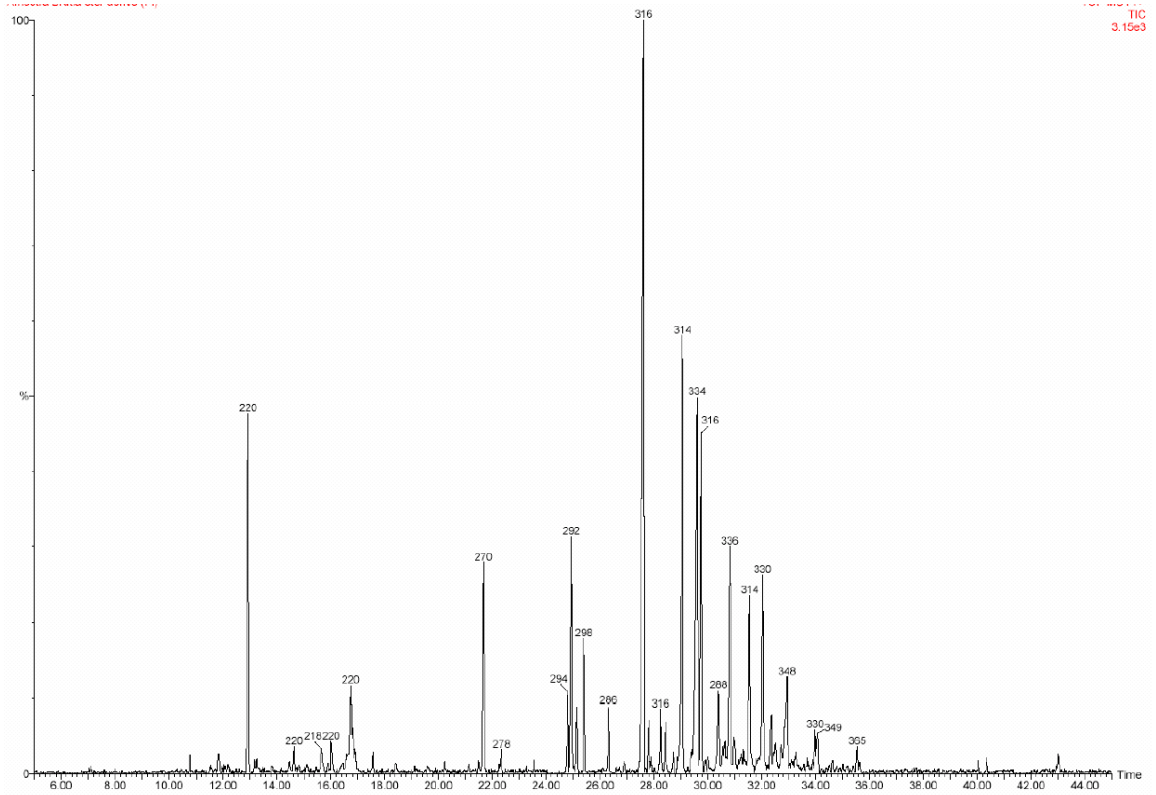

Figure A.22 - 1D-GC/FI-TOFMS TIC from the needles of the *P. brutia* used in the first experience (larval performance; Resin acids). Peak annotations – scan base peak masses.

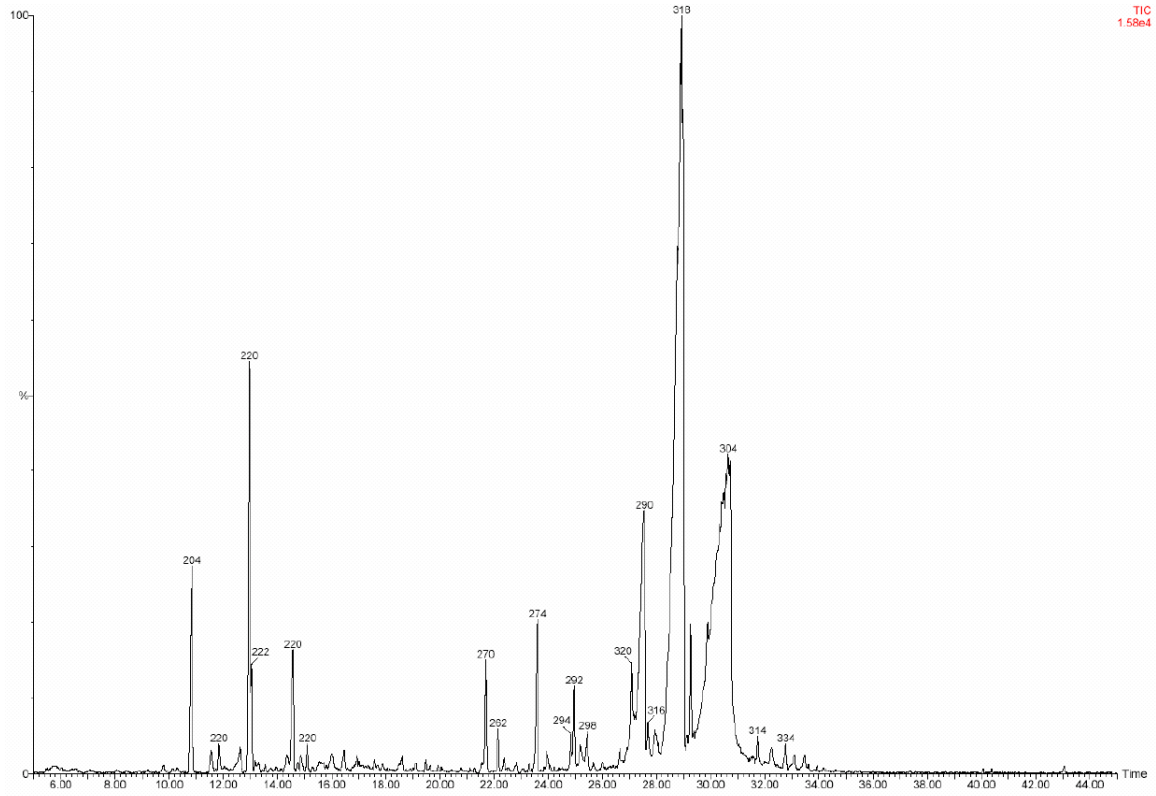

Figure A.23 - 1D-GC/FI-TOFMS TIC from the needles of the *P. halepensis* used in the first experience (larval performance; Resin acids). Peak annotations – scan base peak masses.

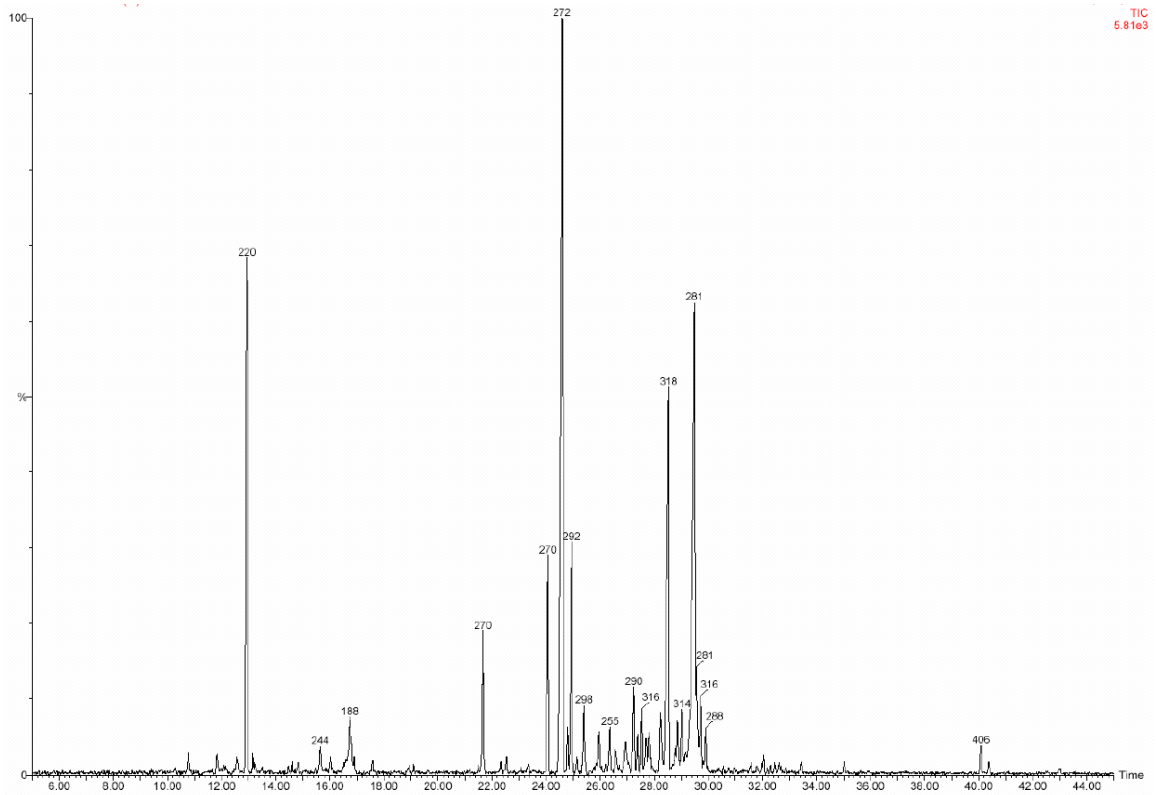

Figure A.24 - 1D-GC/FI-TOFMS TIC from the needles of the *P. pinaster* used in the first experience (larval performance; Resin acids). Peak annotations –scan base peak masses.

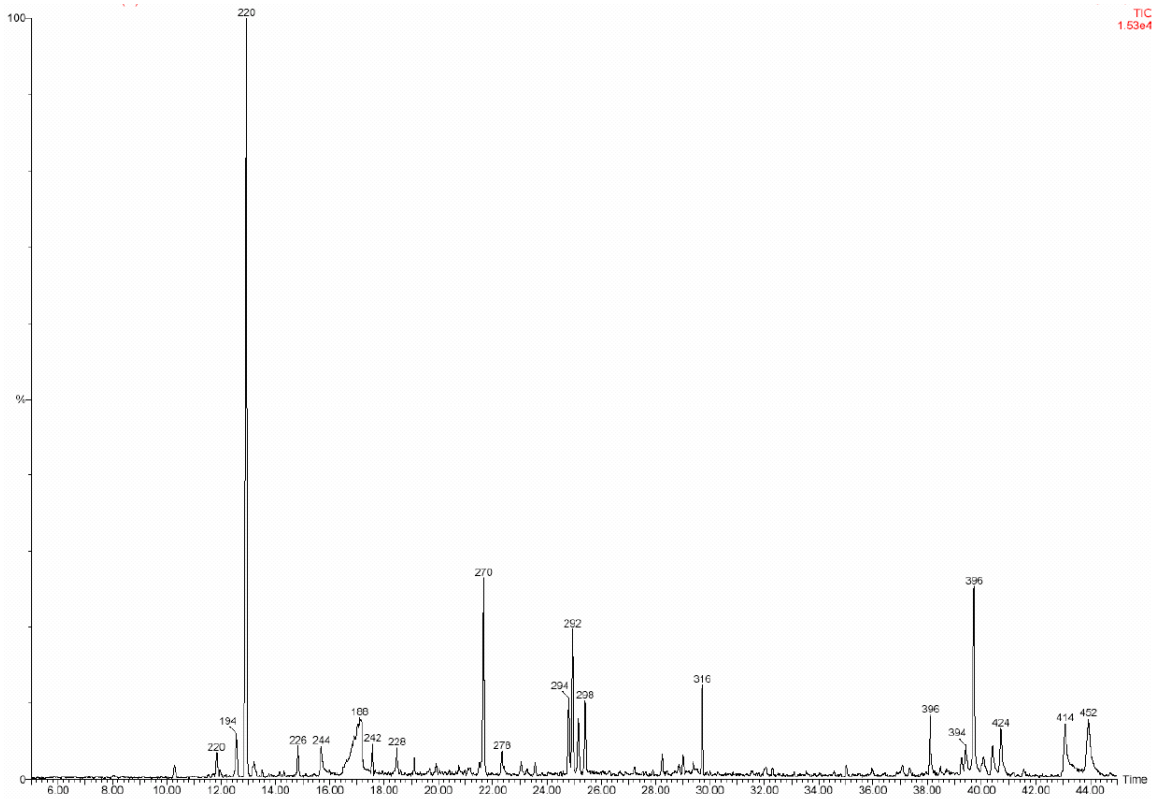

Figure A.25 - 1D-GC/FI-TOFMS TIC from the needles of the *P. pinea* used in the first experience (larval performance; Resin acids). Peak annotations –scan base peak masses.

Appendix B

Table B.1 - Chemical standards used for analyte identification.

Chemical standards	Chemical standards	Chemical standards
(-)-Mirtenal	γ-Butirolactone	Methyldecanoate
(-)-*trans*-Caryophyllene	γ-Nonalactone	Myrcene
(-)-α-Cedrene	γ-Terpinene	Nonan-2-ol
(-)-α-Copaene	γ-Valerolactone	Ocimene
(-)-α-Cubebene	γ–Dodecalactone	Octan-1-ol
(-)-α-Pinene	Acetic acid	Octan-2-ol
(-)-β-Citronelol	Anisole	Octanal
(-)-β-Pinene	Butan-1-ol	*p*-Cimene
(+)-Aromadendrene	Butan-2-ol	Pent-1-en-3-one
(+)-Calarene	Camphene	Pentan-2,4-diol
(+)-α-Pinene	Carvacrol	Pentan-2-ol
(+)-α-Terpineol	*cis*-Citral (neral)	Pentan-3-one
(+)-β-Pinene	*cis*-Hex-2-en-1-ol	Phenyl ethyl acetate
(+)-γ-Decanolactone	*cis*-Hex-3-en-1-ol	Phenyletan-1-ol
(+)-γ-Gurjunene	Etanol	Propan-1-ol
Δ-3-Carene	Ethyl acetate	Propan-2-ol
1,8-Cineol (eucalyptol)	Ethyl hexanoate	R-(+)-Limonene
1-Octyl acetate	Ethyldecanoate.	S-(-)-Limonene
2-Ethylfuran	Ethylphen-4-ol	Sabinene
2-Ethylhexan-1-ol	Geraniol	Terpinolene
2-Methylbutan-1-ol	Heptanal	Terpinyl acetate
2-Methylbutyl acetate	Heptanoic acid	Thujene
2-Methylpropan-1-ol	Hexan-1-ol	*trans, trans*-Deca-2,4-dienal
2-Octyl acetate	Hexan-2-ol	*trans*, *trans*-Nona-2,4-dienal
4-Methylpent-3-en-2-one	Hexan-2-ona	*trans*-2-Hexenyl acetate
α-Fenchene	Hexanal	*trans*-Citral (geranial)
α-Phellandrene	Hexanoic acid	*trans*-Hex-2-en-1-al
α-Terpinene	Hexyl acetate	*trans*-Nonen-2-al
α-Terpineol	Isoamyl alcohol	*trans*-Octen-2-al
β-Citronelol	Linalool	Tricyclene
β-Phellandrene*	Linalool oxide I	Whisky lactone A
δ-Decanolactone	Linalool oxide II	Whisky lactone B
δ-Dodecalactone	Verbenone	α-Caryophyllene (α-Humulene)
	Methanol	ASTM D5307 Hydrocarbon mix

*β-Phellandrene was synthesized according to United States Patent 4224240 and United States Patent 4136126

Appendix C

Table C.1 – *Thaumetopoea pityocampa* final weight, biomass consumption, faeces produced, food assimilated (consumption-faeces) (mg dry weight) and survival (%), observed for 2nd instar larvae, fed on four *Pinus* species ($\bar{x}$ ± SE, n = 5) and ANOVA results. Different letters indicate significant differences at $P < 0.05$ (Branco *et al.*, in prep.)

Measure	*Pinus pinaster*	*Pinus brutia*	*Pinus pinea*	*Pinus halepensis*	$F_{3, 16}$	*P*
Initial weight	14.1 ± 0.4^{a}	14.4 ± 0.2^{a}	14.1 ± 0.2^{a}	14.1 ± 0.2^{a}	0.33	0.801
Final weight	30.9 ± 2.0^{b}	33.1 ± 1.7^{b}	37.6 ± 1.1^{c}	19.9 ± 0.5^{a}	26.47	<0.001
Consumption	403.0 ± 37.1^{c}	265.5 ± 7.0^{b}	407.6 ± 27.0^{c}	160.5 ± 18.9^{a}	22.60	<0.001
Weight gain	16.8 ± 1.7^{b}	18.7 ± 1.6^{b}	23.4 ± 1.1^{c}	5.6 ± 0.5^{a}	32.31	<0.001
Faeces produced	284.8 ± 29.7^{c}	175.0 ± 9.8^{b}	214.6 ± 4.7^{b}	66.7 ± 6.0^{a}	32.14	<0.001
Food assimilated	118.2 ± 11.0^{a}	90.5 ± 10.1^{a}	193.0 ± 24.9^{b}	93.8 ± 13.7^{a}	8.82	0.001
Survival (%)	90.0 ± 3.3^{b}	92.7 ± 2.9^{b}	95.3 ± 1.7^{b}	78.0 ± 4.4^{a}	3.73	0.032